Nonlinear Optical Crystals: A Complete Survey

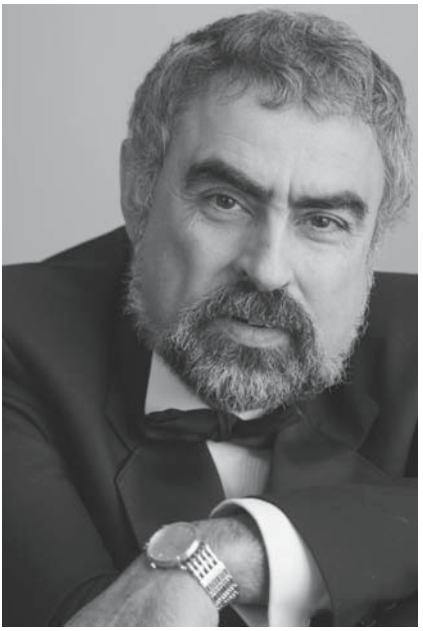

Prof. David N. Nikogosyan, Ph.D., is an SFI (Science Foundation Ireland) Investigator in the Physics Department at University College Cork, Cork, Ireland. He has a 35-year scientific career in nonlinear optics, laser physics and quantum electronics. He has authored 133 peer-reviewed scientific publications, including 11 reviews and 8 books.

David N. Nikogosyan

Nonlinear Optical Crystals: A Complete Survey

Springer

Prof. David N. Nikogosyan, Ph.D.
SFI Investigator
Physics Department
University College Cork
Cork, Ireland.
niko@phys.ucc.ie

ISBN 0-387-22022-4 Printed on acid-free paper.

Printed in the United States of America. (HAM)

9 8 7 6 5 4 3 2 1 SPIN 10948989

springeronline.com

Preface

Many, many years ago, when I was a 12-year-old boy, my father, the renowned sculptor Nikolai Nikogosyan, took my mother and me to visit the famous Soviet diplomat, former Ambassador to the U.K., Prof. Ivan Maisky. At that time my father was creating his sculpture portrait and, as usual, he started a friendship with his model. We were invited to dinner at the ambassador's summer residence ("dacha" in Russian), some 25 miles outside Moscow. I cannot recall in detail that June evening, but I do remember that it was quite bright, and in front of the house, on the round border, the nicely scented scarlet roses were flourishing. But what I can still clearly see through the time distance of 45 years is the ambassador's working room, which housed, besides many other books, the newly published second edition of the *Soviet Encyclopaedia* in luxurious black-leather volumes. I opened one and was immediately captured by the diversity of information: color maps, schemes, photos, illustrations, references, and so forth. "What a treasure!" I thought. When we were returning home, I asked father if it would be possible to purchase such a fantastic set of books, even without luxurious bindings. But he didn't understand my enthusiasm. My mother was more cooperative; she told me that it was too expensive for us and that it would be better if I bought it myself when I would have the means to do so.

Later, in the mid-1960s, when I was studying Physics at Moscow University, I subscribed to the next (the third and last) edition of the *Soviet Encyclopaedia* and during the following 7 or 10 years I purchased it volume by volume (as they were published). I remember the price of a single volume was 5.5 roubles (at that time 8 U.S. dollars by official exchange rate), which formed a noticeable portion of my monthly stipend of 35 roubles.

Nowadays, according to common sense, any encyclopedia is useless. Often, I hear from my students that everything can be found on the Internet. It is, however, a very rough approximation. First of all, on the Internet any small useful seed of information is dissolved in the ocean of useless data, put there without any responsibility or control. The reference data found on the Internet is often incomplete, out of date, and often contradicts similar data from other sources. Anybody who disagrees with me can check it by typing the name of any popular nonlinear optical crystal (e.g., BBO, KTP, lithium niobate, and so forth) into www.google.com and comparing the

different data that appears on the screen. As a result, the Internet user should have a certain erudition to distinguish between numerous data values. The electronic brains of modern computers, though being fantastically fast and genuinely comprehensive, are still rather stupid and unable to make any logical comparison between the different sets of data and to choose the most reliable ones. In other words, in our Internet society, there is still a significant need for scientific books.

From my childhood and throughout all my life (I am 57 now), I was a keen collector. First, it was stamps, then coins, then books, then LPs, then antiques, then rhododendrons (I have a nice collection of 50 varieties in my Irish garden), and so forth. And this crystal survey can be considered as a collection of data, which I have been arranging and completing during the last 25 years. My first review on nonlinear optical crystals [1] appeared in 1977 and 20 years later was selected by SPIE as a milestone publication in the field of optical parametric oscillators [2]. This personal history is probably the reason why I decided to create one more book on nonlinear optical crystals and to spend every day (in reality every evening), during a one and a half year period, behind my home computer. In other words, I like this process (there is no other explanation).

The remarkable property of such a collection is that it belongs to many people simultaneously, as I share it with each reader. I hope that using (reading) my little encyclopedia will bring the readers at least a small part of the great enjoyment, that the compilation of this book gave me.

David N. Nikogosyan
Tower, Blarney
Co. Cork, Ireland
20 December 2003

References

[1] D.N. Nikogosyan: Nonlinear optical crystals (review and summary of data). Kvant. Elektron. **4(1)**, 5–26 (1977) [In Russian, English trans.: Sov. J. Quantum Electron. **7(1)**, 1–13 (1977)].

[2] D.N. Nikogosyan: Nonlinear optical crystals (review and summary of data). In: *Selected Papers on Optical Parametric Oscillations and Amplifiers and Their Applications*, *SPIE Milestone Series*, *Vol. MS140*, ed. by J.H. Hunt (SPIE Optical Engineering Press, Bellingham, Washington, 1997), pp. 191–203.

Contents

Abbreviations

BPM, birefringent phase matching
CW, continuous wave
FiHG, fifth-harmonic generation
FoHG, fourth-harmonic generation
HeXLN, hexagonally poled lithium niobate
MOPA, master oscillator power amplifier
NCPM, non-critical phase matching
OPA, optical parametric amplifier
OPG, optical parametric generator
OPO, optical parametric oscillator
PPKTP, periodically poled potassium titanyl phosphate
PPLN, periodically poled lithium niobate
PPLT, periodically poled lithium tantalate
PPRTA, periodically poled rubidium titanyl arsenate
QPM, quasi phase matching
SFD, self-frequency doubling
SFG, sum-frequency generation
SH, second harmonic
SHG, second-harmonic generation
THG, third-harmonic generation
YAG, yttrium aluminum garnet
YAP, yttrium orthoaluminate
YLF, yttrium lithium fluoride
YSGG, yttrium scandium gallium garnet

1

Introduction

In the past 25 years, I have published 9 reviews and databases on nonlinear optical crystals [1–9]. Therefore, in introducing this new book, I would like to answer probably the most common FAQs of future readers: "Why do we need this new book and what are the most important changes in this crystal survey in comparison with my last database, compiled in 1995 and published by Springer in 1997 and 1999 [8,9]?"

The reason for writing a new book is, first of all, the tremendous development of laser techniques in the past decade. There are three obvious tendencies:

1. A transfer to shorter laser pulses with hundreds (tens) femtoseconds of duration. The shorter pulsewidth leads to an increase of irradiation intensity, which forces nonlinear optical processes to proceed with higher efficiency. At the same time, such transfer dramatically increases the laser pulse–induced damage threshold of nonlinear materials. The short pulse duration makes it necessary to account for the effect of group velocity dispersion. This effect could even be profitable, leading to laser pulse compression in the course of second-harmonic generation (SHG).
2. The development of miniature diode-pumped continuous-wave (CW) laser sources, emitting light in the visible, UV, and near IR ranges. The invention of a new method of phase matching, the so-called quasi-phase matching, allowed use of the highest possible value of the second-order nonlinear coefficient in any crystal material and the ability to obtain phase-matching in any desirable direction (e.g., non-critical phase matching). This significantly increases the efficiency of second-order three-wave interactions (i.e., SHG), allowing the change of frequency of a laser diode with rather high output. Another possible way is to dope the nonlinear optical crystal by a rare-earth ion (which is usually Nd or Yb). Under laser-diode pumping, such doped material generates the fundamental radiation and simultaneously converts it into the second harmonic. Therefore, they are referred to as the self-frequency-doubling crystals.
3. An active search for new nonlinear optical materials, especially among the low-symmetry crystals. In the past decade, important crystals such as GdCOB, YCOB, YAB, BIBO, CLBO, KBBF, LB4, $MgBaF_4$, GaAs, and many others were

introduced or developed. This led to their successful application in quasi-phase matching, self-frequency doubling, deep-UV generation, and so forth.

This book differs from the previous handbook [8,9] first of all by its structure. I omitted the theoretical part as the theory for second-order three-wave interactions in nonlinear crystals is now well established, and other good books have also been written on that subject [10]. I also decided to exclude from consideration all traditional applications of nonlinear optical materials (SHG, SFG, DFG, OPO, and so on), as it would easily increase the book's volume well above any acceptable level.

The second difference is the content of this new database. Forty-three old-fashioned nonlinear optical materials were excluded, and instead, 30 new crystals are now included. For the first time, a special consideration is made for periodically poled and self-frequency-doubling materials. The structure of each crystal file was changed drastically, adding the significant amount of crystallophysical, thermophysical, spectroscopic, electrooptic and magnetooptic information.

This newly written survey of 63 nonlinear optical crystals contains more than 1500 different references with full titles, which for convenience are presented inside each data file. Fifteen percent of all citations refer to years 2000–2003; 41% to the past 9 years (the time passed since the previous data collection). The most frequently cited sources were the journals *Applied Physics Letters* (11.3% of all references), *Optics Letters* (10.0% of all references), and *Optics Communications* (9.8% of all references).

After the survey of crystal properties (Chapters 2–8), Chapter 9, with seven mini-reviews discussing some recent applications of common and novel nonlinear materials (including self-frequency doubling and quasi-phase matching), completes the book.

Finally, I would like to mention my friends and colleagues, listed below in alphabetical order, for their critical comments, valuable discussions, and for sending me related reprints and pdf files. My sincere acknowledgments go to Prof. Gerard Aka (France), Prof. Vladimir Alshits (Russia), Prof. Ladislav Bohaty (Germany), Dr. Patrick Mc Carthy (Ireland), Dr. Subhasis Das (India), Dr. Katia Gallo (U.K.), Dr. Helmut Görner (Germany), Dr. Sergey Grechin (Russia), Dr. Alexander Gribenyukov (Russia), Dr. Stas Ionov (U.S.A.), Dr. Ludmila Isaenko (Russia), Dr. Mitsuru Ishii (Japan), Prof. Kiyoshi Kato (Japan), Dr. Hideo Kimura (Japan), Prof. Takayoshi Kobayashi (Japan), Prof. Lev Kulevskii (Russia), Prof. Nikolay Leonyuk (Russia), Prof. Wenju Liu (China), Ms. Alla Makarova (Russia), Dr. Nikolai Merzliakov (Russia), Dr. Kiminori Mizuuchi (Japan), Prof. Yusuke Mori (Japan), Dr. Eugene Moskovets (U.S.A.), Dr. Tatiana Perova (Ireland), Dr. Katalin Polgár (Hungary), Dr. Mariola Ramirez (Spain), Prof. Martin Richardson (U.S.A.), Prof. Eugenii Ryabov (Russia), Prof. Mark Saffman (U.S.A.), Prof. Solomon Saltiel (Bulgaria), Dr. Ichiro Shoji (Japan), Dr. Yuji Suzuki (Japan), Dr. Eiko Takaoka (Japan), Prof. Daniel Vivien (France), Dr. Richard White (Australia), Dr. Alexander Yelisseyev (Russia), Dr. Masashi Yoshimura (Japan), Dr. Natalia Zaitseva (U.S.A.), and Dr. Anatoly Zayats (U.K.).

I would like to acknowledge separately the help of Ms. Eileen Heathy, Ms. Phil O'Sullivan, and Mr. Garret Cahill from the Inter-Library Loans Service, Boole Library, University College Cork.

I wish especially to thank my Editor, Dr. Hans Koelsch from Springer-NY, for his constructive advice and fruitful cooperation. I am also infinitely grateful to my beloved wife Danielle for her encouragement and patience.

References

[1] D.N. Nikogosyan: Nonlinear optical crystals (review and summary of data). Kvant. Elektron. **4(1)**, 5–26 (1977) [In Russian, English trans.: Sov. J. Quantum Electron. **7(1)**, 1–13 (1977)].

[2] D.N. Nikogosyan, G.G. Gurzadyan: Crystals for nonlinear optics. Biaxial crystals. Kvant. Elektron. **14(8)**, 1529–1541 (1987) [In Russian, English trans.: Sov. J. Quantum Electron. **17(8)**, 970–977 (1987)].

[3] G.G. Gurzadyan, V.G. Dmitriev, D.N. Nikogosyan: *Nonlinear Optical Crystals. Properties and Applications in Quantum Electronics. Handbook* (Radio i Sviyaz, Moscow, 1991), pp. 1–160 [In Russian].

[4] V.G. Dmitriev, G.G. Gurzadyan, D.N. Nikogosyan: *Handbook of Nonlinear Optical Crystals.* Springer Series in Optical Sciences, Vol. 64, ed. by A.E. Siegman (Springer, Berlin, 1991), pp. 1–221.

[5] D.N. Nikogosyan: Beta barium borate (BBO). A review of its properties and applications. Appl. Phys. A **52(6)**, 359–368 (1991).

[6] D.N. Nikogosyan: Lithium triborate (LBO). A review of its properties and applications. Appl. Phys. A **58(3)**, 181–190 (1994).

[7] D.N. Nikogosyan: *Properties of Optical and Laser-Related Materials. A Handbook* (John Wiley & Sons Ltd., Chichester, 1997), pp. 1–594.

[8] D.N. Nikogosyan: Properties of Nonlinear Optical Crystals. In: V.G. Dmitriev, G.G. Gurzadyan, D.N. Nikogosyan: *Handbook of Nonlinear Optical Crystals, Second, Revised and Updated Edition*. Springer Series in Optical Sciences, Vol. 64, ed. by A.E. Siegman (Springer, Berlin, 1997), pp. 67–288.

[9] D.N. Nikogosyan: Properties of Nonlinear Optical Crystals. In: V.G. Dmitriev, G.G. Gurzadyan, D.N. Nikogosyan: *Handbook of Nonlinear Optical Crystals, Third Revised Edition*. Springer Series in Optical Sciences, Vol. 64, ed. by A.E. Siegman (Springer, Berlin, 1999), pp. 67–288.

[10] R.L. Sutherland: *Handbook of Nonlinear Optics* (Marcel Dekker, New York, 1996), pp. 1–685.

2

Basic Nonlinear Optical Crystals

This chapter contains information on the four most widely used nonlinear optical crystals: beta-barium borate (BBO), lithium triborate (LBO), lithium niobate (LN), and potassium titanyl phosphate (KTP). Together with their periodically poled derivatives, periodically poled lithium niobate (PPLN) and periodically poled potassium titanyl phosphate (PPKTP), these materials are employed in at least 75% of all today's practical applications.

All the values of the angular, temperature and spectral acceptances, given in this and in the following chapters, correspond to a 1 cm length of the considered nonlinear crystal.

2.1 β-BaB_2O_4, Beta-Barium Borate (BBO)

Negative uniaxial crystal: $n_o > n_e$
Molecular mass: 222.950
Specific gravity: 3.84 g/cm^3 [1]; 3.849 g/cm^3 [2]; 3.85 g/cm^3 at $T = 293$ K [3]
Point group: $3m$
Lattice constants:
$a = 12.532$ Å [4]; 12.532 ± 0.001 Å [2]; 12.547 Å [5]
$c = 12.717$ Å [4]; 12.726 ± 0.001 Å [2]; 12.736 Å [5]
Mohs hardness: 4 [6], [7]; 4.5 [2]
Melting point: 1368 K [2], [8]

Linear thermal expansion coefficient α_t [3]

T [K]	$\alpha_t \times 10^6$ [K^{-1}], $\parallel c$	$\alpha_t \times 10^6$ [K^{-1}], $\perp c$
293	0.36	−2.54

Mean value of linear thermal expansion coefficient [5]

T [K]	$\alpha_t \times 10^6$ [K^{-1}], $\parallel c$	$\alpha_t \times 10^6$ [K^{-1}], $\perp c$
298–1173	36	4.0

Specific heat capacity c_p at $P = 0.101325$ MPa

T [K]	c_p [J/kgK]	Ref.
298	490	[2]
	496	[9]

Thermal conductivity coefficient

κ [W/mK], $\parallel c$	κ [W/mK], $\perp c$	Ref.
0.8	0.08	[5]
1.6	1.2	[10]

Direct band-gap energy at room temperature: $E_g = 6.2$ eV [11], 6.43 eV [12]
Transparency range:
at 0.5 level: 0.198–2.6 μm for 0.8-cm-long crystal [13]; 0.196–2.2 μm for 0.3-cm-long crystal [2]
at "0" transmittance level: 0.189–3.5 μm [8], [14]
at 0.5 transmittance level: 0.198–2.6 μm [1]

Linear absorption coefficient α

λ [μm]	α [cm^{-1}]	Ref.	Note
0.1934	1.39	[15]	$T = 295$ K
	0.29	[15]	$T = 91$ K
0.213	<0.21	[1]	best crystals
0.264	0.04 ± 0.01	[16]	$\parallel c$
	0.06 ± 0.003	[16]	$\perp c$, o-wave
	0.10 ± 0.003	[16]	$\perp c$, e-wave
0.2661	<0.17	[1]	best crystals
	0.04–0.15	[2]	
0.5321	0.01	[17]	
	<0.01	[9]	
1.0	0.001–0.002	[2]	
1.0642	<0.001	[9]	
2.09	0.0085	[2]	e-wave
	0.07	[2]	o-wave
2.55	0.5	[18]	

Two-photon absorption coefficient β

λ [μm]	τ_p [ns]	$\beta \times 10^{11}$ [cm/W]	Ref.	Note
0.211	0.0009	243 ± 85	[19]	$\theta = 30°$, $\phi = 0°$
0.264	0.0008	93 ± 33	[19]	$\theta = 30°$, $\phi = 0°$
	0.00022	68 ± 6	[20]	$\parallel c$

λ [μm]	τ_p [ns]	$\beta \times 10^{11}$ [cm/W]	Ref.	Note
		66 ± 7	[20]	$\perp c$, o-wave
		47 ± 5	[20]	$\perp c$, e-wave
	0.0002	61	[21]	$\theta = 48°$
0.2661	0.015	90 ± 10	[11]	$\parallel c$
0.3547	0.017	1.0 ± 0.2	[11]	$\parallel c$

Experimental values of refractive indices [5]

λ [μm]	n_o	n_e
0.40466	1.69267	1.56796
0.43583	1.68679	1.56376
0.46782	1.68198	1.56024
0.47999	1.68044	1.55914
0.50858	1.67722	1.55691
0.54607	1.67376	1.55465
0.57907	1.67131	1.55298
0.58930	1.67049	1.55247
0.64385	1.66736	1.55012
0.81890	1.66066	1.54589
0.85212	1.65969	1.54542
0.89435	1.65862	1.54469
1.01400	1.65608	1.54333

Temperature derivative of refractive indices for temperature range 293–353 K [5]

λ [μm]	$dn_o/dT \times 10^6$ [K^{-1}]	$dn_e/dT \times 10^6$ [K^{-1}]
0.4–1.0	−16.6	−9.3

Best set of dispersion relations (λ in μm, $T = 293$ K) [13]:

$$n_o^2 = 2.7359 + \frac{0.01878}{\lambda^2 - 0.01822} - 0.01354\,\lambda^2$$

$$n_e^2 = 2.3753 + \frac{0.01224}{\lambda^2 - 0.01667} - 0.01516\,\lambda^2$$

Sellmeier equations with better accuracy near infrared absorption edge (λ in μm, $T = 293$ K) [22]:

$$n_o^2 = 2.7359 + \frac{0.01878}{\lambda^2 - 0.01822} - 0.01471\,\lambda^2 + 0.0006081\,\lambda^4 - 0.00006740\,\lambda^6$$

$$n_e^2 = 2.3753 + \frac{0.01224}{\lambda^2 - 0.01667} - 0.01627\,\lambda^2 + 0.0005716\,\lambda^4 - 0.00006305\,\lambda^6$$

Other sets of Sellmeier equations are given in [1], [5], [8], [23], [24], [25], [26].

Nonlinear refractive index γ

λ [μm]	$\gamma \times 10^{15}$ [cm^2/W]	Ref.	Note
0.2661	0.025 ± 0.008	[11]	$\parallel c$
0.3547	0.36 ± 0.08	[11]	$\parallel c$
0.5321	0.55 ± 0.10	[11]	$\parallel c$
0.780	0.40 ± 0.05	[27]	[100] direction
	0.32 ± 0.05	[27]	[010] direction
0.850	0.37 ± 0.06	[28]	$\theta = 29.2°$, $\phi = 0°$
1.0642	0.29 ± 0.05	[11]	$\parallel c$

Linear electrooptic coefficients measured at low frequencies (well below the acoustic resonances of BBO crystal, i.e., for the "free" crystal) at room temperature

λ [μm]	r_{22}^{T} [pm/V]	r_{51}^{T} [pm/V]	Ref.	Note
0.5145	2.5 ± 0.1		[29]	$T = 296$ K
0.6328	2.5	<0.04	[30]	
	2.2 ± 0.1		[31]	

Linear electrooptic coefficient measured at high frequencies (well above the acoustic resonances of BBO crystal, i.e., for the "clamped" crystal)

λ [μm]	r_{22}^{S} [pm/V]	Ref.	Note
0.5145	2.1 ± 0.3	[29]	$T = 296$ K
0.6328	2.1 ± 0.1	[31]	

Expressions for the effective second-order nonlinear coefficient in general case (Kleinman symmetry conditions are valid, $d_{31} = d_{15}$) [32]:

$$d_{\mathrm{ooe}} = d_{31} \sin(\theta + \rho) - d_{22} \cos(\theta + \rho) \sin 3\phi$$

$$d_{\mathrm{eoe}} = d_{\mathrm{oee}} = d_{22} \cos^2(\theta + \rho) \cos 3\phi$$

Simplified expressions for the effective second-order nonlinear coefficient (approximation of small birefringence angle, Kleinman symmetry conditions are valid, $d_{31} = d_{15}$) [33]:

$$d_{\mathrm{ooe}} = d_{31} \sin\theta - d_{22} \cos\theta \sin 3\phi$$

$$d_{\mathrm{eoe}} = d_{\mathrm{oee}} = d_{22} \cos^2\theta \cos 3\phi$$

Absolute values of second-order nonlinear coefficients [32]:

$$|d_{22}(0.532\,\mu\mathrm{m})| = 2.6\,\mathrm{pm/V}$$

$$|d_{22}(0.852\,\mu\mathrm{m})| = 2.3\,\mathrm{pm/V}$$

$$|d_{22}(1.064\,\mu\mathrm{m})| = 2.2\,\mathrm{pm/V}$$

$$|d_{22}(1.313\,\mu\mathrm{m})| = 1.9\,\mathrm{pm/V}$$

$$|d_{15}(1.064\,\mu\mathrm{m})| = 0.03\,\mathrm{pm/V}$$

$|d_{31}(1.064\,\mu\text{m})| = 0.04\,\text{pm/V}$

$|d_{33}(1.064\,\mu\text{m})| = 0.04\,\text{pm/V}$

Other values of second-order nonlinear coefficients d_{22}:

$|d_{22}(1.064\,\mu\text{m})| = 2.1 \pm 0.1\,\text{pm/V}$ [34]; $2.2 \pm 0.2\,\text{pm/V}$ [35]; $2.23 \pm 0.16\,\text{pm/V}$ [36]; $2.23 \pm 0.18\,\text{pm/V}$ [37]

$|d_{22}(1.319\,\mu\text{m})| = 1.89 \pm 0.15\,\text{pm/V}$ [37]

Relative signs of d_{22} and d_{31} are opposite [8], [25], [34].

Experimental values of phase-matching angle ($T = 293\,\text{K}$)

Interacting wavelengths [μm]	θ_{exp} [deg]	Ref.
SHG, $o + o \Rightarrow e$		
0.4096 ⇒ 0.2048	90	[13]
0.41 ⇒ 0.205	90	[38]
0.41152 ⇒ 0.20576	82.8	[13]
0.41546 ⇒ 0.20773	79.2	[13]
0.418 ⇒ 0.209	77.3	[39]
0.429 ⇒ 0.2145	71	[40]
0.4765 ⇒ 0.23825	57	[41]
0.488 ⇒ 0.244	54.5	[41]
0.4965 ⇒ 0.24825	52.5	[41]
0.5106 ⇒ 0.2553	50	[42]
	50.6	[43]
0.5145 ⇒ 0.25725	49.5	[41]
0.5321 ⇒ 0.26605	47.3	[5]
	47.5	[13], [44], [45]
	47.6	[46], [47]
	48	[23], [48]
0.589 ⇒ 0.2945	41.5	[49]
0.604 ⇒ 0.302	40	[50]
0.6156 ⇒ 0.3078	39	[51]
0.616 ⇒ 0.308	38	[52]
0.70946 ⇒ 0.35473	32.9	[53], [54]
	33	[44], [55], [56]
	33.1	[47]
	33.3	[18]
	33.7	[57]
0.78 ⇒ 0.39	31	[58]
	30	[59]
0.8 ⇒ 0.4	26.5	[60]
0.946 ⇒ 0.473	24.9	[61]

Interacting wavelengths [μm]	θ_{exp} [deg]	Ref.
1.0642 ⇒ 0.5321	22.7	[5]
	22.8	[4], [13], [44], [47], [62], [63]
SFG, $o + o \Rightarrow e$		
0.73865 + 0.25725 ⇒ 0.1908	81.7	[64]
0.72747 + 0.26325 ⇒ 0.1933	76	[65]
0.5922 + 0.2961 ⇒ 0.1974	88	[66]
0.5964 + 0.2982 ⇒ 0.1988	82.5	[67]
0.5991 + 0.29955 ⇒ 0.1997	80	[66]
0.60465 + 0.30233 ⇒ 0.20155	76.2	[67]
0.5321 + 0.32561 ⇒ 0.202	83.9	[13]
0.6099 + 0.30495 ⇒ 0.2033	73.5	[66]
0.5321 + 0.34691 ⇒ 0.21	71.9	[13]
0.7736 + 0.25787 ⇒ 0.1934	70.7	[15]
0.5321 + 0.35473 ⇒ 0.21284	70	[48]
0.51567 + 0.38675 ⇒ 0.221	64.7	[68]
0.804 + 0.268 ⇒ 0.201	64	[69]
0.75 + 0.375 ⇒ 0.25	61.7	[70]
1.0642 + 0.26605 ⇒ 0.21284	51.1	[13]
0.78 + 0.373 ⇒ 0.2523	47.4	[71], [72]
1.0642 + 0.298 ⇒ 0.23281	46.1	[73]
0.5782 + 0.5106 ⇒ 0.27115	46	[74]
0.59099 + 0.5321 ⇒ 0.28	44.7	[75]
0.78 + 0.43 ⇒ 0.2772	43.4	[76]
1.0642 + 0.35473 ⇒ 0.26605	40.2	[13]
1.0641 + 0.53205 ⇒ 0.3547	31.3	[77]
1.0642 + 0.5321 ⇒ 0.35473	31.1	[5]
	31.3	[13]
	31.4	[57]
2.68823 + 0.5712 ⇒ 0.4711	21.8	[25]
1.41831 + 1.0642 ⇒ 0.608	21	[78]
SHG, $e + o \Rightarrow e$		
0.5321 ⇒ 0.26605	81	[13]
0.70946 ⇒ 0.35473	48	[55]
	48.1	[44]
1.0642 ⇒ 0.5321	31.6	[79]
	32.4	[5]
	32.7	[4], [44]
	32.9	[13]
SFG, $e + o \Rightarrow e$		
1.0642 + 0.35473 ⇒ 0.26605	46.6	[13]
1.0642 + 0.5321 ⇒ 0.35473	38.4	[5]
	38.5	[13]
SFG, $o + e \Rightarrow e$		
1.0642 + 0.5321 ⇒ 0.35473	59.8	[13]

Experimental values of internal angular, temperature, and spectral bandwidths at $T = 293\,\mathrm{K}$

Interacting wavelengths [μm]	θ_{pm} [deg]	$\Delta\theta^{int}$ [deg]	ΔT [°C]	$\Delta\nu$ [cm^{-1}]	Ref.
SHG, $o + o \Rightarrow e$					
$1.0642 \Rightarrow 0.5321$	22.8	0.021	37	9.7	[4]
	21.9	0.028			[23]
	22.7	0.030	51		[5]
$0.5321 \Rightarrow 0.26605$	47.3	0.010	4		[5]
$0.53 \Rightarrow 0.265$	47.6 (298 K)	0.006			[80]
SFG, $o + o \Rightarrow e$					
$1.0641 + 0.53205 \Rightarrow 0.3547$	31.3	0.011			[77]
$1.0642 + 0.5321 \Rightarrow 0.35473$	31.1	0.015	16		[5]
$2.44702 + 0.5712 \Rightarrow 0.4631$	22.1	0.026			[25]
$2.68823 + 0.5712 \Rightarrow 0.4711$	21.8	0.028			[25]
SHG, $e + o \Rightarrow e$					
$1.0642 \Rightarrow 0.5321$	32.7	0.034		8.8	[4]
	32.4	0.046	37		[5]
SFG, $e + o \Rightarrow e$					
$1.0642 + 0.5321 \Rightarrow 0.35473$	38.4	0.020	13		[5]
SFG, $o + e \Rightarrow e$					
$1.0642 + 0.5321 \Rightarrow 0.35473$	58.4	0.050	12		[5]

Temperature variation of phase-matching angle at $T = 293\,\mathrm{K}$ [5]

Interacting wavelengths [μm]	θ_{pm} [deg]	$d\theta_{pm}/dT$ [deg/K]
SHG, $o + o \Rightarrow e$		
$0.5321 \Rightarrow 0.26605$	47.3	0.00250
$1.0642 \Rightarrow 0.5321$	22.7	0.00057
SFG, $o + o \Rightarrow e$		
$1.0642 + 0.5321 \Rightarrow 0.35473$	31.1	0.00099
SHG, $e + o \Rightarrow e$		
$1.0642 \Rightarrow 0.5321$	32.4	0.00120
SFG, $e + o \Rightarrow e$		
$1.0642 + 0.5321 \Rightarrow 0.35473$	38.4	0.00150
SFG, $o + e \Rightarrow e$		
$1.0642 + 0.5321 \Rightarrow 0.35473$	58.4	0.00421

Calculated values of inverse group-velocity mismatch for SHG process in BBO

Interacting wavelengths [μm]	θ_{pm} [deg]	β [fs/mm]
SHG, $o + o \Rightarrow e$		
$1.2 \Rightarrow 0.6$	21.18	54
$1.1 \Rightarrow 0.55$	22.28	76
$1.0 \Rightarrow 0.5$	23.85	104
$0.9 \Rightarrow 0.45$	26.07	141

Interacting wavelengths [μm]	θ_{pm} [deg]	β [fs/mm]
0.8 ⇒ 0.4	29.18	194
0.7 ⇒ 0.35	33.65	275
0.6 ⇒ 0.3	40.47	415
0.5 ⇒ 0.25	52.34	695
SHG, $e + o \Rightarrow e$		
1.2 ⇒ 0.6	29.91	103
1.1 ⇒ 0.55	31.46	130
1.0 ⇒ 0.5	33.73	164
0.9 ⇒ 0.45	36.98	210
0.8 ⇒ 0.4	41.67	276
0.7 ⇒ 0.35	48.74	373
0.6 ⇒ 0.3	60.91	531

Laser-induced bulk damage threshold

λ [μm]	τ_p [ns]	I_{thr} [GW/cm^2]	Ref.	Note
0.2661	10	0.3	[81]	10 Hz
	8	>0.12	[46]	
		2.0	[82]	grown by Czochralski method (CZ-BBO)
		3.0	[82]	grown by flux method (flux-BBO)
		3.4	[82]	CZ-BBO, annealed at 1193 K (50 hours)
0.308	12	>0.2	[83]	
0.3547	10	0.9	[81]	10 Hz
		5	[18]	
	8	25	[84]	1 pulse
		19	[84]	1800 pulses
	0.03	>0.4	[85]	10 Hz
	0.015	>3	[53]	
0.400	0.0002	>150	[60]	10 Hz
0.5106	20	>0.25	[86]	4 kHz
0.51–0.58	20	10	[87]	
0.5145	CW	>0.0004	[88]	
0.5321	10	2.3	[81]	10 Hz
	8	48	[84]	1 pulse
		32	[84]	1800 pulses
	1	7	[23]	
	0.25	10	[6]	
	0.075	>7	[14]	
	0.025	>4.2	[54]	10 Hz
		>4	[63]	

λ [μm]	τ_p [ns]	I_{thr} [GW/cm^2]	Ref.	Note
0.62	0.0002	>50	[89]	
	0.0001	1000 (?)	[90]	
0.6943	0.02	10	[8]	
0.8	0.000025	>3400	[91]	1–5 kHz
0.85	0.00025	>93	[92]	1 kHz
1.054	0.005	50	[93]	
1.0642	14	50	[84]	1 pulse
		23	[84]	1800 pulses
	10	4.5	[81]	10 Hz
		5	[6]	
	1.3	10	[4]	
	1.1	14	[94]	
	1.0	13.5	[6]	
	0.1	10	[6]	
	0.035	>5	[54]	

Laser-induced surface damage threshold

λ [μm]	τ_p [ns]	I_{thr} [GW/cm^2]	Ref.	Note
0.266	10	0.15	[81]	10 Hz
0.355	10	0.50	[81]	10 Hz
0.51–0.58	20	1	[95]	4–14 kHz
0.532	10	1.3	[81]	10 Hz
0.5398	0.015	120–150 (?)	[96]	1 pulse
1.064	10	2.6	[81]	10 Hz
1.0796	0.015	250–350 (?)	[96]	1 pulse

About the crystal

Discovered in 1985 by Chen *et al.* [8], BBO quickly became the most popular crystal for visible and UV applications. We will touch briefly upon the most interesting results obtained recently with this nonlinear material. In [61], the radiation of a Nd:YAG laser ($\lambda = 946$ nm) was frequency-doubled in a 0.4-cm BBO crystal, generating 550 mW of continuous-wave (CW) blue output. In [97], 400 mW of output power at 400 nm was produced via second-harmonic generation (SHG) of CW Ti:sapphire laser in a 0.8-cm-long BBO crystal. Much higher levels of SHG power were reached by SHG of pulsed pump sources with kilohertz frequency rates. Very recently, Watanabe *et al.* [91] investigated the second-harmonic generation of a sub-10-fs Ti:sapphire, and 1.9-mJ pulses at 400 nm with a repetition rate of 1 kHz were obtained, which corresponded to the mean blue power value of 1.9 W. In [43], 5.1 W of quasi-CW UV power at 255 nm was generated via SHG of a copper vapor laser radiation ($P = 32$ W, $\Delta f = 5$ kHz). The third harmonic ($\lambda = 355$ nm, $P = 0.31$ W, $\tau = 23$ ns, $\Delta f = 10$ kHz) of diode-pumped Q-switched Nd:YVO_4 laser radiation was produced in a type I BBO

crystal [77]. In [98], the fourth-harmonic generation (FoHG) ($\lambda = 266$ nm) and fifth-harmonic generation (FiHG) ($\lambda = 213$ nm) of multi-kHz Nd:YAG laser radiation ($\tau = 25$ ns) were realized in 0.7-cm-long BBO crystals; the average power equaled 2.1 W and 0.54 W, respectively.

References

[1] A.E. Kokh, V.A. Mishchenko, V.A. Antsigin, A.M. Yurkin, N.G. Kononova, V.A. Guets, Y.K. Nizienko, A.I. Zakharenko: Growth and investigation of BBO crystals with improved characteristics for UV harmonic generation. Proc. SPIE **3610**, 139–147 (1999).

[2] Data sheet of Cleveland Crystals Inc. Available at www.clevelandcrystals.com.

[3] R. Guo, A.S. Bhalla: Pyroelectric, piezoelectric, and dielectric properties of β-BaB_2O_4 single crystal. J. Appl. Phys. **66(12)**, 6186–6188 (1989).

[4] C. Chen: Chinese lab grows new nonlinear optical borate crystals. Laser Focus World **25(11)**, 129–137 (1989).

[5] D. Eimerl, L. Davis, S. Velsko, E.K. Graham, A. Zalkin: Optical, mechanical, and thermal properties of barium borate. J. Appl. Phys. **62(5)**, 1968–1983 (1987).

[6] R.S. Adhav, S.R. Adhav, J.M. Pelaprat: BBO's nonlinear optical phase-matching properties. Laser Focus **23(9)**, 88–100 (1987).

[7] B.H.T. Chai: Optical Crystals. In: *CRC Handbook of Laser Science and Technology, Supplement 2: Optical Materials*, ed. by M.J. Weber (CRC Press, Boca Raton, 1995), pp. 3–65.

[8] C. Chen, B. Wu, A. Jiang, G. You: A new type ultraviolet SHG crystal β-BaB_2O_4. Scientia Sinica B **28(3)**, 235–243 (1985).

[9] Data sheet of Fujian Castech Crystals, Inc. Available at www.castech.com.

[10] J.D. Beasley: Thermal conductivities of some novel nonlinear optical materials. Appl. Opt. **33(1)**, 1000–1003 (1994).

[11] R. DeSalvo, A.A. Said, D.J. Hagan, E.W. van Stryland, M. Sheik-Bahae: Infrared to ultraviolet measurements of two-photon absorption and n_2 in wide bandgap solids. IEEE J. Quant. Electr. **32(8)**, 1324–1333 (1996).

[12] R.H. French, J.W. Ling, F.S. Ohuchi, C.T. Chen: Electronic structure of β-BaB_2O_4 and LiB_3O_5 nonlinear optical crystals. Phys. Rev. B **44(16)**, 8496–8502 (1991).

[13] K. Kato: Second-harmonic generation to 2048 Å in β-BaB_2O_4. IEEE J. Quant. Electr. **QE-22(7)**, 1013–1014 (1986).

[14] L.J. Bromley, A. Guy, D.C. Hanna: Synchronously pumped optical parametric oscillation in beta barium borate. Opt. Commun. **67(4)**, 316–320 (1988).

[15] H. Kouta, Y. Kuwano: Attaining 186-nm light generation in cooled β-BaB_2O_4 crystal. Opt. Lett. **24(13)**, 1230–1232 (1999).

[16] A. Dragomir, J.G. McInerney, D.N. Nikogosyan: Femtosecond measurements of two-photon absorption coefficients at $\lambda = 264$ nm in glasses, crystals, and liquids. Appl. Opt. **41(21)**, 4365–4376 (2002).

[17] Y.X. Fan, R.C. Eckardt, R.L. Byer, C. Chen, A.D. Jiang: Barium borate optical parametric oscillator. IEEE J. Quant. Electr. **25(6)**, 1196–1199 (1989).

[18] Y.X. Fan, R.C. Eckardt, R.L. Byer, J. Nolting, R. Wallenstein: Visible BaB_2O_4 optical parametric oscillator pumped at 355 nm by a single-axial-mode pulsed source. Appl. Phys. Lett. **53(21)**, 2014–2016 (1988).

[19] A. Dubietis, G. Tamošauskas, A. Varanavičius, G. Valiulis: Two-photon absorbing properties of ultraviolet phase-matchable crystals at 264 and 211 nm. Appl. Opt. **39(15)**, 2437–2440 (2000).

[20] L.I. Isaenko, A. Dragomir, J.G. McInerney, D.N. Nikogosyan: Anisotropy of two-photon absorption in BBO at 264 nm. Opt. Commun. **198(4–6)**, 433–438 (2001).

[21] G. Veitas, A. Dubietis, G. Valiulis, D. Podenas, G. Tamošauskas: Efficient femtosecond pulse generation at 264 nm. Opt. Commun. **138(4–6)**, 333–336 (1997).

[22] D. Zhang, Y. Kong, J. Zhang: Optical parametric properties of 532-nm-pumped beta-barium-borate near the infrared absorption edge. Opt. Commun. **184(5–6)**, 485–491 (2000).

[23] C. Chen, Y.X. Fan, R.C. Eckardt, R.L. Byer: Recent developments in barium borate. Proc. SPIE **681**, 12–19 (1987).

[24] G.C. Bhar, S. Das, U. Chatterjee: Evaluation of beta barium borate crystal for nonlinear optics. Appl. Opt. **28(2)**, 202–204 (1989).

[25] M.-H. Lu, Y.-M. Liu: Infrared up-conversion with beta barium borate crystal. Opt. Commun. **84(3–4)**, 193–198 (1991).

[26] M. Oka, L.Y. Li, W. Wiechmann, N. Eguchi, S. Kubota: All solid-state continuous-wave frequency-quadrupled Nd:YAG laser. IEEE J. Sel. Topics Quant. Electr. **1(3)**, 859–866 (1995).

[27] H.P. Li, C.H. Kam, Y.L. Lam, W. Ji: Femtosecond Z-scan measurements of nonlinear refraction in nonlinear optical materials. Opt. Mater. **15(4)**, 237–242 (2001).

[28] M. Sheik-Bahae, M. Ebrahimzadeh: Measurements of nonlinear refraction in the second-order $\chi^{(2)}$ materials $KTiOPO_4$, $KNbO_3$, β-BaB_2O_4, and LiB_3O_5. Opt. Commun. **142 (4–6)**, 294–298 (1997).

[29] C.A. Ebbers: Linear electro-optic effect in β-BaB_2O_4. Appl. Phys. Lett. **52(23)**, 948–1949 (1988).

[30] H. Nakatani, W. Bosenberg, L.K. Cheng, C.L. Tang: Linear electro-optic effect in barium metaborate. Appl. Phys. Lett. **52(16)**, 1288–1290 (1988).

[31] M. Abarkan, J.P. Salvestrini, M.D. Fontana, M. Aillerie: Frequency and wavelength dependences of electro-optic coefficients in inorganic crystals. Appl. Phys. B **76(7)**, 765–769 (2003).

[32] I. Shoji, H. Nakamura, K. Ohdaira, T. Kondo, R. Ito, T. Okamoto, K. Tatsuki, S. Kubota: Absolute measurement of second-order nonlinear-optical coefficients of β-BaB_2O_4 for visible to ultraviolet second-harmonic wavelengths. J. Opt. Soc. Am. B **16(4)**, 620–624 (1999).

[33] J.E. Midwinter, J. Warner: The effects of phase matching method and of uniaxial crystal symmetry on the polar distribution of second-order non-linear optical polarization. Brit. J. Appl. Phys. **16(11)**, 1135–1142 (1965).

[34] R.S. Klein, G.E. Kugel, A. Maillard, A. Sifi, K. Polgar: Absolute non-linear optical coefficients measurements of BBO single crystal and determination of angular acceptance by second harmonic generation. Opt. Mater. **22(2)**, 163–169 (2003).

[35] R.C. Eckardt, H. Masuda, Y.X. Fan, R.L. Byer: Absolute and relative nonlinear optical coefficients of KDP, KD*P, BaB_2O_4, $LiIO_3$, MgO:$LiNbO_3$, and KTP measured by phase-matched second-harmonic generation. IEEE J. Quant. Electr. **26(5)**, 922–933 (1990).

[36] S.P. Velsko, M. Webb, L. Davis, C. Huang: Phase-matched harmonic generation in lithium triborate (LBO). IEEE J. Quant. Electr. **27(9)**, 2182–2192 (1991).

[37] W.J. Alford, A.V. Smith: Wavelength variation of the second-order nonlinear coefficients of $KNbO_3$, $KTiOPO_4$, $KTiOAsO_4$, $LiNbO_3$, $LiIO_3$, β-BaB_2O_4, KH_2PO_4, and LiB_3O_5 crystals: a test of Miller wavelength scaling. J. Opt. Soc. Am. B **18(4)**, 524–533 (2001).

[38] K. Miyazaki, H. Sakai, T. Sato: Efficient deep-ultraviolet generation by frequency doubling in β-BaB_2O_4 crystals. Opt. Lett. **11(12)**, 797–799 (1986).

[39] H. Yamamoto, K. Toyoda, K. Matsubara, M. Watanabe, S. Urabe: Development of a tunable 209 nm continuous-wave light source using two-stage frequency doubling of a Ti:sapphire laser. Jpn. J. Appl. Phys. **41(6A)**, 3710–3713 (2002).

[40] K. Matsubara, U. Tanaka, H. Imajo, K. Hayasaka, R. Ohmukai, M. Watanabe, S. Urabe: An all-solid-state tunable 214.5-nm continuous-wave light source by using two-stage frequency doubling of a diode laser. Appl. Phys. B **67(1)**, 1–4 (1998).

[41] G. Xinan, Y. Shuzhong, B. Wu: Autocorrelation measurements of mode-locked Ar^+ laser pulses with a novel frequency doubling crystal β-BaB_2O_4. Chin. J. Lasers **13(12)**, 771–773 (1986) [In Chinese, English trans.: Chinese Physics - Lasers **13(12)**, 892–894 (1986)].

[42] A.A. Isaev, D.R. Jones, C.E. Little, G.G. Petrash, C.G. Whyte, K.I. Zemskov: 1.3 W average power at 255 nm by second harmonic generation in BBO by a copper HyBrID laser. Opt. Commun. **132(3–4)**, 302–306 (1996).

[43] N. Huot, C. Jonin, N. Sanner, E. Baubeau, E. Audouard, P. Laporte: High UV average power at 15 kHz by frequency doubling of a copper HyBrID vapor laser in β-barium borate. Opt. Commun. **211(1–6)**, 277–282 (2002).

[44] L.K. Cheng, W.R. Bosenberg, C.L. Tang: Broadly tunable optical parametric oscillation in β-BaB_2O_4. Appl. Phys. Lett. **53(3)**, 175–177 (1988).

[45] H. Masuda, N. Umezu, K. Kimura, S. Kubota: High-repetition-rate, 192–197 nm pulse generation in β-BaB_2O_4 by intracavity sum-frequency-mixing of a Ti:sapphire laser with a frequency-quadrupled Nd:YAG laser. In: *Advanced Solid-State Lasers, OSA Trends in Optics and Photonics Series, Vol. 26*, ed. by M.M. Fejer, H. Injeyan, U. Keller (OSA, Washington DC, 1999), pp. 63–69.

[46] W.R. Bosenberg, L.K. Cheng, C.L. Tang: Ultraviolet optical parametric oscillation in β-BaB_2O_4. Appl. Phys. Lett. **54(1)**, 13–15 (1989).

[47] A. Fix, T. Schroder, R. Wallenstein: The optical parametric oscillators of beta barium borate and lithium triborate: new sources of powerful tunable laser radiation in the ultraviolet, visible and near infrared. Laser und Optoelektronik **23(3)**, 106–110 (1991).

[48] D.A.V. Kliner, F. Di Teodoro, J.P. Koplow, S.W. Moore, A.V. Smith: Efficient second, third, fourth, and fifth harmonic generation of a Yb-doped fiber amplifier. Opt. Commun. **210(3–6)**, 393–398 (2002).

[49] S.J. Rehse, S.A. Lee: Generation of 125 mW frequency stabilized continuous-wave tunable laser light at 295 nm by frequency doubling in a BBO crystal. Opt. Commun. **213 (4–6)**, 347–350 (2002).

[50] H.J. Muschenborn, W. Theiss, W. Demtroder: A tunable UV-light source for laser spectroscopy using second harmonic generation in β-BaB_2O_4. Appl. Phys. B **50(5)**, 365–369 (1990).

[51] M. Ebrahimzadeh, A.J. Henderson, M.H. Dunn: An excimer-pumped β-BaB_2O_4 optical parametric oscillator tunable from 354 nm to 2.370 μm. IEEE J. Quant. Electr. **26(7)**, 1241–1252 (1990).

[52] A.J.S. McGonigle, A.A. Anrews, D.W. Coutts, G.P. Hogan, K.S. Johnston, J.D. Moorhouse, C.E. Webb: Compact 2.5-W 10-kHz Nd:YLF-pumped dye laser. Appl. Opt. **41(9)**, 1714–1717 (2002).

[53] J.Y. Huang, J.Y. Zhang, Y.R. Shen, C. Chen, B. Wu: High-power, widely tunable, picosecond coherent source from optical parametric amplification in barium borate. Appl. Phys. Lett. **57(19)**, 1961–1963 (1990).

[54] J.Y. Zhang, J.Y. Huang, Y.R. Shen, C. Chen: Optical parametric generation and amplification in barium borate and lithium triborate crystals. J. Opt. Soc. Am. B **10(9)**, 1758–1764 (1993).
[55] H. Vanherzeele, C. Chen: Widely tunable parametric generation in beta barium borate. Appl. Opt. **27(13)**, 2634–2636 (1988).
[56] H. Komine: Average power scaling for ultraviolet-pumped β-barium borate and lithium triborate optical parametric oscillators. J. Opt. Soc. Am. B **10(9)**, 1751–1757 (1993).
[57] G.C. Bhar, S. Das, U. Chatterjee: Noncollinear third harmonic generation and tunable second harmonic generation in barium borate. J. Appl. Phys. **66(10)**, 5111–5113 (1989).
[58] V. Krylov, O. Ollikainen, J. Gallus, U. Wild, A. Rebane, A. Kalintsev: Efficient noncollinear parametric amplification of weak femtosecond pulses in the visible and near-infrared spectral range. Opt. Lett. **23(2)**, 100–102 (1998).
[59] V. Krylov, J. Gallus, U.P. Wild, A. Kalintsev, A. Rebane: Femtosecond noncollinear and collinear parametric generation and amplification in BBO crystal. Appl. Phys. B **70(2)**, 163–168 (2000).
[60] Y.-C. Chen, X.-J. Fang, J. Li, X.-Y. Liang, H.-L. Zhang, B.-H. Feng, X.-L. Zhang, L.-A. Wu, Z.-Y. Xu: Efficient femtosecond optical parametric generator with a birefringent delay compensator. Appl. Opt. **40(15)**, 2579–2582 (2001).
[61] T. Kellner, F. Heine, G. Huber: Efficient laser performance of Nd:YAG at 946 nm and intracavity frequency doubling with $LiJO_3$, β-BaB_2O_4, and LiB_3O_5. Appl. Phys. B **65(6)**, 789–792 (1997).
[62] G.C. Bhar, S. Das, U. Chatterjee: Noncollinear phase-matched second-harmonic generation in beta barium borate. Appl. Phys. Lett. **54(15)**, 1383–1384 (1989).
[63] X.D. Zhu, L. Deng: Broadly tunable picosecond pulses generated in a β-BaB_2O_4 optical parametric amplifier pumped by 0.532 μm pulses. Appl. Phys. Lett. **61(13)**, 1490–1492 (1992).
[64] M. Watanabe, K. Hayasaka, H. Imajo, J. Umezu, S. Urabe: Generation of continuous-wave coherent radiation tunable down to 190.8 nm in β-BaB_2O_4. Appl. Phys. B **53(1)**, 11–13 (1991).
[65] I.V. Tomov, T. Anderson, P.M. Rentzepis: High repetition rate picosecond laser system at 193 nm. Appl. Phys. Lett. **61(10)**, 1157–1159 (1992).
[66] W.L. Glab, J.P. Hessler: Efficient generation of 200-nm light in β-BaB_2O_4. Appl. Opt. **26(16)**, 3181–3182 (1987).
[67] U. Heitmann, M. Kotteritzsch, S. Heitz, A. Hese: Efficient generation of tunable VUV laser radiation below 205 nm by SFG in BBO. Appl. Phys. B **55(5)**, 419–423 (1992).
[68] H. Kitano, H. Kawai, K. Miramitsu, S. Owa, M. Yoshimura, Y. Mori, T. Sasaki: 387-nm generation in $Gd_xY_{1-x}Ca_4O(BO_3)_3$ crystal and its utilization for 193-nm light source. Jpn. J. Appl. Phys. **42(2B)**, L166–L169 (2003).
[69] M. Hacker, T. Feurer, R. Sauerbrey, T. Lucza, G. Szabo: Programmable femtosecond laser pulses in the ultraviolet. J. Opt. Soc. Am. B **18(6)**, 866–871 (2001).
[70] S. Sayama, M. Ohtsu: Tunable UV CW generation by frequency tripling of a Ti:sapphire laser. Opt. Commun. **137(4–6)**, 295–298 (1997).
[71] T. Fujii, H. Kumagai, K. Midorikawa, M. Obara: Development of a high-power deep-ultraviolet continuous-wave coherent light source for laser cooling of silicon atoms. Opt. Lett. **25(19)**, 1457–1459 (2000).
[72] H. Kumagai, K. Midorikawa, T. Iwane, M. Obara: Efficient sum-frequency generation of continuous-wave single-frequency coherent light at 252 nm with dual wavelength enhancement. Opt. Lett. **28(20)**, 1969–1971 (2003).

[73] J.F. Pinto, L. Esterowitz, T.J. Carrig: Extended wavelength coverage of a Ce^{3+}:LiCAF laser between 223 and 243 nm by sum frequency mixing in β-barium borate. Appl. Opt. **37(6)**, 1060–1061 (1998).

[74] D.W. Coutts, M.D. Ainsworth, J.A. Piper: Sum frequency mixing of copper vapor laser output in KDP and β-BBO. IEEE J. Quant. Electr. **25(9)**, 1985–1987 (1989).

[75] S. Lu, Y. Yuan, Y. Tang, W. Xu, C. Wu: Mixing frequency generation of 271.0–291.5 nm in β-BaB_2O_4. In: *Proceedings of the Topical Meeting on Laser Materials and Laser Spectroscopy*, ed. by Z. Wang, Z. Zhang (World Scientific, Singapore, 1989), pp. 77–79.

[76] S. Sayama, M. Ohtsu: Tunable UV CW generation at 276 nm wavelength by frequency conversion of laser diodes. Opt. Commun. **145(1–6)**, 95–97 (1998).

[77] Y.-L. Jia, J.-L. He, H.-T. Wang, S.-N. Zhu, Y.-Y. Zhu: Single pass third-harmonic generation of 310 mW of 355 nm with an all-solid-state laser. Chin. Phys. Lett. **18(12)**, 1589–1591 (2001).

[78] K. Kurokawa, M. Nakazawa: Femtosecond 1.4–1.6 μm infrared pulse generation at a high repetition rate by difference frequency generation. Appl. Phys. Lett. **55(1)**, 7–9 (1989).

[79] G.C. Bhar, S. Das, U. Chatterjee: Second harmonic generation from non-collinear orthogonally polarized Nd:YAG laser radiation in β-BaB_2O_4. J. Phys. D **22(4)**, 562–563 (1989).

[80] S.C. Matthews, J.S. Sorce: Fourth harmonic conversion of 1.06 μm in BBO and KD*P. Proc. SPIE **1220**, 137–147 (1990).

[81] H. Kouta: Wavelength dependence of repetitive-pulse laser-induced damage threshold in β-BaB_2O_4. Appl. Opt. **38(3)**, 545–547 (1999).

[82] H. Kouta, Y. Kuwano: Improvement of laser-induced damage threshold in CZ-BBO by reducing the light scattering center with annealing. In: *Advanced Solid-State Lasers, OSA Trends in Optics and Photonics Series, Vol. 19*, ed. by W.R. Bosenberg, M.M. Fejer (OSA, Washington DC, 1998), pp. 28–31.

[83] H. Komine: Optical parametric oscillation in a beta-barium borate crystal pumped by an XeCl excimer laser. Opt. Lett. **13(8)**, 643–645 (1988).

[84] H. Nakatani, W.R. Bosenberg, L.K. Cheng, C.L. Tang: Laser-induced damage in beta barium metaborate. Appl. Phys. Lett. **53(26)**, 2587–2589 (1988).

[85] F. Huang, L. Huang: Picosecond optical parametric generation and amplification in LiB_3O_5 and β-BaB_2O_4. Appl. Phys. Lett. **61(15)**, 1769–1771 (1992).

[86] K. Kuroda, T. Omatsu, T. Shimura, M. Chihara, I. Ogura: Second harmonic generation of a copper vapor laser in barium borate. Opt. Commun. **75(1)**, 42–46 (1990).

[87] D.W. Coutts, M.D. Ainsworth, J.A. Piper: Enhanced efficiency of UV second harmonic and sum frequency generation from copper vapor lasers. IEEE J. Quant. Electr. **26(9)**, 1555–1558 (1990).

[88] Y. Taira: High-power continuous-wave ultraviolet generation by frequency doubling of an argon laser. Jpn. J. Appl. Phys. **31(6A)**, L682–L684 (1992).

[89] W. Joosen, H.J. Bakker, L.D. Noordam, H.G. Muller, H.B. van Linden van den Heuvell: Parametric generation in β-barium borate of intense femtosecond pulses near 800 nm. J. Opt. Soc. Am. B **8(10)**, 2087–2093 (1991).

[90] T.R. Zhang, H.R. Choo, M.C. Downer: Phase and group velocity matching for second harmonic generation of femtosecond pulses. Appl. Opt. **29(27)**, 3927–3933 (1990).

[91] T. Kanai, X. Zhou, T. Sekikawa, S. Watanabe, T. Togashi: Generation of subterawatt sub-10-fs blue pulses at 1–5 kHz by broadband frequency doubling. Opt. Lett. **28(16)**, 1484–1486 (2003).

[92] M.A. Krumbügel, J.N. Sweetser, D.N. Fittinghoff, K.W. DeLong, R. Trebino: Ultrafast optical switching by use of fully phase-matched cascaded second-order nonlinearities in a polarization-gate geometry. Opt. Lett. **22(4)**, 245–247 (1997).

[93] P. Qiu, A. Penzkofer: Picosecond third-harmonic light generation in β-BaB_2O_4. Appl. Phys. B **45(4)**, 225–236 (1988).
[94] M. Yoshimura, T. Kamimura, K. Murase, Y. Mori, H. Yoshida, M. Nakatsuka, T. Sasaki: Bulk laser damage in $CsLiB_6O_{10}$ crystal and its dependence on crystal structure. Jpn. J. Appl. Phys. **38(2A)**, L129–L131 (1999).
[95] D.W. Coutts, J.A. Piper: One watt average power by second harmonic and sum frequency generation from a single medium scale copper vapor laser. IEEE J. Quant. Electr. **28(8)**, 1761–1764 (1992).
[96] G.G. Gurzadyan, A.S. Oganesyan, A.V. Petrosyan, R.O. Sharkhatunyan: Growth of β-barium borate crystals and study of their nonlinear properties. Zh. Tekh. Fiz. **61(3)**, 152–154 (1991) [In Russian, English trans.: Sov. Phys.-Tech. Phys. **36(3)**, 341–342 (1991)].
[97] W.-L. Zhou, Y. Mori, T. Sasaki, S. Nakai: High-efficiency intracavity continuous-wave ultraviolet generation using crystals $CsLiB_6O_{10}$, β-BaB_2O_4, and LiB_3O_5. Opt. Commun. **123(4–6)**, 583–586 (1996).
[98] L.B. Chang, S.C. Wang, A.H. Kung: Efficient compact watt-level deep-ultraviolet laser generated from a multi-kHz Q-switched diode-pumped solid-state laser system. Opt. Commun. **209(4–6)**, 397–401 (2002).

2.2 LiB_3O_5, Lithium Triborate (LBO)

Negative biaxial crystal: $2V_z = 109.2°$ at $\lambda = 0.5321\,\mu m$ [1]
Molecular mass: 119.371
Specific gravity: 2.474 g/cm^3 [2]
Point group: *mm*2
Lattice constants:
$a = 8.46$ Å [3]; 8.49 Å [4]; 8.461 Å at $T = 273$ K [5]; 8.4473 ± 0.0007 Å [2]
$b = 7.38$ Å [3]; 7.42 Å [4]; 7.412 Å at $T = 273$ K [5]; 7.3788 ± 0.0006 Å [2]
$c = 5.13$ Å [3]; 5.17 Å [4]; 5.179 Å at $T = 273$ K [5]; 5.1395 ± 0.0005 Å [2]
Assignment of dielectric and crystallographic axes: $X, Y, Z \Rightarrow a, c, b$
Mohs hardness: 6 [2]; 7 [6]
Vickers hardness [7]:
400–450 ($\|X$)
650–700 ($\|Y$)
Melting point: 1107 K [2], [8]

Linear thermal expansion coefficient α_t [5]

T [K]	$\alpha_t \times 10^6$ [K^{-1}], $\|X$	$\alpha_t \times 10^6$ [K^{-1}], $\|Y$	$\alpha_t \times 10^6$ [K^{-1}], $\|Z$
273	107.1	−95.4	33.7
323	108.2	−88.0	33.6
373	108.3	−80.9	33.2
423	107.3	−74.0	32.6
473	105.3	−67.3	31.7
523	102.3	−60.7	30.5
573	98.2	−54.4	29.1
673	87.0	−42.3	25.5

T [K]	$\alpha_t \times 10^6$ [K^{-1}], $\parallel X$	$\alpha_t \times 10^6$ [K^{-1}], $\parallel Y$	$\alpha_t \times 10^6$ [K^{-1}], $\parallel Z$
723	79.8	−36.5	23.3
773	71.6	−30.9	20.9
873	52.1	−20.3	15.3
923	40.8	−15.3	12.1
973	28.5	−10.6	8.7
1023	15.1	−5.9	5.0
1073	0.8	−1.5	1.1

Mean value of linear thermal expansion coefficient α_t for temperature range 298–423 K [4]:

$\alpha_t = 66.4 \times 10^{-6}\,\mathrm{K}^{-1}$ (along X)

$\alpha_t = -52.8 \times 10^{-6}\,\mathrm{K}^{-1}$ (along Y)

$\alpha_t = 27.3 \times 10^{-6}\,\mathrm{K}^{-1}$ (along Z)

Temperature dependence of linear thermal expansion coefficient for temperature range 273–1073 K (T in K) [5]:

$$\alpha_t\,(\parallel X) = 1.071 \times 10^{-4} + 3.204 \times 10^{-8}(T - 273) - 2.063 \times 10^{-10}\,(T - 273)^2$$

$$\alpha_t\,(\parallel Y) = -9.535 \times 10^{-5} - 1.481 \times 10^{-7}\,(T - 273) - 3.489 \times 10^{-11}\,(T - 273)^2$$

$$\alpha_t\,(\parallel Z) = 3.374 \times 10^{-5} + 3.400 \times 10^{-10}\,(T - 273) - 5.067 \times 10^{-11}\,(T - 273)^2$$

Specific heat capacity c_p at $P = 0.101325$ MPa [2]

T [K]	c_p [J/kgK]
298	1060

Thermal conductivity coefficient:

$\kappa = 3.5$ W/mK [9]

$\kappa = 2.7$ W/mK($\parallel X$) [2]

$\kappa = 3.1$ W/mK($\parallel Y$) [2]

$\kappa = 4.5$ W/mK ($\parallel Z$) [2]

Direct band-gap energy at room temperature: $E_g = 7.75$ eV [6], 7.78 eV [10]
Transparency range:

at 0.5 level: 0.16–2.3 μm for 0.3 cm long crystal [2]

at "0" transmittance level: 0.155–3.2 μm [1], [11]

Linear absorption coefficient α [12]

λ [μm]	α [cm^{-1}]
0.35–0.36	0.0031
1.0642	0.00035

Two-photon absorption coefficient β [13]

λ [μm]	τ_p [ns]	$\beta \times 10^{11}$ [cm/W]	Note
0.211	0.0009	103 ± 36	$\theta = 90°, \phi = 30°$
0.264	0.0008	15 ± 5	$\theta = 90°, \phi = 30°$

Experimental values of refractive indices

λ [μm]	n_X	n_Y	n_Z	Ref.
0.2537	1.6335	1.6582	1.6792	[1]
0.2894	1.6209	1.6467	1.6681	[1]
0.2968	1.6182	1.6450	1.6674	[1]
0.3125	1.6097	1.6415	1.6588	[1]
0.3341	1.6043	1.6346	1.6509	[1]
0.3650	1.59523	1.62518	1.64025	[12]
	1.5954	1.6250	1.6407	[1]
0.4000	1.58995	1.61918		[12]
0.4047	1.5907	1.6216	1.6353	[1]
0.4358	1.5859	1.6148	1.6297	[1]
0.4500	1.58449	1.61301	1.62793	[12]
0.4861	1.5817	1.6099	1.6248	[1]
0.5000	1.58059	1.60862	1.62348	[12]
0.5250	1.57906	1.60686		[12]
0.5321	1.57868	1.60642	1.62122	[12]
	1.5785	1.6065	1.6212	[1]
0.5461	1.5780	1.6057	1.6206	[1]
0.5500	1.57772	1.60535	1.62014	[12]
0.5780	1.5765	1.6039	1.6187	[1]
0.5893	1.5760	1.6035	1.6183	[1]
0.6000	1.57541	1.60276	1.61753	[12]
0.6328	1.5742	1.6014	1.6163	[1]
0.6563	1.5734	1.6006	1.6154	[1]
0.7000		1.59893	1.61363	[12]
0.8000	1.56959	1.59615	1.61078	[12]
0.9000	1.56764	1.59386	1.60843	[12]
1.0000	1.56586	1.59187	1.60637	[12]
1.0642	1.56487	1.59072	1.60515	[12]
	1.5656	1.5905	1.6055	[1]
1.1000	1.56432	1.59005	1.60449	[12]

Best set of dispersion relations (λ in μm, $T = 293$ K) [14]:

$$n_X^2 = 2.4542 + \frac{0.01125}{\lambda^2 - 0.01135} - 0.01388\,\lambda^2$$

$$n_Y^2 = 2.5390 + \frac{0.01277}{\lambda^2 - 0.01189} - 0.01849\,\lambda^2 + 4.3025 \times 10^{-5}\,\lambda^4 - 2.9131 \times 10^{-5}\,\lambda^6$$

$$n_Z^2 = 2.5865 + \frac{0.01310}{\lambda^2 - 0.01223} - 0.01862\,\lambda^2 + 4.5778 \times 10^{-5}\,\lambda^4 - 3.2526 \times 10^{-5}\,\lambda^6$$

Other sets of Sellmeier equations are given in [1], [11], [12], [15], [16], [17], [18], [19], [20], [21], [22], [23], [24].

Temperature derivative of refractive indices:

for spectral range 0.4–1.0 μm and temperature range 293–338 K (λ in μm) [12]:

$dn_X/dT = -1.8 \times 10^{-6}\,\mathrm{K}^{-1}$
$dn_Y/dT = -13.6 \times 10^{-6}\,\mathrm{K}^{-1}$
$dn_Z/dT = -(6.3 + 2.1\,\lambda) \times 10^{-6}\,\mathrm{K}^{-1}$

for spectral range 0.4–1.0 μm and temperature range 293–383 K (λ in μm) [14]:

$dn_X/dT = -(3.76\,\lambda - 2.3) \times 10^{-6}\,\mathrm{K}^{-1}$
$dn_Y/dT = -(19.40 - 6.01\,\lambda) \times 10^{-6}\,\mathrm{K}^{-1}$
$dn_Z/dT = -(9.70 - 1.50\,\lambda) \times 10^{-6}\,\mathrm{K}^{-1}$

for $\lambda = 0.6328\,\mu$m and temperature range 293–473 K (λ in μm, T in K) [25]:

$$dn_X/dT = \left[0.20342 - 1.9697 \times 10^{-2}(T - 273) - 1.4415 \times 10^{-5}(T - 273)^2\right] \times 10^{-6}\,\mathrm{K}^{-1}$$

$$dn_Y/dT = -\left[10.748 + 7.1034 \times 10^{-2}(T - 273) + 5.7387 \times 10^{-5}(T - 273)^2\right] \times 10^{-6}\,\mathrm{K}^{-1}$$

$$dn_Z/dT = -\left[\begin{array}{l} 0.85998 + 1.5476 \times 10^{-1}(T - 273) - 9.4675 \\ \quad \times 10^{-4}(T - 273)^2 + 2.2375 \times 10^{-6}(T - 273)^3 \end{array}\right] \times 10^{-6}\,\mathrm{K}^{-1}$$

Nonlinear refractive index γ

λ [μm]	$\gamma \times 10^{15}$ [cm^2/W]	Ref.	Note
0.780	0.26 ± 0.03	[26]	[100] direction
	0.19 ± 0.03	[26]	[010] direction
0.850	0.19 ± 0.04	[27]	$\theta = 90°$, $\phi = 31.7°$

Expressions for the effective second-order nonlinear coefficient in principal planes of LBO crystal (Kleinman symmetry conditions are not valid) [28]:

XY plane: $d_{ooe} = d_{32} \cos\phi$

YZ plane: $d_{oeo} = d_{eoo} = d_{15} \cos\theta$

XZ plane, $\theta < V_z$: $d_{eoe} = d_{oee} = d_{24} \sin^2\theta + d_{15} \cos^2\theta$

XZ plane, $\theta > V_z$: $d_{eeo} = d_{32} \sin^2\theta + d_{31} \cos^2\theta$

Expressions for the effective second-order nonlinear coefficient in principal planes of LBO crystal (Kleinman symmetry conditions are valid, $d_{15} = d_{31}$ and $d_{24} = d_{32}$) [28]:

XY plane: $d_{ooe} = d_{32} \cos\phi$

YZ plane: $d_{oeo} = d_{eoo} = d_{31} \cos\theta$

XZ plane, $\theta < V_z$: $d_{eoe} = d_{oee} = d_{32} \sin^2\theta + d_{31} \cos^2\theta$

XZ plane, $\theta > V_z$: $d_{eeo} = d_{32} \sin^2\theta + d_{31} \cos^2\theta$

Expressions for the effective second-order nonlinear coefficient in arbitrary direction inside the LBO crystal are given in [28].
Second-order nonlinear coefficients [29]:

$| d_{31}(1.0642\,\mu\text{m}) | = 0.67\,\text{pm/V}$

$| d_{32}(1.0642\,\mu\text{m}) | = 0.85\,\text{pm/V}$

$| d_{33}(1.0642\,\mu\text{m}) | = 0.04\,\text{pm/V}$

The signs of LBO second-order nonlinear coefficients d_{15}, d_{31} and d_{24}, d_{32}, d_{33} are opposite [29].

Experimental values of phase-matching angles ($T = 293\,\text{K}$)

Interacting wavelengths [μm]	ϕ_{exp} [deg]	θ_{exp} [deg]	Ref.
XY plane, $\theta = 90°$			
SHG, $o + o \Rightarrow e$			
$1.908 \Rightarrow 0.954$	23.8		[16]
$1.5 \Rightarrow 0.75$	7		[16]
$1.0796 \Rightarrow 0.5398$	10.6		[16]
	10.7		[1], [30]
$1.0642 \Rightarrow 0.5321$	11.3		[12]
	11.4		[20], [31], [32]
	11.6		[11], [16], [33]
	11.8		[34]
$0.946 \Rightarrow 0.473$	19.4		[35], [36]
	19.5		[37], [38]

Interacting wavelengths [μm]	ϕ_{exp} [deg]	θ_{exp} [deg]	Ref.
0.930 ⇒ 0.465	21.3		[39]
0.896 ⇒ 0.448	23.25		[40]
0.88 ⇒ 0.44	24.53		[40]
0.850 ⇒ 0.425	27		[41]
0.84 ⇒ 0.42	27.92		[40]
0.836 ⇒ 0.418	28.3		[42]
0.80 ⇒ 0.40	31.70		[40]
0.794 ⇒ 0.397	32.3		[43]
0.786 ⇒ 0.393	33		[44]
0.78 ⇒ 0.39	33.70		[40]
0.7735 ⇒ 0.38675	34.4		[45]
0.75 ⇒ 0.375	37.13		[40]
	37		[46]
0.746 ⇒ 0.373	37.5		[47], [48]
0.7094 ⇒ 0.3547	41.8		[16]
	41.9		[49]
	42		[50]
	43.5		[51]
0.63 ⇒ 0.315	55.6		[52]
0.555 ⇒ 0.2775	86		[16]
0.554 ⇒ 0.277	90		[53]
SFG, $o + o \Rightarrow e$			
1.3414 + 0.6707 ⇒ 0.44713	20		[19]
1.0642 + 0.5321 ⇒ 0.35473	37		[54]
	37.1		[19]
	37.2		[11], [12]
1.053 + 0.5265 ⇒ 0.351	38.2		[55]
1.0642 + 0.35473 ⇒ 0.26605	60.7		[11]
	61		[16]
0.86 + 0.43 ⇒ 0.2867	61		[41]
1.3188 + 0.26605 ⇒ 0.22139	70.2		[11]
0.21284 + 2.35524 ⇒ 0.1952	50.3		[19]
0.21284 + 1.90007 ⇒ 0.1914	63.8		[19]
0.21284 + 1.58910 ⇒ 0.18774	88		[19]
YZ plane, $\phi = 90°$			
SHG, $o + e \Rightarrow o$			
1.908 ⇒ 0.954		46.2	[16]
1.5 ⇒ 0.75		14.7	[16]
1.0796 ⇒ 0.5398		19.2	[16]
1.0642 ⇒ 0.5321		19.9	[12]
		20.5	[11]
		20.6	[56]
		21.0	[16]
SFG, $o + e \Rightarrow o$			
1.0641 + 0.53205 ⇒ 0.3547		42	[57]

Interacting wavelengths [μm]	ϕ_{exp} [deg]	θ_{exp} [deg]	Ref.
		42.7	[58]
$1.0642 + 0.5321 \Rightarrow 0.35473$		42.2	[11]
		42.5	[19]
		43.2	[12]
XZ plane, $\phi = 0°$, $\theta < V_z$			
SHG, $e + o \Rightarrow e$			
$1.3414 \Rightarrow 0.6707$		3.6	[59]
		4.2	[16]
		5.0	[33]
$1.3188 \Rightarrow 0.6594$		5.2	[11]
$1.3 \Rightarrow 0.65$		5.4	[33]
XZ plane, $\phi = 0°$, $\theta > V_z$			
SHG, $e + e \Rightarrow o$			
$1.3414 \Rightarrow 0.6707$		86.1	[59], [60]
		86.3	[16]
		86.6	[33]
$1.3188 \Rightarrow 0.6594$		86.0	[11]
$1.3 \Rightarrow 0.65$		86.1	[33]
$1.24 \Rightarrow 0.62$		86	[61]

Experimental values of non-critical phase matching (NCPM) temperature

Interacting wavelengths [μm]	T [°C]	Ref.
along *X* axis		
SHG, type I		
$1.547 \Rightarrow 0.7735$	117	[45]
$1.46 \Rightarrow 0.73$	50	[62]
$1.252 \Rightarrow 0.626$	3.5	[63]
$1.25 \Rightarrow 0.625$	−2.9	[20], [31]
$1.215 \Rightarrow 0.6075$	21	[20]
$1.211 \Rightarrow 0.6055$	20	[11]
$1.206 \Rightarrow 0.603$	24	[64]
$1.2 \Rightarrow 0.6$	24.3	[20], [31]
$1.15 \Rightarrow 0.575$	61.1	[20], [31]
$1.135 \Rightarrow 0.5675$	77.4	[34]
$1.11 \Rightarrow 0.555$	108.2	[20], [31]
$1.0796 \Rightarrow 0.5398$	112	[1]
$1.0642 \Rightarrow 0.5321$	134 (?)	[65]
	148	[20], [31]
	148.5	[66], [67]
	149	[34], [68]
	149.5	[69]
	151	[56]

Interacting wavelengths [μm]	T [°C]	Ref.
1.047 ⇒ 0.5235	166.5	[70]
	167	[71]
	≈170	[72]
	172	[73]
	175	[74]
	176.5	[75]
	180	[76]
1.025 ⇒ 0.5125	190.3	[20], [31]
SFG, type I		
1.908 + 1.0642 ⇒ 0.6832	81	[34]
1.444 + 1.08 ⇒ 0.6179	23	[77]
1.135 + 1.0642 ⇒ 0.5491	112	[34]
1.547 + 0.7735 ⇒ 0.5157	141	[45]
DFG, type I		
0.532 − 0.8 ⇒ 1.588	135	[78]
along Z axis		
SHG, type II		
1.342 ⇒ 0.671	35	[79]
1.3 ⇒ 0.65	46	[62]

Experimental values of internal angular, temperature, and spectral bandwidths

Interacting wavelengths [μm]	T [°C]	$\Delta\varphi^{\text{int}}$ [deg]	$\Delta\theta^{\text{int}}$ [deg]	ΔT [°C]	Ref.
along X axis					
SHG, type I					
1.46 ⇒ 0.73	50			6	[62]
1.252 ⇒ 0.626	3.5			9	[63]
1.206 ⇒ 0.603	24			13	[64]
1.135 ⇒ 0.5675	77.4			4.7	[34]
1.0642 ⇒ 0.5321	148	3.54	2.57	3.9	[31]
	148.5			2.7	[66]
	148.5			4.2	[67]
	149	2.3	1.9	4.0	[34]
	149.5			4.1	[69]
	151	2.1	2.1	2.9	[56]
1.047 ⇒ 0.5235	175			3.5	[74]
	176.5			3.5	[75]
SFG, type I					
1.908 + 1.0642 ⇒ 0.6832	81			7.4	[34]
1.444 + 1.08 ⇒ 0.6179	23	4.2	3.0		[77]
1.135 + 1.0642 ⇒ 0.5491	112			5.0	[34]
DFG, type I					
0.532 − 0.8 ⇒ 1.588	135			3.8	[78]

Experimental values of internal angular, temperature, and spectral bandwidths

Interacting wavelengths [μm]	ϕ_{pm} [deg]	θ_{pm} [deg]	$\Delta\varphi^{int}$ [deg]	$\Delta\theta^{int}$ [deg]	ΔT [°C]	$\Delta\nu$ [cm^{-1}]	Ref.
XY plane, $\theta = 90°(T = 293\,K)$							
SHG, $o + o \Rightarrow e$							
$1.0796 \Rightarrow 0.5398$	10.7		0.31				[30]
$1.0642 \Rightarrow 0.5321$	10.8		0.27	2.63			[56]
	11.4		0.24	1.79			[20]
	11.6				5.8		[11]
			0.34	2.64	6.7	8.8	[80]
$0.886 \Rightarrow 0.443$	24.1				7.8	15.9	[40]
$0.870 \Rightarrow 0.435$	25.4		0.12				[81]
			0.10				[40]
$0.78 \Rightarrow 0.39$	33.7		0.08				[81]
			0.07				[40]
$0.7605 \Rightarrow 0.38025$	35.9				15.3	10.5	[40]
$0.715 \Rightarrow 0.3575$	41		0.06				[81]
SFG, $o + o \Rightarrow e$							
$1.0642 + 0.3547 \Rightarrow 0.2661$	60.7				3.8		[11]
YZ plane, $\phi = 90°(T = 293\,K)$							
SHG, $o + e \Rightarrow o$							
$1.0642 \Rightarrow 0.5321$		20.6	3.20	0.77			[56]
			3.00	0.81		11.5	[80]
					6.2		[11]
SFG, $o + e \Rightarrow o$							
$1.0641 + 0.53205 \Rightarrow 0.3547$		42	0.79	0.16	6		[57]
$1.0642 + 0.5321 \Rightarrow 0.35473$		42.2		0.18			[11]
		41	3.07	0.18			[15]

Calculated values of inverse group-velocity mismatch for SHG process in LBO

Interacting wavelengths [μm]	ϕ_{pm} [deg]	θ_{pm} [deg]	β [fs/mm]
XY plane, $\theta = 90°$			
SHG, $o + o \Rightarrow e$			
$1.2 \Rightarrow 0.6$	2.36		18
$1.1 \Rightarrow 0.55$	9.37		37
$1.0 \Rightarrow 0.5$	15.74		59
$0.9 \Rightarrow 0.45$	22.94		86
$0.8 \Rightarrow 0.4$	31.69		123
$0.7 \Rightarrow 0.35$	43.38		175
$0.6 \Rightarrow 0.3$	62.63		257
YZ plane, $\phi = 90°$			
SHG, $o + e \Rightarrow o$			
$1.1 \Rightarrow 0.55$		15.98	82

Interacting wavelengths [μm]	ϕ_{pm} [deg]	θ_{pm} [deg]	β [fs/mm]
1.0 ⇒ 0.5		28.96	106
0.9 ⇒ 0.45		45.36	139
0.8 ⇒ 0.4		76.88	186

Laser-induced surface-damage threshold

λ [μm]	τ_p [ns]	I_{thr} [GW/cm^2]	Ref.	Note
0.2661	12	>0.04	[82]	
	0.07	>3	[83]	
0.308	17	>0.05	[84]	
		>0.06	[85]	
	10	>0.1	[86]	
	0.0003	47,000	[87]	sharp focusing
0.3547	18	>0.18	[88]	10 Hz
	10	>0.04	[49]	
		>0.2	[89]	
	8	>0.1	[17]	
	7	>0.14	[90]	
	0.03	>9.4	[91]	10 Hz
		>18	[92]	10 Hz
	0.015	>2.8	[51]	
	0.018	>5	[50]	
	0.025	>6	[93]	10 Hz
0.5145	CW	>0.00003	[94]	
0.5235	0.055	>1.1	[76]	500 Hz
		>5	[95]	500 Hz
0.5321	CW	>0.0004	[69]	
	60	>0.07	[96]	900 Hz
	10	>0.22	[33]	
	0.1	>4.5	[97]	500 Hz
	0.035	>3.1	[66]	
	0.015	>4.4	[18]	
0.592	0.0005	>50	[98]	1 kHz
0.605	0.0002	>25	[99]	
0.616	0.0004	31,000	[87]	sharp focusing
		35,000	[100]	sharp focusing
		38,000	[101]	sharp focusing
0.652	0.02	>0.81	[21]	
0.7–0.9	10	>0.03	[40]	10 Hz
0.71–0.87	25	1.1–1.4	[81]	25 Hz
0.72–0.85	0.001	>8	[102]	

λ [μm]	τ_p [ns]	I_{thr} [GW/cm^2]	Ref.	Note
0.77–0.83	0.00005	>22	[103]	80 MHz
1.0642	CW	>0.001	[69]	
	60	>0.06	[96]	1333 Hz
	18	>0.6	[88]	10 Hz
	9	>0.9	[104]	10 Hz
	8	>0.5	[56]	
	1.3	19	[80]	
	1.1	45	[105]	bulk damage
	0.1	25	[1]	
	0.035	>4.8	[66]	
	0.025	>3.3	[93]	10 Hz
1.0796	5	20	[106]	1–25 Hz
	0.04	30	[87]	

About the crystal

In comparison with BBO, the applications of LBO mainly concentrated around SHG of near IR radiation and OPO in visible and near-IR ranges. We will give some characteristic examples. In recent experiments, lithium triborate was used for CW frequency doubling of Nd:YVO_4 laser ($\lambda = 1342$ nm) [79], Nd:$YAlO_3$ laser ($\lambda = 1341.4$ nm) [60], Nd:YAG laser ($\lambda = 946$ nm) [35], InGaAs diode-laser oscillator ($\lambda = 930$ nm) [39], and Ti:sapphire laser ($\lambda = 746$ nm) [47]. The obtained CW SH output power ranged from 0.6 to 1.2 W. The LBO crystal was also employed for SHG of a diode-pumped high-average-power Q-switched Nd:YAG laser ($\lambda = 1064$ nm); the green output power of 138 W was generated [107]. Though a KTP crystal used for this application produces more SH power, the advantage of LBO is the absence of photochromic damage (gray-tracking). As a result, the output green power does not decrease with time.

In [108], the LBO-based OPO was pumped by the second harmonic of a mode-locked ps Nd:YLF laser ($\lambda = 527$ nm, $P = 5.6$ W, $\tau = 35$ ps, $\Delta f = 76$ MHz). The signal and idler output were tunable from 750 to 930 nm and from 1220 to 1770 nm, respectively. A signal output power of up to 1.6 W was obtained. In [58], the LBO-based OPO was synchronously pumped by the third harmonic of a mode-locked ps Nd:YVO_4 laser ($\lambda = 355$ nm, $P = 9.0$ W, $\tau = 7.5$ ps, $\Delta f = 84$ MHz). The tunability range of a signal wave was 457–479 nm, the signal output power reached 5.0 W at 462 nm, and the idler output power equaled 1.7 W at 1535 nm.

References

[1] C. Chen, Y. Wu, A. Jiang, B. Wu, G. You, R. Li, S. Lin: New nonlinear-optical crystal: LiB_3O_5. J. Opt. Soc. Am. B **6(4)**, 616–621 (1989).

[2] Data sheet of Cleveland Crystals Inc. Available at www.clevelandcrystals.com.
[3] Y.-N. Xu, W.Y. Ching: Electronic structure and optical properties of LiB_3O_5. Phys. Rev. B **41(8)**, 5471–5474 (1990).
[4] R. Guo, S.A. Markgraf, Y. Furukawa, M. Sato, A.S. Bhalla: Pyroelectric, dielectric, and piezoelectric properties of LiB_3O_5. J. Appl. Phys. **78(12)**, 7234–7239 (1995).
[5] L. Wei, D. Guiqing, H. Qingzhen, Z. An, L. Jingkui: Anisotropic thermal expansion of LiB_3O_5. J. Phys. D **23(8)**, 1073–1075 (1990).
[6] B.H.T. Chai: Optical Crystals. In: CRC Handbook of Laser Science and Technology, Supplement 2: Optical Materials, ed. by M.J. Weber (CRC Press, Boca Raton, 1995), pp. 3–65.
[7] Y. Mori, S. Nakajima, A. Miyamoto, M. Inagaki, T. Sasaki, H. Yoshida, S. Nakai: Generation of ultraviolet light using a new nonlinear optical crystal $CsLiB_6O_{10}$. Proc. SPIE, **2633**, 299–307 (1995).
[8] Data sheet of Fujian Castech Crystals, Inc. Available at www.castech.com.
[9] J.D. Beasley: Thermal conductivities of some novel nonlinear optical materials. Appl. Opt. **33(1)**, 1000–1003 (1994).
[10] R.H. French, J.W. Ling, F.S. Ohuchi, C.T. Chen: Electronic structure of β-BaB_2O_4 and LiB_3O_5 nonlinear optical crystals. Phys. Rev. B **44(16)**, 8496–8502 (1991).
[11] K. Kato: Tunable UV generation to 0.2325 μm in LiB_3O_5. IEEE J. Quant. Electr. **26(7)**, 1173–1175 (1990).
[12] S.P. Velsko, M. Webb, L. Davis, C. Huang: Phase-matched harmonic generation in lithium triborate (LBO). IEEE J. Quant. Electr. **27(9)**, 2182–2192 (1991).
[13] A. Dubietis, G. Timošauskas, A. Varanavičius, G. Valiulis: Two-photon absorbing properties of ultraviolet phase-matchable crystals at 264 and 211 nm. Appl. Opt. **39(15)**, 2437–2440 (2000).
[14] K. Kato: Temperature-tuned 90° phase-matching properties of LiB_3O_5. IEEE J. Quant. Electr. **30(12)**, 2950–2952 (1994).
[15] B. Wu, N. Chen, C. Chen, D. Deng, Z. Xu: Highly efficient ultraviolet generation at 355 nm in LiB_3O_5. Opt.Lett. **14(19)**, 1080–1081 (1989).
[16] S. Lin, B. Wu, F. Xie, C. Chen: Phase-matching retracing behavior: new features in LiB_3O_5. Appl. Phys. Lett. **59(13)**, 1541–1543 (1991).
[17] F. Hanson, D. Dick: Blue parametric generation from temperature-tuned LiB_3O_5. Opt. Lett. **16(4)**, 205–207 (1991).
[18] S. Lin, J.Y. Huang, J. Ling, C. Chen, Y.R. Shen: Optical parametric amplification in a lithium triborate crystal tunable from 0.65 to 2.5 μm. Appl. Phys. Lett. **59(22)**, 2805–2807 (1991).
[19] B. Wu, F. Xie, C. Chen, D. Deng, Z. Xu: Generation of tunable coherent vacuum ultraviolet radiation in LiB_3O_5 crystal. Opt. Commun. **88(4–6)**, 451–454 (1992).
[20] T. Ukachi, R.J. Lane, W.R. Bosenberg, C.L. Tang: Phased-matched second-harmonic generation and growth of a LiB_3O_5 crystal. J. Opt. Soc. Am. B **9(7)**, 1128–1133 (1992).
[21] H. Mao, B. Wu, C. Chen, D. Zhang, P. Wang: Broadband optical parametric amplification in LiB_3O_5. Appl. Phys. Lett. **62(16)**, 1866–1868 (1993).
[22] G.C. Bhar, P.K. Datta, A.M. Rudra: Noncollinear ultraviolet generation in a lithium borate crystal. Appl. Phys. B **57(6)**, 431–434 (1993).
[23] T. Schröder, K.-J. Boller, A. Fix, R. Wallenstein: Spectral properties and numerical modeling of a critically phase-matched nanosecond LiB_3O_5 optical parametric oscillator. Appl. Phys. B **58(5)**, 425–438 (1994).
[24] I.T. Bodnar, A.U. Sheleg, L.V. Losovskaya: Refractive indices of lithium triborate in a temperature range of 20–600°C. Opt. Spektrosk. **86(4)**, 571–573 (1999) [In Russian, English trans.: Opt. Spectrosc. **86(4)**, 640–642 (1999)].

[25] Y. Tang, Y. Cui, M.H. Dunn: Thermal dependence of the principal refractive indices of lithium triborate. J. Opt. Soc. Am. B **12(4)**, 638–643 (1995).
[26] H.P. Li, C.H. Kam, Y.L. Lam, W. Ji: Femtosecond Z-scan measurements of nonlinear refraction in nonlinear optical materials. Opt. Mater. **15(4)**, 237–242 (2001).
[27] M. Sheik-Bahae, M. Ebrahimzadeh: Measurements of nonlinear refraction in the second-order $\chi^{(2)}$ materials $KTiOPO_4$, $KNbO_3$, β-BaB_2O_4, and LiB_3O_5. Opt. Commun. **142(4–6)**, 294–298 (1997).
[28] V.G. Dmitriev, D.N. Nikogosyan: Effective nonlinearity coefficients for three-wave interactions in biaxial crystals of *mm*2 point group symmetry. Opt. Commun. **95(1– 3)**, 173–182 (1993).
[29] D.A. Roberts: Simplified characterization of uniaxial and biaxial nonlinear optical crystals: a plea for standardization of nomenclature and conventions. IEEE J. Quant. Electr. **28(10)**, 2057–2074 (1992).
[30] S. Lin, Z. Sun, B. Wu, C. Chen: The nonlinear optical characteristics of a LiB_3O_5 crystal. J. Appl. Phys. **67(2)**, 634–638 (1990).
[31] T. Ukachi, R.J. Lane, W.R. Bosenberg, C.L. Tang: Measurements of noncritically phase-matched second-harmonic generation in a LiB_3O_5 crystal. Appl. Phys. Lett. **57(10)**, 980–982 (1990).
[32] N. Pavel, J. Saikawa, T. Taira: Diode end-pumped passively Q-switched Nd:YAG laser intra-cavity frequency doubled by LBO crystal. Opt. Commun. **195(1–4)**, 233–240 (2001).
[33] K. Kato: Parametric oscillation in LiB_3O_5 pumped at 0.532 μm. IEEE J. Quant. Electr. **26(12)**, 2043–2045 (1990).
[34] J.T. Lin, J.L. Montgomery, K. Kato: Temperature-tuned noncritically phase-matched frequency conversion in LiB_3O_5 crystal. Opt. Commun. **80(2)**, 159–165 (1990).
[35] D.-H. Li, P.-X. Li, Z.-G. Zhang, S.-W. Zhang: Compact high-power blue light from a diode-pumped intracavity-doubled Nd:YAG laser. Chin. Phys. Lett. **19(11)**, 1632–1634 (2002).
[36] P.-X. Li, D.-H. Li, Z.-G. Zhang, S.-W. Zhang: Diode-pumped compact CW frequency-doubled Nd:YAG laser in the Watt range at 473 nm. Chin. Phys. Lett. **20(7)**, 1064–1066 (2003).
[37] T. Kellner, F. Heine, G. Huber: Efficient laser performance of Nd:YAG at 946 nm and intracavity frequency doubling with $LiJO_3$, β-BaB_2O_4, and LiB_3O_5. Appl. Phys. B **65(6)**, 789–792 (1997).
[38] X.-C. Lin, R.-N. Li, D.-F. Cui, A.-Y. Yao, Y. Feng, Y. Bi, Z.-Y. Xu: Highly-efficient blue-light generation by intracavity frequency doubling with LiB_3O_5. Chin. Phys. Lett. **19(8)**, 1106–1107 (2002).
[39] D. Woll, B. Beier, K.-J. Boller, R. Wallenstein, M. Hagberg, S. O'Brien: 1 W of blue 465-nm radiation generated by frequency doubling of the output of a high-power diode laser in critically phase-matched LiB_3O_5. Opt. Lett. **24(10)**, 691–693 (1999).
[40] D.-W. Chen, J.T. Lin: Temperature-tuned phase-matching properties of LiB_3O_5 for Ti:sapphire laser frequency doubling. IEEE J. Quant. Electr. **29(2)**, 307–310 (1993).
[41] F. Balembois, M. Gaignet, F. Louradour, V. Couderc, A. Barthelemy, P. Georges, A. Brun: Tunable picosecond UV source at 10 kHz based on an all-solid-state diode-pumped laser system. Appl. Phys. B **65(2)**, 255–258 (1997).
[42] H. Yamamoto, K. Toyoda, K. Matsubara, M. Watanabe, S. Urabe: Development of a tunable 209 nm continuous-wave light source using two-stage frequency doubling of a Ti:sapphire laser. Jpn. J. Appl. Phys. **41(6A)**, 3710–3713 (2002).
[43] T. Kaing, M. Houssin: Ring cavity enhanced second harmonic generation of a diode laser using LBO crystal. Opt. Commun. **157(1–6)**, 155–160 (1998).

[44] P.L. Ramazza, S. Ducci, A. Zavatta, M. Bellini, F.T. Arecchi: Second-harmonic generation from a picosecond Ti:Sa laser in LBO: conversion efficiency and spatial properties. Appl. Phys. B **75(1)**, 53–58 (2002).
[45] H. Kitano, H. Kawai, K. Miramitsu, S. Owa, M. Yoshimura, Y. Mori, T. Sasaki: 387-nm generation in $Gd_xY_{1-x}Ca_4O(BO_3)_3$ crystal and its utilization for 193-nm light source. Jpn. J. Appl. Phys. **42(2B)**, L166–L169 (2003).
[46] S. Sayama, M. Ohtsu: Tunable UV CW generation by frequency tripling of a Ti:sapphire laser. Opt. Commun. **137(4–6)**, 295–298 (1997).
[47] Y. Asakawa, H. Kumagai, K. Midorikawa, M. Obara: 50% frequency doubling efficiency of 1.2-W CW Ti:sapphire laser at 746 nm. Opt. Commun. **217(1–6)**, 311–315 (2003).
[48] T. Fujii, H. Kumagai, K. Midorikawa, M. Obara: Development of a high-power deep-ultraviolet continuous-wave coherent light source for laser cooling of silicon atoms. Opt. Lett. **25(19)**, 1457–1459 (2000).
[49] Y. Wang, Z. Xu, D. Deng, W. Zheng, B. Wu, C. Chen: Visible optical parametric oscillation in LiB_3O_5. Appl. Phys. Lett. **59(5)**, 531–533 (1991).
[50] H.-J. Krause, W. Daum: Efficient parametric generation of high-power coherent picosecond pulses in lithium borate tunable from 0.405 to 2.4 μm. Appl. Phys. Lett. **60(18)**, 2180–2182 (1992).
[51] J.Y. Zhang, J.Y. Huang, Y.R. Shen, C. Chen, B. Wu: Picosecond optical parametric amplification in lithium triborate. Appl. Phys. Lett. **58(3)**, 213–215 (1991).
[52] W.S. Pelouch, T. Ukachi, E.S. Wachman, C.L. Tang: Evaluation of LiB_3O_5 for second-harmonic generation of femtosecond optical pulses. Appl. Phys. Lett. **57(2)**, 111–113 (1990).
[53] A. Borsutzky, R. Brunger, C. Huang, R. Wallenstein: Harmonic and sum-frequency generation of pulsed laser radiation in BBO, LBO and KD*P. Appl. Phys. B **52(1)**, 55–62 (1991).
[54] D.A.V. Kliner, F. Di Teodoro, J.P. Koplow, S.W. Moore, A.V. Smith: Efficient second, third, fourth, and fifth harmonic generation of a Yb-doped fiber amplifier. Opt. Commun. **210(3–6)**, 393–398 (2002).
[55] D. Wang, C. Grässer, R. Beigang, R. Wallenstein: The generation of tunable blue ps-light-pulses from a CW mode-locked LBO optical parametric oscillator. Opt. Commun. **138(1–3)**, 87–90 (1997).
[56] V.A. Dyakov, M.K. Dzhafarov, A.A. Lukashev, A.A. Podshivalov, V.I. Pryalkin: Conversion of the frequency of laser radiation in lithium triborate LiB_3O_5 crystals. Kvant. Elektron. **18(3)**, 339–341 (1991) [In Russian, English trans.: Sov. J. Quantum Electron. **21(3)**, 307–308 (1991)].
[57] J.J. McFerran, A.N. Luiten: Efficient continuous-wave ultraviolet generation in LiB_3O_5 and RbD_2AsO_4. Appl. Opt. **39(18)**, 3115–3119 (2000).
[58] B. Ruffing, A. Nebel, R. Wallenstein: High-power picosecond LiB_3O_5 optical parametric oscillators tunable in the blue spectral range. Appl. Phys. B **72(2)**, 137–149 (2001).
[59] Q. Zheng, H. Tan, L. Zhao, L. Quan: Diode-pumped 671 nm laser frequency doubled by CPM LBO. Opt. Laser Technol. **34(4)**, 329–331 (2002).
[60] G. Zhang, H. Shen, R. Zeng, C. Huang, W. Lin, J. Huang: The study of 1341.4 nm Nd:$YalO_3$ laser intracavity frequency doubling by LiB_3O_5. Opt. Commun. **183(5–6)**, 461–466 (2000).
[61] X. Liu, L. Qian, F.W. Wise: Efficient generation of 50-fs red pulses by frequency doubling in LiB_3O_5. Opt. Commun. **144(4–6)**, 265–268 (1997).
[62] S. French, M. Ebrahimzadeh, A. Miller: Visible picosecond pulse generation in a frequency doubled optical parametric oscillator based on LiB_3O_5. Opt. Commun. **128(1–3)**, 166–176 (1996).

[63] V. Shcheslavskiy, V. Petrov, F. Noack, N. Zhavoronkov: An all-solid-state laser system for generation of 100 μJ femtosecond pulses near 625 nm at 1 kHz. Appl. Phys. B **69(2)**, 167–169 (1999).
[64] N. Zhavoronkov, V. Petrov, F. Noack: Powerful and tunable operation of a 1-2-kHz repetition-rate gain-switched Cr:forsterite laser and its frequency doubling. Appl. Opt. **38(15)**, 3285–3293 (1999).
[65] M. Tsunekane, S. Kimura, M. Kimura, N. Taguchi, H. Inaba: Broadband tuning of a continuous-wave, doubly resonant, lithium triborate optical parametric oscillator from 791 to 1620 nm. Appl. Opt. **37(27)**, 6459–6462 (1998).
[66] J.Y. Huang, Y.R. Shen, C. Chen, B. Wu: Noncritically phase-matched second-harmonic generation and optical parametric amplification in a lithium triborate crystal. Appl. Phys. Lett. **58(15)**, 1579–1581 (1991).
[67] I. Gontijo: Determination of important parameters for second harmonic generation in LBO. Opt. Commun. **108(4–6)**, 324–328 (1994).
[68] Y. Bi, H.-B. Zhang, Z.-P. Sun, Z.-R.-G.-T. Bao, H.-Q. Li, Y.-P. Kong, X.-C. Lin, G.-L. Wang, J. Zhang, W. Hou, R.-N. Li, D.-F. Cui, Z.-Y. Xu, L.-W. Song, P. Zhang, J.-F. Cui, Z.-W. Fan: High-power blue light generation by external frequency doubling of an optical parametric oscillator. Chin. Phys. Lett. **20(11)**, 1957–1959 (2003).
[69] S.T. Yang, C.C. Pohalski, E.K. Gustafson, R.L. Byer, R.S. Feigelson, R.J. Raymakers, R.K. Route: 6.5-W, 532-nm radiation by CW resonant external-cavity second-harmonic generation of an 18-W Nd:YAG laser in LiB_3O_5. Opt. Lett. **16(19)**, 1493–1495 (1991).
[70] G.J. Hall, A.I. Ferguson: LiB_3O_5 optical parametric oscillator pumped by a Q-switched frequency-doubled all-solid-state laser. Opt. Lett. **18(18)**, 1511–1513 (1993).
[71] G.P.A. Malcolm, M. Ebrahimzadeh, A.I. Ferguson: Efficient frequency conversion of mode-locked diode-pumped lasers and tunable all-solid-state laser sources. IEEE J. Quant. Electr. **28(4)**, 1172–1178 (1992).
[72] K.F. Wall, J.S. Smucz, B. Pati, Y. Isyanova, P. Moulton, J.G. Manni: A quasi-continuous-wave deep ultraviolet laser source. IEEE J. Quant. Electr. **39(9)**, 1160–1169 (2003).
[73] A. Robertson, A.I. Ferguson: Synchronously pumped all-solid-state lithium triborate optical parametric oscillator in a ring configuration. Opt. Lett. **19(2)**, 117–119 (1994).
[74] S.D. Butterworth, M.J. McCarthy, D.C. Hanna: Widely tunable synchronously pumped optical parametric oscillator. Opt. Lett. **18(17)**, 1429–1431 (1993).
[75] M.J. McCarthy, S.D. Butterworth, D.C. Hanna: High-power widely-tunable picosecond pulses from an all-solid-state synchronously-pumped optical parametric oscillator. Opt. Commun. **102(3–4)**, 297–303 (1993).
[76] M. Ebrahimzadeh, G.J. Hall, A.I. Ferguson: Temperature-tuned noncritically phase-matched picosecond LiB_3O_5 optical parameter oscillator. Appl. Phys. Lett. **60(12)**, 1421–1423 (1992).
[77] H.M. Kretschmann, F. Heine, G. Huber, T. Halldorsson: All-solid-state continuous-wave doubly resonant all-intracavity sum-frequency mixer. Opt. Lett. **22(19)**, 1461–1463 (1997).
[78] J. Hong, A.D.O. Bawagan, S. Charbonneau, A. Stolow: Broadly tunable femtosecond pulse generation in the near and mid-infrared. Appl. Opt. **36(9)**, 1894–1897 (1997).
[79] A. Agnesi, A. Guandalini, G. Reali: Efficient 671-nm pump source by intracavity doubling of a diode-pumped Nd:YVO_4 laser. J. Opt. Soc. Am. B **19(5)**, 1078–1082 (2002).
[80] C. Chen: Chinese lab grows new nonlinear optical borate crystals. Laser Focus World **25(11)**, 129–137 (1989).
[81] G.A. Skripko, S.G. Bartoshevich, I.V. Mikhnyuk, I.G. Tarazevich: LiB_3O_5: a highly efficient frequency converter for Ti:sapphire lasers. Opt. Lett. **16(22)**, 1726–1728 (1991).

[82] Y. Tang, Y. Cui, M.H. Dunn: Lithium triborate optical parametric oscillator pumped at 266 nm. Opt. Lett. **17(3)**, 192–194 (1992).
[83] J. Izawa, K. Midorikawa, M. Obara, K. Toyoda: Picosecond ultraviolet optical parametric generation using a type-II phase-matched lithium triborate crystal for an injection seed of VUV lasers. IEEE J. Quant. Electr. **33(11)**, 1997–2001 (1997).
[84] G. Robertson, A. Henderson, M.H. Dunn: Broadly tunable LiB_3O_5 optical parametric oscillator. Appl. Phys. Lett. **60(3)**, 271–273 (1992).
[85] G. Robertson, A. Henderson, M. Dunn: Attainment of high efficiencies in optical parametric oscillators. Opt. Lett. **16(20)**, 1584–1586 (1991).
[86] M. Ebrahimzadeh, G. Robertson, M.H. Dunn: Efficient ultraviolet LiB_3O_5 optical parametric oscillator. Opt. Lett. **16(10)**, 767–769 (1991).
[87] I.M. Bayanov, V.M. Gordienko, M.S. Djidjoev, V.A. Dyakov, S.A. Magnitskii, V.I. Pryalkin, A.P. Tarasevitch: Parametric generation of high-peak-power femtosecond light pulses in LBO crystal. Proc. SPIE **1800**, 2–17 (1991).
[88] Y. Cui, M.H. Dunn, C.J. Norrie, W. Sibbett, B.D. Sinclair, Y. Tang, J.A.C. Terry: All-solid-state optical parametric oscillator for the visible. Opt. Lett. **17(9)**, 646–648 (1992).
[89] Y. Cui, D.E. Withers, C.F. Rae, C.J. Norrie, Y. Tang, B.D. Sinclair, W. Sibbett, M.H. Dunn: Widely tunable all-solid-state optical parametric oscillator for the visible and near infrared. Opt. Lett. **18(2)**, 122–124 (1993).
[90] A. Fix, T. Schröder, R. Wallenstein: The optical parametric oscillators of beta barium borate and lithium triborate: new sources of powerful tunable laser radiation in the ultraviolet, visible and near infrared. Laser und Optoelektronik **23(3)**, 106–110 (1991).
[91] F. Huang, L. Huang: Picosecond optical parametric generation and amplification in LiB_3O_5 and β-BaB_2O_4. Appl. Phys. Lett. **61(15)**, 1769–1771 (1992).
[92] F. Huang, L. Huang, B.-I. Yin, Y. Hua: Generation of 415.9-482.6 nm tunable intense picosecond single pulse in LiB_3O_5. Appl. Phys. Lett. **62(7)**, 672–674 (1993).
[93] H.-J. Krause, W. Daum: High-power source of coherent picosecond light pulses tunable from 0.41 to 12.9 μm. Appl. Phys. B **56(1)**, 8–13 (1993).
[94] F.G. Colville, A.J. Henderson, M.J. Padgett, J. Zhang, M.H. Dunn: Continuous-wave parametric oscillation in lithium triborate. Opt. Lett. **18(3)**, 205–207 (1993).
[95] M. Ebrahimzadeh, G.J. Hall, A.I. Ferguson: Singly resonant, all-solid-state, mode-locked LiB_3O_5 optical parametric oscillator tunable from 652 nm to 2.65 μm. Opt. Lett. **17(9)**, 652–654 (1992).
[96] F. Hanson, P. Poirier: Efficient intracavity frequency doubling of a high- repetition-rate diode-pumped Nd:YAG laser. Opt. Lett. **19(19)**, 1526–1528 (1994).
[97] H. Zhou, J. Zhang, T. Chen, C. Chen, Y.R. Shen: Picosecond, narrow-band, widely tunable optical parametric oscillator using a temperature-tuned lithium borate crystal. Appl. Phys. Lett. **62(13)**, 1457–1459 (1993).
[98] G.P. Banfi, C. Solcia, P. Di Trapani, R. Danielius, A. Piskarskas, R. Righini, R. Torre: Travelling-wave parametric conversion of microjoule pulses with LBO. Opt. Commun. **118(3–4)**, 353–359 (1995).
[99] G.P. Banfi, R. Danielius, A. Piskarskas, P. Di Trapani, P. Foggi, R. Righini: Femtosecond traveling-wave parametric generation with lithium triborate. Opt. Lett. **18(19)**, 1633–1635 (1993).
[100] S.A. Akhmanov, I.M. Bayanov, V.M. Gordienko, V.A. Dyakov, S.A. Magnitskii, V.I. Pryalkin, A.P. Tarasevitch: Parametric generation of femtosecond pulses by LBO crystal in the near IR. In: *Ultrafast Processes in Spectroscopy 1991, IOP Conf. Ser. No. 126*, ed. by A. Laubereau, A. Seilmeier (IOP Publishing, Bristol, 1992), pp. 67–70.

[101] V.M. Gordienko, S.A. Magnitskii, A.P. Tarasevitch: Injection-locked femtosecond parametric oscillators on LBO crystal; towards 10^{17} W cm^{-2}. In: *Frontiers in Nonlinear Optics. The Sergei Akhmanov Memorial Volume*, ed. by H. Walther, N. Koroteev, M.O. Scully (IOP Publishing, Bristol, 1993), pp. 286–292.
[102] A. Nebel, R. Beigang: External frequency conversion of cw mode-locked Ti:Al_2O_3 laser radiation. Opt. Lett. **16(22)**, 1729–1731 (1991).
[103] J. Jiang, T. Hasama: High repetition-rate femtosecond optical parametric oscillator based on LiB_3O_5. Opt. Commun. **211(1–6)**, 295–302 (2002).
[104] F. Xie, B. Wu, G. You, C. Chen: Characterization of LiB_3O_5 crystal for second-harmonic generation. Opt. Lett. **16(16)**, 1237–1239 (1991).
[105] M. Yoshimura, T. Kamimura, K. Murase, Y. Mori, H. Yoshida, M. Nakatsuka, T. Sasaki: Bulk laser damage in $CsLiB_6O_{10}$ crystal and its dependence on crystal structure. Jpn. J. Appl. Phys. **38(2A)**, L129-L131 (1999).
[106] S.V. Muraviov, A.A. Babin, F.I. Feldstein, A.M. Yurkin, V.A. Kamenskii, A.Y. Malyshev, M.S. Kitai, N.M. Bityurin: Efficient conversion to the fifth harmonic of spatially multi-mode radiation of a repetitively pulsed Nd:YAP laser. Kvant. Elektron. **25(6)**, 535–536 (1998) [In Russian, English trans.: Quantum Electron. **28(6)**, 520–521 (1998)].
[107] S. Konno, T. Kojima, S. Fujikawa, K. Yasui: High-brightness 138-W green laser based on an intracavity-frequency-doubled diode-side-pumped Q-switched Nd:YAG laser. Opt. Lett. **25(2)**, 105–107 (2000).
[108] T.W. Tukker, C. Otto, J. Greve: A narrow-bandwidth optical parametric oscillator. Opt. Commun. **154(1–3)**, 83–86 (1998).

2.3 $LiNbO_3$, Lithium Niobate (LN)

Negative uniaxial crystal: $n_o > n_e$
Molecular mass: 147.846
Specific gravity:

4.628 g/cm^3 at $T = 296$ K [1]

4.620 ± 0.020 g/cm^3 at $T = 300$ K (stoichiometric LN) [2]

4.617 ± 0.020 g/cm^3 at $T = 300$ K (congruent LN) [2]

4.635 ± 0.005 g/cm^3 at $T = 298$ K (stoichiometric LN) [3], 4.648 ± 0.005 g/cm^3 at $T = 298$ (K congruent LN, mole ratio Li/Nb = 0.940) [3]

Point group: $3m$
Lattice constants:

$a = 5.14829 \pm 0.00002$ Å [4], $c = 13.8631 \pm 0.0004$ Å [4]

$a = 5.1489$ Å (congruent LN) [5], $c = 13.8631$ Å (congruent LN) [5]

$a = 5.1502 \pm 0.0005$ Å (congruent LN) [2], $c = 13.8636 \pm 0.0010$ Å (congruent LN) [2]

$a = 5.15052 \pm 0.00006$ Å (congruent LN, mole ratio Li/Nb = 0.940) [3],

$c = 13.86496 \pm 0.00003$ Å (congruent LN, mole ratio Li/Nb $= 0.940$) [3]

$a = 5.1483 \pm 0.0005$ Å (stoichiometric LN) [2], $c = 13.8573 \pm 0.0010$ Å (stoichiometric LN) [2]

$a = 5.14739 \pm 0.00008$ Å (stoichiometric LN) [3]$c = 13.85614 \pm 0.00009$ Å (stoichiometric LN) [3]

Mohs hardness: 5 [6], [7]; 5–5.5 [8]
Vickers hardness: 630 ± 30 kgf/mm^2 at indenter load 15–200 g [9]

Solubility in 100 g H_2O [7]

T [K]	s [g]
273	0.0034
298	0.0041
323	0.0064
348	0.0089
373	0.0109

Melting point: 1530 K [10]; 1533 K [11]
Curie temperature: 1411 K (congruent LN, mole ratio Li/Nb $= 0.942$) [12]; 1438 K (congruent LN) [5]; 1466 K (stoichiometric LN) [13]; 1466 ± 2 K (stoichiometric LN, mole ratio Li/Nb $= 0.988$) [12]; 1475 K (stoichiometric LN) [14]
Dependence of Curie temperature on Li concentration ([Li] in mol%, 46% < [Li] < 50%, T_c in K) [15]: $T_c = -473.57 + 39.064\,[\mathrm{Li}]$

Linear thermal expansion coefficient

T [K]	$\alpha_t \times 10^6$ [K^{-1}], $\parallel c$	$\alpha_t \times 10^6$ [K^{-1}], $\perp c$	Ref.
100	1.0	1.9	[16]
200	3.8	8.5	[16]
300	4.0	15.7	[16]
	4.1	15.0	[10]
400	2.0	17.5	[16]
600	2.0	19.0	[16]

Mean value of linear thermal expansion coefficient [4]

T [K]	$\alpha_t \times 10^6$ [K^{-1}], $\parallel c$	$\alpha_t \times 10^6$ [K^{-1}], $\perp c$
297–873	≈ 2	
297–1073		16.7

Thermal expansion $\parallel c$ for temperature range 298 K $< T <$ 773 K [5]:

$$L(T) = L(T_0)\left\{1 + \alpha(T - 298) + \beta(T - 298)^2\right\}$$

where T in K, $T_0 = 298$ K, $\alpha = 7.5 \times 10^{-6}$ K^{-1}, $\beta = -7.7 \times 10^{-9}$ K^{-2}.

Thermal expansion $\perp c$ for temperature range 298 K $< T <$ 773 K [5]:

$$L(T) = L(T_0)\left\{1 + \alpha(T - 298) + \beta(T - 298)^2\right\}$$

where T in K, $T_0 = 298$ K, $\alpha = 15.4 \times 10^{-6}\,\mathrm{K}^{-1}$, $\beta = 5.3 \times 10^{-9}\,\mathrm{K}^{-2}$.

Specific heat capacity c_p at $P = 0.101325$ MPa [17]

T [K]	c_p [J/kgK]
80	136
100	218
150	379
200	514
250	592
270	619
290	639
300	648
340	682
390	718

Thermal conductivity coefficient

T [K]	κ [W/mK]	Ref.	Note
300	4.4	[17]	$\parallel c$
	4.5	[17]	$\perp c$
	4.6	[18]	

Band-gap energy at room temperature (direct transition): $E_g = 3.9$ eV [19]; 4.0 eV [20], [6]; 4.3 eV [21]
Band-gap energy at room temperature (indirect transition): $E_g = 3.3$ eV [21]
Transparency range at "0" transmittance level: 0.4–5.5 μm [22], [23]
UV transmittance cutoff for stoichiometric LN is at 0.3 μm [14]

UV transmittance cutoff at $\alpha = 20\,\mathrm{cm}^{-1}$ level as a function of relative molar Li concentration in LN ($T = 295$ K) [24]

$\frac{[\mathrm{Li}]}{[\mathrm{Li}] + [\mathrm{Nb}]}$ [%]	λ [μm]
47.8	324
48.5	320
49.2	314
49.7	309
50.0	303

Linear absorption coefficient α

λ [μm]	α [cm^{-1}]	Ref.	Note
0.326	2.0	[2]	congruent LN
0.5145	0.025	[25]	
	0.019–0.025	[26]	$\parallel c$
	0.035–0.045	[26]	e-wave, $\perp c$
0.6594	0.0021–0.0044	[26]	$\parallel c$
	0.0085–0.0096	[26]	e-wave, $\perp c$
1.0642	0.0019–0.0023	[26]	$\parallel c$
	0.0014–0.0019	[26]	e-wave, $\perp c$
	0.0042	[27]	$\parallel c$
	0.0028	[27]	$\perp c$
	0.0011	[27]	$\parallel c$, best crystals
1.3188	0.0018–0.0044	[26]	$\parallel c$
	0.0017–0.0110	[26]	e-wave, $\perp c$
4.0	0.08	[28], [29]	e-wave
	$\approx$0.1	[30]	e-wave
5.0	0.94	[28], [29]	e-wave
5.3	$\approx$3	[31]	e-wave

Two-photon absorption coefficient β

λ [μm]	τ_p [ns]	$\beta \times 10^{11}$ [cm/W]	Ref.	Note
0.5288	0.007	15	[32]	
0.53	0.01	500 (?)	[33]	
0.5321	10	290	[34]	o-wave
	10	160	[34]	e-wave
	0.025	350 (?)	[35]	
		25	[36]	o-wave
	0.022	38 ± 8	[19]	$\mathbf{E} \parallel c$
0.6943	30	1000	[37]	

Experimental values of refractive indices

λ [μm]	n_o	n_e
for lithium-rich lithium niobate (mole ratio Li/Nb = 0.996) grown by vapor transport equilibration at $T = 298$ K [38]		
0.3250	2.6360	2.4670
0.4545	2.3751	2.2608
0.4579	2.3719	2.2584
0.4658	2.3658	2.2530
0.4727	2.3604	2.2489
0.4765	2.3573	2.2465
0.4880	2.3495	2.2398
0.4965	2.3437	2.2352

λ [μm]	n_o	n_e
0.5017	2.3405	2.2329
0.5145	2.3334	2.2270
0.6328	2.2878	2.1890
1.0642	2.2339	2.1440
for lithium niobate grown from stoichiometric melt (mole ratio Li/Nb ≈ 1.0) at $T = 293$ K [22]		
0.42	2.4089	2.3025
0.45	2.3780	2.2772
0.50	2.3410	2.2457
0.55	2.3132	2.2237
0.60	2.2967	2.2082
0.70	2.2716	2.1874
0.80	2.2571	2.1745
0.90	2.2448	2.1641
1.00	2.2370	2.1567
1.20	2.2269	2.1478
1.40	2.2184	2.1417
1.60	2.2113	2.1361
1.80	2.2049	2.1306
2.00	2.1974	2.1250
2.20	2.1909	2.1183
2.40	2.1850	2.1129
2.60	2.1778	2.1071
2.80	2.1703	2.1009
3.00	2.1625	2.0945
3.20	2.1543	2.0871
3.40	2.1456	2.0804
3.60	2.1363	2.0725
3.80	2.1263	2.0642
4.00	2.1155	2.0553
for lithium niobate grown from congruent melt (mole ratio Li/Nb = 0.946) at $T = 293$ K [39]		
0.43584	2.39276	2.29278
0.54608	2.31657	2.22816
0.63282	2.28647	2.20240
1.1523	2.2273	2.1515
3.3913	2.1451	2.0822
for lithium niobate grown from congruent melt (mole ratio Li/Nb = 0.946) at $T = 297.5$ K [40]		
0.40463	2.4317	2.3260
0.43584	2.3928	2.2932
0.46782	2.3634	2.2683

λ [μm]	n_o	n_e
0.47999	2.3541	2.2605
0.50858	2.3356	2.2448
0.54607	2.3165	2.2285
0.57696	2.3040	2.2178
0.57897	2.3032	2.2171
0.58756	2.3002	2.2147
0.64385	2.2835	2.2002
0.66782	2.2778	2.1953
0.70652	2.2699	2.1886
0.80926	2.2541	2.1749
0.87168	2.2471	2.1688
0.93564	2.2412	2.1639
0.95998	2.2393	2.1622
1.01400	2.2351	2.1584
1.09214	2.2304	2.1545
1.15392	2.2271	2.1517
1.15794	2.2269	2.1515
1.28770	2.2211	2.1464
1.43997	2.2151	2.1413
1.63821	2.2083	2.1356
1.91125	2.1994	2.1280
2.18428	2.1912	2.1211
2.39995	2.1840	2.1151
2.61504	2.1765	2.1087
2.73035	2.1724	2.1053
2.89733	2.1657	2.0999
3.05148	2.1594	2.0946

Temperature derivatives of refractive indices for lithium-rich lithium niobate (mole ratio Li/Nb = 0.996) grown by vapor transport equilibration at $T = 298$ K [38]

λ [μm]	$dn_o/dT \times 10^6$ [K^{-1}]	$dn_e/dT \times 10^6$ [K^{-1}]
0.3250	87	129
0.4545	19	62
0.6328	5.2	43
1.0642	1.4	39

Temperature derivatives of refractive indices for lithium niobate grown from stoichiometric melt (mole ratio Li/Nb ≈ 1.0) at $T = 293$ K

λ [μm]	$dn_o/dT \times 10^6$ [K^{-1}]	$dn_e/dT \times 10^6$ [K^{-1}]	Ref.
0.45–0.70	20	76	[41]
0.6328	8	50	[23]

Sellmeier equations (λ in μm):

for lithium-rich lithium niobate (mole ratio Li/Nb = 0.996) grown by vapor transport equilibration ($0.325\,\mu\text{m} < \lambda < 1.064\,\mu\text{m}$, $T = 298$ K) [38]:

$$n_o^2 = 4.91296 + \frac{0.116275}{\lambda^2 - 0.048398} - 0.0273\,\lambda^2$$

$$n_e^2 = 4.54528 + \frac{0.091649}{\lambda^2 - 0.046079} - 0.0303\,\lambda^2$$

for lithium niobate grown from stoichiometric melt (mole ratio Li/Nb ≈ 1.0, $0.4\,\mu\text{m} < \lambda < 4.0\,\mu\text{m}$, $T = 293$ K) [42]:

$$n_o^2 = 4.91300 + \frac{0.118717}{\lambda^2 - 0.045932} - 0.0278\,\lambda^2$$

$$n_e^2 = 4.57906 + \frac{0.099318}{\lambda^2 - 0.042286} - 0.0224\,\lambda^2$$

for congruent LN (mole ratio Li/Nb = 0.937, $0.4\,\mu\text{m} < \lambda < 5.0\,\mu\text{m}$, $T = 294$ K) [43]:

$$n_o^2 = 1 + \frac{2.6734\,\lambda^2}{\lambda^2 - 0.01764} + \frac{1.2290\,\lambda^2}{\lambda^2 - 0.05914} + \frac{12.614\,\lambda^2}{\lambda^2 - 474.6}$$

$$n_e^2 = 1 + \frac{2.9804\,\lambda^2}{\lambda^2 - 0.02047} + \frac{0.5981\,\lambda^2}{\lambda^2 - 0.0666} + \frac{8.9543\,\lambda^2}{\lambda^2 - 416.08}$$

Other sets of dispersion relations for congruent $LiNbO_3$ at room temperature are given in [39], [40].

Temperature-dependent Sellmeier equations (λ in μm, T in K):

for lithium-rich lithium niobate (mole ratio Li/Nb = 0.996) grown by vapor transport equilibration ($0.325\,\mu\text{m} < \lambda < 1.064\,\mu\text{m}$) [38]:

$$n_o^2 = 4.913 + 1.6 \times 10^{-8}\left(T^2 - 88506.25\right) + \frac{0.1163 + 0.94 \times 10^{-8}\left(T^2 - 88506.25\right)}{\lambda^2 - \left[0.2201 + 3.98 \times 10^{-8}\left(T^2 - 88506.25\right)\right]^2} - 0.0273\,\lambda^2$$

$$n_e^2 = 4.546 + 2.72 \times 10^{-7}\left(T^2 - 88506.25\right) + \frac{0.0917 + 1.93 \times 10^{-8}\left(T^2 - 88506.25\right)}{\lambda^2 - \left[0.2148 + 5.3 \times 10^{-8}\left(T^2 - 88506.25\right)\right]^2} - 0.0303\,\lambda^2$$

for lithium niobate grown from stoichiometric melt (mole ratio Li/Nb ≈ 1.0) for wavelengths $0.4\,\mu\text{m} < \lambda < 4.0\,\mu\text{m}$ [42]:

$$n_o^2 = 4.9130 + \frac{0.1173 + 1.65 \times 10^{-8}\, T^2}{\lambda^2 - \left(0.212 + 2.7 \times 10^{-8}\, T^2\right)^2} - 0.0278\,\lambda^2$$

$$n_e^2 = 4.5567 + 2.605 \times 10^{-7}\, T^2 + \frac{0.0970 + 2.70 \times 10^{-8}\, T^2}{\lambda^2 - \left(0.201 + 5.4 \times 10^{-8}\, T^2\right)^2} - 0.0224\,\lambda^2$$

for lithium niobate grown from congruent melt (mole ratio Li/Nb = 0.946) for wavelengths $0.4\,\mu\text{m} < \lambda < 3.05\,\mu\text{m}$ [44]:

$$n_o^2 = 4.9048 + 2.1429 \times 10^{-8}\left(T^2 - 88506.25\right) + \frac{0.11775 + 2.2314 \times 10^{-8}\left(T^2 - 88506.25\right)}{\lambda^2 - \left[0.21802 - 2.9671 \times 10^{-8}\left(T^2 - 88506.25\right)\right]^2} - 0.027153\,\lambda^2$$

$$n_e^2 = 4.5820 + 2.2971 \times 10^{-7}\left(T^2 - 88506.25\right) + \frac{0.09921 + 5.2716 \times 10^{-8}\left(T^2 - 88506.25\right)}{\lambda^2 - \left[0.21090 - 4.9143 \times 10^{-8}\left(T^2 - 88506.25\right)\right]^2} - 0.021940\,\lambda^2$$

Infrared-corrected temperature-dependent Sellmeier equation for extraordinary refractive index for congruent LN (mole ratio Li/Nb = 0.937) [28]:

$$n_e^2 = 5.35583 + 4.629 \times 10^{-7}\left(T^2 - 88601.4756\right) + \frac{0.100473 + 3.862 \times 10^{-8}\left(T^2 - 88601.4756\right)}{\lambda^2 - \left[0.20692 - 0.89 \times 10^{-8}\left(T^2 - 88601.4756\right)\right]^2} + \frac{100 + 2.657 \times 10^{-5}\left(T^2 - 88601.4756\right)}{\lambda^2 - (11.34927)^2} - 1.5334 \times 10^{-2}\,\lambda^2$$

Temperature-dependent dispersion relations for LN of different composition (mole ratio Li/Nb = 0.8871.0) for wavelengths $0.4\,\mu\text{m} < \lambda < 1.2\,\mu\text{m}$ and temperature range $50\,\text{K} < T < 600\,\text{K}$ are given in [28], [48].

Nonlinear refractive index γ [19]

λ [μm]	$\gamma \times 10^{15}$ [cm^2/W]	Note
0.5321	8.3 ± 1.3	$\mathbf{k} \parallel X$, $\mathbf{E} \parallel Z$
1.0642	0.91 ± 0.13	$\mathbf{k} \parallel X$, $\mathbf{E} \parallel Z$

Linear electrooptic coefficients measured at low frequencies (well below the acoustic resonances of LN crystal, i.e., for the "free" crystal) at room temperature

λ [μm]	r_{13}^T [pm/V]	r_{22}^T [pm/V]	r_{33}^T [pm/V]	r_{51}^T [pm/V]	Ref.	Note
0.6328	+9.6	+6.8	+30.9	+32.6	[46]	
	+9.7		+31.4		[47]	congruent LN

λ [μm]	r_{13}^T [pm/V]	r_{22}^T [pm/V]	r_{33}^T [pm/V]	r_{51}^T [pm/V]	Ref.	Note
	+10.0	+6.81	+32.2		[48]	
	+10.0 ± 0.8		+31.5 ± 1.4		[49]	congruent LN
	+10.5 ± 0.07		+31.4 ± 0.2		[50]	congruent LN
	+10.4 ± 0.8		+38.3 ± 1.4		[49]	stoichiometric LN
	+10.9 ± 1.0		+34.0 ± 2.5		[51]	
		+3.3		+32 ± 2	[52]	
		+6.4 ± 0.3			[53]	congruent LN
		+6.7			[54], [55]	
		+6.8 ± 0.4			[53]	stoichiometric LN
1.047	+8		+24.6		[47]	congruent LN
1.1523		+5.4			[46]	
3.3913		+3.1			[46]	

Linear electrooptic coefficients measured at high frequencies (well above the acoustic resonances of LN crystal, i.e., for the "clamped" crystal) at room temperature

λ [μm]	r_{13}^S [pm/V]	r_{22}^S [pm/V]	r_{33}^S [pm/V]	r_{51}^S [pm/V]	Ref.	Note
0.6328	7.68		28.8	18.2 (?)	[56]	
	8.6	3.4	30.8	28	[57]	
		3.8 ± 0.2			[53]	congruent LN
		4.5 ± 0.2			[53]	stoichiometric LN
1.1523	6.65		27.2		[56]	
3.3913	5.32–6.5	3.1	25.5–28	23	[56]	

Dependence of linear electrooptic coefficient r_{22}^T measured at 1 kHz as a function of relative molar Li concentration in LN [58]

λ [μm]	$\frac{[Li]}{[Li]+[Nb]}$ [%]	r_{22}^T [pm/V]
0.6328	48.51	6.07
	48.69	4.67
	48.90	1.51
	49.09	1.97
	49.36	6.50
	49.95	9.89

Coercive field value:

≈21 kV/mm (congruent LN) [59], [60];

≈4 kV/mm (stoichiometric LN) [61]

Expressions for the effective second-order nonlinear coefficient in general case (Kleinman symmetry conditions are valid, $d_{15} = d_{24} = d_{31} = d_{32}$) [62]:

$$d_{\mathrm{ooe}} = d_{31}\sin(\theta + \rho) - d_{22}\cos(\theta + \rho)\sin 3\phi$$

$$d_{\mathrm{eoe}} = d_{\mathrm{oee}} = d_{22}\cos^2(\theta + \rho)\cos 3\phi$$

Simplified expressions for the effective second-order nonlinear coefficient (approximation of small birefringence angle, Kleinman symmetry conditions are valid, $d_{15} = d_{24} = d_{31} = d_{32}$) [63]:

$$d_{\mathrm{ooe}} = d_{31}\sin\theta - d_{22}\cos\theta\sin 3\phi$$

$$d_{\mathrm{eoe}} = d_{\mathrm{oee}} = d_{22}\cos^2\theta\cos 3\phi$$

Absolute values of second-order nonlinear coefficients for lithium niobate grown from congruent melt (mole ratio Li/Nb = 0.946) [64]:

$$|\, d_{31}(0.852\,\mu\mathrm{m}) \,| = 4.8\,\mathrm{pm/V}$$

$$|\, d_{33}(0.852\,\mu\mathrm{m}) \,| = 25.7\,\mathrm{pm/V}$$

$$|\, d_{31}(1.064\,\mu\mathrm{m}) \,| = 4.6\,\mathrm{pm/V}$$

$$|\, d_{33}(1.064\,\mu\mathrm{m}) \,| = 25.2\,\mathrm{pm/V}$$

$$|\, d_{31}(1.313\,\mu\mathrm{m}) \,| = 3.2\,\mathrm{pm/V}$$

$$|\, d_{33}(1.313\,\mu\mathrm{m}) \,| = 19.5\,\mathrm{pm/V}$$

Values of second-order nonlinear coefficients for lithium niobate grown from congruent melt (mole ratio Li/Nb = 0.946) [65], [66]:

$$d_{22}(1.064\,\mu\mathrm{m}) = 2.10 \pm 0.21\,\mathrm{pm/V}$$

$$d_{31}(1.064\,\mu\mathrm{m}) = -4.35 \pm 0.44\,\mathrm{pm/V}$$

$$d_{33}(1.064\,\mu\mathrm{m}) = -27.2 \pm 2.7\,\mathrm{pm/V}$$

Values of second-order nonlinear coefficients for lithium niobate grown from stoichiometric melt (mole ratio Li/Nb = 1.000) [22], [66]:

$$d_{22}(1.058\,\mu\mathrm{m}) = 2.46 \pm 0.23\,\mathrm{pm/V}$$

$$d_{31}(1.058\,\mu\mathrm{m}) = -4.64 \pm 0.66\,\mathrm{pm/V}$$

$$d_{33}(1.058\,\mu\mathrm{m}) = -41.7 \pm 7.8\,\mathrm{pm/V}$$

Experimental values of phase-matching angle

Interacting wavelengths [μm]	θ_{exp} [deg]	Ref.
lithium-rich lithium niobate (mole ratio Li/Nb = 0.996, $T = 295$ K)		
SHG, $o + o \Rightarrow e$		
1.0642 ⇒ 0.5321	67.5	[38]

Interacting wavelengths [μm]	θ_{exp} [deg]	Ref.
stoichiometric melt (mole ratio Li/Nb ≈ 1.0, $T = 293$ K)		
SHG, $o + o \Rightarrow e$		
1.118 ⇒ 0.559	71.7	[42]
1.1523 ⇒ 0.57615	67.6	[42]
	68	[22]
	69	[11]
SFG, $o + o \Rightarrow e$		
2.17933 + 0.8529 ⇒ 0.613	55	[67]
4.0 + 0.72394 ⇒ 0.613	47.5	[67]
congruent melt (mole ratio Li/Nb = 0.946), $T = 293$ K		
SHG, $o + o \Rightarrow e$		
1.1523 ⇒ 0.57615	72	[11]
2.12 ⇒ 1.06	43.8	[68]
2.1284 ⇒ 1.0642	44.6	[69]
	47	[70]
SFG, $o + o \Rightarrow e$		
1.95160 + 1.0642 ⇒ 0.68867	52.7	[71]
2.57887 + 1.0642 ⇒ 0.75333	48.1	[71]
3.22241 + 1.0642 ⇒ 0.80000	46.5	[71]
4.19039 + 1.0642 ⇒ 0.84867	47	[71]

Note: The phase-matching (PM) angle values are strongly dependent on melt stoichiometry.

Experimental values of NCPM temperature

Interacting wavelengths [μm]	T [°C]	Ref.
lithium-rich lithium niobate (mole ratio Li/Nb = 0.996)		
SHG, $o + o \Rightarrow e$		
0.954 ⇒ 0.477	−62.5	[38]
1.0642 ⇒ 0.5321	233.7	[27], [15]
	238	[38]
1.3188 ⇒ 0.6594	520	[38]
stoichiometric melt (mole ratio Li/Nb ≈ 1.0)		
SHG, $o + o \Rightarrow e$		
1.029 ⇒ 0.5145	15	[72]
1.058 ⇒ 0.529	0	[73]
1.0642 ⇒ 0.5321	43	[74]
	72	[75]
1.084 ⇒ 0.542	97	[76]
1.118 ⇒ 0.559	153.5	[42]
1.1523 ⇒ 0.57615	193	[73]
	208	[42]
	211	[75]

Interacting wavelengths [μm]	T [°C]	Ref.
congruent melt (mole ratio Li/Nb = 0.946)		
SHG, $o + o \Rightarrow e$		
1.029 ⇒ 0.5145	−66	[72]
1.0576 ⇒ 0.5288	−14	[32]
1.0642 ⇒ 0.5321	−8	[77]
	6	[78]
	11.5	[74]
1.084 ⇒ 0.542	38	[79]
	42	[77]
	46	[72]
1.1523 ⇒ 0.57615	172	[77]
	174	[40]

Note: The NCPM temperature values are strongly dependent on melt stoichiometry.

Experimental value of internal angular bandwidth [80]

Interacting wavelengths [μm]	$\Delta\theta^{\text{int}}$ [deg]
SHG, $o + o \Rightarrow e$	
1.06 ⇒ 0.53	0.040

Experimental values of temperature and spectral bandwidths

Interacting wavelengths [μm]	T [°C]	θ_{pm} [deg]	ΔT [°C]	$\Delta\nu_1$ [cm^{-1}]	Ref.
SHG, $o + o \Rightarrow e$					
1.06 ⇒ 0.53	20	68		3.2	[80]
1.0642 ⇒ 0.5321	−1.6	90	0.74		[81]
	51	90	0.72		[82]
	234	90	0.52		[27]
1.084 ⇒ 0.542	38	90	0.74		[72]
	46	90	0.74		[79]
1.1523 ⇒ 0.57615	172	90	0.66		[77]
SFG, $o + o \Rightarrow e$					
1.7 + 0.6943 ⇒ 0.493	70	90	1.6	7.9	[83]
2.65 + 0.488 ⇒ 0.4115	90	90		2.9	[84]

Laser-induced bulk damage threshold

λ [μm]	τ_{p} [ns]	I_{thr} [GW/cm^2]	Ref.	Note
0.53	0.007	>10	[85]	
0.5321	0.002	>70	[86]	10 Hz
0.59–0.596	≈10	>0.35	[86]	10 Hz
0.6943	25	0.15	[87]	1 pulse
1.06	30	0.06	[88]	25 pulses

Laser-induced bulk damage threshold

λ [μm]	τ_p [ns]	I_{thr} [GW/cm^2]	Ref.	Note
		0.12	[88]	10 pulses
		0.17	[89]	
		0.47	[88]	1 pulse
	10–30	0.3	[90]	
	14	10–13	[91]	100-μm beam-waist diameter
		36	[91]	21-μm beam-waist diameter
	10	0.25	[92]	
	0.006	>10	[68]	
1.0642	30	15–20	[93]	with coating
	20	>0.1	[69]	
	10	0.5–2	[94]	
	7	0.84	[95]	
		0.43	[96]	100 Hz
1.56	50	0.35	[97]	300 Hz, 80-μm beam-waist diameter

Laser-induced surface damage threshold

λ [μm]	τ_p [ns]	$I_{thr} \times 10^{-12}$ [W/m^2]	Ref.	Note
1.0642	12	111	[98]	[100] direction, 30-μm beam-waist diameter
	10	5–30	[94]	
	7	8.4	[95]	

About the crystal

$LiNbO_3$ was one of the first crystals especially synthesized for nonlinear frequency conversion [22], [99]. It was successfully used in the first OPO system [100] and became a very popular nonlinear material at the end of the 1960s / beginning of the 1970s. However, when more effective and damage-resistant crystals (KTP, BBO, LBO) were introduced, they completely replaced bulk LN in applications. After that, it is really amazing that the periodically poled LN (PPLN), due to a very high value of effective second-order nonlinear coefficient along the optical axis (up to 20 pm/V), became in the 1990s one of the most popular nonlinear materials. Ironically, the method of quasi-phase matching (QPM) in periodically poled materials was proposed by Bloembergen *et al.* as early as 1962 [101], even before the birefringent phase matching, and only the absence of poling methods at that time stopped the development of this approach. In 1980, a Chinese group discovered an enhancement of SHG in periodically poled LN [102], and a decade later the first applications of PPLN for SHG, [103], [104], [105], [106]; DFG, [107], [108]; and OPO [109] were reported. At the moment, there are hundreds of works devoted to

PPLN and its applications; for the reviews on QPM and PPLN, see [110], [111], [112].

Lithium niobate has some principal disadvantages, namely, a low level of laser damage threshold and also a susceptibility to photorefractive damage [113], [114]. To avoid the photorefractive effects, LN (or PPLN) elements should be kept at elevated temperatures, typically between 140 and 230°C [115], [116], [117], [118]. Another way is doping by MgO (see Magnesium-Oxide–Doped Lithium Niobate). It was shown that the photorefractive damage threshold of 1.8 mol% MgO-doped stoichiometric LN is 4 orders of magnitude higher than that of undoped stoichiometric and congruent LN [12]. A similar effect on photorefractive damage threshold increase was observed in ZnO-doped LN [119], [120].

References

[1] L.G. van Uitert, J.J. Rubin, W.A. Bonner: Growth of $Ba_2NaNb_5O_{15}$ single crystals for optical applications. IEEE J. Quant. Electr. **QE-4(10)**, 622–627 (1968).

[2] D. Redfield, W.J. Burke: Optical absorption edge of $LiNbO_3$. J. Appl. Phys. **45(10)**, 4566–4571 (1974).

[3] S.C. Abrahams, P. Marsh: Defect structure dependence on composition of lithium niobate. Acta Crystallogr. B **42(1)**, 61–68 (1986).

[4] S.C. Abrahams, H.J. Levinstein, J.M. Reddy: Ferroelectric lithium niobate. V. Polycrystal X-ray diffraction study between 24° and 1200°. J. Phys. Chem. Solids **27(6–7)**, 1019–1026 (1966).

[5] Y.S. Kim, R.T. Smith: Thermal expansion of lithium tantalate and lithium niobate crystals. J. Appl. Phys. **40(11)**, 4637–4641 (1969).

[6] B.H.T. Chai: Optical Crystals. In: *CRC Handbook of Laser Science and Technology, Supplement 2: Optical Materials*, ed. by M.J. Weber (CRC Press, Boca Raton, 1995), pp. 3–65.

[7] Y.S. Kuzminov: *Lithium Niobate and Lithium Tantalate. Materials for Nonlinear Optics* (Nauka, Moscow, 1975) [In Russian].

[8] V.G. Dmitriev, G.G. Gurzadyan, D.N. Nikogosyan: *Handbook of Nonlinear Optical Crystals; Third Revised Edition* (Springer, Berlin, 1999).

[9] K.G. Subhadra, K. Kishan Rao, D.B. Sirdeshmukh: Systematic hardness studies on lithium niobate crystals. Bull. Mater. Sci. **23(2)**, 147–150 (2000).

[10] S.S. Ballard, J.S. Browder: Thermal Properties. In: *CRC Handbook of Laser Science and Technology, Vol. IV, Optical Materials: Part 2*, ed. by M.J. Weber (CRC Press, Boca Raton, 1987), pp. 49–54

[11] A.M. Prokhorov, Y.S. Kuzminov: *Physics and Chemistry of Crystalline Lithium Niobate* (Adam Hilger, Bristol, 1990).

[12] K. Niwa, Y. Furukawa, S. Takekawa, K. Kitamura: Growth and characterization of MgO doped near stoichiometric $LiNbO_3$ crystals as a new nonlinear optical crystal. J. Cryst. Growth **208(1–4)**, 493–500 (2000).

[13] K. Polgar, A. Peter, I. Földvari: Crystal growth and stoichiometry of $LiNbO_3$ prepared by the flux method. Opt. Mater. **19(1)**, 7–11 (2002).

[14] G. Ravi, R. Jayavel, S. Takekawa, M. Nakamura, K. Kitamura: Effect of niobium substitution in stoichiometric lithium tantalate (SLT) single crystals. J. Cryst. Growth **250(1–2)**, 146–151 (2003).

[15] P.F. Bordui, R.G. Norwood, D.H. Jundt, M.M. Fejer: Preparation and characterization of off-congruent lithium niobate crystals. J. Appl. Phys. **71(2)**, 875–879 (1992).
[16] *Physical Quantities. Handbook*, ed. by I.S. Grigoriev, E.Z. Meilikhov (Energoatomizdat, Moscow, 1991) [In Russian].
[17] V.V. Zhdanova, V.P. Klyuev, V.V. Lemanov, I.A. Smirnov, V.V. Tikhonov: Thermal properties of lithium niobate crystals. Fiz. Tverd. Tela **10(6)**, 1725–1728 (1968). [In Russian, English trans.: Sov. Phys. - Solid State **10(6)**, 1360–1362 (1968)].
[18] A.A. Blistanov, V.S. Bondarenko, N.V. Perelomova, F.N. Strizhevskaya, V.V. Tchkalova, M.P. Shaskolskaya: *Acoustic Crystals* (Nauka, Moscow, 1982). [In Russian].
[19] R. DeSalvo, A.A. Said, D.J. Hagan, E.W. van Stryland, M. Sheik-Bahae: Infrared to ultraviolet measurements of two-photon absorption and n_2 in wide bandgap solids. IEEE J. Quant. Electr. **32(8)**, 1324–1333 (1996).
[20] E.W. van Stryland, L.L. Chase: Two-Photon Absorption. Inorganic Materials. In: *CRC Handbook of Laser Science and Technology, Supplement 2: Optical Materials*, ed. by M.J. Weber (CRC Press, Boca Raton, 1995) pp. 299–328.
[21] S. Kase, K. Ohi: Optical absorption and interband Faraday rotation in $LiTaO_3$ and $LiNbO_3$. Ferroelectrics **8(1–2)**, 419–420 (1974).
[22] G.D. Boyd, R.C. Miller, K. Nassau, W.L. Bond, A. Savage: $LiNbO_3$: an efficient phase matchable nonlinear optical material. Appl. Phys. Lett. **5(11)**, 234–236 (1964).
[23] G.V. Ageev, R.P. Bashuk, A.S. Bebchuk, N.S. Voidetskaya, D.A. Gromov, Y.N. Solovieva, A.V. Chesnokov: Optical and electrooptical properties of some alkali and alkaline earth niobates and tantalates. In: *Nonlinear Optics*, ed. by R.V. Khokhlov (Nauka, Novosibirsk, 1968) pp. 211–217 [In Russian].
[24] L. Kovacs, G. Ruschhaupt: K. Polgar, G. Corradi, M. Wöhlecke: Composition dependence of the ultraviolet absorption edge in lithium niobate. Appl. Phys. Lett. **70(21)**, 2801–2803 (1997).
[25] Y.C. See, S. Guha, J. Falk: Limits to the NEP of an intracavity $LiNbO_3$ upconverter. Appl. Opt. **19(9)**, 1415–1418 (1980).
[26] D.J. Gettemy, W.C. Harker, G. Lindholm, N.P. Barnes: Some optical properties of KTP, $LiIO_3$, and $LiNbO_3$. IEEE J. Quant. Electr. **24(11)**, 2231–2237 (1988).
[27] D.H. Jundt, M.M. Fejer, R.L. Byer, R.G. Norwood, P.F. Bordui: 69% efficient continuous-wave second-harmonic generation in lithium-rich lithium niobate. Opt. Lett. **16(23)**, 1856–1858 (1991).
[28] D.H. Jundt: Temperature-dependent Sellmeier equation for the index of refraction, n_e, in congruent lithium niobate. Opt. Lett. **22(20)**, 1553–1555 (1997).
[29] L.E. Myers, R.C. Eckardt, M.M. Fejer, R.L. Byer, W.R. Bosenberg: Multigrating quasi-phase-matched optical parametric oscillator in periodically poled $LiNbO_3$. Opt. Lett. **21(8)**, 591–593 (1996).
[30] G. Hansson, D.D. Smith: Mid-infrared-wavelength generation in 2-μm pumped periodically poled lithium niobate. Appl. Opt. **37(24)**, 5743–5746 (1998).
[31] L. Lefort, K. Puech, S.D. Butterworth, G.W. Ross, P.G.R. Smith, D.C. Hanna, D.H. Jundt: Efficient, low-threshold synchronously-pumped parametric oscillation in periodically-poled lithium niobate over the 1.3 μm to 5.3 μm range. Opt. Commun. **152(1–3)**, 55–58 (1998).
[32] A. Seilmeier, W. Kaiser: Generation of tunable picosecond light pulses covering the frequency range between 2700 and 32000 cm^{-1}. Appl. Phys. **23(2)**, 113–119 (1980).
[33] D. von der Linde, A.M. Glass, K.F. Rodgers: Multiphoton photorefractive processes for optical storage in $LiNbO_3$. Appl. Phys. Lett. **25(3)**, 155–157 (1974).
[34] N.M. Bityurin, V.I. Bredikhin, V.N. Genkin: Nonlinear optical absorption and energy structure of $LiNbO_3$ and α-$LiIO_3$ crystals. Kvant. Elektron. **5(11)**, 2453–2457 (1978) [In Russian, English trans.: Sov. J. Quantum Electron. **8(11)**, 1377–1379 (1978)].

[35] H. Kurz, D. von der Linde: Nonlinear optical excitation of photovoltaic $LiNbO_3$. Ferroelectrics **21(1–4)**, 621–622 (1978).
[36] H. Li, F. Zhou, X. Zhang, W. Ji: Picosecond Z-scan study of bound electronic Kerr effect in $LiNbO_3$ crystal associated with two-photon absorption. Appl. Phys. B **64(6)**, 659–662 (1997).
[37] V.V. Arseniev, V.S. Dneprovskii, D.N. Klyshko, A.N. Penin: Nonlinear absorption and restriction of light intensity in semiconductors. Zh. Eksp. Teor. Fiz. **56(3)**, 760–765 (1969) [In Russian, English trans.: Sov. Phys. - JETP **29(3)**, 413–415 (1969)].
[38] D.H. Jundt, M.M. Fejer, R.L. Byer: Optical properties of lithium-rich lithium niobate fabricated by vapor transport equilibration. IEEE J. Quant. Electr. **26(1)**, 135–138 (1990).
[39] D.S. Smith, H.D. Riccius, R.P. Edwin: Refractive indices of lithium niobate. Opt. Commun. **17(3)**, 332–335 (1976); Errata. Opt. Commun. **20(1)**, 188 (1977).
[40] D.F. Nelson, R.M. Mikulyak: Refractive indices of congruently melting lithium niobate. J. Appl. Phys. **45(8)**, 3688–3689 (1974).
[41] J.E. Midwinter: Lithium niobate: effects of composition on the refractive indices and optical second-harmonic generation. J. Appl. Phys. **39(7)**, 3033–3038 (1968).
[42] M.V. Hobden, J. Warner: The temperature dependence of the refractive indices of pure lithium niobate. Phys. Lett. **22(3)**, 243–244 (1966).
[43] D.E. Zelmon, D.L. Small, D. Jundt: Infrared corrected Sellmeier coefficients for congruently grown lithium niobate and 5 mol.% magnesium oxide-doped lithium niobate. J. Opt. Soc. Am. B **14(12)**, 3319–3322 (1997).
[44] G.J. Edwards, M. Lawrence: A temperature-dependent dispersion equation for congruently grown lithium niobate. Opt. Quant. Electron. **16(4)**, 373–375 (1984).
[45] U. Schlarb, K. Betzler: Refractive indices of lithium niobate as a function of temperature, wavelength, and composition: a generalized fit. Phys. Rev. B **48(21)**, 15613–15620 (1993).
[46] A. Yariv, P. Yeh: *Optical Waves in Crystals* (John Wiley & Sons, New York, 1984).
[47] A. Mendez, A. Garcia-Cabanes, E. Dieguez, J.M. Cabrera: Wavelength dependence of electro-optic coefficients in congruent and stoichiometric $LiNbO_3$. Electron. Lett. **35(6)**, 498–499 (1999).
[48] J.D. Zook, D. Chen, G.N. Otto: Temperature dependence and model of electro-optic effect in $LiNbO_3$. Appl. Phys. Lett. **11(5)**, 159–161 (1967).
[49] T. Fujiwara, M. Takahashi, M. Ohama, A.J. Ikushima, Y. Furukawa, K. Kitamura: Comparison of electro-optic effect between stoichiometric and congruent $LiNbO_3$. Electron. Lett. **35(6)**, 499–501 (1999).
[50] J.A. de Toro, M.D. Serrano, A. Garcia Cabanes, J.M. Cabrera: Accurate interferometric measurement of electrooptic coefficients: application to quasi-stoichiometric $LiNbO_3$. Opt. Commun. **154(1–3)**, 23–27 (1998).
[51] K. Onuki, N. Uchida, T. Saku: Interferometric method for measuring electro-optic coefficients in crystals. J. Opt. Soc. Am. **62(9)**, 1030–1032 (1972).
[52] E. Bernal, G.D. Chen, T.C. Lee: Low frequency electro-optic and dielectric constants of lithium niobate. Phys. Lett. **21(3)**, 259–260 (1966).
[53] M. Abarkan, J.P. Salvestrini, M.D. Fontana, M. Aillerie: Frequency and wavelength dependences of electro-optic coefficients in inorganic crystals. Appl. Phys. B **76(7)**, 765–769 (2003).
[54] P.V. Lenzo, E.G. Spencer, K. Nassau: Electro-optic coefficients in single-domain ferroelectric lithium niobate. J. Opt. Soc. Am. **56(5)**, 633–635 (1966).
[55] R.S. Weis, T.K. Gaylord: Lithium niobate: summary of physical properties and crystal structure. Appl. Phys. A **37(4)**, 191–203 (1985).

[56] I.P. Kaminow: Tables of Linear Electrooptic Coefficients. In: *CRC Handbook of Laser Science and Technology, Vol. III, Optical Materials: Part 2*, ed. by M.J. Weber (CRC Press, Boca Raton, 1986), pp. 253–278.

[57] E.H. Turner: High-frequency electro-optic coefficients of lithium niobate. Appl. Phys. Lett. **8(11)**, 303–304 (1966).

[58] F. Abdi, M. Aillerie, P. Bourson, M.D. Fontana, K. Polgar: Electro-optic properties in pure $LiNbO_3$ crystals from the congruent to the stoichiometric composition. J. Appl. Phys. **84(4)**, 2251–2254 (1998).

[59] T. Hatanaka, K. Nakamura, T. Taniuchi, H. Ito, Y. Furukawa, K. Kitamara: Quasi-phase-matched optical parametric oscillation with periodically poled stoichiometric $LiTaO_3$. Opt. Lett. **25(9)**, 651–653 (2000).

[60] J.-P. Meyn, C. Laue, R. Knappe, R. Wallenstein, M.M. Fejer: fabrication of periodically poled lithium tantalate for UV generation with diode lasers. Appl. Phys. B **73(2)**, 111–114 (2001).

[61] K. Nakamura, T. Hatanaka, H. Ito: High output energy quasi-phase-matched optical parametric oscillator using diffusion-bonded periodically poled and single domain $LiNbO_3$. Jpn. J. Appl. Phys. **40(4A)**, L337–L339 (2001).

[62] I. Shoji, H. Nakamura, K. Ohdaira, T. Kondo, R. Ito, T. Okamoto, K. Tatsuki, S. Kubota: Absolute measurement of second-order nonlinear-optical coefficients of β-BaB_2O_4 for visible to ultraviolet second-harmonic wavelengths. J. Opt. Soc. Am. B **16(4)**, 620–624 (1999).

[63] J.E. Midwinter, J. Warner: The effects of phase matching method and of uniaxial crystal symmetry on the polar distribution of second-order non-linear optical polarization. Brit. J. Appl. Phys. **16(11)**, 1135–1142 (1965).

[64] I. Shoji, T. Kondo, A. Kitamoto, M. Shirane, R. Ito: Absolute scale of second-order nonlinear-optical coefficients. J. Opt. Soc. Am. B **14(9)**, 2268–2294 (1997).

[65] R.C. Miller, W.A. Nordland, P.M. Bridenbaugh: Dependence of second-harmonic-generation coefficients of $LiNbO_3$ on melt composition. J. Appl. Phys. **42(11)**, 4145–4147 (1971).

[66] D.A. Roberts: Simplified characterization of uniaxial and biaxial nonlinear optical crystals: a plea for standardization of nomenclature and conventions. IEEE J. Quant. Electr. **28(10)**, 2057–2074 (1992).

[67] D.S. Moore, S.C. Schmidt: Tunable subpicosecond infrared pulse generation to 4 μm. Opt. Lett. **12(7)**, 480–482 (1987).

[68] A. Laubereau, L. Greiter, W. Kaiser: Intense tunable picosecond pulses in the infrared. Appl. Phys. Lett. **25(1)**, 87–89 (1974).

[69] R.L. Herbst, R.N. Fleming, R.L. Byer: A 1.4–4.0-μm high-energy angle-tuned $LiNbO_3$ parametric oscillator. Appl. Phys. Lett. **25(9)**, 520–522 (1974).

[70] Z.I. Ivanova, V. Kabelka, S.A. Magnitskii, A. Piskarskas, V. Smilgiavichyus, N.M. Rubinina, V.G. Tunkin: Parametric generation of infrared picosecond pulses in $LiNbO_3$ crystals. Kvant. Elektron. **4(11)**, 2469–2472 (1977) [In Russian, English trans.: Sov. J. Quantum Electron. **7(11)**, 1414–1416 (1977)].

[71] K. Kato: High-efficiency high-power difference-frequency generation at 2–4 μm in $LiNbO_3$. IEEE J. Quant. Electr. **QE-16(10)**, 1017–1018 (1980).

[72] P.M. Bridenbaugh, J.R. Carruthers, J.M. Dziedzic, F.R. Nash: Spatually uniform and alterable SHG phase-matching temperatures in lithium niobate. Appl. Phys. Lett. **17(3)**, 104–106 (1970).

[73] R.C. Miller, G.D. Boyd, A. Savage: Nonlinear optical interactions in $LiNbO_3$ without double refraction. Appl. Phys. Lett. **6(4)**, 77–79 (1965).

[74] H. Fay, W.J. Alfred, H.M. Dess: Dependence of second-harmonic phase-matching temperature in $LiNbO_3$ crystals on melt composition. Appl. Phys. Lett. **12(3)**, 89–92 (1968).

[75] N.B. Angert, O.F. Butyagin, V.P. Zorenko, A.P. Kudryavtseva, V.R. Kushnir, S.R. Rustamov: Phase-matching angles and temperatures of lithium metaniobate crystals of different stoichiometries. Kvant. Elektron. **No.5**, 128–129 (1971) [In Russian, English trans.: Sov. J. Quantum Electron. **1(5)**, 542–543 (1971)].

[76] J.C. Bergman, A. Ashkin, A.A. Ballman, J.M. Dziedzic, H.J. Levinstein, R.G. Smith: Curie temperature, birefringence, and phase-matching temperature variations in $LiNbO_3$ as a function of melt stoichiometry. Appl. Phys. Lett. **12(3)**, 92–94 (1968).

[77] R.L. Byer, J.F. Young, R.S. Feigelson: Growth of high-quality $LiNbO_3$ crystals from the congruent melt. J. Appl. Phys. **41(6)**, 2320–2325 (1970).

[78] T.R. Volk, N.M. Rubinina, A.I. Kholodnykh: Efficient laser frequency converters made of nonphotorefractive lithium niobate. Kvant. Elektron. **15(8)**, 1705–1706 (1988) [In Russian, English trans.: Sov. J. Quantum Electron. **18(8)**, 1061–1062 (1988)].

[79] F.R. Nash, G.D. Boyd, M. Sargent III, P.M. Bridenbaugh: Effect of optical inhomogeneities on phase matching in nonlinear crystals. J. Appl. Phys. **41(6)**, 2564–2576 (1970).

[80] W.F. Hagen, P.C. Magnante: Efficient second-harmonic generation with diffraction-limited and high-spectral-radiance Nd-glass lasers. J. Appl. Phys. **40(1)**, 219–224 (1969).

[81] E.O. Ammann, S. Guch, Jr.: 1.06-0.53 μm second harmonic generation using congruent lithium niobate. Appl. Phys. Lett. **52(17)**, 1374–1376 (1988).

[82] V.A. Dyakov, V.I. Pryalkin, A.I. Kholodnykh: Potassium niobate optical parametric oscillator pumped by the second harmonic of a garnet laser. Kvant. Elektron. **8(4)**, 715–721 (1981) [In Russian, English trans.: Sov. J. Quantum Electron. **11(4)**, 433–436 (1981)].

[83] J.E. Midwinter, J. Warner: Up-conversion of near infra-red to visible radiation in lithium meta-niobate. J. Appl. Phys. **38(2)**, 519–523 (1967).

[84] E.N. Antonov, V.G. Koloshnikov, D.N. Nikogosyan: Nonlinear frequency converter as infrared spectrometer and detector. Opt. Spektrosk. **36(4)**, 768–772 (1974) [In Russian, English trans.: Opt. Spectrosc. USSR **36(4)**, 446–448 (1974)].

[85] T. Kushida, Y. Tanaka, M. Ojima, Y. Nakazaki: Generation of widely tunable picosecond pulses by optical parametric effect. Jpn. J. Appl. Phys. **14(7)**, 1097–1098 (1975).

[86] M. Berg, C.B. Harris, T.W. Kenny, P.L. Richards:Generation of intense tunable picosecond pulses in the far-infrared. Appl. Phys. Lett. **47(3)**, 206–208 (1985).

[87] J. Falk, J.E. Murray: Single-cavity noncollinear optical parametric oscillation. Appl. Phys. Lett. **14(8)**, 245–247 (1969).

[88] G.M. Zverev, E.A. Levchuk, V.A. Pashkov, Y.D. Poryadin: Laser-radiation-induced damage to the surface of lithium niobate and tantalate single crystals. Kvant. Elektron. **No. 2**, 94–96 (1972) [In Russian, English trans.: Sov. J. Quantum Electron. **2(2)**, 167–169 (1972)].

[89] G.M. Zverev, S.A. Kolyadin, E.A. Levchuk, L.A. Skvortsov: Influence of the surface layer on the optical strength of lithium niobate. Kvant. Elektron. **4(9)**, 1882–1889 (1977) [In Russian, English trans.: Sov. J. Quantum Electron. **7(9)**, 1071–1075 (1977)].

[90] S.J. Brosnan, R.L. Byer: Optical parametric oscillator threshold and linewidth studies. IEEE J. Quant. Electr. **QE-15(6)**, 415–431 (1979).

[91] G.M. Zverev, E.A. Levchuk, E.K. Maldutis: Destruction of KDP, ADP, and $LiNbO_3$ crystals by powerful laser radiation. Zh. Eksp. Teor. Fiz. **57(3)**, 730–736 (1969) [In Russian, English trans.: Sov. Phys. - JETP **30(3)**, 400–403 (1970)].

[92] G.M. Zverev: Materials for quantum electronics (yttrium-aluminium garnet, lithium niobate). Izv. Akad. Nauk SSSR, Ser. Fiz. **44(8)**, 1614–1621 (1980) [In Russian, English trans.: Bull. Acad. Sci. USSR, Phys. Ser. **44(8)**, 49–54 (1980)].

[93] M.J. Soileau: Mechanism of laser-induced failure in antireflection-coated $LiNbO_3$ crystals. Appl. Opt. **20(6)**, 1030–1033 (1981).

[94] R.M. Wood, R.T. Taylor, R.L. Rouse: Laser damage in optical materials at 1.06 μm. Opt. Laser Technol. **7(3)**, 105–111 (1975).

[95] M. Bass: Nd:YAG laser-irradiation-induced damage to $LiNbO_3$ and KDP. IEEE J. Quant. Electr. **QE-7(7)**, 350–359 (1971).

[96] L.E. Myers, G.D. Miller, R.C. Eckardt, M.M. Fejer, R.L. Byer, W.R. Bosenberg: Quasi-phase-matched 1.064-μm-pumped optical parametric oscillator in bulk periodically poled $LiNbO_3$. Opt. Lett. **20(1)**, 52–54 (1995).

[97] P.E. Britton, D. Taverner, K. Puech, D.J. Richardson, P.G.R. Smith, G.W. Ross, D.C. Hanna: Optical parametric oscillation in periodically poled lithium niobate driven by a diode-pumped Q-switched erbium fiber laser. Opt. Lett. **23(8)**, 582–584 (1998).

[98] M. Bass, H.H. Barrett: Avalanche breakdown and the probabilistic nature of laser-induced damage. IEEE J. Quant. Electr. **QE-8(3)**, 338–343 (1972).

[99] A.A. Ballman: Growth of piezoelectric and ferroelectric materials by Czochralski technique. J. Am. Ceram. Soc. **48(2)**, 112–113 (1965).

[100] J.A. Giordmaine, R.C. Miller: Tunable coherent parametric oscillation in $LiNbO_3$ at optical frequencies. Phys. Rev. Lett. **14(24)**, 973–976 (1965).

[101] J.A. Armstrong, N. Bloembergen, J. Ducuing, P.S. Pershan: Interactions between light waves in a nonlinear dielectric. Phys. Rev. **127(6)**, 1918–1939 (1962).

[102] D. Feng, N.-B. Ming, J.-F. Hong, Y.-S. Yang, J.-S. Zhu, Z. Yang, Y.-N. Wang: Enhancement of second-harmonic generation in $LiNbO_3$ crystals with periodic laminar ferroelectric domains. Appl. Phys. Lett. **37(7)**, 607–609 (1980).

[103] D.H. Jundt, G.A. Magel, M.M. Fejer, R.L. Byer: Periodically poled $LiNbO_3$ for high-efficiency second-harmonic generation. Appl. Phys. Lett. **59(21)**, 2657–2659 (1991).

[104] W.K. Burns, R.W. McElhanon, L. Goldberg: Second harmonic generation in field poled, quasi-phase-matched, bulk $LiNbO_3$. IEEE Photon. Technol. Lett. **6(2)**, 252–254 (1994).

[105] V. Pruneri, J. Webjörn, P.S.J. Russell, J.R.M. Barr, D.C. Hanna: Intracavity second harmonic generation of 0.532 μm in bulk periodically poled lithium niobate. Opt. Commun. **116(1–3)**, 159–162 (1995).

[106] V. Pruneri, R. Koch, P.G. Kazansky, W.A. Clarkson, P.S.J. Russell, D.C. Hanna: 49 mW of CW blue light generated by first-order quasi-phase-matched frequency doubling of a diode-pumped 946-nm Nd:YAG laser. Opt. Lett. **20(23)**, 2375–2377 (1995).

[107] L. Goldberg, W.K. Burns, R.W. McElhanon: Difference-frequency generation of tunable mid-infrared radiation in bulk periodically poled $LiNbO_3$. Opt. Lett. **20(11)**, 1280–1282 (1995).

[108] L. Goldberg, W.K. Burns, R.W. McElhanon: Wide acceptance bandwidth difference frequency generation in quasi-phase-matched $LiNbO_3$. Appl. Phys. Lett. **67(20)**, 2910–2912 (1995).

[109] L.E. Myers, G.D. Miller, R.C. Eckardt, M.M. Fejer, R.L. Byer, W.R. Bosenberg: Quasi-phase-matched 1.064-μm-pumped optical parametric oscillator in bulk periodically poled $LiNbO_3$. Opt. Lett. **20(1)**, 52–54 (1995).

[110] M.M. Fejer, G.A. Magel, D.H. Jundt, R.L. Byer: Quasi-phase-matched second harmonic generation: tuning and tolerances. IEEE. J. Quant. Electr. **28(11)**, 2631–2654 (1992).

[111] L.E. Myers, R.C. Eckardt, M.M. Fejer, R.L. Byer, W.R. Bosenberg, J.W. Pierce: Quasi-phase-matched optical parametric oscillators in bulk periodically poled $LiNbO_3$. J. Opt. Soc. Am. B **12(11)**, 2102–2116 (1995).
[112] L.E. Myers, W.R. Bosenberg: Periodically poled lithium niobate and quasi-phase-matched optical parametric oscillators. IEEE. J. Quant. Electr. **33(10)**, 1663–1672 (1997).
[113] A. Ashkin, G.D. Boyd, J.M. Dziedzic, R.G. Smith, A.A. Ballman, J.J. Levinstein, K. Nassau: Optically-induced refractive index inhomogeneities in $LiNbO_3$ and $LiTaO_3$. Appl. Phys. Lett. **9(1)**, 72–74 (1966).
[114] A.M. Glass: The photorefractive effect. Opt. Eng. **17(5)**, 470–479 (1978).
[115] G.D. Miller, R.G. Batchko, W.M. Tulloch, D.R.Weise, M.M. Fejer, R.L. Byer: 42%-efficient single-pass CW second-harmonic generation in periodically poled lithium niobate. Opt. Lett. **22(24)**, 1834–1836 (1997).
[116] W.R. Bosenberg, J.I. Alexander, L.E. Myers, R.W. Wallace: 2.5-W, continuous-wave, 629-nm solid-state laser source. Opt. Lett. **23(3)**, 207–209 (1998).
[117] P. Schlup, S.D. Butterworth, I.T. McKinnie: Efficient single-frequency pulsed periodically poled lithium niobate optical parametric oscillator. Opt. Commun. **154(4)**, 191–195 (1998).
[118] U. Bäder, J.-P. Meyn, J. Bartschke, T. Weber, A. Borsutzky, R. Wallenstein, R.G. Batchko, M.M. Fejer, R.L. Byer: Nanosecond periodically poled lithium niobate optical parametric generator pumped at 532 nm by a single-frequency passively Q-switched Nd:YAG laser. Opt. Lett. **24(22)**, 1608–1610 (1999).
[119] T.R. Volk, V.I. Pryalkin, N.M. Rubinina: Optical-damage-resistant $LiNbO_3$:Zn crystal. Opt. Lett. **15(18)**, 996–998 (1990).
[120] Y. Zhang, Y.H. Xu, M.H. Li, Y.Q. Zhao: Growth and properties of Zn doped lithium niobate crystal. J. Cryst. Growth **233(3)**, 537–540 (2001).

2.4 $KTiOPO_4$, Potassium Titanyl Phosphate (KTP)

Positive biaxial crystal: $2V_z = 37.4°$ at $\lambda = 0.5461\ \mu m$ [1]
Molecular mass: 197.949
Specific gravity: 2.945 g/cm^3 [2], [3]; 3.023 g/cm^3 [4]; 3.024 g/cm^3 [5]; 3.03 g/cm^3 [6]
Point group: $mm2$
Lattice constants:
$a = 12.814$ Å [7]; 12.8157 Å [6]; 12.8164 ± 0.0014 Å at $T = 298$ K [8]; 12.822 Å [9]
$b = 6.404$ Å [7]; 6.4027 Å [6]; 6.4033 ± 0.0006 Å at $T = 298$ K [8]; 6.4054 Å [9]
$c = 10.616$ Å [7]; 10.5866 Å [6]; 10.5897 ± 0.0014 Å at $T = 298$ K [8]; 10.589 Å [9]
Assignment of dielectric and crystallographic axes: $X, Y, Z \Rightarrow a, b, c$
Mohs hardness: 5 [3]
Vickers hardness: 531 [4]; 566 [10]
Knoop hardness: 702 [4]
Melting point (decomposition on melting): 1421 K [9]; 1423 K [7]; 1445 K [11]

Curie temperature: 1211 K [12]; 1213 K [13]; 1189 K (lowest potassium concentration in initial flux composition, [K]/[P] = 1) [14]; 1231 K (highest potassium concentration in initial flux composition, [K]/[P] = 2) [14]

Linear thermal expansion coefficient [7]

$\alpha_t \times 10^6$ [K^{-1}], $\parallel X$	$\alpha_t \times 10^6$ [K^{-1}], $\parallel Y$	$\alpha_t \times 10^6$ [K^{-1}], $\parallel Z$
11	9	0.6

Linear thermal expansion coefficient [15]

T [K]	$\alpha_t \times 10^6$ [K^{-1}], $\parallel X$	$\alpha_t \times 10^6$ [K^{-1}], $\parallel Y$	$\alpha_t \times 10^6$ [K^{-1}], $\parallel Z$
373	8.7	10.5	−0.2

Thermal expansion along the X axis for temperature range 298 K $< T <$ 473 K [16]:

$$L(T) = L(T_0)\{1 + \alpha(T - 298) + \beta(T - 298)^2\}$$

where T in K, $T_0 = 298$ K, $\alpha = (6.7 \pm 0.7) \times 10^{-6}$ K^{-1}, $\beta = (11 \pm 2) \times 10^{-9}$ K^{-2}

Specific heat capacity c_p at $P = 0.101325$ MPa

T [K]	c_p [J/kgK]	Ref.
298	688	[4]
	727	[17]
	729	[7]

Thermal conductivity coefficient [7]

κ [W/mK], $\parallel X$	κ [W/mK], $\parallel Y$	κ [W/mK], $\parallel Z$
2	3	3.3

Band-gap energy at room temperature: $E_g = 3.54$ eV [18]; 3.8 eV [19]
Transparency range at "0" transmittance level: 0.35–4.5 μm [20], [21] with the orthophosphate overtone at 3.5 μm [13]
UV transmission cutoff ($\alpha = 2$ cm^{-1}) is at 0.352 μm ($\mathbf{E}\parallel X$); 0.359 μm ($\mathbf{E}\parallel Y$); 0.365 μm ($\mathbf{E}\parallel Z$) [22]

Linear absorption coefficient

λ [μm]	α [cm^{-1}]	Ref.	Note
0.4	0.025–0.036	[23]	depending on Pt impurity
0.423	0.151 ± 0.024	[24]	flux-grown PPKTP
0.43–0.78	<0.004	[25]	oxygen annealing + cerium doping
0.473	0.021–0.067	[22]	flux-grown, $\mathbf{E}\parallel X$
	0.023–0.053	[22]	flux-grown, $\mathbf{E}\parallel Y$
	0.034–0.085	[22]	flux-grown, $\mathbf{E}\parallel Z$

λ [μm]	α [cm^{-1}]	Ref.	Note
	0.037	[22]	hydrothermally grown, $\mathbf{E}\parallel X$
	0.049	[22]	hydrothermally grown, $\mathbf{E}\parallel Y$
	0.076	[22]	hydrothermally grown, $\mathbf{E}\parallel Z$
0.5145	0.013	[26]	along *a* axis
	0.027	[26]	along *b* axis
	0.026	[26]	along *c* axis
0.53–0.78	<0.005	[25]	oxygen annealing
0.5321	0.04	[27]	along SHG direction
	<0.02	[7]	
	0.009–0.036	[22]	flux-grown, $\mathbf{E}\parallel X$
	0.011–0.024	[22]	flux-grown, $\mathbf{E}\parallel Y$
	0.019–0.039	[22]	flux-grown, $\mathbf{E}\parallel Z$
	0.017	[22]	hydrothermally grown, $\mathbf{E}\parallel X$
	0.025	[22]	hydrothermally grown, $\mathbf{E}\parallel Y$
	0.040	[22]	hydrothermally grown, $\mathbf{E}\parallel Z$
0.6594	0.0065	[26]	along *a* axis
	0.0087	[26]	along *b* axis
	0.0065	[26]	along *c* axis
0.846	0.018 ± 0.009	[24]	flux-grown PPKTP
1.06	<0.01	[6]	
1.0642	<0.006	[7]	
	0.005	[27]	along SHG direction
	0.0002	[26]	along *a* axis
	0.0005	[26]	along *b* axis
	0.0004	[26]	along *c* axis
	0.0003	[28]	
1.0796	0.012	[29]	along SHG direction
1.3188	0.0015	[26]	along *a* axis
	0.0004	[26]	along *b* axis
	0.001	[26]	along *c* axis
3.297	0.59	[30]	

Two-photon absorption coefficient β

λ [μm]	τ_p [ns]	$\beta \times 10^{11}$ [cm/W]	Ref.	Note
0.5321	0.022	10 ± 2	[19]	$\mathbf{k}\parallel X$, $\mathbf{E}\parallel Z$
	0.021	24 ± 4.8	[31]	[100] direction
		16 ± 3.2	[31]	[010] direction
		14 ± 2.8	[31]	[110] direction
0.6	0.0012	3.5	[32]	$\theta = 67.3°$, $\phi = 0°$

Experimental values of refractive indices for flux-grown KTP

λ [μm]	n_X	n_Y	n_Z	Ref.
0.4047	1.8249	1.8410	1.9629	[1]

λ [μm]	n_X	n_Y	n_Z	Ref.
0.4358	1.8082	1.8222	1.9359	[1]
0.4916	1.7883	1.8000	1.9044	[1]
0.5343	1.7780	1.7887	1.8888	[1]
0.53975	1.7764	1.7869	1.8863	[33]
0.5410	1.7767	1.7873	1.8869	[1]
0.5461	1.7756	1.7860	1.8850	[1]
0.5770	1.7703	1.7803	1.8769	[1]
0.5790	1.7699	1.7798	1.8764	[1]
0.5853	1.7689	1.7787	1.8749	[1]
0.5893	1.7684	1.7780	1.8740	[1]
0.6234	1.7637	1.7732	1.8672	[1]
0.6328	1.7622	1.7714	1.8649	[33]
0.6410	1.7617	1.7709	1.8641	[1]
0.6939	1.7565	1.7652	1.8564	[1]
0.6943	1.7564	1.7652	1.8564	[1]
0.7050	1.7555	1.7642	1.8550	[1]
1.0640	1.7381	1.7458	1.8302	[1]
1.0642	1.7379	1.7454	1.8297	[33]
1.0795	1.7375	1.7450	1.8291	[33]
1.3414	1.7314	1.7387	1.8211	[33]

Temperature derivative of refractive indices for flux-grown KTP

λ [μm]	T [K]	$dn_X/dT \times 10^6$ [K^{-1}]	$dn_Y/dT \times 10^6$ [K^{-1}]	$dn_Z/dT \times 10^6$ [K^{-1}]	Ref.
0.6328	302–399	9.6 ± 1.1	13.0 ± 0.7	22.4 ± 0.9	[34]
1.0642	288–313	6.1	8.3	14.5	[35]

Best set of Sellmeier equations for flux-grown KTP for 0.43–3.54 μm range (λ in μm, $T = 293$ K) [36]:

$$n_X^2 = 3.29100 + \frac{0.04140}{\lambda^2 - 0.03978} + \frac{9.35522}{\lambda^2 - 31.45571}$$

$$n_Y^2 = 3.45018 + \frac{0.04341}{\lambda^2 - 0.04597} + \frac{16.98825}{\lambda^2 - 39.43799}$$

$$n_Z^2 = 4.59423 + \frac{0.06206}{\lambda^2 - 0.04763} + \frac{110.80672}{\lambda^2 - 86.12171}$$

Other sets of dispersion relations are given in [1], [21], [33], [37], [38], [39], [40], [41], [42], [43], [44], [45], [46].

Infrared-corrected Sellmeier equation for refractive index n_Z in spectral range $0.38\,\mu m < \lambda < 4.5\,\mu m$ (λ in μm, $T = 293$ K) [47]:

$$n_Z^2 = 1 + \frac{1.71645\,\lambda^2}{\lambda^2 - 0.013346} + \frac{0.5924\,\lambda^2}{\lambda^2 - 0.06503} + \frac{0.3226\,\lambda^2}{\lambda^2 - 67.1208} - 0.01133\,\lambda^2$$

Another infrared-corrected Sellmeier equation for refractive index n_Z is given in [48]. Temperature derivative of refractive indices for flux-grown KTP for $T = 293$ to 353 K and for spectral range $0.43\,\mu\text{m} < \lambda < 1.58\,\mu\text{m}$ (λ in μm) [36]:

$$\frac{dn_X}{dT} = \left(\frac{0.1717}{\lambda^3} - \frac{0.5353}{\lambda^2} + \frac{0.8416}{\lambda} + 0.1627\right) \times 10^{-5} K^{-1}$$

$$\frac{dn_Y}{dT} = \left(\frac{0.1997}{\lambda^3} - \frac{0.4063}{\lambda^2} + \frac{0.5154}{\lambda} + 0.5425\right) \times 10^{-5} K^{-1}$$

for spectral range $0.53\,\mu\text{m} < \lambda < 1.57\,\mu\text{m}$ (λ in μm) [36]:

$$\frac{dn_Z}{dT} = \left(\frac{0.9221}{\lambda^3} - \frac{2.9220}{\lambda^2} + \frac{3.6677}{\lambda} - 0.1897\right) \times 10^{-5} K^{-1}$$

for spectral range $1.32\,\mu\text{m} < \lambda < 3.53\,\mu\text{m}$ (λ in μm) [36]:

$$\frac{dn_Z}{dT} = \left(-\frac{0.5523}{\lambda} + 3.3920 - 1.7101\,\lambda + 0.3424\,\lambda^2\right) \times 10^{-5} K^{-1}$$

Nonlinear refractive index γ

λ [μm]	$\gamma \times 10^{15}$ [cm^2/W]	Ref.	Note
0.5321	2.3 ± 0.4	[19]	$\mathbf{k} \parallel X$, $\mathbf{E} \parallel Z$
0.780	1.20 ± 0.16	[49]	[100] direction
	0.94 ± 0.16	[49]	[010] direction
0.850	1.08 ± 0.20	[50]	$\theta = 90°$, $\phi = 23°$
1.0642	1.4	[51]	XY-plane
	1.4 ± 0.28	[31]	[110] direction
	1.8 ± 0.36	[31]	[010] direction
	2.1 ± 0.42	[31]	[100] direction
	2.4 ± 0.5	[19]	$\mathbf{k} \parallel Z$, $\mathbf{E} \parallel Y$
	3.1	[18]	

Linear electrooptic coefficients measured at low frequencies (well below the acoustic resonances of KTP crystal, i.e., for the "free" crystal) at room temperature [7], [52]

λ [μm]	r_{13}^{T} [pm/V]	r_{23}^{T} [pm/V]	r_{33}^{T} [pm/V]	r_{42}^{T} [pm/V]	r_{51}^{T} [pm/V]
0.6328	$+9.5 \pm 0.5$	$+15.7 \pm 0.8$	$+36.3 \pm 1.8$	9.3 ± 0.9	7.3 ± 0.7

Linear electrooptic coefficients measured at high frequencies (well above the acoustic resonances of KTP crystal, i.e., for the "clamped" crystal) at room temperature [7]

λ [μm]	r_{13}^{S} [pm/V]	r_{23}^{S} [pm/V]	r_{33}^{S} [pm/V]	r_{42}^{S} [pm/V]	r_{51}^{S} [pm/V]
0.6328	$+8.8 \pm 0.8$	$+13.8 \pm 1.4$	$+35.0 \pm 3.5$	8.8 ± 1.8	6.9 ± 1.4

Coercive field value: $\approx$2 kV/mm [53], [54], [55]

Expressions for the effective second-order nonlinear coefficient in principal planes of KTP crystal (Kleinman symmetry conditions are not valid) [56]:

XY plane

$$d_{\mathrm{eoe}} = d_{\mathrm{oee}} = d_{15}\sin^2\phi + d_{24}\cos^2\phi$$

YZ plane

$$d_{\mathrm{oeo}} = d_{\mathrm{eoo}} = d_{15}\sin\theta$$

XZ plane, $\theta < V_{\mathrm{z}}$

$$d_{\mathrm{ooe}} = d_{32}\sin\theta$$

XZ plane, $\theta > V_{\mathrm{z}}$

$$d_{\mathrm{oeo}} = d_{\mathrm{eoo}} = d_{24}\sin\theta$$

Expressions for the effective second-order nonlinear coefficient in principal planes of KTP crystal (Kleinman symmetry conditions are valid, $d_{15} = d_{31}$ and $d_{24} = d_{32}$) [56]:

XY plane

$$d_{\mathrm{eoe}} = d_{\mathrm{oee}} = d_{31}\sin^2\phi + d_{32}\cos^2\phi$$

YZ plane

$$d_{\mathrm{oeo}} = d_{\mathrm{eoo}} = d_{31}\sin\theta$$

XZ plane, $\theta < V_{\mathrm{z}}$

$$d_{\mathrm{ooe}} = d_{32}\sin\theta$$

XZ plane, $\theta > V_{\mathrm{z}}$

$$d_{\mathrm{oeo}} = d_{\mathrm{eoo}} = d_{32}\sin\theta$$

Effective second-order nonlinear coefficient for three-wave interactions in the arbitrary direction of KTP crystal is given in [56].

Absolute values of second-order nonlinear coefficients [57]:

$$d_{15}(0.852\,\mu\mathrm{m}) = 1.9 \pm 0.1\,\mathrm{pm/V}$$

$$d_{24}(0.852\,\mu\mathrm{m}) = 3.9 \pm 0.2\,\mathrm{pm/V}$$

$$d_{33}(0.852\,\mu\mathrm{m}) = 16.6 \pm 0.8\,\mathrm{pm/V}$$

$$d_{15}(1.064\,\mu\mathrm{m}) = 1.9 \pm 0.1\,\mathrm{pm/V}$$

$$d_{24}(1.064\,\mu\mathrm{m}) = 3.7 \pm 0.2\,\mathrm{pm/V}$$

$$d_{31}(1.064\,\mu\mathrm{m}) = 2.2 \pm 0.1\,\mathrm{pm/V}$$

$$d_{32}(1.064\,\mu\mathrm{m}) = 3.7 \pm 0.2\,\mathrm{pm/V}$$

$$d_{33}(1.064\,\mu\mathrm{m}) = 14.6 \pm 0.7\,\mathrm{pm/V}$$

$d_{15}(1.313\,\mu\text{m}) = 1.4 \pm 0.1\,\text{pm/V}$

$d_{24}(1.313\,\mu\text{m}) = 2.6 \pm 0.1\,\text{pm/V}$

$d_{33}(1.313\,\mu\text{m}) = 11.1 \pm 0.6\,\text{pm/V}$

The signs of KTP second-order nonlinear coefficients are all the same [58].
Other reliable values of second-order nonlinear coefficients:

$d_{24}(0.6\,\mu\text{m}) = 4.2\,\text{pm/V}$ [32]

$d_{15}(1.064\,\mu\text{m}) = 1.8\,\text{pm/V}$ [58]

$d_{24}(1.054\,\mu\text{m}) = 4.1 \pm 0.4\,\text{pm/V}$ [59]

$d_{24}(1.064\,\mu\text{m}) = 3.4\,\text{pm/V}$ [58]; $3.9 \pm 0.3\,\text{pm/V}$ [60]; $4.2 \pm 0.2\,\text{pm/V}$ [61]

$d_{33}(1.064\,\mu\text{m}) = 17.4\,\text{pm/V}$ [58]

$d_{15}(1.32\,\mu\text{m}) = 1.2 \pm 0.1\,\text{pm/V}$ [45]

$d_{24}(1.32\,\mu\text{m}) = 2.4 \pm 0.2\,\text{pm/V}$ [45]

Experimental values of phase-matching angle ($T = 293\,\text{K}$):

Interacting wavelengths [μm]	ϕ_{exp} [deg]	θ_{exp} [deg]	Ref.
hydrothermally grown KTP			
XY plane, $\theta = 90°$			
SHG, $e + o \Rightarrow e$			
$1.053 \Rightarrow 0.5265$	34		[62]
$1.062 \Rightarrow 0.531$	25		[6]
$1.0642 \Rightarrow 0.5321$	24		[39]
	26		[2], [63], [64]
SFG, $e + o \Rightarrow e$			
$1.3188 + 0.6594 \Rightarrow 0.4396$	3.8		[65]
YZ plane, $\phi = 90°$			
SFG, $o + e \Rightarrow o$			
$1.3188 + 0.6594 \Rightarrow 0.4396$		65.1	[65]
$1.338 + 0.669 \Rightarrow 0.446$		63.2	[65]
XZ plane, $\phi = 0°, \theta > V_z$			
SFG, $o + e \Rightarrow o$			
$1.3188 + 0.6594 \Rightarrow 0.4396$		87.7	[65]
$1.338 + 0.669 \Rightarrow 0.446$		79.9	[65]
$1.0642 + 1.4581 \Rightarrow 0.6152$		78	[66]
$1.0642 + 1.4762 \Rightarrow 0.6184$		76.6	[66]
$1.0642 + 1.5918 \Rightarrow 0.6378$		75.8	[66]
flux-grown KTP			
XY plane, $\theta = 90°$			
SHG, $e + o \Rightarrow e$			
$1.0641 \Rightarrow 0.53205$	23.5		[67]

Interacting wavelengths [μm]	ϕ_{exp} [deg]	θ_{exp} [deg]	Ref.
	23.6		[68]
1.0642 ⇒ 0.5321	23.0		[69]
	23.2		[1]
	23.3		[70]
	24.1		[71]
	24.7		[72]
	25.0		[3]
	25.2		[20], [39], [73]
	25.3		[10]
YZ plane, $\phi = 90°$			
SHG, $o + e \Rightarrow o$			
1.0642 ⇒ 0.5321		69.0	[74]
		69.2	[39]
1.068 ⇒ 0.534		67.8	[74]
1.182 ⇒ 0.591		57.4	[74]
1.3188 ⇒ 0.6594		50.0	[39]
1.5 ⇒ 0.75		44.6	[74]
XZ plane, $\phi = 0°$, $\theta > V_z$			
SHG, $o + e \Rightarrow o$			
1.0796 ⇒ 0.5398		85.3	[75]
		86.7	[33]
1.235 ⇒ 0.6175		65	[76]
1.3188 ⇒ 0.6594		58.3	[39]
		58.6	[77]
		58.9	[78]
1.3414 ⇒ 0.6707		58.7	[33]
		58.9	[79]
1.54 ⇒ 0.77		53	[80]
1.90768 ⇒ 0.95384		51.1	[78]
2.05 ⇒ 1.025		50.8	[78]
2.1284 ⇒ 1.0642		53.7	[81]
		54	[78]
SFG, $o + e \Rightarrow o$			
1.3188 + 0.6594 ⇒ 0.4396		87.1	[65]
		87.6	[39]
1.338 + 0.669 ⇒ 0.446		79.8	[65]
1.3414 + 0.6707 ⇒ 0.44713		78.1	[82]
1.0642 + 1.90768 ⇒ 0.68333		77.2	[78]
1.0796 + 1.3414 ⇒ 0.59817		74.9	[33]
1.54 + 0.78 ⇒ 0.51776		61	[83]
1.90768 + 2.40688 ⇒ 1.0642		58.6	[78]
1.770 + 0.76 ⇒ 0.5321		55	[84]
1.58053 + 1.54 ⇒ 0.78		52.1	[83]
1.90768 + 1.0642 ⇒ 0.68333		48.7	[78]

Experimental values of NCPM temperature and corresponding temperature bandwidth

Interacting wavelengths [μm]	T [°C]	ΔT [°C]	Ref.
hydrothermally grown KTP			
along X axis			
SFG, type II			
$1.3188^Y + 0.6594^Z \Rightarrow 0.4396^Y$	47	8.5	[65]
$1.338^Y + 0.669^Z \Rightarrow 0.446^Y$	463	8.5	[65]
along Y axis			
SHG, type II			
$0.9943^X + 0.9943^Z \Rightarrow 0.49715^X$	20	175	[85]
SFG, type II			
$1.0642^X + 0.809^Z \Rightarrow 0.45961^X$	20	122	[86]
flux-grown KTP			
along X axis			
SHG, type II			
$1.0796^Y + 1.0796^Z \Rightarrow 0.5398^Y$	153 (?)	20	[75]
	63	30	[87]
$1.08^Y + 1.08^Z \Rightarrow 0.54^Y$	≈20		[88]
SFG, type II			
$1.090^Y + 1.039^Z \Rightarrow 0.5321^Y$	20		[89]
	20		[90]
$2.15^Z + 1.04^Y \Rightarrow 0.70094^Y$	20		[91]
$2.402^Z + 1.08^Y \Rightarrow 0.745^Y$	≈20		[88]
$2.75^Z + 1.16^Y \Rightarrow 0.816^Y$	≈20		[92]
$2.756^Z + 1.182^Y \Rightarrow 0.827^Y$	≈20		[93]
$3.09^Z + 1.38^Y \Rightarrow 0.95396^Y$	20		[91]
$3.297^Z + 1.571^Y \Rightarrow 1.047^Y$	20		[94]
$3.276^Z + 1.539^Y \Rightarrow 1.0642^Y$	20		[94]
$3.303^Z + 1.57^Y \Rightarrow 1.0642^Y$	≈20		[95]
$3.290^Z + 1.573^Y \Rightarrow 1.0642^Y$	≈20		[96]
$1.182^Y + 0.827^Z \Rightarrow 0.487^Y$	≈20		[93]
$1.3188^Y + 0.6594^Z \Rightarrow 0.4396^Y$	60.2	8.5	[65]
	53	10.1	[77]
$1.32^Y + 0.66^Z \Rightarrow 0.44^Y$	128	8.7	[77]
$1.338^Y + 0.669^Z \Rightarrow 0.446^Y$	484	8.5	[65]
along Y axis			
SHG, type II			
$0.99^X + 0.99^Z \Rightarrow 0.495^X$	20		[37]
SFG, type II			
$1.0642^X + 0.8068^Z \Rightarrow 0.4589^X$	20		[37]
$1.0642^X + 0.808^Z \Rightarrow 0.45929^X$	20		[39]
$1.0642^X + 0.9691^Z \Rightarrow 0.5072^X$	20		[37]

Note: superscripts of interacting wavelengths represent polarization directions.

Experimental values of internal angular, temperature and spectral bandwidths

Interacting wavelengths [μm]	ϕ_{pm} [deg]	θ_{pm} [deg]	$\Delta\phi^{int}$ [deg]	$\Delta\theta^{int}$ [deg]	ΔT [°C]	$\Delta\nu$ [cm^{-1}]	Ref.
XY plane, $\theta = 90°$ ($T = 293$ K)							
SHG, $e + o \Rightarrow e$							
$1.0582 \Rightarrow 0.5921$			0.43	2.01			[97]
$1.062 \Rightarrow 0.531$	25		0.49	2.23	25	4.9	[6]
$1.0642 \Rightarrow 0.5321$	23		0.53		20		[69]
	23				23.3		[98]
	23.2		0.58	1.82	24		[1]
	23.3		0.43		20	4.0	[70]
	25					6.2	[3]
	25.2				25		[20]
	25.2		0.42		17.5		[73]
	25.2		0.52	2.52	25.7		[10]
YZ plane, $\phi = 90°$ ($T = 293$ K)							
SHG, $o + e \Rightarrow o$							
$0.9943 \Rightarrow 0.49715$		90	5.70	2.96	175	7.1	[85]
$1.0642 \Rightarrow 0.5321$		69			100		[99]
		69		0.11			[74]
$2.532 \Rightarrow 1.266$		56		0.20		30.7	[100]
SFG, type II							
$1.0642^X + 0.809^Z \Rightarrow 0.45961^X$		90	6.13	2.72		$17.6(\Delta\nu_2)$	[86]
XZ plane, $\phi = 0°$, $\theta > V_z$							
SHG, $o + e \Rightarrow o$							
$1.0796 \Rightarrow 0.5398$ ($T = 293$ K)		85.3		0.34			[75]
($T = 426$ K)		90		1.70			[75]

Note: superscripts of interacting wavelengths represent polarization directions.

Calculated values of inverse group-velocity mismatch for SHG process in flux-grown KTP

Interacting wavelengths [μm]	ϕ_{pm} [deg]	θ_{pm} [deg]	β [fs/mm]
XY plane, $\theta = 90°$			
SHG, $e + o \Rightarrow e$			
$1.0 \Rightarrow 0.5$	73.18		475
$1.05 \Rightarrow 0.525$	35.03		434
YZ plane, $\phi = 90°$			
SHG, $o + e \Rightarrow o$			
$1.0 \Rightarrow 0.5$		83.17	490
$1.1 \Rightarrow 0.55$		64.36	361
$1.2 \Rightarrow 0.6$		56.22	329
$1.3 \Rightarrow 0.65$		51.02	228
$1.4 \Rightarrow 0.7$		47.46	186

Interacting wavelengths [μm]	ϕ_{pm} [deg]	θ_{pm} [deg]	β [fs/mm]
1.5 ⇒ 0.75		45.02	153
1.6 ⇒ 0.8		43.40	126
1.7 ⇒ 0.85		42.44	103
1.8 ⇒ 0.9		41.99	84
1.9 ⇒ 0.95		41.98	83
2.0 ⇒ 1.0		42.35	100
XZ plane, $\phi = 0°, \theta > V_z$			
SHG, $o + e \Rightarrow o$			
1.1 ⇒ 0.55		80.31	391
1.2 ⇒ 0.6		67.47	307
1.3 ⇒ 0.65		61.25	246
1.4 ⇒ 0.7		57.32	200
1.5 ⇒ 0.75		54.70	164
1.6 ⇒ 0.8		52.99	135
1.7 ⇒ 0.85		51.94	111
1.8 ⇒ 0.9		51.42	90
1.9 ⇒ 0.95		51.32	81
2.0 ⇒ 1.0		51.57	98

Laser-induced damage threshold for hydrothermally grown KTP

λ [μm]	τ_p [ns]	I_{thr} [GW/cm^2]	Ref.	Note
0.526	0.03	30	[40]	
		30	[7]	10 Hz
0.72–0.99	0.00014	>35	[101]	76 MHz
1.0642	125000	0.001	[102]	
	30	0.15	[103]	
	20	>0.15	[104]	
	11	2–3	[105]	10 Hz

Laser-induced bulk damage threshold for flux-grown KTP

λ [μm]	τ_p [ns]	I_{thr} [GW/cm^2]	Ref.	Note
0.5235	0.0035	>8	[106]	50 Hz
0.526	0.03	10	[7]	10 Hz
0.5321	400,000	0.001	[107]	in the presence of 1.0642 μm beam
	50,000	0.0025	[107]	in the presence of 1.0642 μm beam
	220	0.051	[108]	1.2 kHz, with fundamental beam
	220	0.089	[108]	1.2 kHz, PPKTP, with fundamental beam
	14	0.05	[73]	60 pulses

λ [μm]	τ_p [ns]	I_{thr} [GW/cm^2]	Ref.	Note
	8	2.0–3.2	[109]	2 Hz
	3	>0.6	[110]	100 Hz, coated PPKTP
	0.06	>1.8	[71]	5 Hz
0.74–0.84	0.0002	>200	[111]	1 kHz
0.75–0.85	0.000045	>16	[112]	84 MHz
0.816	0.000085	>50	[92]	76 MHz
	0.00009	>1000	[92]	250 kHz
1.053	0.1	>7	[113]	1 kHz
1.0642	30	>3.3	[78]	
	25	>0.6	[114]	250,000 pulses, bulk darkening
		>0.3	[114]	3,500,000 pulses, bulk darkening
	20	0.15	[73]	60 pulses
	17	2.8 ± 0.1	[115]	1 Hz, 10,000 shots, commercial KTP
		6.2 ± 0.1	[115]	1 Hz, 10,000 shots, high-purity KTP
	16	>0.14	[116]	1 Hz
	15	>0.5	[96]	2.5 Hz
	11	2.4–3.5	[109]	2 Hz
	10	0.9–1.0	[69]	
	9	31	[117]	1 pulse
	5	>0.9	[118]	20 Hz, PPKTP
	1	15	[1]	1 pulse
		>15	[119]	
1.235	35	>0.5	[76]	20 Hz

Laser-induced surface damage threshold for flux-grown KTP

λ [μm]	τ_p [ns]	I_{thr} [GW/cm^2]	Ref.	Note
0.5291	18	0.08–0.1	[97]	
0.5321	8	1.4–2.2	[109]	2 Hz
1.0582	25	0.18–0.22	[97]	
1.0642	11	1.5–2.2	[109]	2 Hz
	1.3	4.6	[120]	
1.618	0.022	50 ± 10	[121]	10 Hz

Laser-induced gray-tracking threshold in flux-grown KTP

λ [μm]	τ_p [ns]	I_{thr} [GW/cm^2]	Ref.	Note
0.5145	CW	0.000026	[122], [123]	$\mathbf{E}\perp Z$, $\theta = 90°$, $\phi = 23.4°$
		0.000130	[122], [123]	$\mathbf{E}\perp Z$, $\theta = 90°$, $\phi = 23.4°$
0.5321	75	0.015	[124]	6.3 kHz, $\theta = 90°$, $\phi = 23.1°$
		0.125	[124]	1 kHz, $\theta = 90°$, $\phi = 23.1°$
	25	0.045	[114]	10 Hz, $\theta = 90°$, $\phi = 23°$
	20	0.05–0.1	[125]	20 Hz, $\theta = 90°$, $\phi = 23°$

Laser-induced gray-tracking threshold in flux-grown KTP

λ [μm]	τ_p [ns]	I_{thr} [GW/cm^2]	Ref.	Note
	10	0.08	[126]	10 Hz, $\theta = 90°$, $\phi = 23°$
	1	>0.1	[64]	3.7 kHz, $\theta = 90°$, $\phi = 26°$
	0.026	2	[84]	10 Hz, $\theta = 55°$, $\phi = 0°$

About the crystal

KTP is one of the main basic nonlinear crystals; it has widely been used during the 1980s and 1990s in frequency conversion devices. One of the few disadvantages of KTP is its susceptibility to photochromic damage, known as gray- or grey-tracking, which occurs under green pulsed or CW laser irradiation, most commonly at 532 or 514.5 nm irradiation (for the recent review, see [127]). The gray-tracks do not form at temperatures above 150°C [128], [129], and vanish quickly under annealing at elevated temperatures [127], [130]. In addition to the photochromic effect, photorefractive damage is also present in KTP [129].

In recent years, diode-laser-pumped, Nd:YAG laser–based, KTP frequency-doubled, green laser sources became very important due to a high efficiency (optical-to-electrical efficiency ~5–10%) and high average output power (up to 300 W at 532 nm) [131], [132], [133]. The disadvantage of a KTP frequency doubler is its susceptibility to gray-tracking. As a result, the output green power slowly deteriorates, that is, in [134] from 106 W to 97.4 W after 100 hours of continuous operation.

In 1994 [53], a periodically poled KTP (PPKTP) was introduced. KTP (regarding QPM) possesses such unique properties as a low coercive field value (which allows the fabrication of large-aperture poled crystals), an absence of photorefractive damage (which allows the operation at room temperature), and a much higher laser damage threshold (in comparison with LN). The major drawback of PPKTP is the relatively short length of elements, usually about 10 mm or even less. Nevertheless, PPKTP was used in variety of applications. We can list here some pioneering works on QPM SHG [108], [135], [136], [137], [138], QPM DFG [48], [139], and QPM OPO [110], [140], [141], [142], [143], [144] in periodically poled KTP crystals.

References

[1] T.Y. Fan, C.E. Huang, B.Q. Hu, R.C. Eckardt, Y.X. Fan, R.L. Byer, R.S. Feigelson: Second harmonic generation and accurate index of refraction measurements in flux-grown $KTiOPO_4$. Appl. Opt. **26(12)**, 2390–2394 (1987).

[2] Y.S. Liu, D. Dentz, R. Belt: High-average-power intracavity second-harmonic generation using $KTiOPO_4$ in an acousto-optically Q-switched Nd:YAG laser oscillator at 5 kHz. Opt. Lett. **9(3)**, 76–78 (1984).

[3] D.N. Dovchenko, V.A. Dyakov, V.I. Pryalkin: Growth and applications of potassium titanyl phosphate crystals. Izv. Akad. Nauk SSSR, Ser. Fiz. **52(2)**, 225–230 (1988) [In Russian, English trans.: Bull. Acad. Sci. USSR, Phys. Ser. **52(2)**, 13–17 (1988)].

[4] J.C. Jacco: $KTiOPO_4$ (KTP)—past, present and future. Proc. SPIE **968**, 93–99 (1988).

[5] B.H.T. Chai: Optical Crystals. In: *CRC Handbook of Laser Science and Technology, Supplement 2: Optical Materials*, ed. by M.J. Weber (CRC Press, Boca Raton, 1995), pp. 3–65.
[6] R.F. Belt, G. Gashurov, Y.S. Liu: KTP as a harmonic generator of Nd:YAG lasers. Laser Focus **21(10)**, 110–124 (1985).
[7] J.D. Bierlein, H. Vanherzeele: Potassium titanyl phosphate: properties and new applications. J. Opt. Soc. Am. B **6(4)**, 622–633 (1989).
[8] I.V. Voloshina, R.G. Gerr, M.Y. Antipin, V.G. Tsirelson, N.I .Pavlova, Y.T. Struchkov, R.P. Ozerov, I.S. Rez: Electron density distribution in a nonlinear $KTiOPO_4$ crystal according to precision X-ray data. Kristallogr. **30(4)**, 668–676 (1985) [In Russian, English trans.: Sov. Phys. - Crystallogr. **30(4)**, 389–393 (1985)].
[9] L.K. Cheng, E.M. McCarron III, J. Calabrese, J.D. Bierlein, A.A. Ballman: Development of the nonlinear optical crystal $CsTiOAsO_4$. I. Structural stability. J. Crystal Growth **132(1–2)**, 280–288 (1993).
[10] Y. Kitaoka, T. Sasaki, S. Nakai, Y. Goto: New nonlinear optical crystal thienylchalcone and its harmonic generation properties. Appl. Phys. Lett. **59(1)**, 19–21 (1991).
[11] I. Bhaumik, S. Ganesamoorthy, R. Bhatt, R. Sundar, A.K. Karnal, V.K. Wadhawan: Novel seeding technique for growing $KTiOPO_4$ single crystals by the TSSG method. J. Cryst. Growth **243(3–4)**, 522–525 (2002).
[12] J.D. Bierlein, H. Vanherzeele, A.A. Ballman: Linear and nonlinear optical properties of flux-grown $KTiOAsO_4$. Appl. Phys. Lett. **54(9)**, 783–785 (1989).
[13] L.K. Cheng, J.D. Bierlein: KTP and isomorphs—recent progress in device and material development. Ferroelectrics **142(1–2)**, 209–228 (1993).
[14] M. Roth, N. Angert, M. Tseitlin, A. Alexandrovski: On the optical quality of KTP crystals for nonlinear optical and electro-optic applications. Opt. Mater. **16(1–2)**, 131–136 (2001).
[15] Data sheet of Molecular Technology GmbH. Available at www.mt-berlin.com.
[16] S. Emanueli, A. Arie: Temperature-dependent dispersion equations for $KTiOPO_4$ and $KTiOAsO_4$. Appl. Opt. **42(33)**, 6661–6665 (2003).
[17] J.D. Bierlein: Potassium titanyl phosphate (KTP): properties, recent advances and new applications. Proc. SPIE **1104**, 2–12 (1989).
[18] M. Sheik-Bahae, D.C. Hutchings, D.J. Hagan, E.W. Van Stryland: Dispersion of bound electron nonlinear refraction in solids. IEEE J. Quant. Electr. **27(6)**, 1296–1309 (1991).
[19] R. DeSalvo, A.A. Said, D.J. Hagan, E.W. van Stryland, M. Sheik-Bahae: Infrared to ultraviolet measurements of two-photon absorption and n_2 in wide bandgap solids. IEEE J. Quant. Electr. **32(8)**, 1324–1333 (1996).
[20] A.L. Aleksandrovskii, S.A. Akhmanov, V.A. Dyakov, N.I. Zheludev, V.I. Pryalkin: Efficient nonlinear optical converters made of potassium titanyl phosphate. Kvant. Elektron. **12(7)**, 1333–1334 (1985) [In Russian, English trans.: Sov. J. Quantum Electron. **15(7)**, 885–886 (1985)].
[21] K. Kato: Parametric oscillation at 3.2 μm in KTP pumped at 1.064 μm. IEEE J. Quant. Electr. **27(5)**, 1137–1140 (1991).
[22] G. Hansson, H. Karlsson, S. Wang, F. Laurell: Transmission measurements in KTP and isomorphic compounds. Appl. Opt. **39(27)**, 5058–5069 (2000).
[23] A. Miyamoto, Y. Mori, T. Sasaki, S. Nakai: Improvement of optical transmission of $KTiOPO_4$ crystals by growth in nitrogen ambient. Appl. Phys. Lett. **69(8)**, 1032–1034 (1996).
[24] F. Torabi-Goudarzi, E. Riis: Efficient CW high-power frequency doubling in periodically poled KTP. Opt. Commun. **227(4–6)**, 389–403 (2003).

[25] P.F. Bordui, R. Blachman, R.G. Norwood: Improved optical transmission of $KTiOPO_4$ crystals through cerium-doping and oxygen annealing. Appl. Phys. Lett. **61(12)**, 1369–1371 (1992).
[26] D.J. Gettemy, W.C. Harker, G. Lindholm, N.P. Barnes: Some optical properties of KTP, $LiIO_3$, and $LiNbO_3$. IEEE J. Quant. Electr. **24(11)**, 2231–2237 (1988).
[27] P.E. Perkins, T.S. Fahlen: 20-W average-power KTP intracavity-doubled Nd:YAG laser. J. Opt. Soc. Am. B **4(7)**, 1066–1071 (1987).
[28] T. Kojima, S. Fujikawa, K. Yasui: Stabilization of a high-power diode-side-pumped intracavity-frequency-doubled CW Nd:YAG laser by compensating for thermal lensing of a KTP crystal and Nd:YAG rods. IEEE J. Quant. Electr. **35(3)**, 377–380 (1999).
[29] C.H. Huang, H.Y. Shen, Z.D. Zeng, Y.P. Zhou, R.R. Zeng, G.F. Yu, A.D. Jiang, T.B. Chen: Measurement of the total absorption coefficient of a KTP crystal. Opt. Laser Technol. **22(5)**, 345–347 (1990).
[30] M.S. Webb, P.F. Moulton, J.J. Kasinski, R.L. Burnham, G. Loiacono, R. Stolzenberger: High-average-power $KTiOAsO_4$ optical parametric oscillator. Opt. Lett. **23(15)**, 1161–1163 (1998).
[31] R. DeSalvo, M. Sheik-Bahae, A.A. Said, D.J. Hagan, E.W. Van Stryland: Z-scan measurements of the anisotropy of nonlinear refraction and absorption in crystals. Opt. Lett. **18(3)**, 194–196 (1993).
[32] T. Nishikawa, N. Uesugi: Effects of walk-off and group velocity difference on the optical parametric generation in $KTiOPO_4$ crystals. J. Appl. Phys. **77(10)**, 4941–4947 (1995).
[33] H.Y. Shen, Y.P. Zhou, W.X. Lin, Z.D. Zeng, R.R. Zeng, G.F. Yu, C.H. Huang, A.D. Jiang, S.Q. Jia, D.Z. Shen: Second harmonic generation and sum frequency mixing of dual wavelength Nd:$YAlO_3$ laser in flux grown $KTiOPO_4$ crystal. IEEE J. Quant. Electr. **28(1)**, 48–51 (1992).
[34] Z. Zeng, H. Shen, H. Xu, Y. Zhou, C. Huang, D. Shen: Measurements of the refractive index and its thermal coefficient for $KTiOPO_4$. J. Synth. Cryst. **16(3)**, 274–277 (1987) [In Chinese].
[35] W. Wiechmann, S. Kubota, T. Fukui, H. Masuda: Refractive-index temperature derivatives of potassium titanyl phosphate. Opt. Lett. **18(15)**, 1208–1210 (1993).
[36] K. Kato, E. Takaoka: Sellmeier and thermo-optic dispersion formulas for KTP. Appl. Opt. **41(24)**, 5040–5044 (2002).
[37] K. Kato: Second-harmonic and sum-frequency generation to 4950 and 4589 Å in KTP. IEEE J. Quant. Electr. **QE-24(1)**, 3–4 (1988).
[38] H. Liao, H. Shen, T. Lian, Y. Zhou, C. Huang, R. Zeng, G. Yu: Accurate values for the index of refraction and the optimum phase match parameters in a flux grown $KTiOPO_4$ crystal. Opt. Laser Technol. **20(2)**, 103–104 (1988).
[39] D.W. Anthon, C.D. Crowder: Wavelength dependent phase matching in KTP. Appl. Opt. **27(13)**, 2650–2652 (1988).
[40] H. Vanherzeele, J.D. Bierlein, F.C. Zumsteg: Index of refraction measurement and parametric generation in hydrothermally-grown KTP. Appl. Opt. **27(16)**, 3314–3316 (1988).
[41] V.A. Dyakov, V.V. Krasnikov, V.I. Pryalkin, M.S. Pshenichnikov, T.B. Razumikhina, V.S. Solomatin, A.I. Kholodnykh: Sellmeier equation and tuning characteristics of KTP crystal frequency converters in the 0.4–4.0 μm range. Kvant. Elektron. **15(9)**, 1703–1704 (1988) [In Russian, English trans.: Sov. J. Quantum Electron. **18(9)**, 1059–1060 (1988)].
[42] G. Ghosh: Temperature dispersion in KTP for nonlinear devices. IEEE Phot. Technol. Lett. **7(1)**, 68–70 (1995).
[43] L. Carrion, J.P. Girardeau-Montaut: Performance of a new picosecond KTP optical parametric generator and amplifier. Opt. Commun. **152(4–6)**, 347–350 (1998).

[44] B. Boulanger, J.P. Feve, G. Marnier, C. Bonnin, P. Villeval, J.J. Zondy: Absolute measurement of quadratic nonlinearities from phase-matched second-harmonic generation in a single KTP crystal cut as a sphere. J. Opt. Soc. Am. B **14(6)**, 1380–1386 (1997).

[45] B. Boulanger, J.P. Feve, G. Marnier, B. Menaert: Methodology for optical studies of nonlinear crystals: application to the isomorph family $KTiOPO_4$, $KTiOAsO_4$, $RbTiOAsO_4$ and $CsTiOAsO_4$. Pure Appl. Opt. **7(2)**, 239–256 (1998).

[46] D.Y. Zhang, H.Y. Shen, W. Liu, G.F. Zhang, W.Z. Chen, G. Zhang, R.R. Zeng, C.H. Huang, W.X. Lin, J.K. Liang: The principal refractive indices and nonlinear optical phase matched properties of Nb:KTP crystals. Opt. Mater. **15(2)**, 99–102 (2000).

[47] M. Katz, D. Eger, M.B. Ogon, A. Hardy: Refractive dispersion curve measurement of $KTiOPO_4$ using periodically segmented waveguides and periodically poled crystals. J. Appl. Phys. **90(1)**, 53–58 (2001).

[48] K. Fradkin, A. Arie, A. Skliar, G. Rosenman: Tunable midinfrared source by difference frequency generation in bulk periodically poled $KTiOPO_4$. Appl. Phys. Lett. **74(7)**, 914–916 (1999); Errata, Appl. Phys. Lett. **74(18)**, 2723 (1999).

[49] H.P. Li, C.H. Kam, Y.L. Lam, W. Ji: Femtosecond Z-scan measurements of nonlinear refraction in nonlinear optical materials. Opt. Mater. **15(4)**, 237–242 (2001).

[50] M. Sheik-Bahae, M. Ebrahimzadeh: Measurements of nonlinear refraction in the second-order $\chi^{(2)}$ materials $KTiOPO_4$, $KNbO_3$, β-BaB_2O_4, and LiB_3O_5. Opt. Commun. **142(4–6)**, 294–298 (1997).

[51] R. Adair, L.L. Chase, S.A. Payne: Nonlinear refractive index of optical crystals. Phys. Rev. B **39(5)**, 3337–3350 (1989).

[52] L.K. Cheng, L.T. Cheng, J. Galperin, P.A. Morris Hotsenpiller, J.D. Bierlein: Crystal growth and characterization of $KTiOPO_4$ isomorphs from the self-fluxes. J. Cryst. Growth **137(1–2)**, 107–115 (1994).

[53] Q. Chen, W.P. Risk: Periodic poling of $KTiOPO_4$ using an applied electric field. Electron. Lett. **30(18)**, 1516–1517 (1994).

[54] H. Karlsson, F. Laurell: Electric field poling of flux grown $KTiOPO_4$. Appl. Phys. Lett. **71(24)**, 3474–3476 (1997).

[55] J. Hellström, V. Pasiskevicius, F. Laurell, H. Karlsson: Efficient nanosecond optical parametric oscillators based on periodically poled KTP emitting in the 1.8–2.5-μm spectral range. Opt. Lett. **24(17)**, 1233–1235 (1999).

[56] V.G. Dmitriev, D.N. Nikogosyan: Effective nonlinearity coefficients for three-wave interactions in biaxial crystals of mm2 point group symmetry. Opt. Commun. **95 (1–3)**, 173–182 (1993).

[57] I. Shoji, T. Kondo, A. Kitamoto, M. Shirane, R. Ito: Absolute scale of second-order nonlinear-optical coefficients. J. Opt. Soc. Am. B **14(9)**, 2268–2294 (1997).

[58] A. Anema, T. Rasing: Relative signs of the nonlinear coefficients of potassium titanyl phosphate. Appl. Opt. **36(24)**, 5902–5904 (1997).

[59] E.C. Cheung, K. Koch, G.T. Moore, J.M. Liu: Measurements of second-order nonlinear optical coefficients from the spectral brightness of parametric fluorescence. Opt. Lett. **19(3)**, 168–170 (1994).

[60] W.J. Alford, A.V. Smith: Wavelength variation of the second-order nonlinear coefficients of $KNbO_3$, $KTiOPO_4$, $KTiOAsO_4$, $LiNbO_3$, $LiIO_3$, β-BaB_2O_4, KH_2PO_4, and LiB_3O_5 crystals: a test of Miller wavelength scaling. J. Opt. Soc. Am. B **18(4)**, 524–533 (2001).

[61] T. Nishikawa, N. Uesugi: Effects of walk-off and group velocity difference on the optical parametric generation in $KTiOPO_4$ crystals. J. Appl. Phys. **77(10)**, 4941–4947 (1995).

[62] H. Vanherzeele: Optimization of a CW mode-locked frequency-doubled Nd:YLF laser. Appl. Opt. **27(17)**, 3608–3615 (1988).

[63] P.E. Perkins, T.S. Fahlen: Half watt average power at 25 kHz from fourth harmonic of Nd:YAG. IEEE J. Quant. Electr. **QE-21(10)**, 1636–1638 (1985).
[64] D.A.V. Kliner, F. Di Teodoro, J.P. Koplow, S.W. Moore, A.V. Smith: Efficient second, third, fourth, and fifth harmonic generation of a Yb-doped fiber amplifier. Opt. Commun. **210(3–6)**, 393–398 (2002).
[65] R.A. Stolzenberger, C.C. Hsu, N. Peyghambarian, J.J.E. Reid, R.A. Morgan: Type II sum frequency generation in flux and hydrothermally grown KTP at 1.319 and 1.338 μm. IEEE Photon. Technol. Lett. **1(12)**, 446–448 (1989).
[66] K. Kurokawa, M. Nakazawa: Femtosecond 1.4–1.6 μm infrared pulse generation at a high repetition rate by difference frequency generation. Appl. Phys. Lett. **55(1)**, 7–9 (1989).
[67] H. Wang, Y. Ma, Z. Zhai, J. Gao, C. Xie, K. Peng: Tunable continuous-wave doubly resonant optical parametric oscillator by use of a semimonolithic KTP crystal. Appl. Opt. **41(6)**, 1124–1127 (2002).
[68] Y.-L. Jia, J.-L. He, H.-T. Wang, S.-N. Zhu, Y.-Y. Zhu: Single pass third-harmonic generation of 310 mW of 355 nm with an all-solid-state laser. Chin. Phys. Lett. **18(12)**, 1589–1591 (2001).
[69] O.I. Lavrovskaya, N.I. Pavlova, A.V. Tarasov: Second harmonic generation of light from an YAG:Nd^{3+} laser in an optically biaxial crystal $KTiOPO_4$. Kristallogr. **31(6)**, 1145–1151 (1986) [In Russian, English trans.: Sov. Phys. - Crystallogr. **31(6)**, 678–682 (1986)].
[70] R.A. Stolzenberger: Nonlinear optical properties of flux grown $KTiOPO_4$. Appl. Opt. **27(18)**, 3883–3886 (1988).
[71] L.J. Bromley, A. Guy, D.C. Hanna: Synchronously pumped optical parametric oscillation in KTP. Opt. Commun. **70(4)**, 350–354 (1989).
[72] Y. Huo, F. Chen, S. He, D. Shen, X. Ma, Y. Lu: Realizing intracavity frequency doubling and Q switching by KTP. Proc. SPIE **3556**, 31–36 (1998).
[73] Y.A. Galaichuk, V.A. Dyakov, N.I. Likholit, V.S. Ovechko, R.A. Petrenko, T.V. Rozhdestvenskaya, V.L. Strizhevskii, A.I. Khilchevskii, Y.N. Yashkir: $KTiOPO_4$ as an optical-frequency converter. Izv. Akad. Nauk SSSR, Ser. Fiz. **52(3)**, 560–563 (1988) [In Russian, English trans.: Bull. Akad. Sci. USSR, Phys. Ser. **52(3)**, 131–133 (1988)].
[74] T. Nishikawa, N. Uesugi, H. Ito: Angle tuning characteristics of second-harmonic generation in $KTiOPO_4$. Appl. Phys. Lett. **55(19)**, 1943–1945 (1989).
[75] V.M. Garmash, G.A. Ermakov, N.I. Pavlova, A.V. Tarasov: Efficient second-harmonic generation in potassium titanyl-phosphate crystals with noncritical matching. Pisma Zh. Tekh. Fiz. **12(20)**, 1222–1225 (1986) [In Russian, English trans.: Sov. Tech. Phys. Lett. **12(10)**, 505–506 (1986)].
[76] I.T. McKinnie, A.L. Oien: Tunable red-yellow laser based on second harmonic generation of Cr:forsterite in KTP. Opt. Commun. **141(3–4)**, 157–161 (1997).
[77] J.P. Feve, B. Boulanger, X. Cabirol, B. Menaert, G. Marnier, C. Bonnin, P. Villeval: Non-critically phase-matched cascaded THG at 440 nm in $KTiOP_{1-y}As_yO_4$ crystals. Opt. Commun. **115(3–4)**, 323–326 (1995).
[78] R. Burnham, R.A. Stolzenberger, A. Pinto: Infrared optical parametric oscillator in potassium titanyl phosphate. IEEE Photon. Technol. Lett. **1(1)**, 27–28 (1989).
[79] Q. Zheng, H. Tan, L. Zhao, L. Quan: Diode-pumped 671 nm laser frequency doubled by CPM LBO. Opt. Laser Technol. **34(4)**, 329–331 (2002).
[80] W. Wang, K. Nakagawa, Y. Toda, M. Ohtsu: 1.5 μm diode laser-based nonlinear frequency conversions by using potassium titanyl phosphate. Appl. Phys. Lett. **61(16)**, 1886–1888 (1992).

[81] J.T. Lin, J.L. Montgomery: Generation of tunable mid-IR (1.8–2.4 μm) laser radiation from optical parametric oscillation in KTP. Opt. Commun. **75(3–4)**, 315–320 (1990).
[82] W.X. Lin, H.Y. Shen, Y.P. Zhou, R.R. Zeng, G.F. Yu, C.H. Huang, Z.D. Zeng, W.J. Zhang: Tripling the harmonic generation of a 1341.4 nm Nd:YAP laser in $LiIO_3$ and KTP crystals to get 447.1 nm blue coherent radiation. Opt. Commun. **82(3–4)**, 333–336 (1991).
[83] W. Wang, M. Ohtsu: Frequency-tunable sum- and difference-frequency generation by using two diode lasers and a KTP crystal. Opt. Commun. **102(3–4)**, 304–308 (1993).
[84] L. Carrion, J.-P. Girardeau-Montaut: Gray-track damage in potassium titanyl-phosphate under a picosecond regime at 532 nm. Appl. Phys. Lett. **77(8)**, 1074–1076 (2000).
[85] W.P. Risk, R.N. Payne, W. Lenth, C. Harder, H. Meier: Noncritically phase-matched frequency doubling using 994 nm dye and diode laser radiation in $KTiOPO_4$. Appl. Phys. Lett. **55(12)**, 1179–1181 (1989).
[86] J.-C. Baumert, F.M. Schellenberg, W. Lenth, W.P. Risk, G.C. Bjorklund: Generation of blue CW coherent radiation by sum frequency mixing in $KTiOPO_4$. Appl. Phys. Lett. **51(26)**, 2192–2194 (1987).
[87] Z.Y. Ou, S.F. Pereira, E.S. Polzik, H.J. Kimble: 85% efficiency for CW frequency doubling from 1.08 to 0.54 μm. Opt. Lett. **17(9)**, 640-642 (1992).
[88] T. Kartaloğlu, K.G. Köprülü, O. Aytür: Phase-matched self-doubling optical parametric oscillator. Opt. Lett. **22(5)**, 280–282 (1997).
[89] S.T. Yang, R.C. Eckardt, R.L. Byer: Power and spectral characteristics of continuous-wave parametric oscillators: the doubly to singly resonant transition. J. Opt. Soc. Am. B **10(9)**, 1684–1695 (1993).
[90] S.T. Yang, R.C. Eckardt, R.L. Byer: Continuous-wave singly resonant optical parametric oscillator pumped by a single-frequency resonantly doubled Nd:YAG laser. Opt. Lett. **18(12)**, 971–973 (1993).
[91] K. Kato, M. Masutani: Widely tunable 90º phase-matched KTP parametric oscillator. Opt. Lett. **17(3)**, 178–179 (1992).
[92] G.R. Holtom, R.A. Crowell, X.S. Xie: High-repetition-rate femtosecond optical parametric-amplifier system near 3 μm. J. Opt. Soc. Am. B **12(9)**, 1723–1731 (1995).
[93] K.G. Köprülü, T. Kartaloglu, Y. Dikmelik, O. Aytür: Single-crystal sum-frequency-generating optical parametric oscillator. J. Opt. Soc. Am. B **16(9)**, 1546–1552 (1999).
[94] J.A.C. Terry, Y. Cui, Y. Yang, W. Sibbett, M.H. Dunn: Low-threshold operation of an all-solid-state KTP optical parametric oscillator. J. Opt. Soc. Am. B **11(5)**, 758–769 (1994).
[95] R. Dabu, C. Fenic, A. Stratan: Intracavity pumped nanosecond optical parametric oscillator emitting in the eye-safe range. Appl. Opt. **40(24)**, 4334–4340 (2001).
[96] V.L. Naumov, A.M. Onishchenko, A.S. Podstavkin, A.V. Shestakov: High-efficiency parametric converter based on KTP crystals. Kvant. Elektron. **30(7)**, 632–634 (2000) [In Russian, English trans.: Quantum Electron. **30(7)**, 632–634 (2000)].
[97] G.I. Dyakonov, V.A. Maslov, V.A. Mikhailov, S.K. Pak, V.N. Semenenko, I.A. Shcherbakov: Highly-efficient YSGG:Cr:Nd laser with frequency doubling in a KTP crystal. Kvant. Elektron. **16(8)**, 1601–1603 (1989) [In Russian, English trans.: Sov. J. Quantum Electron. **19(8)**, 1031–1032 (1989)].
[98] S.G. Grechin, V.G. Dmitriev, V.A. Dyakov, V.I. Pryalkin: Temperature-independent phase matching for second-harmonic generation in a KTP crystal. Kvant. Elektron. **26(1)**, 77–81 (1999) [In Russian, English trans.: Quantum Electron. **29(1)**, 77–81 (1999)].
[99] K. Kato: Temperature insensitive SHG at 0.5321 μm in KTP. IEEE J. Quant. Electr. **28**, 1974–1976 (1992).

[100] J.-J. Zondy, M. Abed, A. Clairon: Type II frequency doubling of $\lambda = 1.30\,\mu$m and $\lambda = 2.53\,\mu$m in flux-grown potassium titanyl phosphate. J. Opt. Soc. Am. B **11(10)**, 2004–2015 (1994).

[101] Y. Wang, V. Petrov, Y.J. Ding, Y. Zheng, J.B. Khurgin, W.P. Risk: Ultrafast generation of blue light by efficient second-harmonic generation in periodically-poled bulk and waveguide potassium titanyl phosphate. Appl. Phys. Lett. **73(7)**, 873–875 (1998).

[102] S.E. Moody, J.M. Eggleston, J.F. Seamans: Long-pulse second-harmonic generation in KTP. IEEE J. Quant. Electr. **QE-23(3)**, 335–340 (1987).

[103] T.A. Driscoll, H.J. Hoffman, R.E. Stone, P.E. Perkins: Efficient second-harmonic generation in KTP crystals. J. Opt. Soc. Am. B **3(5)**, 683–686 (1986).

[104] F.C. Zumsteg, J.D. Bierlein, T.E. Gier: $K_xRb_{1-x}TiOPO_4$: a new nonlinear optical material. J. Appl. Phys. **47(11)**, 4980–4985 (1976).

[105] F. Ahmed: Laser damage threshold of $KTiOPO_4$. Appl. Opt. **28(1)**, 119–122 (1989).

[106] C. Rauscher, T. Roth, R. Laenen, A. Laubereau: Tunable femtosecond-pulse generation by an optical parametric oscillator in the saturation regime. Opt. Lett. **20(19)**, 2003–2005 (1995).

[107] S. Favre, T.C. Sidler, R.-P. Salathe: High-power long-pulse second harmonic generation and optical damage with free-running Nd:YAG laser. IEEE J. Quant. Electr. **39(6)**, 733–740 (2003).

[108] V. Pasiskevicius, S. Wang, J.A. Tellefsen, F. Laurell, H. Karlsson: Periodically poled flux grown KTP for Nd:YAG frequency doubling. Appl. Opt. **37(30)**, 7116–7119 (1998).

[109] P. Yankov, D. Schumov, A. Nenov, A. Monev: Laser damage tests of large flux-grown $KTiOPO_4$ crystals. Opt. Lett. **18(21)**, 1771–1773 (1993).

[110] M. Oba, M. Kato, Y. Maruyama: Optical parametric oscillator with periodically poled $KTiOPO_4$ pumped by 100 Hz Nd:YAG green laser. Jpn. J. Appl. Phys. **41(8A)**, L881–L883 (2002).

[111] V. Petrov, F. Noack, R. Stolzenberger: Seeded femtosecond optical parametric amplification in the mid-infrared spectral region above $3\,\mu$m. Appl. Opt. **36(6)**, 1164–1172 (1997).

[112] J. Jiang, T. Hasama: Femtosecond optical parametric oscillator with a repetition rate of 504 MHz. Jpn. J. Appl. Phys. **41(3A)**, 1365–1368 (2002).

[113] K. Finsterbusch, R. Urschel, H. Zacharias: Tunable, high-power, narrow-band picosecond IR radiation by optical parametric amplification in KTP. Appl. Phys. B **74(4–5)**, 319–322 (2002).

[114] J.C. Jacco, D.R. Rockafellow, E.A. Teppo: Bulk-darkening threshold of flux-grown $KTiOPO_4$. Opt. Lett. **16(17)**, 1307–1309 (1991).

[115] X.B. Hu, H. Liu, J.Y Wang, H.J. Zhang, H.D. Jiang, S.S. Jiang, Q. Li, Y.L. Tian, Y.Y. Huang, W.X. Huang, W. He: Comparative study of $KTiOPO_4$ crystals. Opt. Mater. **23(1–2)**, 369–372 (2003).

[116] J. Sorce, K. Palombo, S. Matthews, E. Gregor: Phase conjugate laser producing 1 J at 532 nm with 80% second-harmonic-generation efficiency. In: *OSA Proceedings on Advanced Solid-State Lasers, Vol.13*, ed. by L.L. Chase, A.A. Pinto (OSA, Washington DC, 1992), pp. 366–368.

[117] R.J. Bolt, M. van der Mooren: Single shot bulk damage threshold and conversion efficiency measurements on flux grown $KTiOPO_4$ (KTP). Opt. Commun. **100(1–4)**, 399–410 (1993).

[118] J. Hellström, G. Karlsson, V. Pasiskevicius, F. Laurell: Optical parametric amplification in periodically poled $KTiOPO_4$ seeded by an Er-Yb:glass microchip laser. Opt. Lett. **26(6)**, 352–354 (2001).

[119] D. Eimerl, S. Velsko, L. Davis, F. Wang, G. Loiacono, G. Kennedy: Deuterated L-arginine phosphate: a new efficient nonlinear crystal. IEEE J. Quant. Electr. **25(2)**, 179–193 (1989).

[120] C. Chen: Chinese lab grows new nonlinear optical borate crystals. Laser Focus World **25(11)**, 129–137 (1989).

[121] J.P. Feve, B. Boulanger, Y. Guillien: Efficient energy conversion for cubic third-harmonic generation that is phase-matched in $KTiOPO_4$. Opt. Lett. **25(18)**, 1373–1375 (2000).

[122] X. Mu, Y.J. Ding, J. Wang, Y. Li, J. Wei, J.B. Khurgin: Investigation of damage mechanisms for $KTiOPO_4$ crystals under irradiation of a CW argon laser. Proc. SPIE **3610**, 9–14 (1999).

[123] X.B. Hu, J.Y. Wang, H.J. Zhang, H.D. Jiang, H. Liu, X.D. Mu, Y.J. Ding: Dependence of photochromic damage on polarization in $KTiOPO_4$ crystals. J. Cryst. Growth **247(1–2)**, 137–140 (2003).

[124] J.P. Feve, B. Boulanger, G. Marnier, H. Albrecht: Repetition rate dependence of gray-tracking in $KTiOPO_4$ during second-harmonic generation at 532 nm. Appl. Phys. Lett. **70(3)**, 277–279 (1997).

[125] G.M. Loiacono, D.N. Loiacono, T. McGee, M. Babb: Laser damage formation in $KTiOPO_4$ and $KTiOAsO_4$: grey tracks. J. Appl. Phys. **72(7)**, 2705–2712 (1992).

[126] B. Boulanger, M.M. Fejer, R. Blachman, P.F. Bordui: Study of $KTiOPO_4$ gray-tracking at 1064, 532, and 355 nm. Appl. Phys. Lett. **65(19)**, 2401–2403 (1994).

[127] B. Boulanger, I. Rousseau, J.P. Feve, M. Maglione, M. Menaert, G. Marnier: Optical studies of laser-induced gray-tracking in KTP. IEEE J. Quant. Electr. **35(3)**, 281–286 (1999).

[128] N.B. Angert, V.M. Garmash, N.I. Pavlova, A.V. Tarasov: Influence of color centers on the optical properties of KTP crystals and on the efficiency of the laser radiation frequency conversion in these crystals. Kvant. Elektron. **18(4)**, 470–472 (1991) [In Russian, English trans.: Sov. J. Quantum Electron. **21(4)**, 426–428 (1991)].

[129] J.K. Tyminski: Photorefractive damage in KTP used as second-harmonic generator. J. Appl. Phys. **70(10)**, 5570–5576 (1991).

[130] R. Blachman, P.F. Bordui, M.M. Fejer: Laser-induced photochromic damage in potassium titanyl phosphate. Appl. Phys. Lett. **64(11)**, 1318–1320 (1994).

[131] B.J. Le Garrec, G.J. Raze, P.Y. Thro, M. Gilbert: High-average-power diode-array-pumped frequency-doubled YAG laser. Opt. Lett. **21(24)**, 1990–1992 (1996).

[132] R.J.S. Pierre, D.W. Mordaunt, H. Injeyan, J.G. Berg, R.C. Hilyard, M.E. Weber, M.G. Wickham, G.M. Harpole, R. Senn: Diode array pumped kilowatt laser. IEEE J. Sel. Topics Quant. Electr. **3(1)**, 53–58 (1997).

[133] E.C. Honea, C.A. Ebbers, R.J. Beach, J.A. Speth, J.A. Skidmore, M.A. Emmanuel, S.A. Payne: Analysis of an intracavity-doubled diode-pumped Q-switched Nd:YAG laser producing more than 100 W of power at 0.532 μm. Opt. Lett. **23(15)**, 1203–1205 (1998).

[134] Y. Hirano, N. Pavel, S. Yamamoto, Y. Koyata, T. Tajime: 100-W, 100-h external green generation with Nd:YAG rod master-oscillator power-amplifier system. Opt. Commun. **184(1–4)**, 231–236 (2000).

[135] A. Arie, G. Rosenman, V. Mahal, A. Skliar, M. Oron, M. Katz, D. Eger: Green and ultraviolet quasi-phase-matched second harmonic generation in bulk periodically-poled $KTiOPO_4$. Opt. Commun. **142(4–6)**, 265–268 (1997).

[136] A. Englander, R. Lavi, M. Katz, M. Oron, D. Eger, E. Lebiush, G. Rosenman, A. Skliar: Highly efficient doubling of a high-repetition-rate diode-pumped laser with bulk periodically poled KTP. Opt. Lett. **22(21)**, 1598–1599 (1997).

[137] A. Arie, G. Rosenman, A. Korenfeld, A. Skliar, M. Oron, M. Katz, D. Eger: Efficient resonant frequency doubling of a CW Nd:YAG laser in bulk periodically poled $KTiOPO_4$. Opt. Lett. **23(1)**, 28–30 (1998).

[138] S. Wang, V. Pasiskevicius, F. Laurell, H. Karlsson: Ultraviolet generation by first-order frequency doubling in periodically poled $KTiOPO_4$. Opt. Lett. **23(24)**, 1883–1885 (1998).

[139] G.M. Gibson, G.A. Turnbull, M. Ebrahimzadeh, M.H. Dunn, H. Karlsson, G. Arvidsson, F. Laurell: Temperature-tuned difference-frequency mixing in periodically poled $KTiOPO_4$. Appl. Phys. B **67(5)**, 675–677 (1998).

[140] T. Kartaloglu, K.G. Köprülü, O. Aytür, M. Sundheimer, W.P. Risk: Femtosecond optical parametric oscillator based on periodically poled $KTiOPO_4$. Opt. Lett. **23(1)**, 61–63 (1998).

[141] A. Garashi, A. Arie, A. Skliar, G. Rosenman: Continuous-wave optical parametric oscillator based on periodically poled $KTiOPO_4$. Opt. Lett. **23(22)**, 1739–1741 (1998).

[142] D.R. Weise, U. Strößner, A. Peters, J. Mlynek, S. Schiller, A. Arie, A. Skliar, G. Rosenman: Continuous-wave 532-nm-pumped singly resonant optical parametric oscillator with periodically poled $KTiOPO_4$. Opt. Commun. **184(1–4)**, 329–333 (2000).

[143] J. Hellström, V. Pasiskevicius, H. Karlsson, F. Laurell: High-power optical parametric oscillation in large-aperture periodically poled $KTiOPO_4$. Opt. Lett. **25(3)**, 174–176 (2000).

[144] G.W. Baxter, P. Schlup, I.T. McKinnie, J. Hellström, F. Laurell: Single-mode near-infrared optical parametric oscillator amplifier based on periodically poled $KTiOPO_4$. Appl. Opt. **40(36)**, 6659–6662 (2001).

3

Main Infrared Materials

This chapter includes the most important infrared nonlinear materials, namely, silver thiogallate (AGS), silver gallium selenide (AGSe), zinc germanium phosphide (ZGP), and gallium selenide (GaSe).

3.1 $AgGaS_2$, Silver Thiogallate (AGS)

Negative uniaxial crystal: $n_o > n_e$ (at $\lambda < 0.497\,\mu m$ $n_e > n_o$)
Molecular mass: 241.723
Specific gravity: 4.58 g/cm^3 [1]; 4.7 g/cm^3 [2]; 4.702 g/cm^3 [3]
Point group: $\bar{4}2\,m$
Lattice constants:
$a = 5.742$ Å [4]; 5.755 Å [5]; 5.757 Å [2], [6]
$c = 10.26$ Å [4]; 10.28 Å [5]; 10.304 Å [2]; 10.305 Å [6]
$a = 5.75722 \pm 0.00003$ Å at $T = 298$ K [1]
$c = 10.3036 \pm 0.0002$ Å at $T = 298$ K [1]
Mohs hardness: 3–3.5
Melting point: 1235 ± 2 K [1]; 1238 K $\pm$ 2 K [7]; 1269 K [8]; 1270 K [9]; 1271 K [10]; 1323 K [11]

Mean value of linear thermal expansion coefficient α_t [7]

T [K]	$\alpha_t \times 10^6$ [K^{-1}], $\parallel c$	$\alpha_t \times 10^6$ [K^{-1}], $\perp c$
298–523	−13.2	12.7
298–773	−15.2	17.3
298–973	−16.7	20.1

Specific heat capacity at $P = 0.101325$ MPa [12]

T [K]	c_p [J/kgK]
292	404

Thermal conductivity coefficient κ [13]

T [K]	κ [W/mK], $\parallel c$	κ [W/mK], $\perp c$
293	1.4	1.5

Band-gap energy at room temperature: $E_g = 2.62$ eV [14]; 2.75 eV [1]; 2.76 eV [9]; 2.655 eV ($\mathbf{E}\perp c$) [15]; 2.572 eV ($\mathbf{E}\parallel c$) [15]
Transparency range:
at $\alpha = 1\,\mathrm{cm}^{-1}$ level: 0.48–11.4 μm [8]
at $\alpha = 3\,\mathrm{cm}^{-1}$ level: 0.50–13.2 μm [14]
at "0" transmittance level: 0.47–13 μm [16]

Linear absorption coefficient α

λ [μm]	α [cm^{-1}]	Ref.	Note
0.5–13	<0.1	[17]	
0.6–0.65	0.04	[18]	
0.6–12	<0.09	[16]	
0.633	0.02–0.05	[9]	typical crystals
	0.015–0.017	[9]	best crystals
0.633	0.05	[19]	
0.7–9	0.01	[20]	
0.8–9	0.01–0.02	[9]	typical crystals
	0.015	[9]	best crystals
0.845	0.01	[12]	
0.9–8.5	<0.9	[11]	
1.0642	0.01	[19]	
	0.01–0.02	[21]	typical crystals
	0.001–0.009	[9]	typical crystals
	0.0005–0.005	[21]	best crystals
	<0.0005	[9]	best crystals
1.15	0.02–0.07	[22]	
1.26	0.26	[23]	*e*-wave
1.8	<0.1	[15]	*e*-wave
1.9	0.05–0.15	[9]	typical crystals, *e*-wave
	0.03	[9]	best crystals, *e*-wave
2.1	<0.02	[15]	*e*-wave
2.15	0.08–0.25	[9]	typical crystals, *e*-wave
	0.05	[9]	best crystals, *e*-wave
2.8	0.012–0.024	[9]	typical crystals
	0.009	[9]	best crystals
4–8.5	<0.04	[18]	
4.64	0.03	[24]	
9.27	0.19	[24]	

λ [μm]	α [cm^{-1}]	Ref.	Note
9.55	<0.1	[25]	
10.2	0.43	[23]	*o*-wave
10.6	0.6	[9]	best crystals

Two-photon absorption coefficient β

λ [μm]	τ_p [ns]	$\beta \times 10^{11}$ [cm/W]	Ref.	Note
0.8	0.0002	350	[26]	*o*-wave
0.8–0.87	0.0002	18	[27]	

Experimental values of refractive indices [6]

λ [μm]	n_o	n_e	λ [μm]	n_o	n_e	λ [μm]	n_o	n_e
0.490	2.7148	2.7287	1.200	2.4414	2.3881	4.500	2.4003	2.3461
0.500	2.6916	2.6867	1.300	2.4359	2.3819	5.000	2.3955	2.3419
0.525	2.6503	2.6239	1.400	2.4315	2.3781	5.500	2.3938	2.3401
0.550	2.6190	2.5834	1.500	2.4280	2.3745	6.000	2.3908	2.3369
0.575	2.5944	2.5537	1.600	2.4252	2.3716	6.500	2.3874	2.3334
0.600	2.5748	2.5303	1.800	2.4206	2.3670	7.000	2.3827	2.3291
0.625	2.5577	2.5116	2.000	2.4164	2.3637	7.500	2.3787	2.3252
0.650	2.5437	2.4961	2.200	2.4142	2.3684	8.000	2.3757	2.3219
0.675	2.5310	2.4824	2.400	2.4119	2.3583	8.500	2.3699	2.3163
0.700	2.5205	2.4706	2.600	2.4102	2.3567	9.000	2.3663	2.3121
0.750	2.5049	2.4540	2.800	2.4094	2.3559	9.500	2.3606	2.3064
0.800	2.4909	2.4395	3.000	2.4080	2.3545	10.00	2.3548	2.3012
0.850	2.4802	2.4279	3.200	2.4068	2.3534	10.50	2.3486	2.2948
0.900	2.4716	2.4192	3.400	2.4062	2.3522	11.00	2.3417	2.2880
0.950	2.4644	2.4118	3.600	2.4046	2.3511	11.50	2.3329	2.2789
1.000	2.4582	2.4053	3.800	2.4024	2.3491	12.00	2.3266	2.2716
1.100	2.4486	2.3954	4.000	2.4024	2.3488	12.50	2.3177	

Experimental values of refractive indices [28]

λ [μm]	n_o	n_e	λ [μm]	n_o	n_e
0.6328	2.5476	2.5039	5.2955	2.3945	2.3405
1.0642	2.4513	2.3982	9.2714	2.3627	2.3074
1.1523	2.4443	2.3911	10.5910	2.3476	2.2919
3.3913	2.4055	2.3519	10.6321	2.3471	2.2914

Optical activity [16], [29]: $\rho = 522\,\text{deg/mm}$ at isotropic point ($n_o = n_e, \lambda = 0.4973\,\mu\text{m}$)

Best set of Sellmeier equations (λ in μm, $0.58\,\mu\text{m} < \lambda < 10.59\,\mu\text{m}$, $T = 293$ K) [30]:

$$n_o^2 = 5.7975 + \frac{0.2311}{\lambda^2 - 0.0688} - 0.00257\,\lambda^2$$

$$n_e^2 = 5.5436 + \frac{0.2230}{\lambda^2 - 0.0946} - 0.00261\,\lambda^2$$

Dispersion relations for a broader wavelength range ($0.54\,\mu\text{m} < \lambda < 12.9\,\mu\text{m}$) [24], [28]:

$$n_o^2 = 5.79419 + \frac{0.23114}{\lambda^2 - 0.06882} - 2.4534 \times 10^{-3}\,\lambda^2 + 3.1814 \times 10^{-7}\,\lambda^4 - 9.7051 \times 10^{-9}\,\lambda^6$$

$$n_e^2 = 5.54120 + \frac{0.22041}{\lambda^2 - 0.09824} - 2.5240 \times 10^{-3}\,\lambda^2 + 3.6214 \times 10^{-7}\,\lambda^4 - 8.3605 \times 10^{-9}\,\lambda^6$$

Other sets of Sellmeier equations are given in [23], [31], [32], [33], [34], [35], [36]. Temperature derivative of refractive indices for spectral range 0.56–10.59 μm and temperature range 293–473 K (λ in μm) [30]:

$$\frac{dn_o}{dT} = \left(\frac{0.3180}{\lambda^3} + \frac{2.8968}{\lambda^2} - \frac{0.8685}{\lambda} + 15.2679\right) \times 10^{-5} K^{-1}$$

$$\frac{dn_e}{dT} = \left(\frac{6.1742}{\lambda^3} - \frac{12.0868}{\lambda^2} + \frac{8.2485}{\lambda} + 14.4365\right) \times 10^{-5} K^{-1}$$

Other thermo-optic dispersion formulas are given in [31], [36], [37].

Linear electrooptic coefficients measured at low frequencies (well below the acoustic resonances of $AgGaS_2$ crystal, i.e., for the "free" crystal) at room temperature [38]

λ [μm]	r_{41}^T [pm/V]	r_{63}^T [pm/V]
0.6328	4.0 ± 0.2	3.0 ± 0.1

Expressions for the effective second-order nonlinear coefficient in general case (Kleinman symmetry conditions are valid, $d_{14} = d_{25} = d_{36}$) [39]:

$$d_{ooe} = -d_{36} \sin(\theta + \rho) \sin 2\phi$$

$$d_{eoe} = d_{oee} = 2d_{36} \sin(\theta + \rho) \cos(\theta + \rho) \cos 2\phi$$

Simplified expressions for the effective second-order nonlinear coefficient (approximation of small birefringence angle, Kleinman symmetry conditions are valid, $d_{14} = d_{25} = d_{36}$) [40]:

$$d_{ooe} = -d_{36} \sin\theta \sin 2\phi$$

$$d_{eoe} = d_{oee} = d_{36} \sin 2\theta \cos 2\phi$$

Values of second-order nonlinear coefficients:
$d_{36}(1.054\,\mu m) = 23.6 \pm 2.4\,pm/V$ [41]
$d_{36}(2.53\,\mu m) = 13.7 \pm 2.2\,pm/V$ [23]
$d_{36}(10.6\,\mu m) = 0.134 \times d_{36}(GaAs) \pm 15\% = 11.1 \pm 1.7\,pm/V$ [6], [42]
$d_{36}(10.6\,\mu m) = 0.15 \times d_{36}(GaAs) \pm 20\% = 12.5 \pm 2.5\,pm/V$ [42], [43]
Other values on second-order nonlinear coefficient of $AgGaS_2$ given below **do not agree** with recent relative measurements in LIS, $LiInSe_2$ and $HgGaS_4$ crystals:
$d_{36}(1.2\,\mu m) = 31 \pm 5\,pm/V$ [44]
$d_{36}(9.2714\,\mu m) = 0.84 \pm 0.10 \times d_{36}(AgGaSe_2) = 34.8 \pm 4.0\,pm/V$ [24], [45]
$d_{36}(10.591\,\mu m) = 0.84 \pm 0.10 \times d_{36}(AgGaSe_2) = 32.0 \pm 4.0\,pm/V$ [24], [45]

Experimental values of phase-matching angle ($T = 293\,K$)

Interacting wavelengths [μm]	θ_{exp} [deg]	Ref.
SHG, $o + o \Rightarrow e$		
2.0970 ⇒ 1.0485	56.1	[24]
2.1284 ⇒ 1.0642	54.7	[24]
3.3913 ⇒ 1.69565	34.1	[24]
	33	[16]
5.2955 ⇒ 2.64775	32.7	[28]
9.2714 ⇒ 4.6357	54.2	[28]
10.5710 ⇒ 5.2855	68.2	[28]
10.5910 ⇒ 5.2955	68.5	[28]
10.6 ⇒ 5.3	67	[43]
	67.5	[10]
	68	[16]
	70.8	[6]
10.6321 ⇒ 5.31605	69.1	[28]
11.10 ⇒ 5.55	78.5	[28]
SFG, $o + o \Rightarrow e$		
11.538 + 1.17233 ⇒ 1.0642	34.7	[35]
10.5910 + 5.2955 ⇒ 3.5303	43.4	[28]
9.9 + 1.19237 ⇒ 1.0642	35.9	[46]
8.7 + 1.21252 ⇒ 1.0642	37	[47]
6.24 + 1.28301 ⇒ 1.0642	41.1	[48]
5.89 + 1.29888 ⇒ 1.0642	42.1	[46]
4.8 + 1.36735 ⇒ 1.0642	44	[47]
4.0 + 1.44996 ⇒ 1.0642	47.7	[48]
3.09 + 1.62325 ⇒ 1.0642	51	[34]
2.53 + 1.83683 ⇒ 1.0642	53.4	[34]
6.85 + 1.0642 ⇒ 0.92110	42	[49]
4.43 + 1.0642 ⇒ 0.85807	55	[49]
6.6 + 0.77593 ⇒ 0.6943	60	[50]
4.8 + 0.81171 ⇒ 0.6943	75.5	[50]

Interacting wavelengths [μm]	θ_{exp} [deg]	Ref.
$11.66329 + 0.617 \Rightarrow 0.586$	64	[51]
$10.12478 + 0.622 \Rightarrow 0.586$	70	[51]
SFG, $e + o \Rightarrow e$		
$10.9 + 1.17934 \Rightarrow 1.0642$	38.3	[52]
$8.8 + 1.21060 \Rightarrow 1.0642$	40.3	[52]
$7.0 + 1.25500 \Rightarrow 1.0642$	43.6	[52]
$5.2 + 1.33803 \Rightarrow 1.0642$	50.6	[52]
$10.6 + 1.0642 \Rightarrow 0.96711$	39.8	[53]
$9.6 + 1.0642 \Rightarrow 0.95800$	41.5	[53]
$10.6 + 0.6943 \Rightarrow 0.65162$	55	[54]

Experimental values of internal angular and spectral bandwidths at $T = 293$ K

Interacting wavelengths [μm]	θ_{pm} [deg]	$\Delta\theta^{int}$ [deg]	$\Delta\nu_1$ [cm^{-1}]	Ref.
SHG, $o + o \Rightarrow e$				
$10.6 \Rightarrow 5.3$	67.5	0.41		[16]
SFG, $o + o \Rightarrow e$				
$10.53 + 0.589 \Rightarrow 0.56589$	90	2.34		[33]
$10.619 + 0.634 \Rightarrow 0.598$	90		1.73	[18]
$10.6 + 0.598 \Rightarrow 0.566$	90		1.5	[55]
$10.6 + 0.5968 \Rightarrow 0.565$	90		1.44	[56]
DFG, $e - o \Rightarrow o$				
$0.6943 - 0.8177 \Rightarrow 4.6$	82.7	0.42		[50]
$0.87163 - 1.0642 \Rightarrow 4.817$	52		5.9	[49]
$1.0642 - 1.283 \Rightarrow 6.24$	41.1		9.8	[48]
DFG, $e - o \Rightarrow e$				
$0.76 - 0.8301 \Rightarrow 9.0$	46.5	0.4	11 ($\Delta\nu_3$)	[57]
$0.80 - 0.8707 \Rightarrow 9.85$			2.9	[58]
$0.80 - 0.8715 \Rightarrow 9.75$			3.4	[27]
$0.80 - 0.8853 \Rightarrow 8.3$			3.1	[58]

Temperature variation of phase-matching angle [53]

Interacting wavelengths [μm]	T [°C]	θ_{pm} [deg]	$d\theta_{pm}/dT$ [deg/K]
SFG, $e + o \Rightarrow e$			
$10.6 + 1.0642 \Rightarrow 0.9671$	20	39.8	0.03

Temperature tuning of noncritical SFG [44]

Interacting wavelengths [μm]	$d\lambda_1/dT$ [nm/K]
SHG, $o + o \Rightarrow e$	
$7.8 + 0.65 \Rightarrow 0.6$	$\approx$4

Experimental values of temperature bandwidth [30]

Interacting wavelengths [μm]	θ_{exp} [deg]	ΔT [°C]
SHG, $o + o \Rightarrow e$		
10.591 ⇒ 5.2955	68.5	139
10.2466 ⇒ 5.1233	64.3	135
9.5525 ⇒ 4.77625	57.4	123
9.2714 ⇒ 4.6357	55.0	118
5.2955 ⇒ 2.64775	33.2	59
3.5303 ⇒ 1.76515	33.7	22

Experimental values of temperature bandwidth for noncritical sum-frequency generation (SFG) process

Interacting wavelengths [μm]	T [°C]	ΔT [°C]	Ref.
SFG, $o + o \Rightarrow e$			
10.591 + 0.5983 ⇒ 0.56632		2.5	[37]
3.2627 + 1.0642 ⇒ 0.8025	192	6.4	[30]

Laser-induced surface-damage threshold

λ [μm]	τ_p [ns]	I_{thr} [GW/cm^2]	Ref.	Note
0.59	500	0.02	[51]	10 pulses
0.598	3	0.015	[55]	
0.625	500	0.025–0.036	[51]	10 pulses
0.6943	30	0.0006	[54]	1 Hz, 1000 pulses
	10	0.01	[50]	100 pulses
		0.02	[31]	
0.75	50	0.025	[20]	
0.8	30	0.01	[57]	10 Hz
0.8–0.87	0.0002	>60	[27]	
1.06	35	0.02–0.025	[31]	
1.0642	100	0.002	[59]	10 Hz, 3000 pulses
	20	0.01	[34]	10 Hz
	17.5	>0.012	[60]	1000 pulses
	15	0.02	[10]	
	12	0.035	[52]	10 Hz
	11	0.03–0.05	[61]	10 Hz, 50 pulses
	10	0.03	[21]	10 Hz
	8	0.034–0.06	[61]	single pulse
	0.025	>0.7	[35]	10 Hz
	0.023	>0.075	[62]	10 Hz
	0.021	>2	[49]	
	0.020	3	[46]	
	0.002	>1	[63]	

λ [μm]	τ_p [ns]	I_{thr} [GW/cm^2]	Ref.	Note
2	6	0.017	[64]	uncoated crystal
		0.035	[64]	coated crystal
2.079	180	0.0014	[24]	5 Hz, uncoated crystal
9.27	50	>0.044	[24]	1 Hz, uncoated crystal
9.55	30	0.18	[25]	SHG direction
10.6	220	0.025	[60]	1000 pulses
	150	0.01	[33]	
		0.02	[65]	

Laser-induced bulk-damage threshold [21]

λ [μm]	τ_p [ns]	I_{thr} [GW/cm^2]
1.064	10	>0.5

About the crystal

In recent years, AGS was widely used for DFG and OPO; below, we will list only the best technical achievements. In [66], the signal and idler wavelengths of BBO OPA, pumped by 50 fs 150 kHz pulses from a Ti:sapphire laser ($\lambda = 800$ nm), were mixed in a 0.1-cm-long type II silver thiogallate crystal to get the tunability range 2.4–12 μm. In [64], the signal and idler wavelengths of LN OPO, pumped by a Nd:YAG laser (8 ns, 30 Hz), were used for DFG. The tunability range was 2.4–12 μm with a maximum difference-frequency pulse energy of 95 μJ near 7.5 μm. The highest idler pulse energy, reached for AGS-based OPO, was 400 μJ near 6 μm [59]. In the same work, the widest idler tunability range of 3.9–11.3 μm was reported. The authors of [59] used a nanosecond Nd:YAG laser (1.064 μm, 30 ns, 10 Hz) and a 2-cm-long type II AGS crystal. In [67], a Q-switched mode-locked Nd:YAG laser ($\lambda = 1.064$ μm, $P = 8$ W) was used for pumping a 3-cm-long type I $AgGaS_2$ crystal. The highest mean power of around 600 mW was reached at an idler wavelength of 4.06 μm. At the same time, the mean power at a signal wavelength of 1.44 μm approached 1.5 W.

References

[1] *Physical-Chemical Properties of Semiconductors. Handbook.* (Nauka, Moscow, 1979) [In Russian].
[2] D.M. Bercha, Y.V. Voroshilov, V.Y. Slivka, I.D. Turyanitsa: *Complex Chalcogenides and Chalcohalogenides*, ed. by D.V. Chepur (Vishcha Shkola, Lvov, 1983) [In Russian].
[3] B.H.T. Chai: Optical Crystals. In: *CRC Handbook of Laser Science and Technology, Supplement 2: Optical Materials*, ed. by M.J. Weber (CRC Press, Boca Raton, 1995) pp. 3–65.
[4] V.I. Gavrilenko, A.M. Grekhov, D.B. Korbutyak, V.G. Litovchenko: *Optical Properties of Semiconductors. Handbook.* (Naukova Dumka, Kiev, 1987) [In Russian].
[5] *Chemist's Handbook, Vol. I*, ed. by B.P. Nikolskii (Goskhimizdat, Leningrad, 1962) [In Russian].

[6] G.D. Boyd, H. Kasper, J.H. McFee: Linear and nonlinear optical properties of $AgGaS_2$, $CuGaS_2$ and $CuInS_2$, and the theory of the wedge technique for the measurement of nonlinear coefficients. IEEE J. Quant. Electr. **QE-7(12)**, 563–573 (1971).
[7] P. Korczak, C.B. Staff: Liquid encapsulated Czochralski growth of silver thiogallate. J. Cryst. Growth **24–25**, 386–389 (1974).
[8] R.S. Feigelson, R.K. Route: Recent developments in the growth of chalcopyrite crystals for nonlinear infrared applications. Opt. Eng. **26(2)**, 113–119 (1987).
[9] G.C. Catella, D. Burlage: Crystal growth and optical properties of $AgGaS_2$ and $AgGaSe_2$. MRS Bulletin **23(7)**, 28–36 (1998).
[10] D.S. Chemla, P.J. Kupecek, D.S. Robertson, R.C. Smith: Silver thiogallate, a new material with potential for infrared devices. Opt. Commun. **3(1)**, 29–31 (1971).
[11] H. Matthes, R. Viehmann, N. Marschall: Improved optical quality of $AgGaS_2$. Appl. Phys. Lett. **26(5)**, 237–239 (1975).
[12] A. Douillet, J.-J. Zondy, A. Yelisseyev, S. Lobanov, L. Isaenko: Stability and frequency tuning of thermally loaded continuous-wave $AgGaS_2$ optical parametric oscillators. J. Opt. Soc. Am. B **16(9)**, 1481–1498 (1999).
[13] J.D. Beasley: Thermal conductivities of some novel nonlinear optical materials. Appl. Opt. **33(6)**, 1000–1003 (1994).
[14] G.C. Bhar, R.C. Smith: Optical properties of II-IV-V_2 and I-III-VI_2 crystals with particular reference to transmission limits. Phys. Stat. Solidi A **13(1)**, 157–168 (1972).
[15] Data sheet of Cleveland Crystals Inc. Available at www.clevelandcrystals.com.
[16] V.V. Badikov, O.N. Pivovarov, Y.V. Skokov, O.V. Skrebneva, N.K. Trotsenko: Some optical properties of silver thiogallate single crystals. Kvant. Elektron. **2(3)**, 618–621 (1975) [In Russian, English trans.: Sov. J. Quantum Electron. **5(3)**, 350–351 (1975)].
[17] E.S. Voronin, V.S. Solomatin, N.I. Cherepov, V.V. Shuvalov, V.V. Badikov, O.N. Pivovarov: Conversion of infrared radiation in an $AgGaS_2$ crystal. Kvant. Elektron. **2(5)**, 1090–1092 (1975) [In Russian, English trans.: Sov. J. Quantum Electron. **5(5)**, 597–598 (1975)].
[18] P. Canarelli, Z. Benko, R. Curl, F.K. Tittel: Continuous-wave infrared laser spectrometer based on difference frequency generation in $AgGaS_2$ for high-resolution spectroscopy. J. Opt. Soc. Am. B **9(2)**, 197–202 (1992).
[19] A.H. Hielscher, C.E. Miller, D.C. Bayard, U. Simon, K.P. Smolka, R.F. Curl, F.K. Tittel: Optimisation of a midinfrared high-resolution difference-frequency laser spectrometer. J. Opt. Soc. Am. B **9(11)**, 1962–1967 (1992).
[20] A.O. Okorogu, S.B. Mirov, W. Lee, D.I. Crouthamel, N. Jenkins, A.Y. Dergachev, K.L. Vodopyanov, V.V. Badikov: Tunable middle infrared downconversion in GaSe and $AgGaS_2$. Opt. Commun. **155(4–6)**, 307–312 (1998).
[21] S. Chandra, T.H. Allik, G. Catella, J.A. Hutchinson: Tunable output around 8 μm from a single step $AgGaS_2$ OPO pumped at 1.064 μm. In: *Advanced Solid-State Lasers, OSA Trends in Optics and Photonics Series, Vol. 19*, ed. by W.R. Bosenberg, M.M. Fejer (OSA, Washington DC, 1998), pp. 282–284.
[22] V.V. Badikov, P.S. Blinov, A.A. Kosterev, V.S. Letokhov, A.L. Malinovskii, E.A. Ryabov: Efficient parametric generators of picosecond mid-infrared pulses based on $AgGaS_2$ crystals. Kvant. Elektron. **24(6)**, 537–540 (1997) [In Russian, English trans.: Quantum Electron. **27(6)**, 523–526 (1997)].
[23] J.-J. Zondy, D. Touahri, O. Acef: Absolute value of the d_{36} nonlinear coefficient of $AgGaS_2$: prospect for a low-threshold doubly resonant oscillator-based 3:1 frequency divider. J. Opt. Soc. Am. B **14(10)**, 2481–2497 (1997).
[24] A. Harasaki, K. Kato: New data on the nonlinear optical constant, phase-matching, and optical damage of $AgGaS_2$. Jpn. J. Appl. Phys. **36(2)**, 700–703 (1997).

[25] Y.M. Andreev, V.V. Badikov, V.G. Voevodin, L.G. Geiko, P.P. Geiko, M.V. Ivashchenko, A.I. Karapuzikov, I.V. Sherstov: Radiation resistance of nonlinear crystals at a wavelength of 9.55 μm. Kvant. Elektron. **31(12)**, 1075–1078 (2001) [In Russian, English trans.: Quantum Electron. **31(12)**, 1075–1078 (2001)].

[26] F. Rotermund, V. Petrov, F. Noack, L. Isaenko, A. Yelisseyev, S. Lobanov: Optical parametric generation of femtosecond pulses up to 9 μm with $LiInS_2$ pumped at 800 nm. Appl. Phys. Lett. **78(18)**, 2623–2625 (2001).

[27] J. Song, J.F. Xia, Z. Zhang, D. Strickland: Mid-infrared pulses generated from the mixing output of an amplified, dual-wavelength Ti:sapphire system. Opt. Lett. **27(3)**, 200–202 (2002).

[28] K. Kato, H. Shirahata: Nonlinear IR generation in $AgGaS_2$. Jpn. J. Appl. Phys. **35(9A)**, 4645–4648 (1996).

[29] V.V. Badikov, I.N. Matveev, S.M. Pshenichnikov, O.V. Skrebneva, N.K. Trotsenko, N.D. Ustinov: Dispersion of birefringence and the optical activity of $AgGa(S_{1-x}Se_x)_2$ crystals. Kristallogr. **26(3)**, 537–539 (1981) [In Russian, English trans.: Sov. Phys. - Crystallogr. **26(3)**, 304–305 (1981)].

[30] E. Takaoka, K. Kato: Thermo-optic dispersion formula for $AgGaS_2$. Appl. Opt. **38(21)**, 4577–4580 (1999).

[31] G.C. Bhar, R.C. Smith: Silver thiogallate ($AgGaS_2$)—Part II: linear optical properties. IEEE J. Quant. Electr. **QE-10(7)**, 546–550 (1974).

[32] G.C. Bhar: Refractive index interpolation in phase-matching. Appl. Opt. **15(2)**, 305–307 (1976).

[33] T. Itabe, J.L. Bufton: Phase-matching measurements for 10-μm upconversion in $AgGaS_2$. Appl. Opt. **23(18)**, 3044–3047 (1984).

[34] Y.X. Fan, R.C. Eckardt, R.L. Byer, R.K. Route, R.S. Feigelson: $AgGaS_2$ infrared parametric oscillator. Appl. Phys. Lett. **45(4)**, 313–315 (1984).

[35] H.-J. Krause, W. Daum: High-power source of coherent picosecond light pulses tunable from 0.41 to 12.9 μm. Appl. Phys. B **56(1)**, 8–13 (1993).

[36] J.-J. Zondy, D. Touahri: Updated thermo-optic coefficients of $AgGaS_2$ from temperature-tuned noncritical $3\omega - \omega \rightarrow 2\omega$ infrared parametric amplification. J. Opt. Soc. Am. B **14(6)**, 1331–1338 (1997).

[37] G.C. Bhar, D.K. Ghosh, P.S. Ghosh, D. Schmitt: Temperature effects in $AgGaS_2$ nonlinear devices. Appl. Opt. **22(16)**, 2492–2494 (1983).

[38] V.M. Cound, P.H. Davies, K.F. Hulme, D. Robertson: The electrooptic coefficients of silver thiogallate ($AgGaS_2$). J. Phys. C **3(4)**, L83–L84 (1970).

[39] R.C. Eckardt, H. Masuda, Y.X. Fan, R.L. Byer: Absolute and relative nonlinear optical coefficients of KDP, KD*P, BaB_2O_4, $LiIO_3$, MgO:$LiNbO_3$, and KTP measured by phase-matched second-harmonic generation. IEEE J. Quant. Electr. **26(5)**, 922–933 (1990).

[40] J.E. Midwinter, J. Warner: The effects of phase matching method and of uniaxial crystal symmetry on the polar distribution of second-order non-linear optical polarization. Brit. J. Appl. Phys. **16(11)**, 1135–1142 (1965).

[41] E.C. Cheung, K. Koch, G.T. Moore, J.M. Liu: Measurements of second-order nonlinear optical coefficients from the spectral brightness of parametric fluorescence. Opt. Lett. **19(3)**, 168–170 (1994).

[42] D.A. Roberts**:** Simplified characterization of uniaxial and biaxial nonlinear optical crystals: a plea for standardization of nomenclature and conventions. IEEE J. Quant. Electr. **28(10)**, 2057–2074 (1992).

[43] P.J. Kupeček, C.A. Schwartz, D.S. Chemla: Silver thiogallate ($AgGaS_2$)—Part I: nonlinear optical properties. IEEE J. Quant. Electr. **QE-10(7)**, 540–545 (1974).

[44] P. Canarelli, Z. Benko, A.H. Hielscher, R.F. Curl, F.K. Tittel: Measurements of nonlinear coefficient and phase matching characteristics of $AgGaS_2$. IEEE J. Quant. Electr. **28(1)**, 52–55 (1992).
[45] K. Kato: Second-harmonic and sum-frequency generation in $ZnGeP_2$. Appl. Opt. **36(12)**, 2506–2510 (1997).
[46] T. Elsaesser, A. Seilmeier, W. Kaiser, P. Koidl, G. Brandt: Parametric generation of tunable picosecond pulses in the medium infrared using $AgGaS_2$ crystals. Appl. Phys. Lett. **44(4)**, 383–385 (1984).
[47] H.J. Bakker, J.T.M. Kennis, H.J. Kop, A. Lagendijk: Generation of intense picosecond pulses tunable between 1.2 and 8.7 μm. Opt. Commun. **86(1)**, 58–64 (1991).
[48] T. Elsaesser, H. Lobentanzer, A. Seilmeier: Generation of tunable picosecond pulses in the medium infrared by down-conversion in $AgGaS_2$. Opt. Commun. **52(5)**, 355–359 (1985).
[49] A.G. Yodh, H.W.K. Tom, G.D. Aumiller, R.S. Miranda: Generation of tunable mid-infrared picosecond pulses at 76 MHz. J. Opt. Soc. Am. B **8(8)**, 1663–1667 (1991).
[50] D.C. Hanna, V.V. Rampal, R.C. Smith: Tunable infrared down-conversion in silver thiogallate. Opt. Commun. **8(2)**, 151–153 (1973).
[51] D.C. Hanna, V.V. Rampal, R.C. Smith: Tunable medium infrared generation in silver thiogallate ($AgGaS_2$) by down-conversion of flash-pumped dye-laser radiation. IEEE J. Quant. Electr. **QE-10(4)**, 461–462 (1974).
[52] K. Kato: High-power difference-frequency generation at 5–11 μm in $AgGaS_2$. IEEE J. Quant. Electr. **QE-20(7)**, 698–699 (1984).
[53] G.C. Bhar, S. Das, U. Chatterjee, R.S. Feigelson, R.K. Route: Synchronous and non-collinear infrared upconversion in $AgGaS_2$. Appl. Phys. Lett. **54(16)**, 1489–1491 (1989).
[54] S.A. Andreev, I.N. Matveev, I.P. Nekrasov, S.M. Pshenichnikov, N.P. Sopina: Parametric conversion of infrared radiation in an $AgGaS_2$ crystal. Kvant. Elektron. **4(3)**, 657–659 (1977) [In Russian, English trans.: Sov. J. Quantum Electron. **7(3)**, 366–368 (1977)].
[55] W. Jantz, P. Koidl: Efficient up-conversion of 10.6-μm radiation into the green spectral range. Appl. Phys. Lett. **31(2)**, 99–101 (1977).
[56] A.P. Gorchakov, A.A. Popesku, V.S. Solomatin: Nonlinear spectroscopy based on a silver thiogallate crystal. Kvant. Elektron. **5(2)**, 413–415 (1978) [In Russian, English trans.: Sov. J. Quantum Electron. **8(2)**, 236–237 (1978)].
[57] N. Saito, K. Akagawa, S. Wada, H. Tashiro: Difference-frequency generation by mixing dual-wavelength pulses emitting from an electronically tuned Ti:sapphire laser. Appl. Phys. B **69(2)**, 93–97 (1999).
[58] J.F. Xia, J. Song, D. Strickland: Development of a dual-wavelength Ti:sapphire multi-pass amplifier and its application to intense mid-infrared generation. Opt. Commun. **206(1–3)**, 149–157 (2002).
[59] K.L. Vodopyanov, J.P. Maffetone, I. Zwieback, W. Ruderman: $AgGaS_2$ optical parametric oscillator continuously tunable from 3.9 to 11.3 μm. Appl. Phys. Lett. **75(9)**, 1204–1206 (1999).
[60] D.C. Hanna, B. Luther-Davies, H.N. Rutt, R.C. Smith, C.R. Stanley: Q-switched laser damage of infrared nonlinear materials. IEEE J. Quant. Electr. **QE-8(3)**, 317–324 (1972).
[61] P.B. Phua, R.F. Wu, T.C. Chong, B.X. Xu: Nanosecond $AgGaS_2$ optical parametric oscillator with more than 4 micron output. Jpn. J. Appl. Phys. **36(12B)**, L1661–L1664 (1997).
[62] K.G. Spears, X. Zhu, X. Yang, L. Wang: Picosecond infrared generation from Nd:YAG and a visible short-cavity dye laser. Opt. Commun. **66(2–3)**, 167–171 (1988).
[63] T. Dahinten, U. Plödereder, A. Seilmeier, K.L. Vodopyanov, K.R. Allakhverdiev, Z.A. Ibragimov: Infrared pulses of 1 picosecond duration tunable between 4 μm and 18 μm. IEEE J. Quant. Electr. **29(7)**, 2245–2250 (1993).

[64] S. Haidar, K. Nakamura, E. Niwa, K. Masumoto, H. Ito: Mid-infrared (5–12-μm) and limited (5.5–8.5-μm) single-knob tuning generated by difference frequency mixing in single-crystal $AgGaS_2$. Appl. Opt. **38(9)**, 1798–1801 (1999).
[65] H. Kildal, G.W. Iseler: Laser-induced surface damage of infrared nonlinear materials. Appl. Opt. **15(12)**, 3062–3065 (1976).
[66] B. Golubovic, M.K. Reed: All-solid-state generation of 100-kHz tunable mid-infrared 50-fs pulses in type I and type II $AgGaS_2$. Opt. Lett. **23(22)**, 1760–1762 (1998).
[67] K.J. McEwan: High-power synchronously pumped $AgGaS_2$ optical parametric oscillator. Opt. Lett. **23(9)**, 667–669 (1998).

3.2 $AgGaSe_2$, Silver Gallium Selenide (AGSe)

Negative uniaxial crystal: $n_o > n_e$ (at $\lambda < 0.804\,\mu m$ $n_e > n_o$)
Molecular mass: 335.511
Specific gravity: 5.70 g/cm^3 [1], [2]; 5.71 g/cm^3 [3], 5.76 g/cm^3 [4]
Point group: $\bar{4}2m$
Lattice constants:
$a = 5.9220$ Å [5]; 5.99202 ± 0.00018 Å [6]
$c = 10.8803$ Å [5]; 10.88626 ± 0.00030 Å [6]
Mohs hardness: 3–3.5
Melting point: 1123 K [3]; 1124 K [2]; 1129 K [7]; 1133 K [8]

Mean value of linear thermal expansion coefficient α_t

T [K]	$\alpha_t \times 10^6$ [K^{-1}], $\parallel c$	$\alpha_t \times 10^6$ [K^{-1}], $\perp c$	Ref.
298–423	−8.1	19.8	[9]
	−6.4	23.4	[4]
298–573	−9.6	24.6	[9]
	−15.7	16.3	[10]
423–773	−12.6	28.0	[9]
423–873	−16.0	18.0	[4]

Specific heat capacity c_p at $P = 0.101325$ MPa [11]

T [K]	c_p [J/kgK]
300	297
400	311
500	318

Thermal conductivity coefficient κ [12]

T [K]	κ [W/mK], $\parallel c$	κ [W/mK], $\perp c$
293	1.0	1.1

Band-gap energy at room temperature: $E_g = 1.65$ eV [3]; 1.72 [13]; 1.8 eV [14]; 1.803 eV [15]; 1.83 eV [2];
1.713 eV ($\mathbf{E} \perp c$) [16]; 1.689 eV($\mathbf{E} \| c$) [16]
Transparency range:
at $\alpha = 1\,\text{cm}^{-1}$ level: 0.76–17 μm [7]
at $\alpha = 3\,\text{cm}^{-1}$ level: 0.78–18 μm [13]
at "0" transmittance level: 0.71–19 μm [8], [17]

Linear absorption coefficient α

λ [μm]	α [cm^{-1}]	Ref.	Note
1	<0.02	[18]	
1–11	0.01–0.18	[2]	typical values
1.06	0.018	[19]	*e*-wave
1.064	0.012–0.2	[2]	typical values
	0.006	[2]	best value
1.3	0.002	[20]	*o*-wave, OPO direction
	0.002	[20]	*e*-wave, OPO direction
1.45–1.6	<0.015	[19]	*o*-wave, *e*-wave
1.8	<0.02	[16]	*e*-wave
1.9	0.012–0.2	[2]	typical values, *e*-wave
	0.01	[2]	best value, *e*-wave
2.0	0.012	[21]	*o*-wave, OPO direction
	0.030	[21]	*e*-wave, OPO direction
	0.004	[22]	
2–5	<0.05	[23]	
2.05	0.015–0.058	[24]	
	<0.01	[25]	
2.1	0.06–0.07	[17]	
	<0.05	[26]	
	0.012–0.072	[27]	
2.15	0.03–0.08	[2]	typical values, *e*-wave
	0.0135	[19]	*e*-wave
	0.01	[2]	best value, *e*-wave
2.2	0.002–0.004	[20]	*o*-wave, OPO direction
	0.02–0.05	[20]	*e*-wave, OPO direction
2.8	0.008–0.012	[2]	typical values
	0.006	[2]	best value
4.65	0.05	[28]	SHG direction
4.775	<0.02	[29]	
5–11	<0.02	[18]	
9.2–10.8	0.02	[30]	*o*-wave
9.3	0.05	[28]	SHG direction
9.5	0.03	[31]	
9.55	<0.1	[32]	SHG direction
	<0.02	[29]	

λ [μm]	α [cm^{-1}]	Ref.	Note
10.6	0.089	[33]	
	<0.02	[16]	
	0.01–0.06	[34]	
	0.01–0.018	[2]	typical values
	0.007	[2]	best value
	0.002	[8]	

Two-photon absorption coefficient β

λ [μm]	τ_p [ns]	$\beta \times 10^{11}$ [cm/W]	Ref.	Note
1.06	~10	140 (?)	[15]	$\perp c$, *e*-wave
1.08	0.04	2500	[35]	$\parallel c$
1.319	70	3600	[36]	*o*-wave, Eksma sample
		1800	[36]	*e*-wave, Eksma sample
		1800	[36]	*o*-wave, Cleveland Crystals sample
		600	[36]	*e*-wave, Cleveland Crystals sample
1.338	70	3000	[36]	*o*-wave, Eksma sample
		1300	[36]	*e*-wave, Eksma sample
1.395	15	3700	[36]	*o*-wave, Eksma sample
1.540	15	800	[36]	*o*-wave, Eksma sample
1.590	15	200	[36]	*o*-wave, Eksma sample
		80	[36]	*e*-wave, Eksma sample

Experimental values of refractive indices [5]

λ [μm]	n_o	n_e	λ [μm]	n_o	n_e
0.725	2.8452	2.8932	2.800	2.6261	2.5943
0.750	2.8191	2.8415	3.000	2.6245	2.5925
0.800	2.7849	2.7866	3.200	2.6231	2.5912
0.850	2.7598	2.7522	3.400	2.6221	2.5899
0.900	2.7406	2.7275	3.600	2.6213	2.5889
0.950	2.7252	2.7085	3.800	2.6203	2.5876
1.000	2.7132	2.6934	4.000	2.6189	2.5863
1.100	2.6942	2.6712	4.500	2.6166	2.5840
1.200	2.6806	2.6554	5.000	2.6144	2.5819
1.300	2.6705	2.6438	5.500	2.6128	2.5800
1.400	2.6624	2.6347	6.000	2.6113	2.5784
1.600	2.6516	2.6224	6.500	2.6094	2.5765
1.800	2.6432	2.6131	7.000	2.6070	2.5743
2.000	2.6376	2.6071	7.500	2.6049	2.5723
2.200	2.6336	2.6027	8.000	2.6032	2.5704
2.400	2.6304	2.5992	8.500	2.6009	2.5681
2.600	2.6286	2.5968	9.000	2.5988	2.5659

λ [μm]	n_o	n_e	λ [μm]	n_o	n_e
9.500	2.5964	2.5635	12.00	2.5837	2.5505
10.00	2.5939	2.5608	12.50	2.5805	2.5473
10.50	2.5917	2.5585	13.00	2.5771	2.5439
11.00	2.5890	2.5555	13.50	2.5731	2.5404
11.50	2.5868	2.5536			

Optical activity [37]: $\rho = 7$ deg/mm at isotropic point ($n_o = n_e$, $\lambda = 0.804\,\mu$m)

Temperature derivative of refractive indices

λ [μm]	T [K]	$dn_o/dT \times 10^6$ [K^{-1}]	$dn_e/dT \times 10^6$ [K^{-1}]	Ref.
2.05			57 ± 9	[24]
3.3913	308	45	76	[17]

Nonlinear refractive index γ [38]

λ [μm]	$\gamma \times 10^{15}$ [cm^2/W]
1.55	35

Best set of Sellmeier equations (λ in μm, $T = 293$ K) [19], [39]:

$$n_o^2 = 6.8507 + \frac{0.4297}{\lambda^2 - 0.1584} - 0.00125\,\lambda^2$$

$$n_e^2 = 6.6792 + \frac{0.4598}{\lambda^2 - 0.2122} - 0.00126\,\lambda^2$$

In [40], [41], improved dispersion relations for 11–16 μm wavelength range are given. Other sets of dispersion relations are given in [10], [18], [42], [43], [44].
Temperature derivative of refractive indices for spectral range 2.05–10.59 μm and temperature range 293–393 K (λ in μm) [45]:

$$dn_o/dT = (0.046\,\lambda + 7.514) \times 10^{-5} K^{-1}$$

$$dn_e/dT = (0.061\,\lambda + 7.984) \times 10^{-5} K^{-1}$$

Linear electrooptic coefficients measured at low frequencies (well below the acoustic resonances of $AgGaSe_2$ crystal, i.e., for the "free" crystal) at room temperature [46]

λ [μm]	r_{41}^T [pm/V]	r_{63}^T [pm/V]
1.15	4.5	3.9

Expressions for the effective second-order nonlinear coefficient in general case (Kleinman symmetry conditions are valid, $d_{14} = d_{25} = d_{36}$) [47]:

$$d_{ooe} = -d_{36} \sin(\theta + \rho) \sin 2\phi$$

$$d_{eoe} = d_{oee} = 2d_{36} \sin(\theta + \rho) \cos(\theta + \rho) \cos 2\phi$$

Simplified expressions for the effective second-order nonlinear coefficient (approximation of small birefringence angle, Kleinman symmetry conditions are valid, $d_{14} = d_{25} = d_{36}$) [48]:

$$d_{\mathrm{ooe}} = -d_{36} \sin\theta \sin 2\phi$$

$$d_{\mathrm{eoe}} = d_{\mathrm{oee}} = d_{36} \sin 2\theta \cos 2\phi$$

Absolute values of second-order nonlinear coefficient:
$d_{36}(9.2714\,\mu\mathrm{m}) = 41.4 \pm 2.0\,\mathrm{pm/V}$ [49], [39]
$d_{36}(10.591\,\mu\mathrm{m}) = 39.5 \pm 1.9\,\mathrm{pm/V}$ [49], [39]

Experimental values of phase-matching angle ($T = 293\,\mathrm{K}$)

Interacting wavelengths [μm]	θ_{exp} [deg]	Ref.
SHG, $o + o \Rightarrow e$		
$10.63 \Rightarrow 5.315$	55.9	[42]
$10.6114 \Rightarrow 5.3057$	55.6	[39]
$10.6 \Rightarrow 5.3$	57.5	[8]
$10.591 \Rightarrow 5.2955$	55.5	[39]
$10.55 \Rightarrow 5.275$	55.3	[42]
$10.3 \Rightarrow 5.15$	53.7	[42]
$10.21 \Rightarrow 5.15$	53.1	[42]
$9.66 \Rightarrow 4.83$	~49	[50]
$9.64 \Rightarrow 4.82$	50.0	[44]
$9.5525 \Rightarrow 4.77625$	49.6	[39]
$9.55 \Rightarrow 4.775$	48.8	[44]
$9.5039 \Rightarrow 4.75195$	49.3	[39]
$9.31 \Rightarrow 4.655$	48.3	[44]
$9.2824 \Rightarrow 4.6412$	48.3	[39]
$9.2714 \Rightarrow 4.6357$	48.2	[39]
$9.2007 \Rightarrow 4.60035$	47.9	[39]
$6 \Rightarrow 3$	42.2	[42]
$5.2955 \Rightarrow 2.64775$	41.3	[39]
$5.2 \Rightarrow 2.6$	40.3	[42]
$4.6357 \Rightarrow 2.31785$	44.6	[39]
$4.1 \Rightarrow 2.05$	49.7	[25]
	50.0	[39]
$3.3913 \Rightarrow 1.69565$	65.8	[39]
SFG, $o + o \Rightarrow e$		
$12.15 + 10.63 \Rightarrow 5.67$	61	[42]
$10.63 + 5.33 \Rightarrow 3.55$	42.7	[42]
$5.515 + 3.3913 \Rightarrow 2.1$	≈48	[17]
$4.84 + 3.55 \Rightarrow 2.0479$	49.2	[25]
$5.13 + 2.685 \Rightarrow 1.763$	61.3	[51]
$6.00 + 2.586 \Rightarrow 1.807$	56	[51]

Interacting wavelengths [μm]	θ_{exp} [deg]	Ref.
$7.43 + 2.484 \Rightarrow 1.862$	49.5	[51]
$9.93 + 2.384 \Rightarrow 1.923$	45.8	[51]
$6.95 + 1.66 \Rightarrow 1.34$	≈78	[25]
$7.4 + 1.604 \Rightarrow 1.318$	80	[8]
$8.8 + 1.550 \Rightarrow 1.318$	70	[8]
$12.3 + 1.476 \Rightarrow 1.318$	60	[8]

Experimental values of internal angular and spectral bandwidths

Interacting wavelengths [μm]	$\Delta\theta^{int}$ [deg]	$\Delta\nu_1$ [cm^{-1}]	Ref.
SHG, $o + o \Rightarrow e$			
$9.3 \Rightarrow 4.65$	0.85		[28]
$10.25 \Rightarrow 5.125$	0.85		[34]
SFG, $o + o \Rightarrow e$			
$5.515 + 3.3913 \Rightarrow 2.1$	0.54		[17]
$10.6 + 1.318 \Rightarrow 1.1722$	1.2		[52]
DFG, $e - o \Rightarrow o$			
$1.2899 - 1.5715 \Rightarrow 7.2$		14.8	[53]

Experimental values of temperature bandwidth [45]

Interacting wavelengths [μm]	θ_{exp} [deg]	ΔT [°C]
SHG, $o + o \Rightarrow e$		
$10.591 \Rightarrow 5.2955$	55.5	350
$5.2955 \Rightarrow 2.6478$	41.3	230
SHG, $e + o \Rightarrow e$		
$5.2955 \Rightarrow 2.6478$	72.2	260
SFG, $o + o \Rightarrow e$		
$10.591 + 5.2955 \Rightarrow 3.5303$	42.4	390
$10.591 + 3.5303 \Rightarrow 2.6478$	41.3	220
SFG, $e + o \Rightarrow e$		
$10.591 + 5.2955 \Rightarrow 3.5303$	56.6	550
$10.591 + 3.5303 \Rightarrow 2.6478$	50.4	260

Laser-induced surface-damage threshold

λ [μm]	τ_p [ns]	I_{thr} [GW/cm^2]	Ref.	Note
1.0642	35	0.011	[42]	1000 pulses
		0.03	[42]	single pulse
	23	0.013–0.04	[25]	
1.57	6	>0.02	[54]	5 kHz

λ [μm]	τ_p [ns]	I_{thr} [GW/cm^2]	Ref.	Note
2.0	30	0.0083	[21]	5 kHz, uncoated crystal
		<0.013	[21]	5 kHz, coated crystal
	20–30	0.02–0.03	[22]	
2.05	55	0.006–0.01	[26]	
	50	0.025	[25]	
2.097	180	0.007	[39]	5 Hz
2.1	180	0.0094	[27]	uncoated crystal
		0.017	[27]	coated crystal
	50	0.013	[17]	
2.79	40	0.025	[23]	
9.2–10.8	CW	0.00004	[30]	
9.27	50	0.05	[39]	1 Hz
9.3	50	0.03	[28]	1 Hz
9.5	30	0.033	[31]	
9.55	30	0.15	[32]	SHG direction
10.2	CW	0.00001–0.00004	[55]	uncoated crystal
		0.00006	[55]	coated crystal
10.25	75	0.012	[34]	10 pulses
10.6	150	0.01–0.02	[56]	

Laser-induced bulk-damage threshold [30]

λ [μm]	τ_p [ns]	I_{thr} [GW/cm^2]
9.2–10.8	CW	0.0001

About the crystal

In comparison with AGS, AGSe has a longer transmission in the IR range, up to 17 μm instead of 11.4 μm (at 1 cm^{-1} level). Therefore, silver gallium selenide is widely used not only for DFG and OPO but also for SHG of CO_2 laser radiation. In [30], the CW second-harmonic output of about 6 mW in the 4.6–5.4-μm range was generated in a 1.9-cm-long AGSe crystal. In [29], the 2-ns pulses of a CO_2 laser ($\lambda = 9.55$ μm) were used, and the second-harmonic pulse energy, generated in a 4-cm-long crystal, reached 100 mJ. Difference-frequency generation is achieved by mixing idler and signal output waves of OPO in AGSe [57], [58]. In [57], KTP-based OPO pumped by a mode-locked Ti:sapphire laser was used, and the tunability range of 8–18 μm was obtained. In [58], $LiNbO_3$-based OPO was employed, and the difference-frequency wavelength was tuned in the 5–18 μm range. The ASGe-based OPO was pumped either by 1.57 μm output of KTP OPO [54] or by 1.55-μm output of CTA OPO [38]. In the first case, the tunability range of 5–18 μm with IR pulse energies up to 1.2 mJ was obtained. In the second experiment, the tunability range was 4–8 μm, and the mean IR power reached 35 mW at 4.55 μm.

References

[1] B.H.T. Chai: Optical Crystals. In: *CRC Handbook of Laser Science and Technology, Supplement 2: Optical Materials*, ed. by M.J. Weber (CRC Press, Boca Raton, 1995), pp. 3–65.

[2] G.C. Catella, D. Burlage: Crystal growth and optical properties of $AgGaS_2$ and $AgGaSe_2$. MRS Bulletin **23(7)**, 28–36 (1998).

[3] *Physical-Chemical Properties of Semiconductors. Handbook*. (Nauka, Moscow, 1979) [In Russian].

[4] D. Eimerl, J. Marion, E.K. Graham, H.A. McKinstry, S. Haussühl: Elastic components and thermal fracture of $AgGaSe_2$ and d-LAP. IEEE J. Ouant. Electr. **27(1)**, 142–145 (1991).

[5] G.D. Boyd, H.M. Kasper, J.H. McFee, F.G. Storz: Linear and nonlinear optical properties of some ternary selenides. IEEE J. Quant. Electr. **QE-8(12)**, 900–908 (1972).

[6] V.I. Gavrilenko, A.M. Grekhov, D.B. Korbutyak, V.G. Litovchenko: *Optical Properties of Semiconductors. Handbook*. (Naukova Dumka, Kiev, 1987) [In Russian].

[7] R.S. Feigelson, R.K. Route: Recent developments in the growth of chalcopyrite crystals for nonlinear infrared applications. Opt. Eng. **26(2)**, 113–119 (1987).

[8] R.L. Byer, M.M. Choy, R.L. Herbst, D.S. Chemla, R.S. Feigelson: Second harmonic generation and infrared mixing in $AgGaSe_2$. Appl. Phys. Lett. **24(2)**, 65–68 (1974).

[9] G.W. Iseler: Thermal expansion and seeded Bridgman growth of $AgGaSe_2$. J. Cryst. Growth **41(1)**, 146–150 (1977).

[10] P.G. Schunemann, S.D. Setzler, T.M. Pollak: Phase-matched crystal growth of $AgGaSe_2$ and $AgGa_{1-x}In_xSe_2$. J. Cryst. Growth **211(1–4)**, 257–264 (2000).

[11] H. Neumann, G. Kühn, W. Möller: High-temperature specific heat of $AgInS_2$ and $AgGaSe_2$. Cryst. Res. Technol. **20(9)**, 1225–1229 (1985).

[12] J.D. Beasley: Thermal conductivities of some novel nonlinear optical materials. Appl. Opt. **33(6)**, 1000–1003 (1994).

[13] G.C. Bhar, R.C. Smith: Optical properties of II-IV-V_2 and I-III-VI_2 crystals with particular reference to transmission limits. Phys. Stat. Solidi A **13(1)**, 157–168 (1972).

[14] E.W. van Stryland, L.L. Chase: Two-Photon Absorption. Inorganic Materials. In: *CRC Handbook of Laser Science and Technology, Supplement 2: Optical Materials*, ed. by M.J. Weber (CRC Press, Boca Raton, 1995) pp. 299–328.

[15] A. Miller, G.S. Ash: Two-photon absorption and short pulse stimulated recombination in $AgGaSe_2$. Opt. Commun. **33(3)**, 297–300 (1980).

[16] Data sheet of Cleveland Crystals Inc. Available at www.clevelandcrystals.com.

[17] N.P. Barnes, D.J. Gettemy, J.R. Hietanen, R.A. Iannini: Parametric amplification in $AgGaSe_2$. Appl. Opt. **28(23)**, 5162–5168 (1989).

[18] V.V. Badikov, V.B. Laptev, V.L. Panyutin, E.A. Ryabov, G.S. Shevyrdyaeva, O.B. Scherbina: Growth and optical properties of nonlinear silver selenogallate single crystals. Kvant. Elektron. **19(8)**, 782–784 (1992) [In Russian, English trans.: Sov. J. Quantum Electron. **22(8)**, 722–724 (1992)].

[19] H. Komine, J.M. Fukumoto, W.H. Long, Jr., E.A. Stappaerts: Noncritically phase matched mid-infrared generation in $AgGaSe_2$. IEEE J. Sel. Topics Quant. Electr. **1(1)**, 44–49 (1995).

[20] G.C. Catella, L.R. Shiozawa, J.R. Hietanen, R.C. Eckardt, R.K. Route, R.S. Feigelson, D.G. Cooper, C.L. Marquardt: Mid-IR absorption in $AgGaSe_2$ optical parametric oscillator crystal. Appl. Opt. **32(21)**, 3948–3951 (1993).

[21] P.A. Budni, M.G. Knights, E.P. Chicklis, K.L. Schepler: Kilohertz AgGaSe2 optical parametric oscillator pumped at 2 μm. Opt. Lett. **18(13)**, 1068–1070 (1993).

[22] U. Simon, Z. Benko, M.W. Sigrist, R.F. Curl, F.K. Tittel: Design consideration of an infrared spectrometer based on difference-frequency generation in $AgGaSe_2$. Appl. Opt. **32(33)**, 6650–6655 (1993).

[23] J. Kirton: A 2.54 μm-pumped type II $AgGaSe_2$ mid-IR optical parametric oscillator. Opt. Commun. **115(1–2)**, 93–98 (1995).

[24] C.L. Marquardt, D.G. Cooper, P.A. Budni, M.G. Knights, K.L. Schepler, R. DeDomenico, G.C. Catella: Thermal lensing in silver gallium selenide parametric oscillator crystal. Appl. Opt. **33(15)**, 3192–3197 (1994).

[25] R.C. Eckardt, Y.X. Fan, R.L. Byer, C.L. Marquardt, M.E. Storm, L. Esterowitz: Broadly tunable infrared parametric oscillator using $AgGaSe_2$. Appl. Phys. Lett. **49(11)**, 608–610 (1986).

[26] P.G. Schunemann, K.L. Schepler, P.A. Budni: Nonlinear frequency conversion performance of $AgGaSe_2$, $ZnGeP_2$, and $CdGeAs_2$. MRS Bulletin **23(7)**, 45–49 (1998).

[27] B.C. Ziegler, K.L. Schepler: Transmission and damage-threshold measurements in $AgGaSe_2$ at 2.1 μm. Appl. Opt. **30(34)**, 5077–5080 (1991).

[28] Y.M. Andreev, V.V. Butuzov, G.A. Verozubova, A.I. Gribenyukov, S.V. Davydov, V.P. Zakharov: Generation of the second harmonic of pulsed CO_2-laser radiation in $AgGaSe_2$ and $ZnGeP_2$ single crystals. Laser Phys. **5(5)**, 1014–1019 (1995).

[29] H.P. Chou, R.C. Slater, Y. Wang: High-energy, fourth-harmonic generation using CO_2 lasers. Appl. Phys. B **66(5)**, 555–559 (1998).

[30] S.Y. Tochitsky, V.O. Petukhov, V.A. Gorobets, V.V. Churakov, V.N. Yakimovich: Efficient continuous-wave frequency doubling of a tunable CO_2 laser in $AgGaSe_2$. Appl. Opt. **36(9)**, 1882–1888 (1997).

[31] D.A. Russell, R. Ebert: Efficient generation and heterodyne detection of 4.75-μm light with second-harmonic generation. Appl. Opt. **32(33)**, 6638–6644 (1993).

[32] Y.M. Andreev, V.V. Badikov, V.G. Voevodin, L.G. Geiko, P.P. Geiko, M.V. Ivashchenko, A.I. Karapuzikov, I.V. Sherstov: Radiation resistance of nonlinear crystals at a wavelength of 9.55 μm. Kvant. Elektron. **31(12)**, 1075–1078 (2001) [In Russian, English trans.: Quantum Electron. **31(12)**, 1075–1078 (2001)].

[33] N.P. Barnes, R.C. Eckardt, D.J. Gettemy, L.B. Edgett: Absorption coefficients and the temperature variation of the refractive index difference of nonlinear optical crystals. IEEE J. Quant. Electr. **QE-15(10)**, 1074–1076 (1979).

[34] R.C. Eckardt, Y.X. Fan, R.L. Byer, R.K. Route, R.S. Feigelson, J. van der Laan: Efficient second harmonic generation of 10-μm radiation in $AgGaSe_2$. Appl. Phys. Lett. **47(8)**, 786–788 (1985).

[35] A.A. Bugaev, G.K. Averkieva, V.D. Prochukhan: Two-photon absorption and nonstationary energy transfer in the ternary semiconductor $AgGaSe_2$. Fiz. Tverd. Tela **37(8)**, 2495–2502 (1995) [In Russian, English trans.: Phys. Solid State **37(8)**, 1367–1370 (1995)].

[36] S. Pearl, S. Fastig, Y. Ehrlich, R. Lavi: Limited efficiency of a silver selenogallate optical parametric oscillator caused by two-photon absorption. Appl. Opt. **40(15)**, 2490–2492 (2001).

[37] V.V. Badikov, I.N. Matveev, S.M. Pshenichnikov, O.V. Skrebneva, N.K. Trotsenko, N.D. Ustinov: Dispersion of birefringence and the optical activity of $AgGa(S_{1-x}Se_x)_2$ crystals. Kristallogr. **26(3)**, 537–539 (1981) [In Russian, English trans.: Sov. Phys.-Crystallogr. **26(3)**, 304–305 (1981)].

[38] S. Marzenell, R. Beigang, R. Wallenstein: Synchronously pumped femtosecond optical oscillator based on $AgGaSe_2$ tunable from 2 μm to 8 μm. Appl. Phys. B **69(5–6)**, 423–428 (1999).

[39] A. Harasaki, K. Kato: New data on the nonlinear optical constant, phase-matching, and optical damage of $AgGaS_2$. Jpn. J. Appl. Phys. **36(2)**, 700–703 (1997).
[40] H.W. Wang, M.H. Lu: The refractive index of extraordinary wave for $AgGaSe_2$ crystal in 11–16 μm range. Opt. Commun. **192(3–6)**, 357–363 (2001).
[41] H.W. Wang, M.H. Lu: A two-stage up-convertor made of $AgGaSe_2$ and β-BBO crystals. Appl. Phys. B **70(1)**, 15–21 (2001).
[42] H. Kildal, J.C. Mikkelsen: The nonlinear optical coefficient, phasematching and optical damage in chalcopyrite $AgGaSe_2$. Opt. Commun. **9(3)**, 315–318 (1973).
[43] G.C. Bhar: Refractive index interpolation in phase-matching. Appl. Opt. **15(2)**, 305–307 (1976).
[44] Y.M. Andreev, I.S. Baturin, P.P. Geiko, A.I. Gusamov: Frequency doubling of CO_2-laser radiation in new nonlinear crystal $AgGa_xIn_{1-x}Se_2$. Kvant. Elektron. **29(1)**, 66–70 (1999) [In Russian, English trans.: Quantum Electron. **29(10)**, 904–908 (1999)].
[45] E. Tanaka, K. Kato: Thermo-optic dispersion formula of $AgGaSe_2$ and its practical applications. Appl. Opt. **37(3)**, 561–564 (1998).
[46] H. Horinaka, H. Sonomura, T. Miyauchi: Linear electro-optic effect of $AgGaSe_2$. Jpn. J. Appl. Phys. **21(10)**, 1485–1488 (1982).
[47] R.C. Eckardt, H. Masuda, Y.X. Fan, R.L. Byer: Absolute and relative nonlinear optical coefficients of KDP, KD*P, BaB_2O_4, $LiIO_3$, MgO:$LiNbO_3$, and KTP measured by phase-matched second-harmonic generation. IEEE J. Quant. Electr. **26(5)**, 922–933 (1990).
[48] J.E. Midwinter, J. Warner: The effects of phase matching method and of uniaxial crystal symmetry on the polar distribution of second-order non-linear optical polarization. Brit. J. Appl. Phys. **16(11)**, 1135–1142 (1965).
[49] K. Kato: Second-harmonic and sum-frequency generation in $ZnGeP_2$. Appl. Opt. **36(12)**, 2506–2510 (1997).
[50] G.C. Bhar, S. Das, U. Chatterjee, P.K. Datta, Y.N. Andreev: Noncritical second harmonic generation of CO_2 laser radiation in mixed chalcopyrite crystal. Appl. Phys. Lett. **63(10)**, 1316–1318 (1993).
[51] A. Bianchi, M. Garbi: Down-conversion in the 4–18 μm range with GaSe and $AgGaSe_2$ nonlinear crystals. Opt. Commun. **30(1)**, 122–124 (1979).
[52] G.C. Bhar, S. Das, R.K. Route, R.S. Feigelson: Synchronous pulsed infrared detection in $AgGaSe_2$ crystal using 1.318 μm pump. Appl. Phys. B **65(4–5)**, 471–473 (1997).
[53] B. Sumpf, D. Rehle, T. Kelz, H.-D. Kronfeldt: A tunable diode-laser spectrometer for the MIR region near 7.2 μm applying difference-frequency in $AgGaSe_2$. Appl. Phys. B **67(3)**, 369–373 (1998).
[54] S. Chandra, T.H. Alik, G. Catella, R. Utano, J.A. Hutchinson: Continuously tunable, 6–14 μm silver-gallium selenide optical parametric oscillator pumped at 1.57 μm. Appl. Phys. Lett. **71(5)**, 584–586 (1997).
[55] J.-J. Zondy: Experimental investigation of single and twin $AgGaSe_2$ crystals for CW 10.2 μm SHG. Opt. Commun. **119(3–4)**, 320–326 (1995).
[56] H. Kildal, G.W. Iseler: Laser-induced surface damage of infrared nonlinear materials. Appl. Opt. **15(12)**, 3062–3065 (1976).
[57] J.M. Fraser, D. Wang, A. Hache, G.R. Allan, H.M. van Driel: Generation of high-repetition-rate femtosecond pulses from 8 to 18 μm. Appl. Opt. **36(21)**, 5044–5047 (1997).
[58] K.S. Abedin, S. Haidar, Y. Konno, C. Takyu, H. Ito: Difference frequency generation of 5–18 μm in a $AgGaSe_2$ crystal. Appl. Opt. **37(9)**, 1642–1646 (1998).

3.3 $ZnGeP_2$, Zinc Germanium Phosphide (ZGP)

Positive uniaxial crystal: $n_e > n_o$
Molecular mass: 199.928
Specific gravity: 4.12 g/cm^3 [1]; 4.162 g/cm^3 [2]; 4.175 g/cm^3 [3]
Point group: $\bar{4}2m$
Lattice constants:
$a = 5.465$ Å [4]; 5.465 Å [1]; 5.466 Å [5]
$c = 10.708$ Å [4]; 10.717 Å [1]; 10.722 Å [5]
Mohs hardness: 5.5
Knoop (or Vickers) hardness: 1020 at indenter load 50 g [6]
Melting point: 1293 K [1]; 1298 K [7]; 1300 ± 3 K [1], [8]; 1298–1301 K [9]; 1313 K [2]

Mean value of linear thermal expansion coefficient [6]

ΔT [K]	$\alpha_t \times 10^6$ [K^{-1}], $\parallel c$	$\alpha_t \times 10^6$ [K^{-1}], $\perp c$
293–573	15.9	17.5
573–873	8.08	9.1

Specific heat capacity at $P = 0.101325$ MPa:
$c_p = 392$ J/kgK [2]
$c_p = 464$ J/kgK [3]

Thermal conductivity coefficient κ [10]

T [K]	κ [W/mK], $\parallel c$	κ [W/mK], $\perp c$
293	36	35

Band-gap energy at $T = 300$ K: $E_g = 2.0$ eV [1]; 2.1 eV [1]
Transparency range at "0" transmittance level: 0.74–12 μm [11], [12]

Linear absorption coefficient α

λ [μm]	α [cm^{-1}]	Ref.	Note
1.064	1.52	[13]	
	1.06	[14]	best crystals
1.9	0.8–0.95	[15]	
2.0	0.15	[16]	*o*-wave, best crystals
	0.16	[17]	
2.05	0.35	[18]	
	0.26	[19]	*o*-wave
	0.23	[20]	
	0.2	[8]	*o*-wave, after annealing
	<0.1	[20]	best crystals
	0.09	[14]	best crystals
	0.02–0.04	[21]	after annealing and radiation processing

λ [μm]	α [cm^{-1}]	Ref.	Note
2.08	0.62	[22]	*o*-wave, mean value
	1.20	[22]	*e*-wave, mean value
2.15	0.6	[23]	
	0.09–0.25	[24]	typical crystals, *o*-wave
	0.03	[24]	best crystals, *o*-wave
2.39	0.55	[25]	
2.5	0.11	[8]	*o*-wave, as-grown crystals
2.5–8	<0.1	[26]	
2.5–8.3	<0.2	[27]	
2.5–8.5	<0.1	[28]	
2.73	0.03	[20]	
2.75	0.3	[29]	
2.79	0.06	[30]	
2.8	0.01	[24]	best crystals, *o*-wave
2.8–8.3	<0.1	[31]	
3–8	0.005–0.15	[32]	
	<0.1	[33]	
	<0.01	[14]	
3.15	0.17	[29]	
3.5–3.9	0.41	[34]	*o*-wave, SFG direction
3.5	0.4	[35]	
3.8	0.1–0.18	[15]	
3.9–4.5	0.10	[29]	
4–8.5	<0.05	[36]	
4.5–8	0.03	[37]	best samples
4.65	0.4	[38]	
	0.1–0.2	[39]	
	0.01–0.05	[40]	SHG direction
4.78	<0.055	[25]	
	0.16	[41]	
5.3–6.1	0.32	[34]	*e*-wave, SFG direction
5.5–6.3	0.10	[29]	
7.8	0.15	[29]	
8.24	0.02	[20]	
8.3	0.45	[29]	
8.3–9.5	<0.3	[27]	
9	0.9	[29]	
9.2	0.51	[19]	
9.28	0.4	[26]	
9.3	0.8	[38]	
	0.7	[40]	SHG direction
	0.4–0.5	[39]	
	0.48	[42]	*e*-wave
9.5	0.39	[42]	*e*-wave
9.55	0.26	[43]	SHG direction

λ [μm]	α [cm^{-1}]	Ref.	Note
	0.56	[41]	
9.6	0.33	[19]	
9.7	0.33	[42]	*e*-wave
10.0	0.45	[36]	
10.3	0.42	[44]	
10.4	0.6	[23]	
10.6	0.9	[35]	
	0.83	[34]	*e*-wave, SFG direction
	0.65	[19]	
10.7	0.88	[42]	*e*-wave
11.1	1.2	[36]	

Two-photon absorption coefficient β [45]

λ [μm]	τ_p [ns]	$\beta \times 10^{11}$ [cm/W]
1.3	0.00013	25

Experimental values of refractive indices [11]

λ [μm]	n_o	n_e	λ [μm]	n_o	n_e
0.64	3.5052	3.5802	3.40	3.1263	3.1647
0.66	3.4756	3.5467	3.60	3.1257	3.1632
0.68	3.4477	3.5160	3.80	3.1237	3.1616
0.70	3.4233	3.4885	4.00	3.1223	3.1608
0.75	3.3730	3.4324	4.20	3.1209	3.1595
0.80	3.3357	3.3915	4.50	3.1186	3.1561
0.85	3.3063	3.3593	4.70	3.1174	3.1549
0.90	3.2830	3.3336	5.00	3.1149	3.1533
0.95	3.2638	3.3124	5.50	3.1131	3.1518
1.00	3.2478	3.2954	6.00	3.1101	3.1480
1.10	3.2232	3.2688	6.50	3.1057	3.1445
1.20	3.2054	3.2493	7.00	3.1040	3.1420
1.30	3.1924	3.2346	7.50	3.0994	3.1378
1.40	3.1820	3.2244	8.00	3.0961	3.1350
1.60	3.1666	3.2077	8.50	3.0919	3.1311
1.80	3.1562	3.1965	9.00	3.0880	3.1272
2.00	3.1490	3.1889	9.50	3.0836	3.1231
2.20	3.1433	3.1829	10.00	3.0788	3.1183
2.40	3.1388	3.1780	10.50	3.0738	3.1137
2.60	3.1357	3.1745	11.00	3.0689	3.1087
2.80	3.1327	3.1717	11.50	3.0623	3.1008
3.00	3.1304	3.1693	12.00	3.0552	3.0949
3.20	3.1284	3.1671			

Temperature derivative of refractive indices [11]

λ [μm]	$dn_o/dT \times 10^6$ [K^{-1}]	$dn_e/dT \times 10^6$ [K^{-1}]	λ [μm]	$dn_o/dT \times 10^6$ [K^{-1}]	$dn_e/dT \times 10^6$ [K^{-1}]
0.64	359.4	375.8	3.40	144.0	154.6
0.66	312.3	373.4	3.60	155.8	162.9
0.68	295.2	325.3	3.80	145.8	165.3
0.70	286.3	318.2	4.00	142.6	150.2
0.75	262.2	282.6	4.20	135.7	151.4
0.80	246.9	264.3	4.50	153.1	166.0
0.85	241.2	253.9	4.70	155.1	167.1
0.90	223.4	246.1	5.00	150.5	164.3
0.95	213.2	242.6	5.50	144.9	154.2
1.00	211.8	230.1	6.00	145.8	163.0
1.10	201.1	220.8	6.50	156.0	161.3
1.20	186.3	205.1	7.00	128.5	150.1
1.30	168.4	201.2	7.50	181.5	185.9
1.40	153.4	165.5	8.00	161.0	174.3
1.60	151.0	167.5	8.50	151.6	173.7
1.80	132.0	144.0	9.00	155.6	175.0
2.00	141.9	152.9	9.50	162.7	171.1
2.20	146.0	152.8	10.00	165.3	184.1
2.40	141.4	154.9	10.50	154.0	168.4
2.60	151.3	168.0	11.00	152.5	163.4
2.80	154.8	160.5	11.50	147.4	183.2
3.00	132.6	139.6	12.00	142.4	165.9
3.20	149.4	162.8			

Sellmeier equations (λ in μm, $1.5\,\mu m < \lambda < 10.59\,\mu m$, $T = 293$ K) [46]:

$$n_o^2 = 11.6413 + \frac{0.69363}{\lambda^2 - 0.21967} + \frac{1586.06}{\lambda^2 - 832.75}$$

$$n_e^2 = 12.1438 + \frac{0.75255}{\lambda^2 - 0.21913} + \frac{2061.68}{\lambda^2 - 951.07}$$

Other sets of dispersion relations for room temperature are given in [18], [36], [47], [48], [49], [50], [51], [52]; for temperatures for $T = 93$ K, 173 K, 373 K, 473 K, 673 K in [53]; for $T = 343$ K in [54].

Temperature derivatives of the refractive indices upon heating from room temperature to T [K] for the spectral range 1.5–10.25 μm [46]:

$$dn_o/dT = (11.4188/\lambda^3 - 12.8971/\lambda^2 + 7.2947/\lambda + 14.2082) \times 10^{-5} \times [1 + 3.36 \times 10^{-3}(T - 293)]$$

$$dn_e/dT = (10.3798/\lambda^3 - 10.1785/\lambda^2 + 6.3877/\lambda + 15.6688)) \times 10^{-5} \times [1 + 3.28 \times 10^{-3}(T - 293)]$$

Linear electrooptic coefficients measured at high frequencies (well above the acoustic resonances of $ZnGeP_2$ crystal, i.e., for the "clamped" crystal) at room temperature [55]

λ [μm]	r_{41}^S [pm/V]	r_{63}^S [pm/V]
3.3913	1.6	−0.8

Expressions for the effective second-order nonlinear coefficient in general case (Kleinman symmetry conditions are valid, $d_{14} = d_{25} = d_{36}$) [56], [57]:

$$d_{\mathrm{eeo}} = 2d_{36}\sin(\theta+\rho)\cos(\theta+\rho)\cos 2\phi$$

$$d_{\mathrm{oeo}} = d_{\mathrm{eoo}} = -d_{36}\sin(\theta+\rho)\sin 2\phi$$

Simplified expressions for the effective second-order nonlinear coefficient (approximation of small birefringence angle, Kleinman symmetry conditions are valid, $d_{14} = d_{25} = d_{36}$) [57]:

$$d_{\mathrm{eeo}} = d_{36}\sin 2\theta\cos 2\phi$$

$$d_{\mathrm{oeo}} = d_{\mathrm{eoo}} = -d_{36}\sin\theta\sin 2\phi$$

Values of second-order nonlinear coefficient:

$$d_{36}(5.2955\,\mu\mathrm{m}) = 1.70 \pm 0.17 \times d_{36}(\mathrm{AgGaSe_2}) = 70 \pm 7\,\mathrm{pm/V}\ [49]$$

$$d_{36}(9.6\,\mu\mathrm{m}) = 75 \pm 8\,\mathrm{pm/V}\ [41]$$

$$d_{36}(10.6\,\mu\mathrm{m}) = 0.83 \times d_{36}(\mathrm{GaAs}) \pm 15\% = 68.9 \pm 10.3\,\mathrm{pm/V}\ [11], [58]$$

Experimental values of phase-matching angle ($T = 293$ K)

Interacting wavelengths [μm]	θ_{exp} [deg]	Ref.
SHG, $e + e \Rightarrow o$		
3.9278 ⇒ 1.9639	57.8 ± 0.3	[15], [49]
4.34 ⇒ 2.17	55.8 ± 0.2	[23]
4.64 ⇒ 2.32	47.5	[59]
4.775 ⇒ 2.3875	49.2	[25]
5.2955 ⇒ 2.64775	46.8	[49]
9.2 ⇒ 4.6	63.8	[60]
9.3054 ⇒ 4.6527	61.3	[28]
	61.3	[48]
	62.7–64.4	[39]
	63	[49]
	64	[38]
9.5 ⇒ 4.75	62.1	[28]
	62.1	[48]
	66.8	[60]
9.5524 ⇒ 4.7762	65.3	[49]
9.6036 ⇒ 4.8018	64.9	[39]
	65.8	[49]

Interacting wavelengths [μm]	θ_{exp} [deg]	Ref.
10.2 ⇒ 5.1	72	[28]
10.3035 ⇒ 5.15175	74.3	[44]
	74.5	[49]
10.5514 ⇒ 5.2757	79.2	[49]
10.5910 ⇒ 5.2955	80.1	[49]
SFG, $e + e \Rightarrow o$		
10.668 + 4.34 ⇒ 3.085	54.3 ± 0.2	[23]
10.5910 + 5.2955 ⇒ 3.53033	52.1	[49]
10.5910 + 3.53033 ⇒ 2.64775	48.4	[49]
9.74 + 4.2039 ⇒ 2.9365	49.6	[12]
5.2955 + 3.53033 ⇒ 2.1182	51.7	[49]
SFG, $o + e \Rightarrow o$		
6.74 + 5.2036 ⇒ 2.9365	76	[61]
6.45 + 5.3908 ⇒ 2.9365	79.2	[27]
6.25 + 5.5389 ⇒ 2.9365	84.0	[27]
6.15 + 5.6199 ⇒ 2.9365	85.5	[27]
6.29 + 5.0173 ⇒ 2.791	76	[31]
6.19 + 5.0828 ⇒ 2.791	77.6	[31]
6.06 + 5.1739 ⇒ 2.791	80.5	[31]
6.015 + 5.207 ⇒ 2.791	84	[62]
5.95 + 5.2569 ⇒ 2.791	83.4	[31]
5.90 + 5.2965 ⇒ 2.791	87	[31]
10.5910 + 1.0642 ⇒ 0.96703	84	[35]

Experimental values of internal angular bandwidth

Interacting wavelengths [μm]	$\Delta\theta^{int}$ [deg]	Ref.
SHG, $e + e \Rightarrow o$		
3.8 ⇒ 1.9	1.33	[15]
4.34 ⇒ 2.17	1.05	[23]
5.3 ⇒ 2.65	0.69	[59]
7.8 ⇒ 3.9	0.5	[29]
9.3 ⇒ 4.65	0.74–0.80	[39]
	0.83	[40]
	1.15	[38]
9.55 ⇒ 4.775	0.89	[41]
9.6 ⇒ 4.8	0.8	[39]
10.2 ⇒ 5.1	1.35	[28]
10.3 ⇒ 5.15	1.20	[44]
SFG, $e + e \Rightarrow o$		
10.668 + 4.34 ⇒ 3.085	1.23	[23]
SFG, $o + e \Rightarrow o$		
10.6 + 1.064 ⇒ 0.967	0.55	[35]

Experimental values of spectral bandwidth

Interacting wavelengths [μm]	$\Delta\nu$ [cm^{-1}]	Ref.
SHG, $e + e \Rightarrow o$		
4.34 ⇒ 2.17	7.9	[23]
10.2 ⇒ 5.1	4.9	[28]

Experimental values of temperature bandwidth [49]

Interacting wavelengths [μm]	θ_{exp} [deg]	ΔT [°C]	Ref.
SHG, $e + e \Rightarrow o$			
10.5910 ⇒ 5.2955	80.1	44	[49]
10.3035 ⇒ 5.15175	74.5	45	[49]
10.2 ⇒ 5.1	72	50	[28]
9.6036 ⇒ 4.8018	65.8	48	[49]
SFG, $o + e \Rightarrow o$			
10.5910 + 1.0642 ⇒ 0.96703	84	81.9	[35]

Temperature variation of phase-matching angle

Interacting wavelengths [μm]	$d\theta_{\text{pm}}/dT$ [deg/K]	Ref.
SHG, $e + e \Rightarrow o$		
9.2 ⇒ 4.6	0.014	[60]
10.3 ⇒ 5.15	0.072	[28]
10.6 ⇒ 5.3	0.107	[28]
SFG, $o + e \Rightarrow o$		
10.6 + 1.0642 ⇒ 0.9671	0.007	[35]

Laser-induced surface-damage threshold

λ [μm]	τ_{p} [ns]	I_{thr} [GW/cm^2]	Ref.	Note
1.0642	30	>0.003	[63]	12.5 Hz
	10	0.003	[11]	
1.3	0.00013	>150	[45]	1 kHz
1.66	0.00013	>100	[45]	1 kHz
2.05	30	0.013–0.016	[19]	5 kHz
	10	>0.074	[64]	10 kHz
2.79	50	>0.014	[30]	10 Hz
		0.018	[30]	10 Hz
	0.15	30	[31]	
	0.1	35	[16], [62]	1 Hz
2.8	70	0.056	[22]	1 Hz, uncoated sample
		0.08	[22]	1 Hz, coated samples

λ [μm]	τ_p [ns]	I_{thr} [GW/cm^2]	Ref.	Note
2.94	0.11	30	[61]	
		30	[12]	
5.3–6.1	CW	>0.00001	[59]	
		0.00025	[34]	
7.8	5000	10	[29]	
9.2–10.8	CW	>0.00008	[42]	
9.28	2	1.25	[26]	
9.3	100	0.012	[38]	100 Hz
	50	>0.06	[40]	1 Hz
9.3–10.6	125	0.025	[44]	20 Hz
		0.03–0.04	[44]	2 Hz
9.55	220	0.078	[41], [65]	
	30	0.14	[43]	SHG direction
10.2–10.8	CW	>0.000001	[28]	
	100,000–10,000,000	0.06	[28]	1500 Hz
10.6	CW	>0.00000001	[63]	
		0.0002	[34]	

About the crystal

The intensive research recently conducted by Schunemann [14], [19], and Gribenyukov [8], [21], resulted in a decreased IR absorption of ZGP crystal in the 2.05-μm region (down to 0.02–0.04 cm^{-1}). This allowed Vodopyanov to improve significantly the characteristics of ZGP-based singly resonant OPO systems, pumped by Er,Cr:YSGG laser ($\lambda = 2.8\,\mu$m). The tunability of OPO based on type I phase-matching was 3.8–12.4 μm, whereas for type II phase-matching the range 4–10 μm was achieved [66]. The IR pulse energy in the 6–8 μm range reached 300 μJ for the repetition rate 25 Hz [67]. In [68], an all–solid-state diode-pumped Nd:YAG laser pumped a PPLN-based OPO, the idler wavelength of the latter ($\lambda = 2.3$ to 3.7 μm) was used for the pumping of singly-resonant ZGP-based OPO (repetition rate, 1–10 kHz). The output pulses possessed energy of more than 20 μJ and were tunable in the 6–8 μm range.

References

[1] *Physical-Chemical Properties of Semiconductors. Handbook*. (Nauka, Moscow, 1979) [In Russian].

[2] Data sheet of Inrad, Inc. Available at www.inrad.com.

[3] J.E. Tucker, C.L. Marquardt, S.R. Bowman, B.J. Feldman: Transient thermal lens in a ZnGeP2 crystal. Appl. Opt. **34(15)**, 2678–2682 (1995).

[4] V.I. Gavrilenko, A.M. Grekhov, D.B. Korbutyak, V.G. Litovchenko: *Optical Properties of Semiconductors. Handbook*. (Naukova Dumka, Kiev, 1987) [In Russian].

[5] G.D. Boyd, E. Buehler, F.G. Storz, J.H. Wernick: Linear and nonlinear optical properties of ternary $A^{II}B^{IV}C_2^V$ chalcopyrite semiconductors. IEEE J. Quant. Electr. **QE-8(4)**, 419–426 (1972).

[6] I.I. Kozhina, A.S. Borshchevskii: High-temperature x-ray investigations of $A^{II}B^{IV}C_2^V$ compounds. Vestnik LGU **No.22**, 87–92 (1971) [In Russian].
[7] H.M. Hobgood, T. Henningsen, R.N. Thomas, R.H. Hopkins, M.C. Ohmer, W.C. Mitchel, D.W. Fischer, S.M. Hegde, F.K. Hopkins: $ZnGeP_2$ grown by the liquid encapsulated Czochralski method. J. Appl. Phys. **73(8)**, 4030-4036 (1993).
[8] Y.M. Andreev, G.A. Verozubova, A.I. Gribenyukov, V.V. Korotkova: $ZnGeP_2$ crystals for infrared laser radiation frequency conversion. J. Korean Phys. Soc. **33(3)**, 356–361 (1998).
[9] G.A. Verozubova, A.I. Gribenyukov, V.V. Korotkova, M.P. Ruzaikin: $ZnGeP_2$ synthesis and growth from melt. Mater. Sci. Eng. B **48(3)**, 191–197 (1997).
[10] J.D. Beasley: Thermal conductivities of some novel nonlinear optical materials. Appl. Opt. **33(6)**, 1000–1003 (1994).
[11] G.D. Boyd, E. Buehler, F.G. Storz: Linear and nonlinear optical properties of $ZnGeP_2$ and CdSe. Appl. Phys. Lett. **18(7)**, 301–304 (1971).
[12] K.L. Vodopyanov: Parametric generation of tunable infrared radiation in $ZnGeP_2$ and GaSe pumped at 3 μm. J. Opt. Soc. Am. B **10(9)**, 1723–1729 (1993).
[13] W. Shi, Y.J. Ding: Continuously tunable and coherent terahertz radiation by means of phase-matched difference-frequency generation in zinc germanium phosphide. Appl. Phys. Lett. **83(5)**, 848–851 (2003).
[14] P.G. Schunemann, T.M. Pollak: Ultralow gradient HGF-grown $ZnGeP_2$ and $CdGeAs_2$ and their optical properties. MRS Bulletin **23(7)**, 23–27 (1998).
[15] Y.M. Andreev, S.D. Velikanov, A.S. Elutin, A.F. Zapolskii, D.V. Konkin, S.N. Mikshin, S.V. Smirnov, Y.N. Frolov, V.V. Shchurov: Second harmonic generation from DF laser radiation in $ZnGeP_2$. Kvant. Elektron. **19(11)**, 1110 (1992) [In Russian, English trans.: Quantum Electron. **22(11)**, 1035 (1992)].
[16] Y.M. Andreev, G.C. Bhar, A.I. Gribenyukov, G.A. Verozubova, K.L. Vodopyanov: Nonlinear tunable parametric luminescence in $ZnGeP_2$ crystals. Proc. SPIE **3403**, 336–340 (1997).
[17] R.F. Wu, K.S. Lai, E. Lau, H.F. Wong, W.J. Xie, Y.L. Lim, K.W. Lim, L. Chia: Multi-watt ZGP OPO based on diffusion bonded walkoff compensated KTP OPO and Nd:YALO laser. In: *Advanced Solid-State Lasers, OSA Trends in Optics and Photonics Series, Vol. 68*, ed. by M.E. Fermann, L.R. Marshall (OSA, Washington DC, 2002), pp. 194–197.
[18] N.P. Barnes, K.E. Murray, M.G. Jani, P.G. Schunemann, T.M. Pollak: $ZnGeP_2$ parametric oscillator. J. Opt. Soc. Am. B **15(1)**, 232–238 (1998).
[19] P.G. Schunemann, K.L. Schepler, P.A. Budni: Nonlinear frequency conversion performance of $AgGaSe_2$, $ZnGeP_2$, and $CdGeAs_2$. MRS Bulletin **23(7)**, 45–49 (1998).
[20] P.A. Ketteridge, P.A. Budni, P.G. Schunemann, M.L. Lemons, T.M. Pollak, E.P. Chicklis: Tunable all solid state average power ZGP OPO at 2.7 and 8.5 microns. In: *Advanced Solid-State Lasers, OSA Trends in Optics and Photonics Series, Vol. 19*, ed. by W.R. Bosenberg, M.M. Fejer (OSA, Washington DC, 1998), pp. 233–235.
[21] A.I. Gribenyukov: Nonlinear optical $ZnGeP_2$ crystals: the history of technology. Atmos. Oceanic Opt. **15(1)**, 61–68 (2002).
[22] R.D. Peterson, K.L. Schepler, J.L. Brown, P.G. Schunemann: Damage properties of $ZnGeP_2$ at 2 μm. J. Opt. Soc. Am. B **12(11)**, 2142–2146 (1995).
[23] Y.M. Andreev, V.G. Voevodin, P.P. Geiko, A.I. Gribenyukov, V.V. Zuev, A.S. Solodukhin, S.A. Trushin, V.V. Churakov, S.F. Shubin: Transformation of the frequencies of nontraditional (4.3 and 10.4 μm) CO_2 laser radiation bands in $ZnGeP_2$. Kvant. Elektron.

14(11), 2137–2138 (1987) [In Russian, English trans.: Sov. J. Quantum Electron. **17(11)**, 1362–1363 (1987)].

[24] G.C. Catella, D. Burlage: Crystal growth and optical properties of $AgGaS_2$ and $AgGaSe_2$. MRS Bulletin **23(7)**, 28–36 (1998).

[25] H.P. Chou, R.C. Slater, Y. Wang: High-energy, fourth-harmonic generation using CO_2 lasers. Appl. Phys. B **66(5)**, 555–559 (1998).

[26] Y.M. Andreev, V.Y. Baranov, V.G. Voevodin, P.P. Geiko, A.I. Gribenyukov, S.V. Izyumov, S.M. Kozochkin, V.D. Pismenny, Y.A. Satov, A.P. Streltsov: Efficient generation of the second harmonic of a nanosecond CO_2 laser radiation pulse. Kvant. Elektron. **14(11)**, 2252–2254 (1987) [In Russian, English trans.: Sov. J. Quantum Electron. **17(11)**, 1435–1436 (1987)].

[27] K.L. Vodopyanov, V.G. Voevodin, A.I. Gribenyukov, L.A. Kulevskii: Picosecond parametric superluminescence in the $ZnGeP_2$ crystal. Izv. Akad. Nauk SSSR, Ser. Fiz. **49(3)**, 569-572 (1985) [In Russian, English trans.: Bull. Acad. Sci. USSR, Phys. Ser. **49(3)**, 146-149 (1985)].

[28] Y.M. Andreev, V.G. Voevodin, A.I. Gribenyukov, O.Y. Zyryanov, I.I. Ippolitov, A.N. Morozov, A.V. Sosnin, G.S. Khmelnitskii: Efficient generation of the second harmonic of tunable CO_2 laser radiation in $ZnGeP_2$. Kvant. Elektron. **11(8)**, 1511–1512 (1984) [In Russian, English trans.: Sov. J. Quantum Electron. **14(8)**, 1021–1022 (1984)].

[29] J.M. Auerhammer, A.F.G. van der Meer, P.W. van Amersfoort, Q.H.F. Vrehen, E.R. Eliel: Efficient frequency doubling of ps-pulses from a free-electron laser in $ZnGeP_2$. Opt. Commun. **118(1–2)**, 85–89 (1995).

[30] T.H. Allik, S. Chandra, D.M. Rines, P.G. Schunemann, J.A. Hutchinson, R. Utano: Tunable 7–12-μm optical parametric oscillator using a Cr,Er:YSGG laser to pump CdSe and $ZnGeP_2$ crystals. Opt. Lett. **22(9)**, 597–599 (1997).

[31] K.L. Vodopyanov, V.G. Voevodin, A.I. Gribenyukov, L.A. Kulevskii: High-efficiency picosecond parametric superradiance emitted by a $ZnGeP_2$ crystal in 5–6.3 μm range. Kvant. Elektron. **14(9)**, 1815–1819 (1987) [In Russian, English trans.: Sov. J. Quantum Electron. **17(9)**, 1159–1161 (1987)].

[32] G.A. Verozubova, A.I. Gribenyukov, V.V. Korotkova, O. Semchinova, D. Uffmann: Synthesis and growth of $ZnGeP_2$ crystals for nonlinear optical applications. J. Cryst. Growth **213(3–4)**, 334–339 (2000).

[33] Y.M. Andreev, A.D. Belykh, V.G. Voevodin, P.P. Geiko, A.I. Gribenyukov, V.A. Gurashvili, S.V. Izyumov: Doubling of the emission of CO lasers with the efficiency of 3%. Kvant. Elektron. **14(4)**, 782–783 (1987) [In Russian, English trans.: Sov. J. Quantum Electron. **17(4)**, 490–491 (1987)].

[34] Y.M. Andreev, V.G. Voevodin, A.I. Gribenyukov, V.P. Novikov: Mixing of frequencies of CO_2 and CO lasers in $ZnGeP_2$ crystals. Kvant. Elektron. **14(6)**, 1177–1179 (1987) [In Russian, English trans.: Sov. J. Quantum Electron. **17(6)**, 748–749 (1987)].

[35] G.D. Boyd, W.B. Gandrud, E. Buehler: Phase-matched upconversion of 10.6-μm radiation in $ZnGeP_2$. Appl. Phys. Lett. **18(10)**, 446–448 (1971).

[36] S.V. Zakharov, A.E. Negin, P.G. Filippov, E.F. Zhilis: Sellmeier equation and conversion of the radiation of a repetitively pulsed tunable TEA CO_2 laser into the second harmonic in a $ZnGeP_2$ crystal. Kvantovaya Elektron. **28(3)**, 251–255 (1999) [English trans.: Quantum Electron. **29(9)**, 806–810 (1999)].

[37] V.E. Zuev, M.V. Kabanov, Y.M. Andreev, V.G. Voevodin, P.P. Geiko, A.I. Gribenyukov, V.V. Zuev: Applications of efficient parametric IR-laser frequency converters. Izv. Akad. Nauk SSSR, Ser. Fiz. **52(6)**, 1142–1148 (1988) [In Russian, English trans.: Bull. Acad. Sci. USSR, Phys. Ser. **52(6)**, 87–92 (1988)].

[38] A.A. Barykin, S.V. Davydov, V.P. Dorokhov, V.P. Zakharov, V.V. Butuzov: Generation of the second harmonic of CO_2 laser pulses in a $ZnGeP_2$ crystal. Kvant. Elektron. **20(8)**, 794–800 (1993) [In Russian, English trans.: Quantum Electron. **23**, 688–693 (1993)].

[39] Y.M. Andreev, A.N. Bykanov, A.I. Gribenyukov, V.V. Zuev, V.D. Karyshev, A.V. Kisletsov, I.O. Kovalev, V.I. Konov, G.P. Kuzmin, A.A. Nesterenko, A.E. Osorgin, Y.M. Starodumov, N.I. Chapliev: Conversion of pulsed laser radiation from the 9.3–9.6 μm range to the second harmonic in $ZnGeP_2$ crystals. Kvant. Elektron. **17(4)**, 476–480 (1990) [In Russian, English trans.: Sov. J. Quantum Electron. **20(4)**, 410–414 (1990)].

[40] Y.M. Andreev, V.V. Butuzov, G.A. Verozubova, A.I. Gribenyukov, S.V. Davydov, V.P. Zakharov: Generation of the second harmonic of pulsed CO_2-laser radiation in $AgGaSe_2$ and $ZnGeP_2$ single crystals. Laser Phys. **5(5)**, 1014–1019 (1995).

[41] P.D. Mason, D.J. Jackson, E.K. Gorton: CO_2 laser frequency doubling in $ZnGeP_2$. Opt. Commun. **110(1–2)**, 163–166 (1994).

[42] S.Y. Tochitsky, V.O. Petukhov, V.A. Gorobets, V.V. Churakov, V.N. Yakimovich: Efficient continuous-wave frequency doubling of a tunable CO_2 laser in $AgGaSe_2$. Appl. Opt. **36(9)**, 1882–1888 (1997).

[43] Y.M. Andreev, V.V. Badikov, V.G. Voevodin, L.G. Geiko, P.P. Geiko, M.V. Ivashchenko, A.I. Karapuzikov, I.V. Sherstov: Radiation resistance of nonlinear crystals at a wavelength of 9.55 μm. Kvant. Elektron. **31(12)**, 1075–1078 (2001) [In Russian, English trans.: Quantum Electron. **31(12)**, 1075–1078 (2001)].

[44] G.B. Abdullaev, K.R. Allakhverdiev, M.E. Karasev, V.I. Konov, L.A. Kulevskii, N.B. Mustafaev, P.P. Pashinin, A.M. Prokhorov, Y.M. Starodumov, N.I. Chapliev: Efficient generation of the second harmonic of CO_2 laser radiation in a GaSe crystal. Kvant. Elektron. **16(4)**, 757–763 (1989) [In Russian, English trans.: Sov. J. Quantum Electron. **19(4)**, 494–498 (1989)].

[45] V. Petrov, F. Rotermund, F. Noack, P. Schunemann: Femtosecond parametric generation in $ZnGeP_2$. Opt. Lett. **24(6)**, 414–416 (1999).

[46] K. Kato, E. Takaoka, N. Umemura: New Sellmeier and thermo-optic dispersion formulas for $ZnGeP_2$. In: *Conference on Lasers and Electrooptics CLEO/QELS 2003, Technical Digest* (OSA, Washington DC, 2003), paper CTuM17.

[47] G.C. Bhar: Refractive index interpolation in phase-matching. Appl. Opt. **15(2)**, 305–307 (1976).

[48] G.C. Bhar, L.K. Samanta, D.K. Ghosh, S. Das: Tunable parametric $ZnGeP_2$ crystal oscillator. Kvant. Elektron. **14(7)**, 1361–1363 (1987) [In Russian, English trans.: Sov. J. Quantum Electron. **17(7)**, 860–861 (1987)].

[49] K. Kato: Second-harmonic and sum-frequency generation in $ZnGeP_2$. Appl. Opt. **36(12)**, 2506–2510 (1997).

[50] G. Ghosh: Sellmeier coefficients for the birefringence and refractive indices of $ZnGeP_2$ nonlinear crystal at different temperatures. Appl. Opt. **37(7)**, 1205–1212 (1998).

[51] D.E. Zelmon, E.A. Hanning, P.G. Schunemann: Refractive-index measurements and Sellmeier coefficients for zinc germanium phosphide from 2 to 9 μm with implications for phase matching in optical frequency-conversion devices. J. Opt. Soc. Am. B **18(9)**, 1307–1310 (2001).

[52] S. Das, G.C. Bhar, S. Gangopadhyay, C. Ghosh: Linear and nonlinear optical properties of $ZnGeP_2$ crystal for infrared laser device applications: revisited. Appl. Opt. **42(21)**, 4335–4340 (2003).

[53] G.C. Bhar, G.C. Ghosh: Temperature dependent phase-matched nonlinear optical devices using CdSe and $ZnGeP_2$. IEEE J. Quant. Electr. **QE-16(8)**, 838–843 (1980).

[54] G.C. Bhar, G. Ghosh: Temperature-dependent Sellmeier coefficients and coherence lengths for some chalcopyrite crystals. J. Opt. Soc. Am. **69(5)**, 730–733 (1979).

[55] E.H. Turner, E. Buehler, H. Kasper: Electro-optic behavior and dielectric constants of $ZnGeP_2$ and $CuGaS_2$. Phys. Rev. B **9(2)**, 558–561 (1974).

[56] R.C. Eckardt, H. Masuda, Y.X. Fan, R.L. Byer: Absolute and relative nonlinear optical coefficients of KDP, KD*P, BaB_2O_4, $LiIO_3$, MgO:$LiNbO_3$, and KTP measured by phase-matched second-harmonic generation. IEEE J. Quant. Electr. **26(5)**, 922–933 (1990).

[57] J.E. Midwinter, J. Warner: The effects of phase matching method and of uniaxial crystal symmetry on the polar distribution of second-order non-linear optical polarization. Brit. J. Appl. Phys. **16(11)**, 1135–1142 (1965).

[58] D.A. Roberts: Simplified characterization of uniaxial and biaxial nonlinear optical crystals: a plea for standardization of nomenclature and conventions. IEEE J. Quant. Electr. **28(10)**, 2057–2074 (1992).

[59] Y.M. Andreev, T.V. Vedernikova, A.A. Betin, V.G. Voevodin, A.I. Gribenyukov, O.Y. Zyryanov, I.I. Ippolitov, V.I. Masychev, O.V. Mitropolskii, V.P. Novikov, M.A. Novikov, A.V. Sosnin: Conversion of CO_2 and CO laser radiation in a $ZnGeP_2$ crystal to the 2.3–3.1 μm spectral range. Kvant. Elektron. **12(7)**, 1535–1537 (1985) [In Russian, English trans.: Sov. J. Quantum Electron. **15(7)**, 1014–1015 (1985)].

[60] G.C. Bhar, S. Das, U. Chatterjee, K.L. Vodopyanov: Temperature-tunable second-harmonic generation in zinc germanium diphosphide. Appl. Phys. Lett. **54(4)**, 313–314 (1989).

[61] K.L. Vodopyanov, L.A. Kulevskii, V.G. Voevodin, A.I. Gribenyukov, K.R. Allakhverdiev, T.A. Kerimov: High efficiency middle IR parametric superradiance in $ZnGeP_2$ and GaSe crystals pumped by an erbium laser. Opt. Commun. **83(5–6)**, 322–326 (1991).

[62] K.L. Vodopyanov, Y.A. Andreev, G.C. Bhar: Parametric superluminescence in a $ZnGeP_2$ crystal with temperature tuning and pumping by an erbium laser. Kvant. Elektron. **20(9)**, 879–881 (1993) [In Russian, English trans.: Quantum Electron. **23(9)**, 763–765 (1993)].

[63] N.P. Andreeva, S.A. Andreev, I.N. Matveev, S.M. Pshenichnikov, N.D. Ustinov: Parametric conversion of infrared radiation in zinc germanium diphosphide. Kvant. Elektron. **6(2)**, 357–359 (1979) [In Russian, English trans.: Sov. J. Quantum Electron. **9(2)**, 208–210 (1979)].

[64] P.A. Budni, L.A. Pomeranz, M.L. Lemons, P.G. Schunemann, T.M. Pollak, E.P. Chicklis: 10 W mid-IR holmium pumped $ZnGeP_2$ OPO. In: *Advanced Solid-State Lasers, OSA Trends in Optics and Photonics Series, Vol. 19*, ed. by W.R. Bosenberg, M.M. Fejer (OSA, Washington DC 1998), pp. 226–229.

[65] P.D. Mason, D.J. Jackson, E.K. Gorton: CO_2 laser frequency doubling in $ZnGeP_2$. Erratum. Opt. Commun. **114(5–6)**, 529 (1995).

[66] K.L. Vodopyanov, F. Ganikhanov, J.P. Maffetone, I. Zwieback, W. Ruderman: $ZnGeP_2$ optical parametric oscillator with 3.8–12.4-μm tunability. Opt. Lett. **25(11)**, 841–843 (2000).

[67] M.W. Todd, R.A. Provencal, T.G. Owano, B.A. Paldus, A. Kachanov, K.L. Vodopyanov, M. Hunter, S.L. Coy, J.I. Steinfeld, J.T. Arnold: Application of mid-infrared cavity-ringdown spectroscopy to trace explosives vapor detection using a broadly-tunable (6–8 μm) optical parametric oscillator. Appl. Phys. B **75(2–3)**, 367–376 (2002).

[68] K.L. Vodopyanov, P.G. Schunemann: Broadly tunable noncritically phase-matched $ZnGeP_2$ optical parametric oscillator with a 2-μJ pump threshold. Opt. Lett. **28(6)**, 441–443 (2003).

3.4 GaSe, Gallium Selenide

Negative uniaxial crystal: $n_o > n_e$
Molecular mass: 148.683
Specific gravity: 5.03 g/cm^3 [1]
Point group: $\bar{6}2m$
Lattice constants [2]:
$a = 3.755$ Å
$c = 15.94$ Å
Mohs hardness: ≈ 0
Melting point: 1211 K [2]; 1233 K [2]

Linear thermal expansion coefficient [1]

T [K]	$\alpha_t \times 10^6$ [K^{-1}], $\parallel c$	$\alpha_t \times 10^6$ [K^{-1}], $\perp c$
300	9.15	10.85

Thermal conductivity coefficient κ [3]

T [K]	κ [W/mK], $\parallel c$	κ [W/mK], $\perp c$
293	16.2	2.0

Band-gap energy at room temperature: $E_g = 2.0$ eV [17]; 2.09 eV [2]
Transparency range at "0" transmittance level: 0.62–20 μm [4]

Linear absorption coefficient α

λ [μm]	α [cm^{-1}]	Ref.
0.65–18	<1	[5]
0.7	<0.3	[6]
0.7–0.8	0.3	[7]
1.06	0.45	[8]
	<0.25	[9]
	<0.1	[10]
1.5–12	<0.03	[7]
1.9	0.1	[8]
2	<0.1	[10]
9.3–10.6	<0.05	[11]
9.55	<0.1	[12]
10	<0.1	[10]
10.6	0.081	[13]

Temperature dependence of linear absorption coefficient at $\lambda = 0.6328$ μm for the range 283–343 K (T in K) [14]: $\alpha(T) = 7.39 \exp[0.0558 \times (T - 273)]$

Two-photon absorption coefficient β

λ [μm]	τ_p [ns]	$\beta \times 10^{11}$ [cm/W]	Ref.	Note
0.700	0.070	600	[15]	$\parallel c$
	0.0002	216	[16]	$\parallel c$
0.725	0.0002	190	[16]	$\parallel c$
0.750	0.0002	78	[16]	$\parallel c$
0.775	0.0002	50	[16]	$\parallel c$
0.800	0.0002	56	[16]	$\parallel c$
0.825	0.0002	45	[16]	$\parallel c$
0.850	0.0002	43	[16]	$\parallel c$
0.875	0.0002	48	[16]	$\parallel c$
0.900	0.0002	68	[16]	$\parallel c$
1.06	20	11000	[17]	

Experimental values of refractive indices [5]

λ [μm]	n_o	n_e
0.6328	2.97	2.74
1.1523	2.90	2.54
3.3913	2.81	2.46

Temperature derivative of refractive index for ordinary wave at $T = 75$ to 300 K [18]

λ [μm]	$dn_o/dT \times 10^6$ [K^{-1}]
0.6	182.7
0.8	134.6
1.0	117.3
2.0	95.4

Temperature dependence of n_o at $\lambda = 0.6328\,\mu$m for the range 298–373 K (T in K) [14]:

$$n_o = 2.93323 + 2.55921 \times 10^{-4}(T - 273) - 3.26264 \times 10^{-6}(T - 273)^2 + 8.06267 \times 10^{-8}(T - 273)^3 - 5.20204 \times 10^{-10}(T - 273)^4$$

Sellmeier equations (λ in μm, $T = 293$ K) [19]:

$$n_o^2 = 7.4437 + \frac{0.3757}{\lambda^2 - 0.1260} - 0.00154\,\lambda^2$$

$$n_e^2 = 5.7608 + \frac{0.2908}{\lambda^2 - 0.1628} - 0.00131\,\lambda^2$$

Other dispersion relations are given in [5], [9], [20].

Temperature derivative of refractive indices for spectral range 0.9–14 μm and temperature range 293–393 K (λ in μm) [19]:

$$\frac{dn_o}{dT} = \left(\frac{0.69}{\lambda^3} + \frac{3.43}{\lambda^2} - \frac{2.03}{\lambda} + 9.65\right) \times 10^{-5}\,\mathrm{K}^{-1}$$

$$\frac{dn_e}{dT} = \left(\frac{16.75}{\lambda^3} + \frac{41.31}{\lambda^2} - \frac{7.51}{\lambda} + 7.32\right) \times 10^{-5}\,\mathrm{K}^{-1}$$

Verdet constant at $T = 298$ K [21]

λ [μm]	V [degree/Tm]
0.6265	21420
0.6275	19170
0.6287	17420
0.6306	15170
0.6328	13420
0.6356	12330
0.6381	11830
0.6420	10830
0.6459	10250
0.6494	9920

Expressions for the effective second-order nonlinear coefficient [22]:

$$d_{\mathrm{ooe}} = d_{22} \cos\theta \sin 3\phi$$

$$d_{\mathrm{eoe}} = d_{\mathrm{oee}} = d_{22} \cos^2\theta \cos 3\phi$$

Second-order nonlinear coefficient:

$$|d_{22}(10.6\,\mu\mathrm{m})| = 3 \times |d_{31}(\mathrm{CdSe})| \pm 20\% = 54 \pm 11\,\mathrm{pm/V}\ [5],\ [23]$$

Experimental values of phase-matching angle ($T = 293$ K)

Interacting wavelengths [μm]	θ_{exp} [deg]	Ref.
SHG, $o + o \Rightarrow e$		
2.36 ⇒ 1.18	18.7	[5]
5.30 ⇒ 2.65	10.2	[5]
9.30 ⇒ 4.65	12.8	[11]
9.60 ⇒ 4.80	13.2	[11]
10.3 ⇒ 5.15	14.0	[11]
10.6 ⇒ 5.3	12.7	[5]
	14.4	[11]
SFG, $o + o \Rightarrow e$		
17.4 + 3.5327 ⇒ 2.9365	13	[4], [24]

Interacting wavelengths [μm]	θ_{exp} [deg]	Ref.
$11.6 + 3.9318 \Rightarrow 2.9365$	10	[4], [24]
$10.8 + 2.3611 \Rightarrow 1.9375$	10.7	[8]
$7.4 + 2.4859 \Rightarrow 1.8608$	11.2	[8]
$5 + 2.7039 \Rightarrow 1.7549$	12.4	[8]
$10.1 + 1.1895 \Rightarrow 1.0642$	13.3	[25]
$7.15 + 1.2503 \Rightarrow 1.0642$	15	[25]
$19.1 + 1.1144 \Rightarrow 1.053$	11.5	[26]
$12 + 1.1543 \Rightarrow 1.053$	12	[26]
$5.8 + 1.2866 \Rightarrow 1.053$	15.7	[26]
$10.6 + 1.0642 \Rightarrow 0.96711$	13.6	[9]
$4.9 + 1.0642 \Rightarrow 0.8743$	18.8	[9]
$17.17 + 0.7235 \Rightarrow 0.6943$	15.2	[6]
$9.99 + 0.7462 \Rightarrow 0.6943$	18.3	[6]
SFG, $e + o \Rightarrow e$		
$15.5 + 1.1427 \Rightarrow 1.0642$	12.4	[25]
$12.0 + 1.1678 \Rightarrow 1.0642$	13.3	[25]
$9.4 + 1.2001 \Rightarrow 1.0642$	14.4	[25]
$7.4 + 1.2430 \Rightarrow 1.0642$	16.4	[25]
$10.6 + 1.0642 \Rightarrow 0.96711$	14.4	[9]
$18.28 + 0.7217 \Rightarrow 0.6943$	15.2	[6]
$11.10 + 0.7406 \Rightarrow 0.6943$	18.6	[6]

Experimental values of internal angular bandwidth

Interacting wavelengths [μm]	$\Delta\theta^{int}$ [deg]	Ref.
SHG, $o + o \Rightarrow e$		
$10.3 \Rightarrow 5.15$	0.146	[11]
SFG, $o + o \Rightarrow e$		
$7 + 2.51 \Rightarrow 1.8475$	0.086	[8]
$12.5 + 0.7351 \Rightarrow 0.6943$	0.021	[6]

Experimental values of temperature bandwidth [19]

Interacting wavelengths [μm]	ΔT [°C]
SHG, $o + o \Rightarrow e$	
$10.591 \Rightarrow 5.2955$	172
$5.2955 \Rightarrow 2.6478$	218
$3.5303 \Rightarrow 1.76515$	15
SFG, $o + o \Rightarrow e$	
$10.591 + 3.5303 \Rightarrow 2.6478$	228

Interacting wavelengths [μm]	ΔT [°C]
SFG, $e + o \Rightarrow e$	
$5.2955 + 3.5303 \Rightarrow 2.6478$	14
SFG, $o + e \Rightarrow e$	
$5.2955 + 3.5303 \Rightarrow 2.6478$	10

Laser-induced surface-damage threshold

λ [μm]	τ_p [ns]	I_{thr} [GW/cm^2]	Ref.	Note
0.683	6	0.082	[15]	100 pulses
0.6943	30	0.02	[6]	
0.7	0.07	7	[15]	100 pulses
0.75	50	0.02	[7]	
0.8	60	0.008	[15]	100 pulses
1.053	0.002	>1.0	[26]	1 Hz
1.06	20	>0.01	[17]	
1.0642	10	0.03	[9]	
2.36	40	>0.005	[5]	
2.80	0.1	>4	[27]	3 Hz
2.94	0.11	30	[4], [24]	1 Hz
9.55	30	0.12	[12]	$\parallel c$
10.6	CW	>0.0005	[28]	
	125	0.03	[11]	2–20 Hz

About the crystal

GaSe is known by its lateral structure [29]. Nevertheless, it is the one of the best nonlinear crystals for mid-IR generation via OPG or DFG. Recently, Vodopyanov [30], [31], reported double-pass traveling-wave GaSe-based OPG pumped by 100-ps, 3-mJ pulses of an Er,Cr:YSGG laser, operating at 2.8 μm. The achieved tunability region of the OPG covered 3.3–19 μm. In DFG experiments made in past 5 years, the continuously tunable mid-IR range was permanently increased from 9 to 18 μm [32] to 7 to 20 μm [33] and finally to 2.7 to 28.7 μm [34].

References

[1] *Physical-Chemical Properties of Semiconductors. Handbook*. (Nauka, Moscow, 1979) [In Russian].

[2] *Physical Quantities. Handbook*, ed. by I.S. Grigoriev and E.Z. Meilikhov (Energoatomizdat, Moscow, 1991) [In Russian].

[3] G.D Guseinov, A.I. Rasulov: Heat conductivity of GaSe monocrystals. Phys. Stat. Solidi **18(2)**, 911–922 (1966).

[4] K.L. Vodopyanov, L.A. Kulevskii, V.G. Voevodin, A.I. Gribenyukov, K.R. Allakhverdiev, T.A. Kerimov: High efficiency middle IR parametric superradiance in $ZnGeP_2$ and GaSe crystals pumped by an erbium laser. Opt. Commun. **83(5–6)**, 322–326 (1991).

[5] G.B. Abdullaev, L.A. Kulevskii, A.M. Prokhorov, A.D. Saveliev, E.Y. Salaev, V.V. Smirnov: GaSe, a new effective material for nonlinear optics. Pisma Zh. Eksp. Teor. Fiz. **16(3)**, 130–133 (1972) [In Russian, English trans.: JETP Lett. **16(3)**, 90–92 (1972)].

[6] G.B. Abdullaev, L.A. Kulevskii, P.V. Nikles, A.M. Prokhorov, A.D. Saveliev, E.Y. Salaev, V.V. Smirnov: Difference frequency generation in a GaSe crystal with continuous tuning in the 560–1050 cm^{-1} range. Kvant. Elektron. **3(1)**, 163–167 (1976) [In Russian, English trans.: Sov. J. Quantum Electron. **6(1)**, 88–90 (1976)].

[7] A.O. Okorogu, S.B. Mirov, W. Lee, D.I. Crouthamel, N. Jenkins, A.Y. Dergachev, K.L. Vodopyanov, V.V. Badikov: Tunable middle infrared downconversion in GaSe and $AgGaS_2$. Opt. Commun. **155(4–6)**, 307–312 (1998).

[8] A. Bianchi, A. Ferrario, M. Musci: 4–12 μm tunable down-conversion in GaSe from a $LiNbO_3$ parametric oscillator. Opt. Commun. **25(2)**, 256–258 (1978).

[9] G.B. Abdullaev, K.R. Allakhverdiev, L.A. Kulevskii, A.M. Prokhorov, E.Y. Salaev, A.D. Saveliev, V.V. Smirnov: Parametric conversion of infrared radiation in a GaSe crystal. Kvant. Elektron. **2(6)**, 1228–1233 (1975) [In Russian, English trans.: Sov. J. Quantum Electron. **5(6)**, 665–668 (1975)].

[10] A. Bianchi, M. Garbi: Down-conversion in the 4–18 μm range with GaSe and $AgGaSe_2$ nonlinear crystals. Opt. Commun. **30(1)**, 122–124 (1979).

[11] G.B. Abdullaev, K.R. Allakhverdiev, M.E. Karasev, V.I. Konov, L.A. Kulevskii, N.B. Mustafaev, P.P. Pashinin, A.M. Prokhorov, Y.M. Starodumov, N.I. Chapliev: Efficient generation of the second harmonic of CO_2 laser radiation in a GaSe crystal. Kvant. Elektron. **16(4)**, 757–763 (1989) [In Russian, English trans.: Sov. J. Quantum Electron. **19(4)**, 494–498 (1989)].

[12] Y.M. Andreev, V.V. Badikov, V.G. Voevodin, L.G. Geiko, P.P. Geiko, M.V. Ivashchenko, A.I. Karapuzikov, I.V. Sherstov: Radiation resistance of nonlinear crystals at a wavelength of 9.55 μm. Kvant. Elektron. **31(12)**, 1075–1078 (2001) [In Russian, English trans.: Quantum Electron. **31(12)**, 1075–1078 (2001)].

[13] N.P. Barnes, R.C. Eckardt, D.J. Gettemy, L.B. Edgett: Absorption coefficients and the temperature variation of the refractive index difference of nonlinear optical crystals. IEEE J. Quant. Electr. **QE-15(10)**, 1074–1076 (1979).

[14] M.A. Hernandez, M.V. Andres, A. Segura, V. Munoz: Temperature dependence of refractive index and absorption coefficient of GaSe at 633 nm. Opt. Commun. **118(3–4)**, 335–337 (1995).

[15] K.L. Vodopyanov, S.B. Mirov, V.G. Voevodin, P.G. Schunemann: Two-photon absorption in GaSe and $CdGeAs_2$. Opt. Commun. **155(1–3)**, 47–50 (1998).

[16] I.B. Zotova, Y.J. Ding: Spectral measurements of two-photon absorption coefficients for CdSe and GaSe crystals. Appl. Opt. **40(36)**, 6654–6658 (2001).

[17] F. Adduci, I.M. Catalano, A. Cingolani, A. Minafra: Direct and indirect two-photon processes in layered semiconductors. Phys. Rev. B **15(2)**, 926–931 (1977).

[18] G. Antonioli, D. Bianchi, P. Franzosi: Temperature variation of refractive index in GaSe. Appl. Opt. **18(22)**, 3847–3850 (1979).

[19] E. Takaoka, K. Kato: Temperature phase-matching properties for harmonic generation in GaSe. Jpn. J. Appl. Phys. **38(5A)**, 2755–2759 (1999).

[20] K.L. Vodopyanov, L.A. Kulevskii: New dispersion relationships for GaSe in the 0.65–18 μm spectral region. Opt. Commun. **118(3–4)**, 375–378 (1995).

[21] A. Balbin Villaverde, D.A. Donatti: GaSe Faraday rotation near the absorption edge. J. Chem. Phys. **72(10)**, 5341–5342 (1980).

[22] J.E. Midwinter, J. Warner: The effects of phase matching method and of uniaxial crystal symmetry on the polar distribution of second-order non-linear optical polarization. Brit. J. Appl. Phys. **16(11)**, 1135–1142 (1965).

[23] D.A. Roberts: Simplified characterization of uniaxial and biaxial nonlinear optical crystals: a plea for standardization of nomenclature and conventions. IEEE J. Quant. Electr. **28(10)**, 2057–2074 (1992).

[24] K.L. Vodopyanov: Parametric generation of tunable infrared radiation in $ZnGeP_2$ and GaSe pumped at 3 μm. J. Opt. Soc. Am. B **10(9)**, 1723–1729 (1993).

[25] Y.A. Gusev, A.V. Kirpichnikov, S.N. Konoplin, S.I. Marennikov, P.V. Nikles, Y.N. Polivanov, A.M. Prokhorov, A.D. Saveliev, R.S. Sayakhov, V.V. Smirnov, V.P. Chebotaev: Tunable mid-IR difference frequency generator. Pisma Zh. Tekh. Fiz. **6(19–20)**, 1262–1265 (1980) [In Russian, English trans.: Sov. Tech. Phys. Lett. **6(10)**, 541–542 (1980)].

[26] T. Dahinten, U. Plödereder, A. Seilmeier, K.L. Vodopyanov, K.R. Allakhverdiev, Z.A. Ibragimov: Infrared pulses of 1 picosecond duration tunable between 4 μm and 18 μm. IEEE J. Quant. Electr. **29(7)**, 2245–2250 (1993).

[27] K.L. Vodopyanov, V.G. Voevodin: 2.8 μm laser pumped type I and type II travelling-wave optical parametric generator in GaSe. Opt. Commun. **114(3–4)**, 333–335 (1995).

[28] J.-J. Zondy: Experimental investigation of single and twin $AgGaSe_2$ crystals for CW 10.2 μm SHG. Opt. Commun. **119(3–4)**, 320–326 (1995).

[29] L. Kador, D. Haarer, K.R. Allakhverdiev, E.Y. Salaev: Phase-matched second-harmonic generation at 789.5 nm in a GaSe crystal. Appl. Phys. Lett. **69(6)**, 731–733 (1996).

[30] K.L. Vodopyanov, V. Chazapis: Extra-wide tuning range optical parametric oscillator. Opt. Commun. **135(13)**, 98–102 (1997).

[31] K.L. Vodopyanov: Mid-infrared optical parametric generator with extra-wide (2.7–28.7 μm) tunability: applications for spectroscopy of two-dimensional electrons in quantum wells. J. Opt. Soc. Am. B **16(9)**, 1579–1586 (1999).

[32] R.A. Kaindl, D.C. Smith, M. Joschko, M.P. Hasselbeck, M. Woerner, T. Elsaesser: Femtosecond infrared pulses tunable from 9 to 18 μm at an 88-MHZ repetition rate. Opt. Lett. **23(11)**, 861–863 (1998).

[33] R.A. Kaindl, F. Eickemeyer, M. Woerner, T. Elsaesser: Broadband phase-matched difference frequency mixing of femtosecond pulses in GaSe: experiment and theory. **75(8)**, 1060–1062 (1999).

[34] W. Shi, Y.J. Ding, X. Mu, N. Fernelius: Tunable and coherent nanosecond radiation in the range of 2.7–28.7 μm based on difference-frequency generation in gallium selenide. Appl. Phys. Lett. **80(21)**, 3889–3891 (2002).

4

Often-Used Crystals

This chapter relates to other frequently used nonlinear optical crystals, such as potassium dihydrogen phosphate (KDP) and its most popular analogs ammonium dihydrogen phosphate (ADP) and deuterated potassium dihydrogen phosphate (DKDP); the recently developed cesium lithium borate (CLBO), an analog of lithium niobate, magnesium-oxide–doped lithium niobate (MgLN), an analog of KTP, potassium titanyl arsenate (KTA); and finally potassium niobate (KN).

4.1 KH_2PO_4, Potassium Dihydrogen Phosphate (KDP)

Negative uniaxial crystal: $n_o > n_e$
Molecular mass: 136.086
Specific gravity: 2.3325 g/cm^3 [1]; 2.338 g/cm^3 [2]; 2.3383 g/cm^3 at 293 K [3]
Point group: $\bar{4}2m$ ($mm2$ at $T < 122$ K [4])
Lattice constants:
point group $\bar{4}2m$:
$a = 7.448$ Å [5]; 7.452 Å [6]; 7.453 Å [4]; 7.4529 ± 0.0002 Å at $T = 296$ K [7]
$c = 6.977$ Å [5]; 6.959 Å [6]; 6.959 Å [4]; 6.9751 ± 0.0006 Å at $T = 296$ K [7]
point group $mm2$:
$a = 10.44$ Å [8]
$b = 10.53$ Å [8]
$c = 6.90$ Å [8]

Variation in KDP lattice constants for crystals from different commercial sources [9]

Firm	a [Å]	c [Å]
Inrad	7.460	6.965
Cleveland Crystals #1	7.451	6.950
Cleveland Crystals #2	7.439	6.962

Mohs hardness: 1.5 [10]; 2.5 [11], [12]
Vickers hardness [13]:
122 ± 17 along a direction
183 ± 12 along c direction

Solubility in 100 g H_2O [3]

T [K]	s [g]
298	33

Melting point: 525 K [3]; 526 K [14], [15]
Curie temperature: 122 K [16]; 122.6 K [17]; 123 K [7], [17], [18]; [19]

Linear thermal expansion coefficient [4]

T [K]	$\alpha_t \times 10^6$ [K^{-1}], $\parallel c$	$\alpha_t \times 10^6$ [K^{-1}], $\perp c$
200	39	22
250	41	24.6
270	41.6	25.6
280	41.9	26.0
290	42.1	26.4
300	42.4	26.8

Mean value of linear thermal expansion coefficient

T [K]	$\alpha_t \times 10^6$ [K^{-1}], $\parallel c$	$\alpha_t \times 10^6$ [K^{-1}], $\perp c$	Ref.
123–293	42	20	[4]
123–298	39.2	22	[19]
223–323	44.0	24.9	[19]
223–373		26.6	[4]
233–363	44.6		[4]

Specific heat capacity c_p at $P = 0.101325$ MPa

T [K]	c_p [J/kgK]	Ref.
80	341	[14]
150	552	[14]
250	764	[14]
298	857	[14]
306	879	[15]

Thermal conductivity coefficient [3]

T [K]	κ [W/mK], $\parallel c$	κ [W/mK], $\perp c$
302	1.21	
319		1.34
428	1.30	1.76

Band-gap energy at room temperature: $E_g = 6.95$ eV [20]; 7.0 eV [21], [10]
Transparency range at $\alpha = 1\,\text{cm}^{-1}$ level: 0.176–1.4 μm [22], [7]
Transparency range at 0.5 transmittance level for 0.2-cm-long crystal: 0.176–1.55 μm [1]

Linear absorption coefficient α

λ [μm]	α [cm^{-1}]	Ref.	Note
0.212	0.2	[23]	
0.25725	0.01–0.2	[24]	*e*-wave, $\perp c$
	0.009	[25]	
	0.007	[26]	*e*-wave, $\perp c$
0.263	0.03	[27]	
0.3513	0.003	[28]	*e*-wave, $\perp c$
0.5145	0.0001	[25]	
	0.00005	[24]	*o*-wave
0.5265	0.01	[29]	*o*-wave
0.6943	0.008	[30]	
0.78	0.024	[4]	
0.89	0.015	[4]	
0.94	0.01	[31]	
1.053	0.05	[29]	*o*-wave
	0.03	[27]	
1.054	0.058	[28]	*o*-wave
	0.02	[28]	*e*-wave, $\perp c$
1.06	0.03	[4]	
1.0642	0.03	[32]	
	0.058	[33]	*o*-wave
	0.006	[33]	*e*-wave
1.22	0.1	[34]	*o*-wave
1.3152	0.3	[35]	
1.32	0.1	[34]	*e*-wave, $\perp c$

Two-photon absorption coefficient β

λ [μm]	τ_p [ns]	$\beta \times 10^{11}$ [cm/W]	Ref.	Note
0.211	0.0009	136 ± 48	[36]	$\theta = 41°, \phi = 45°$
0.216	0.015	60 ± 5	[37]	
0.263	0.6	60	[27]	
0.2635	0.5	50	[38]	
0.264	0.0008	26 ± 9	[36]	$\theta = 41°, \phi = 45°$
0.2661	0.015	27 ± 8	[20]	$\theta = 41°, \phi = 45°$
	0.6	40–80	[39]	
0.270	0.015	28 ± 3	[40]	
0.3547	0.017	0.59 ± 0.21	[20]	*e*-wave, $\perp c$

Experimental values of refractive indices at $T = 298$ K [41]

λ [μm]	n_o	n_e	λ [μm]	n_o	n_e
0.2138560	1.60177	1.54615	0.3906410		1.48089
0.2288018	1.58546		0.4046561	1.52341	1.47927
0.2446905	1.57228		0.4077811	1.52301	1.47898
0.2464068	1.57105		0.4358350	1.51990	1.47640
0.2536519	1.56631	1.51586	0.4916036		1.47254
0.2800869	1.55263	1.50416	0.5460740	1.51152	1.46982
0.2980628	1.54618	1.49824	0.5769580	1.50987	
0.3021499	1.54433	1.49708	0.5790654	1.50977	1.46856
0.3035781		1.49667	0.6328160	1.50737	1.46685
0.3125663	1.54117	1.49434	1.0139750	1.49535	1.46041
0.3131545	1.54098	1.49419	1.1287040	1.49205	1.45917
0.3341478		1.48954	1.1522760	1.49135	1.45893
0.3650146	1.52932	1.48432	1.3570700	1.48455	
0.3654833	1.52923	1.48423	1.5231000		1.45521
0.3662878	1.52909	1.48409	1.5295250		1.45512

Temperature derivative of refractive indices [42]

λ [μm]	$dn_o/dT \times 10^5$ [K^{-1}]	$dn_e/dT \times 10^5$ [K^{-1}]
0.405	−3.27	−3.15
0.436	−3.27	−2.88
0.546	−3.28	−2.90
0.578	−3.25	−2.87
0.633	−3.94	−2.54

Temperature dependencies of the refractive indices upon cooling from room temperature to T [K]:

for the spectral range 0.365–0.690 μm [42]:

$$n_o(T) = n_o(298) + 0.402 \times 10^{-4}\{[n_o(298)]^2 - 1.432\}(298 - T)$$
$$n_e(T) = n_e(298) + 0.221 \times 10^{-4}\{[n_e(298)]^2 - 1.105\}(298 - T)$$

for the spectral range 0.436–0.589 μm [43]:

$$n_o(T) = n_o(300) + 10^{-4}(143.3 - 0.618T + 4.81 \times 10^{-4}T^2)$$
$$n_e(T) = n_e(300) + 10^{-4}(153.3 - 0.969T + 1.57 \times 10^{-3}T^2)$$

Best set of dispersion relations (λ in μm, $T = 293$ K) [41]:

$$n_o^2 = 2.259276 + \frac{13.00522\lambda^2}{\lambda^2 - 400} + \frac{0.01008956}{\lambda^2 - (77.26408)^{-1}}$$

$$n_e^2 = 2.132668 + \frac{3.2279924\lambda^2}{\lambda^2 - 400} + \frac{0.008637494}{\lambda^2 - (81.42631)^{-1}}$$

Other sets of dispersion relations are given in [9], [44], [45], [46], [47].

Temperature-dependent Sellmeier equations (λ in μm, T in K) [45]:

$$n_o^2 = (1.44896 + 3.185 \times 10^{-5}T) + \frac{(0.84181 - 1.4114 \times 10^{-4}T)\lambda^2}{\lambda^2 - (0.0128 - 2.13 \times 10^{-7}T)} + \frac{(0.90793 + 5.75 \times 10^{-7}T)\lambda^2}{\lambda^2 - 30}$$

$$n_e^2 = (1.42961 - 1.152 \times 10^{-5}T) + \frac{(0.72722 - 6.139 \times 10^{-5}T)\lambda^2}{\lambda^2 - (0.01213 + 3.104 \times 10^{-7}T)} + \frac{(0.22543 - 1.98 \times 10^{-7}T)\lambda^2}{\lambda^2 - 30}$$

Nonlinear refractive index γ

λ [μm]	$\gamma \times 10^{15}$ [cm^2/W]	Ref.	Note
0.5321	0.25 ± 0.08	[48]	$\theta = 78°$
	0.28 ± 0.08	[48]	$\theta = 41°$
	0.28 ± 0.08	[49]	
1.0642	0.20	[50]	*o*-wave
	0.22	[50]	*e*-wave
	0.26 ± 0.08	[48]	$\theta = 90°$
	0.28	[51]	
	0.29 ± 0.09	[52]	
	0.44 ± 0.13	[48]	$\theta = 78°$
	0.46 ± 0.14	[48]	$\theta = 59°$
	1.0 (?)	[53]	

Linear electrooptic coefficients measured at low frequencies (well below the acoustic resonances of KDP crystal, i.e., for the "free" crystal) at room temperature

λ [μm]	r_{41}^T [pm/V]	r_{63}^T [pm/V]	Ref.	Note
0.20		-10.7	[54]	$T = 283$ K
0.25		-10.5	[54]	$T = 283$ K
0.500		-9.2	[55]	
0.5461	-8.77 ± 0.14		[56]	
		-10.3	[57]	
0.556	-8.6 ± 0.2		[58]	$T = 295$ K
		-10.5 ± 0.2	[58]	$T = 295$ K
0.6328	-8		[59]	
	-8.6 ± 0.2		[60]	$T = 295$ K
		-9.4 ± 0.4	[61]	
		-9.9 ± 0.2	[60]	$T = 295$ K
		-11	[59]	
0.700		-9.4	[55]	
3.3913		-9.7	[57]	

Linear electrooptic coefficient measured at high frequencies (well above the acoustic resonances of KDP crystal, i.e., for the "clamped" crystal) at room temperature

λ [μm]	r_{63}^{S} [pm/V]	Ref.
0.5461	-8.5 ± 2.4	[62]
	-9.7	[63]
0.6328	-8.8 ± 0.5	[64]

Half-wave retardation voltage at longitudinal modulation

λ [μm]	$V_{\lambda/2}$ [kV]	Ref.
0.4358	6.04 ± 0.06	[56]
0.5461	7.5	[63]
	7.65 ± 0.08	[56]
0.578	8.17 ± 0.08	[56]

Verdet constant ($\|c$)

λ [μm]	T [K]	V [degree/Tm]	Ref.
0.6328	293	221 ± 5	[2]
		213	[65]
	298	207	[66]

Note: The measurements in [65] were done at room temperature.

Calculated Verdet constants ($\|c$) [67]

λ [μm]	V [degree/Tm]
0.193	3875
0.222	2487
0.248	1800
0.308	1030
0.351	758

Lineshift under ns SRS: $\Delta\nu = 915\,\mathrm{cm}^{-1}$ [68]
Expressions for the effective second-order nonlinear coefficient in general case (Kleinman symmetry conditions are valid, $d_{14} = d_{25} = d_{36}$) [69]:

$$d_{\mathrm{ooe}} = -d_{36}\sin(\theta + \rho)\sin 2\phi$$

$$d_{\mathrm{eoe}} = d_{\mathrm{oee}} = 2d_{36}\sin(\theta + \rho)\cos(\theta + \rho)\cos 2\phi$$

Simplified expressions for the effective second-order nonlinear coefficient (approximation of small birefringence angle, Kleinman symmetry conditions are valid, $d_{14} = d_{25} = d_{36}$) [70]:

$$d_{\mathrm{ooe}} = -d_{36}\sin\theta\sin 2\phi$$

$$d_{\mathrm{eoe}} = d_{\mathrm{oee}} = d_{36}\sin 2\theta\cos 2\phi$$

Absolute values of second-order nonlinear coefficient:
$d_{36}(1.319\,\mu m) = 0.31 \pm 0.02$ pm/V [71]
$d_{36}(1.0642\,\mu m) = 0.38$ pm/V [69]; 0.39 pm/V [72]
0.39 ± 0.03 pm/V [73]; 0.40 ± 0.02 pm/V [71]

Experimental values of phase-matching angle ($T = 293$ K)

Interacting wavelengths [μm]	θ_{exp} [deg]	Ref.
SHG, $o + o \Rightarrow e$		
$0.517 \Rightarrow 0.2585$	90	[44]
$0.6576 \Rightarrow 0.3288$	53.6	[35]
$0.6943 \Rightarrow 0.34715$	50.4	[74]
$0.8707 \Rightarrow 0.43535$	42.4	[75]
$1.06 \Rightarrow 0.53$	41	[76], [77]
$1.3152 \Rightarrow 0.6576$	44.3	[35]
SFG, $o + o \Rightarrow e$		
$1.415 + 0.22027 \Rightarrow 0.1906$	88.7	[78]
$1.3648 + 0.6943 \Rightarrow 0.46019$	40.9	[75]
$1.3152 + 0.6576 \Rightarrow 0.4384$	42.2	[35]
$1.0642 + 0.2707 \Rightarrow 0.21581$	87.6	[79]
$1.0642 + 0.5321 \Rightarrow 0.35473$	47.3	[80]
$1.06 + 0.53 \Rightarrow 0.35333$	47.5	[77]
$0.6576 + 0.4384 \Rightarrow 0.26304$	74	[81]
SHG, $e + o \Rightarrow e$		
$1.3152 \Rightarrow 0.6576$	61.4	[35]
$1.06 \Rightarrow 0.53$	59	[77]
SFG, $e + o \Rightarrow e$		
$1.0642 + 0.5321 \Rightarrow 0.35473$	58.3	[80]
$1.06 + 0.53 \Rightarrow 0.35333$	59.3	[77]

Experimental values of NCPM temperature

Interacting wavelengths [μm]	T [°C]	Ref.
SHG, $o + o \Rightarrow e$		
$0.5145 \Rightarrow 0.25725$	−13.7	[26]
	−11	[24]
$0.517 \Rightarrow 0.2585$	20	[44]
$0.5321 \Rightarrow 0.26605$	177	[82], [83]
SFG, $o + o \Rightarrow e$		
$1.06 + 0.265 \Rightarrow 0.212$	−70	[23]
$1.0642 + 0.26605 \Rightarrow 0.21284$	−40	[84]
	−35	[85]
$1.0796 + 0.2699 \Rightarrow 0.21592$	60	[86]

Experimental values of internal angular and temperature bandwidths

Interacting wavelengths [μm]	T [°C]	θ_{pm} [deg]	$\Delta\theta^{int}$ [deg]	ΔT [°C]	Ref.
SHG, $o + o \Rightarrow e$					
1.1523 ⇒ 0.57615	20	41	0.074		[87]
1.0642 ⇒ 0.5321	20	41	0.070		[69]
	25			23 ± 1	[88]
1.064 ⇒ 0.532	20	41	0.069		[89]
1.06 ⇒ 0.53	20	41	0.063		[76]
			0.065 ± 0.003		[90]
1.054 ⇒ 0.527	25	41	0.060		[91]
0.5321 ⇒ 0.26605	25			1.7 ± 0.1	[88]
	177	90		1.9	[82]
	177	90		2	[83]
0.53 ⇒ 0.265	20	77	0.059		[92]
	20	77	0.066	1.2 (?)	[93]
SFG, $o + o \Rightarrow e$					
1.0642 + 0.5321 ⇒ 0.35473	25			5.5 ± 0.2	[88]
1.054 + 0.527 ⇒ 0.35133	25	48	0.046		[91]
1.0796 + 0.2699 ⇒ 0.21592	60	90		1.3	[86]
SHG, $e + o \Rightarrow e$					
1.0642 ⇒ 0.5321	25			18.3 ± 1.7	[88]
1.06 ⇒ 0.53	20	59	0.129		[92]
			0.133 ± 0.002		[90]
1.054 ⇒ 0.527	25	59	0.126		[91]
SFG, $e + o \Rightarrow e$					
1.0642 + 0.5321 ⇒ 0.35473	25			5.2 ± 0.2	[88]
1.06 + 0.53 ⇒ 0.35333	20	59	0.062	2.2 (?)	[93]
1.054 + 0.527 ⇒ 0.35133	25	59	0.059		[91]

Experimental values of spectral bandwidth

Interacting wavelengths [μm]	T [°C]	θ_{pm} [deg]	$\Delta\nu$ [cm^{-1}]	Ref.
SHG, $o + o \Rightarrow e$				
1.06 ⇒ 0.53	20	41	178	[76]
0.53 ⇒ 0.265	20	77	4.7	[92]
SHG, $e + o \Rightarrow e$				
1.06 ⇒ 0.53	20	59	101.5	[92]

Temperature variation of phase-matching angle

Interacting wavelengths [μm]	T [°C]	θ_{pm} [deg]	$d\theta_{pm}/dT$ [deg/K]	Ref.
SHG, $o + o \Rightarrow e$				
1.0642 ⇒ 0.5321	25		0.0028	[88]
1.06 ⇒ 0.53		41	0.00365 ± 0.00003	
1.054 ⇒ 0.527	25	41	0.0046	[91]
0.5321 ⇒ 0.26605	25		0.0382	[88]
0.5265 ⇒ 0.26325		80	0.0602	[27]

Interacting wavelengths [μm]	T [°C]	θ_{pm} [deg]	$d\theta_{pm}/dT$ [deg/K]	Ref.
SFG, $o + o \Rightarrow e$				
$1.0642 + 0.5321 \Rightarrow 0.35473$	25		0.0073	[88]
$1.054 + 0.527 \Rightarrow 0.35133$	25	48	0.0046	[91]
SHG, $e + o \Rightarrow e$				
$1.0642 \Rightarrow 0.5321$	25	59	0.0069 ± 0.0003	[94]
	25		0.0069	[88]
$1.06 \Rightarrow 0.53$	20	59	0.0057	[92]
			0.0097 ± 0.0003	[90]
$1.054 \Rightarrow 0.527$	25	59	0.0085	[91]
	20	59	0.0069	[28]
SFG, $e + o \Rightarrow e$				
$1.0642 + 0.5321 \Rightarrow 0.35473$	25	58	0.0106 ± 0.0003	[94]
	25		0.0117	[88]
$1.054 + 0.527 \Rightarrow 0.35133$	25	59	0.0152	[91]
	20	59	0.0075	[28]

Temperature tuning of noncritical SHG [44]

Interacting wavelengths [μm]	$d\lambda_1/dT$ [nm/K]
SHG, $o + o \Rightarrow e$	
$0.517 \Rightarrow 0.2585$	0.048

Temperature variation of birefringence for the noncritical SHG process

Interacting wavelengths [μm]	$d(n_2^e - n_1^o)/dT \times 10^{-5}$ [K^{-1}]	Ref.
$0.5145 \Rightarrow 0.25725$	1.745	[95]
$0.5321 \Rightarrow 0.26605$	1.2	[82]

Electro-optic tuning sensitivity for SHG process [90]

Interacting wavelengths [μm]	$d\theta_{pm}/d\boldsymbol{E}$ [deg · cm/kV]
SHG, $o + o \Rightarrow e$	
$1.06 \Rightarrow 0.53$	0.00293 ± 0.00002
SHG, $e + o \Rightarrow e$	
$1.06 \Rightarrow 0.53$	≈ 0

Calculated values of phase-matching and "walk-off" angles

Interacting wavelengths [μm]	θ_{pm} [deg]	ρ_1 [deg]	ρ_3 [deg]
SHG, $o + o \Rightarrow e$			
$0.5321 \Rightarrow 0.26605$	76.60		0.808
$0.5782 \Rightarrow 0.2891$	64.03		1.391
$0.6328 \Rightarrow 0.3164$	56.15		1.611

Interacting wavelengths [μm]	θ_{pm} [deg]	ρ_1 [deg]	ρ_3 [deg]
$0.6594 \Rightarrow 0.3297$	53.43		1.657
$0.6943 \Rightarrow 0.34715$	50.55		1.687
$1.0642 \Rightarrow 0.5321$	41.21		1.603
$1.3188 \Rightarrow 0.6594$	44.70		1.549
SFG, $o + o \Rightarrow e$			
$0.5782 + 0.5105 \Rightarrow 0.27112$	72.46		1.025
$1.0642 + 0.5321 \Rightarrow 0.35473$	47.28		1.712
$1.3188 + 0.6594 \Rightarrow 0.4396$	42.05		1.657
SHG, $e + o \Rightarrow e$			
$1.0642 \Rightarrow 0.5321$	58.98	1.149	1.404
$1.3188 \Rightarrow 0.6594$	61.85	0.922	1.269
SFG, $e + o \Rightarrow e$			
$1.0642 + 0.5321 \Rightarrow 0.35473$	58.23	1.166	1.521
$1.3188 + 0.6594 \Rightarrow 0.4396$	49.42	1.104	1.634

Calculated values of inverse group-velocity mismatch for SHG process in KDP

Interacting wavelengths [μm]	θ_{pm} [deg]	β [fs/mm]
SHG, $o + o \Rightarrow e$		
$1.2 \Rightarrow 0.6$	42.45	42
$1.1 \Rightarrow 0.55$	41.38	17
$1.0 \Rightarrow 0.5$	41.22	9
$0.9 \Rightarrow 0.45$	42.24	40
$0.8 \Rightarrow 0.4$	44.91	77
$0.7 \Rightarrow 0.35$	50.14	128
$0.6 \Rightarrow 0.3$	60.40	208
SHG, $e + o \Rightarrow e$		
$1.2 \Rightarrow 0.6$	59.54	89
$1.1 \Rightarrow 0.55$	58.87	67
$1.0 \Rightarrow 0.5$	59.75	89
$0.9 \Rightarrow 0.45$	62.97	118
$0.8 \Rightarrow 0.4$	70.71	158

Laser-induced bulk-damage threshold

λ [μm]	τ_p [ns]	I_{thr} [GW/cm^2]	Ref.	Note
0.2661	8	2.3	[96]	
	0.75	7	[13]	$\mathbf{k} \perp c$, $\mathbf{E} \parallel c$
0.3547	0.85	5.1–6.2	[13]	
	0.017	5000–24,000	[49]	sharp focusing
0.355	7.6	5.1	[97]	$\parallel c$, large-tank boules
		2.9	[97]	$\theta = 58°$, large-tank boules
0.52	330	0.2	[98]	
0.5265	20	3	[29]	
	0.6	9	[29]	

λ [μm]	τ_p [ns]	I_{thr} [GW/cm^2]	Ref.	Note
0.527	0.5	>14	[99]	
0.53	10	34–57	[100]	21-μm beam-waist diameter
	0.2	17	[101]	
	0.005	1000	[102]	
0.5321	1.0	6–20	[13]	depends on irradiation direction and light polarization
	0.6	>8	[39]	
	0.03	30	[103]	
	0.021	2200	[49]	sharp focusing
0.596	330	0.24	[98]	
	20	3	[98]	
0.6943	20	>0.4	[104]	
	5–25	0.10–0.14	[30]	
1.053	25	4	[29]	
	1.1	10.6–20.9	[13]	depends on irradiation direction and light polarization
	1	18	[29]	
	1	15–20	[105]	UV irradiation of KDP solution
	1	20	[106]	
1.054	3	>3.3	[107]	
	1	>5.1	[107]	
	0.14	>7	[108]	
1.06	60	0.2	[109]	
	30	17–34	[110]	sharp focusing
	14	2.5–5	[100]	100-μm beam-waist diameter
		17–35	[100]	21-μm beam-waist diameter
	12–25	>0.25	[76]	
	0.5	>3	[111]	
	0.2	23	[101]	
	0.003	7000–10,000	[110]	sharp focusing
1.0642	20	0.3–0.6	[112]	
	10	6.4–18.5	[113]	
	7	2.7	[114]	
	1.3	8	[115]	
	1.1	16	[116]	
	1	3–7	[112]	
		5	[117]	
	0.1	7	[118]	
		>100	[51]	
	0.03	2000	[53]	sharp focusing
1.0796	5	16	[86]	

Laser-induced surface damage threshold

λ [μm]	τ_p [ns]	I_{thr} [GW/cm^2]	Ref.	Note
0.2484	20	0.45	[119]	1.5-mm beam-waist diameter
0.2661	0.7	8.6	[119]	
0.6943	5–25	1–5	[30]	

λ [μm]	τ_p [ns]	I_{thr} [GW/cm^2]	Ref.	Note
1.0642	12	14.4	[120]	$\parallel c$, 30-μm beam-waist diameter
	10	3.9–18.5	[113]	

About the crystal

KDP (together with its analogs DKDP and ADP) is one of the oldest nonlinear optical materials [8], [121]. It was widely applied in the first experiments made in the 1960s, and it is still in use, especially in the experiments on inertial-confinement fusion [122], where damage-resistant and wide-aperture SHG and THG crystals are needed. For these purposes, the methods of rapid KDP growth, up to 50 mm/day with crystal sizes up to 90 cm, were developed [123], [124], [125].

References

[1] Data sheet of Cleveland Crystals Inc. Available at www.clevelandcrystals.com.

[2] S. Haussühl, W. Effgen: Faraday effect in cubic crystals. Additivity rule and phase transitions. Z. Kristallogr. **183(1–4)**, 153–174 (1988).

[3] E.M. Voronkova, B.N. Grechushnikov, G.I. Distler, I.P. Petrov: *Optical Materials for Infrared Technique* (Nauka, Moscow, 1965) [In Russian].

[4] A.A. Blistanov, V.S. Bondarenko, N.V. Perelomova, F.N. Strizhevskaya, V.V. Tchkalova, M.P. Shaskolskaya: *Acoustic Crystals* (Nauka, Moscow, 1982) [In Russian].

[5] *Handbook of Optical Constants of Solids II*, ed. by E.D. Palik (Academic Press, Boston, 1991).

[6] S. Haussühl: Elastische und thermoelastische Eigenschaften von KH_2PO_4, KH_2AsO_4, $NH_4H_2PO_4$, $NH_4H_2AsO_4$ und RbH_2PO_4. Z. Kristallogr. **120(6)**, 401–414 (1964) [In German].

[7] T.R. Sliker, S.R. Burlage: Some dielectric and optical properties of KD_2PO_4. J. Appl. Phys. **34(7)**, 1837–1840 (1963).

[8] F. Jona, G. Shirane: *Ferroelectric Crystals* (Pergamon Press, Oxford, 1962).

[9] K.W. Kirby, L.G. DeShazer: Refractive indices of 14 nonlinear crystals isomorphic to KH_2PO_4. J. Opt. Soc. Am. B **4(7)**, 1072–1078 (1987).

[10] B.H.T. Chai: Optical Crystals. In: *CRC Handbook of Laser Science and Technology, Supplement 2: Optical Materials*, ed. by M.J. Weber (CRC Press, Boca Raton, 1995) pp. 3–65.

[11] V.G. Dmitriev, G.G. Gurzadyan, D.N. Nikogosyan: *Handbook of Nonlinear Optical Crystals, Third Revised Edition* (Springer, Berlin, 1999).

[12] D. Yuan, D. Xu, M. Liu, F. Qi, W. Yu, W. Hou, Y. Bing, S. Sun, M. Jiang: Structure and properties of a complex crystal for laser diode frequency doubling: cadmium mercury thiocyanate. Appl. Phys. Lett. **70(5)**, 544–546 (1997).

[13] H. Yoshida, T. Jitsuno, H. Fujita, M. Nakatsuka, M. Yoshimura, T. Sasaki, K. Yoshida: Investigation of bulk laser damage in KDP crystal as a function of laser irradiation direction, polarization and wavelength. Appl. Phys. B, **70(2)**, 195–201 (2000).

[14] *Physical Quantities. Handbook*, ed. by I.S. Grigoriev, E.Z. Meilikhov (Energoatomizdat, Moscow, 1991) [In Russian].

[15] S.S. Ballard, J.S. Browder: Thermal Properties. In: *CRC Handbook of Laser Science and Technology, Vol. IV, Optical Materials: Part 2*, ed. by M.J. Weber (CRC Press, Boca Raton, 1987) pp. 49–54.

[16] A.S. Sonin, A.S. Vasilevskaya: *Electrooptic Crystals* (Atomizdat, Moscow, 1971) [In Russian].

[17] I.P. Kaminow: Tables of Linear Electrooptic Coefficients. In: *CRC Handbook of Laser Science and Technology, Vol. III, Optical Materials: Part 2*, ed. by M.J. Weber (CRC Press, Boca Raton, 1986) pp. 253–278.

[18] I.P. Kaminow, G.O. Harding: Complex dielectric constant of KH_2PO_4 at 9.2 Gc/sec. Phys. Rev. **129(4)**, 1562–1566 (1963).

[19] W.R. Cook, Jr.: Thermal expansion of crystals with KH_2PO_4 structure. J. Appl. Phys. **38(4)**, 1637–1642 (1967).

[20] P. Liu, W.L. Smith, H. Lotem, J.H. Bechtel, N. Bloembergen, R.S. Adhav: Absolute two-photon absorption coefficients at 355 and 266 nm. Phys. Rev. B **17(12)**, 4620–4632 (1978).

[21] E.W. van Stryland, L.L. Chase: Two-Photon Absorption. Inorganic Materials. In: *CRC Handbook of Laser Science and Technology, Supplement 2: Optical Materials*, ed. by M.J. Weber (CRC Press, Boca Raton, 1995) pp. 299–328.

[22] W.L. Smith: KDP and ADP transmission in the vacuum ultraviolet. Appl. Opt. **16(7)**, 798 (1977).

[23] A.G. Akmanov, S.A. Akhmanov, B.V. Zhdanov, A.I. Kovrigin, N.K. Podsotskaya, R.V. Khokhlov: Generation of coherent radiation at $\lambda = 2120$Å by cascade frequency conversion. Pisma Zh. Eksp. Teor. Fiz. **10(6)**, 244–249 (1969) [In Russian, English trans.: JETP Lett. **10(6)**, 154–156 (1969)].

[24] M.W. Dowley, E.B. Hodges: Studies of high-power CW and quasi-CW parametric UV generation by ADP and KDP in argon-ion laser cavity. IEEE J. Quant. Electr. **QE-4(10)**, 552–558 (1968).

[25] P. Huber: High power in the near ultraviolet using efficient SHG. Opt. Commun. **15(2)**, 196–200 (1975).

[26] E.F. Labuda, A.M. Johnson: Continuous second-harmonic generation of $\lambda = 2572$Å using Ar^{2+} laser. IEEE J. Quant. Electr. **QE-3(4)**, 164–167 (1967).

[27] D. Bruneau, A.M. Tournade, E. Fabre: Fourth harmonic generation of a large-aperture Nd:glass laser. Appl. Opt. **24(22)**, 3740–3745 (1985).

[28] P.J. Wegner, M.A. Henesian, D.R. Speck, C. Bibeau, R.B. Ehrlich, C.W. Laumann, J.K. Lawson, T.L. Weiland: Harmonic conversion of large-aperture 1.05-μm laser beams for inertion-confinement fusion research. Appl. Opt. **31(30)**, 6414–6426 (1992).

[29] A. Yokotani, T. Sasaki, K. Yoshida, S. Nakai: Extremely high damage threshold of a new nonlinear crystal L-arginine phosphate and its deuterium compound. Appl. Phys. Lett. **55(26)**, 2692–2693 (1989).

[30] T.M. Christmas, J.M. Ley: Laser-induced damage in XDP materials. Electron. Lett. **7(18)**, 544–546 (1971).

[31] E.N. Volkova, V.V. Fadeev: Linear absorption coefficient of some nonlinear optical crystals. In: *Nonlinear Optics*, ed. by R.V. Khokhlov (Nauka, Novosibirsk, 1968) pp. 185–187 [In Russian].

[32] C. Chen, Y.X. Fan, R.C. Eckardt, R.L. Byer: Recent developments in barium borate. Proc. SPIE **681**, 12–19 (1987).

[33] C.A. Ebbers, J. Happe, N. Nielsen, S.P. Velsko: Optical absorption at 1.06 μm in highly deuterated potassium dihydrogen phosphate. Appl. Opt. **31(12)**, 1960–1964 (1992).

[34] G. Dikchyus, E. Zhilinskas, A. Piskarskas, V. Sirutkaitis: Statistical properties and stabilization of a picosecond phosphate-glass laser with 2 Hz repetition frequency. Kvant. Elektron. **6(8)**, 1610–1619 (1979) [In Russian, English trans.: Sov. J. Quantum Electron. **9(8)**, 950–955 (1979)].

[35] E.E. Fill: Generation of higher harmonics of iodine laser radiation. Opt. Commun. **33(3)**, 321–322 (1980).

[36] A. Dubietis, G. Tamošauskas, A. Varanavičius, G. Valiulis: Two-photon absorbing properties of ultraviolet phase-matchable crystals at 264 and 211 nm. Appl. Opt. **39(15)**, 2437–2440 (2000).

[37] G.G. Gurzadyan, R.K. Ispiryan: Two-photon absorption peculiarities of potassium dihydrogen phosphate crystal at 216 nm. Appl. Phys. Lett. **59(6)**, 630–631 (1991).

[38] I.A. Begishev, R.A. Ganeev, A.A. Gulamov, E.A. Erofeev, S.R. Kamalov, T. Usmanov, A.D. Khadzhaev: The neodymium laser fifth harmonic generation and two-photon absorption in KDP and ADP crystals. Kvant. Elektron. **15(2)**, 353–361 (1988) [In Russian, English trans.: Sov. J. Quantum Electron. **18(2)**, 224–228 (1988)].

[39] G.J. Linford, B.C. Johnson, J.S. Hildum, W.E. Martin, K. Snyder, R.D. Boyd, W.L. Smith, C.L. Vercimak, D. Eimerl, J.T. Hunt: Large aperture harmonic conversion experiments at Lawrence Livermore National Laboratory. Appl. Opt. **21(20)**, 3633–3643 (1982).

[40] G.G. Gurzadyan, R.K. Ispiryan: Two-photon absorption in potassium dihydrophosphate, potassium pentaborate and quartz crystals at 270 and 216 nm. Int. J. Nonl. Opt. Phys. **1(3)**, 533–540 (1992).

[41] F. Zernike, Jr.: Refractive indices of ammonium dihydrogen phosphate and potassium dihydrogen phosphate between 2000Å and 1.5 μm. J. Opt. Soc. Am. **54(10)**, 1215–1220 (1964).

[42] R.A. Philips: Temperature variations of the index of refraction of ADP, KDP, and deuterated KDP. J. Opt. Soc. Am. **56(5)**, 629–632 (1966).

[43] M. Yamazaki, T. Ogawa: Temperature dependences of the refractive indices of $NH_4H_2PO_4$, KH_2PO_4, and partially deuterated KH_2PO_4. J. Opt. Soc. Am. **56(10)**, 1407–1408 (1966).

[44] N.P. Barnes, D.J. Gettemy, R.S. Adhav: Variations of the refractive index with temperature and the tuning rate for KDP isomorphs. J. Opt. Soc. Am. **72(7)**, 895–898 (1982).

[45] G.C. Ghosh, G.C. Bhar: Temperature dispersion in ADP, KDP, and KD*P for nonlinear devices. IEEE J. Quant. Electr. **QE-18(2)**, 143–145 (1982).

[46] D. Eimerl: Electro-optic, linear and nonlinear optical properties of KDP and its isomorphs. Ferroelectrics **72(1–4)**, 95–139 (1987).

[47] D.A. Roberts: Dispersion equations for nonlinear optical crystals: KDP, $AgGaSe_2$, and $AgGaS_2$. Appl. Opt. **35(24)**, 4677–4688 (1966).

[48] R.A. Ganeev, I.A. Kulagin, A.I. Ryasnyansky, R.I. Tugushev, T. Usmanov: Characterization of nonlinear optical parameters of KDP, $LiNbO_3$ and BBO crystals. Opt. Commun. **229(1–6)**, 403–412 (2004).

[49] W.L. Smith, J.H. Bechtel, N. Bloembergen: Picosecond laser-induced breakdown at 5321 and 3547Å: observation of frequency-dependent behavior. Phys. Rev. B **15(8)**, 4039–4055 (1977).

[50] R. Adair, L.L. Chase, S.A. Payne: Nonlinear refractive index of optical crystals. Phys. Rev. B **39(5)**, 3337–3350 (1989).

[51] D. Milam, M. Weber: Time-resolved interferometric measurements of the nonlinear refractive index in laser materials. Opt. Commun. **18(1)**, 172–173 (1976).

[52] D. Milam, M.J. Weber: Measurement of nonlinear refractive-index coefficients using time-resolved interferometry: application to optical materials for high-power neodymium lasers. J. Appl. Phys. **47(6)**, 2497–2501 (1976).
[53] W.L. Smith, J.H. Bechtel, N. Bloembergen: Dielectric-breakdown threshold and nonlinear-refractive-index measurements with picosecond laser pulses. Phys. Rev. B **12(2)**, 706–714 (1975).
[54] R. Onaka, H. Ito: Pockels effect of KDP and ADP in the ultraviolet region. J. Phys. Soc. Japan **41(4)**, 1303–1309 (1976).
[55] O.G. Vlokh: Dispersion of electro-optic coefficient r_{63} in ADP and KDP crystals. Kristallogr. **7(4)**, 632–633 (1962) [In Russian, English trans.: Sov. Phys.-Crystallogr. **7(4)**, 509–511 (1962)].
[56] J.H. Ott, T.R. Sliker: Linear electro-optic effect in KH_2PO_4 and its isomorphs. J. Opt. Soc. Am. **54(12)**, 1442–1444 (1964).
[57] A. Yariv, P. Yeh: *Optical Waves in Crystals* (John Wiley & Sons, New York, 1984).
[58] R.O'B. Carpenter: The electro-optic effect in uniaxial crystals of the dihydrogen phosphate type. III. Measurements of coefficients. J. Opt. Soc. Am. **40(4)**, 225–229 (1950).
[59] G.W.C. Kaye, T.H. Laby: *Tables of Physical and Chemical Constants* (Longman Group Ltd., London, 1995).
[60] E.N. Volkova, I.A. Velichko: Electrooptical properties of potassium dihydrogen phosphate crystals having different degrees of deuteration. Kristallogr. **18(2)**, 409–410 (1973) [In Russian, English trans.: Sov. Phys.-Crystallogr. **18(2)**, 256–257 (1973)].
[61] K. Onuki, N. Uchida, T. Saku: Interferometric method for measuring electro-optic coefficients in crystals. J. Opt. Soc. Am. **62(9)**, 1030–1032 (1972).
[62] Y.V. Pisarevskii, G.A. Tregubov, Y.V. Shaldin: The electro-optical properties of $NH_4H_2PO_4$, KH_2PO_4 and $N_4(CH_2)_6$ crystals in UHF fields. Fiz. Tverd. Tela **7(2)**, 661–663 (1965) [In Russian, English trans.: Sov. Phys.-Solid State **7(2)**, 530–531 (1965)].
[63] S. Musikant: *Optical Materials. An Introduction to Selection and Application* (Marcel Dekker, Inc., New York, 1985).
[64] R.D. Rosner, E.H. Turner, I.P. Kaminow: Clamped electrooptic coefficients of KDP and quartz. Appl. Opt. **6(4)**, 778 (1967).
[65] E. Munin, A. Balbin Villaverde: Magneto-optical rotatory dispersion of some non-linear crystals. J. Phys.: Condens. Matter **3(27)**, 5099–5106 (1991).
[66] M. Koralewski: Dispersion of the Faraday rotation in KDP-type crystals by pulse high magnetic field. Phys. Stat. Solidi A **65(1)**, K49–K53 (1981).
[67] J.L. Dexter, J. Landry, D.G. Cooper, J. Reintjes: Ultraviolet optical isolators utilizing KDP-isomorphs. Opt. Commun. **80(2)**, 115–118 (1990).
[68] M.K. Srivastava, R.W. Crow: Raman susceptibility measurements and stimulated Raman effect in KDP. Opt. Commun. **8(1)**, 82–84 (1973).
[69] R.C. Eckardt, H. Masuda, Y.X. Fan, R.L. Byer: Absolute and relative nonlinear optical coefficients of KDP, KD*P, BaB_2O_4, $LiIO_3$, MgO:$LiNbO_3$, and KTP measured by phase-matched second-harmonic generation. IEEE J. Quant. Electr. **26(5)**, 922–933 (1990).
[70] J.E. Midwinter, J. Warner: The effects of phase matching method and of uniaxial crystal symmetry on the polar distribution of second-order non-linear optical polarization. Brit. J. Appl. Phys. **16(11)**, 1135–1142 (1965).
[71] W.J. Alford, A.V. Smith: Wavelength variation of the second-order nonlinear coefficients of $KNbO_3$, $KTiOPO_4$, $KTiOAsO_4$, $LiNbO_3$, $LiIO_3$, β-BaB_2O_4, KH_2PO_4, and LiB_3O_5 crystals: a test of Miller wavelength scaling. J. Opt. Soc. Am. B **18(4)**, 524–533 (2001).
[72] I. Shoji, T. Kondo, A. Kitamoto, M. Shirane, R. Ito: Absolute scale of second-order nonlinear-optical coefficients. J. Opt. Soc. Am. B **14(9)**, 2268–2294 (1997).

[73] R.J. Gehr, A.V. Smith: Separated-beam nonphase-matched second-harmonic method of characterizing nonlinear optical coefficients. J. Opt. Soc. Am. B **15(8)**, 2298–2307 (1998).

[74] V.S. Suvorov, A.S. Sonin: Nonlinear optical materials. Kristallogr. **11(5)**, 832–848 (1966) [In Russian, English trans.: Sov. Phys.-Crystallogr. **11(5)**, 711–723 (1966)].

[75] F.M. Johnson, J.A. Duardo: Infrared detection by parametric up-conversion. Laser Focus **3(6)**, 31–37 (1967).

[76] W.F. Hagen, P.C. Magnante: Efficient second-harmonic generation with diffraction-limited and high-spectral-radiance Nd-glass lasers. J. Appl. Phys. **40(1)**, 219–224 (1969).

[77] A.P. Sukhorukov, I.V. Tomov: Tripling of optical frequencies. II. Experimental investigation of a cascade tripler. Opt. Spektrosk. **28(6)**, 1211–1213 (1970) [In Russian, English trans.: Opt. Spectrosc. USSR **28(6)**, 651–653 (1970)].

[78] Y. Takagi, M. Sumitani, N. Nakashima, K. Yoshihara: Efficient generation of picosecond coherent tunable radiation between 190 and 212 nm by sum frequency mixing from Raman and optical parametric radiations. IEEE J. Quant. Electr. **QE-21(3)**, 193–195 (1985).

[79] G.A. Massey, J.C. Johnson: Wavelength-tunable optical mixing experiments between 208 nm and 259 nm. IEEE J. Quant. Electr. **QE-12(11)**, 721–727 (1976).

[80] M. Okada, S. Ieiri: Efficiency in the optical mixing between waves at 1.06 μm and 0.53 μm. Jpn. J. Appl. Phys. **10(6)**, 808 (1971).

[81] E. Fill, J. Wildenauer: Generation of the fifth and sixth harmonics of iodine laser pulses. Opt. Commun. **47(6)**, 412–413 (1983).

[82] V.I. Bredikhin, V.N. Genkin, S.P. Kuznetsov, M.A. Novikov: 90° phase-matching in $KD_{2x}H_{2(1-x)}PO_4$ crystals upon doubling of the second harmonic of a Nd laser. Pisma Zh. Tekh. Phys. **3(9)**, 407–409 (1977) [In Russian, English trans.: Sov. Tech. Phys. Lett. **3(5)**, 165–166 (1977)].

[83] V.I. Bredikhin, G.L. Galushkina, V.N. Genkin, S.P. Kuznetsov: 90° phase-matching upon frequency doubling in $Rb_xK_{(1-x)}H_2PO_4$ crystals. Pisma Zh. Tekh. Phys. **5(7–8)**, 505–508 (1979) [In Russian, English trans.: Sov. Tech. Phys. Lett. **5(4)**, 207–208 (1977)].

[84] M.D. Jones, G.A. Massey: Milliwatt-level 213 nm source based on a repetitively Q-switched, CW-pumped Nd:YAG laser. IEEE J. Quant. Electr. **QE-15(4)**, 204–206 (1979).

[85] G.A. Massey, M.D. Jones, J.C. Johnson: Generation of pulse bursts at 212.8 nm by intracavity modulation of an Nd:YAG laser. IEEE J. Quant. Electr. **QE-14(7)**, 527–532 (1978).

[86] S.V. Muraviov, A.A. Babin, F.I. Feldstein, A.M. Yurkin, V.A. Kamenskii, A.Y. Malyshev, M.S. Kitai, N.M. Bityurin: Efficient conversion to the fifth harmonic of spatially multimode radiation of a repetitively pulsed Nd:YAP laser. Kvant. Elektron. **25(6)**, 535–536 (1998) [In Russian, English trans.: Quantum Electron. **28(6)**, 520–521 (1998)].

[87] A. Ashkin, G.D. Boyd, J.M. Dziedzic: Observation of continuous optical harmonic generation with gas lasers. Phys. Rev. Lett. **11(1)**, 14–17 (1963).

[88] M. Webb: Temperature sensitivity of KDP for phase-matched frequency conversion of 1 μm laser light. IEEE J. Quant. Electr. **30(8)**, 1934–1942 (1994).

[89] U. Deserno, S. Haussühl: Phase-matchable optical nonlinearity in strontium formate and strontium formate dihydrate. IEEE J. Quant. Electr. **QE-9(6)**, 598–601 (1973).

[90] M.J. Chu, S.S. Lee: Thermo-optic and electro-optic tuning sensitivities of the second-harmonic generation in KH_2PO_4 crystal measured by diverging beam technique. J. Appl. Phys. **57(7)**, 2647–2649 (1985).

[91] R.S. Craxton, S.D. Jacobs, J.E. Rizzo, R. Boni: Basic properties of KDP crystal related to the frequency conversion of 1 μm laser radiation. IEEE J. Quant. Electr. **QE-17(9)**, 1782–1786 (1981).

[92] R.B. Andreev, V.D. Volosov, A.G. Kalintsev: Spectral, angular, and temperature characteristics of HIO_3, $LiIO_3$, CDA, DKDP, KDP and ADP non-linear crystals in second- and fourth-harmonic generation. Opt. Spektrosk. **37(2)**, 294–299 (1974) [In Russian, English trans.: Opt. Spectrosc. USSR **37(2)**, 169–171 (1974)].

[93] R.B. Andreev, V.D. Volosov, V.N. Krylov: Temperature stabilization of ADP and KDP crystals in cascade UV generation. Zh. Tekh. Fiz. **47(9)**, 1977–1978 (1977) [In Russian, English trans.: Sov. Phys.-Tech. Phys. **22(9)**, 1146 (1977)].

[94] A. Yokotani, T. Sasaki, T. Yamanaka, C. Yamanaka: Temperature dependence of phase-matching angle of second and third harmonic generation in type-II KDP crystal. Jpn. J. Appl. Phys. **25(1)**, 161–162 (1986).

[95] M.W. Dowley: Parametric fluorescence in ADP and KDP excited by 2573Å CW pump. Opto-electron. **1(4)**, 179–181 (1969).

[96] R.M. Wood: *Laser Damage in Optical Materials* (Adam Hilger, Bristol, 1986).

[97] M. Runkel, A.K. Burnham: Differences in bulk damage probability distributions between tripler and z-cuts of KDP and DKDP at 355 nm. Proc. SPIE **4347**, 408–419 (2001).

[98] L. Armstrong, S.E. Neister, R. Adhav: Measuring CFP dye laser damage thresholds on UV doubling crystals. Laser Focus **18(12)**, 49–53 (1982).

[99] B.F. Bareika, I.A. Begishev, S.A. Burdulis, A.A. Gulamov, E.A. Erofeev, A.S. Piskarskas, V.A. Sirutkaitis, T. Usmanov: Highly efficient parametric generation during pumping with high-power subnanosecond pulses. Pisma Zh. Tekh. Phys. **12(2)**, 186–189 (1986) [In Russian, English trans.: Sov. Tech. Phys. Lett. **12(2)**, 78–79 (1986)].

[100] G.M. Zverev, E.A. Levchuk, E.K. Maldutis: Destruction of KDP, ADP, and $LiNbO_3$ crystals by powerful laser radiation. Zh. Eksp. Teor. Fiz. **57(3)**, 730–736 (1969) [In Russian, English trans.: Sov. Phys.-JETP **30(3)**, 400–403 (1970)].

[101] V.D. Volosov, V.N. Krylov, V.A. Serebryakov, D.V. Sokolov: High-efficiency emission of the second and fourth harmonics of high power picosecond pulses. Pisma Zh. Eksp. Teor. Fiz. **19(1)**, 38–41 (1974) [In Russian, English trans.: JETP Lett. **19(1)**, 23–25 (1974)].

[102] K.P. Burneika, M.V. Ignatavichyus, V.I. Kabelka, A.S. Piskarskas, A.Y. Stabinis: Parametric generation of ultrashort pulses of tunable-frequency radiation. Pisma Zh. Eksp. Teor. Fiz. **16(7)**, 365–367 (1972) [In Russian, English trans.: JETP Lett. **16(7)**, 257–258 (1972)].

[103] V. Kabelka, A. Kutka, A. Piskarskas, V. Smilgiavichyus, Y. Yasevichyute: Parametric generation of picosecond light pulses with an energy conversion greater than 50%. Kvant. Elektron. **6(8)**, 1735–1739 (1979) [In Russian, English trans.: Sov. J. Quantum Electron. **9(8)**, 1022–1024 (1979)].

[104] V.D. Volosov, Y.E. Kamach, E.N. Kozlovsky, V.M. Ovchinnikov: The efficient generation of second harmonic of ruby laser radiation. Opt. Mekh. Promyshl. **36(10)**, 3–4 (1969) [In Russian, English trans.: Sov. J. Opt. Technol. **36(5)**, 656–657 (1969)].

[105] A. Yokotani, T. Sasaki, K. Yoshida, T. Yamanaka, C. Yamanaka: Improvement of the bulk laser damage threshold of potassium dihydrogen phosphate crystals by ultraviolet irradiation. Appl. Phys. Lett. **48(16)**, 1030–1032 (1986).

[106] Y. Nishida, A. Yokotani, T. Sasaki, K. Yoshida, T. Yamanaka, C. Yamanaka: Improvement of the bulk laser damage threshold of potassium dihydrogen phosphate crystal by reducing the organic impurities in growth solution. Appl. Phys. Lett. **52(6)**, 420–421 (1988).

[107] C.E. Barker, B.M. van Wonterghem, J.M. Auerbach, R.J. Foley, J.R. Murray, J.H. Campbell, J.A. Caird, D.R. Speck, B. Woods: Design and performance of the Beamlet laser third harmonic frequency converter. Proc. SPIE **2633**, 398–404 (1995).

[108] W. Seka, S.D. Jacobs, J.E. Rizzo, R. Boni, R.S. Craxton: Demonstration of high efficiency third harmonic conversion of high power Nd-glass laser radiation. Opt. Commun. **34(3)**, 469–473 (1980).

[109] V.D. Volosov, E.V. Nilov: Effect of the spatial structure of a laser beam on the generation of the second harmonic in ADP and KDP crystals. Opt. Spektrosk. **21(6)**, 715–719 (1966) [In Russian, English trans.: Opt. Spectrosc. USSR **21(6)**, 392–394 (1966)].

[110] R.Y. Orlov, I.B. Skidan, L.S. Telegin: Investigation of breakdown in dielectrics produced by ultrashort laser pulses. Zh. Eksp. Teor. Fiz. **61(2)**, 784–790 (1971) [In Russian, English trans.: Sov. Phys.-JETP **34(2)**, 418–421 (1972)].

[111] S.A. Akhmanov, I.A. Begishev, A.A. Gulamov, E.A. Erofeev, B.V. Zhdanov, V.I. Kuznetsov, L.N. Rashkovich, T.V. Usmanov: Highly-efficient parametric frequency conversion of light in large-aperture crystals grown by a fast method. Kvant. Elektron. **11(9)**, 1701–1702 (1984) [In Russian, English trans.: Sov. J. Quantum Electron. **14(9)**, 1145–1146 (1984)].

[112] J.E. Swain, S.E. Stokowski, D. Milam, G.C. Kennedy: The effect of baking and pulsed laser irradiation on the bulk laser damage threshold of potassium dihydrogen phosphate crystals. Appl. Phys. Lett. **41(1)**, 12–14 (1982).

[113] R.M. Wood, R.T. Taylor, R.L. Rouse: Laser damage in optical materials at 1.06 μm. Opt. Laser Technol. **7(3)**, 105–111 (1975).

[114] M. Bass: Nd:YAG laser-irradiation-induced damage to $LiNbO_3$ and KDP. IEEE J. Quant. Electr. **QE-7(7)**, 350–359 (1971).

[115] C. Chen: Chinese lab grows new nonlinear optical borate crystals. Laser Focus World **25(11)**, 129–137 (1989).

[116] M. Yoshimura, T. Kamimura, K. Murase, Y. Mori, H. Yoshida, M. Nakatsuka, T. Sasaki: Bulk laser damage in $CsLiB_6O_{10}$ crystal and its dependence on crystal structure. Jpn. J. Appl. Phys. **38(2A)**, L129–L131 (1999).

[117] D. Eimerl, S. Velsko, L. Davis, F. Wang, G. Loiacono, G. Kennedy: Deuterated L-arginine phosphate: a new efficient nonlinear crystal. IEEE J. Quant. Electr. **25(2)**, 179–193 (1989).

[118] C. Chen, Y. Wu, A. Jiang, B. Wu, G. You, R. Li, S. Lin: New nonlinear-optical crystal: LiB_3O_5. J. Opt. Soc. Am. B **6(4)**, 616–621 (1989).

[119] F. Rainer, W.H. Lowdermilk, D. Milam: Bulk and surface damage thresholds of crystals and glasses at 248 nm. Opt. Eng. **22(4)**, 431–434 (1983).

[120] M. Bass, H.H. Barrett: Avalanche breakdown and the probabilistic nature of laser-induced damage. IEEE J. Quant. Electr. **QE-8(3)**, 338–343 (1972).

[121] L.N. Rashkovich: *KDP-family Single Crystals* (Adam Hilger, Bristol, 1991).

[122] J.J. De Yoreo, A.K. Burnham, P.K. Whitman: Developing KH_2PO_4 and KD_2PO_4 crystals for the world's most powerful laser. Int. Mater. Rev. **47(3)**, 113–152 (2002).

[123] N. Zaitseva, L. Carman, I. Smolsky, R. Torres, M. Yan: The effect of impurities and supersaturation on the rapid growth of KDP crystals. J. Cryst. Growth **204(4)**, 512–524 (1999).

[124] N. Zaitseva, J. Atherton, L. Carman, M. Runkel, R. Ryon, I. Smolsky, H. Spears, R. Torres, M. Yan: Rapid growth of KDP and DKDP crystals: the connection between growth quality conditions and crystal quality. Nonl. Opt. **23(3–4)**, 269–284 (2000).

[125] N. Zaitseva, L. Carman: Rapid growth of KDP-type crystals. Progr. Cryst. Growth Character. Mater. **43(1)**, 1–118 (2001).

4.2 $NH_4H_2PO_4$, Ammonium Dihydrogen Phosphate (ADP)

Negative uniaxial crystal: $n_o > n_e$
Molecular mass: 115.026
Specific gravity: 1.798 g/cm^3 [1]; 1.799 g/cm^3 [2]; 1.803 g/cm^3 at 293 K [3]
Point group: $\bar{4}2m$ (222 at $T < 125$ K [4])
Lattice constants ($\bar{4}2m$):
$a = 7.495$ Å [5]; 7.510 Å [6]; 7.50 Å [4]; 7.4991 ± 0.0004 Å at $T = 293$ K [7]
$c = 7.548$ Å [5]; 7.564 Å [6]; 7.58 Å [4]; 7.5493 ± 0.0012 Å at $T = 293$ K [7]
Mohs hardness: 1 [8]; 2 [9]

Solubility in 100 g H_2O

T [K]	s [g]	Ref.
273	22.7	[3]
293	36.8	[8]
373	173.2	[3]

Melting point: 463 K [10]
Curie temperature: 147 K [7]; 148 K [11], [12]

Linear thermal expansion coefficient [4]

T [K]	$\alpha_t \times 10^6$ [K^{-1}], $\parallel c$	$\alpha_t \times 10^6$ [K^{-1}], $\perp c$
293	4	37

Mean value of linear thermal expansion coefficient [7]

T [K]	$\alpha_t \times 10^6$ [K^{-1}], $\parallel c$	$\alpha_t \times 10^6$ [K^{-1}], $\perp c$
148–298	10.7	27.2
223–323	4.2	32.0

Specific heat capacity c_p at $P = 0.101325$ MPa [13]

T [K]	c_p [J/kgK]
80	405
250	1088
298	1236

Thermal conductivity coefficient [3]

T [K]	κ [W/mK], $\parallel c$	κ [W/mK], $\perp c$
315	0.71	1.26
340	0.71	1.34

Band-gap energy at room temperature: $E_g = 6.8$ eV [14]; 6.81 eV [15]
Transparency range at $\alpha = 1$ cm^{-1} level: 0.184–1.3 μm [11], [16]
Transparency range at 0.5 transmittance level for 0.2-cm-long crystal: 0.184–1.5 μm [2]

Linear absorption coefficient α

λ [μm]	α [cm^{-1}]	Ref.	Note
0.25725	0.01	[17]	
	0.002	[18]	e-wave, $\perp c$
0.265	0.07	[19]	e-wave, $\perp c$
0.2661	0.035	[20]	
0.5145	0.0005	[17]	
	0.00005	[18]	o-wave, $\perp c$
0.6943	0.032	[21]	
0.79	0.03	[4]	
0.89	0.038	[4]	
1.027	0.086	[22]	
1.06	0.1	[4]	
1.083	0.208	[22]	
1.144	0.150	[22]	

Two-photon absorption coefficient β

λ [μm]	τ_p [ns]	$\beta \times 10^{11}$ [cm/W]	Ref.	Note
0.2635	0.5	35	[23]	
0.2661	0.030	6 ± 1	[24]	
		11 ± 3	[20]	
	0.015	24 ± 7	[15]	$\theta = 42°, \phi = 45°$
0.308	0.120	23 ± 5	[25]	
0.3547	0.017	0.68 ± 0.24	[15]	e-wave, $\perp c$

Experimental values of refractive indices at $T = 298$ K [26], [27]

λ [μm]	n_o	n_e	λ [μm]	n_o	n_e
0.2138560	1.62598	1.56738	0.4046561	1.53969	1.49159
0.2288018	1.60785	1.55138	0.4077811	1.53925	1.49123
0.2536519	1.58688	1.53289	0.4358350	1.53578	1.48831
0.2967278	1.56462	1.51339	0.4916036		1.48390
0.3021499	1.56270	1.51163	0.5460740	1.52662	1.48079
0.3125663	1.55917	1.50853	0.5769590	1.52478	1.47939
0.3131545	1.55897	1.50832	0.5790654	1.52466	1.47930
0.3341478	1.55300	1.50313	0.6328160	1.52195	1.47727
0.3650146	1.54615	1.49720	1.0139750	1.50835	1.46895
0.3654833	1.54608	1.49712	1.1287040	1.50446	1.46704
0.3662878	1.54592	1.49698	1.1522760	1.50364	1.46666
0.3906410	1.54174				

Temperature derivatives of refractive indices [28]

λ [μm]	$dn_o/dT \times 10^5$ [K^{-1}]	$dn_e/dT \times 10^5$ [K^{-1}]
0.405	−4.78	≈0
0.436	−4.94	≈0
0.546	−5.23	≈0
0.578	−4.60	≈0
0.633	−5.08	≈0

Temperature dependencies of the refractive indices upon cooling from room temperature to T [K]:

for the spectral range 0.365–0.690 μm [29]:

$$n_o(T) = n_o(298) + 0.713 \times 10^{-2}\left\{[n_o(298)]^2 - 3.0297\,[n_o(298)] + 2.3004\right\} \times (298 - T)$$

$$n_e(T) = n_e(298) + 0.675 \times 10^{-6}[n_e(298)]^2\,(298 - T)$$

for the spectral range 0.436–0.589 μm [30]:

$$n_o(T) = n_o(300) + 10^{-4}\left(141.8 - 0.322\,T - 5.02 \times 10^{-4}\,T^2\right)$$

$$n_e(T) = n_e(300) - 10^{-4}\left(2.5 - 0.01763\,T + 2.901 \times 10^{-5}\,T^2\right)$$

Best set of dispersion relations (λ in μm, $T = 293$ K) [26], [27]:

$$n_o^2 = 2.302842 + \frac{15.102464\lambda^2}{\lambda^2 - 400} + \frac{0.011125165}{\lambda^2 - (75.450861)^{-1}}$$

$$n_e^2 = 2.163510 + \frac{5.919896\lambda^2}{\lambda^2 - 400} + \frac{0.009616676}{\lambda^2 - (76.98751)^{-1}}$$

Other sets of dispersion relations are given in [28], [31], [32], [33].

Temperature-dependent Sellmeier equations (λ in μm, T in K) [31]:

$$n_o^2 = \left(1.6996 - 8.7835 \times 10^{-4}T\right) + \frac{\left(0.64955 + 7.2007 \times 10^{-4}T\right)\lambda^2}{\lambda^2 - \left(0.01723 - 1.40526 \times 10^{-5}T\right)} + \frac{\left(1.10624 - 1.179 \times 10^{-4}T\right)\lambda^2}{\lambda^2 - 30}$$

$$n_e^2 = \left(1.42036 - 1.089 \times 10^{-5}T\right) + \frac{\left(0.74453 + 5.14 \times 10^{-6}T\right)\lambda^2}{\lambda^2 - \left(0.013 - 2.471 \times 10^{-7}T\right)} + \frac{\left(0.42033 - 9.99 \times 10^{-7}T\right)\lambda^2}{\lambda^2 - 30}$$

Linear electrooptic coefficients measured at low frequencies (well below the acoustic resonances of ADP crystal, i.e., for the "free" crystal) at room temperature

λ [μm]	r_{41}^T [pm/V]	r_{63}^T [pm/V]	Ref.	Note
0.20		−8.5	[34]	$T = 286$ K
0.25		−8.6	[34]	$T = 286$ K

λ [μm]	r_{41}^{T} [pm/V]	r_{63}^{T} [pm/V]	Ref.	Note
0.30		−8.2	[34]	$T = 286$ K
0.488	−22.9 ± 0.2	−8.07 ± 0.1	[35]	$T = 298$ K
0.500		−7.8	[36]	
0.5461		−8.56	[37]	
	−23.76		[37]	
	−24.5 ± 0.4		[38]	
0.556		−8.47 ± 0.17	[39]	$T = 295$ K
	−20.8 ± 0.3 (?)		[39]	$T = 295$ K
0.61–1.15		−8.55 ± 0.15	[40]	
0.6328		−7.83	[37]	
		−7.9	[36]	
	−22.2 ± 0.2	−8.14 ± 0.1	[35]	$T = 298$ K
	−23.1 ± 0.3		[41]	$T = 293$ K
	−23.41		[37]	

Linear electrooptic coefficient measured at high frequencies (well above the acoustic resonances of ADP crystal, i.e., for the "clamped" crystal) at room temperature

λ [μm]	r_{63}^{S} [pm/V]	Ref.
0.5461	−4.1 ± 0.4 (?)	[42]
	−5.1 ± 1.5	[43]
	−5.5	[44]

Half-wave retardation voltage at longitudinal modulation

λ [μm]	$V_{\lambda/2}$ [kV]	Ref.
0.488	8.4	[35]
0.5	8.27	[39]
0.5461	9.0	[44]
0.6	10.0	[39]
0.6328	11.0	[35]

Verdet constant ($\|c$)

λ [μm]	T [K]	V [degree/Tm]	Ref.
0.6328	293	251 ± 5	[1]
	298	230	[45]

Calculated Verdet constant ($\|c$) [46]

λ [μm]	V [degree/Tm]
0.193	4023
0.222	2573
0.248	1858

λ [μm]	V [degree/Tm]
0.308	1061
0.351	781

Expressions for the effective second-order nonlinear coefficient in general case (Kleinman symmetry conditions are valid, $d_{14} = d_{25} = d_{36}$) [47]:

$$d_{\mathrm{ooe}} = -d_{36}\sin(\theta + \rho)\sin 2\phi$$

$$d_{\mathrm{eoe}} = d_{\mathrm{oee}} = 2d_{36}\sin(\theta + \rho)\cos(\theta + \rho)\cos 2\phi$$

Simplified expressions for the effective second-order nonlinear coefficient (approximation of small birefringence angle, Kleinman symmetry conditions are valid, $d_{14} = d_{25} = d_{36}$) [48]:

$$d_{\mathrm{ooe}} = -d_{36}\sin\theta\sin 2\phi$$

$$d_{\mathrm{eoe}} = d_{\mathrm{oee}} = d_{36}\sin 2\theta\cos 2\phi$$

Absolute values of second-order nonlinear coefficient:

$d_{36}(0.6328\ \mu\mathrm{m}) = 0.55 \pm 0.02$ pm/V [49]

$d_{36}(1.0642\ \mu\mathrm{m}) = 0.46 \pm 0.03$ pm/V [49]; 0.47 pm/V [50]

Experimental values of phase-matching angle ($T = 293$ K)

Interacting wavelengths [μm]	θ_{exp} [deg]	Ref.
SHG, $o + o \Rightarrow e$		
0.524 ⇒ 0.262	90	[28]
0.530 ⇒ 0.265	81.7	[51]
0.6943 ⇒ 0.34715	51.9	[52]
0.7035 ⇒ 0.35175	50.5	[53]
1.06 ⇒ 0.53	41.9	[52]
	42	[54]
SHG, $o + o \Rightarrow e$		
1.0642 + 0.5321 ⇒ 0.35473	46.9	[55]
1.0642 + 0.2810 ⇒ 0.22230	90	[56]
0.81219 + 0.34715 ⇒ 0.24320	90	[57]
SHG, $e + o \Rightarrow e$		
1.0642 + 0.5321 ⇒ 0.35473	60.2	[55]

Experimental values of NCPM temperature

Interacting wavelengths [μm]	T [°C]	Ref.	Note
SHG, $o + o \Rightarrow e$			
0.4920 ⇒ 0.2460	−116	[58]	
0.4965 ⇒ 0.24825	−93.2	[59]	
0.5017 ⇒ 0.25085	−68.4	[59]	

Interacting wavelengths [μm]	T [°C]	Ref.	Note
0.5145 ⇒ 0.25725	−11.7	[60]	
	−10.2	[59]	
	−9.2	[18]	
0.524 ⇒ 0.262	20	[28]	
0.52534 ⇒ 0.26267	30	[61]	
0.53 ⇒ 0.265	43	[19]	
	47	[51]	
	48	[62]	
	49.6	[63]	
0.5321 ⇒ 0.26605	47.1	[64]	
	49.5	[65]	
	50	[66]	
	51.2	[67]	0.1–1 Hz
	44.6	[67]	20 Hz
	51–52	[68]	
0.5398 ⇒ 0.2699	79	[69]	1–25 Hz
0.548 ⇒ 0.274	100	[61]	
0.557 ⇒ 0.2785	120	[70]	
SFG, $o + o \Rightarrow e$			
1.0642 + 0.26605 ⇒ 0.21284	−55	[71]	

Experimental values of internal angular and temperature bandwidths

Interacting wavelengths [μm]	T [°C]	θ_{pm} [deg]	$\Delta\theta^{int}$ [deg]	ΔT [°C]	Ref.
SHG, $o + o \Rightarrow e$					
1.06 ⇒ 0.53	20	42	0.057		[54]
0.5321 ⇒ 0.26605	49.5	90		0.60	[65]
	51	90	1.086	0.53	[67]
0.53 ⇒ 0.265	20	82	0.118		[72]
	20	82	0.088		[73]
	20	82	0.089	0.63	[51]

Experimental values of spectral bandwidth

Interacting wavelengths [μm]	T [°C]	θ_{pm} [deg]	$\Delta\nu$ [cm^{-1}]	Ref.
SHG, $o + o \Rightarrow e$				
1.06 ⇒ 0.53	20	42	178	[54]
0.53 ⇒ 0.265	20	82	4.9	[73]

Temperature variation of phase-matching angle [51]

Interacting wavelengths [μm]	T [°C]	θ_{pm} [deg]	$d\theta_{pm}/dT$ [deg/K]
SHG, $o + o \Rightarrow e$			
0.53 ⇒ 0.265	20	82	0.14
	47	90	1.10

Temperature tuning of noncritical SHG [28]

Interacting wavelengths [μm]	$d\lambda_1/dT$ [nm/K]
SHG, $o + o \Rightarrow e$	
$0.524 \Rightarrow 0.262$	0.306

Temperature tuning of noncritical SFG [74]

Interacting wavelengths [μm]	$d\lambda_3/dT$ [nm/K]
SHG, $o + o \Rightarrow e$	
$0.6943 + 0.39961 \Rightarrow 0.25363$	0.171

Temperature variation of birefringence for noncritical SHG process (0.5145 μm $\Rightarrow$ 0.25725 μm, $o + o \Rightarrow e$): $d(n_2^{\mathrm{e}} - n_1^{\mathrm{o}})/dT = 5.65 \times 10^{-5}\ \mathrm{K}^{-1}$ [60]

Calculated values of phase-matching and "walk-off" angles

Interacting wavelengths [μm]	θ_{pm} [deg]	ρ_1 [deg]	ρ_3 [deg]
SHG, $o + o \Rightarrow e$			
$0.5321 \Rightarrow 0.26605$	80.15		0.639
$0.5782 \Rightarrow 0.2891$	65.28		1.427
$0.6328 \Rightarrow 0.3164$	56.91		1.703
$0.6594 \Rightarrow 0.3297$	54.07		1.762
$0.6943 \Rightarrow 0.34715$	51.09		1.803
$1.0642 \Rightarrow 0.5321$	41.74		1.746
$1.3188 \Rightarrow 0.6594$	45.45		1.694
SFG, $o + o \Rightarrow e$			
$0.5782 + 0.5105 \Rightarrow 0.27112$	74.84		0.955
$1.0642 + 0.5321 \Rightarrow 0.35473$	47.82		1.836
$1.3188 + 0.6594 \Rightarrow 0.4396$	42.56		1.794
SHG, $e + o \Rightarrow e$			
$1.0642 \Rightarrow 0.5321$	61.39	1.230	1.449
$1.3188 \Rightarrow 0.6594$	65.63	0.968	1.250
SFG, $e + o \Rightarrow e$			
$1.0642 + 0.5321 \Rightarrow 0.35473$	59.85	1.272	1.582
$1.3188 + 0.6594 \Rightarrow 0.4396$	50.86	1.274	1.748

Calculated values of inverse group-velocity mismatch for SHG process in ADP

Interacting wavelengths [μm]	θ_{pm} [deg]	β [fs/mm]
SHG, $o + o \Rightarrow e$		
$1.2 \Rightarrow 0.6$	43.10	49
$1.1 \Rightarrow 0.55$	41.94	21
$1.0 \Rightarrow 0.5$	41.71	8
$0.9 \Rightarrow 0.45$	42.68	42
$0.8 \Rightarrow 0.4$	45.34	85
$0.7 \Rightarrow 0.35$	50.67	142

Interacting wavelengths [μm]	θ_{pm} [deg]	β [fs/mm]
0.6 ⇒ 0.3	61.39	233
SHG, $e + o \Rightarrow e$		
1.2 ⇒ 0.6	62.50	105
1.1 ⇒ 0.55	61.39	78
1.0 ⇒ 0.5	62.02	95
0.9 ⇒ 0.45	65.24	127
0.8 ⇒ 0.4	73.80	173

Laser-induced bulk-damage threshold

λ [μm]	τ_p [ns]	I_{thr} [GW/cm^2]	Ref.	Note
0.265	30	>1	[19]	
0.2661	0.03	>10	[75]	
0.53	10	120–220	[76]	21-μm beam-waist diameter
	0.5	>13	[77]	
0.5321	3	>0.75	[68]	30 Hz
	0.6	>8	[78]	
	0.03	>8	[24]	
0.5398	5	6	[69]	SHG direction
0.6	330	1.8	[79]	
0.6943	5–25	0.15–0.24	[21]	
1.06	60	0.5	[80]	
	14	10–18	[76]	100-μm beam-waist diameter
		70–130	[76]	21-μm beam-waist
1.0642	10	>4.5	[81]	

Laser-induced surface damage threshold

λ [μm]	τ_p [ns]	I_{thr} [GW/cm^2]	Ref.	Note
0.2484	20	0.2	[82]	1.5-mm beam-waist diameter
0.6943	5–25	1–5.4	[21]	
1.0642	12	6.4	[83]	$\parallel c$, 30-μm beam-waist diameter
10	2.2 to >4.5		[81]	

About the crystal

ADP is the analog of KDP with a slightly higher second-order nonlinear coefficient.

References

[1] S. Haussühl, W. Effgen: Faraday effect in cubic crystals. Additivity rule and phase transitions. Z. Kristallogr. **183(1–4)**, 153–174 (1988).

[2] Data sheet of Cleveland Crystals Inc. Available at www.clevelandcrystals.com.

[3] E.M. Voronkova, B.N. Grechushnikov, G.I. Distler, I.P. Petrov: *Optical Materials for Infrared Technique* (Nauka, Moscow, 1965) [In Russian].

[4] A.A. Blistanov, V.S. Bondarenko, N.V. Perelomova, F.N. Strizhevskaya, V.V. Tchkalova, M.P. Shaskolskaya: *Acoustic Crystals* (Nauka, Moscow, 1982) [In Russian].

[5] S. Haussühl: Elastische und thermoelastische Eigenschaften von KH_2PO_4, KH_2AsO_4, $NH_4H_2PO_4$, $NH_4H_2AsO_4$ und RbH_2PO_4. Z. Kristallogr. **120(6)**, 401–414 (1964) [In German].

[6] *Handbook of Optical Constants of Solids II*, ed. by E.D. Palik (Academic Press, Boston, 1991).

[7] W.R. Cook, Jr.: Thermal expansion of crystals with KH_2PO_4 structure. J. Appl. Phys. **38(4)**, 1637–1642 (1967).

[8] B.H.T. Chai: Optical Crystals. In: *CRC Handbook of Laser Science and Technology, Supplement 2: Optical Materials*, ed. by M.J. Weber (CRC Press, Boca Raton, 1995) pp. 3–65.

[9] V.G. Dmitriev, G.G. Gurzadyan, D.N. Nikogosyan: *Handbook of Nonlinear Optical Crystals, Third Revised Edition* (Springer, Berlin, 1999).

[10] S.S. Ballard, J.S. Browder: Thermal Properties. In: *CRC Handbook of Laser Science and Technology, Vol. IV, Optical Materials: Part 2*, ed. by M.J. Weber (CRC Press, Boca Raton, 1987), pp. 49–54.

[11] A.S. Sonin, A.S. Vasilevskaya: *Electrooptic Crystals* (Atomizdat, Moscow, 1971) [In Russian].

[12] I.P. Kaminow: Tables of Linear Electrooptic Coefficients. In: *CRC Handbook of Laser Science and Technology, Vol. III, Optical Materials: Part 2*, ed. by M.J. Weber (CRC Press, Boca Raton, 1986), pp. 253–278.

[13] *Physical Quantities. Handbook*, ed. by I.S. Grigoriev and E.Z. Meilikhov (Energoatomizdat, Moscow, 1991) [In Russian].

[14] E.W. van Stryland, L.L. Chase: Two-Photon Absorption. Inorganic Materials. In: *CRC Handbook of Laser Science and Technology, Supplement 2: Optical Materials*, ed. by M.J. Weber (CRC Press, Boca Raton, 1995), pp. 299–328.

[15] P. Liu, W.L. Smith, H. Lotem, J.H. Bechtel, N. Bloembergen, R.S. Adhav: Absolute two-photon absorption coefficients at 355 and 266 nm. Phys. Rev. B **17(12)**, 4620–4632 (1978).

[16] W.L. Smith: KDP and ADP transmission in the vacuum ultraviolet. Appl. Opt. **16(7)**, 798 (1977).

[17] P. Huber: High power in the near ultraviolet using efficient SHG. Opt. Commun. **15(2)**, 196–200 (1975).

[18] M.W. Dowley, E.B. Hodges: Studies of high-power CW and quasi-CW parametric UV generation by ADP and KDP in argon-ion laser cavity. IEEE J. Quant. Electr. **QE-4(10)**, 552–558 (1968).

[19] B.V. Zhdanov, V.V. Kalitin, A.I. Kovrigin, S.M. Pershin: Parametric light generator tunable from 3980 to 7920 Å. Pisma Zh. Tekh. Phys. **1(18)**, 847–851 (1975) [In Russian, English trans.: Sov. Tech. Phys. Lett. **1(9)**, 368–369 (1975)].

[20] J. Reintjes, R.C. Eckardt: Two-photon absorption in ADP and KD*P at 266.1 nm. IEEE J. Quant. Electr. **QE-13(9)**, 791–793 (1977).

[21] T.M. Christmas, J.M. Ley: Laser-induced damage in XDP materials. Electron. Lett. **7(18)**, 544–546 (1971).
[22] E.N. Volkova, V.V. Fadeev: Linear absorption coefficient of some nonlinear optical crystals. In: *Nonlinear Optics*, ed. by R.V. Khokhlov (Nauka, Novosibirsk, 1968), pp. 185–187 [In Russian].
[23] I.A. Begishev, R.A. Ganeev, A.A. Gulamov, E.A. Erofeev, S.R. Kamalov, T. Usmanov, A.D. Khadzhaev: The neodymium laser fifth harmonic generation and two-photon absorption in KDP and ADP crystals. Kvant. Elektron. **15(2)**, 353–361 (1988) [In Russian, English trans.: Sov. J. Quantum Electron. **18(2)**, 224–228 (1988)].
[24] J. Reintjes, R.C. Eckardt: Efficient harmonic generation from 532 to 266 nm in ADP and KD*P. Appl. Phys. Lett. **30(2)**, 91–93 (1977).
[25] Y.P. Kim, M.H.R. Hutchinson: Intensity-induced nonlinear effects in UV window materials. Appl. Phys. B **49(5)**, 469–478 (1989).
[26] F. Zernike, Jr.: Refractive indices of ammonium dihydrogen phosphate and potassium dihydrogen phosphate between 2000 Å and 1.5 μm. J. Opt. Soc. Am. **54(10)**, 1215–1220 (1964).
[27] F. Zernike, Jr.: Refractive indices of ammonium dihydrogen phosphate and potassium dihydrogen phosphate between 2000 Å and 1.5 μm. Erratum. J. Opt. Soc. Am. **55(2)**, 210–211 (1965).
[28] N.P. Barnes, D.J. Gettemy, R.S. Adhav: Variations of the refractive index with temperature and the tuning rate for KDP isomorphs. J. Opt. Soc. Am. **72(7)**, 895–898 (1982).
[29] R.A. Philips: Temperature variations of the index of refraction of ADP, KDP, and deuterated KDP. J. Opt. Soc. Am. **56(5)**, 629–632 (1966).
[30] M. Yamazaki, T. Ogawa: Temperature dependences of the refractive indices of $NH_4H_2PO_4$, KH_2PO_4, and partially deuterated KH_2PO_4. J. Opt. Soc. Am. **56(10)**, 1407–1408 (1966).
[31] G.C. Ghosh, G.C. Bhar: Temperature dispersion in ADP, KDP, and KD*P for nonlinear devices. IEEE J. Quant. Electr. **QE-18(2)**, 143–145 (1982).
[32] D. Eimerl: Electro-optic, linear and nonlinear optical properties of KDP and its isomorphs. Ferroelectrics **72(1–4)**, 95–139 (1987).
[33] K.W. Kirby, L.G. DeShazer: Refractive indices of 14 nonlinear crystals isomorphic to KH_2PO_4. J. Opt. Soc. Am. B **4(7)**, 1072–1078 (1987).
[34] R. Onaka, H. Ito: Pockels effect of KDP and ADP in the ultraviolet region. J. Phys. Soc. Japan **41(4)**, 1303–1309 (1976).
[35] Z. Li, X. Huang, D. Wu, K. Xiong: Large crystal growth and measurement of electro-optical coefficients of ADP. J. Cryst. Growth **222(3)**, 524–527 (2001).
[36] O.G. Vlokh: Dispersion of electro-optic coefficient r_{63} in ADP and KDP crystals. Kristallogr. **7(4)**, 632–633 (1962) [In Russian, English trans.: Sov. Phys.-Crystallogr. **7(4)**, 509–511 (1962)].
[37] A. Yariv, P. Yeh: *Optical Waves in Crystals* (John Wiley & Sons, New York, 1984).
[38] J.H. Ott, T.R. Sliker: Linear electro-optic effect in KH_2PO_4 and its isomorphs. J. Opt. Soc. Am. **54(12)**, 1442–1444 (1964).
[39] R.O'B. Carpenter: The electro-optic effect in uniaxial crystals of the dihydrogen phosphate type. III. Measurements of coefficients. J. Opt. Soc. Am. **40(4)**, 225–229 (1950).
[40] H. Koetser: Measurement of r_{63} for ADP up to electric breakdown. Electron. Lett. **3(2)**, 54–55 (1967).
[41] J.M. Ley: Low-voltage light-amplitude modulation. Electron. Lett. **2(1)**, 12–13 (1966).
[42] L. Silverstein, M. Sucher: Determination of the Pockels electro–optic coefficient in ADP at 5.5 GHz. Electron. Lett. **2(12)**, 437–438 (1966).

[43] Y.V. Pisarevskii, G.A. Tregubov, Y.V. Shaldin: The electro-optical properties of $NH_4H_2PO_4$, KH_2PO_4 and $N_4(CH_2)_6$ crystals in UHF fields. Fiz. Tverd. Tela **7(2)**, 661–663 (1965) [In Russian, English trans.: Sov. Phys.-Solid State **7(2)**, 530–531 (1965)].

[44] S. Musikant: *Optical Materials. An Introduction to Selection and Application* (Marcel Dekker, Inc., New York, 1985).

[45] M. Koralewski: Dispersion of the Faraday rotation in KDP-type crystals by pulse high magnetic field. Phys. Stat. Solidi A **65(1)**, K49–K53 (1981).

[46] J.L. Dexter, J. Landry, D.G. Cooper, J. Reintjes: Ultraviolet optical isolators utilizing KDP-isomorphs. Opt. Commun. **80(2)**, 115–118 (1990).

[47] R.C. Eckardt, H. Masuda, Y.X. Fan, R.L. Byer: Absolute and relative nonlinear optical coefficients of KDP, KD*P, BaB_2O_4, $LiIO_3$, $MgO:LiNbO_3$, and KTP measured by phase-matched second-harmonic generation. IEEE J. Quant. Electr. **26(5)**, 922–933 (1990).

[48] J.E. Midwinter, J. Warner: The effects of phase matching method and of uniaxial crystal symmetry on the polar distribution of second-order non-linear optical polarization. Brit. J. Appl. Phys. **16(11)**, 1135–1142 (1965).

[49] K. Hagimoto, A. Mito: Determination of the second-order susceptibility of ammonium dihydrogen phosphate and α-quartz at 633 and 1064 nm. Appl. Opt. **34(36)**, 8276–8282 (1995).

[50] D.A. Roberts: Simplified characterization of uniaxial and biaxial nonlinear optical crystals: a plea for standardization of nomenclature and conventions. IEEE J. Quant. Electr. **28(10)**, 2057–2074 (1992).

[51] R.B. Andreev, V.D. Volosov, V.N. Krylov: Temperature stabilization of ADP and KDP crystals in cascade UV generation. Zh. Tekh. Fiz. **47(9)**, 1977–1978 (1977) [In Russian, English trans.: Sov. Phys.-Tech. Phys. **22(9)**, 1146 (1977)].

[52] V.S. Suvorov, A.S. Sonin: Nonlinear optical materials. Kristallogr. **11(5)**, 832–848 (1966) [In Russian, English trans.: Sov. Phys.-Crystallogr. **11(5)**, 711–723 (1966)].

[53] F. Wondrazek, A. Seilmeier, W. Kaiser: Picosecond light pulses tunable from the violet to near infrared. Appl. Phys. B **32(1)**, 39–42 (1983).

[54] W.F. Hagen, P.C. Magnante: Efficient second-harmonic generation with diffraction-limited and high-spectral-radiance Nd-glass lasers. J. Appl. Phys. **40(1)**, 219–224 (1969).

[55] M. Okada, S. Ieiri: Efficiency in the optical mixing between waves at 1.06 μm and 0.53 μm. Jpn. J. Appl. Phys. **10(6)**, 808 (1971).

[56] G.A. Massey, J.C. Johnson: Wavelength-tunable optical mixing experiments between 208 and 259 nm. IEEE J. Quant. Electr. **QE-12(11)**, 721–727 (1976).

[57] R.E. Stickel, Jr., F.B. Dunning: Generation of tunable coherent radiation below 250 nm at MW power levels. Appl. Opt. **17(9)**, 1313–1314 (1978).

[58] R.K. Jain, T.K. Gustafson: Efficient generation of continuously tunable coherent radiation in the 2460–2650 Å spectral range. IEEE J. Quant. Electr. **QE-12(9)**, 555–556 (1976).

[59] R.K. Jain, T.K. Gustafson: Second-harmonic generation of several argon-ion laser lines. IEEE J. Quant. Electr. **QE-9(8)**, 859–861 (1973).

[60] M.W. Dowley: Parametric fluorescence in ADP and KDP excited by 2573 Å CW pump. Opto-electron. **1(4)**, 179–181 (1969).

[61] R.W. Wallace: Generation of tunable UV from 2610 to 3150 Å. Opt. Commun. **4(4)**, 316–318 (1971).

[62] G.V. Venkin, L.L. Kulyuk, D.I. Maleev: Investigation of stimulated Raman scattering in gases excited by fourth harmonic of neodymium laser radiation. Kvant. Elektron. **2(11)**, 2475–2480 (1975) [In Russian, English trans.: Sov. J. Quantum Electron. **5(11)**, 1348–1351 (1975)].

[63] B.G. Huth, Y.C. Kiang: 90° phase matching for second-harmonic conversion to the ultraviolet. J. Appl. Phys. **40(12)**, 4976–4977 (1969).

[64] G.A. Massey, M.D. Jones, J.C. Johnson: Generation of pulse bursts at 212.8 nm by intracavity modulation of an Nd:YAG laser. IEEE J. Quant. Electr. **QE-14(7)**, 527–532 (1978).

[65] D.P. Schinke: Generation of ultraviolet light using the Nd:YAG laser. IEEE J. Quant. Electr. **QE-8(2)**, 86–87 (1972).

[66] A.H. Kung: Generation of tunable picosecond VUV radiation. Appl. Phys. Lett. **25(11)**, 653–655 (1974).

[67] K. Kato: Conversion of high power Nd:YAG laser radiation to the UV at 2661 Å. Opt. Commun. **13(4)**, 361–362 (1975).

[68] J.M. Yarborough, G.A. Massey: Efficient high-gain parametric generation in ADP continuously tunable across the visible spectrum. Appl. Phys. Lett. **18(10)**, 438–440 (1971).

[69] S.V. Muraviov, A.A. Babin, F.I. Feldstein, A.M. Yurkin, V.A. Kamenskii, A.Y. Malyshev, M.S. Kitai, N.M. Bityurin: Efficient conversion to the fifth harmonic of spatially multimode radiation of a repetitively pulsed Nd:YAP laser. Kvant. Elektron. **25(6)**, 535–536 (1998) [In Russian, English trans.: Quantum Electron. **28(6)**, 520–521 (1998)].

[70] R.S. Adhav: Materials for optical harmonic generation. Laser Focus **19(6)**, 73–78 (1983).

[71] G.A. Massey: Efficient upconversion of long-wavelength UV light into the 200–235 nm band. Appl. Phys. Lett. **24(8)**, 371–373 (1974).

[72] V.D. Volosov, V.N. Krylov, V.A. Serebryakov, D.V. Sokolov: High-efficiency emission of the second and fourth harmonics of high power picosecond pulses. Pisma Zh. Eksp. Teor. Fiz. **19(1)**, 38–41 (1974) [In Russian, English trans.: JETP Lett. **19(1)**, 23–25 (1974)].

[73] R.B. Andreev, V.D. Volosov, A.G. Kalintsev: Spectral, angular, and temperature characteristics of HIO_3, $LiIO_3$, CDA, DKDP, KDP and ADP non-linear crystals in second- and fourth-harmonic generation. Opt. Spektrosk. **37(2)**, 294–299 (1974) [In Russian, English trans.: Opt. Spectrosc. USSR **37(2)**, 169–171 (1974)].

[74] T. Sato: Continuously tunable ultraviolet radiation at 2535 Å. J. Appl. Phys. **44(5)**, 2257–2259 (1973).

[75] T.A. Rabson, H.J. Ruiz, P.L. Shah, F.K. Tittel: Efficient second harmonic generation of picosecond laser pulses. Appl. Phys. Lett. **20(8)**, 282–284 (1972).

[76] G.M. Zverev, E.A. Levchuk, E.K. Maldutis: Destruction of KDP, ADP, and $LiNbO_3$ crystals by powerful laser radiation. Zh. Eksp. Teor. Fiz. **57(3)**, 730–736 (1969) [In Russian, English trans.: Sov. Phys.-JETP **30(3)**, 400–403 (1970)].

[77] S.A. Akhmanov, I.A. Begishev, A.A. Gulamov, E.A. Erofeev, B.V. Zhdanov, V.I. Kuznetsov, L.N. Rashkovich, T.V. Usmanov: Highly-efficient parametric frequency conversion of light in large-aperture crystals grown by a fast method. Kvant. Elektron. **11(9)**, 1701–1702 (1984) [In Russian, English trans.: Sov. J. Quantum Electron. **14(9)**, 1145–1146 (1984)].

[78] G.J. Linford, B.C. Johnson, J.S. Hildum, W.E. Martin, K. Snyder, R.D. Boyd, W.L. Smith, C.L. Vercimak, D. Eimerl, J.T. Hunt: Large aperture harmonic conversion experiments at Lawrence Livermore National Laboratory. Appl. Opt. **21(20)**, 3633–3643 (1982).

[79] L. Armstrong, S.E. Neister, R. Adhav: Measuring CFP dye laser damage thresholds on UV doubling crystals. Laser Focus **18(12)**, 49–53 (1982).

[80] V.D. Volosov, E.V. Nilov: Effect of the spatial structure of a laser beam on the generation of the second harmonic in ADP and KDP crystals. Opt. Spektrosk. **21(6)**, 715–719 (1966) [In Russian, English trans.: Opt. Spectrosc. USSR **21(6)**, 392–394 (1966)].

[81] R.M. Wood, R.T. Taylor, R.L. Rouse: Laser damage in optical materials at 1.06 μm. Opt. Laser Technol. **7(3)**, 105–111 (1975).

[82] F. Rainer, W.H. Lowdermilk, D. Milam: Bulk and surface damage thresholds of crystals and glasses at 248 nm. Opt. Eng. **22(4)**, 431–434 (1983).
[83] M. Bass, H.H. Barrett: Avalanche breakdown and the probabilistic nature of laser-induced damage. IEEE J. Quant. Electr. **QE–8(3)**, 338–343 (1972).

4.3 KD_2PO_4, Deuterated Potassium Dihydrogen Phosphate (DKDP)

Negative uniaxial crystal: $n_o > n_e$
Molecular mass: 138.098
Specific gravity: 2.355 g/cm^3 [1]; 2.3555 g/cm^3 [2]
Point group: $\bar{4}2m$
Lattice constants [3], [4]:
$a = 7.4697 \pm 0.0003$ Å at $T = 298$ K
$c = 6.9766 \pm 0.0005$ Å at $T = 298$ K
Mohs hardness: 1.5 [5]; 2.5 [1]
Curie temperature: 222 ± 1 K [3]; 222 K [4]; 222 K at 99.8% deuteration [6]; 216.3 K at 98% deuteration [6]

Linear thermal expansion coefficient [7]

$\alpha_t \times 10^6$ [K^{-1}], $\parallel c$	$\alpha_t \times 10^6$ [K^{-1}], $\perp c$
44	24.9

Mean value of linear thermal expansion coefficient [4]

T [K]	$\alpha_t \times 10^6$ [K^{-1}], $\parallel c$	$\alpha_t \times 10^6$ [K^{-1}], $\perp c$
223–298	39.5	19.4
223–323	40.7	20.1

Thermal conductivity coefficient [8]

κ [W/mK], $\parallel c$	κ [W/mK], $\perp c$
1.86	2.09

Band-gap energy at room temperature: $E_g = 7.0$ eV [9]
Transparency range at $\alpha = 1$ cm^{-1} level: ≈0.2 to ≈1.8 μm [3], [10]
Transparency range at 0.5 transmittance level for 0.2-cm-long crystal: <0.2 to 2.15 μm [2]

Linear absorption coefficient α

λ [μm]	α [cm^{-1}]	Ref.	Note
0.2661	0.035	[11]	
0.5321	0.004–0.005	[12]	98–99% deuteration
	<0.001	[7]	

λ [μm]	α [cm^{-1}]	Ref.	Note
0.6943	<0.004	[13]	80–95% deuteration
0.82–1.21	<0.015	[14]	
0.94	0.005	[14]	
1.0642	0.004–0.005	[12]	98–99% deuteration
	0.012	[7]	*o*-wave
	0.0019	[15]	*o*-wave, 98% deuteration
	0.0013	[15]	*o*-wave, 99.5% deuteration
	<0.001	[7]	*e*-wave
	0.0004	[15]	*e*-wave, 98% deuteration
	0.0003	[15]	*e*-wave, 99.5% deuteration
1.315	0.025	[16]	
1.57	0.1	[17]	*o*-wave, 95% deuteration
1.74	0.1	[17]	*e*-wave, 95% deuteration

Two-photon absorption coefficient β

λ [μm]	τ_p [ns]	$\beta \times 10^{11}$ [cm/W]	Ref.	Note
0.2661	0.030	2 ± 1	[18]	
		2.7 ± 0.7	[11]	
0.3547	0.017	0.54 ± 0.19	[19]	*e*-wave, $\perp c$

Experimental values of refractive indices at $T = 298$ K [20]

λ [μm]	n_o	n_e	λ [μm]	n_o	n_e
0.4047	1.5189	1.4776	0.5461	1.5079	1.4683
0.4078	1.5185	1.4772	0.5779	1.5063	1.4670
0.4358	1.5155	1.4747	0.6234	1.5044	1.4656
0.4916	1.5111	1.4710	0.6907	1.5022	1.4639

Temperature derivatives of refractive indices [21]

λ [μm]	$dn_o/dT \times 10^5$ [K^{-1}]	$dn_e/dT \times 10^5$ [K^{-1}]
0.405	−3.00	−1.86
0.436	−3.37	−2.13
0.546	−2.99	−1.95
0.578	−3.00	−2.52
0.633	−3.16	−2.03

Temperature dependencies of the refractive indices upon cooling from room temperature to T [K]:

for the spectral range 0.365–0.690 μm [20]:

$$n_o(T) = n_o(298) + 0.228 \times 10^{-4}\{[n_o(298)]^2 - 1.047\}(298 - T)$$

$$n_e(T) = n_e(298) + 0.955 \times 10^{-5}[n_e(298)]^2(298 - T)$$

for the spectral range 0.436–0.589 μm [22]:

$$n_o(T) = n_o(300) + 10^{-4}(85.2 - 0.0695\,T - 7.25 \times 10^{-4}\,T^2)$$
$$n_e(T) = n_e(300) - 10^{-4}(21.8 - 0.445\,T + 1.24 \times 10^{-3}\,T^2)$$

Best set of dispersion relations (λ in μm, $T = 293$ K) [23]

$$n_o^2 = 2.240921 + \frac{2.246956\lambda^2}{\lambda^2 - (11.26591)^2} + \frac{0.009676}{\lambda^2 - (0.124981)^2}$$

$$n_e^2 = 2.126019 + \frac{0.784404\lambda^2}{\lambda^2 - (11.10871)^2} + \frac{0.008578}{\lambda^2 - (0.109505)^2}$$

Other sets of dispersion relations are given in [8], [21], [24]
Temperature-dependent Sellmeier equations (λ in μm, T in K) [24]:

$$n_o^2 = (1.55934 + 3.3935 \times 10^{-4}\,T) + \frac{(0.71098 - 4.1655 \times 10^{-4}\,T)\lambda^2}{\lambda^2 - (0.01407 + 6.4904 \times 10^{-6}\,T)} + \frac{(0.67671 + 4.8281 \times 10^{-5}\,T)\lambda^2}{\lambda^2 - 30}$$

$$n_e^2 = (1.68647 + 3.43 \times 10^{-6}\,T) + \frac{(0.46629 - 6.26 \times 10^{-5}\,T)\lambda^2}{\lambda^2 - (0.01663 + 1.3626 \times 10^{-6}\,T)} + \frac{(0.59614 + 2.41 \times 10^{-7}\,T)\lambda^2}{\lambda^2 - 30}$$

Linear electrooptic coefficients measured at low frequencies (well below the acoustic resonances of DKDP crystal, i.e., for the "free" crystal) at room temperature

λ [μm]	r_{41}^T [pm/V]	r_{63}^T [pm/V]	Ref.	Note
0.5461	-8.8 ± 0.4		[25]	83–92% deuteration
	-8.8		[26]	
		-26.4 ± 0.7	[3]	$T = 295$ K
		-26.8	[26]	
0.500		-25.6 ± 1.3	[27]	90% deuteration
0.6328	-10.7 ± 0.3		[6]	98% deuteration, $T = 295$ K
		-23.8 ± 0.6	[28]	
		-24.1	[29]	
		-25.8 ± 0.2	[6]	98% deuteration, $T = 295$ K
		-26.4 ± 0.7	[6]	99.8% deuteration, $T = 295$ K

Linear electrooptic coefficient measured at high frequencies (well above the acoustic resonances of DKDP crystal, i.e., for the "clamped" crystal) at room temperature

λ [μm]	r_{63}^S [pm/V]	Ref.	Note
0.500	-24.0 ± 1.2	[27]	90% deuteration
0.6328	-24.1	[26]	

Half-wave retardation voltage at longitudinal modulation

λ [μm]	$V_{\lambda/2}$ [kV]	Ref.
0.5	2.7	[3]
0.5461	2.98	[30]

Verdet constant at $T = 298\,\mathrm{K}$ ($\|c$) [31]

λ [μm]	V [degree/Tm]	Note
0.6328	237	80% deuteration
	241	85% deuteration
	247	95% deuteration

Calculated Verdet constants ($\|c$) [32]

λ [μm]	V [degree/Tm]
0.193	4271
0.222	2795
0.248	2043
0.308	1185
0.351	877

Expressions for the effective second-order nonlinear coefficient in general case (Kleinman symmetry conditions are valid, $d_{14} = d_{25} = d_{36}$) [33]:

$$d_{\mathrm{ooe}} = -d_{36}\sin(\theta + \rho)\sin 2\phi$$

$$d_{\mathrm{eoe}} = d_{\mathrm{oee}} = 2d_{36}\sin(\theta + \rho)\cos(\theta + \rho)\cos 2\phi$$

Simplified expressions for the effective second-order nonlinear coefficient (approximation of small birefringence angle, Kleinman symmetry conditions are valid, $d_{14} = d_{25} = d_{36}$) [34]:

$$d_{\mathrm{ooe}} = -d_{36}\sin\theta\sin 2\phi$$

$$d_{\mathrm{eoe}} = d_{\mathrm{oee}} = d_{36}\sin 2\theta\cos 2\phi$$

Absolute value of second-order nonlinear coefficient [33], [35]:

$$d_{36}(1.0642\,\mu\mathrm{m}) = 0.37\,\mathrm{pm/V}$$

Experimental values of phase-matching angle ($T = 293\,\mathrm{K}$)

Interacting wavelengths [μm]	θ_{exp} [deg]	Ref.
SHG, $o + o \Rightarrow e$		
$0.530 \Rightarrow 0.265$	90	[36]
$0.5321 \Rightarrow 0.26605$	88	[37]
$0.6943 \Rightarrow 0.34715$	52	[38]
$1.062 \Rightarrow 0.531$	37.1	[39]

Interacting wavelengths [μm]	θ_{exp} [deg]	Ref.
SHG, $e + o \Rightarrow e$		
1.3152 ⇒ 0.6576	51.3	[40]

Experimental values of NCPM temperature

Interacting wavelengths [μm]	T [°C]	Ref.	Note
SHG, $o + o \Rightarrow e$			
0.528 ⇒ 0.264	−30	[36]	
0.5321 ⇒ 0.26605	42	[41]	99% deuteration
	45	[42]	95% deuteration
	46	[43]	99% deuteration
	49.8	[44]	>95% deuteration
	60.8	[45]	90% deuteration
0.536 ⇒ 0.268	100	[36]	

Experimental values of internal angular and temperature bandwidths

Interacting wavelengths [μm]	T [°C]	θ_{pm} [deg]	$\Delta\theta^{int}$ [deg]	ΔT [°C]	Ref.
SHG, $o + o \Rightarrow e$					
1.0642 ⇒ 0.5321	20	37	0.081		[33]
0.5321 ⇒ 0.26605	60.8	90		1.8	[45]
	45	90		1.9	[42]
0.53 ⇒ 0.265	25	85.4	0.099		[46]
SHG, $e + o \Rightarrow e$					
1.0642 ⇒ 0.5321	20	54	0.131		[47]
	20		0.126		[48]
1.06 ⇒ 0.53	20	60	0.143		[49]

Experimental value of spectral bandwidth [49]

Interacting wavelengths [μm]	T [°C]	θ_{pm} [deg]	$\Delta\nu$ [cm^{-1}]
SHG, $e + o \Rightarrow e$			
1.06 ⇒ 0.53	20	60	74.8

Temperature variation of phase-matching angle [49]

Interacting wavelengths [μm]	T [°C]	θ_{pm} [deg]	$d\theta_{pm}/dT$ [deg/K]
SHG, $e + o \Rightarrow e$			
1.06 ⇒ 0.53	20	60	0.0063

Temperature tuning of noncritical SHG [21]

Interacting wavelengths [μm]	$d\lambda_1/dT$ [nm/K]
SHG, $o + o \Rightarrow e$	
0.519 ⇒ 0.2595	0.068

Calculated values of phase-matching and "walk-off" angles

Interacting wavelengths [μm]	θ_{pm} [deg]	ρ_1 [deg]	ρ_3 [deg]
SHG, $o + o \Rightarrow e$			
$0.5321 \Rightarrow 0.26605$	86.20		0.225
$0.5782 \Rightarrow 0.2891$	66.87		1.197
$0.6328 \Rightarrow 0.3164$	57.53		1.467
$0.6594 \Rightarrow 0.3297$	54.31		1.522
$0.6943 \Rightarrow 0.34715$	50.86		1.558
$1.0642 \Rightarrow 0.5321$	36.60		1.450
$1.3188 \Rightarrow 0.6594$	36.36		1.412
SFG, $o + o \Rightarrow e$			
$0.5782 + 0.5105 \Rightarrow 0.27112$	77.88		0.695
$1.0642 + 0.5321 \Rightarrow 0.35473$	46.82		1.587
$1.3188 + 0.6594 \Rightarrow 0.4396$	39.18		1.515
SHG, $e + o \Rightarrow e$			
$1.0642 \Rightarrow 0.5321$	53.47	1.286	1.427
$1.3188 \Rightarrow 0.6594$	51.70	1.222	1.420
SFG, $e + o \Rightarrow e$			
$1.0642 + 0.5321 \Rightarrow 0.35473$	59.38	1.174	1.378
$1.3188 + 0.6594 \Rightarrow 0.4396$	47.70	1.254	1.527

Calculated values of inverse group-velocity mismatch for SHG process in DKDP

Interacting wavelengths [μm]	θ_{pm} [deg]	β [fs/mm]
SHG, $o + o \Rightarrow e$		
$1.2 \Rightarrow 0.6$	35.94	<1
$1.1 \Rightarrow 0.55$	36.28	18
$1.0 \Rightarrow 0.5$	37.47	38
$0.9 \Rightarrow 0.45$	39.79	63
$0.8 \Rightarrow 0.4$	43.75	96
$0.7 \Rightarrow 0.35$	50.37	143
$0.6 \Rightarrow 0.3$	62.54	218
SHG, $e + o \Rightarrow e$		
$1.2 \Rightarrow 0.6$	51.62	55
$1.1 \Rightarrow 0.55$	52.73	71
$1.0 \Rightarrow 0.5$	55.37	92
$0.9 \Rightarrow 0.45$	60.41	120
$0.8 \Rightarrow 0.4$	70.43	159

Laser-induced bulk-damage threshold

λ [μm]	τ_p [ns]	I_{thr} [GW/cm^2]	Ref.	Note
0.2661	0.03	>10	[11]	
0.351	3	>2.9	[50]	80% deuteration

λ [μm]	τ_p [ns]	I_{thr} [GW/cm^2]	Ref.	Note
0.355	7.6	3.5	[51]	$\parallel c$, small-tank boules
		2.2	[52]	$\parallel c$, conventional growth, 150 pulses
		1.9	[51]	$\parallel c$, large-tank boules
		1.8	[52]	$\parallel c$, rapid growth, 150 pulses
		1.9	[51]	$\theta = 58°$, small-tank boules
		1.4	[52]	$\theta = 58°$, conventional growth, 150 pulses
		0.9	[51]	$\theta = 58°$, large-tank boules
		0.9	[52]	$\theta = 58°$, rapid growth, 150 pulses
0.527	1.7	>0.5	[53]	$\theta = 37°$, 89% deuteration
0.5321	30	>0.05	[54]	
	8	17	[55]	
	0.6	>8	[56]	
	0.03	>8	[18]	
0.6	330	0.3	[57]	
0.6943	5–25	0.16–0.26	[13]	
1.062	0.007	>1	[39]	
1.0642	40	>0.25	[54]	
	18	>0.1	[12]	
	14	8	[55]	
	10	1.5–18	[58]	
	1	6	[48]	
	0.25	>3	[12]	
1.315	1	1.5	[40]	

Laser-induced surface damage threshold

λ [μm]	τ_p [ns]	I_{thr} [GW/cm^2]	Ref.	Note
0.2484	20	0.15	[59]	1.5-mm beam-waist diameter
0.6943	5–25	1.2–5.8	[13]	95% deuteration
1.0642	10	0.7–4.3	[58]	

About the crystal

DKDP is the analog of KDP with a higher transmission in the IR range due to the deuteration.

References

[1] V.G. Dmitriev, G.G. Gurzadyan, D.N. Nikogosyan: *Handbook of Nonlinear Optical Crystals, Third Revised Edition* (Springer, Berlin, 1999).

[2] Data sheet of Cleveland Crystals Inc. Available at www.clevelandcrystals.com.
[3] T.R. Sliker, S.R. Burlage: Some dielectric and optical properties of KD_2PO_4. J. Appl. Phys. **34(7)**, 1837–1840 (1963).
[4] W.R. Cook, Jr.: Thermal expansion of crystals with KH_2PO_4 structure. J. Appl. Phys. **38(4)**, 1637–1642 (1967).
[5] B.H.T. Chai: Optical Crystals. In: *CRC Handbook of Laser Science and Technology, Supplement 2: Optical Materials*, ed. by M.J. Weber (CRC Press, Boca Raton, 1995), pp. 3–65.
[6] E.N. Volkova, I.A. Velichko: Electrooptical properties of potassium dihydrogen phosphate crystals having different degrees of deuteration. Kristallogr. **18(2)**, 409–410 (1973) [In Russian, English trans.: Sov. Phys. - Crystallogr. **18(2)**, 256–257 (1973)].
[7] D. Eimerl: High average power harmonic generation. IEEE J. Quant. Electr. **QE-23(5)**, 575–592 (1987).
[8] D. Eimerl: Electro-optic, linear and nonlinear optical properties of KDP and its isomorphs. Ferroelectrics **72(1–4)**, 95–139 (1987).
[9] E.W. van Stryland, L.L. Chase: Two-Photon Absorption. Inorganic Materials. In: *CRC Handbook of Laser Science and Technology, Supplement 2: Optical Materials*, ed. by M.J. Weber (CRC Press, Boca Raton, 1995) pp. 299–328.
[10] A.S. Sonin, A.S. Vasilevskaya: *Electrooptic Crystals* (Atomizdat, Moscow, 1971) [In Russian].
[11] J. Reintjes, R.C. Eckardt: Two-photon absorption in ADP and KD*P at 266.1 nm. IEEE J. Quant. Electr. **QE-13(9)**, 791–793 (1977).
[12] J.P. Machewirth, R. Webb, D. Anafi: High power harmonics produced with high efficiency in KD*P. Laser Focus: **12(5)**, 104–107 (1976).
[13] T.M. Christmas, J.M. Ley: Laser-induced damage in XDP materials. Electron. Lett. **7(18)**, 544–546 (1971).
[14] E.N. Volkova, V.V. Fadeev: Linear absorption coefficient of some nonlinear optical crystals. In: *Nonlinear Optics*, ed. by R.V. Khokhlov (Nauka, Novosibirsk, 1968), pp. 185–187 [In Russian].
[15] C.A. Ebbers, J. Happe, N. Nielsen, S.P. Velsko: Optical absorption at 1.06 μm in highly deuterated potassium dihydrogen phosphate. Appl. Opt. **31(12)**, 1960–1964 (1992).
[16] G. Brederlow, E. Fill, K.J. Witte: *The High-Power Iodine Laser* (Springer, Berlin, 1983).
[17] G. Dikchyus, E. Zhilinskas, A. Piskarskas, V. Sirutkaitis: Statistical properties and stabilization of a picosecond phosphate-glass laser with 2 Hz repetition frequency. Kvant. Elektron. **6(8)**, 1610–1619 (1979) [In Russian, English trans.: Sov. J. Quantum Electron. **9(8)**, 950–955 (1979)].
[18] J. Reintjes, R.C. Eckardt: Efficient harmonic generation from 532 to 266 nm in ADP and KD*P. Appl. Phys. Lett. **30(2)**, 91–93 (1977).
[19] P. Liu, W.L. Smith, H. Lotem, J.H. Bechtel, N. Bloembergen, R.S. Adhav: Absolute two photon absorption coefficients at 355 and 266 nm. Phys. Rev. B **17(12)**, 4620–4632 (1978).
[20] R.A. Philips: Temperature variations of the index of refraction of ADP, KDP, and deuterated KDP. J. Opt. Soc. Am. **56(5)**, 629–632 (1966).
[21] N.P. Barnes, D.J. Gettemy, R.S. Adhav: Variations of the refractive index with temperature and the tuning rate for KDP isomorphs. J. Opt. Soc. Am. **72(7)**, 895–898 (1982).
[22] M. Yamazaki, T. Ogawa: Temperature dependences of the refractive indices of $NH_4H_2PO_4$, KH_2PO_4, and partially deuterated KH_2PO_4. J. Opt. Soc. Am. **56(10)**, 1407–1408 (1966).
[23] K.W. Kirby, L.G. DeShazer: Refractive indices of 14 nonlinear crystals isomorphic to KH_2PO_4. J. Opt. Soc. Am. B **4(7)**, 1072–1078 (1987).

[24] G.C. Ghosh, G.C. Bhar: Temperature dispersion in ADP, KDP, and KD*P for nonlinear devices. IEEE J. Quant. Electr. **QE-18(2)**, 143–145 (1982).
[25] J.H. Ott, T.R. Sliker: Linear electro-optic effect in KH_2PO_4 and its isomorphs. J. Opt. Soc. Am. **54(12)**, 1442–1444 (1964).
[26] A. Yariv, P. Yeh: *Optical Waves in Crystals* (John Wiley & Sons, New York, 1984).
[27] T.M. Christmas, C.G. Wildey: Precise pulse-transmission mode control of a ruby laser. Electron. Lett. **6(22)**, 152–153 (1970).
[28] K. Onuki, N. Uchida, T. Saku: Interferometric method for measuring electro-optic coefficients in crystals. J. Opt. Soc. Am. **62(9)**, 1030–1032 (1972).
[29] G.W.C. Kaye, T.H. Laby: *Tables of Physical and Chemical Constants* (Longman Group Ltd., London, 1995).
[30] S. Musikant: *Optical Materials. An Introduction to Selection and Application* (Marcel Dekker, Inc., New York, 1985).
[31] M. Koralewski: Dispersion of the Faraday rotation in KDP-type crystals by pulse high magnetic field. Phys. Stat. Solidi A **65(1)**, K49–K53 (1981).
[32] J.L. Dexter, J. Landry, D.G. Cooper, J. Reintjes: Ultraviolet optical isolators utilizing KDP-isomorphs. Opt. Commun. **80(2)**, 115–118 (1990).
[33] R.C. Eckardt, H. Masuda, Y.X. Fan, R.L. Byer: Absolute and relative nonlinear optical coefficients of KDP, KD*P, BaB_2O_4, $LiIO_3$, MgO:$LiNbO_3$ and KTP measured by phase-matched second-harmonic generation. IEEE J. Quant. Electr. **26(5)**, 922–933 (1990).
[34] J.E. Midwinter, J. Warner: The effects of phase matching method and of uniaxial crystal symmetry on the polar distribution of second-order non-linear optical polarization. Brit. J. Appl. Phys. **16(11)**, 1135–1142 (1965).
[35] D.A. Roberts: Simplified characterization of uniaxial and biaxial nonlinear optical crystals: a plea for standardization of nomenclature and conventions. IEEE J. Quant. Electr. **28(10)**, 2057–2074 (1992).
[36] R.S. Adhav: Materials for optical harmonic generation. Laser Focus **19(6)**, 73–78 (1983).
[37] D.A.V. Kliner, F. Di Teodoro, J.P. Koplow, S.W. Moore, A.V. Smith: Efficient second, third, fourth, and fifth harmonic generation of a Yb-doped fiber amplifier. Opt. Commun. **210(3–6)**, 393–398 (2002).
[38] V.S. Suvorov, A.S. Sonin: Nonlinear optical materials. Kristallogr. **11(5)**, 832–848 (1966) [In Russian, English trans.: Sov. Phys. - Crystallogr. **11(5)**, 711–723 (1966)].
[39] T.A. Rabson, H.J. Ruiz, P.L. Shah, F.K. Tittel: Efficient second harmonic generation of picosecond laser pulses. Appl. Phys. Lett. **20(8)**, 282–284 (1972).
[40] E.E. Fill: Generation of higher harmonics of iodine laser radiation. Opt. Commun. **33(3)**, 321–322 (1980).
[41] M.D. Jones, G.A. Massey: Milliwatt-level 213 nm source based on a repetitively Q-switched, CW-pumped Nd:YAG laser. IEEE J. Quant. Electr. **QE-15(4)**, 204–206 (1979).
[42] V.I. Bredikhin, V.N. Genkin, S.P. Kuznetsov, M.A. Novikov: 90° phase-matching in $KD_{2x}H_{2(1-x)}PO_4$ crystals upon doubling of the second harmonic of a Nd laser. Pisma Zh. Tekh. Phys. **3(9)**, 407–409 (1977) [In Russian, English trans.: Sov. Tech. Phys. Lett. **3(5)**, 165–166 (1977)].
[43] G.A. Massey, M.D. Jones, J.C. Johnson: Generation of pulse bursts at 212.8 nm by intracavity modulation of an Nd:YAG laser. IEEE J. Quant. Electr. **QE-14(7)**, 527–532 (1978).
[44] P.E. Perkins, T.S. Fahlen: Half watt average power at 25 kHz from fourth harmonic of Nd:YAG. IEEE J. Quant. Electr. **QE-21(10)**, 1636–1638 (1985).
[45] Y.S. Liu, W.B. Jones, J.P. Chernoch: High-efficiency high-power coherent UV generation at 266 nm in 90° phase-matched deuterated KDP. Appl. Phys. Lett. **29(1)**, 32–34 (1976).

[46] S.C. Matthews, J.S. Sorce: Fourth harmonic conversion of 1.06 μm in BBO and KD*P. Proc. SPIE **1220**, 137–147 (1990).
[47] R.M. Kogan, T.G. Crow: A 1 J high-brightness frequency-doubled Nd:YAG laser. Appl. Opt. **17(6)**, 927–930 (1978).
[48] R.S. Adhav, S.R. Adhav, J.M. Pelaprat: BBO's nonlinear optical phase-matching properties. Laser Focus **23(9)**, 88–100 (1987).
[49] R.B. Andreev, V.D. Volosov, A.G. Kalintsev: Spectral, angular, and temperature characteristics of HIO_3, $LiIO_3$, CDA, DKDP, KDP and ADP non-linear crystals in second- and fourth-harmonic generation. Opt. Spektrosk. **37(2)**, 294–299 (1974) [In Russian, English trans.: Opt. Spectrosc. USSR **37(2)**, 169–171 (1974)].
[50] C.E. Barker, B.M. van Wonterghem, J.M. Auerbach, R.J. Foley, J.R. Murray, J.H. Campbell, J.A. Caird, D.R. Speck, B. Woods: Design and performance of the Beamlet laser third harmonic frequency converter. Proc. SPIE **2633**, 398–404 (1995).
[51] M. Runkel, A.K. Burnham: Differences in bulk damage probability distributions between tripler and z-cuts of KDP and DKDP at 355 nm. Proc. SPIE **4347**, 408–419 (2001).
[52] A.K. Burnham, M. Runkel, M.D. Feit, A.M. Rubenchik, R.L. Floyd, T.A. Land, W.J. Siekhaus, R.A. Hawley-Fedder: Laser-induced damage in deuterated potassium dihydrogen phosphate. Appl. Opt. **42(27)**, 5483–5495 (2003).
[53] G. Freidman, N. Andreev, V. Bespalov, V. Bredikhin, V. Ginzburg, E. Katin, E. Khazanov, A. Korytin, V. Lozhkarev, O. Palashov, A. Poteomkin, A. Sergeev, I. Yakovlev: Multicascade broadband optical parametric chirped pulse amplifier based on KD*P crystals. Proc. SPIE **4972**, 90–101 (2003).
[54] Y.S. Liu, W.B. Jones, J.P. Chernoch: High-efficiency high-power coherent UV generation at 266 nm in 90° phase-matched deuterated KDP. Appl. Phys. Lett. **29(1)**, 32–34 (1976).
[55] H. Nakatani, W.R. Bosenberg, L.K. Cheng, C.L. Tang: Laser-induced damage in beta barium metaborate. Appl. Phys. Lett. **53(12)**, 2587–2589 (1988).
[56] G.J. Linford, B.C. Johnson, J.S. Hildum, W.E. Martin, K. Snyder, R.D. Boyd, W.L. Smith, C.L. Vercimak, D. Eimerl, J.T. Hunt: Large aperture harmonic conversion experiments at Lawrence Livermore National Laboratory. Appl. Opt. **21(20)**, 3633–3643 (1982).
[57] L. Armstrong, S.E. Neister, R. Adhav: Measuring CFP dye laser damage thresholds on UV doubling crystals. Laser Focus **18(12)**, 49–53 (1982).
[58] R.M. Wood, R.T. Taylor, R.L. Rouse: Laser damage in optical materials at 1.06 μm. Opt. Laser Technol. **6(3)**, 105–111 (1975).
[59] F. Rainer, W.H. Lowdermilk, D. Milam: Bulk and surface damage thresholds of crystals and glasses at 248 nm. Opt. Eng. **22(4)**, 431–434 (1983).

4.4 $CsLiB_6O_{10}$, Cesium Lithium Borate (CLBO)

Negative uniaxial crystal: $n_o > n_e$
Molecular mass: 364.706
Specific gravity: 2.461 g/cm^3 (calculated) [1]); 2.472 g/cm^3 (calculated) [2]
Point group: $\bar{4}2m$
Lattice constants [3]:
$a = 10.494 \pm 0.001$ Å
$c = 8.939 \pm 0.002$ Å
Vickers hardness:
140–170 (along [001] direction) [3]

230–260 (along [100] direction) [3]
270 (for the crystals with high bulk laser damage threshold) [4]
Mohs hardness: 5.5 [5]
Melting point: 1118 K [6]; 1121 K [7]
Band-gap energy: 6.9 eV [8]
Transparency range at "0" transmittance level: 0.18–2.75 μm [9]

Two-photon absorption coefficient β [10]

λ [μm]	τ_p [ns]	$\beta \times 10^{11}$ [cm/W]
0.2	0.00014	120 ± 20

Experimental values of refractive indices at $T = 293$ K [11]

λ [μm]	n_o	n_e	λ [μm]	n_o	n_e
0.420	1.5058	1.4517	0.610	1.4935	1.4414
0.450	1.5030	1.4493	0.6328	1.4928	1.4409
0.480	1.5006	1.4474	0.670	1.4915	1.4398
0.500	1.4991	1.4462	0.700	1.4907	1.4392
0.532	1.4971	1.4445	0.720	1.4902	1.4387
0.560	1.4957	1.4434	1.064	1.4838	1.4340
0.590	1.4943	1.4422			

Temperature derivative of refractive indices for temperature range 293–373 K and spectral range 0.2128–1.3382 μm (in $10^{-6}\,K^{-1}$) [12]:

$$\frac{dn_o}{dT} = -12.48 - \frac{0.328}{\lambda}$$

$$\frac{dn_e}{dT} = -8.36 + \frac{0.047}{\lambda} - \frac{0.039}{\lambda^2} + \frac{0.014}{\lambda^3}$$

Other expressions for temperature derivative of refractive indices are given in [13].
Best set of Sellmeier equations ($T = 293$ K, λ in μm, $0.1914\,\mu m < \lambda < 2.09\,\mu m$) [12]:

$$n_o^2 = 2.2104 + \frac{0.01018}{\lambda^2 - 0.01424} - 0.01258\,\lambda^2$$

$$n_e^2 = 2.0588 + \frac{0.00838}{\lambda^2 - 0.01363} - 0.00607\,\lambda^2$$

Other sets of dispersion relations are given in [7], [9], [11], [13], [14], [15].
Expressions for the effective second-order nonlinear coefficient in general case (Kleinman symmetry conditions are valid, $d_{14} = d_{25} = d_{36}$) [16]:

$$d_{ooe} = -d_{36}\sin(\theta + \rho)\sin 2\phi$$

$$d_{eoe} = d_{oee} = 2d_{36}\sin(\theta + \rho)\cos(\theta + \rho)\cos 2\phi$$

Simplified expressions for the effective second-order nonlinear coefficient (approximation of small birefringence angle, Kleinman symmetry conditions are valid, $d_{14} = d_{25} = d_{36}$) [17]:

$$d_{\mathrm{ooe}} = -d_{36} \sin\theta \sin 2\phi$$

$$d_{\mathrm{eoe}} = d_{\mathrm{oee}} = d_{36} \sin 2\theta \cos 2\phi$$

Absolute values of second-order nonlinear coefficients [18]:
$d_{36}(0.532\,\mu\mathrm{m}) = 0.92\,\mathrm{pm/V}$
$d_{14}(0.852\,\mu\mathrm{m}) = 0.69\,\mathrm{pm/V}$
$d_{36}(0.852\,\mu\mathrm{m}) = 0.83\,\mathrm{pm/V}$
$d_{36}(1.064\,\mu\mathrm{m}) = 0.74\,\mathrm{pm/V}$

Experimental values of NCPM temperature

Interacting wavelengths [μm]	T [°C]	Ref.
SFG, $o + o \Rightarrow e$		
$1.047 + 0.24114 \Rightarrow 0.196$	4	[19]
$1.047 + 0.2416 \Rightarrow 0.1963$	34	[20]
$1.047 + 0.2431 \Rightarrow 0.1973$	150	[19]

Experimental values of phase-matching temperature, internal angular and temperature bandwidths

Interacting wavelengths [μm]	θ_{pm} [deg]	T [°C]	$\Delta\theta^{\mathrm{int}}$ [deg]	ΔT [°C]	Ref.
SHG, $o + o \Rightarrow e$					
$0.946 \Rightarrow 0.473$	90	−15		5.0	[21]
$0.5235 \Rightarrow 0.26175$	64.8	≈160			[22]
$0.5321 \Rightarrow 0.26605$	62	≈140			[6]
	61.4	20	0.023		[11]
				6.2	[12]
$1.0642 \Rightarrow 0.5321$	29.5	20	0.043		[11]
				52.7	[12]
$1.3382 \Rightarrow 0.6691$	27.7	20		68.7	[12]
SFG, $o + o \Rightarrow e$					
$1.0642 + 0.26605 \Rightarrow 0.21284$	67.3	20		3.6	[12]
$1.547 + 0.221 \Rightarrow 0.19338$	61.7	150			[23]
$1.9079 + 0.2128 \Rightarrow 0.1914$	55	20		1.2	[12]
$1.0642 + 0.35473 \Rightarrow 0.26605$	50.6	20		6.1	[12]
$1.0642 + 0.5321 \Rightarrow 0.35473$	39.1	20		18.0	[12]
SHG, $e + o \Rightarrow e$					
$1.0642 \Rightarrow 0.5321$	42.4	20		49.4	[12]
SFG, $e + o \Rightarrow e$					
$1.9079 + 0.2128 \Rightarrow 0.1914$	57.4	20		1.1	[12]
$1.0642 + 0.5321 \Rightarrow 0.35473$	48.9	20		17.0	[12]

Laser-induced bulk damage threshold

λ [μm]	τ_p [ns]	I_{thr} [GW/cm^2]	Ref.	Note
0.2	0.00014	>250	[10]	1 kHz
0.266	8	17–19	[4]	solution-stirring growth
	0.75	6.4	[8]	
	0.75	9–10	[24]	dislocation density ~1.5 × 10^4 cm^{-3}
	0.75	15–20	[24]	dislocation density (0.7 to 1) ×10^4 cm^{-3}
	0.75	25	[25]	solution-stirring TSSG growth
0.511	20	>0.5	[26]	12 kHz
0.527	0.0015	>47	[27]	1/6 Hz
0.532	70	>0.043	[28]	1 kHz
	7	>0.13	[29]	10 Hz
	0.014	130–520	[30]	train of 80 pulses
0.5395	7	>0.67	[31]	10 Hz
0.576	8	>0.1	[32]	10 Hz
0.800	CW	>0.0000038	[33]	
	0.0014	>600	[10]	1 kHz
1.053	0.0015	>100	[27]	
1.064	CW	0.000088	[11]	
	13	>0.35	[34]	10 Hz
	7	>0.37	[35]	10 Hz
	1.1	16–19	[8]	along [100] direction
	1.1	29	[8]	along [001] direction

Laser-induced surface damage threshold

λ [μm]	τ_p [ns]	I_{thr} [GW/cm^2]	Ref.	Note
0.266	8	1.4–1.6	[4]	conventional crystals
		2.0	[4]	solution-stirring growth
		1.3–1.5	[36]	conventional crystals, mechanical polishing
		2.3	[36]	conventional crystals, ion-beam etching
		1.9	[36]	high-quality crystals, mechanical polishing
		2.9	[36]	high-quality crystals, ion-beam etching

About the crystal

CLBO was grown first in 1995 in Japan by the top-seeded Kyropolous method [3], [7], [9]. Conventionally, it is produced by top-seeded solution growth (TSSG) or

solution-stirring TSSG (SS-TSSG) methods [24], [25]. This UV nonlinear material is much easier to grow than BBO and LBO crystals. The main application of $CsLiB_6O_{10}$ is the frequency conversion of visible and near-IR laser radiation to the UV range. In 1996–1998, Japanese scientists used CLBO for second-, fourth-, and fifth-harmonic generation of nanosecond Nd:YAG laser radiation. They managed to generate pulses with energies 1.55, 0.5, and 0.23 J at 532, 266, and 213 nm, respectively [29], [35]. Second- and third-harmonic generation of 3-ps, 1053-nm laser radiation with efficiencies of 70% and 20% was achieved in 7- and 5-mm-long CLBO crystals, respectively [37]. Using CLBO for SHG and SFG, it is possible to create high-power nanosecond UV sources, operating with kilohertz repetition rate; for example, 20 W at 266 nm [38], 15 W at 255 nm [26], 3 W at 242 nm [19], and 1.5 W at 196 nm [19]. The Chinese investigators studied CLBO-based ps UV-laser pumped (266 or 355 nm) OPG/OPA systems [15]. Though they have realized a rather wide OPO tuning range (347–1137 nm for 266-nm pump and 447–1725 nm for 355-nm pump), they have observed that the amplification factor for CLBO crystal at 450 nm is 7 times lower than for BBO, probably due to the difference in the effective nonlinear coefficient. Very recently, CLBO was used for eight-harmonic generation of a 1.547-nm laser-source via SFG between radiations at fundamental frequency and its seventh harmonic [23].

One of the disadvantages of $CsLiB_6O_{10}$ is its deterioration due to water absorption at room temperature. To prevent this, CLBO crystal should be kept at elevated temperatures, 140–160°C [26], [38], [39]. The experiments done according to this approach [39] demonstrated more than 1 month's stable operation of a CLBO doubler without any degradation of SHG performance. Additional significant increase of SHG efficiency (2.3 times) could be achieved by compensation of thermally induced phase mismatch in a CLBO crystal, kept at elevated temperatures, by room-temperature nitrogen gas flow cooling [40]. In [21], SHG in CLBO crystal was achieved at −15°C. In this case, the crystal and the vacuum-tight vessel were processed at a high temperature (150°C), then the vessel was backfilled with dry nitrogen at atmospheric pressure and sealed.

Another way to protect CLBO from atmospheric moisture is to use a Si–Cd film [31], which was applied by spraying, and then the crystal was dried in a furnace at 120 °C and normal pressure for 24 hours.

References

[1] T. Sasaki, Y. Mori, I. Kuroda, S. Nakajima, K. Yamaguchi, S. Watanabe, S. Nakai: Caesium lithium borate: a new nonlinear optical crystal. Acta Crystallogr. C **51(11)**, 2222–2224 (1995).

[2] J.-M. Tu, D.A. Keshler: $CsLiB_6O_{10}$: a noncentrosymmetric polyborate. Mat. Res. Bull. **30(2)**, 209–215 (1995).

[3] Y. Mori, I. Kuroda, S. Nakajima, T. Sasaki, S. Nakai: Growth of a new nonlinear optical crystal: cesium lithium borate. J. Cryst. Growth **156(3)**, 307–309 (1995).

[4] M. Nishioka, S. Fukumoto, F. Kawamura, M. Yoshimura, Y. Mori, T. Sasaki: Improvement of laser-induced damage tolerance in $CsLiB_6O_{10}$ for high-power UV laser source. In: *Conference on Lasers and Electrooptics CLEO/QELS 2003*, Technical Digest (OSA, Washington DC, 2003), paper CTuF2.

[5] N.A. Pylneva, N.G. Kononova, A.M. Yurkin, A.E. Kokh, G.G. Bazarova, V.I. Danilov, I.A. Lisova, N.L. Tsirkina: Top-seeded solution growth of CLBO crystals. Proc. SPIE **3610**, 148–155 (1999).

[6] T. Sasaki, Y. Mori, M. Yoshimura: Progress in the growth of a $CsLiB_6O_{10}$ crystal and its application to ultraviolet light generation. Opt. Mater. **23(1–2)**, 343–351 (2003).

[7] Y. Mori, I. Kuroda, S. Nakajima, T. Sasaki, S. Nakai: New nonlinear optical crystal: cesium lithium borate. Appl. Phys. Lett. **67(13)**, 1818–1820 (1995).

[8] M. Yoshimura, T. Kamimura, K. Murase, Y. Mori, H. Yoshida, M. Nakatsuka, T. Sasaki: Bulk laser damage in $CsLiB_6O_{10}$ crystal and its dependence on crystal structure. Jpn. J. Appl. Phys. **38(2A)**, L129-L131 (1999).

[9] Y. Mori, S. Nakajima, A. Miyamoto, M. Inagaki, T. Sasaki, H. Yoshida, S. Nakai: Generation of ultraviolet light by using new nonlinear optical crystal $CsLiB_6O_{10}$. Proc. SPIE **2633**, 299–307 (1995).

[10] V. Petrov, F. Noack, F. Rotermund, M. Tanaka, Y. Okada: Sum-frequency generation of femtosecond pulses in $CsLiB_6O_{10}$ down to 175 nm. Appl. Opt. **39(27)**, 5076–5079 (2000).

[11] G. Ryu, C.S. Yoon, T.P.J. Han, H.G. Gallagher: Growth and characterisation of $CsLiB_6O_{10}$ (CLBO) crystals. J. Cryst. Growth **191(3)**, 492–500 (1998).

[12] N. Umemura, K. Yoshida, T. Kamimura, Y. Mori, T. Sasaki, K. Kato: New data of phase-matching properties of $CsLiB_6O_{10}$. In: *Advanced Solid-State Lasers, OSA Trends in Optics and Photonics Series*, *Vol. 26*, ed. by M.M. Fejer, H. Injeyan, U. Keller (OSA, Washington DC, 1999), pp. 715–719.

[13] N. Umemura, K. Kato: Ultraviolet generation tunable to 0.185 μm in $CsLiB_6O_{10}$. Appl. Opt. **36(27)**, 6794–6796 (1997).

[14] Y. Mori, I. Kuroda, S. Nakajima, T. Sasaki, S. Nakai: Nonlinear optical properties of cesium lithium borate. Jpn. J. Appl. Phys. **34(3A)**, L296–L298 (1995).

[15] J.-Y. Zhang, Y. Kong, Z. Xu, D. Shen: Optical parametric properties of ultraviolet-pumped cesium lithium borate crystals. Appl. Opt. **41(3)**, 475–482 (2002).

[16] R.C. Eckardt, H. Masuda, Y.X. Fan, R.L. Byer: Absolute and relative nonlinear optical coefficients of KDP, KD*P, BaB_2O_4, $LiIO_3$, MgO:$LiNbO_3$, and KTP measured by phase-matched second-harmonic generation. IEEE J. Quant. Electr. **26(5)**, 922–933 (1990).

[17] J.E. Midwinter, J. Warner: The effects of phase matching method and of uniaxial crystal symmetry on the polar distribution of second-order non-linear optical polarization. Brit. J. Appl. Phys. **16(11)**, 1135–1142 (1965).

[18] I. Shoji, H. Nakamura, R. Ito, T. Kondo, M. Yoshimura, Y. Mori, T. Sasaki: Absolute measurement of second-harmonic nonlinear-optical coefficients of $CsLiB_6O_{10}$ for visible-to-ultraviolet second-harmonic wavelengths. J. Opt. Soc. Am. B **18(3)**, 302–307 (2001).

[19] J. Sakuma, K. Deki, A. Finch, Y. Ohsako, T. Yokota: All-solid-state, high-power, deep-UV laser system based on cascaded sum-frequency mixing in $CsLiB_6O_{10}$ crystals. Appl. Opt. **39(30)**, 5505–5511 (2001).

[20] J. Sakuma, A. Finch, Y. Ohsako, K. Deki, M. Yoshino, M. Horiguchi, T. Yokota, Y. Mori, T. Sasaki: All-solid-state, 1-W, 5-kHz laser source below 200 nm. In: *Advanced Solid-State Lasers, OSA Trends in Optics and Photonics Series, Vol. 26*, ed. by M.M. Fejer, H. Injeyan, U. Keller (OSA, Washington DC, 1999), pp. 89–92.

[21] D.C. Gerstenberger, T.M. Trautmann, M.S. Bowers: Noncritically phase-matched second-harmonic generation in cesium lithium borate. Opt. Lett. **28(14)**, 1242–1244 (2003).

[22] K.F. Wall, J.S. Smucz, B. Pati, Y. Isyanova, P. Moulton, J.G. Manni: A quasi-continuous-wave deep ultraviolet laser source. IEEE J. Quant. Electr. **39(9)**, 1160–1169 (2003).

[23] H. Kitano, H. Kawai, K. Miramitsu, S. Owa, M. Yoshimura, Y. Mori, T. Sasaki: 387-nm generation in $Gd_xY_{1-x}Ca_4O(BO_3)_3$ crystal and its utilization for 193-nm light source. Jpn. J. Appl. Phys. **42(2B)**, L166–L169 (2003).

[24] T. Kamimura, R. Ono, Y.K. Yap, M. Yoshimura, Y. Mori, T. Sasaki: Influence of crystallinity on the bulk laser-induced damage threshold and absorption of laser light in $CsLiB_6O_{10}$ crystals. Jpn. J. Appl. Phys. **40(2A)**, L111–L113 (2001).

[25] R. Ono, T. Kamimura, S. Fukumoto, Y.K. Yap, M. Yoshimura, Y. Mori, T. Sasaki, K. Yoshida: Effect of crystallinity on the bulk laser damage and UV absorption of CLBO crystals. J. Cryst. Growth **237–239,** 645–648 (2002).

[26] D.J.W. Brown, M.J. Withford: High-average-power (15-W) 255-nm source based on second-harmonic generation of a copper laser master oscillator power amplifier system in cesium lithium borate. Opt. Lett. **26(23)**, 1885–1887 (2001).

[27] L.B. Sharma, H. Daido, Y. Kato, S. Nakai, T. Zhang, Y. Mori, T. Sasaki: Fourth-harmonic generation of picosecond glass laser pulses with cesium lithium borate crystals. Appl. Phys. Lett. **69(25)**, 3812–3814 (1996).

[28] S. Konno, Y. Inoue, T. Kojima, S. Fujikawa, K. Yasui: Efficient high-pulse-energy green-beam generation by intracavity frequency doubling of a quasi-continuous-wave laser-diode-pumped Nd:YAG laser. Appl. Opt. **40(24)**, 4341–4343 (2001).

[29] Y.K. Yap, M. Inagaki, S. Nakajima, Y. Mori, T. Sasaki: High-power fourth- and fifth-harmonic generation of a Nd:YAG laser by means of a $CsLiB_6O_{10}$. Opt. Lett. **21(17)**, 1348–1350 (1996).

[30] T. Srinivasan-Rao, M. Babzien, F. Sakai, Y. Mori, T. Sasaki: Conversion efficiency and damage threshold measurements of $CsLiB_6O_{10}$ with a train of laser pulses. Appl. Phys. Lett. **71(14)**, 1927–1929 (1997).

[31] A.E. Kokh, N.G. Kononova, I.A. Lisova, S.V. Muraviov: $CsLiB_6O_{10}$ crystal: fourth- and fifth-harmonic generation of Nd:YAG laser. Proc. SPIE **4268**, 43–48 (2001).

[32] S. Chandra, T.H. Allik, J.A. Hutchinson, J. Fox, C. Swim: Tunable ultraviolet laser source based on solid-state dye laser technology and $CsLiB_6O_{10}$ harmonic generation. Opt. Lett. **22(4)**, 209–211 (1997).

[33] W.-L. Zhou, Y. Mori, T. Sasaki, S. Nakai: High-efficiency intracavity continuous-wave ultraviolet generation using crystals $CsLiB_6O_{10}$, β-BaB_2O_4 and LiB_3O_5. Opt. Commun. **123(4–6)**, 583–586 (1996).

[34] H. Kiriyama, F. Nakano, K. Yamakawa: High-efficiency frequency doubling of a Nd:YAG laser in a two-pass quadrature frequency-conversion scheme using $CsLiB_6O_{10}$ crystals. J. Opt. Soc. Am. B **19(8)**, 1857–1864 (2002).

[35] Y.K. Yap, S. Hamamura, A. Taguchi, Y. Mori, T. Sasaki: $CsLiB_6O_{10}$ crystal for frequency doubling the Nd:YAG laser. Opt. Commun. **145(1–6)**, 101–104 (1998).

[36] T. Kamimura, S. Fukumoto, R. Ono, Y.K. Yap, M. Yoshimura, Y. Mori, T. Sasaki, K. Yoshida: Enhancement of $CsLiB_6O_{10}$ surface-damage resistance by improved crystallinity and ion-beam etching. Opt. Lett. **27(8)**, 616–618 (2002).

[37] T. Zhang, Y. Motoki, L.B. Sharma, H. Daido, Y. Kato, Y. Mori, T. Sasaki: 351 nm wavelength generation of picosecond laser pulses. Electron. Lett. **32(5)**, 452–454 (1996).

[38] T. Kojima, S. Konno, S. Fujikawa, K. Yoshizawa, Y. Mori, T. Sasaki, M. Tanaka, Y. Okada: 20-W ultraviolet-beam generation by fourth-harmonic generation of an all-solid-state laser. Opt. Lett. **25(1)**, 58–60 (2000).

[39] Y.K. Yap, T. Inoue, H. Sakai, Y. Kagebayashi, Y. Mori, T. Sasaki, K. Deki, M. Horiguchi: Long-term operation of $CsLiB_6O_{10}$ at elevated crystal temperature. Opt. Lett. **23(1)**, 34–36 (1998).

[40] Y.K. Yap, K. Deki, N. Kitatochi, Y. Mori, T. Sasaki: Alleviation of thermally induced phase mismatch in $CsLiB_6O_{10}$ crystal by means of temperature-profile compensation. Opt. Lett. **23(13)**, 1016–1018 (1998).

4.5 MgO:LiNbO$_3$, Magnesium-Oxide–Doped Lithium Niobate (MgLN)

Negative uniaxial crystal: $n_o > n_e$
Point group: $3m$

Curie temperature and UV absorption cutoff at $\alpha = 20\,\text{cm}^{-1}$ as a function of MgO concentration (in mol%) in stoichiometric and congruent LN crystals [1]

[MgO]	T_c [K]	λ_{cutoff} [μm]
stoichiometric LN		
0	1466 ± 2	0.306
0.8	1479 ± 2	0.304
2.0	1486 ± 1	0.301
3.3	1485 ± 1	0.303
4.6	1480 ± 2	
congruent LN		
0	1411	0.316
>5	1486	

Transparency range at "0" transmittance level for congruent LN crystals: 0.32–5 μm [2], [3], [4]

Linear absorption coefficient α

λ [μm]	α [cm^{-1}]	Ref.
0.5321	0.02	[5]
1.0642	<0.01	[5]
	<0.003	[6]

Experimental values of refractive indices for crystal with 5 mol% MgO and mole ratio Li/Nb = 0.97 [3]

λ [μm]	n_o	n_e
0.4358	2.3863	2.2802
0.4916	2.3403	2.2416
0.5461	2.3114	2.2172
0.5770	2.2988	2.2068
0.5790	2.2980	2.2062
0.6328	2.2816	2.1922
0.6943	2.2678	2.1805

λ [μm]	n_o	n_e
0.8400	2.2460	2.1622
1.0642	2.2272	2.1463

Experimental values of refractive indices for crystal with 5 mol% MgO and mole ratio Li/Nb = 0.946 (congruent melt) [4]

λ [μm]	n_o	n_e	λ [μm]	n_o	n_e
0.4047	2.4247	2.3111	0.5790	2.2982	2.2056
0.4078	2.4202	2.3073	0.5893	2.2945	2.2027
0.4358	2.3863	2.2795	0.6234	2.2840	2.1938
0.4861	2.3441	2.2444	0.6563	2.2756	2.1867
0.4916	2.3404	2.2412	0.6907	2.2681	2.1802
0.4962	2.3376	2.2389	0.6943	2.2669	2.1793
0.5461	2.3112	2.2167	1.0640	2.2237	2.1456
0.5770	2.2989	2.2063			

Refractive indices of 5 mol% MgO-doped congruent $LiNbO_3$ at different temperatures (293 K, 348 K, 389 K, 428 K) are given in [7].

Temperature derivatives of refractive indices for 5 mol% MgO-doped congruent $LiNbO_3$ [7]

λ [μm]	$dn_o/dT \times 10^6$ [K^{-1}]	$dn_e/dT \times 10^6$ [K^{-1}]
0.53975	16.663	72.763
0.6328	12.121	64.866
1.0795	4.356	54.190
1.3414	5.895	52.665

Best set of Sellmeier equations (5 mol% MgO, mole ratio Li/Nb = 0.937, congruent melt, λ in μm, 0.4 μm $< \lambda <$ 5.0 μm, T = 294 K) [8]:

$$n_o^2 = 1 + \frac{2.2454\,\lambda^2}{\lambda^2 - 0.01242} + \frac{1.3005\,\lambda^2}{\lambda^2 - 0.05313} + \frac{6.8972\,\lambda^2}{\lambda^2 - 331.33}$$

$$n_e^2 = 1 + \frac{2.4272\,\lambda^2}{\lambda^2 - 0.01478} + \frac{1.4617\,\lambda^2}{\lambda^2 - 0.05612} + \frac{9.6536\,\lambda^2}{\lambda^2 - 371.216}$$

Other sets of dispersion relations for MgO-doped congruent $LiNbO_3$ at room temperature are given in [9] for 0–9 mol% MgO, in [3], [4] for 5 mol% MgO, in [10], [11] for 7 mol% MgO.
Sellmeier equations for MgO-doped (0–4.6 mol%) stoichiometric $LiNbO_3$ for the wavelength range 0.44–1.05 μm are given in [12].
Temperature-dependent Sellmeier equations (5–7 mol% MgO, congruent melt, λ in μm, 0.4 μm $< \lambda <$ 4.0 μm, T in K, 273 K $< T <$ 673 K) [13]:

$$n_o^2 = 4.9130 + \frac{1.173 \times 10^5 + 1.65 \times 10^{-2}\, T^2}{\lambda^2 - (2.12 \times 10^2 + 2.7 \times 10^{-5}\, T^2)^2} - 2.78 \times 10^{-8}\, \lambda^2$$

$$n_e^2 = 4.5567 + \frac{0.97 \times 10^5 + 2.7 \times 10^{-2}\, T^2}{\lambda^2 - (2.01 \times 10^2 + 5.4 \times 10^{-5}\, T^2)^2} - 2.24 \times 10^{-8}\, \lambda^2$$

$$+2.605 \times 10^{-7}\, T^2 - 2.1432 \times 10^{-4}\, T_{\mathrm{NCPM}} - 4.07 \times T_{\mathrm{NCPM}}^2$$

where T_{NCPM} (in °C) is the temperature of non-critical phase-matching for $1.064\,\mu\mathrm{m} \Rightarrow 0.532\,\mu\mathrm{m}$ SHG interaction.
Other temperature-dependent Sellmeier equations for 5 mol% MgO-doped congruent LiNbO$_3$ are given in [7], [14], [15].

Nonlinear refractive index γ [16]

λ [μm]	$\gamma \times 10^{15}$ [cm^2/W]	Note
0.780	2.0 ± 0.3	[100] direction
	2.0 ± 0.3	[010] direction

Coercive field value for 5 mol% MgO-doped congruent LiNbO$_3$: ≈4.5 kV/mm [17].

Dependence of coercive field value for 5 mol% MgO-doped congruent LiNbO$_3$ on crystal temperature [18]

T [K]	P [kV/mm]
298	4.5
353	2.4
393	1.8
443	1.3

Expressions for the effective second-order nonlinear coefficient in general case (Kleinman symmetry conditions are valid, $d_{15} = d_{24} = d_{31} = d_{32}$) [19]:

$$d_{\mathrm{ooe}} = d_{31} \sin(\theta + \rho) - d_{22} \cos(\theta + \rho) \sin 3\phi$$

$$d_{\mathrm{eoe}} = d_{\mathrm{oee}} = d_{22} \cos^2(\theta + \rho) \cos 3\phi$$

Simplified expressions for the effective second-order nonlinear coefficient (approximation of small birefringence angle, Kleinman symmetry conditions are valid, $d_{15} = d_{24} = d_{31} = d_{32}$) [20]:

$$d_{\mathrm{ooe}} = d_{31} \sin\theta - d_{22} \cos\theta \sin 3\phi$$

$$d_{\mathrm{eoe}} = d_{\mathrm{oee}} = d_{22} \cos^2\theta \cos 3\phi$$

Absolute values of second-order nonlinear coefficients for 5 mol% MgO:LiNbO$_3$ [21]:

$|d_{31}(0.852\,\mu\mathrm{m})| = 4.9\,\mathrm{pm/V}$
$|d_{33}(0.852\,\mu\mathrm{m})| = 28.4\,\mathrm{pm/V}$
$|d_{31}(1.064\,\mu\mathrm{m})| = 4.4\,\mathrm{pm/V}$

$|d_{33}(1.064\,\mu\text{m})| = 25.0\,\text{pm/V}$
$|d_{31}(1.313\,\mu\text{m})| = 3.4\,\text{pm/V}$
$|d_{33}(1.313\,\mu\text{m})| = 20.3\,\text{pm/V}$

Experimental values of phase-matching angle ($T = 293\,\text{K}$)

Interacting wavelengths [μm]	θ_{exp} [deg]	Ref.	Note
SHG, $o + o \Rightarrow e$			
1.0642 ⇒ 0.5321	74.5	[4]	5 mol% MgO, congruent LN
	76	[5]	5 mol% MgO
	76.5	[3]	5 mol% MgO, Li/Nb = 0.97
	82.3	[10]	7 mol% MgO
1.0795 ⇒ 0.53975	75.1	[7]	5 mol% MgO, congruent LN
1.0796 ⇒ 0.5398	74	[3]	5 mol% MgO, Li/Nb = 0.97
1.3414 ⇒ 0.6707	54	[7]	5 mol% MgO, congruent LN

Note: The PM angle values are strongly dependent on melt stoichiometry.

Experimental values of NCPM temperature

Interacting wavelengths [μm]	T [°C]	Ref.	Note
SHG, $o + o \Rightarrow e$			
1.047 ⇒ 0.5235	75.3	[22]	
1.0642 ⇒ 0.5321	25.4	[23]	0.6 mol% MgO, congruent LN
	78.5	[24]	7 mol% MgO, along X
	85–109	[13]	>5 mol% MgO
	107	[5], [6], [25], [26]	5 mol% MgO
	110	[27]	5 mol% MgO
	110.6	[28]	5 mol% MgO
	110.8	[29]	7 mol% MgO
	113	[30]	
	116	[31]	
1.0795 ⇒ 0.53975	115	[7]	5 mol% MgO, congruent LN

Note: The PM temperature values are strongly dependent on melt stoichiometry.

Experimental values of angular and temperature bandwidths

Interacting wavelengths [μm]	T [°C]	θ_{pm} [deg]	$\Delta\theta^{\text{int}}$ [deg]	ΔT [°C]	Ref.	Note
SHG, $o + o \Rightarrow e$						
1.0642 ⇒ 0.5321	20	76	0.063		[5]	5 mol% MgO
	25.4	90		0.68	[23]	0.6 mol% MgO
	107	90	2.160	0.73	[5]	5 mol% MgO
	110.6	90		0.73	[28]	5 mol% MgO

Laser-induced damage threshold

λ [μm]	τ_p [ns]	I_{thr} [GW/cm^2]	Ref.	Note
0.5321	CW	>0.002	[12]	1 mol% MgO, Li/Nb = 1.38
		>0.002	[12]	2 mol% MgO, Li/Nb = 1.0
		0.002	[12]	5 mol% MgO, congruent LN
		>0.006	[32]	1.8 mol% MgO, Li/Nb = 0.96–0.99
	≈20	0.34	[5]	5 mol% MgO
0.778	0.002	>10	[33]	7 mol% MgO
0.780	0.00015	>15	[16]	
0.78–0.84	0.0001	>130	[34]	1 kHz, 7 mol% MgO
1.0642	25	>0.025	[23]	0.6 mol% MgO, congruent LN
	≈20	0.61	[5]	5 mol% MgO
	20	>0.039	[10]	10 Hz, 5 mol% MgO
	0.04	>0.8	[23]	0.6 mol% MgO, congruent LN
	0.03	>0.14	[10]	5 Hz, 5 mol% MgO
1.56	0.00008	>1.36	[35]	1 kHz, 5 mol% MgO

Note: Under CW 0.532-μm irradiation, the bulk photorefractive damage was investigated.

About the crystal

One of the most important drawbacks of popular $LiNbO_3$ crystal is its susceptibility to photorefractive damage (optically induced change of refractive index, usually under exposure with blue or green CW light) [36]. The usual way to eliminate this effect is to keep LN crystals at elevated temperatures (400 K or more). Another way to prevent photorefractive damage is MgO-doping (usually at levels of around 5 mol% for congruent LN). What is good is that such MgO-doped congruent $LiNbO_3$ crystals have a much lower coercive field value than undoped LN crystals. However, the large amounts of MgO-doping subsequently cause difficulty in growing crystals of high optical quality. Recently, it was shown [12] that stoichiometric $LiNbO_3$ crystals, doped with only 1 mol% MgO, possess higher photorefractive damage threshold than 5 mol% MgO-doped congruent LN samples.

Let us briefly consider the two latest records, achieved recently by a Japanese group, which developed the PPMgLN crystals with extremely small values of the grating period (down to 1.4 μm). In [37], 1.2-mW CW UV light ($\lambda = 341.5$ nm) was generated via first-order QPM SHG in a 2-mm-thick, 10-mm-long crystal at fundamental power of 141 mW. In [38], 890 mW at 531 nm was generated in a 2-mm-thick, 10-mm-long PPMgLN by single pass frequency doubling of a diode end-pumped Nd:$GdVO_4$ laser. According to the authors of [38], this is the highest CW power ever obtained by QPM SHG at room temperature.

References

[1] K. Niwa, Y. Furukawa, S. Takekawa, K. Kitamura: Growth and characterization of MgO doped near stoichiometric $LiNbO_3$ crystals as a new nonlinear optical crystal. J. Cryst. Growth **208(1–4)**, 493–500 (2000).

[2] K. Mizuuchi, A. Morikawa, T. Sugita, K. Yamamoto: Generation of 360-nm ultraviolet light in first-order periodically poled bulk MgO:$LiNbO_3$. Opt. Lett. **28(11)**, 935–937 (2003).

[3] A.L. Aleksandrovskii, G.I. Ershova, G.K. Kitaeva, S.P. Kulik, I.I. Naumova, V.V. Tarasenko: Dispersion of the refractive indices of $LiNbO_3$:Mg and $LiNbO_3$:Y crystals. Kvant. Elektron. **18(2)**, 254–256 (1991) [In Russian, English trans.: Sov. J. Quantum Electron. **21(2)**, 225–227 (1991)].

[4] Y. Chang, J. Wen, H. Wang, B. Li: Refractive index measurement and second harmonic generation in a series of $LiNbO_3$:Mg (5 mol%) crystals. Chin. Phys. Lett. **9(8)**, 427–430 (1992).

[5] J.L. Nightingale, W.J. Silva, G.E. Reade, A. Rybicki, W.J. Kozlovsky, R.L. Byer: Fifty percent conversion efficiency second harmonic generation in magnesium oxide doped lithium niobate. Proc. SPIE **681**, 20–24 (1986).

[6] W.J. Kozlovsky, C.D. Nabors, R.L. Byer: Efficient second harmonic generation of a diode-laser-pumped cw Nd:YAG laser using monolithic MgO:$LiNbO_3$ external resonant cavities. IEEE J. Quant. Electr. **24(6)**, 913–919 (1988).

[7] H.Y. Shen, H. Xu, Z.D. Zheng, W.X. Lin, R.F. Wu, G.F. Hu: Measurement of refractive indices and thermal refractive-index coefficients of $LiNbO_3$ crystal doped with 5 mol% MgO. Appl. Opt. **31(31)**, 6695–6697 (1992).

[8] D.E. Zelmon, D.L. Small, D. Jundt: Infrared corrected Sellmeier coefficients for congruently grown lithium niobate and 5 mol% magnesium oxide-doped lithium niobate. J. Opt. Soc. Am. B **14(12)**, 3319–3322 (1997).

[9] U. Schlarb, K. Betzler: Influence of the defect structure on the refractive indices of undoped and MgO-doped lithium niobate. Phys. Rev. B **50(2)**, 751–757 (1994).

[10] J.Q. Yao, W.Q. Shi, J.E. Millerd, G.F. Hu, E. Garmire, M. Birnbaum: Room temperature 1.06–0.53 μm second harmonic generation with MgO:$LiNbO_3$. Opt. Lett. **15(23)**, 1339–1341 (1990).

[11] S. Lin, Y. Tanaka, S. Takeuchi, T. Suzuki: Improved dispersion equation for MgO:$LiNbO_3$ crystal in the infrared spectral range derived from sum and difference frequency mixing. IEEE J. Quant. Electr. **32(1)**, 124–126 (1996).

[12] M. Nakamura, S. Higuchi, S. Takekawa, K. Terabe, Y. Furukawa, K. Kitamura: Optical damage resistance and refractive indices in near-stoichiometric MgO-doped $LiNbO_3$. Jpn. J. Appl. Phys. **41(1A/B)**, L49–L51 (2002).

[13] J.-Q. Yao, Y.-Z. Yu, P. Wang, T. Wang, B.-G. Zhang, X. Ding, J. Chen, H.J. Peng, H.S. Kwok: Nearly-noncritical phase matching in MgO:$LiNbO_3$ optical parametric oscillators. Chin. Phys. Lett. **18(9)**, 1214–1217 (2001).

[14] R.C. Eckardt, C.D. Nabors, W.J. Kozlovsky, R.L. Byer: Optical parametric oscillator frequency tuning and control. J. Opt. Soc. Am. B **8(3)**, 646–667 (1991).

[15] D.Y. Sugak, A.O. Matkovskii, I.M. Solskii, I.V. Stefanskii, V.M. Gaba, A.T. Mikhalevich, V.V. Grabovski, V.I. Prokhorenko, B.N. Kopko, V.Y. Oliinyk: Growth and investigation of $LiNbO_3$:MgO single crystals. Proc. SPIE **2795**, 257–264 (1996).

[16] H.P. Li, C.H. Kam, Y.L. Lam, W. Ji: Femtosecond Z-scan measurements of nonlinear refraction in nonlinear optical materials. Opt. Mater. **15(4)**, 237–242 (2001).

[17] H. Ishizuki, T. Taira, S. Kurimura, J.H. Ro, M. Cha: Periodic poling in 3-mm-thick MgO:$LiNbO_3$ crystals. Jpn. J. Appl. Phys. **42(2A)**, L108-L110 (2003).

[18] H. Ishizuki, I. Shoji, T. Taira: Periodical poling of 3 mm-thick MgO:$LiNbO_3$ crystals for high-power nonlinear wavelength conversion. In: *CLEO/Europe 2003, Technical Digest* (OSA, Washington DC, 2003), paper CE2–2-MON.

[19] I. Shoji, H. Nakamura, K. Ohdaira, T. Kondo, R. Ito, T. Okamoto, K. Tatsuki, S. Kubota: Absolute measurement of second-order nonlinear-optical coefficients of β-BaB_2O_4 for visible to ultraviolet second-harmonic wavelengths. J. Opt. Soc. Am. B **16(4)**, 620–624 (1999).
[20] J.E. Midwinter, J. Warner: The effects of phase matching method and of uniaxial crystal symmetry on the polar distribution of second-order non-linear optical polarization. Brit. J. Appl. Phys. **16(11)**, 1135–1142 (1965).
[21] I. Shoji, T. Kondo, A. Kitamoto, M. Shirane, R. Ito: Absolute scale of second-order nonlinear-optical coefficients. J. Opt. Soc. Am. B **14(9)**, 2268–2294 (1997).
[22] G.T. Maker, A.I. Ferguson: Ti:sapphire laser pumped by a frequency-doubled diode-pumped Nd:YLF laser. Opt. Lett. **15(7)**, 375–377 (1990).
[23] B.K. Rhee, J.-S. Lee, G.-T. Joo: Room-temperature 1.06–0.53 μm second-harmonic generation in $LiNbO_3$ with 0.6 mole% MgO doping. Proc. SPIE **3610**, 156–163 (1999).
[24] M. Tsunekane, S. Kimura, M. Kimura, N. Taguchi, H. Inaba: Continuous-wave, broadband tuning from 788 to 1640 nm by a doubly resonant, MgO:$LiNbO_3$ optical parametric oscillator. Appl. Phys. Lett. **72(26)**, 3414–3416 (1998).
[25] W.J. Kozlovsky, C.D. Nabors, R.C. Eckardt, R.L. Byer: Monolithic MgO:$LiNbO_3$ doubly resonant optical parametric oscillator pumped by a frequency-doubled diode-laser-pumped Nd:YAG laser. Opt. Lett. **14(1)**, 66–68 (1989).
[26] C.D. Nabors, R.C. Eckardt, W.J. Kozlovsky, R.L. Byer: Efficient, single-axial-mode operation of a monolithic MgO:$LiNbO_3$ optical parametric oscillator. Opt. Lett. **14(20)**, 1134–1136 (1989).
[27] D.C. Gerstenberger, G.E. Tye, R.W. Wallace: Efficient second-harmonic conversion of CW single-frequency Nd:YAG laser light by frequency locking to a monolithic ring frequency doubler. Opt. Lett. **16(13)**, 992–994 (1991).
[28] R.C. Eckardt, H. Masuda, Y.X. Fan, R.L. Byer: Absolute and relative nonlinear optical coefficients of KDP, KD*P, BaB_2O_4, $LiIO_3$, MgO:$LiNbO_3$, and KTP measured by phase-matched second-harmonic generation IEEE J. Quant. Electr. **26(5)**, 922–933 (1990).
[29] A. Porzio, C. Altucci, M. Autiero, A. Chiummo, C. De Lisio, S. Solimeno: Tunable twin beams generated by a type-I OPO. Appl. Phys. B **73(7)**, 763–766 (2001).
[30] D.C. Gerstenberger, R.W. Wallace: Continuous-wave operation of a doubly resonant lithium niobate optical parametric oscillator system tunable from 966 to 1185 nm. J. Opt. Soc. Am. B **10(9)**, 1681–1683 (1993).
[31] G.T. Maker, A.I. Ferguson: Efficient frequency doubling of a diode laser-pumped mode-locked Nd:YAG laser using an external resonant cavity. Opt. Commun. **76(5–6)**, 369–375 (1990).
[32] Y. Furukawa, K. Kitamura, S. Takekawa, K. Niwa, H. Hatano: Stoichiometric MgO:$LiNbO_3$ as an effective material for nonlinear optics. Opt. Lett. **23(24)**, 1892–1894 (1998).
[33] S. Lin, T. Suzuki: Tunable picosecond mid-infrared pulses generated by optical parametric generation/amplification in MgO:$LiNbO_3$ crystals. Opt. Lett. **21(8)**, 579–581 (1996).
[34] V. Petrov, F. Rotermund, F. Noack: Femtosecond traveling-wave optical parametric amplification in MgO:$LiNbO_3$. Appl. Opt. **37(36)**, 8504–8511 (1998).
[35] S. Ashihara, T. Shimura, K. Kuroda, N.E. Yu, S. Kurimura, K. Kitamura, J.H. Ro, M. Cha, T. Taira: Group-velocity-matched cascaded quadratic nonlinearities of femtosecond pulses in periodically poled MgO:$LiNbO_3$. Opt. Lett. **28(16)**, 1442–1444 (2003).
[36] A.M. Glass: The photorefractive effect. Opt. Eng. **17(5)**, 470–479 (1978).
[37] K. Mizuuchi, A. Morikawa, T. Sugita, K. Yamamoto: Efficient second-harmonic generation of 340-nm light in a 1.4-μm periodically poled bulk MgO:$LiNbO_3$. Jpn. J. Appl. Phys. **42(2A)**, L90–L91 (2003).

[38] K. Mizuuchi, A. Morikawa, T. Sugita, K. Yamamoto, N. Pavel, I. Shoji, T. Taira: High-power continuous wave green generation by single-pass frequency doubling of a Nd:$GdVO_4$ laser in a periodically poled MgO:$LiNbO_3$ operating at room temperature. Jpn. J. Appl. Phys. **42(11A)**, L1296–L1298 (2003).

4.6 $KTiOAsO_4$, Potassium Titanyl Arsenate (KTA)

Positive biaxial crystal: $2V_z = 40.4°$ at $\lambda = 0.5321\,\mu m$
Molecular mass: 241.897
Specific gravity: $3.454\,g/cm^3$ [1]
Point group: $mm2$
Lattice constants:
$a = 13.103$ Å [2]; 13.125 Å [3]; 13.127 Å [4]
$b = 6.558$ Å [2]; 6.5716 Å [3]; 6.5713 Å [4]
$c = 10.746$ Å [2]; 10.786 Å [3]; 10.789 Å [4]
Assignment of dielectric and crystallographic axes: $X, Y, Z \Rightarrow a, b, c$
Curie temperature: 1153 K [2]; 1149 K ($\|c$), 1151 K ($\|a$), 1153 K ($\|b$) [5]
Thermal expansion along the X axis for temperature range $298\,K < T < 473\,K$ [6]:

$$L(T) = L_0\left[1 + \alpha(T - 298) + \beta(T - 298)^2\right]$$

where T in K, $T_0 = 298\,K$, $\alpha = (7.6 \pm 0.6) \times 10^{-6}\,K^{-1}$, $\beta = (8.4 \pm 1.2) \times 10^{-9}\,K^{-2}$.
Transparency range at "0" transmittance level: $0.35 - 5.2\,\mu m$ [2], [7]; $0.35 - 5.3\,\mu m$ [8], [5]
UV transmission cutoff ($\alpha = 2\,cm^{-1}$) is at $0.377\,\mu m$ ($\mathbf{E}\|X$); $0.385\,\mu m$ ($\mathbf{E}\|Y$); $0.393\,\mu m$ ($\mathbf{E}\|Z$) [9].

Linear absorption coefficient α

λ [μm]	α [cm^{-1}]	Ref.	Note
0.473	0.008	[9]	$\mathbf{E}\|X$
	0.014	[9]	$\mathbf{E}\|Y$
	0.016	[9]	$\mathbf{E}\|Z$
0.532	0.005	[9]	$\mathbf{E}\|X$
	0.005	[9]	$\mathbf{E}\|Y$
	0.005	[9]	$\mathbf{E}\|Z$
4.0	0.2	[10]	
5.0	1.0	[10]	

Experimental values of refractive indices [11]

λ [μm]	n_X	n_Y	n_Z
0.6328	1.8083	1.8142	1.9048

Traditional Sellmeier equations (λ in μm, $T = 293$ K) [12]:

$$n_X^2 = 3.1413 + \frac{0.04683}{\lambda^2 - 0.04055} - 0.01023\,\lambda^2$$

$$n_Y^2 = 3.1593 + \frac{0.04828}{\lambda^2 - 0.04710} - 0.01049\,\lambda^2$$

$$n_Z^2 = 3.4435 + \frac{0.06571}{\lambda^2 - 0.05435} - 0.01460\,\lambda^2$$

More accurate dispersion relations (λ in μm, $0.4\,\mu\text{m} < \lambda < 5.3\,\mu\text{m}$ for n_X and n_Y, $0.4\,\mu\text{m} < \lambda < 3.6\,\mu\text{m}$ for n_Z, $T = 293$ K) [13], [14]:

$$n_X^2 = 2.1495 + \frac{1.0203\,\lambda^{1.9951}}{\lambda^{1.9951} - 0.042378} + \frac{0.5531\,\lambda^{1.9567}}{\lambda^{1.9567} - 72.3045}$$

$$n_Y^2 = 2.1308 + \frac{1.0564\,\lambda^{2.0017}}{\lambda^{2.0017} - 0.042523} + \frac{0.6927\,\lambda^{1.7261}}{\lambda^{1.7261} - 54.8505}$$

$$n_Z^2 = 2.1931 + \frac{1.2382\,\lambda^{1.8920}}{\lambda^{1.8920} - 0.059171} + \frac{0.5088\,\lambda^{2.0000}}{\lambda^{2.0000} - 53.2898}$$

Other sets of dispersion relations are given in [4], [11], [15], [16], [17], [18].
Infrared-corrected Sellmeier equation for refractive index n_Z (λ in μm, $T = 293$ K) [19]:

$$n_Z^2 = 1.214331 + \frac{2.225328\,\lambda^2}{\lambda^2 - (0.178542)^2} + \frac{0.310017\,\lambda^2}{\lambda^2 - (8.989998)^2} - 0.009381\,\lambda^2$$

Nonlinear refractive index γ [20], [21]

λ [μm]	$\gamma \times 10^{15}$ [cm^2/W]	Note
0.780	1.7 ± 0.3	[100] direction
	1.7 ± 0.3	[010] direction

Linear electrooptic coefficients measured at low frequencies (well below the acoustic resonances of KTA crystal, i.e., for the "free" crystal) at room temperature [17]

λ [μm]	r_{13}^{T} [pm/V]	r_{23}^{T} [pm/V]	r_{33}^{T} [pm/V]
0.6328	11.5 ± 1.2	15.4 ± 1.5	37.5 ± 3.8

Expressions for the effective second-order nonlinear coefficient in principal planes of KTA crystal (Kleinman symmetry conditions are not valid) [22]:

XY plane

$$d_{\mathrm{eoe}} = d_{\mathrm{oee}} = d_{15}\sin^2\phi + d_{24}\cos^2\phi$$

YZ plane

$$d_{\mathrm{oeo}} = d_{\mathrm{eoo}} = d_{15}\sin\theta$$

XZ plane, $\theta < V_z$

$$d_{ooe} = d_{32} \sin\theta$$

XZ plane, $\theta < V_z$

$$d_{oeo} = d_{eoo} = d_{24} \sin\theta$$

Expressions for the effective second-order nonlinear coefficient in principal planes of KTA crystal (Kleinman symmetry conditions are valid, $d_{15} = d_{31}$ and $d_{24} = d_{32}$) [22]:

XY plane

$$d_{eoe} = d_{oee} = d_{31} \sin^2\phi + d_{32} \cos^2\phi$$

YZ plane

$$d_{oeo} = d_{eoo} = d_{31} \sin\theta$$

XZ plane, $\theta < V_z$

$$d_{ooe} = d_{32} \sin\theta$$

XZ plane, $\theta > V_z$

$$d_{oeo} = d_{eoo} = d_{32} \sin\theta$$

Effective second-order nonlinear coefficient for three-wave interactions in the arbitrary direction of KTA crystal is given in [22].
The signs of KTA second-order nonlinear coefficients are probably all the same [23].
Absolute and relative values of second-order nonlinear coefficients:

$d_{15}(1.064\,\mu\text{m}) = 1.3 \times d_{15}(\text{KTP}) = 2.5 \pm 0.2\,\text{pm/V}$ [4], [24]

$d_{24}(1.064\,\mu\text{m}) = (1.8 \pm 0.1) \times d_{15}(\text{KTA}) = 4.4 \pm 0.2\,\text{pm/V}$ [4], [24]

$d_{31}(1.064\,\mu\text{m}) = 2.8 \pm 0.3\,\text{pm/V}$ [11]

$d_{31}(1.064\,\mu\text{m}) = (1.3 \pm 0.1) \times d_{31}(\text{KTP}) = 2.9 \pm 0.2\,\text{pm/V}$ [24], [25]

$d_{32}(1.064\,\mu\text{m}) = 4.2 \pm 0.4\,\text{pm/V}$ [11]

$d_{32}(1.064\,\mu\text{m}) = (1.8 \pm 0.1) \times d_{31}(\text{KTA}) = 5.1 \pm 0.3\,\text{pm/V}$ [24], [25]

$d_{33}(1.064\,\mu\text{m}) = 16.2 \pm 1.0\,\text{pm/V}$ [11]

$d_{15}(1.32\,\mu\text{m}) = 1.2 \times d_{15}(\text{KTP}) = 1.7 \pm 0.1\,\text{pm/V}$ [16], [24]

$d_{24}(1.32\,\mu\text{m}) = 1.7 \times d_{15}(\text{KTP}) = 2.4 \pm 0.2\,\text{pm/V}$ [16], [24]

Experimental values of phase-matching angle ($T = 293$ K)

Interacting wavelengths [μm]	ϕ_{exp} [deg]	θ_{exp} [deg]	Ref.
XY plane, $\theta = 90°$			
SFG, $e + o \Rightarrow e$			
$1.3188 + 0.6594 \Rightarrow 0.4396$	62.5		[12]
$1.0642 + 1.9079 \Rightarrow 0.6831$	15.7		[12]
YZ plane, $\phi = 90°$			
SHG, $o + e \Rightarrow o$			
$1.0745 \Rightarrow 0.53725$		90	[12]
$1.1523 \Rightarrow 0.57615$		69.2	[12]
$1.3188 \Rightarrow 0.6594$		56	[16]
		55.9	[12]
		55.9	[11]
		55.7	[15]
$3.3913 \Rightarrow 1.69565$		63.5	[12]
SFG, $o + e \Rightarrow o$			
$1.3188 + 0.6594 \Rightarrow 0.4396$		79.8	[12]
$1.0642 + 1.9079 \Rightarrow 0.6831$		72.1	[12]
XZ plane, $\phi = 0°$, $\theta > V_z$			
SHG, $o + e \Rightarrow o$			
$1.1422 \Rightarrow 0.5711$		90	[12]
$1.1523 \Rightarrow 0.57615$		82.9	[4]
$1.3188 \Rightarrow 0.6594$		65	[15]
		64.6	[5]
		64.2	[4]
		63.1	[12]
$3.3913 \Rightarrow 1.69565$		70.6	[12]

Experimental values of internal angular bandwidth

Interacting wavelengths [μm]	θ_{pm} [deg]	$\Delta\theta^{int}$ [deg]	Ref.
YZ plane, $\phi = 90°$			
SHG, $o + e \Rightarrow o$			
$1.3188 \Rightarrow 0.6594$	56	0.086	[16]
	55.9	0.093	[11]

Laser-induced damage threshold

λ [μm]	τ_p [ns]	I_{thr} [GW/cm^2]	Ref.	Note
0.74–0.84	0.0002	>200	[26]	1 kHz
0.77–0.9	0.0012	>0.3	[27]	81 MHz
0.78	0.00015	>20	[21]	76 MHz
0.85	2	>1	[28]	
1.0642	18	>0.12	[29]	100 Hz
	8	>1.2	[10]	20 Hz, 1000 pulses

About the crystal

Unlike KTP, KTA is mainly used for birefringent phase matching. Main advantages of KTA in comparison with KTP are slightly higher values of second-order nonlinear coefficients [4], [25], [11], [24], a longer IR cutoff wavelength, and the absence of significant absorption at 3.5 μm [9]. Until now, only few works were devoted to PPKTA [19], [30].

References

[1] B.H.T. Chai: Optical Crystals. In: *CRC Handbook of Laser Science and Technology, Supplement 2: Optical Materials*, ed. by M.J. Weber (CRC Press, Boca Raton, 1995), pp. 3–65.

[2] J.D. Bierlein, H. Vanherzeele, A.A. Ballman: Linear and nonlinear optical properties of flux-grown $KTiOAsO_4$. Appl. Phys. Lett. **54(9)**, 783–785 (1989).

[3] L.K. Cheng, E.M. McCarron III, J. Calabrese, J.D. Bierlein, A.A. Ballman: Development of the nonlinear optical crystal $CsTiOAsO_4$. I. Structural stability. J. Cryst. Growth **132(1–2)**, 280–288 (1993).

[4] K. Kato: Second-harmonic and sum-frequency generation in $KTiOAsO_4$. IEEE J. Quant. Electr. **30(4)**, 881–883 (1994).

[5] J. Wei, J. Wang, Y. Liu, L. Shi, M. Wang, Z. Shao: Growth, second harmonic and sum frequency generation operations of potassium titanyl arsenate crystal. Chin. Phys. Lett. **11(2)**, 95–98 (1994).

[6] S. Emanueli, A. Arie: Temperature-dependent dispersion equations for $KTiOPO_4$ and $KTiOAsO_4$. Appl. Opt. **42(33)**, 6661–6665 (2003).

[7] A.H. Kung: Efficient conversion of high-power narrow-band Ti:sapphire laser radiation to the mid-infrared in $KTiOAsO_4$. Opt. Lett. **20(10)**, 1107–1109 (1995).

[8] L.K. Cheng, J.D. Bierlein: KTP and isomorphs—recent progress in device and material development. Ferroelectrics **142(1–2)**, 209–228 (1993).

[9] G. Hansson, H. Karlsson, S. Wang, F. Laurell: Transmission measurements in KTP and isomorphic compounds. Appl. Opt. **39(27)**, 5058–5069 (2000).

[10] W.R. Bosenberg, L.K. Cheng, J.D. Bierlein: Optical parametric frequency conversion properties of $KTiOAsO_4$. Appl. Phys. Lett. **65(22)**, 2765–2767 (1994).

[11] L.K. Cheng, L.-T. Cheng, J.D. Bierlein, F.C. Zumsteg, A.A. Ballman: Properties of doped and undoped crystals of single domain $KTiOAsO_4$. Appl. Phys. Lett. **62(4)**, 346–348 (1993).

[12] K. Kato, N. Umemura, E. Tanaka: 90° phase-matched mid-infrared parametric oscillation in undoped $KTiOAsO_4$. Jpn. J. Appl. Phys. **36(4A)**, L403–L405 (1997).

[13] J.P. Feve, B. Boulanger, O. Pacaud, I. Rousseau, B. Menaert, G. Marnier: Refined Sellmeier equations from phase-matching measurements over the complete transparency range of $KTiOAsO_4$, $RbTiOAsO_4$, and $CsTiOAsO_4$. In: *Advanced Solid-State Lasers, OSA Trends in Optics and Photonics Series, Vol. 34*, ed. by H. Injeyan, U. Keller, C. Marshall (OSA, Washington DC, 2000), pp. 575–577.

[14] J.-P. Feve, B. Boulanger, O. Pacaud, I. Rousseau, B. Menaert, G. Marnier, P. Villeval, C. Bonnin, G.M. Loiacono, D.N. Loiacono: Phase-matching measurements and Sellmeier equations over the complete transparency range of $KTiOAsO_4$, $RbTiOAsO_4$, and $CsTiOAsO_4$. J. Am. Opt. Soc. B **17(5)**, 775–780 (2000).

[15] B. Boulanger, G. Marnier, B. Menaert, X. Gabirol, J.P. Feve, C. Bonnin, P. Villeval: Collinear L.C. type II phase-matching for SHG in $KTiOAsO_4$: demonstration of its impossibility at 1.064 μm and first experiments at 1.32 μm. Comparison with $KTiOPO_4$. Nonl. Opt. **4(2)**, 133–142 (1993).
[16] L.-T. Cheng, L.K. Cheng, J.D. Bierlein: Linear and nonlinear optical properties of the arsenate isomorphs of KTP. Proc. SPIE **1863**, 43–53 (1993).
[17] L.K. Cheng, L.T. Cheng, J. Galperin, P.A. Morris Hotsenpiller, J.D. Bierlein: Crystal growth and characterization of $KTiOPO_4$ isomorphs from the self-fluxes. J. Cryst. Growth **137(1–2)**, 107–115 (1994).
[18] D.L. Fenimore, K.L. Schepler, U.B. Ramabadran, S.R. McPherson: Infrared corrected Sellmeier coefficients for potassium titanyl arsenate. J. Opt. Soc. Am. B **12(5)**, 794–796 (1995).
[19] K. Fradkin-Kashi, A. Arie, P. Urenski, G. Rosenman: Mid-infrared difference-frequency generation in periodically poled $KTiOAsO_4$ and application to gas sensing. Opt. Lett. **25(10)**, 743–745 (2000).
[20] H.P. Li, C.H. Kam, Y.L. Lam, F. Zhou, W. Ji: Nonlinear refraction of undoped and Fe-doped $KTiOAsO_4$ crystals in the femtosecond regime. Appl. Phys. B **70(3)**, 385–388 (2000).
[21] H.P. Li, C.H. Kam, Y.L. Lam, W. Ji: Femtosecond Z-scan measurements of nonlinear refraction in nonlinear optical materials. Opt. Mater. **15(4)**, 237–242 (2001).
[22] V.G. Dmitriev, D.N. Nikogosyan: Effective nonlinearity coefficients for three-wave interactions in biaxial crystals of $mm2$ point group symmetry. Opt. Commun. **95(1–3)**, 173–182 (1993).
[23] A. Anema, T. Rasing: Relative signs of the nonlinear coefficients of potassium titanyl phosphate. Appl. Opt. **36(24)**, 5902–5904 (1997).
[24] I. Shoji, T. Kondo, A. Kitamoto, M. Shirane, R. Ito: Absolute scale of second-order nonlinear-optical coefficients. J. Opt. Soc. Am. B **14(9)**, 2268–2294 (1997).
[25] J. Wang, J. Wei, Y. Liu, X. Yin, X. Hu, Z. Shao, M. Jiang: A survey of research on KTP and its analogue crystals. Progr. Cryst. Growth Character. Mater. **40(1–4)**, 3–15 (2000).
[26] V. Petrov, F. Noack, R. Stolzenberger: Seeded femtosecond optical parametric amplification in the mid-infrared spectral region above 3 μm. Appl. Opt. **36(6)**, 1164–1172 (1997).
[27] S. French, A. Miller, M. Ebrahimzade: Picosecond near- to mid-infrared optical parametric oscillator using $KTiOAsO_4$. Opt. Quant. Electron. **29(11–12)**, 999–1021 (1997).
[28] A.H. Kung: Narrow band mid-infrared generation using $KTiOAsO_4$. Appl. Phys. Lett. **65(4)**, 1082–1084 (1994).
[29] M.S. Webb, P.F. Moulton, J.J. Kasinski, R.L. Burnham, G. Loiacono, R. Stolzenberger: High-average-power $KTiOAsO_4$ optical parametric oscillator. Opt. Lett. **23(15)**, 1161–1163 (1998).
[30] G. Rosenman, A. Skliar, Y. Findling, P. Urenski, A. Englander, P.A. Thomas, Z.W. Hu: Periodically poled $KTiAsO_4$ crystals for optical parametric oscillation. J. Phys. D **32(14)**, L49–L52 (1999).

4.7 $KNbO_3$, Potassium Niobate (KN)

Negative biaxial crystal: $2V_z = 66.78°$ at $\lambda = 0.5321$ μm [1]
Molecular mass: 188.150

Specific gravity: 4.617 g/cm^3 [2]
Point group: $mm2$ (223 K $< T <$ 496 K)
Lattice constants:
$a = 5.6896$ Å [3]; 5.697 Å [4]; 5.7061 Å [5]
$b = 3.9692$ Å [3]; 3.971 Å [4]; 3.9794 Å [5]
$c = 5.7256$ Å [3]; 5.722 Å [4]; 5.7319 Å [5]
Assignment of dielectric and crystallographic axes: $X, Y, Z \Rightarrow b, a, c$
Melting temperature: 1333 K [6]
Curie temperature: 498 K [7]
Specific heat capacity c_p at $P = 0.101325$ MPa: $c_p = 767$ J/kgK [8]
Thermal conductivity coefficient:
$\kappa > 3.5$ W/mK [9];
$\kappa = 4$ W/mK [8]
Transparency range at "0" transmittance level: ≈0.4 to >4 μm [3], [10]
IR cutoff wavelength is at 5.5 μm ($\|a$ or $\|c$) [11]

Linear absorption coefficient α

λ [μm]	α [cm^{-1}]	Ref.	Note
0.42–1.06	<0.05	[12]	
0.423	0.13 ± 0.02	[13]	along a axis, $\mathbf{E}\|c$
0.458–0.515	0.04–0.07	[8]	
0.8–1.1	0.001–0.003	[8]	
0.82	0.015	[14]	
0.846	0.000034 ± 0.000022	[13]	along a axis, $\mathbf{E}\|b$
1.0642	0.0018–0.0025	[9]	along b axis
3.0	0.05	[11]	along c axis
	0.03	[11]	along a axis
3.5	0.05	[11]	along c axis
	0.02	[11]	along a axis
4.0	0.08	[11]	along c axis
	0.08	[11]	along a axis
4.5	0.27	[11]	along c axis
	0.45	[11]	along a axis
5.0	1.21	[11]	along c axis
	1.85	[11]	along a axis
5.5	7.60	[11]	along c axis
	4.90	[11]	along a axis

Two-photon absorption coefficient β (along a axis) [13]

λ [μm]	τ_p [ns]	$\beta \times 10^{11}$ [cm/W]
0.846	CW	320 ± 50

Experimental values of refractive indices at $T = 295\,\mathrm{K}$ [3]

λ [μm]	n_X	n_Y	n_Z
0.430	2.4974	2.4145	2.2771
0.488	2.4187	2.3527	2.2274
0.514	2.3951	2.3337	2.2121
0.633	2.3296	2.2801	2.1687
0.860	2.2784	2.2372	2.1338
1.064	2.2576	2.2195	2.1194
1.500	2.2341	2.1992	2.1029
2.000	2.2159	2.1832	2.0899
2.500	2.1981	2.1674	2.0771
3.000	2.1785	2.1498	2.0630

Best set of dispersion relations (λ in μm, $T = 295\,\mathrm{K}$) [11], [15]:

$$n_X^2 = 4.9856 + \frac{0.15266}{\lambda^2 - 0.06331} - 0.02831\,\lambda^2 + 2.0754 \times 10^{-6}\,\lambda^4 - 1.2131 \times 10^{-6}\lambda^6$$

$$n_Y^2 = 4.8353 + \frac{0.12808}{\lambda^2 - 0.05674} - 0.02528\,\lambda^2 + 1.8590 \times 10^{-6}\,\lambda^4 - 1.0689 \times 10^{-6}\lambda^6$$

$$n_Z^2 = 4.4222 + \frac{0.09972}{\lambda^2 - 0.05496} - 0.01976\,\lambda^2$$

Other sets of dispersion relations are given in [1], [3], [16], [17].

Temperature-dependent Sellmeier equations (λ in μm, T in K) [18]:

$$n_X^2 = 1 + \frac{(2.5389409 + 3.8636303 \times 10^{-6} F)\lambda^2}{\lambda^2 - (0.1371639 + 1.767 \times 10^{-7} F)^2} + \frac{(1.4451842 - 3.909336 \times 10^{-6} F - 1.2256136 \times 10^{-4}\,G)\lambda^2}{\lambda^2 - (0.2725429 + 2.38 \times 10^{-7} F - 6.78 \times 10^{-5}\,G)^2} - (2.837 \times 10^{-2} - 1.22 \times 10^{-8} F)\lambda^2 - 3.3 \times 10^{-10} F\lambda^4$$

$$n_Y^2 = 1 + \frac{(2.6386669 + 1.6708469 \times 10^{-6} F)\lambda^2}{\lambda^2 - (0.1361248 + 0.796 \times 10^{-7} F)^2} + \frac{(1.1948477 - 1.3872635 \times 10^{-6} F - 0.90742707 \times 10^{-4} G)\lambda^2}{\lambda^2 - (0.2621917 + 1.231 \times 10^{-7} F - 1.82 \times 10^{-5} G)^2} - (2.513 \times 10^{-2} - 0.558 \times 10^{-8} F)\lambda^2 - 4.4 \times 10^{-10} F\lambda^4$$

$$n_Z^2 = 1 + \frac{(2.370517 + 2.8373545 \times 10^{-6} F)\lambda^2}{\lambda^2 - (0.1194071 + 1.75 \times 10^{-7} F)^2} + \frac{(1.048952 - 2.1303781 \times 10^{-6} F - 1.8258521 \times 10^{-4} G)\lambda^2}{\lambda^2 - (0.2553605 + 1.89 \times 10^{-7} F - 2.48 \times 10^{-5} G)^2} - (1.939 \times 10^{-2} - 0.27 \times 10^{-8} F)\lambda^2 - 5.7 \times 10^{-10} F \lambda^4$$

where $F = T^2 - 295.15^2$, $G = T - 295.15$.

Temperature derivative of refractive indices for spectral range 0.42–5.3 μm and temperature range 295–473 K and corresponding equations for calculation of temperature-induced refractive index change (λ in μm, T in K) [15]:

$$\frac{dn_X}{dT} = \left(\frac{0.3041}{\lambda} - 3.1012\right) \times 10^{-5}\,\mathrm{K}^{-1}$$

$$\frac{dn_Y}{dT} = \left(\frac{2.5929}{\lambda^3} - \frac{4.7381}{\lambda^2} + \frac{4.1254}{\lambda} + 1.3788\right) \times 10^{-5}\,\mathrm{K}^{-1}$$

$$\frac{dn_Z}{dT} = \left(\frac{1.4087}{\lambda^3} - \frac{5.1523}{\lambda^2} + \frac{8.7432}{\lambda} + 2.2350\right) \times 10^{-5}\,\mathrm{K}^{-1}$$

$$\Delta n_X = \frac{dn_X}{dT}\left[(T - 295.15) - 0.32 \times 10^{-3}(T - 295.15)^2\right]$$

$$\Delta n_Y = \frac{dn_Y}{dT}\left[(T - 295.15) + 2.20 \times 10^{-3}(T - 295.15)^2)\right]$$

$$\Delta n_Z = \frac{dn_Z}{dT}\left[(T - 295.15) + 2.71 \times 10^{-3}(T - 295.15)^2\right]$$

Nonlinear refractive index γ [19]

λ [μm]	$\gamma \times 10^{15}$ [cm^2/W]	Note
0.850	1.87 ± 0.35	along Y

Linear electrooptic coefficients measured at low frequencies (well below the acoustic resonances of $KNbO_3$ crystal, i.e., for the "free" crystal) at room temperature [20]

λ [μm]	r_{13}^{T} [pm/V]	r_{23}^{T} [pm/V]	r_{33}^{T} [pm/V]	r_{42}^{T}[pm/V]	r_{51}^{T} [pm/V]
0.6328	$+28 \pm 2$	$+1.3 \pm 0.5$	64 ± 5	380 ± 50	105 ± 13

Linear electrooptic coefficients measured at high frequencies (well above the acoustic resonances of $KNbO_3$ crystal, i.e., for the "clamped" crystal) at room temperature [20]

λ [μm]	R_{13}^{S} [pm/V]	r_{23}^{S} [pm/V]	r_{33}^{S} [pm/V]	r_{42}^{S} [pm/V]	r_{51}^{S} [pm/V]
0.6328	10 ± 2	2 ± 1	25 ± 8	270 ± 40	23 ± 3

Coercive field value: 0.5 kV/mm [21]; 0.55 kV/mm [6]
Expressions for the effective second-order nonlinear coefficient in principal planes of potassium niobate crystal (Kleinman symmetry conditions are not valid) [22]:

XY plane

$d_{eeo} = d_{32} \sin^2 \phi + d_{31} \cos^2 \phi$

YZ plane

$d_{ooe} = d_{32} \sin \theta$

XZ plane, $\theta < V_z$

$d_{oeo} = d_{eoo} = d_{15} \sin \theta$

XZ plane, $\theta > V_z$

$d_{ooe} = d_{31} \sin \theta$

Expressions for the effective second-order nonlinear coefficient in principal planes of potassium niobate crystal (Kleinman symmetry conditions are valid, $d_{15} = d_{31}$ and $d_{24} = d_{32}$) [22]:

XY plane

$d_{eeo} = d_{32} \sin^2 \phi + d_{31} \cos^2 \phi$

YZ plane

$d_{ooe} = d_{32} \sin \theta$

XZ plane, $\theta < V_z$

$d_{oeo} = d_{eoo} = d_{31} \sin \theta$

XZ plane, $\theta > V_z$

$d_{ooe} = d_{31} \sin \theta$

Effective second-order nonlinear coefficient for three-wave interactions in the arbitrary direction of $KNbO_3$ crystal is given in [22].

The signs of $KNbO_3$ second-order nonlinear coefficients are all negative [10], [23].

Absolute values of second-order nonlinear coefficients [24]:

$|d_{32}(0.852\,\mu m)| = 11.0 \pm 0.6\,pm/V$

$|d_{33}(0.852\,\mu m)| = 22.3 \pm 1.1\,pm/V$

$|d_{24}(1.064\,\mu m)| = 12.5 \pm 0.6\,pm/V$

$|d_{32}(1.064\,\mu m)| = 10.8 \pm 0.6\,pm/V$

$|d_{33}(1.064\,\mu m)| = 19.6 \pm 1.0\,pm/V$

$|d_{32}(1.313\,\mu m)| = 9.2 \pm 0.5\,pm/V$

$|d_{33}(1.313\,\mu m)| = 16.1 \pm 0.8\,pm/V$

Relative values of second-order nonlinear coefficients:

$|d_{15}(1.064\,\mu m)| = (41.2 \pm 0.8) \times d_{11}(SiO_2) = 12.4 \pm 0.2\,pm/V$ [16], [25]

$|d_{15}(1.064\,\mu m)| = 9.2 \pm 0.2\,pm/V$ [26]

$|d_{24}(1.064\,\mu m)| = (42.8 \pm 0.8) \times d_{11}(SiO_2) = 12.8 \pm 0.2\,pm/V$ [16], [25]

$|d_{24}(1.064\,\mu m)| = 13.0 \pm 0.4\,pm/V$ [26]

$|d_{31}(1.064\,\mu m)| = (39.5 \pm 0.6) \times d_{11}(SiO_2) = 11.9 \pm 0.2\,pm/V$ [16], [25]

$|d_{31}(1.064\,\mu m)| = 8.9 \pm 0.4\,pm/V$ [26]

$|d_{32}(1.064\,\mu m)| = (45.7 \pm 0.6) \times d_{11}(SiO_2) = 13.7 \pm 0.2\,pm/V$ [16], [25]

$|d_{32}(1.064\,\mu m)| = 12.4 \pm 0.3\,pm/V$ [26]

$|d_{33}(1.064\,\mu m)| = (68.5 \pm 0.6) \times d_{11}(SiO_2) = 20.6 \pm 0.2\,pm/V$ [16], [25]

$|d_{33}(1.064\,\mu m)| = 21.9 \pm 0.5\,pm/V$ [26]

Experimental values of phase-matching angle ($T = 293$ K)

Interacting wavelengths [μm]	ϕ_{exp} [deg]	θ_{exp} [deg]	Ref.
XY plane, $\theta = 90°$			
SHG, $e + e \Rightarrow o$			
0.946 ⇒ 0.473	≈30		[27]
4.7599 ⇒ 2.37995	69.9		[11]
YZ plane, $\phi = 90°$			
SHG, $o + o \Rightarrow e$			
0.86 ⇒ 0.43		83.5	[28]
0.89 ⇒ 0.445		70.7	[28]
0.92 ⇒ 0.46		64	[28]
0.94 ⇒ 0.47		60.5	[28]
1.0642 ⇒ 0.5321		46.4	[11]
		≈47	[1]
1.3188 ⇒ 0.6594		30.6	[11]
1.3382 ⇒ 0.6691		29.7	[15]
3.5303 ⇒ 1.76515		37.3	[11]
4.7291 ⇒ 2.36455		77.3	[11]
SFG, $o + o \Rightarrow e$			
1.3188 + 0.6594 ⇒ 0.4396		62.3	[11]
1.3188 + 1.0642 ⇒ 0.5889		37.7	[11]
4.7762 + 3.1841 ⇒ 1.9105		46.6	[11]
5.2955 + 3.5303 ⇒ 2.1182		59.5	[11]
XZ plane, $\phi = 0°, \theta > V_z$			
SHG, $o + o \Rightarrow e$			
1.0642 ⇒ 0.5321		70.4	[4]
		71	[1], [12], [16]
		71.4	[11]
		71.5	[29]
1.3188 ⇒ 0.6594		56.8	[11]
1.3382 ⇒ 0.6691		56.2	[15]
3.5303 ⇒ 1.76515		58.8	[11]
SFG, $o + o \Rightarrow e$			
1.3188 + 1.0642 ⇒ 0.5889		62.6	[11]
5.2955 + 3.5303 ⇒ 2.1182		86.1	[11]

Experimental values of NCPM temperature

Interacting wavelengths [μm]	T [°C]	Ref.
along *X* axis		
SHG, type I		
0.972 ⇒ 0.486	−20	[30]
0.982 ⇒ 0.491	18.7	[31]
	20	[23]

Interacting wavelengths [μm]	T [°C]	Ref.
0.986 ⇒ 0.493	20	[32]
0.988 ⇒ 0.494	20	[12]
1.047 ⇒ 0.5235	162	[33]
1.0642 ⇒ 0.5321	178	[34]
	181 ± 2	[1]
	182	[4]
	184 ± 2	[35]
	188	[36]
along Y axis		
SHG, type I		
0.8385 ⇒ 0.41925	−34.2	[37]
0.8406 ⇒ 0.4203	−28.3	[38]
0.842 ⇒ 0.421	−22.8	[39]
0.846 ⇒ 0.423	−11.5	[13]
0.856 ⇒ 0.428	15	[40]
0.857 ⇒ 0.4285	20	[41]
0.8593 ⇒ 0.42965	20	[37]
0.86 ⇒ 0.43	22	[32]
0.8615 ⇒ 0.43075	30	[42]
0.862 ⇒ 0.431	34	[43]
0.879 ⇒ 0.4395	70	[43]
0.9289 ⇒ 0.46445	158	[37]
0.95 ⇒ 0.475	180	[32]
SFG, type I		
0.6764 + 1.0642 ⇒ 0.41355	−4	[44]
0.6943 + 1.0642 ⇒ 0.42017	27.2	[44]

Experimental values of internal angular bandwidth [23]

Interacting wavelengths [μm]	T [°C]	θ_{pm} [deg]	$\Delta\theta^{int}$ [deg]	$\Delta\phi^{int}$ [deg]
XZ plane, $\phi = 0°$				
SHG, $o + o \Rightarrow e$				
1.0642 ⇒ 0.5321	20	71	0.013–0.014	
along Y axis				
SHG, type I				
0.857 ⇒ 0.4285	20	90	0.659	1.117

Experimental values of temperature bandwidth

Interacting wavelengths [μm]	T [°C]	θ_{pm} [deg]	ΔT [°C]	Ref.
along X axis				
SHG, type I				
0.982 ⇒ 0.491	18.7	90	0.95	[31]
1.0642 ⇒ 0.5321	181	90	0.27–0.32	[1]

Interacting wavelengths [μm]	T [°C]	θ_{pm} [deg]	ΔT [°C]	Ref.
	182	90	0.28	[4]
	184	90	0.28–0.29	[35]
	188	90	0.34	[36]
along Y axis				
SHG, type I				
$0.8385 \Rightarrow 0.41925$	−34.2	90	0.27	[37]
$0.842 \Rightarrow 0.421$	−22.8	90	0.30	[39]
$0.855 \Rightarrow 0.4275$	26.4 (?)	90	0.265	[12]
$0.92 \Rightarrow 0.46$	163.5 (?)	90	0.285	[12]
SFG, type I				
$0.6764 + 1.0642 \Rightarrow 0.41355$	−4	90	0.35	[44]

Experimental values of temperature bandwidth at $T = 295$ K [15]

Interacting wavelengths [μm]	θ_{exp} [deg]	ΔT [°C]
YZ plane, $\phi = 90°$		
SHG, $o + o \Rightarrow e$		
$1.0642 \Rightarrow 0.5321$	46.4	0.39
$1.3382 \Rightarrow 0.6691$	29.7	0.59
$3.5303 \Rightarrow 1.76515$	37.1	2.3
SFG, $o + o \Rightarrow e$		
$5.2955 + 3.5303 \Rightarrow 2.1182$	59.5	2.4
XZ plane, $\phi = 0°$, $\theta > V_z$		
SHG, $o + o \Rightarrow e$		
$1.0642 \Rightarrow 0.5321$	71.4	0.77
$1.3382 \Rightarrow 0.6691$	56.2	2.2
$3.5303 \Rightarrow 1.76515$	58.9	10.1

Temperature tuning of noncritical SHG [23]:

along X axis: $\lambda_1 = 0.97604 + 2.53 \times 10^{-4}\, T + 1.146 \times 10^{-6}\, T^2$

along Y axis: $\lambda_1 = 0.85040 + 2.94 \times 10^{-4}\, T + 1.234 \times 10^{-6}\, T^2$

where λ_1 in μm, T in °C.

Temperature variation of birefringence for noncritical SHG process [12]:

along X axis (1.0642 μm ⇒ 0.5321 μm):

$$\frac{d\,[n_Z(2\omega) - n_Y(\omega)]}{dT} = 1.10 \times 10^{-4}\,\mathrm{K}^{-1}$$

along Y axis (0.92 μm ⇒ 0.46 μm):

$$\frac{d\,[n_Z(2\omega) - n_X(\omega)]}{dT} = 1.43 \times 10^{-4}\,\mathrm{K}^{-1}$$

Laser-induced surface-damage threshold

λ [μm]	τ_p [ns]	I_{thr} [GW/cm^2]	Ref.	Note
0.527	0.5	8.8–9.4	[45]	along b axis, $\mathbf{E}\parallel c$
		12–15	[45]	along b axis, $\mathbf{E}\perp c$
0.5321	25	0.15–0.18	[35]	
	10	0.055	[34]	
0.8	0.0002	>200	[46]	1 kHz
1.047	11	>0.03	[33]	4 kHz, 2000 hours
1.054	0.7	11	[45]	along a axis, $\mathbf{E}\perp c$
		18	[45]	along b axis, $\mathbf{E}\perp c$
		37	[45]	along b axis, $\mathbf{E}\parallel c$
1.0642	25	0.15–0.18	[35]	
	0.1	>100	[23]	

About the crystal

A decade ago, potassium niobate was widely used for the frequency doubling of CW diode laser radiation. Nowadays, for this purpose, the periodically poled nonlinear materials, such as PPLN and PPKTP, are mainly employed. Recently, the fabrication of periodically poled KN was also reported [6], [21].

References

[1] Y. Uematsu: Nonlinear optical properties of $KNbO_3$ single crystals in the orthorhombic phase. Jpn. J. Appl. Phys. **13(9)**, 1362–1368 (1974).

[2] B.H.T. Chai: Optical Crystals. In: *CRC Handbook of Laser Science and Technology, Supplement 2: Optical Materials*, ed. by M.J. Weber (CRC Press, Boca Raton, 1995), pp. 3–65.

[3] B. Zysset, I. Biaggio, P. Günter: Refractive indices of orthorhombic $KNbO_3$. I. Dispersion and temperature dependence. J. Opt. Soc. Am. B **9(3)**, 380–386 (1992).

[4] Y. Uematsu, T. Fukuda: Nonlinear optical properties of $KNbO_3$ single crystals. Jpn. J. Appl. Phys. **10(4)**, 507 (1971).

[5] *Chemist's Handbook, Vol. I*, ed. by B.P. Nikolskii (Goskhimizdat, Leningrad, 1962) [In Russian].

[6] J.H. Kim, C.S. Yoon: Domain switching characteristics and fabrication of periodically poled potassium niobate for second-harmonic generation. Appl. Phys. Lett. **81(18)**, 3332–3334 (2002).

[7] M.D. Ewbank, M.J. Rosker, G.L. Bennett: Frequency tuning a mid-infrared optical parametric oscillator by the electro-optic effect. J. Opt. Soc. Am. B **14(3)**, 666–671 (1997).

[8] L.E. Busse, L. Goldberg, M.R. Surette, G. Mizell: Absorption losses in MgO-doped and undoped potassium niobate. J. Appl. Phys. **75(2)**, 1102–1110 (1994).

[9] Y. Uematsu, T. Fukuda: Characteristics and performance of $KNbO_3$-Nd:YAG intracavity second harmonic generation. Jpn. J. Appl. Phys. **12(6)**, 841–844 (1973).

[10] W.R. Bosenberg, R.H. Jarman: Type-II phase-matched $KNbO_3$ optical parametric oscillator. Opt. Lett. **18(16)**, 1323–1325 (1993).

[11] N. Umemura, K. Yoshida, K. Kato: Phase-matching properties of $KNbO_3$ in the mid-infrared. Appl. Opt. **38(6)**, 991–994 (1999).

[12] K. Kato: High-efficiency second-harmonic generation at 4250–4680 Å in $KNbO_3$. IEEE J. Quant. Electr. **QE-15(6)**, 410–411 (1979).
[13] A.D. Ludlow, H.M. Nelson, S.D. Bergeson: Two-photon absorption in potassium niobate. J. Opt. Soc. Am. B **18(12)**, 1813–1820 (2001).
[14] J.J.E. Reid: Resonantly enhanced, frequency doubling of an 820 nm GaAlAs diode laser in a potassium lithium niobate crystal. Appl. Phys. Lett. **62(1)**, 19–21 (1993).
[15] N. Umemura, K. Yoshida, K. Kato: Thermo-optic dispersion formula of $KNbO_3$ for mid-infrared OPO. Proc. SPIE **3889**, 472–480 (2000).
[16] J.-C. Baumert, J. Hoffnagle, P. Günter: Nonlinear optical effects in $KNbO_3$ crystals at $Al_xGa_{1-x}As$, dye, ruby and Nd:YAG laser wavelengths. Proc. SPIE **492**, 374–385 (1984).
[17] G. Ghosh: Dispersion of thermo-optic coefficients in a potassium niobate nonlinear crystal. Appl. Phys. Lett. **65(26)**, 3311–3313 (1994).
[18] D.H. Jundt, P. Günter, B. Zysset: A temperature-dependent dispersion equation for $KNbO_3$. Nonl. Opt. **4(4)**, 341–345 (1993).
[19] M. Sheik-Bahae, M. Ebrahimzadeh: Measurements of nonlinear refraction in the second-order $\chi^{(2)}$ materials $KTiOPO_4$, $KNbO_3$, β-BaB_2O_4, and LiB_3O_5. Opt. Commun. **142(4–6)**, 294–298 (1997).
[20] I.P. Kaminow: Tables of Linear Electrooptic Coefficients. In: *CRC Handbook of Laser Science and Technology, Vol. III, Optical Materials: Part 2*, ed. by M.J. Weber (CRC Press, Boca Raton, 1986), pp. 253–278.
[21] J.-P. Meyn, M.E. Klein, D. Woll, R. Wallenstein, D. Rytz: Periodically poled potassium niobate for second-harmonic generation at 463 nm. Opt. Lett. **24(16)**, 1154–1156 (1999).
[22] V.G. Dmitriev, D.N. Nikogosyan: Effective nonlinearity coefficients for three-wave interactions in biaxial crystals of $mm2$ point group symmetry. Opt. Commun. **95(1–3)**, 173–182 (1993).
[23] I. Biaggio, P. Kerkoc, L.-S. Wu, P. Günter, B. Zysset: Refractive indices of orthorhombic $KNbO_3$. II. Phase-matching configurations for NLO interactions. J. Opt. Soc. Am. B **9(4)**, 507–517 (1992).
[24] I. Shoji, T. Kondo, A. Kitamoto, M. Shirane, R. Ito: Absolute scale of second-order nonlinear-optical coefficients. J. Opt. Soc. Am. B **14(9)**, 2268–2294 (1997).
[25] D.A. Roberts: Simplified characterization of uniaxial and biaxial nonlinear optical crystals: a plea for standardization of nomenclature and conventions. IEEE J. Quant. Electr. **28(10)**, 2057–2074 (1992).
[26] M.V. Pack, D.J. Armstrong, A.V. Smith: Measurement of the $\chi^{(2)}$ tensor of the potassium niobate crystal. J. Opt. Soc. Am. **20(10)**, 2109–2116 (2003).
[27] W.P. Risk, R. Pon, W. Lenth: Diode laser pumped blue-light source at 473 nm using intracavity frequency doubling of a 946 nm Nd:YAG laser. Appl. Phys. Lett. **54(17)**, 1625–1627 (1989).
[28] Y. Lu, Q. Zhao, Y. Li, H. He, Q. Zou, Z. Lu, Z. Geng: Second-harmonic generation in $KNbO_3$ crystals. Opt. Eng. **32(4)**, 713–716 (1993).
[29] S. Haidar, H. Ito: Periodically poled lithium niobate optical parametric oscillator pumped at 0.532 μm and use of its output to produce tunable 4.6–8.3 μm in $AgGaS_2$ crystal. Opt. Commun. **202(1–3)**, 227–231 (2002).
[30] C. Zimmermann, T.W. Hansch, R. Byer, S. O'Brien, D. Welch: Second harmonic generation at 972 nm using a distributed Bragg reflection semiconductor laser. Appl. Phys. Lett. **61(23)**, 2741–2743 (1992).
[31] D. Fluck, T. Pliska, P. Günter: Compact 10 mW all-solid-state 491 nm laser based on frequency doubling a master oscillator power amplifier laser diode. Opt. Commun. **123(4–6)**, 624–628 (1996).

[32] P. Günter: Near-infrared noncritically phase-matched second-harmonic generation in $KNbO_3$. Appl. Phys. Lett. **34(10)**, 650–652 (1979).
[33] W. Seelert, P. Kortz, D. Rytz, B. Zysset, D. Ellgehausen, G. Mizell: Second-harmonic generation and degradation in critically phase-matched $KNbO_3$ with a diode-pumped Q-switched Nd:YLF laser. Opt. Lett. **17(20)**, 1432–1434 (1992).
[34] K. Kato: High-efficiency high-power parametric oscillation in $KNbO_3$. IEEE J. Quant. Electr. **QE-18(4)**, 451–452 (1982).
[35] V.A. Dyakov, V.I. Pryalkin, A.I. Kholodnykh: Potassium niobate optical parametric oscillator pumped by the second harmonic of a garnet laser. Kvant. Elektron. **8(4)**, 715–721 (1981) [In Russian, English trans.: Sov. J. Quantum Electron. **11(4)**, 433–436 (1981)].
[36] I. Biaggio, H. Looser, P. Günter: Intracavity frequency doubling of a diode pumped Nd:YAG laser using a $KNbO_3$ crystal. Ferroelectrics **94**, 157–161 (1989).
[37] J.-C. Baumert, P. Günter, H. Melchior: High efficiency second-harmonic generation in $KNbO_3$ crystals. Opt. Commun. **48(3)**, 215–220 (1983).
[38] A. Hemmerich, D.H. McIntyre, C. Zimmermann, T.W. Hansch: Second-harmonic generation and optical stabilization of a diode laser in an external ring resonator. Opt. Lett. **15(7)**, 372–374 (1990).
[39] M.K. Chun, L. Goldberg, J.F. Weller: Second-harmonic generation at 421 nm using injection-locked GaAlAs laser array and $KNbO_3$. Appl. Phys. Lett. **53(13)**, 1170–1171 (1988).
[40] W.J. Kozlovsky, W. Lenth, E.E. Latta, A. Moser, G.L. Bona: Generation of 41 mW of blue radiation by frequency doubling of a GaAlAs diode laser. Appl. Phys. Lett. **56(23)**, 2291–2292 (1990).
[41] J.-C. Baumert, J. Hoffnagle, P. Günter: High-efficiency intracavity doubling of a Styril-9 dye laser radiation with $KNbO_3$ crystals. Appl. Opt. **24(9)**, 1299–1301 (1985).
[42] P. Günter, P.M. Asbeck, S.K. Kurtz: Second-harmonic generation with $Ga_{1-x}Al_xAs$ lasers and $KNbO_3$ crystals. Appl. Phys. Lett. **35(6)**, 461–463 (1979).
[43] L. Goldberg, L. Busse, D. Mehuys: Blue light generation by frequency doubling of AlGaAs broad area amplifier emission. Appl. Phys. Lett. **60(9)**, 1037–1039 (1992).
[44] J.-C. Baumert, P. Günter: Noncritically phase-matched sum frequency generation and image up-conversion in $KNbO_3$ crystals. Appl. Phys. Lett. **50(10)**, 554–556 (1987).
[45] U. Ellenberger, R. Weber, J.E. Balmer, B. Zysset, D. Ellgehausen, G.J. Mizell: Pulsed optical damage threshold of potassium niobate. Appl. Opt. **31(36)**, 7563–7569 (1992).

5

Periodically Poled Crystals and "Wafer" Materials

This chapter comprises the nonlinear optical crystals used for quasi-phase matching, besides the previously discussed LN, KTP, MgLN, KTA, and KN. These include lithium tantalate (LT), rubidium titanyl arsenate (RTA), barium titanate, magnesium barium fluoride, and gallium arsenide.

5.1 $LiTaO_3$, Lithium Tantalate (LT)

Negative uniaxial crystal: $n_o > n_e$
Molecular mass: 235.886
Specific gravity: 7.43 g/cm^3 [1]; 7.454 g/cm^3 [2]
Point group: $3m$
Lattice constants:
$a = 5.143$ Å [3]; 5.1543 Å [4]
$c = 13.756$ Å [3]; 13.7835 Å [4]
Mohs hardness: 6 [1]; 6.7 [2]
Vickers hardness: 766 [2]

Solubility in 100 g H_2O [3]

T [K]	s [g]
273	0.0012
298	0.0025
323	0.0054
248	0.0090
373	0.0120

Melting point: 1923 K [2]
Curie temperature: 874–880 K [4]; 874 K (congruent LT, [Li]/[Ta] = 0.942) [5]; 877 K (congruent LT, [Li]/[Ta] = 0.942) [6], [7]; 958 K (stoichiometric LT) [5]; 960 K (stoichiometric LT) [6]; 961 K (stoichiometric LT) [7]; 963 K (stoichiometric LT) [8]

Linear thermal expansion coefficient [9]

T [K]	$\alpha_t \times 10^6$ [K^{-1}], $\parallel c$	$\alpha_t \times 10^6$ [K^{-1}], $\perp c$
300	4.2	12.0

Mean value of linear thermal expansion coefficient [2]

T [K]	$\alpha_t \times 10^6$ [K^{-1}], $\parallel c$	$\alpha_t \times 10^6$ [K^{-1}], $\perp c$
273–773		15.4–16.1

Thermal expansion $\parallel c$ for temperature range 298 K $< T <$ 773 K [4]:

$$L(T) = L\,(T_0)\left\{1 + \alpha(T - 298) + \beta(T - 298)^2\right\}$$

where T in K, $T_0 = 298$ K, $\alpha = 2.2 \times 10^{-6}$ K^{-1}, $\beta = -5.9 \times 10^{-9}$ K^{-2}.
Thermal expansion $\perp c$ for temperature range 298 K $< T <$ 773 K [4]:

$$L(T) = L\,(T_0)\left\{1 + \alpha(T - 298) + \beta(T - 298)^2\right\}$$

where T in K, $T_0 = 298$ K, $\alpha = 16.2 \times 10^{-6}$ K^{-1}, $\beta = 5.9 \times 10^{-9}$ K^{-2}.

Specific heat capacity c_p at $P = 0.101325$ MPa [2]

T [K]	c_p [J/kgK]
298	426

Thermal conductivity coefficient [10]

T [K]	κ [W/mK]
300	5

Band-gap energy at room temperature (direct transition): $E_g = 4.9$ eV [11]
Band-gap energy at room temperature (indirect transition): $E_g = 4.1$ eV [11]
UV transmittance cutoff for stoichiometric LT is at 0.26 μm [6]
UV transmittance cutoff at 1 cm^{-1} level is at 0.29 μm [12]
Transparency range at " 0" transmittance level: 0.28–5.5 μm [8]

Linear absorption coefficient α

λ [μm]	α [cm^{-1}]	Ref.	Note
0.325	1.7	[13]	
0.5145	0.005–0.03	[12]	
1.064	0.001–0.003	[12]	
	0.0015	[10]	stoichiometric LT

Experimental values of refractive indices [14]

λ [μm]	n_o	n_e	λ [μm]	n_o	n_e
0.45	2.2420	2.2468	2.0	2.1066	2.1115
0.50	2.2160	2.2205	2.2	2.1009	2.1053
0.60	2.1834	2.1878	2.4	2.0951	2.0993
0.70	2.1652	2.1696	2.6	2.0891	2.0936
0.80	2.1538	2.1578	2.8	2.0825	2.0871
0.90	2.1454	2.1493	3.0	2.0755	2.0799
1.00	2.1391	2.1432	3.2	2.0680	2.0727
1.20	2.1305	2.1341	3.4	2.0601	2.0649
1.40	2.1236	2.1273	3.6	2.0513	2.0561
1.60	2.1174	2.1213	3.8	2.0424	2.0473
1.80	2.1120	2.1170	4.0	2.0335	2.0377

Sellmeier equations for stoichiometric LT (λ in μm, $0.44\,\mu\text{m} < \lambda < 1.05\,\mu\text{m}$, $T = 293\,\text{K}$) [7]:

$$n_o^2 = 4.5281 + \frac{0.079841}{\lambda^2 - 0.047857} - 0.032690\,\lambda^2$$

$$n_e^2 = 4.5096 + \frac{0.082712}{\lambda^2 - 0.041306} - 0.031587\,\lambda^2$$

n_o for congruent LT ([Li]/[Ta] = 0.942) is almost the same as for stoichiometric LT, whereas n_e for congruent LT is larger than that of stoichiometric LT [7].
Other Sellmeier equations are given in [15], [16].
Temperature-dependent dispersion relation for extraordinary refractive index in stoichiometric LT (λ in μm, T in K, $0.39\,\mu\text{m} < \lambda < 4.1\,\mu\text{m}$, $303\,\text{K} < T < 473\,\text{K}$) [8]:

$$n_e^2(\lambda, T) = 4.502483 + \frac{0.007294 + 3.483933 \times 10^{-8}\,T^2}{\lambda^2 - \left[0.185087 + 1.607839 \times 10^{-8}\,T^2\right]^2} + \frac{0.073423}{\lambda^2 - 0.199595^2} + \frac{0.001}{\lambda^2 - 7.99724^2} - 0.02357\,\lambda^2$$

Similar dispersion relation for extraordinary refractive index in stoichiometric LT with slightly different coefficients is given by the same authors in [17].
Temperature-dependent dispersion relation for extraordinary refractive index in congruent LT (λ in μm, T in K, $0.39\,\mu\text{m} < \lambda < 4.1\,\mu\text{m}$, $303\,\text{K} < T < 473\,\text{K}$) [17]:

$$n_e^2(\lambda, T) = 4.514261 + \frac{0.011901 + 1.82194 \times 10^{-8}\,T^2}{\lambda^2 - \left[0.110744 + 1.5662 \times 10^{-8}\,T^2\right]^2} + \frac{0.076144}{\lambda^2 - 0.195596^2} - 0.02323\,\lambda^2$$

Other temperature-dependent dispersion relation for extraordinary refractive index is given in [13].

Nonlinear refractive index γ [18]

λ [μm]	$\gamma \times 10^{15}$ [cm^2/W]	Note
0.8	3.0 ± 0.6	*e*-wave
	1.7 ± 0.3	*o*-wave

Linear electrooptic coefficients measured at low frequencies (well below the acoustic resonances of LT crystal, i.e., for the "free" crystal) at room temperature

λ [μm]	r_{13}^{T} [pm/V]	r_{22}^{T} [pm/V]	r_{33}^{T} [pm/V]	r_{51}^{T} [pm/V]	Ref.
0.6328	$+8.4 \pm 0.9$	≈ 0	$+30.5 \pm 0.9$		[19]
		$+0.1 \pm 0.01$			[20]
3.3913	+4.5	+0.3	+27	+15	[21]

Linear electrooptic coefficients measured at high frequencies (well above the acoustic resonances of LT crystal, i.e., for the " clamped" crystal) at room temperature

λ [μm]	r_{13}^{S} [pm/V]	r_{22}^{S} [pm/V]	r_{33}^{S} [pm/V]	r_{51}^{S} [pm/V]	Ref.
0.6328	6.2	≈ 0	28.5	8.4	[22]
	7.0		30.3		[23]
		1.0 ± 0.1			[20]
1.1523	5.2	≈ 0	26.7	8.9	[22]
3.3913	4.4		25.2	7.0	[22]

Coercive field value:
1.7 kV/mm (stoichiometric LT) [17]; 1.7–4.5 kV/mm (stoichiometric LT) [8]
21 kV/mm (congruent LT) [24]; ≈22 kV/mm (congruent LT) [5]
Absolute values of second-order nonlinear coefficients for lithium tantalate [25]:

$|\, d_{33}(0.852\,\mu\text{m})\, | = 15.1\,\text{pm/V}$
$|\, d_{31}(1.064\,\mu\text{m})\, | = 0.85\,\text{pm/V}$
$|\, d_{33}(1.064\,\mu\text{m})\, | = 13.8\,\text{pm/V}$
$|\, d_{33}(1.313\,\mu\text{m})\, | = 10.7\,\text{pm/V}$

Laser-induced surface-damage threshold [26]

λ [μm]	τ_p [ns]	I_{thr} [GW/cm^2]	Note
1.06	30	0.14	25 pulses
		0.22	10 pulses
		0.47	1 pulse

About the crystal

Lithium tantalate is very similar to lithium niobate; however, its birefringence is lower, and, therefore, it is not possible to realize normal birefringent phase-matching in this crystal. However, this crystal became very popular with the invention of quasi-phase matching. In addition to a very low coercive field value (1.7 kV/mm for stoichiometric

LT and less than 1.5 kV/mm for stoichiometric LT with 1 mol% MgO), this crystal possesses higher UV transmittance, which allows realization of different quasi-phase-matched processes in periodically poled LT (PPLT) with second harmonic or sum frequency, lying in the UV range. For example, in [27] and [13], SHG at 340 and 325 nm was produced, respectively. In [28], via two-stage third harmonic generation of Nd:YVO_4 laser radiation in dual-periodic PPLT, sum-frequency at 355 nm was obtained. Very recently, using aperiodically poled LT (APPLT) and a $NdYVO_4$ laser, generating at 1064 and 1342 nm, three nonlinear processes (two SHG and one SFG) were quasi-phase-matched [29]. This resulted in simultaneous generation of three wavelengths, so-called traffic signal lights, in green (532 nm), yellow (593 nm), and red (671 nm) spectral regions. It should be noted also that no photorefractive damage was observed in LT at temperatures above 170 °C [13].

References

[1] B.H.T. Chai: Optical Crystals. In: *CRC Handbook of Laser Science and Technology, Supplement 2: Optical Materials*, ed. by M.J. Weber (CRC Press, Boca Raton, 1995), pp. 3–65.

[2] A.A. Blistanov, V.S. Bondarenko, N.V. Perelomova, F.N. Strizhevskaya, V.V. Tchkalova, M.P. Shaskolskaya: *Acoustic Crystals* (Nauka, Moscow, 1982) [In Russian].

[3] Y.S. Kuzminov: *Lithium Niobate and Lithium Tantalate. Materials for Nonlinear Optics* (Nauka, Moscow, 1975).

[4] Y.S. Kim, R.T. Smith: Thermal expansion of lithium tantalate and lithium niobate crystals. J. Appl. Phys. **40(11)**, 4637–4641 (1969).

[5] T. Hatanaka, K. Nakamura, T. Taniuchi, H. Ito, Y. Furukawa, K. Kitamara: Quasi-phase-matched optical parametric oscillation with periodically poled stoichiometric $LiTaO_3$. Opt. Lett. **25(9)**, 651–653 (2000).

[6] G. Ravi, R. Jayavel, S. Takekawa, M. Nakamura, K. Kitamura: Effect of niobium substitution in stoichiometric lithium tantalate (SLT) single crystals. J. Cryst. Growth **250(1–2)**, 146–151 (2003).

[7] M. Nakamura, S. Higuchi, S. Takekawa, K. Terabe, Y. Furukawa, K. Kitamura: Refractive indices in undoped and MgO-doped near-stoichiometric $LiTaO_3$ crystals. Jpn. J. Appl. Phys. **41(4B)**, L465–L467 (2002).

[8] A. Bruner, D. Eger, M.B. Oron, P. Blau, M. Katz, S. Ruschin: Temperature-dependent Sellmeier equation for the refractive index of stoichiometric lithium tantalate. Opt. Lett. **28(3)**, 194–196 (2003).

[9] *Physical Quantities. Handbook*, ed. by I.S. Grigoriev, E.Z. Meilikhov (Energoatomizdat, Moscow, 1991) [In Russian].

[10] P. Blau, S. Pearl, A. Englander, A. Bruner, D. Eger: Average power effects in periodically poled crystals. Proc. SPIE **4972**, 34–41 (2003).

[11] S. Kase, K. Ohi: Optical absorption and interband Faraday rotation in $LiTaO_3$ and $LiNbO_3$. Ferroelectrics **8(1–2)**, 419–420 (1974).

[12] A.L. Alexandrovski, G. Foulon, L.E. Myers, R.K. Route, M.M. Fejer: UV and visible absorption in $LiTaO_3$. Proc. SPIE **3610**, 44–51 (1999).

[13] J.-P. Meyn, M.M. Fejer: Tunable ultraviolet radiation by second-harmonic generation in periodically poled lithium tantalate. Opt. Lett. **22(16)**, 1214–1216 (1997).

[14] W.L. Bond: Measurement of the refractive indices of several crystals. J. Appl. Phys. **36(5)**, 1674–1677 (1965).

[15] S. Matsumoto, E.J. Lim, H.M. Hertz, M.M. Fejer: Quasi phase-matched second harmonic generation of blue light in electrically periodically-poled lithium tantalate waveguides. Electron. Lett. **27(22)**, 2040–2042 (1991).
[16] K.S. Abedin, H. Ito: Temperature-dependent dispersion relation of ferroelectric lithium tantalate. J. Appl. Phys. **80(11)**, 6561–6563 (1996).
[17] A. Bruner, D. Eger, M. Oron, P. Blau, M. Katz, S. Ruschin: Refractive index dispersion measurements of congruent and stoichiometric $LiTaO_3$. Proc. SPIE **4628**, 66–73 (2002).
[18] S. Ashihara, J. Nishina, T. Shimura, K. Kuroda, T. Sugita, K. Mizuuchi, K. Yamamoto: Nonlinear refraction of femtosecond pulses due to quadratic and cubic nonlinearities in periodically poled lithium tantalate. Opt. Commun. **222(1–6)**, 421–427 (2003).
[19] K. Onuki, N. Uchida, T. Saku: Interferometric method for measuring electro-optic coefficients in crystals. J. Opt. Soc. Am. **62(9)**, 1030–1032 (1972).
[20] M. Abarkan, J.P. Salvestrini, M.D. Fontana, M. Aillerie: Frequency and wavelength dependencies of electro-optic coefficients in inorganic crystals. Appl. Phys. B **76(7)**, 765–769 (2003).
[21] A. Yariv, P. Yeh: *Optical Waves in Crystals* (John Wiley & Sons, New York, 1984).
[22] I.P. Kaminow: Tables of Linear Electrooptic Coefficients. In: *CRC Handbook of Laser Science and Technology, Vol. III, Optical Materials: Part 2*, ed. by M.J. Weber (CRC Press, Boca Raton, 1986), pp. 253–278.
[23] P.V. Lenzo, E.H. Turner, E.G. Spencer, A.A. Ballman: Electrooptic coefficients and elastic-wave propagation in single-domain ferroelectric lithium tantalate. Appl. Phys. Lett. **8(4)**, 81–82 (1966).
[24] J.-P. Meyn, C. Laue, R. Knappe, R. Wallenstein, M.M. Fejer: Fabrication of periodically poled lithium tantalate for UV generation with diode lasers. Appl. Phys. B. **73(2)**, 111–114 (2001).
[25] I. Shoji, T. Kondo, A. Kitamoto, M. Shirane, R. Ito: Absolute scale of second-order nonlinear-optical coefficients. J. Opt. Soc. Am. B **14(9)**, 2268–2294 (1997).
[26] G.M. Zverev, E.A. Levchuk, V.A. Pashkov, Y.D. Poryadin: Laser-radiation-induced damage to the surface of lithium niobate and tantalate single crystals. Kvant. Elektron. **No. 2**, 94–96 (1972) [In Russian, English trans.: Sov. J. Quantum Electron. **2(2)**, 167–169 (1972)].
[27] K. Mizuuchi, K. Yamamoto: Generation of 340-nm light by frequency doubling of a laser diode in bulk periodically poled $LiTaO_3$. Opt. Lett. **21(2)**, 107–109 (1996).
[28] Z.W. Liu, S.N. Zhu, Y.Y. Zhu, Y.Q. Qin, J.L. He, C. Zhang, H.T. Wang, N.B. Ming, X.Y. Liang, Z.Y. Xu: Quasi-CW ultraviolet generation in a dual-periodic $LiTaO_3$ superlattice by frequency tripling. Jpn. J. Appl. Phys. **40(12)**, 6841–6844 (2001).
[29] J.-L. He, J. Liao, H. Liu, J. Du, F. Xu, H.-T. Wang, S.N. Zhu, Y.Y. Zhu, N.B. Ming: Simultaneous CW red, yellow, and green light generation, "traffic signal lights", by frequency doubling and sum-frequency mixing in an aperiodically poled $LiTaO_3$. Appl. Phys. Lett. **83(2)**, 228–230 (2003).

5.2 $RbTiOAsO_4$, Rubidium Titanyl Arsenate (RTA)

Positive biaxial crystal: $2V_z = 39.2°$ at $\lambda = 0.532\,\mu m$
Molecular mass: 288.266
Specific gravity: 4.018 g/cm^3 [1]; 4.05 g/cm^3 [2]

Point group: *mm*2
Lattice constants:
$a = 13.2428$ Å [2]; 13.257 Å [3];
$b = 6.6685$ Å [2]; 6.6780 Å [3]
$c = 10.7642$ Å [2]; 10.765 Å [3]
Assignment of dielectric and crystallographic axes: $X, Y, Z \Rightarrow a, b, c$
Melting point: 1383 K [3]

Thermal conductivity coefficient [4]

T [K]	κ [W/mK]
300	1.6

Transparency range at "0" transmittance level: 0.35–5.3 μm [5]; 0.35–5.1 μm [2]; 0.38–5.1 μm [6]
UV transmission cutoff ($\alpha = 2\,\mathrm{cm}^{-1}$) is at 0.358 μm ($\mathbf{E}\|X$); 0.366 μm ($\mathbf{E}\|Y$); 0.371 μm ($\mathbf{E}\|Z$) [7]

Linear absorption coefficient α [7]

λ [μm]	α [cm^{-1}]	Note
0.473	0.012	$\mathbf{E}\|X$
	0.002	$\mathbf{E}\|Y$
	0.005	$\mathbf{E}\|Z$
0.532	0.015	$\mathbf{E}\|X$
	0.002	$\mathbf{E}\|Y$
	0.002	$\mathbf{E}\|Z$

Experimental values of refractive indices at $T = 293$ K

λ [μm]	n_X	n_Y	n_Z	Ref.
0.48613		1.8720	1.9643	[2]
0.5320	1.8476	1.8578	1.9444	[2]
0.54607	1.8444	1.8543	1.9397	[2]
0.58756	1.8364	1.8456	1.9279	[2]
0.6328	1.8294	1.8363	1.9185	[8]
0.65628	1.8267	1.8352	1.9142	[2]
1.06400	1.8041	1.8114	1.8846	[2]
			1.8808	[9]

Temperature derivatives of refractive index n_Z [4]

λ [μm]	$dn_Z/dT \times 10^6$ [K^{-1}]
1.064	2
1.5	0.3

Highly accurate Sellmeier equations (λ in μm, $T = 293$ K) [10]:

$$n_X^2 = 3.21992 + \frac{0.04763}{\lambda^2 - 0.04063} - 0.01035\,\lambda^2$$

$$n_Y^2 = 3.24185 + \frac{0.05056}{\lambda^2 - 0.04532} - 0.01062\,\lambda^2$$

$$n_Z^2 = 7.00229 + \frac{0.06787}{\lambda^2 - 0.05241} + \frac{917.9906}{\lambda^2 - 261.3629}$$

Other sets of dispersion relations are given in [5], [9], [11], [12], [13], [14].
Temperature derivative of refractive indices for RTA for $T = 293$ to 393 K and:
for spectral range $0.45\,\mu\text{m} < \lambda < 1.62\,\mu\text{m}$ (λ in μm) [10]:

$$\frac{dn_X}{dT} = \left(\frac{0.4287}{\lambda^3} - \frac{0.9181}{\lambda^2} + \frac{0.6685}{\lambda} + 1.9687\right) \times 10^{-5} K^{-1}$$

$$\frac{dn_Y}{dT} = \left(\frac{0.5138}{\lambda^3} - \frac{1.1054}{\lambda^2} + \frac{0.8035}{\lambda} + 1.9591\right) \times 10^{-5} K^{-1}$$

for spectral range $0.45\,\mu\text{m} < \lambda < 3.2\,\mu\text{m}$ (λ in μm) [10]:

$$\frac{dn_Z}{dT} = \left(\frac{1.5905}{\lambda^3} - \frac{4.2423}{\lambda^2} + \frac{4.2161}{\lambda} + 1.7355\right) \times 10^{-5} K^{-1}$$

Linear electrooptic coefficients measured at low frequencies (well below the acoustic resonances of RTA crystal, i.e., for the "free" crystal) at room temperature

λ [μm]	r_{13}^{T} [pm/V]	r_{23}^{T} [pm/V]	r_{33}^{T} [pm/V]	r_{51}^{T} [pm/V]	r_{42}^{T} [pm/V]	Ref.
0.6328	13.5 ± 1.4	17.5 ± 1.8	40.5 ± 4.1			[12]
	10.8 ± 1.0	17.3 ± 1.0	40.0 ± 1.5	12.3 ± 1.0	14.6 ± 1.0	[8]

Coercive field value: 1.76 kV/mm [15]
Expressions for the effective second-order nonlinear coefficient in principal planes of RTA crystal (Kleinman symmetry conditions are not valid) [16]:

XY plane

$$d_{\mathrm{eoe}} = d_{\mathrm{oee}} = d_{15} \sin^2\phi + d_{24} \cos^2\phi$$

YZ plane

$$d_{\mathrm{oeo}} = d_{\mathrm{eoo}} = d_{15} \sin\theta$$

XZ plane, $\theta < V_z$

$$d_{\mathrm{ooe}} = d_{32} \sin\theta$$

XZ plane, $\theta > V_z$

$$d_{\mathrm{oeo}} = d_{\mathrm{eoo}} = d_{24} \sin\theta$$

Expressions for the effective second-order nonlinear coefficient in principal planes of RTA crystal (Kleinman symmetry conditions are valid, $d_{15} = d_{31}$ and $d_{24} = d_{32}$) [16]:

XY plane

$$d_{eoe} = d_{oee} = d_{31} \sin^2 \phi + d_{32} \cos^2 \phi$$

YZ plane

$$d_{oeo} = d_{eoo} = d_{31} \sin \theta$$

XZ plane, $\theta < V_z$

$$d_{ooe} = d_{32} \sin \theta$$

XZ plane, $\theta > V_z$

$$d_{oeo} = d_{eoo} = d_{32} \sin \theta$$

Effective second-order nonlinear coefficient for three-wave interactions in the arbitrary direction of RTA crystal is given in [16].

The signs of RTA second-order nonlinear coefficients are probably all the same [17].

Absolute and relative values of second-order nonlinear coefficients:

$d_{31}(1.064\,\mu m) = 2.3 \pm 0.5\,pm/V$ [11]
$d_{31}(1.064\,\mu m) = 3.55 \times d_{36}(KDP) = 1.4\,pm/V$ [2], [18]
$d_{32}(1.064\,\mu m) = 3.8 \pm 0.7\,pm/V$ [11]
$d_{32}(1.064\,\mu m) = 11.71 \times d_{36}(KDP) = 4.6\,pm/V$ [2], [18]
$d_{33}(1.064\,\mu m) = 15.8 \pm 1.6\,pm/V$ [11]
$d_{33}(1.064\,\mu m) = 31.05 \times d_{36}(KDP) = 12.1\,pm/V$ [2], [18]

Experimental value of effective second-order nonlinear coefficient for specific phase-matching direction (SHG, type I, $1.0642 \Rightarrow 0.5321\,\mu m$) in RTA crystal [2]

Phase-matching direction	d_{eff} [pm/V]
$\theta = 52.7°$, $\phi = 39.8°$	1.33

Experimental values of phase-matching angle and temperature bandwidth

Interacting wavelengths [μm]	ϕ_{exp} [deg]	θ_{exp} [deg]	ΔT [°C]	Ref.
XY plane, $\theta = 90°$				
SFG, $e + o \Rightarrow e$				
$1.6132 + 0.6412 \Rightarrow 0.4588$	5.7		14.6	[10]
YZ plane, $\phi = 90°$				
SHG, $o + e \Rightarrow o$				
$1.3188 \Rightarrow 0.6594$		61.2	35.2	[10]

Interacting wavelengths [μm]	ϕ_{exp} [deg]	θ_{exp} [deg]	ΔT [°C]	Ref.
SFG, $o + e \Rightarrow o$				
$1.3188 + 1.0642 \Rightarrow 0.58895$		65.3	59.3	[10]
$1.6132 + 1.0642 \Rightarrow 0.6412$		52.0	39.8	[10]
$1.6132 + 0.6412 \Rightarrow 0.4588$		64.9	16.9	[10]
SFG, $e + o \Rightarrow o$				
$3.1271 + 1.6132 \Rightarrow 1.0642$		69.1	61.0	[10]
XZ plane, $\phi = 0°, \theta > V_z$				
SHG, $o + e \Rightarrow o$				
$1.3188 \Rightarrow 0.6594$		73.7		[6]
		73.5	29.3	[10]
SFG, $o + e \Rightarrow o$				
$1.3188 + 1.0642 \Rightarrow 0.58895$		82.0	47.8	[10]
$1.6132 + 1.0642 \Rightarrow 0.6412$		62.2	26.8	[10]
SFG, $e + o \Rightarrow o$				
$3.1271 + 1.6132 \Rightarrow 1.0642$		86.2	54.3	[10]
DFG, $o - e \Rightarrow o$				
$1.0642 - 1.5108 \Rightarrow 3.6$		45.1		[5]
$1.0642 - 1.4500 \Rightarrow 4.0$		44.8		[5]

Laser-induced damage threshold

λ [μm]	τ_p [ns]	I_{thr} [GW/cm^2]	Ref.	Note
0.74–0.84	0.0002	>200	[19]	1 kHz
1.064	10–20	>0.4	[20]	PPRTA
	5.5	>0.1	[15]	1 kHz, PPRTA

About the crystal

Successful poling of a flux-grown RTA crystal was demonstrated in 1996 [21]. Like PPKTP, it offers some practical advantages over periodically poled lithium niobate such as about one order less coercive field value, which allows production of PPRTA crystals with higher apertures [15], low susceptibility to thermal lensing and phase mismatch, and absence of photorefractive damage, which permits stable operation at room temperature. In comparison with PPKTP, periodically poled RTA crystals possess a longer IR cutoff wavelength (≈5.2 μm instead of ≈4.4 μm for KTP) and lack of IR absorption at 3.5 μm [7]. Such properties make PPRTA especially suitable for mid-IR OPO [4], [15], [22], [23], [24], [25], [26] and DFG [14], [20] systems. The only disadvantage of currently available PPRTA crystals is their relatively short length (below 20 mm) compared with the 50-mm length of standard PPLN elements.

References

[1] B.H.T. Chai: Optical Crystals. In: *CRC Handbook of Laser Science and Technology, Supplement 2: Optical Materials*, ed. by M.J. Weber (CRC Press, Boca Raton, 1995), pp. 3–65.

[2] J. Han, Y. Liu, M. Wang, D. Nie: Flux growth and properties of $RbTiOPO_4$ (RTA) crystals. J. Cryst. Growth **128(1–4)**, 864–866 (1993).
[3] L.K. Cheng, E.M. McCarron III, J. Calabrese, J.D. Bierlein, A.A. Ballman: Development of the nonlinear optical crystal $CsTiOAsO_4$. I. Structural stability. J. Cryst. Growth **132(1–2)**, 280–288 (1993).
[4] A. Carleton, D.J.M. Stothard, I.D. Lindsay, M. Ebrahimzadeh, M.H. Dunn: Compact, continuous-wave, singly resonant optical parametric oscillator based on periodically poled $RbTiOAsO_4$ in a Nd:YVO_4 laser. Opt. Lett. **28(7)**, 555–557 (2003).
[5] D.L. Fenimore, K.L. Schepler, D. Zelmon, S. Kük, U.B. Ramabadran, P. von Richter, D. Small: Rubidium titanyl arsenate difference-frequency generation and validation of new Sellmeier coefficients. J. Opt. Soc. Am B **13(9)**, 1935–1940 (1996).
[6] J. Wang, J. Wei, Y. Liu, X. Yin, X. Hu, Z. Shao, M. Jiang: A survey of research on KTP and its analogue crystals. Progr. Cryst. Growth Character. Mater. **40(1–4)**, 3–15 (2000).
[7] G. Hansson, H. Karlsson, S. Wang, F. Laurell: Transmission measurements in KTP and isomorphic compounds. Appl. Opt. **39(27)**, 5058–5069 (2000).
[8] X. Yin, J.Y. Wang: Electro-optic property of $RbTiOPO_4$ (RTA) crystal. Nonl. Opt. **23(2)**, 93–96 (2000).
[9] J.-P. Feve, B. Boulanger, O. Pacaud, I. Rousseau, B. Menaert, G. Marnier, P. Villeval, C. Bonnin, G.M. Loiacono, D.N. Loiacono: Phase-matching measurements and Sellmeier equations over the complete transparency range of $KTiOAsO_4$, $RbTiOAsO_4$, and $CsTiOAsO_4$. J. Am. Opt. Soc. B **17(5)**, 775–780 (2000).
[10] K. Kato, E. Takaoka, N. Umemura: Thermo-optic dispersion formula for $RbTiOAsO_4$. Jpn. J. Appl. Phys. **42(10)**, 6420–6423 (2003).
[11] L.-T. Cheng, L.K. Cheng, J.D. Bierlein: Linear and nonlinear optical properties of the arsenate isomorphs of KTP. Proc. SPIE **1863**, 43–53 (1993).
[12] L.K. Cheng, L.T. Cheng, J. Galperin, P.A. Morris Hotsenpiller, J.D. Bierlein: Crystal growth and characterization of $KTiOPO_4$ isomorphs from the self-fluxes. J. Cryst. Growth **137(1–2)**, 107–115 (1994).
[13] J.P. Feve, B. Boulanger, O. Pacaud, I. Rousseau, B. Menaert, G. Marnier: Refined Sellmeier equations from phase-matching measurements over the complete transparency range of $KTiOAsO_4$, $RbTiOAsO_4$, and $CsTiOAsO_4$. In: *Advanced Solid-State Lasers, OSA Trends in Optics and Photonics Series, Vol. 34*, ed. by H. Injeyan, U. Keller, C. Marshall (OSA, Washington DC, 2000), pp. 575–577.
[14] K. Fradkin-Kashi, A. Arie, P. Urenski, G. Rosenman: Characterization of optical and nonlinear properties of periodically-poled $RbTiOAsO_4$ in the mid-infrared range via difference-frequency generation. Appl. Phys. B **71(2)**, 251–255 (2000).
[15] H. Karlsson, M. Olson, G. Arvidsson, F. Laurell, U. Bäder, A. Borsutzky, R. Wallenstein, S. Wickström, M. Gustafsson: Nanosecond optical parametric oscillator based on large-aperture periodically poled $RbTiOAsO_4$. Opt. Lett. **24(5)**, 330–332 (1999).
[16] V.G. Dmitriev, D.N. Nikogosyan: Effective nonlinearity coefficients for three-wave interactions in biaxial crystals of *mm*2 point group symmetry. Opt. Commun. **95(1–3)**, 173–182 (1993).
[17] A. Anema, T. Rasing: Relative signs of the nonlinear coefficients of potassium titanyl phosphate. Appl. Opt. **36(24)**, 5902–5904 (1997).
[18] I. Shoji, T. Kondo, A. Kitamoto, M. Shirane, R. Ito: Absolute scale of second-order nonlinear-optical coefficients. J. Opt. Soc. Am. B **14(9)**, 2268–2294 (1997).
[19] V. Petrov, F. Noack, R. Stolzenberger: Seeded femtosecond optical parametric amplification in the mid-infrared spectral region above 3 μm. Appl. Opt. **36(6)**, 1164–1172 (1997).

[20] W. Chen, G. Mouret, D. Boucher, F.K. Tittel: Mid-infrared trace gas detection using continuous-wave difference frequency generation in periodically poled $RbTiOAsO_4$. Appl. Phys. B **72(7)**, 873–876 (2001).

[21] H. Karlsson, F. Laurell, P. Henriksson, G. Arvidsson: Frequency doubling in periodically poled $RbTiOAsO_4$. Electron. Lett. **32(6)**, 556–557 (1996).

[22] D.T. Reid, Z. Penman, M. Ebrahimzadeh, W. Sibbett, H. Karlsson, F. Laurell: Broadly tunable infrared femtosecond optical parametric oscillator based on periodically poled $RbTiOAsO_4$. Opt. Lett. **22(18)**, 1397–1399 (1997).

[23] D.T. Reid, G.T. Kennedy, A. Miller, W. Sibbett, M. Ebrahimzadeh: Widely tunable, near- to mid-infrared femtosecond and picosecond optical parametric oscillators using periodically poled $LiNbO_3$ and $RbTiOAsO_4$. IEEE J. Sel. Topics Quant. Electr. **4(2)**, 238–248 (1998).

[24] G.T. Kennedy, D.T. Reid, A. Miller, M. Ebrahimzadeh, H. Karlsson, G. Arvidsson, F. Laurell: Near- to mid-infrared picosecond optical parametric oscillator based on periodically poled $RbTiOAsO_4$. Opt. Lett. **23(7)**, 503–505 (1998).

[25] T.J. Edwards, G.A. Turnbull, M.H. Dunn, M. Ebrahimzadeh, H. Karlsson, G. Arvidsson, F. Laurell: Continuous-wave singly resonant optical parametric oscillator based on periodically poled $RbTiOAsO_4$. Opt. Lett. **23(11)**, 837–839 (1998).

[26] P. Loza-Alvarez, D.T. Reid, M. Ebrahimzadeh, W. Sibbett, H. Karlsson, P. Henriksson, G. Arvidsson, F. Laurell: Periodically poled $RbTiOAsO_4$ femtosecond optical parametric oscillator tunable from 1.38 to 1.58 μm. Appl. Phys. B **68(2)**, 177–180 (1999).

5.3 $BaTiO_3$, Barium Titanate

Negative uniaxial crystal: $n_o > n_e (278\,K < T < 393\,K)$

Molecular mass: 233.208

Specific gravity: 5.9 g/cm^3 [1]; 6.02 g/cm^3 at $278\,K < T < 393\,K$ [2]; 6.017 g/cm^3 at $T > 393\,K$ [2]

Point group [2]:

$3m$ at $T < 183\,K$

$mm2$ at $183\,K < T < 278\,K$

$4mm$ at $278\,K < T < 393\,K$

$m3m$ at $T > 393\,K$

Lattice constants for point group $4mm$:

$a = 3.985$ Å [2]; 3.9920 Å [3]; 3.994 Å [4]

$c = 4.020$ Å [2]; 4.0361 Å [3]; 4.038 Å [4]

Mohs hardness: 5 [5]

Vickers hardness: 200–580 [4]

Solubility in water: insoluble [2]

Melting point: 1870 K [6]; 1898 K [4], [2]

Curie temperature: 393 K [7]; 405 K [8]; 406 ± 2 K [9]

Linear thermal expansion coefficient

T [K]	$\alpha_t \times 10^6$ [K^{-1}]	Ref.
300	11.4	[10]
393	8.6	[4]
400	8.6	[10]
473	9.4	[4]
623	10.8	[4]
673	11.3	[4]
773	12.3	[10]
873	13.2	[4]
973	14.2	[4]
1073	15.1	[4]

Mean value of linear thermal expansion coefficient [2]

T [K]	$\alpha_t \times 10^6$ [K^{-1}]
113–174	8.8
174–277	11.4
277–293	11.4
303–395	5.1
397–583	10.3

Specific heat capacity c_p at $P = 0.101325$ MPa

T [K]	c_p [J/kgK]	Ref.
80	135	[10]
100	185	[4]
125	239	[4]
150	286	[10]
	288	[4]
175	322	[6]
	327	[4]
250	409	[10]
300	439	[5]
350	454	[2]
400	484	[10]
600	520	[10]
1000	549	[10]

Thermal conductivity coefficient

T [K]	κ [W/mK]	Ref.
293	1.34	[6]
401	0.67	[4]

Band-gap energy at room temperature: $E_g = 3.1$ eV [11]
Transparency range at $\alpha = 1\,\mathrm{cm}^{-1}$ level: 0.4–9 μm [9]

Linear absorption coefficient α

λ [μm]	α [cm^{-1}]	Ref.	Note
0.41	1.0	[9]	$T = 306$ K, $\mathbf{E}\parallel c$
0.423	1.0	[9]	$T = 306$ K, $\mathbf{E}\perp c$
0.5145	2.14	[12]	$\mathbf{E}\perp c$
	1.16	[12]	$\mathbf{E}\parallel c$

Two-photon absorption coefficient β [11]

λ [μm]	τ_p [ns]	$\beta \times 10^{11}$ [cm/W]	Note
0.596	0.001	10	$\perp c$, $\mathbf{E}\perp c$

Experimental values of refractive indices

λ [μm]	n_o	n_e	Ref.
0.5145	2.494	2.431	[13]
0.55	2.458	2.399	[9]
0.589	2.428	2.371	[14]

Temperature derivative of refractive indices [12]

λ [μm]	ΔT [K]	$\mathrm{d}n_o/\mathrm{d}T \times 10^6$ [K^{-1}]	$\mathrm{d}n_e/\mathrm{d}T \times 10^6$ [K^{-1}]
0.5145	298–319	≈ 0	
	297–315		140

Corrected Sellmeier equations (λ in μm) [15]:

$$n_o^2 = 3.05840 + \frac{2.27326\,\lambda^2}{\lambda^2 - 0.07409} - 0.02428\,\lambda^2$$

$$n_e^2 = 3.02479 + \frac{2.14062\,\lambda^2}{\lambda^2 - 0.067007} - 0.02169\,\lambda^2$$

Other sets of dispersion relations are given in [9], [16].

Linear electrooptic coefficients measured at low frequencies (well below the acoustic resonances of $BaTiO_3$ crystal, i.e., for the "free" crystal)

λ [μm]	r_{13}^T [pm/V]	r_{33}^T [pm/V]	r_{51}^T [pm/V]	Ref.	Note
0.5145	19.5 ± 1			[13]	$T = 296$ K
		97 ± 7		[13]	$T = 296$ K
0.5461			1640	[7]	$T = 298$ K

Linear electrooptic coefficients measured at high frequencies (well above the acoustic resonances of $BaTiO_3$ crystal, i.e., for the "clamped" crystal) at room temperature

λ [μm]	r_{13}^S [pm/V]	r_{33}^S [pm/V]	r_{51}^S [pm/V]	Ref.	Note
0.5461			820	[17]	$T = 295$ K
0.6328	8			[18]	
		28		[18]	

Verdet constant at $T = 403$ K [19]

λ [μm]	V [degree/Tm]
0.620	−2920

Coercive field value: ≈0.1 kV/mm [15]
Expression for the effective second-order nonlinear coefficient (Kleinman symmetry conditions are valid, $d_{15} = d_{24} = d_{31} = d_{32}$) [20]:

$$d_{\mathrm{ooe}} = d_{31} \sin\theta$$

Values of second-order nonlinear coefficient [21], recalculated using new absolute values for d_{36}(KDP) [22]:

$$d_{15}(1.06\,\mu\mathrm{m}) = 13.7 \pm 1.2\,\mathrm{pm/V}$$
$$d_{32}(1.06\,\mu\mathrm{m}) = 14.4 \pm 1.2\,\mathrm{pm/V}$$
$$d_{33}(1.06\,\mu\mathrm{m}) = 5.5 \pm 0.4\,\mathrm{pm/V}$$

Laser-induced bulk-damage threshold [11]

λ [μm]	τ_p [ns]	I_{thr} [GW/cm^2]
0.596	0.001	>83

About the crystal

The nonlinear optical properties of barium titanate were known already 40 years ago [21]. However, due to a low birefringence, the normal phase matching in this crystal is not possible. The renewed interest in this crystal [15] is related to the possibility of its use in quasi-phase-matched devices. A low coercive field value (≈0.1 kV/mm) allows the fabrication of waveguides with high apertures. Another advantage is its high transmission in the IR range up to 9 μm.

References

[1] B.H.T. Chai: Optical Crystals. In: *CRC Handbook of Laser Science and Technology, Supplement 2: Optical Materials*, ed. by M.J. Weber (CRC Press, Boca Raton, 1995), pp. 3–65.
[2] A.A. Blistanov, V.S. Bondarenko, N.V. Perelomova, F.N. Strizhevskaya, V.V. Tchkalova, M.P. Shaskolskaya: *Acoustic Crystals* (Nauka, Moscow, 1982) [In Russian].

[3] *Handbook of Optical Constants of Solids II*, ed. by E.D. Palik (Academic Press, Boston, 1991).
[4] E.M. Voronkova, B.N. Grechushnikov, G.I. Distler, I.P. Petrov: *Optical Materials for Infrared Technique* (Nauka, Moscow, 1965) [In Russian].
[5] *Handbook of Optical Materials*, ed. by M.J. Weber (CRC Press, Boca Raton, 2003), pp. 1–512.
[6] S.S. Ballard, J.S. Browder: Thermal Properties. In: *CRC Handbook of Laser Science and Technology, Vol. IV, Optical Materials: Part 2*, ed. by M.J. Weber (CRC Press, Boca Raton, 1987), pp. 49–54.
[7] A.R. Johnston, J.M. Weingart: Determination of the low-frequency linear electro-optic effect in tetragonal $BaTiO_3$. J. Opt. Soc. Am. **55(7)**, 828–834 (1965).
[8] C.J. Johnson: Some dielectric and electro-optic properties of $BaTiO_3$ single crystals. Appl. Phys. Lett. **7(8)**, 221–223 (1965).
[9] S.H. Wemple, M. DiDomenico, Jr., I. Camlibel: Dielectric and optical properties of melt-grown $BaTiO_3$. J. Phys. Chem. Solids **29(10)**, 1797–1803 (1968).
[10] *Physical Quantities. Handbook*, ed. by I.S. Grigoriev, E.Z. Meilikhov (Energoatomizdat, Moscow, 1991) [In Russian].
[11] T.F. Boggess, J.O. White, G.C. Valley: Two-photon absorption and anisotropic transient energy transfer in $BaTiO_3$ with 1-psec excitation. J. Opt. Soc. Am. B **7(12)**, 2255–2258 (1990).
[12] D.W. Rush, B.M. Dugan, G.L. Burdge: Temperature-dependent index-of-refraction changes in $BaTiO_3$. Opt. Lett. **16(17)**, 1295–1297 (1991).
[13] S. Ducharme, J. Feinberg, R.R. Neurgaonkar: Electrooptic and piezoelectric measurements in photorefractive barium titanate and strontium barium titanate. IEEE J. Quant. Electr. **QE-23(12)**, 2116–2121 (1987).
[14] L.V. Deshpande, M.B. Joshi, R.B. Mishra: Angle of polarization and refractive indices of $BaTiO_3$. J. Opt. Soc. Am. **70(9)**, 1163–1166 (1980).
[15] S.D. Setzler, P.G. Schunemann, T.M. Pollak, L.A. Pomeranz, M.J. Missey, D.E. Zelmon: Periodically poled barium titanate as a new nonlinear optical material. In: *Advanced Solid State Lasers, OSA Trends in Optics and Photonics Series, Vol. 26*, ed. by M.M. Fejer, H. Injeyan, U. Keller (OSA, Washington DC, 1999), pp. 676–680.
[16] S. Singh: Nonlinear optical materials. In: *Handbook of Lasers with Selected Data on Optical Technology*, ed. by R.J. Pressley (Chemical Rubber Co., Cleveland, 1971), pp. 489–525.
[17] A.R. Johnston: The strain-free electro-optic effect in single-crystal barium titanate. Appl. Phys. Lett. **7(7)**, 195–197 (1965).
[18] I.P. Kaminow: Tables of Linear Electrooptic Coefficients. In: *CRC Handbook of Laser Science and Technology, Vol. III, Optical Materials: Part 2*, ed. by M.J. Weber (CRC Press, Boca Raton, 1986), pp. 253–278.
[19] M.N. Deeter, G.W. Day, A.H. Rose: Magnetooptic Materials. Crystals and Glasses. In: *CRC Handbook of Laser Science and Technology, Supplement 2, Optical Materials*, ed. by M.J. Weber (CRC Press, Boca Raton, 1995), pp. 367–402.
[20] J.E. Midwinter, J. Warner: The effects of phase matching method and of uniaxial crystal symmetry on the polar distribution of second-order non-linear optical polarization. Brit. J. Appl. Phys. **16(11)**, 1135–1142 (1965)
[21] R.C. Miller, D.A. Kleinman, A. Savage: Quantitative studies of optical harmonic generation in CdS, $BaTiO_3$, and KH_2PO_4 type crystals. Phys. Rev. Lett. **11(4)**, 146–149 (1963).
[22] I. Shoji, T. Kondo, A. Kitamoto, M. Shirane, R. Ito: Absolute scale of second-order nonlinear-optical coefficients. J. Opt. Soc. Am. B **14(9)**, 2268–2294 (1997).

5.4 $MgBaF_4$, Magnesium Barium Fluoride

Negative biaxial crystal: $2V_z = 117.5°$ at $\lambda = 0.5321\,\mu m$ [1]
Molecular mass: 237.629
Point group: *mm*2
Lattice costants [2]:
$a = 4.125\,Å$
$b = 14.509\,Å$
$c = 5.841\,Å$
Assignment of dielectric and crystallographic axes: $X, Y, Z \Rightarrow b, c, a$
Transparency range: <0.14 to ~10 μm [2], [3]

Linear absorption coefficient [3]

λ [μm]	α [cm^{-1}]
0.144	2.0
0.164	1.0
0.178	0.5
0.200	0.2

Experimental values of refraction indices at $T = 295\,K$

λ [μm]	n_X	n_Y	n_Z	Ref.
0.1576299	1.5871	1.6138		[3]
0.4801254	1.4529	1.470467		[3]
0.5017077	1.4519	1.469492		[3]
0.5087240	1.44517	1.469179		[3]
0.5321	1.4508	1.4678	1.4742	[1]
0.5462260	1.4504	1.4678		[3]
0.5877254	1.4492	1.4666		[3]
0.6440250	1.4480	1.4652		[3]
1.0642	1.4436	1.4604	1.4674	[2]

Sellmeier equations for visible range (λ in μm, $T = 293\,K$) [1]:

$$n_X^2 = 2.0770 + \frac{0.00760}{\lambda^2 - 0.0079}$$

$$n_Y^2 = 2.1238 + \frac{0.00860}{\lambda^2}$$

$$n_Z^2 = 2.1462 + \frac{0.00736}{\lambda^2 - 0.0090}$$

Sellmeier equations for the range $0.157 - 1.06\,\mu\text{m}$ (λ in μm, $T = 293$ K) [3]:

$$n_X^2 = 2.07971 + \frac{0.006897}{\lambda^2 - 0.00914}$$

$$n_Y^2 = 2.12832 + \frac{0.0075537}{\lambda^2 - 0.008979}$$

Experimental values of phase-matching angle [1]

Interacting wavelengths [μm]	ϕ_{exp} [deg]	θ_{exp} [deg]
XY plane, $\theta = 90°$		
SHG, $o + o \Rightarrow e$		
$1.0642 \Rightarrow 0.5321$	9.2	
XZ plane, $\phi = 0°$, $\theta < V_z$		
SHG, $e + o \Rightarrow e$		
$1.0642 \Rightarrow 0.5321$		18.9

Experimental values of internal angular bandwidths [1]

Interacting wavelengths [μm]	ϕ_{pm} [deg]	$\Delta\varphi^{\text{int}}$ [deg]	$\Delta\theta^{\text{int}}$ [deg]
XY plane, $\theta = 90°$			
SHG, $o + o \Rightarrow e$			
$1.0642 \Rightarrow 0.5321$	9.2	0.82	2.25

Expressions for the effective second-order nonlinear coefficient in principal planes of $MgBaF_4$ crystal (Kleinman symmetry conditions are not valid) [4]:

XY plane

$$d_{\text{ooe}} = d_{31} \cos\phi$$

YZ plane

$$d_{\text{oeo}} = d_{\text{eoo}} = d_{24} \cos\theta$$

XZ plane, $\theta < V_z$

$$d_{\text{oee}} = d_{\text{eoe}} = d_{15} \sin^2\theta + d_{24} \cos^2\theta$$

XZ plane, $\theta > V_z$

$$d_{\text{eeo}} = d_{31} \sin^2\theta + d_{32} \cos^2\theta$$

Expressions for the effective second-order nonlinear coefficient in the principal planes of $MgBaF_4$ crystal (Kleinman symmetry conditions are valid, $d_{15} = d_{31}$ and $d_{24} = d_{32}$) [4]:

XY plane

$$d_{\text{ooe}} = d_{31} \cos\phi$$

YZ plane

$$d_{\text{oeo}} = d_{\text{eoo}} = d_{32} \cos\theta$$

XZ plane, $\theta < V_z$

$$d_{oee} = d_{eoe} = d_{31}\sin^2\theta + d_{32}\cos^2\theta$$

XZ plane, $\theta > V_z$

$$d_{eeo} = d_{31}\sin^2\theta + d_{32}\cos^2\theta$$

Expressions for the effective second-order nonlinear coefficient in arbitrary direction inside the $MgBaF_4$ crystal are given in [4].
Values of second-order nonlinear coefficients:

$d_{15}(1.064\,\mu m) = 0.07 \times d_{11}(SiO_2) \pm 20\% = 0.021 \pm 0.004$ pm/V [2], [5]
$d_{24}(1.064\,\mu m) = 0.07 \times d_{11}(SiO_2) \pm 20\% = 0.021 \pm 0.004$ pm/V [2], [5]
$d_{24}(1.064\,\mu m) = 0.062 \times d_{36}(KDP) \pm 17\% = 0.024 \pm 0.004$ pm/V [1], [5]
$d_{31}(1.064\,\mu m) = 0.07 \times d_{11}(SiO_2) \pm 20\% = 0.021 \pm 0.004$ pm/V [2], [5]
$d_{31}(1.064\,\mu m) = 0.057 \times d_{36}(KDP) \pm 23\% = 0.022 \pm 0.005$ pm/V [1], [5]
$d_{32}(1.064\,\mu m) = 0.13 \times d_{11}(SiO_2) \pm 20\% = 0.039 \pm 0.008$ pm/V [2], [5]
$d_{32}(1.064\,\mu m) = 0.085 \times d_{36}(KDP) \pm 12\% = 0.033 \pm 0.012$ pm/V [1], [5]
$d_{33}(1.064\,\mu m) = 0.05 \times d_{11}(SiO_2) \pm 20\% = 0.015 \pm 0.003$ pm/V [2], [5]
$d_{33}(1.064\,\mu m) = 0.023 \times d_{36}(KDP) \pm 14\% = 0.009 \pm 0.001$ pm/V [1], [5]

Laser-induced surface-damage threshold

λ [μm]	τ_p [ns]	I_{thr} [GW/cm^2]	Ref.	Note
0.157	10	>0.0002	[3]	$>10^9$ pulses
1.0642	≈20	>1	[2]	

About the crystal

The nonlinear optical properties of this crystal were known since the mid-1970s. However, very recently it was discovered that $MgBaF_4$ has a unique transmission in UV range down to 140 nm [3]. Simultaneously, ferroelectric domain inversion has been demonstrated, proving the possibility of quasi-phase-matching in this material [3].

References

[1] P.S. Bechtold, S. Haussühl: Nonlinear optical properties of orthorhombic barium formate and magnesium barium fluoride. Appl. Phys. **14(4)**, 403–410 (1977).
[2] J.G. Bergman, G.R. Crane, H. Guggenheim: Linear and nonlinear optical properties of ferroelectric $BaMgF_4$ and $BaZnF_4$. J. Appl. Phys. **46(11)**, 4645–4646 (1975).
[3] S.C. Buchter, T.Y. Fan, V. Liberman, J.J. Zayhowski, M. Rothschild, E.J. Mason, A. Cassanho, H.P. Jenssen, J.H. Burnett: Periodically poled $BaMgF_4$ for ultraviolet frequency conversion. Opt. Lett. **26(21)**, 1693–1695 (2001).
[4] V.G. Dmitriev, D.N. Nikogosyan: Effective nonlinearity coefficients for three-wave interactions in biaxial crystals of *mm*2 point group symmetry. Opt. Commun. **95(1–3)**, 173–182 (1993).
[5] D.A. Roberts: Simplified characterization of uniaxial and biaxial nonlinear optical crystals: a plea for standardization of nomenclature and conventions. IEEE J. Quant. Electr. **28(10)**, 2057–2074 (1992).

5.5 GaAs, Gallium Arsenide

Optically isotropic crystal
Molecular mass: 144.645
Specific gravity: $5.3161 \pm 0.0002\,\mathrm{g/cm^3}$ at T = 298 K [1];
$5.3170\,\mathrm{g/cm^3}$ [2]; $5.32\,\mathrm{g/cm^3}$ at T = 293 K [3]
Point group: $\bar{4}3m$
Lattice constant: $a = 5.6534 \pm 0.0002$ Å [1]; 5.65321 ± 0.00003 Å [4]; 5.6535 Å [5]
Mohs hardness: 4.5 [1]
Knoop hardness: 750 at indenter load 25 g [1]; 750 ± 40 [6]; 721 [7]
Solubility in water: insoluble [4]
Melting point: 1510 K [6]; 1511 K [1], [2], [4], [8]; 1513 K [9], [10]; 1520 K [11]

Linear thermal expansion coefficient

T [K]	$\alpha_t \times 10^6$ [K^{-1}]	Ref.
40	−0.50	[1]
50	−0.15	[8]
55	0.00	[1]
100	1.9	[12]
	2.05	[8]
200	4.93	[8]
293	5.7	[12]
300	5.82	[8]
	6.0	[2]
400	6.23	[8]
500	6.5	[12]
600	6.98	[8]
800	7.1	[12]
	7.4	[8]

Mean value of linear thermal expansion coefficient [1]

T [K]	$\alpha_t \times 10^6$ [K^{-1}]
78–290	3.64
291–560	5.74
560–680	7.44

Specific heat capacity c_p at $P = 0.101325$ MPa [9]

T [K]	c_p [J/kgK]
273	318

Thermal conductivity coefficient κ

T [K]	κ [W/mK]	Ref.
300	52	[9]
	52.3	[1]

Thermal conductivity coefficient of n-GaAs ($n = 2 \times 10^{16}\,\mathrm{cm}^{-3}$ at $T = 77\,\mathrm{K}$) [8]

T [K]	κ [W/mK]
80	270
150	105
300	58

Band-gap energy at room temperature (direct transition) $E_g = 1.42\,\mathrm{eV}$ [13], [14], [15]; 1.425 eV [16], [17]; 1.428 eV [2]; 1.43 eV [8], [18], [19]; 1.435 eV [11], [20], [21], [22]
Transparency range at $\alpha = 1\,\mathrm{cm}^{-1}$ level: 1.1–17 μm [23]; 0.95–17 μm [24]

Linear absorption coefficient α

λ [μm]	α [cm^{-1}]	Ref.	Note
0.53	80000	[25]	Si-doped GaAs, $n = 10^{18}\,\mathrm{cm}^{-3}$,$T = 300\,\mathrm{K}$
1.06	0.9	[25]	Si-doped GaAs, $n = 10^{18}\,\mathrm{cm}^{-3}$, $T = 300\,\mathrm{K}$
	1.2	[26]	undoped GaAs
	1.54	[27]	n-type GaAs, [111] direction, $n = 2 \times 10^{17}\,\mathrm{cm}^{-3}$
	1.57	[17]	Si-doped GaAs, $n = 1.5 \times 10^{17}\,\mathrm{cm}^{-3}$, $T = 295\,\mathrm{K}$
	2.5	[28]	$n = 4 \times 10^{16}\,\mathrm{cm}^{-3}$, $T = 300\,\mathrm{K}$
	~3	[29]	O_2-doped with $n = 3 \times 10^{14}\,\mathrm{cm}^{-3}$ and $\rho_0 = 2.4\,\Omega\,\mathrm{cm}$
	4.0	[30]	$n = 4 \times 10^{16}\,\mathrm{cm}^{-3}$
1.0642	0.7	[31]	n-type GaAs, $\mathbf{E} \perp c$
	0.7	[32]	
	1.2	[3]	Cr-doped GaAs, $n = 10^{16}\,\mathrm{cm}^{-3}$, $\rho_0 > 10^7\,\Omega\,\mathrm{cm}$
	1.50 ± 0.15	[33]	
1.318	0.05	[34]	O_2-doped sample
2.7–2.8	0.0032	[35]	$\rho_0 \sim 10^8\,\Omega\,\mathrm{cm}$, bulk absorption
3.8–3.9	0.003	[35]	$\rho_0 \sim 10^8\,\Omega\,\mathrm{cm}$, bulk absorption
5–6	0.016	[36]	bulk absorption
9.2	0.006	[24]	
9.3	0.005	[37]	bulk absorption
9.6	0.008	[24]	
10.6	0.005	[38]	

λ [μm]	α [cm^{-1}]	Ref.	Note
	0.006 ± 0.002	[39]	$\rho_0 = 10^4$ to $10^9\ \Omega$ cm
	0.009	[37]	bulk absorption
	0.01–0.05	[40]	
	0.01–0.20	[41]	
	0.012 ± 0.002	[42]	Cr-doped GaAs, $\rho_0 = 3 \times 10^8\ \Omega$ cm
12.4	0.05	[24]	
13.78	0.15	[24]	
15.9	0.36	[24]	
16.75	0.71	[24]	
17.22	1.09	[24]	

Two-photon absorption coefficient β

λ [μm]	τ_p [ns]	$\beta \times 10^{11}$ [cm/W]	Ref.	Note
1.06	0.005	4500 ± 1000	[17]	$T = 295$ K, Si-doped GaAs, $n = 1.5 \times 10^{17}$ cm^{-3}
	0.008	1500 ± 500	[28]	$n = 4 \times 10^{16}$ cm^{-3}
	0.08	2600	[43]	
	10	3500 ± 300	[44]	O_2-doped sample
1.0642	0.003	2500	[45]	[001] direction, **E**∥[110] direction
	0.028	2200 ± 300	[27]	n-type GaAs, [111] direction, $n = 2 \times 10^{17}$ cm^{-3}
	0.03	3000 ± 500	[31]	n-type GaAs, **E**⊥c
		1800 ± 360	[46]	[100] direction
		2400 ± 480	[46]	[110] direction
		2500 ± 500	[46]	[111] direction
	0.035	2700	[26]	undoped GaAs
	0.038	2300	[47]	[111] direction
	0.04	2600 ± 500	[48]	[110] direction
	0.05	2900	[14]	
	11	3000 ± 900	[33]	
	∼20	∼2000	[49]	
1.318	∼20	3300 ± 1500	[34]	O_2-doped sample
1.32	0.003	1100	[45]	[001] direction, **E**∥ [110] direction

Experimental values of refractive index

λ [μm]	n	Ref.	λ [μm]	n	Ref.
0.895	3.603	[50]	1.000	3.509	[50]
0.900	3.595	[50]	1.020	3.498	[50]
0.910	3.581	[50]	1.040	3.488	[50]
0.920	3.569	[50]	1.060	3.479	[50]
0.940	3.550	[50]	1.100	3.463	[50]
0.960	3.534	[50]	1.150	3.446	[50]
0.980	3.520	[50]	1.200	3.433	[50]

λ [μm]	n	Ref.	λ [μm]	n	Ref.
1.400	3.394	[50]	13.0	2.97	[4]
1.435	3.40	[4]	13.7	2.895	[4]
1.500	3.381	[50]	14.5	2.82	[4]
1.700	3.362	[50]	15.0	2.73	[4]
2.87	3.33	[4]	17.0	2.59	[4]
5.1	3.30	[4]	19.0	2.41	[4]
10.0	3.27	[4]	21.9	2.12	[4]
11.0	3.045	[4]			

Temperature derivative of refractive index

λ [μm]	T [K]	$dn/dT \times 10^6$ [K^{-1}]	Ref.	Note
10.6	293	56 ± 3	[42]	Cr-doped GaAs, $\rho_0 = 3 \times 10^8\ \Omega\,\mathrm{cm}$
	300	100	[51]	

Nonlinear refractive index γ [48], [52]

λ [μm]	$\gamma \times 10^{20}$ [m^2/W]
1.0642	-3260 ± 600

Linear electrooptic coefficient measured at low frequencies (well below the acoustic resonances of GaAs crystal, i.e., for the "free" crystal) at room temperature

λ [μm]	r_{41}^{T} [pm/V]	Ref.
1.0642	-1.17	[53]
1.1523	-1.43	[54]
1.208	-1.25	[53]
1.306	-1.28	[53]
1.50	-1.36	[53]
3.3913	-1.24 ± 0.04	[55]
10.6	-1.51 ± 0.05	[55]
	-1.6	[56]

Linear electrooptic coefficient measured at high frequencies (well above the acoustic resonances of GaAs crystal, i.e., for the "clamped" crystal) at room temperature

λ [μm]	r_{41}^{S} [pm/V]	Ref.
0.95–1.08	-1.2	[57]
1.0642	-1.33	[53]
1.208	-1.41	[53]
1.306	-1.46	[53]
1.50	-1.53	[53]
3.3913	-1.5	[58]

Verdet constant at $T = 293\,\mathrm{K}$

λ [μm]	V [degree/Tm]	Ref.
1.06	5850 ± 290	[59]
	5000	[8]
1.95	1800 ± 180	[59]

Absolute values of second-order nonlinear coefficient:

$d_{36}(1.064\,\mu\mathrm{m}) = 170\,\mathrm{pm/V}$ [60]

$d_{36}(1.533\,\mu\mathrm{m}) = 119\,\mathrm{pm/V}$ [60]

$d_{36}(10.6\,\mu\mathrm{m}) = 83\,\mathrm{pm/V}$ [61]

Laser-induced damage threshold

λ [μm]	τ_p [ns]	I_{thr} [GW/cm^2]	Ref.	Note
0.6943	500000	0.00002	[62]	surface damage
	30	0.072 (?)	[63]	surface damage
	20	0.008 ± 0.002	[64]	surface damage, [100] direction
1.06	300000	0.00011–0.00024	[11]	surface damage, 1000-μm beam-waist diameter
	1000	0.01	[65]	surface damage
	60	0.013 ± 0.005	[64]	surface damage, [100] and [110] directions
	35	0.03 ± 0.01	[59]	surface damage
	20	0.043 ± 0.008	[66]	surface damage
1.0642	45	0.02	[3]	surface damage, 10 pulses, [100] direction
		0.05	[3]	surface damage, 1 pulse, [100] direction
	20	0.045 ± 0.04	[67]	surface damage, 1 pulse, [100] direction
	18	0.04	[68]	
	10	0.024	[69]	surface damage
	0.035	200	[70]	[100] direction
2.76	90	0.08	[71]	
2.8	70	0.079	[72]	
10.6	CW	0.000006	[71]	
		0.000003	[40]	>3-cm beam-waist diameter
		0.00003	[40]	<0.5-cm beam-waist diameter
	200	0.06	[68]	
	150–200	0.07–0.09	[73]	surface damage, 6-cm beam-waist diameter
		0.135–0.18	[73]	surface damage, 500-μm beam-waist diameter

λ [μm]	τ_p [ns]	I_{thr} [GW/cm^2]	Ref.	Note
	150	0.05–0.11	[40]	surface damage, ~2-cm beam-waist diameter
	100	0.01 ± 0.005	[59]	bulk damage, Zn-doped p-typed GaAs $n \approx 10^{19}$ cm^{-3}
		0.03 ± 0.01	[59]	surface damage, n-type GaAs, $n \approx 10^{18}$ cm^{-3}
		0.11–0.8	[71]	
	60	1.6–3.2	[40]	100-μm beam-waist diameter

About the crystal

Though the isotropic nature of GaAs precludes the realization of ordinary birefringent phase matching, the quasi-phase-matching (QPM) is still possible. As early as in 1976, two USA groups [74], [75] reported the application of a stack of properly oriented GaAs plates for SHG of CO_2 laser radiation and made the first successful experiments. In 1993, a more sophisticated method of diffusion bonding of GaAs wafers was proposed [76] and later used in the experiments on QPM SHG [77], [78], [79], QPM SFG [78], and QPM DFG [80].

References

[1] E.M. Voronkova, B.N. Grechushnikov, G.I. Distler, I.P. Petrov: *Optical Materials for Infrared Technique* (Nauka, Moscow, 1965) [In Russian].

[2] *Physical-Chemical Properties of Semiconductors. Handbook* (Nauka, Moscow, 1979) [In Russian].

[3] A.L. Huang, M.F. Becker, R.M. Walser: Laser-induced damage and ion emission of GaAs at 1.06 μm. Appl. Opt. **25(21)**, 3864–3870 (1986).

[4] A.A. Blistanov, V.S. Bondarenko, N.V. Perelomova, F.N. Strizhevskaya, V.V. Tchkalova, M.P. Shaskolskaya: *Acoustic Crystals* (Nauka, Moscow, 1982) [In Russian].

[5] *Handbook of Optical Constants of Solids II*, ed. by E.D. Palik (Academic Press, Boston, 1991).

[6] M. Bertolotti, D. Sette, L. Stagni, G. Vitali: Electron microscope observation of laser damage on GaAs, GaSb and InSb. Radiation Effects **16(3–4)**, 197–202 (1972).

[7] B.H.T. Chai: Optical Crystals. In: *CRC Handbook of Laser Science and Technology, Supplement 2: Optical Materials*, ed. by M.J. Weber (CRC Press, Boca Raton, 1995), pp. 3–65.

[8] *Physical Quantities. Handbook*, ed. by I.S. Grigoriev, E.Z. Meilikhov (Energoatomizdat, Moscow, 1991) [In Russian].

[9] S.S. Ballard, J.S. Browder: Thermal Properties. In: *CRC Handbook of Laser Science and Technology, Vol. IV, Optical Materials: Part 2*, ed. by M.J. Weber (CRC Press, Boca Raton, 1987), pp. 49–54.

[10] S. Musikant: *Optical Materials. An Introduction to Selection and Application* (Marcel Dekker, Inc., New York, 1985).

[11] A.V. Kuanr, S.K. Bansal, G.P. Srivastava: Laser-induced damage in GaAs at 1.06 μm. wavelength: surface effects. Opt. Laser Technol. **28(1)**, 25–34 (1996).

[12] G.W.C. Kaye, T.H. Laby: *Tables of Physical and Chemical Constants* (Longman Group Ltd., London, 1995).
[13] E.W. van Stryland, M.A. Woodall, H. Vanherzeele, M.J. Soileau: Energy band-gap dependence of two-photon absorption. Opt. Lett. **10(10)**, 490–492 (1985).
[14] E.W. van Stryland, L.L. Chase: Two-Photon Absorption. Inorganic Materials. In: *CRC Handbook of Laser Science and Technology, Supplement 2: Optical Materials*, ed. by M.J. Weber (CRC Press, Boca Raton, 1995), pp. 299–328.
[15] K.J. Bachmann: *The Materials Science of Microelectronics* (VCH Publishers, New York, 1995).
[16] H. Burkhard, H.W. Dinges, E. Kuphal: Optical properties of $In_{1-x}Ga_xP_{1-y}As_y$, InP, GaAs, and GaP determined by ellipsometry. J. Appl. Phys. **53(1)**, 655–662 (1982).
[17] A. Penzkofer, A.A. Bugayev: Two-photon absorption and emission dynamics of bulk GaAs. Opt. Quant. Electron. **21(4)**, 283–306 (1989).
[18] A.Z. Grasyuk, I.G. Zubarev, A.B. Mironov, I.A. Poluektov: Spectrum of two-photon interband absorption of laser radiation in GaAs. Fiz. Tekh. Poluprov. **10(2)**, 262–270 (1976) [In Russian, English trans.: Sov. Phys. - Semicond. **10(2)**, 159–163 (1976)].
[19] C. Kittel: *Introduction to Solid State Physics, Seventh Edition* (John Wiley & Sons, New York, 1996).
[20] S.S. Mitra, L.M. Narducci, R.A. Shatas, Y.F. Tsay, A. Vaidyanathan: Nonlinear absorption in direct-gap semiconductors. Appl. Opt. **14(12)**, 3038–3042 (1975).
[21] M. Bertolotti, V. Bogdanov, A. Ferrari, A. Yaskov, N. Nazorova, A. Pikhtin, L. Schirone: Temperature dependence of the refractive index in semiconductors. J. Opt. Soc. Am. B **7(6)**, 918–922 (1990).
[22] A. Vaidyanathan, A.H. Guenther, S.S. Mitra: Two-photon absorption in direct-gap crystals—an addendum. Phys. Rev. B **22(12)**, 6480–6483 (1980).
[23] A.S. Sonin, A.S. Vasilevskaya: *Electrooptic Crystals* (Atomizdat, Moscow, 1971) [In Russian].
[24] *Handbook of Optical Constants of Solids*, ed. by E.D. Palik (Academic Press, Orlando, 1985).
[25] A. Saissy, A. Azema, J. Botineau, F. Gires: Absolute measurement of the 1.06 μm two-photon absorption coefficient in GaAs. Appl. Phys. **15(1)**, 99–102 (1978).
[26] G.C. Valley, T.F. Boggess, J. Dubard, A.L. Smirl: Picosecond pump-probe technique to measure deep-level, free-carrier, and two photon cross sections in GaAs. J. Appl. Phys. **66(6)**, 2407–2413 (1989).
[27] A.A. Bugaev, T.Y. Dunaeva, V.A. Lukoshkin: Influence of nonlinear refraction, absorption by free carriers, and multiple reflection on the determination of the two-photon absorption coefficient of gallium arsenide. Fiz. Tverd. Tela **31(12)**, 9–14 (1989) [In Russian, English trans.: Sov.Phys. - Solid State **31(12)**, 2031–2034 (1989)].
[28] B. Bosacchi, J.S. Bessey, F.C. Jain: Two-photon absorption of neodymium laser radiation in gallium arsenide. J. Appl. Phys. **49(8)**, 4609–4611 (1978).
[29] T.F. Deutsch: Absorption coefficient of infrared laser window materials. J. Phys. Chem. Solids **34(12)**, 2091–2104 (1973).
[30] C.C. Lee, H.Y. Fan: Two-photon absorption and photoconductivity in GaAs and InP. Appl. Phys. Lett. **20(1)**, 18–20 (1972).
[31] J.H. Bechtel, W.L. Smith: Two-photon absorption in semiconductors with picosecond light pulses. Phys. Rev. B **13(8)**, 3515–3522 (1976).
[32] I.M. Catalano, A. Cingolani: Non-parabolic band effect on two-photon absorption in ZnSe and CdTe. Solid State Commun. **43(3)**, 213–215 (1982).
[33] A.F. Stewart, M. Bass: Intensity dependent absorption in semiconductors. Appl. Phys. Lett. **37(11)**, 1040–1043 (1980).

[34] D.A. Kleinman, R.C. Miller, W.A. Nordland: Two-photon absorption of Nd laser radiation in GaAs. Appl. Phys. Lett. **23(5)**, 243–244 (1973).
[35] A. Hordvik, L. Skolnik: Photoacoustic measurements of surface and bulk absorption in HF/DF laser window materials. Appl. Opt. **16(11)**, 2919–2924 (1977).
[36] V.B. Nosov, G.T. Petrovskii, M.V. Serzhantova, A.V. Shatilov: Calorimetric measurements of the volume and surface absorption of infrared materials in the 5–6 μm spectral region. Opt. Mekh. Promyshl. **No. 4**, 42–44 (1989) [In Russian, English trans.: Sov. J. Opt. Technol. **56(4)**, 238–240 (1989)].
[37] C.P. Christensen, R. Joiner, S.T.K. Nieh, W.H. Steier: Investigation of infrared loss mechanism in high-resistivity GaAs. J. Appl. Phys. **45(11)**, 4957–4960 (1974).
[38] A.J. Glass, A.H. Guenther: Laser induced damage of optical elements—a status report. Appl. Opt. **12(4)**, 637–649 (1973).
[39] J. Comly, E. Garmire, A. Yariv: Infrared absorption at 10.6 μm in GaAs. J. Appl. Phys. **38(10)**, 4091–4092 (1968).
[40] N.V. Karlov, E.V. Sisakyan: Optical materials for CO_2 lasers. Izv. Akad. Nauk SSSR, Ser. Fiz. **44(8)**, 1631–1638 (1980) [In Russian, English trans.: Bull. Acad. Sci. USSR, Phys. Ser. **44(8)**, 63–68 (1980)].
[41] M.A. Ilin, N.V. Ovsyannikova, E.V. Sisakyan: Method of measuring the small absorption coefficients of gallium arsenide single crystals. Opt. Mekh. Promyshl. **No. 10**, 57–59 (1977) [In Russian, English trans.: Sov. J. Opt. Technol. **44(10)**, 626–627 (1977)].
[42] R. Weil: Interference of 10.6-μm coherent radiation in a 5-cm long gallium arsenide parallelepiped. J. Appl. Phys. **40(7)**, 2857–2859 (1969).
[43] J.S. Aitchison, M.K. Oliver, E. Kapon, E. Colas, P.W.E. Smith: Role of two-photon absorption in ultrafast semiconductor optical switching devices. Appl. Phys. Lett. **56(14)**, 1305–1307 (1990).
[44] I.G. Zubarev, A.B. Mironov, S.I. Mikhailov: Influence of deep impurity levels on nonlinear absorption of light in GaAs. Fiz. Tekh. Poluprov. **11(2)**, 415–417 (1977) [In Russian, English trans.: Sov. Phys. - Semicond. **11(2)**, 239–240 (1977)].
[45] I.B. Zotova, Y.J. Ding: Spectral two-photon absorption in the range of 1.3–1.75 μm for GaAs. In: *Conference on Lasers and Electrooptics CLEO/QELS 2003, Technical Digest* (OSA, Washington DC, 2003), paper CTuM21.
[46] R. DeSalvo, M. Sheik-Bahae, A.A. Said, D.J. Hagan, E.W. Van Stryland: Z-scan measurements of the anisotropy of nonlinear refraction and absorption in crystals. Opt. Lett. **18(3)**, 194–196 (1993).
[47] E.W. van Stryland, H. Vanherzeele, M.A. Woodall, M.J. Soileau, A.L. Smirl, S. Guha, T.F. Boggess: Two photon absorption, nonlinear refraction, and optical limiting in semiconductors. Opt. Eng. **24(4)**, 613–623 (1985).
[48] A.A. Said, M. Sheik-Bahae, D.J. Hagan, T.H. Wei, J. Wang, J. Young, E.W. van Stryland: Determination of bound-electronic and free-carrier nonlinearities in ZnSe, GaAs, CdTe, and ZnSe. J. Opt. Soc. Am. B **9(3)**, 405–414 (1992).
[49] J.M. Ralston, R.K. Chang: Nd:laser induced absorption in semiconductors and aqueous $PrCl_3$ and $NdCl_3$. Opto-electron. **1(4)**, 182–188 (1969).
[50] D.T.F. Marple: Refractive index of GaAs. J. Appl. Phys. **35(4)**, 1241–1242 (1964).
[51] O.A. Kolosovskii, L.N. Ustimenko: Measurement of the temperature coefficient of the refractive index of infrared materials using a CO_2 laser. Opt. Spektrosk. **33(4)**, 781–782 (1972) [In Russian, English trans.: Opt. Spectrosc. USSR **33(4)**, 430–431 (1972)].
[52] M. Sheik-Bahae, D.C. Hutchings, D.J. Hagan, E.W. van Stryland: Dispersion of bound electron nonlinear refraction in solids. IEEE J. Quant. Electr. **27(6)**, 1296–1309 (1991).
[53] N. Suzuki, K. Tada: Elastooptic and electrooptic properties of GaAs. Jpn. J. Appl. Phys. **23(8)**, 1011–1016 (1984).

[54] A. Yariv, P. Yeh: *Optical Waves in Crystals*. (John Wiley & Sons, New York, 1984).
[55] M. Sugie, K. Tada: Measurements of the linear electrooptic coefficients and analysis of the nonlinear susceptibilities in cubic GaAs and hexagonal CdS. Jpn. J. Appl. Phys. **15(3)**, 421–431 (1976).
[56] I.P. Kaminow: Measurements of the electrooptic effect in CdS, ZnTe and GaAs at 10.6 μm. IEEE J. Quant. Electr. **QE-4(1)**, 23–26 (1968).
[57] E.H. Turner, I.P. Kaminow: Electro-optic effect in GaAs. J. Opt. Soc. Am. **53(4)**, 523 (1963).
[58] I.P. Kaminow: Tables of Linear Electrooptic Coefficients. In: *CRC Handbook of Laser Science and Technology, Vol. III, Optical Materials: Part 2*, ed. by M.J. Weber (CRC Press, Boca Raton, 1986), pp. 253–278.
[59] J.L. Smith, G.A. Tanton: Intense laser flux effect on GaAs. Appl. Phys. **4(4)**, 313–315 (1974).
[60] I. Shoji, T. Kondo, A. Kitamoto, M. Shirane, R. Ito: Absolute scale of second-order nonlinear-optical coefficients. J. Opt. Soc. Am. B **14(9)**, 2268–2294 (1997).
[61] D.A. Roberts: Simplified characterization of uniaxial and biaxial nonlinear optical crystals: a plea for standardization of nomenclature and conventions. IEEE J. Quant. Electr. **28(10)**, 2057–2074 (1992).
[62] M. Bertolotti, F. de Pasquale, P. Marietti, D. Sette, G. Vitali: Laser damage on semiconductor surfaces. J. Appl. Phys. **38(10)**, 4088–4090 (1967).
[63] M. Birnbaum, T.L. Stocker: Reflectivity enhancement of semiconductors by Q-switched ruby lasers. J. Appl. Phys. **39(13)**, 6032–6036 (1968).
[64] J.L. Smith: Surface damage of GaAs from 0.694 and 1.06 μm laser radiations. J. Appl. Phys. **43(8)**, 3399–3402 (1972).
[65] A.M. Bonch-Bruevich, V.P. Kovalev, G.S. Romanov, Y.A. Imas, M.N. Libenson: The change in reflectivity properties of some semiconductors upon laser exposure. Zh. Tekh. Fiz. **38(4)**, 677–685 (1968) [In Russian, English trans.: Sov. Phys. - Tech. Phys. **13(4)**, 507–513 (1968)].
[66] C.L. Sam: Laser damage of GaAs and ZnTe at 1.06 μm. Appl. Opt. **12(4)**, 878–879 (1973).
[67] A. Garg, A. Kapoor, K.N. Tripathi: Laser-induced damage in GaAs. Opt. Laser Technol. **35(1)**, 21–24 (2003).
[68] D.C. Hanna, B. Luther-Davies, H.N. Rutt, R.C. Smith, C.R. Stanley: Q-switched laser damage of infrared nonlinear materials. IEEE J. Quant. Electr. **QE-8(3)**, 317–324 (1972).
[69] R. Tsu, J.E. Baglin, G.J. Lasher, J.C. Tsang: Laser-induced recrystallization and damage in GaAs. Appl. Phys. Lett. **34(2)**, 153–155 (1979).
[70] A.P. Singh, A. Kapoor, K.N. Tripathi, G.R. Kumar: Thermal and mechanical damage of GaAs in picosecond regime. Opt. Laser Technol. **33(6)**, 363–369 (2001).
[71] R.M. Wood: *Laser Damage in Optical Materials* (Adam Hilger, Bristol, 1986).
[72] R.D. Peterson, K.L. Schepler, J.L. Brown, P.G. Schunemann: Damage properties of $ZnGeP_2$ at 2 μm. J. Opt. Soc. Am. B **12(11)**, 2142–2146 (1995).
[73] N.P. Datskevich, N.V. Karlov, G.P. Kuzmin, A.A. Nesterenko, E.V. Sisakyan: The resistance of infrared optical materials to pulsed CO_2 laser light in large irradiated spots. Kratkie Soobshch. Fiz. **No. 6**, 3–7 (1983) [In Russian, English trans.: Sov. Phys. - Lebedev Institute Reports **No. 6**, 1–5 (1983)].
[74] A. Szilagyi, A. Hordvik, H. Schlossberg: A quasi-phase-matching technique for efficient optical mixing and frequency doubling. J. Appl. Phys. **47(5)**, 2025–2032 (1976).
[75] D.E. Thompson, J.D. McMullen, D.B. Anderson: Second-harmonic generation in GaAs "stack of plates" using high-power CO_2 laser radiation. Appl. Phys. Lett. **29(2)**, 113–115 (1976).

[76] L. Gordon, G.L. Woods, R.C. Eckardt, R.R. Route, R.S. Feigelson, M.M. Fejer, R.L. Byer: Diffusion-bonded stacked GaAs for quasi-phase-matched second-harmonic generation of a carbon dioxide laser. Electron. Lett. **29(22)**, 1942–1944 (1993).

[77] E. Lallier, M. Brevignon, J. Lehoux: Efficient second-harmonic generation of a CO_2 laser with quasi-phase-matched GaAs crystal. Opt. Lett. **23(19)**, 1511–1513 (1998).

[78] L. Becouarn, E. Lallier, M. Brevignon, J. Lehoux: Cascaded second-harmonic and sum-frequency generation of a CO_2 laser by use of a single quasi-phase-matched GaAs crystal. Opt. Lett. **23(19)**, 1508–1510 (1998).

[79] A. Romann, M.W. Sigrist: Photoacoustic gas sensing employing fundamental and frequency-doubled radiation of a continuously tunable high-pressure CO_2 laser. Appl. Phys. B **75(2–3)**, 377–383 (2002).

[80] D. Zheng, L.A. Gordon, Y.S. Wu, R.S. Feigelson, M.M. Fejer, R.L. Byer, K.L. Vodopyanov: 16-μm infrared generation by difference-frequency mixing in diffusion-bonded-stacked GaAs. Opt. Lett. **23(13)**, 1010–1012 (1998).

6

Newly Developed and Perspective Crystals

This chapter describes 19 newly developed and perspective nonlinear optical materials such as bismuth triborate (BIBO), potassium aluminum borate (KABO), potassium fluoroboratoberyllate (KBBF), gadolinium calcium oxyborate (GdCOB), yttrium calcium oxyborate (YCOB), lithium tetraborate (LB4), lithium thioindate (LIS), and others.

6.1 BiB_3O_6, Bismuth Triborate (BIBO)

Negative biaxial crystal: $2V_z = 53.5°$ at $\lambda = 0.53975\,\mu m$
Molecular mass: 337.407
Specific gravity: 4.896 g/cm^3 [1]; 5.01 g/cm^3 [2]
Point group: 2
Lattice constants:
$a = 7.116 \pm 0.002$ Å [2]; 7.1203 ± 0.0007 Å [1]
$b = 4.993 \pm 0.002$ Å [2]; 4.9948 ± 0.0007 Å [1]
$c = 6.508 \pm 0.003$ Å [2]; 6.5077 ± 0.0007 Å [1]
$\beta = 105.62°$ [2]; $105.59°$ [1]
Assignment of dielectric and crystallographic axes:
$X \| b$, the axes a and c lie in YZ plane, the angle between them is $\beta = 105.6°$, the angle between the axes Z and a is about 31° (slightly depends on wavelength and/or temperature), the angle between the axes Y and c is 15.2° [7]
Mohs hardness: 5–5.5
Melting point: 999 K [3], 981 ± 5 K [1]

Mean values of linear thermal expansion coefficient α_t (in 10^{-6} K^{-1})

T [K]	α_{11} ($\|a$)	α_{22} ($\|b$)	α_{33} ($\|c$)	$\alpha_{13} = \alpha_{31}$	Ref.
173–573	-28.1 ± 0.5	53.7 ± 0.5	8.5 ± 0.5	-5.5 ± 0.5	[4]
298–573	-25.6	50.4	7.7	-5.33	[5]

Specific heat capacity c_p at $P = 0.101325$ MPa [6]

T [K]	c_p [J/kgK]
323	500
373	540
423	570
473	590

Transparency range at 0.5 level for 0.1-cm-long BIBO crystal: 0.286–2.7 μm [7]
UV transmission cutoff is at 270 nm, IR transmission cutoff at 0.5 level for 0.47 cm long BIBO crystal is at 2.63 μm [1], [8].

Calculated values of refractive indices

λ [μm]	n_X	n_Y	n_Z
0.53975	1.78690	1.81846	1.96134
1.07950	1.75650	1.78309	1.91610

Note: In [9], the BIBO refractive indices at the same wavelengths with respect to vacuum are presented. The above-mentioned refractive indices were calculated using the dispersion relations given below.

Sellmeier equations (λ in μm, $T = 295$ K) [7]:

$$n_X^2 = 3.0722 + \frac{0.0324}{\lambda^2 - 0.0315} - 0.0133\,\lambda^2$$

$$n_Y^2 = 3.1669 + \frac{0.0372}{\lambda^2 - 0.0348} - 0.0175\,\lambda^2$$

$$n_Z^2 = 3.6525 + \frac{0.0511}{\lambda^2 - 0.0370} - 0.0226\,\lambda^2$$

Note: In [7], the BIBO dispersion relations with respect to vacuum are given. The above-mentioned Sellmeier equations (with respect to air) have been obtained from the authors of [7] by private communication.
Experimentally determined values of second-order nonlinear coefficient [7], [9]:

$d_{14}(1.0795\,\mu\text{m}) = (2.4 \pm 0.3)$ pm/V
$d_{16}(1.0795\,\mu\text{m}) = (2.8 \pm 0.2)$ pm/V
$d_{21}(1.0795\,\mu\text{m}) = (2.3 \pm 0.2)$ pm/V
$d_{22}(1.0795\,\mu\text{m}) = (2.53 \pm 0.08)$ pm/V
$d_{23}(1.0795\,\mu\text{m}) = (1.3 \pm 0.1)$ pm/V
$d_{25}(1.0795\,\mu\text{m}) = (2.3 \pm 0.2)$ pm/V
$d_{34}(1.0795\,\mu\text{m}) = (0.9 \pm 0.1)$ pm/V
$d_{36}(1.0795\,\mu\text{m}) = (2.4 \pm 0.3)$ pm/V

The $d_{14}, d_{16}, d_{21}, d_{22}, d_{25}, d_{36}$ coefficients are of the same sign, which is opposite to that of d_{23}, d_{34} coefficients [7], [9].

Experimental values of phase-matching angles

Interacting wavelengths [μm]	θ_{pm} [deg]	Ref.
YZ plane, $\phi = 90°$		
SHG, $o + o \Rightarrow e$		
$1.0642 \Rightarrow 0.5321$	11.1	[6], [8]
	168.9	[6], [8]
$0.946 \Rightarrow 0.473$	161.7	[10]

Note: Due to the BIBO symmetry (point group 2), the spatial distribution of d_{eff} can be fully described by choosing two independent neighbor quadrants, for example, ($0° < \theta < 90°$, $0° < \phi < 90°$) and ($90° < \theta < 180°$, $0° < \phi < 90°$).

Calculated values of effective second-order nonlinear coefficient for some specific phase-matching directions (SHG, type I, $1.0795 \Rightarrow 0.53975\,\mu m$) in BIBO crystal [7], [9]

Phase-matching direction	d_{eff} [pm/V]
$\theta \approx 10°$, $\phi = 90°$	2.3
$\theta \approx 170°$, $\phi = 90°$	3.2

See the note to the previous table.

Calculated values of effective second-order nonlinear coefficient for the specific phase-matching direction (SHG, type I, $0.946 \Rightarrow 0.473\,\mu m$) in BIBO crystal [10]

Phase-matching direction	d_{eff} [pm/V]
$\theta = 161.7°$, $\phi = 90°$	3.34

Experimental values of SHG conversion efficiency (SHG, type I, $1.0642 \Rightarrow 0.5321\,\mu m$, $I = 3.6\,GW/cm^2$) for some specific phase-matching directions [6], [8]

Phase-matching direction	Crystal length [cm]	SHG conversion efficiency [%]
$\theta = 11.1°$, $\phi = 90°$ (*YZ* plane)	0.47	58
$\theta = 168.9°$, $\phi = 90°$ (*YZ* plane)	0.24	67.7

See the note to table above.

Laser-induced bulk damage threshold

λ [μm]	τ_p [ns]	I_{thr} [GW/cm^2]	Ref.
1.064	0.035	>4.7	[8]
		>5	[1]

About the crystal

The newly discovered monoclinic nonlinear crystal BIBO possesses a rather high effective second-order nonlinearity value that exceeds that of BBO and LBO by

1.7 and 4 times, respectively. Therefore, it could find a wide application for SHG of continuous-wave radiation. In [11], 2.8 W of CW blue light ($\lambda = 473$ nm) was generated in BIBO via SHG of a Nd:YAG laser ($\lambda = 946$ nm, P = 4.6 W), end-pumped by 21-W laser diode radiation at 808 nm. In [10], the SHG of the signal wave of a quasi-continuous OPO (777–1036 nm, 10 kHz, 50 ns) was performed in BIBO; as a result, the tuning in the UV range 450–494 nm was achieved with maximum blue output of 1.3 W at 470 nm.

References

[1] B. Teng, J. Wang, Z. Wang, H. Jiang, X. Hu, R. Song, H. Liu, Y. Liu, J. Wei, Z. Shao: Growth and investigation of a new nonlinear optical crystal: bismuth borate BiB_3O_6. J. Cryst. Growth **224(3–4)**, 280–283 (2001).

[2] R. Fröhlich, L. Bohaty, J. Liebertz: Die Kristallstruktur von Wismutborat, BiB_3O_6. Acta Crystallogr. C **40(3)**, 343–344 (1984) [In German].

[3] P. Becker, J. Liebertz, L. Bohaty: Top-seeded growth of bismuth triborate, BiB_3O_6. J. Cryst. Growth **203(1–2)**, 149–155 (1999).

[4] P. Becker, L. Bohaty: Thermal expansion of bismuth triborate. Cryst. Res. Technol. **36(11)**, 1175–1180 (2001).

[5] B. Teng, Z. Wang, H. Jiang, X. Cheng, H. Liu, X. Hu, S. Dong, J. Wang, Z. Shao: Anisotropic thermal expansion of BiB_3O_6. J. Appl. Phys. **91(6)**, 3618–3620 (2002).

[6] B. Teng, J. Wang, Z. Wang, X. Hu, H. Jiang, H. Liu, X. Cheng, S. Dong, Y. Liu, Z. Shao: Crystal growth, thermal and optical performance of BiB_3O_6. J. Cryst. Growth **233(1–2)**, 282–286 (2001).

[7] H. Hellwig, J. Liebertz, L. Bohaty: Linear optical properties of the monoclinic bismuth borate BiB_3O_6. J. Appl. Phys. **88(1)**, 240–244 (2000).

[8] Z. Wang, B. Teng, K. Fu, X. Xu, R. Song, C. Du, H. Jiang, J. Wang, Y. Liu, Z. Shao: Efficient second harmonic generation of pulsed laser radiation in BiB_3O_3 (BIBO) crystal with different phase matching directions. Opt. Commun. **202(1–3)**, 217–220 (2002).

[9] H. Hellwig, J. Liebertz, L. Bohaty: Exceptional large nonlinear optical coefficients in the monoclinic bismuth borate BiB_3O_6 (BIBO). Solid State Commun. **109(4)**, 249–251 (1999).

[10] Y. Bi, H.-B. Zhang, Z.-P. Sun, Z.-R.-G.-T. Bao, H.-Q. Li, Y.-P. Kong, X.-C. Lin, G.-L. Wang, J. Zhang, W. Hou, R.-N. Li, D.-F. Cui, Z.-Y. Xu, L.-W. Song, P. Zhang, J.-F. Cui, Z.-W. Fan: High-power blue light generation by external frequency doubling of an optical parametric oscillator. Chin. Phys. Lett. **20(11)**, 1957–1959 (2003).

[11] C. Czeranowsky, E. Heumann, G. Huber: All-solid-state continuous-wave frequency-doubled Nd:YAG–BIBO laser with 2.8-W output power at 473 nm. Opt. Lett. **28(6)**, 432–434 (2003).

6.2 $K_2Al_2B_2O_7$, Potassium Aluminum Borate (KABO)

Negative uniaxial crystal: $n_o > n_e$
Molecular mass: 265.775
Specific gravity: 2.47 g/cm^3 [1]
Point group: 32

Lattice constants:
$a = 8.530$ Å [2]; 8.55800 ± 0.00002 Å [3]; 8.5598 Å [4]; 8.5657 ± 0.0008 Å [5]; 8.5669 ± 0.0009 Å [6]
$c = 8.409$ Å [2]; 8.45576 ± 0.00003 Å [3]; 8.463 ± 0.001 Å [5]; 8.467 ± 0.001 Å [6]; 8.5048 Å [4]
Mohs hardness: ≈6 [7]; 5.5–6.5 [1]
Solubility in water: insoluble [1]
Melting point: 1383 K [1]

Mean value of linear thermal expansion coefficient [1]

T [K]	$\alpha_t \times 10^6$ [K^{-1}], $\parallel a$	$\alpha_t \times 10^6$ [K^{-1}], $\parallel c$
298–573	8.4	16.5

Specific heat capacity c_p at $P = 0.101325$ MPa [1]

T [K]	c_p [J/kgK]
321	1008.4
568	1390

Transparency range at "0" transmittance level: 0.18–3.6 μm [2]

Experimental values of refractive indices [2]

λ [μm]	n_o	n_e
0.4047	1.57022	1.49643
0.4078	1.56973	1.49600
0.4358	1.56571	1.49294
0.4861	1.56029	1.48887
0.4916	1.55982	1.48848
0.4962	1.55938	1.48816
0.5461	1.55572	1.48536
0.5780	1.55385	1.48398
0.5893	1.55320	1.48354
0.6234	1.55159	1.48234
0.6563	1.55029	1.48136
0.6943	1.54881	1.48033

Temperature derivative of refractive indices for temperature range 293–393 K and spectral range 0.193 μm $< \lambda <$ 1.3382 μm (in 10^{-5} K^{-1}) [8]:

$$\frac{dn_o}{dT} = 1.6101 + 0.0361\,\lambda$$

$$\frac{dn_e}{dT} = 1.9905 + \frac{0.0956}{\lambda} + \frac{0.0083}{\lambda^2} - \frac{0.0015}{\lambda^3}$$

Sellmeier equations (λ in μm, $0.193\,\mu\text{m} < \lambda < 1.3382\,\mu\text{m}$, $T = 293$ K) [8]:

$$n_o^2 = 2.3765 + \frac{0.01303}{\lambda^2 - 0.01852} - 0.01317\,\lambda^2$$

$$n_e^2 = 2.17367 + \frac{0.00950}{\lambda^2 - 0.01530} - 0.00832\,\lambda^2$$

Other dispersion relations are given in [2], [7], [9].
Expressions for the effective second-order nonlinear coefficient (Kleinman symmetry conditions are valid) [10]:

$d_{ooe} = d_{11} \cos\theta \cos 3\phi$

$d_{eoe} = d_{oee} = d_{11} \cos^2\theta \sin 3\phi$

Value of second-order nonlinear coefficient:
$d_{11}(1.064\,\mu\text{m}) = 0.45$ pm/V [2]; 0.47 pm/V [1]; 0.46 ± 0.04 pm/V [8]

Experimental values of phase-matching angle

Interacting wavelengths [μm]	θ_{exp} [deg]	Ref.
SHG, $o + o \Rightarrow e$		
$1.0642 \Rightarrow 0.5321$	27.3	[8]
$0.8 \Rightarrow 0.4$	33.7	[11]
$0.5321 \Rightarrow 0.26605$	57.2	[8], [12]
	58.1	[13]
	58.3	[3]
SFG, $o + o \Rightarrow e$		
$1.0642 + 0.5321 \Rightarrow 0.35473$	36.9	[12]
	37.2	[8]
$1.0642 + 0.26605 \Rightarrow 0.21284$	60.2	[8]
$1.0642 + 0.2358 \Rightarrow 0.1930$	68.9	[8], [9]
SHG, $e + o \Rightarrow e$		
$1.0642 \Rightarrow 0.5321$	39.3	[8]

Experimental values of internal angular, temperature, and spectral bandwidths

Interacting wavelengths [μm]	θ_{pm} [deg]	$\Delta\theta^{int}$ [deg]	ΔT [°C]	$\Delta\nu$ [cm^{-1}]	Ref.
SHG, $o + o \Rightarrow e$					
$1.0642 \Rightarrow 0.5321$	27.3		41.9		[8]
$0.8 \Rightarrow 0.4$	33.7	0.052 ± 0.017		9.4 ± 2.2	[11]
$0.5321 \Rightarrow 0.26605$	57.2		4.1		[8]
SFG, $o + o \Rightarrow e$					
$1.0642 + 0.5321 \Rightarrow 0.35473$	36.9	0.025			[12]
			13.2		[8]
$1.0642 + 0.26605 \Rightarrow 0.21284$	60.2		2.9		[8]
$1.0642 + 0.2358 \Rightarrow 0.193$	68.9	0.011	2.1		[9]
			2.2		[8]

Laser-induced damage threshold

λ [μm]	τ_p [ns]	I_{thr} [GW/cm^2]	Ref.	Note
0.532	0.035	>1.3	[3]	
0.8	0.00005	>170	[11]	5 kHz
1.064	10	>1.0	[2]	10 Hz
		15	[2]	1 pulse

About the crystal

This new nonlinear borate crystal is nonhygroscopic and could easily be cut and polished by standard procedure. Though the second-order nonlinear coefficient in KABO is smaller than that of BBO and CLBO, nevertheless, this material could be useful for the realization of three-wave interactions in the UV range. In [8], 0.22 W of quasi-CW output ($\lambda = 193$ nm) was obtained in a 0.7-cm KABO crystal ($\theta = 68.9°$, $\phi = 0°$) by SFG of a Nd:YAG laser radiation ($P = 18$ W, $\Delta f = 10$ kHz) and the second harmonic of a Nd:YAG laser pumped OPO.

References

[1] C. Zhang, J. Wang, X. Cheng, X. Hu, H. Jiang, Y. Liu, C. Chen: Growth and properties of $K_2Al_2B_2O_7$ crystal. Opt. Mater. **23(1–2)**, 357–362 (2003).

[2] N. Ye, W. Zeng, J. Jiang, B. Wu, C. Chen, B. Feng, X. Zhang: New nonlinear optical crystal $K_2Al_2B_2O_7$. J. Opt. Soc. Am. B **17(5)**, 764–768 (2000).

[3] C. Zhang, J. Wang, X. Hu, H. Jiang, Y. Liu, C. Chen: Growth of large $K_2Al_2B_2O_7$ crystals. J. Cryst. Growth **235(1–4)**, 1–4 (2002).

[4] C. Zhang, J. Wang, X. Hu, H. Liu, J. Wei, Y. Liu, Y. Wu, C. Chen: Top-seeded growth of $K_2Al_2B_2O_7$. J. Cryst. Growth **231(4)**, 439–441 (2001).

[5] Z. Hu, T. Higashiyama, M. Yoshimura, Y.K. Yap, Y. Mori, T. Sasaki: A new nonlinear optical borate crystal $K_2Al_2B_2O_7$ (KAB). Jpn. J. Appl. Phys. **37(10A)**, L1093–L1094 (1998).

[6] Z. Hu, Y. Mori, T. Higashiyama, M. Yoshimura, Y.K.Yap, Y. Kagebayashi, T. Sasaki: $K_2Al_2B_2O_7$—a new nonlinear optical crystal. Proc. SPIE **3556**, 156–161 (1998).

[7] N. Ye, W. Zeng, J. Jiang, B. Wu, C. Chen, B. Feng, X. Zhang: New nonlinear optical crystal $K_2Al_2B_2O_7$: errata. J. Opt. Soc. Am. B **18(1)**, 122 (2001).

[8] N. Umemura, M. Ando, K. Suzuki, E. Takaoka, K. Kato, Z.-G. Hu, M. Yoshimura, Y. Mori, T. Sasaki: 200-mW-average power ultraviolet generation at 0.193 μm in $K_2Al_2B_2O_7$. Appl. Opt. **42(15)**, 2716–2719 (2003).

[9] Z.-G. Hu, M. Yoshimura, Y. Mori, T. Sasaki, K. Kato: Growth of $K_2Al_2B_2O_7$ crystal for UV light generation. Opt. Mater. **23(1–2)**, 353–356 (2003).

[10] J.E. Midwinter, J. Warner: The effects of phase matching method and of uniaxial crystal symmetry on the polar distribution of second-order non-linear optical polarization. Brit. J. Appl. Phys. **16(11)**, 1135–1142 (1965).

[11] P. Kumbhakar, S. Adachi, Z.-G. Hu, M. Yoshimura, Y. Mori, T. Sasaki, T. Kobayashi: Generation of tunable near-UV laser radiation by type-I second-harmonic generation in a new crystal, $K_2Al_2B_2O_7$ (KABO). Jpn. J. Appl. Phys. **42(10B)**, L1255–L1258 (2003).

[12] Z. Hu, N. Ushiyama, Y.K. Yap, M. Yoshimura, Y. Mori, T. Sasaki: The crystal growth and nonlinear optical properties of $K_2Al_2B_2O_7$. J. Cryst. Growth **237–239**, 654–657 (2002).
[13] J. Lu, G. Wang, Z. Hu, C. Chen, J. Wang, C. Zhang, Y. Liu: Efficient 266 nm ultraviolet beam generation in $K_2Al_2B_2O_7$ crystal. Chin. Phys. Lett. **19(5)**, 680–681 (2002).

6.3 $KBe_2BO_3F_2$, Potassium Fluoroboratoberyllate (KBBF)

Negative uniaxial crystal: $n_o > n_e$
Molecular mass: 153.927
Point group: 32
Lattice constants [1]:
$a = 4.427 \pm 0.004$ Å
$c = 18.744 \pm 0.009$ Å
Mohs hardness: ≈0, splits easily along the [001] plane [2]
Melting temperature: 1373 K [3]
Transparency range at "0" transmittance level: 0.155–3.7 μm [2]

Experimental values of refractive indices [4]

λ [μm]	n_o	n_e
0.4047	1.487	1.410
0.4358	1.485	1.408
0.4861	1.482	1.406
0.5461	1.479	1.403
0.5893	1.479	1.401
0.6328	1.478	1.400
0.6563	1.477	1.400

Sellmeier equations (λ in μm) [2], [4]:

$$n_o^2 = 1 + \frac{1.169725\,\lambda^2}{\lambda^2 - 0.0062400} - 0.009904\,\lambda^2$$

$$n_e^2 = 1 + \frac{0.956611\,\lambda^2}{\lambda^2 - 0.0061926} - 0.027849\,\lambda^2$$

Expressions for the effective second-order nonlinear coefficient (Kleinman symmetry conditions are valid) [5]:
$d_{ooe} = d_{11} \cos\theta \cos 3\phi$
$d_{eoe} = d_{oee} = d_{11} \cos^2\theta \sin 3\phi$
Absolute value of second-order nonlinear coefficient:
$d_{11}(1.0642\,\mu\text{m}) = 0.49$ pm/V [6]

Experimental values of phase-matching angle

Interacting wavelengths [μm]	θ_{exp} [deg]	Ref.
SHG, $o + o \Rightarrow e$		
0.345 ⇒ 0.1725	~71	[7]

Interacting wavelengths [μm]	θ_{exp} [deg]	Ref.
0.3546 ⇒ 0.1773	~66.2	[7]
0.3695 ⇒ 0.18475	61	[2]
0.3743 ⇒ 0.18715	59.4	[2]
0.3847 ⇒ 0.19235	56.8	[2]
0.41 ⇒ 0.205	51.5	[2]
0.44 ⇒ 0.22	46	[2]
0.46 ⇒ 0.23	44	[2]
0.48 ⇒ 0.24	41.7	[2]
0.5 ⇒ 0.25	39.6	[2]
0.532 ⇒ 0.266	36.2	[2]
0.55 ⇒ 0.275	34.9	[2]
0.589 ⇒ 0.2945	32.5	[2]
0.6 ⇒ 0.3	32.1	[2]
0.68 ⇒ 0.34	27.6	[2]
0.77 ⇒ 0.385	25.1	[2]
0.85 ⇒ 0.425	23.1	[2]
0.9 ⇒ 0.45	22	[2]
0.95 ⇒ 0.425	21	[2]
1.064 ⇒ 0.532	20.2	[2]
1.342 ⇒ 0.671	18.6	[2]

Experimental values of internal angular bandwidth

Interacting wavelengths [μm]	θ_{pm} [deg]	$\Delta\theta^{int}$ [deg]	Ref.
SHG, $o + o \Rightarrow e$			
0.41 ⇒ 0.205	51.5	0.0119	[2]
0.44 ⇒ 0.22	46	0.0127	[2]
0.46 ⇒ 0.23	44	0.0127	[2]
0.48 ⇒ 0.24	41.7	0.0139	[2]
0.5 ⇒ 0.25	39.6	0.0143	[2]
0.532 ⇒ 0.266	36.2	0.0166	[2]
		0.0152	[8]
0.589 ⇒ 0.2945	32.5	0.0244	[2]
0.9 ⇒ 0.45	22.0	0.0572	[2]
1.064 ⇒ 0.532	20.2	0.0592	[2]
1.342 ⇒ 0.671	18.6	0.0644	[2]

Laser-induced damage threshold

λ [μm]	τ_p [ns]	I_{thr} [GW/cm^2]	Ref.	Note
0.3546	0.01	>0.04	[7]	80 MHz
0.4	0.00005	>17	[9]	1 kHz
0.532	0.035	>4.2	[10]	
		>11.6	[8]	10 Hz

λ [μm]	τ_p [ns]	I_{thr} [GW/cm^2]	Ref.	Note
	0.03	>7	[11]	
1.064	8	>5.0	[2]	along *c*

About the crystal

KBBF is an outstanding nonlinear material that allows generation of deep-UV light. In [7], the radiation at 172.5 nm was obtained by direct SHG and at 163.3 nm by SFG. The main disadvantage of KBBF is its plate-like nature, which makes it very difficult to grow crystals thicker than a millimeter. To overcome the problem of cutting such thin crystals, the special prism-coupling technique was proposed [8], [9], [11].

References

[1] C. Chen, Y. Wang, Y. Xia, B. Wu, D. Tang, K. Wu, Z. Wenrong, L. Yu, L. Mei: New development of nonlinear optical crystals for the ultraviolet region with molecular engineering approach. J. Appl. Phys. **77(6)**, 2268–2272 (1995).
[2] B. Wu, D. Tang, N. Ye, C. Chen: Linear and nonlinear optical properties of the $KBe_2BO_3F_2$ (KBBF) crystal. Opt. Mater. **5(1–2)**, 105–109 (1996).
[3] D. Tang, Y. Xia, B. Wu, C. Chen: Growth of a new UV nonlinear optical crystal: $KBe_2(BO_3)F_2$. J. Cryst. Growth **222(1–2)**, 125–129 (2001).
[4] C. Chen, Z. Xu, D. Deng, J. Zhang, G.K.L. Wong, B. Wu, N. Ye, D. Tang: The vacuum ultraviolet phase-matching characteristics of nonlinear optical $KBe_2BO_3F_2$ crystal. Appl. Phys. Lett. **68(21)**, 2930–2932 (1996).
[5] J.E. Midwinter, J. Warner: The effects of phase matching method and of uniaxial crystal symmetry on the polar distribution of second-order non-linear optical polarization. Brit. J. Appl. Phys. **16(11)**, 1135–1142 (1965).
[6] G. Wang, C. Zhang, C. Chen, Z. Xu, J. Wang: Determination of nonlinear optical coefficients of $KBe_2BO_3F_2$ crystals. Chin. Phys. Lett. **20(2)**, 243–245 (2003).
[7] T. Togashi, T. Kanai, T. Sekikawa, S. Watanabe, C. Chen, C. Zhang, Z. Xu, J. Wang: Generation of vacuum-ultraviolet light by an optically contacted, prism-coupled $KBe_2BO_3F_2$ crystal. Opt. Lett. **28(4)**, 254–256 (2003).
[8] G. Wang, C. Zhang, C. Chen, A. Yao, J. Zhang, Z. Hu, J. Wang: High-efficiency 266-nm output of a $KBe_2BO_3F_2$ crystal. Appl. Opt. **42(21)**, 4331–4334 (2003).
[9] C. Chen, J. Lu, T. Togashi, T. Suganuma, T. Sekikawa, S. Watanabe, Z. Xu, J. Wang: Second-harmonic generation from a $KBe_2BO_3F_2$ crystal in the deep ultraviolet. Opt. Lett. **27(8)**, 637–639 (2002).
[10] J. Lu, G. Wang, Z. Xu, C. Chen, J. Wang, C. Zhang, Y. Liu: High-efficiency fourth-harmonic generation of KBBF crystal. Opt. Commun. **200(1–6)**, 415–418 (2001).
[11] C. Chen, J. Lu, G. Wang, Z. Xu, J. Wang, C. Zhang, Y. Liu: Deep ultraviolet harmonic generation with $KBe_2BO_3F_2$ crystal. Chin. Phys. Lett. **18(8)**, 1081 (2001).

6.4 $BaAlBO_3F_2$, Barium Aluminum Fluoroborate (BABF)

Negative uniaxial crystal: $n_o > n_e$
Molecular mass: 261.117
Point group: $\bar{6}$

Lattice constants [1]:
$a = 4.8879 \pm 0.0006$ Å
$c = 9.403 \pm 0.001$ Å
Transparency range at "0" transmittance level: 0.165 to >1.6 μm [2]

Experimental values of refractive indices [2]

λ [μm]	n_o	n_e	λ [μm]	n_o	n_e
0.230	1.7171	1.6604	0.683	1.6266	1.5834
0.244	1.7045	1.6492	0.733	1.6253	1.5821
0.266	1.6886	1.6364	0.783	1.6240	1.5810
0.300	1.6719	1.6219	0.833	1.6227	1.5805
0.355	1.6548	1.6073	0.933	1.6214	1.5791
0.400	1.6464	1.6004	1.064	1.6193	1.5775
0.440	1.6413	1.5957	1.150	1.6180	1.5770
0.488	1.6369	1.5917	1.250	1.6170	1.5764
0.514	1.6346	1.5901	1.350	1.6154	1.5756
0.532	1.6336	1.5890	1.450	1.6141	1.5743
0.580	1.6307	1.5866	1.547	1.6130	1.5740
0.633	1.6284	1.5850			

Sellmeier equations (λ in μm) [2]:

$$n_o^2 = 2.6213 + \frac{0.01353}{\lambda^2 - 0.01204} - 0.01055\,\lambda^2$$

$$n_e^2 = 2.4833 + \frac{0.01178}{\lambda^2 - 0.00996} - 0.00447\,\lambda^2$$

Expressions for the effective second-order nonlinear coefficient (Kleinman symmetry conditions are valid) [3]:

$$d_{ooe} = d_{11}\cos\theta\cos 3\phi - d_{22}\cos\theta\sin 3\phi$$
$$d_{eoe} = d_{oee} = d_{11}\cos^2\theta\sin 3\phi + d_{22}\cos^2\theta\cos 3\phi$$

Experimental values of phase-matching angle [2]

Interacting wavelengths [μm]	θ_{exp} [deg]
SHG, $o + o \Rightarrow e$	
1.064 ⇒ 0.532	34.1

About the crystal

It was found [2] that in powder state, BABF produces twice as much second-harmonic power than KDP.

References

[1] Z.-G. Hu, M. Yoshimura, Y. Mori, T. Sasaki: Growth of a new nonlinear optical crystal—$BaAlBO_3F_2$. J. Cryst. Growth **260(3–4)**, 287–290 (2004).

[2] Z.-G. Hu, M. Yoshimura, K. Muramatsu, Y. Mori, T. Sasaki: A new nonlinear optical crystal—$BaAlBO_3F_2$ (BABF). Jpn. J. Appl. Phys. **41(10B)**, L1131–L1133 (2002).
[3] J.E. Midwinter, J. Warner: The effects of phase matching method and of uniaxial crystal symmetry on the polar distribution of second-order non-linear optical polarization. Brit. J. Appl. Phys. **16(11)**, 1135–1142 (1965).

6.5 $La_2CaB_{10}O_{19}$, Lanthanum Calcium Borate (LCB)

Positive biaxial crystal: $2V_z = 9.7°$ at $\lambda = 0.5321\,\mu m$
Molecular mass: 729.978
Specific gravity (calculated): $3.665\,g/cm^3$ [1]
Point group: 2
Lattice constants:
$a = 11.043 \pm 0.003$ Å [1]; 11.056 Å [2]
$b = 6.563 \pm 0.002$ Å [1]; 6.577 Å [2]
$c = 9.129 \pm 0.002$ Å [1]; 9.119 Å [2]
Assignment of dielectric and crystallographic axes [3]:
$Y \| b$, the axes a and c lie in XZ plane, the angle between them is $\beta = 91.47°$, the angle between the axes Z and a is 46.03°, the angle between the axes X and c is 47.5°. Similar assignment is given in [4].
Mohs hardness: 6.5 [1]
Melting point: 1338 K [1]
Transparency range at 0.5 level: 0.185–3.0 μm [3]; 0.28–2.45 μm [4]
Sellmeier equations (λ in μm) [3]:

$$n_X^2 = 2.78122 + \frac{0.0163186}{\lambda^2 - 0.0146002} - 0.0162299\,\lambda^2$$

$$n_Y^2 = 2.78533 + \frac{0.0151688}{\lambda^2 - 0.0206079} - 0.0155475\,\lambda^2$$

$$n_Z^2 = 2.96167 + \frac{0.0204238}{\lambda^2 - 0.0136912} - 0.0201447\,\lambda^2$$

Expressions for effective second-order nonlinear coefficient in the principal planes of LCB crystal (approximation of small walk-off angle, Kleinman symmetry conditions are valid, $d_{14} = d_{25} = d_{36}$, $d_{16} = d_{21}$ and $d_{23} = d_{34}$) [5]:

XY plane

$d_{ooe} = d_{23} \cos\phi$

$d_{eoe} = d_{oee} = d_{14} \sin 2\phi$

YZ plane

$d_{eeo} = d_{14} \sin 2\theta$

$d_{oeo} = d_{eoo} = d_{16} \cos\theta$

XZ plane, $\theta < V_z$

$d_{eoe} = d_{oee} = d_{16} \cos^2\theta + d_{23} \sin^2\theta \pm d_{14} \sin 2\theta$

XZ plane, $\theta > V_z$

$$d_{eeo} = d_{16}\cos^2\theta + d_{23}\sin^2\theta \pm d_{14}\sin 2\theta$$

Experimental value of effective second-order nonlinear coefficient for a specific phase-matching direction (SHG, type I, 1.0642 ⇒ 0.5321 μm) in LCB crystal [3]

Phase-matching direction	d_{eff} [pm/V]
$\theta = 34.3°$, $\phi = 7.7°$	1.05

Laser-induced bulk damage threshold [3]

λ [μm]	τ_p [ns]	I_{thr} [GW/cm^2]
1.064	0.035	>8

About the crystal

This newly developed monoclinic crystal possesses high hardness and medium nonlinearity, it is also non-hygroscopic [2]. Shortest obtainable SHG wavelength is at 288 nm [4].

References

[1] Y. Wu, J. Liu, P. Fu, F. Guo, G. Zhao, J. Qin, C. Chen: A new class of nonlinear optical crystals $R_2CaB_{10}O_{19}$ (RCB). Proc. SPIE **3556**, 8–13 (1998).
[2] X.W. Xu, T.C. Chong, G.Y. Zhang, S.D. Cheng, M.H. Li, C.C. Phua: Growth and optical properties of a new nonlinear optical lanthanum borate crystal. J. Cryst. Growth **237–239**, 649–653 (2002).
[3] G. Wang, J. Lu, D. Cui, Z. Xu, Y. Wu, P. Fu, X. Guan, C. Chen: Efficient second harmonic generation in a new nonlinear $La_2CaB_{10}O_{19}$ crystal. Opt. Commun. **209(4–6)**, 481–484 (2002).
[4] Y. Wu, P. Fu, F. Zheng, S. Wan, X. Guan: Growth of a nonlinear optical crystal $La_2CaB_{10}O_{19}$ (LCB). Opt. Mater. **23(1–2)**, 373–375 (2003).
[5] B.V. Bokut: Optical mixing in biaxial crystals. Zh. Prikl. Spektrosk. **7(4)**, 621–624 (1967) [In Russian, English trans.: J. Appl. Spectrosc. **7(4)**, 425–429 (1967)].

6.6 $GdCa_4O(BO_3)_3$, Gadolinium Calcium Oxyborate (GdCOB)

Negative biaxial crystal: $2V_Z = 120.7°$ at $\lambda = 0.546\,\mu m$ [1], [2]
Molecular mass: 509.986
Specific gravity: 3.736 g/cm^3 (calculated) [3]
Point group: *m*
Lattice constants:

$a = 8.106 \pm 0.002$ Å [1]; 8.095 ± 0.007 Å [4]; 8.0937 Å [5]; 8.098 ± 0.002 Å [6]

$b = 16.028 \pm 0.003$ Å [1]; 16.018 ± 0.006 Å [4]; 16.013 Å [5]; 16.019 ± 0.006 Å [6]
$c = 3.557 \pm 0.001$ Å [1]; 3.558 ± 0.008 Å [4]; 3.5579 Å [5]; 3.559 ± 0.007 Å [6]
$\beta = 101.25°$ [1]; $101.26° \pm 0.01°$ [4]; 101.27° [5], [6]

Assignment of dielectric and crystallographic axes:
$Y \| b$, the axes a and c lie in XZ plane, the angle between them is $\beta = 101.27°$, the angle between the axes Z and a is 27.2°, the angle between the axes X and c is 16.2° [7], [8]. A slightly different assignment: $(a, Z) = 26°$, $(c, X) = 15°$, was reported earlier [1], [2].
Mohs hardness: 6.5 [9]
Knoop hardness: 550–715 kg/mm^2 [2]
Melting point: 1753 K [4], [5]; 1756 K (congruent melting) [10]

Mean value of linear thermal expansion coefficient

T [K]	$\alpha_t \times 10^6$ [K^{-1}], $\|a$	$\alpha_t \times 10^6$ [K^{-1}], $\|b$	$\alpha_t \times 10^6$ [K^{-1}], $\|c$	Ref.
293–1133	10.2	8.3	14.3	[11]
293–1273	10.35	7.78	13.10	[6]

Thermal conductivity coefficient at $T = 293$ K

T [K]	κ [W/mK], $\|X$	κ [W/mK], $\|Y$	κ [W/mK], $\|Z$	Ref.
287	2.173			[12]
289			2.401	[12]
291		1.32		[12]
293	2.54	1.32	2.06	[9]
297	2.539			[12]
324	2.227			[12]
345			1.880	[12]
353	2.016			[12]
394			1.799	[12]
403		1.22		[12]
424	2.237			[12]
445			1.807	[12]
474	2.277			[12]
496			1.852	[12]
525			1.789	[12]
526	2.009			[12]
545		1.18		[12]

High transmittance range: 0.32–2.6 μm [13]
In the UV transparency range 0.2–0.32 μm there are three groups of sharp absorption lines centered around 0.25, 0.277, and 0.31 μm [2].
In the IR transparency range 2.6–3.7 μm there are absorption bands at 2.72, 2.9, and 3.25 μm [2], [13].

Experimental values of refractive indices [2]

λ [μm]	n_X	n_Y	n_Z	λ [μm]	n_X	n_Y	n_Z
0.4047	1.7209	1.7476	1.7563	0.5780	1.6966	1.7225	1.7310
0.4358	1.7142	1.7409	1.7493	0.5876	1.6960	1.7218	1.7303
0.4678	1.7089	1.7350	1.7436	0.6439	1.6923	1.7181	1.7265
0.4800	1.7068	1.7333	1.7418	0.6678	1.6910	1.7168	1.7250
0.5086	1.7033	1.7295	1.7379	0.7290	1.6879	1.7133	1.7216
0.5461	1.6992	1.7253	1.7340	0.7960	1.6860	1.7112	1.7197

Best set of Sellmeier equations ($T = 293$ K, λ in μm, $0.4129\,\mu\text{m} < \lambda < 1.3382\,\mu\text{m}$) [14]:

$$n_X^2 = 2.8063 + \frac{0.02315}{\lambda^2 - 0.01378} - 0.00537\,\lambda^2$$

$$n_Y^2 = 2.8959 + \frac{0.02398}{\lambda^2 - 0.01389} - 0.01132\,\lambda^2$$

$$n_Z^2 = 2.9248 + \frac{0.02410}{\lambda^2 - 0.01406} - 0.01139\,\lambda^2$$

Other sets of dispersion relations are given in [1], [2], [5], [8], [15].

Linear electrooptic coefficients measured at low frequencies (well below the acoustic resonances of GdCOB crystal, i.e., for the "free" crystal) at room temperature (in pm/V) [16]

λ [μm]	r_{11}^{T}	r_{21}^{T}	r_{31}^{T}	r_{13}^{T}	r_{23}^{T}	r_{33}^{T}	r_{51}^{T}	r_{53}^{T}	r_{42}^{T}	r_{62}^{T}
0.6328	0.4	0.5	0.6	0.1	0.4	2.0	0.7	1.5	0.5	0.8

Expressions for effective second-order nonlinear coefficient in the principal planes of GdCOB crystal (approximation of small walk-off angle Kleinman symmetry conditions are valid: $d_{12} = d_{26}$, $d_{13} = d_{35}$, $d_{15} = d_{31}$, $d_{24} = d_{32}$) [2], [17]:

XY plane, $\theta = 90°$

$d_{\mathrm{ooe}} = d_{13} \sin\phi$

$d_{\mathrm{eoe}} = d_{\mathrm{oee}} = d_{31} \sin^2\phi + d_{32} \cos^2\phi$

YZ plane, $\phi = 90°$

$d_{\mathrm{eeo}} = d_{13} \sin^2\theta + d_{12} \cos^2\theta$

$d_{\mathrm{oeo}} = d_{\mathrm{eoo}} = d_{31} \sin\theta$

XZ plane, $\phi = 0°$, $V_{\mathrm{z}} > \theta > 0°$

$d_{\mathrm{ooe}} = d_{12} \cos\theta - d_{32} \sin\theta$

XZ plane, $\phi = 0°$, $90° > \theta > V_{\mathrm{z}}$

$d_{\mathrm{oeo}} = d_{\mathrm{eoo}} = d_{12} \cos\theta - d_{32} \sin\theta$

XZ plane, $\phi = 0°$, $180° - V_{\mathrm{z}} > \theta > 90°$; or $\phi = 180°$, $90° > \theta > V_{\mathrm{z}}$

$d_{\mathrm{oeo}} = d_{\mathrm{eoo}} = d_{12} \cos\theta + d_{32} \sin\theta$

XZ plane, $\phi = 0°$, $180° > \theta > 180° - V_{\mathrm{z}}$; or $\phi = 180°$, $V_{\mathrm{z}} > \theta > 0°$

$d_{\mathrm{ooe}} = d_{12} \cos\theta + d_{32} \sin\theta$

Most reliable experimental values of second-order nonlinear coefficients:

$d_{11}(1.0642\,\mu\text{m}) = 0$ [17]
$d_{12}(1.0642\,\mu\text{m}) = 0.24\,\text{pm/V}$ [18]; $0.27\,\text{pm/V}$ [17]; $0.31\,\text{pm/V}$ [19]
$d_{13}(1.0642\,\mu\text{m}) = -0.74\,\text{pm/V}$ [18]; $-0.85\,\text{pm/V}$ [17]; $-0.87\,\text{pm/V}$ [19]
$d_{31}(1.0642\,\mu\text{m}) = 0.20\,\text{pm/V}$ [17]
$d_{32}(1.0642\,\mu\text{m}) = 2.23\,\text{pm/V}$ [17]; $2.26\,\text{pm/V}$ [19]; $2.39\,\text{pm/V}$ [18]
$d_{33}(1.0642\,\mu\text{m}) = -1.87\,\text{pm/V}$ [17]

Experimental values of phase-matching angle and internal angular bandwidth for SHG in principal planes of GdCOB crystal

Interacting wavelengths [μm]	ϕ_{pm} [deg]	θ_{pm} [deg]	$\Delta\varphi^{int}$ [deg]	$\Delta\theta^{int}$ [deg]	Ref.
XY plane, $\theta = 90°$					
SHG, $o + o \Rightarrow e$					
$1.0642 \Rightarrow 0.5321$	46		0.10		[2], [15], [18], [19]
$0.946 \Rightarrow 0.473$	55.9		0.11		[20]
XZ plane, $\phi = 0°$, $\theta < V_z$					
SHG, $o + o \Rightarrow e$					
$1.0642 \Rightarrow 0.5321$		19.7		0.15	[2], [15], [18], [19]

Note: For a biaxial crystal, two angular acceptances exist: one in θ and other in ϕ. The authors have presented only the smallest one.

Experimental values of effective second-order nonlinear coefficient for some phase-matching directions (SHG, type I, $1.0642\,\mu\text{m} \Rightarrow 0.5321\,\mu\text{m}$) in GdCOB crystal

Phase-matching direction	d_{eff} [pm/V]	Ref.
$\theta = 90°$, $\phi = 46°$ (*XY* plane)	0.59	[17]
	0.63	[19]
$\theta = 19.7°$, $\phi = 0°$ (*XZ* plane)	0.48	[19]
	0.50	[17]
$\theta = 160.3°$, $\phi = 0°$ (*XZ* plane)	1.01	[17]
	1.05	[19]
$\theta = 66.8°$, $\phi = 47.4°$	0.68	[17]
$\theta = 67°$, $\phi = 46°$	0.78	[19]
$\theta = 66.8°$, $\phi = 132.6°$	1.51	[6]
	1.68	[17]
$\theta = 67°$, $\phi = 134°$	1.8	[19]

Note: The properties of d_{eff} in the case of GdCOB crystal include mirror and inversion symmetries [21]. This means that the spatial distribution of d_{eff} can fully be described by choosing two independent quadrants, for example, ($0° < \theta < 90°, 0° < \phi < 90°$) and ($0° < \theta < 90°, 90° < \phi < 180°$). After that, the d_{eff} value in each (θ, ϕ) direction in these two quadrants is equal to that in ($180° - \theta$, $180° - \phi$) direction and vice versa. For example, the directions ($\theta = 66.8°$, $\phi = 132.6°$) and ($\theta = 113.2°$, $\phi = 47.4°$) possess equal d_{eff} values.

Laser-induced bulk damage threshold

λ [μm]	τ_p [ns]	I_{thr} [GW/cm^2]	Ref.	Note
0.337	0.015–0.075	>1.35	[10]	
0.532	7	1	[2]	
1.064	6	>1	[15]	10 Hz
	0.035	>6	[17]	
		>8	[22]	
		130	[6]	1 pulse

About the crystal

GdCOB was developed rather recently, in 1996–1997, simultaneously by French and Japanese scientists [1], [4], [5]. Since that time, more than a hundred papers were published devoted to investigation of GdCOB and its closest analog, YCOB. At the moment, these materials are certainly the most investigated ones of point group m. This brought to significant progress in understanding the physics of three-wave interactions in low-symmetry crystals. It was shown that the spatial distribution of d_{eff} for such crystals can fully be described only by choosing *two* independent quadrants, for example, ($0° < \theta < 90°$, $0° < \phi < 90°$) and ($0° < \theta < 90°$, $90° < \phi < 180°$). Second-order nonlinear coefficients of GdCOB were measured, and it was found that the maximum of effective nonlinearity for SHG of Nd:YAG laser radiation lies not in the first quadrant ($0° < \theta < 90°$, $0° < \phi < 90°$) [13], [17], [19]. The expressions for d_{eff} in the principal planes of GdCOB were deduced [17].

The impact of 4% atomic doping of GdCOB by Sr on the intracavity SHG of $Nd:YVO_4$ laser CW light (1064 nm) was investigated in [22], [23]. It was shown that such doping of 6-mm crystal ($\theta = 66.8°$, $\phi = 132.6°$) leads to the significant improvement of SHG conversion efficiency. CW green output of 2.3 W was generated with 13 W fundamental power [22]. The same Sr-doped crystal was used for extracavity SHG of mode-locked Nd:YAG laser. A 55% energy conversion efficiency was achieved at fundamental intensity of 4–8 GW/cm^2, which by 1.4 times exceeds the value for the undoped sample. In [24], 1.2-cm-long 4 at.% Li-doped GdCOB crystal ($\theta = 66.8°$, $\phi = 132.3°$) was used for intracavity SHG of 13 W $Nd:YVO_4$ laser. CW radiation of 2.55 W at 531 nm was generated.

One of the latest technical achievements, connected with GdCOB, is the generation of 2.8-W CW green output ($\lambda = 532$ nm) in 1.2-cm-long crystal ($\theta = 66.8°$, $\phi = 132.3°$) via intercavity SHG of diode-array end-pumped $Nd:YVO_4$ laser ($P = 6.8$ W) [25]. However, the KTP crystal of the same length ($\theta = 90°$, $\phi = 25°$), used in the same configuration, produced about 4.5 W of green light.

References

[1] G. Aka, L. Bloch, J.M. Benitez, P. Crochet, A. Kahn-Harari, D. Vivien, F. salin, P. Coquelin, D. Colin: A new non linear oxoborate crystal, characterized by using femtosecond broadband pulses. In: *Advanced Solid-State Lasers, OSA Trends in Optics and*

Photonics Series, Vol. 1, ed. by S.A. Payne, C. Pollock (OSA, Washington DC, 1996), pp. 336–340.

[2] G. Aka, A. Kahn-Harari, F. Mougel, D. Vivien, F. Salin, P. Coquelin, P. Colin, D. Pelenc, J.P. Damelet: Linear and nonlinear-optical properties of a new gadolinium calcium oxoborate crystal, $Ca_4GdO(BO_3)_3$. J. Opt. Soc. Am. B **14(9)**, 2238–2247 (1997).

[3] A.B. Ilyukhin, B.F. Dzhurinskii: Crystal structures of binary oxoborates $LnCa_4O(BO_3)_3$ (Ln = Gd, Tb, and Lu) and $Eu_2CaO(BO_3)_2$. Zh. Neorg. Khim. **38(6)**, 917–920 (1993) [In Russian, English trans.: Russ. J. Inorg. Chem. **38(6)**, 847–850 (1993)].

[4] G. Aka, A. Kahn-Harari, D. Vivien, J.-M. Benitez, F. Salin, J. Godard: A new nonlinear and neodymium laser self-frequency doubling crystal with congruent melting: $Ca_4GdO(BO_3)_3$ (GdCOB). Eur. J. Solid State Inorg. Chem. **33(8)**, 727–736 (1996).

[5] M. Iwai, T. Kobayashi, H. Furuya, Y. Mori, T. Sasaki: Crystal growth and optical characterization of rare-earth (Re) calcium oxyborate $ReCa_4O(BO_3)_3$ (Re = Y or Gd) as new nonlinear optical material. Jpn. J. Appl. Phys. **36(3A)**, L276-L279 (1997).

[6] J. Zhou, Z. Zhong, J. Xu, J. Luo, W. Hua, S. Fan: Bridgman growth and characterization of nonlinear optical single crystals $Ca_4GdO(BO_3)_3$. Mater. Sci. Eng. B **97(3)**, 283–287 (2003).

[7] Z. Wang, J. Liu, R. Song, X. Xu, X. Sun, H. Jiang, K. Fu, J. Wang, Y. Liu, J. Wei, Z. Shao: The second-harmonic-generation property of $GdCa_4O(BO_3)_3$ crystal with various phase-matching directions. Opt. Commun. **187(4–6)**, 401–405 (2001).

[8] Z. Shao, J. Lu, Z. Wang, J. Wang, M. Jiang: Anisotropic properties of Nd:ReCOB (Re = Y, Gd): a low symmetry self-frequency doubling crystal. Progr. Cryst. Growth Character. Mater. **40(1–4)**, 63–73 (2000).

[9] D. Vivien, G. Aka, A. Kahn-Harari, A. Aron, F. Mougel, J.-M. Benitez, B. Ferrand, R. Klein, G. Kugel, N. Le Nain, M. Jacquet: Crystal growth and optical properties of rare earth calcium oxoborates. J. Cryst. Growth, **237–239**, 621–628 (2002).

[10] T. Łukasiewicz, A. Majchrowski, I.V. Kityk, J. Kroog: Influence of the rare-earth doping on the photoinduced EOEs in the GdCOB. Mater. Lett. **57(13–14)**, 2049–2052 (2003).

[11] C. Wang, H. Zhang, X. Meng, L. Zhu, Y.T. Chow, X. Liu, R. Cheng, Z. Yang, S. Zhang, L. Sun: Thermal, spectroscopic properties and laser performance at 1.06 and 1.33 μm of Nd:$Ca_4YO(BO_3)_3$ and Nd:$Ca_4GdO(BO_3)_3$ crystals. J. Cryst. Growth **220(1–2)**, 114–120 (2000).

[12] F. Auge, F. Druon, F. Balembois, P. Georges, A. Brun, F. Mougel, G. Aka, D. Vivien: Theoretical and experimental investigations of a diode-pumped quasi-three-level laser: the Yb^{3+}-doped $Ca_4GdO(BO_3)_3$ (Yb:GdCOB) laser. IEEE. J. Quant. Electr. **36(5)**, 598–606 (2000).

[13] S. Zhang, Z. Cheng, J. Lu, G. Li, J. Lu, Z. Shao, H. Chen: Studies of the effective nonlinear coefficient of $GdCa_4O(BO_3)_3$ crystal. J. Cryst. Growth **205(3)**, 453–456 (1999).

[14] N. Umemura, H. Nakao, H. Furuya, M. Yoshimura, Y. Mori, T. Sasaki, K. Yoshida, K. Kato: 90° phase-matching properties of $YCa_4O(BO_3)_3$ and $Gd_xY_{1-x}Ca_4O(BO_3)_3$. Jpn. J. Appl. Phys. **40(2A)**, 596–600 (2001).

[15] G. Aka, F. Mougel, D. Pelenc, B. Ferrand, D. Vivien: Comparative evaluation of GdCOB and YCOB nonlinear-optical properties, in principal and out of principal plane configurations, for the 1064 nm Nd:YAG laser frequency conversion. Proc. SPIE **3928**, 108–114 (2000).

[16] X. Yin, J.Y. Wang, H.D. Jiang: Measurement of electro-optic coefficients of low symmetry crystal $GdCa_4O(BO_3)_3$. Opt. Laser Technol. **33(8)**, 563–566 (2001).

[17] Z.P. Wang, J.H. Liu, R.B. Song, H.D. Jiang, S.J. Zhang, K. Fu, C.Q. Wang, J.Y. Wang, Y.G. Liu, J.Q. Wei, H.C. Chen, Z.S. Shao: Anisotropy of nonlinear-optical property of RCOB (R = Gd, Y) crystal. Chin. Phys. Lett. **18(3)**, 385–387 (2001).
[18] F. Mougel, G. Aka, F. Salin, D. Pelenc, B. Ferrand, A. Kahn-Harari, D. Vivien: Accurate second harmonic generation phase matching angles prediction and evaluation of nonlinear coefficients of $YCa_4O(BO_3)_3$ (YCOB) crystal. In: *Advanced Solid State Lasers, OSA Trends in Optics and Photonics Series, Vol. 26*, ed. by M.M. Fejer, H. Injeyan, U. Keller (OSA, Washington DC, 1999), pp. 709–714.
[19] G. Aka, F. Mougel, D. Vivien, R. Klein, G. Kugel, B. Ferrand, D. Pelenc: Conversion efficiency and absolute effective nonlinear optical coefficients of YCOB and GdCOB measured for different type I SHG phase matching configurations. In: *Advanced Solid-State Lasers, OSA Trends in Optics and Photonics Series, Vol. 50*, ed. by C. Marshall (OSA, Washington DC, 2001), pp. 548–553.
[20] E. Reino, E. Verdier, G. Aka, J.M. Benitez, D. Vivien: Frequency conversion for blue laser emission in $Gd_{1-x}Y_xCOB$. In: *Advanced Solid-State Lasers, OSA Trends in Optics and Photonics Series, Vol. 68*, ed. by M.E. Fermann, L.R. Marshall (OSA, Washington DC, 2002), pp. 32–36.
[21] X. Chen, M. Huang, Z. Luo, Y. Huang: Determination of the optimum phase-matching directions for the self-frequency conversion of Nd:GdCOB and Nd:YCOB crystals. Opt. Commun. **196(1–6)**, 299–307 (2001).
[22] J. Liu, Z. Wang, S. Zhang, J. Wang, H. Chen, Z. Shao, M. Jiang: Second-harmonic generation of 1.06 μm in Sr doped $GdCa_4O(BO_3)_3$ crystal. Opt. Commun. **195(1–4)**, 267–271 (2001).
[23] S.-J. Zhang, Z.-X. Cheng, J.-H. Liu, J.-R. Han, J.-Y. Wang, Z.-S. Shao, H.-C. Chen: Effect of strontium ion on the growth and second-harmonic generation properties of $GdCa_4O(BO_3)_3$ crystal. Chin. Phys. Lett. **18(1)**, 63–64 (2001).
[24] J. Liu, Z. Fei, S. Zhang, C. Du, J. Wang, H. Chen, Z. Shao: Investigation on intracavity second-harmonic generation of a new Li-doped $GdCa_4O(BO_3)_3$ crystal. Opt. Laser Technol. **33(8)**, 597–600 (2001).
[25] J. Liu, X. Xu, C.Q. Wang, S. Zhang, J. Wang, H. Chen, Z. Shao, M. Jiang: Intracavity second-harmonic generation of 1.06 μm in $GdCa_4O(BO_3)_3$. Appl. Phys. B. **72(2)**, 163–166 (2001).

6.7 $YCa_4O(BO_3)_3$, Yttrium Calcium Oxyborate (YCOB)

Negative biaxial crystal: $2V_z = 121.1°$ at $\lambda = 0.546\,\mu m$
Molecular mass: 441.642
Specific gravity: 3.31 g/cm^3 [1]
Point group: *m*
Lattice constants:
$a = 8.046$ Å [2]; 8.0770 ± 0.0003 Å [3]
$b = 15.959$ Å [2]; 16.0194 ± 0.0005 Å [3]
$c = 3.517$ Å [2]; 3.5308 ± 0.0001 Å [3]
$\beta = 101.19°$ [2]; $101.167° \pm 0.004°$ [3]
Assignment of dielectric and crystallographic axes:
$Y \| b$, the axes a and c lie in XZ plane, the angle between them is $\beta = 101.167°$, the angle between the axes Z and a is 24.7°, the angle between the axes X and c

is 13.5° [3]. The slightly different assignments: $(a, Z) = 23°$, $(c, X) = 12°$, and $(a, Z) = 23.6°$, $(c, X) = 12.6°$, were reported in [1] and [4], respectively.
Thermal rotation of XZ plane relative to the crystallographic axes (a, c) {around Y axis}[5]:

$$\frac{d\alpha_{\text{ext}}}{dT} = \pm\left(\frac{0.0064}{\lambda^3} - \frac{0.0173}{\lambda^2} + \frac{0.0149}{\lambda} + 0.0043\right) \times 0.0573\,\text{deg/K}$$

where $0.3973\,\mu\text{m} < \lambda < 0.6691\,\mu\text{m}$ and the plus and minus signs refer to two propagation directions, $\phi = 180°$ and $\phi = 0°$.
Mohs hardness: 6–6.5 [6]
Melting point: 1783 K [1], [7]

Mean values of linear thermal expansion coefficient

T [K]	$\alpha_t \times 10^6$ [K^{-1}], $\parallel a$	$\alpha_t \times 10^6$ [K^{-1}], $\parallel b$	$\alpha_t \times 10^6$ [K^{-1}], $\parallel c$	Ref.
293–473	8.39	5.18	9.17	[8]
293–1173	9.9	8.2	12.8	[9]

Specific heat capacity c_p at $P = 0.101325$ MPa [9]

T [K]	c_p [J/kgK]
373	729.7

Thermal conductivity coefficient at $T = 293$ K [6]

κ [W/mK], $\parallel X$	κ [W/mK], $\parallel Y$	κ [W/mK], $\parallel Z$
2.60	2.33	3.01

Thermal conductivity coefficient at $T = 373$ K [9]

κ [W/mK], $\parallel a$	κ [W/mK], $\parallel b$	κ [W/mK], $\parallel c$
1.83	1.72	2.17

High transmittance range: $0.202 - 2.5\,\mu\text{m}$ [10]
In the IR transparency range $2.5 - 3.7\,\mu\text{m}$, there are absorption bands at 2.7, 2.9, and 3.25 μm [11].

Linear absorption coefficient α

λ [μm]	α [cm^{-1}]	Ref.
0.21	1.0	[12]
1.06	0.013	[13]

Best set of Sellmeier equations ($T = 293$ K, λ in μm, $0.3547\,\mu\text{m} < \lambda < 1.9079\,\mu\text{m}$) [10], [14]:

$$n_X^2 = 2.7697 + \frac{0.02034}{\lambda^2 - 0.01779} - 0.00643\,\lambda^2$$

$$n_Y^2 = 2.8741 + \frac{0.02213}{\lambda^2 - 0.01871} - 0.01078\,\lambda^2$$

$$n_Z^2 = 2.9107 + \frac{0.02232}{\lambda^2 - 0.01887} - 0.01256\,\lambda^2$$

Other sets of dispersion relations are given in [2], [3], [4], [7], [12], [15].
Temperature derivative of refractive indices for spectral range 0.3973–1.3382 μm and temperature range 293–393 K (λ in μm) [5]:

$$dn_X/dT = (8.2058 - 5.0188\,\lambda) \times 10^{-6}\,\text{K}^{-1}$$

$$dn_Y/dT = (2.8217 + 1.9154\,\lambda) \times 10^{-6}\,\text{K}^{-1}$$

$$dn_Z/dT = (3.0310 + 1.8399\,\lambda) \times 10^{-6}\,\text{K}^{-1}$$

Expressions for effective second-order nonlinear coefficient in the principal planes of YCOB crystal (approximation of small walk-off angle, Kleinman symmetry conditions are valid: $d_{12} = d_{26}$, $d_{13} = d_{35}$, $d_{15} = d_{31}$, $d_{24} = d_{32}$) [16], [17]:

XY plane, $\theta = 90°$

$d_{\text{ooe}} = d_{13} \sin\phi$

$d_{\text{eoe}} = d_{\text{oee}} = d_{31} \sin^2\phi + d_{32} \cos^2\phi$

YZ plane, $\phi = 90°$

$d_{\text{eeo}} = d_{13} \sin^2\theta + d_{12} \cos^2\theta$

$d_{\text{oeo}} = d_{\text{eoo}} = d_{31} \sin\theta$

XZ plane, $\phi = 0°$, $V_z > \theta > 0°$

$d_{\text{ooe}} = d_{12} \cos\theta - d_{32} \sin\theta$

XZ plane, $\phi = 0°$, $90° > \theta > V_z$

$d_{\text{oeo}} = d_{\text{eoo}} = d_{12} \cos\theta - d_{32} \sin\theta$

XZ plane, $\phi = 0°$, $180° - V_z > \theta > 90°$; or $\phi = 180°$, $90° > \theta > V_z$

$d_{\text{oeo}} = d_{\text{eoo}} = d_{12} \cos\theta + d_{32} \sin\theta$

XZ plane, $\phi = 0°$, $180° > \theta > 180° - V_z$; or $\phi = 180°$, $V_z > \theta > 0°$

$d_{\text{ooe}} = d_{12} \cos\theta + d_{32} \sin\theta$

Most reliable experimental values of second-order nonlinear coefficients:

$d_{11}(1.0642\,\mu\text{m}) = 0$ [17]; ≈ 0 [18]

$d_{12}(1.0642\,\mu\text{m}) = 0.24$ pm/V [17]; 0.34 pm/V [19]; 0.43 pm/V [3]

$d_{13}(1.0642\,\mu\text{m}) = -0.71$ pm/V [19]; -0.73 pm/V [17]; -0.92 pm/V [3]

$d_{31}(1.0642\,\mu\text{m}) = 0.41$ pm/V [17]

$d_{32}(1.0642\,\mu\text{m}) = 2.00$ pm/V [3]; 2.03 pm/V [19]; 2.35 pm/V [17]

$d_{33}(1.0642\,\mu\text{m}) = -1.60$ pm/V [17]

Experimental values of phase-matching angle for SHG and SFG in principal planes of YCOB crystal at $T = 293$ K

Interacting wavelengths [μm]	ϕ_{pm} [deg]	θ_{pm} [deg]	Ref.
XY plane, $\theta = 90°$			
SHG, $o + o \Rightarrow e$			
$1.0642 \Rightarrow 0.5321$	35.0		[3], [7], [19]
$0.7379 \Rightarrow 0.36895$	77.3		[10]
SHG, type I, along *Y*			
$0.724 \Rightarrow 0.362$	90		[20]
SFG, $o + o \Rightarrow e$			
$1.0642 + 0.5321 \Rightarrow 0.3547$	73.2		[11]
	73.6		[10]
	73.7		[5]
	73.8		[21]
SHG, $e + o \Rightarrow e$			
$1.0642 \Rightarrow 0.5321$	73.4		[7]
	74.8		[22]
	75.2		[10]
	75.3		[5]
SHG, type II, along *Y*			
$1.03 \Rightarrow 0.515$	90		[10]
SFG, $e + o \Rightarrow e$			
$1.9079 + 1.0642 \Rightarrow 0.6831$	81.2		[10]
YZ plane, $\phi = 90°$			
SHG, $e + e \Rightarrow o$			
$0.7379 \Rightarrow 0.36895$		66.9	[10]
SFG, $e + e \Rightarrow o$			
$1.0642 + 0.5321 \Rightarrow 0.3547$		58.7	[11]
		59.7	[5]
		59.8	[21]
		59.9	[10]
SHG, $e + o \Rightarrow o$			
$1.0642 \Rightarrow 0.5321$		58.7	[3], [7]
		61.1	[22]
		62.7	[5], [10]
SFG, $e + o \Rightarrow o$			
$1.9079 + 1.0642 \Rightarrow 0.6831$		73.5	[10]
XZ plane, $\phi = 0°$, $\theta < V_Z$			
SHG, type I, along *Z*			
$0.83 \Rightarrow 0.415$		0	[12]
$0.8325 \Rightarrow 0.41625$		0	[10], [5]
SHG, $o + o \Rightarrow e$			
$0.9 \Rightarrow 0.45$		18.7	[5]
$0.954 \Rightarrow 0.477$		24.1	[10]
$1.0642 \Rightarrow 0.5321$		30.8	[10], [5]
		31.7	[3], [7], [19]

Interacting wavelengths [μm]	ϕ_{pm} [deg]	θ_{pm} [deg]	Ref.
1.3382 ⇒ 0.6691		38.2	[10]
		38.3	[5]
SFG, $o + o \Rightarrow e$			
1.0642 + 0.7379 ⇒ 0.4358		17.1	[5]
1.569 + 0.5321 ⇒ 0.3973		18.6	[5]
1.3188 + 0.6594 ⇒ 0.4396		23.0	[10]
1.9079 + 0.5321 ⇒ 0.4161		26.6	[10]

Experimental values of internal angular bandwidth for SHG and SFG in principal planes of YCOB crystal

Interacting wavelengths [μm]	ϕ_{pm} [deg]	θ_{pm} [deg]	$\Delta\varphi^{int}$ [deg]	$\Delta\theta^{int}$ [deg]	Ref.
XY plane, $\theta = 90°$					
SHG, $o + o \Rightarrow e$					
1.0642 ⇒ 0.5321	35.0		0.09		[3], [7], [19]
SHG, $e + o \Rightarrow e$					
1.0642 ⇒ 0.5321	73.4		0.32		[7]
SFG, $o + o \Rightarrow e$					
1.0642 + 0.5321 ⇒ 0.3547	73.2		0.11		[23]
YZ plane, $\phi = 90°$					
SHG, $e + o \Rightarrow o$					
1.0642 ⇒ 0.5321		58.7		0.74	[3], [7]
SFG, $e + e \Rightarrow o$					
1.0642 + 0.5321 ⇒ 0.3547		58.7		0.19	[23]
XZ plane, $\phi = 0°$, $\theta < V_Z$					
SHG, $o + o \Rightarrow e$					
1.0642 ⇒ 0.5321		31.7		0.08	[3], [7], [19]

Note: For a biaxial crystal, two angular acceptances exist: one in θ and other in ϕ. The authors have presented only the smallest one.

Experimental values of internal angular bandwidth for some specific phase-matching direction (SHG, type I, 0.946 μm ⇒ 0.473 μm) in YCOB crystal [24]

Phase-matching direction	Δ [deg]
$\theta = 67.9°$, $\phi = 136.8°$	0.06

Experimental values of temperature bandwidth for SHG and SFG in principal planes of YCOB crystal

Interacting wavelengths [μm]	ΔT [°C]	Ref.	Note
XY plane, $\theta = 90°$			
SHG, $o + e \Rightarrow e$			
1.0642 ⇒ 0.5321	32.7	[10]	

Interacting wavelengths [μm]	ΔT [°C]	Ref.	Note
	32.8	[5]	$\phi = 75.3°$
SFG, $o + o \Rightarrow e$			
$1.0642 + 0.5321 \Rightarrow 0.3547$	8.6	[10]	$\phi = 73.7°$
	9.7	[25]	
	10	[12]	
YZ plane, $\phi = 90°$			
SHG, $o + e \Rightarrow o$			
$1.0642 \Rightarrow 0.5321$	31.5	[10]	$\theta = 62.7°$
	31.7	[14]	
	29.2	[5]	
SFG, $e + e \Rightarrow o$			
$1.0642 + 0.5321 \Rightarrow 0.3547$	6.2	[10]	
	8.5	[23]	
XZ plane, $\phi = 0°$, $\theta < V_Z$ and $\theta > 180° - V_Z$			
SHG, type I, along *Z*			
$0.8325 \Rightarrow 0.41625$	21.6	[5]	
	31.5	[10]	
SHG, $o + o \Rightarrow e$			
$0.9 \Rightarrow 0.45$	24.6	[5]	$\theta = 18.7°$
	45.3	[5]	$\theta = 161.3°$
$1.0642 \Rightarrow 0.5321$	75	[5]	$\theta = 30.8°$
$1.3382 \Rightarrow 0.6691$	61	[5]	$\theta = 141.7°$
SFG, $o + o \Rightarrow e$			
$1.0642 + 0.7379 \Rightarrow 0.4358$	36.5	[5]	$\theta = 162.9°$
$1.569 + 0.5321 \Rightarrow 0.3973$	16.9	[5]	$\theta = 18.6°$
	33.8	[5]	$\theta = 161.4°$

Experimental values of effective second-order nonlinear coefficient for some specific phase-matching directions (SHG, type I, 1.0642 μm ⇒ 0.5321 μm) in YCOB crystal

Phase-matching direction	d_{eff} [pm/V]	Ref.
$\theta = 90°$, $\phi = 35.3°$ (*XY* plane)	0.39	[19]
$\theta = 90°$, $\phi = 35°$ (*XY* plane)	0.42	[17]
$\theta = 31.7°$, $\phi = 0°$ (*XZ* plane)	0.78	[17]
	1.03	[19]
$\theta = 148.3°$, $\phi = 0°$ (*XZ* plane)	1.36	[19]
	1.44	[17]
$\theta = 65°$, $\phi = 36.5°$	1.14	[17]
$\theta = 65.9°$, $\phi = 36.5°$	0.91	[9]
$\theta = 66.3°$, $\phi = 143.5°$	1.45	[9]

Phase-matching direction	d_{eff} [pm/V]	Ref.
$\theta = 67°, \phi = 143.5°$	1.73	[17]
$\theta = 66°, \phi = 145°$	1.8	[19]

Note: The properties of d_{eff} in the case of YCOB crystal include mirror and inversion symmetries [26]. This means that the spatial distribution of d_{eff} can fully be described by choosing two independent quadrants, for example, $(0° < \theta < 90°, 0° < \phi < 90°)$ and $(0° < \theta < 90°, 90° < \phi < 180°)$. After that, the d_{eff} value in each (θ, ϕ) direction in these two quadrants is equal to that in $(180° - \theta, 180° - \phi)$ direction and vice versa. For example, the directions $(\theta = 33°, \phi = 9°)$ and $(\theta = 147°, \phi = 171°)$ possess equal d_{eff} values.

Experimental values of THG conversion efficiency (type I, $1.0642\,\mu m + 0.5321\,\mu m \Rightarrow 0.3547\,\mu m$, $I = 0.8\,GW/cm^2$, $l = 1.04\,cm$) for some specific phase-matching directions in YCOB crystal [21]

Phase-matching direction	THG conversion efficiency [%]
$\theta = 65°, \phi = 82.8°$	2
$\theta = 90°, \phi = 73.8°$ (*XY* plane)	7
$\theta = 111°, \phi = 79.6°$	20
$\theta = 106°, \phi = 77.2°$	26

See the note to the previous table.

Other proof of superiority of $(\theta = 106°, \phi = 77.2°)$ direction for type I THG of 1.06-μm radiation in YCOB is given in [27].

Laser-induced bulk damage threshold

λ [μm]	τ_p [ns]	I_{thr} [GW/cm^2]	Ref.	Note
0.532	6	1	[7]	
1.064	10	85	[9]	1 pulse
	6	>1	[7]	10 Hz
	1.1	18.4	[12]	along Y axis, $\mathbf{E} \| Z$

About the crystal

Japanese scientists introduced YCOB in 1997 [2], and in a short time, more than a hundred works were published devoted to this crystal and its closest analog, GdCOB. At the moment, these nonlinear crystals are certainly the most investigated ones of point group m. This brought significant progress in understanding the physics of three-wave interactions in low-symmetry crystals. It was shown that the spatial distribution of d_{eff} for such crystals can fully be described only by choosing *two* independent quadrants, for example, $(0° < \theta < 90°, 0° < \phi < 90°)$ and $(0° < \theta < 90°, 90° < \phi < 180°)$. Second-order nonlinear coefficients of YCOB were measured, and it was

found that the maximum effective nonlinearity for SHG and THG of Nd:YAG laser radiation does not lie not in the first quadrant ($0° < \theta < 90°$, $0° < \phi < 90°$) [17], [18], [19]. The expressions for d_{eff} in the principal planes of YCOB were deduced [17]. Very recently, it was reported that in this monoclinic crystal, due to the thermal rotation of the *XZ* plane around the *Y* axis, the spatial anisotropy of SHG temperature bandwidth also takes place [5].

One of the latest technical achievements connected with YCOB is the generation of 2.35-W CW green output ($\lambda = 532$ nm) in a 1.2-cm-long crystal ($\theta = 64.5°$, $\phi = 35.5°$) via intercavity SHG of a diode-array end-pumped Nd:YVO_4 laser ($P = 5.6$ W) [13]. Another similar application is THG of $NdYVO_4$ laser radiation [27]. Using the KTP crystal for frequency doubling and a 1.1-cm-long YCOB crystal ($\theta = 106°$, $\phi = 77.2°$), the authors managed to obtain 124 mW of quasi-CW light (pulse repetition frequency 20 kHz) at 355 nm.

References

[1] Q. Ye, B.H.T. Chai: Crystal growth of $YCa_4O(BO_3)_3$ and its orientation. J. Cryst. Growth **197(1–2)**, 228–235 (1999).

[2] M. Iwai, T. Kobayashi, H. Furuya, Y. Mori, T. Sasaki: Crystal growth and optical characterization of rare-earth (Re) calcium oxyborate $ReCa_4O(BO_3)_3$ (Re = Y or Gd) as new nonlinear optical material. Jpn. J. Appl. Phys. **36(3A)**, L276–L279 (1997).

[3] F. Mougel, G. Aka, F. Salin, D. Pelenc, B. Ferrand, A. Kahn-Harari, D. Vivien: Accurate second harmonic generation phase matching angles prediction and evaluation of nonlinear coefficients of $YCa_4O(BO_3)_3$ (YCOB) crystal. In: *Advanced Solid State Lasers, OSA Trends in Optics and Photonics Series, Vol. 26*, ed. by M.M. Fejer, H. Injeyan, U. Keller (OSA, Washington DC, 1999), pp. 709–714.

[4] J. Wang, Z. Shao, J. Wei, X. Hu, Y. Liu, B. Gong, G. Li, J. Lu, M. Guo, M. Jiang: Research on growth and self-frequency doubling of Nd:ReCOB (Re = Y or Gd) crystals. Progr. Cryst. Growth Character. Mater. **40(1–4)**, 17–31 (2000).

[5] N. Umemura, M. Ando, K. Suzuki, E. Takaoka, K. Kato, M. Yoshimura, Y. Mori, T. Sasaki: Temperature-insensitive second-harmonic generation at 0.5321 μm in $YCa_4O(BO_3)_3$. Jpn. J. Appl. Phys. **42(8)**, 5040–5042 (2003).

[6] Q. Ye, L. Shah, J. Eichenholz, D. Hammons, R. Peale, M. Richardson, A. Chin, B.H.T. Chai: Investigation of diode-pumped, self-frequency doubled RGB lasers from Nd:YCOB crystals. Opt. Commun. **164(1–3)**, 33–37 (1999).

[7] G. Aka, F. Mougel, D. Pelenc, B. Ferrand, D. Vivien: Comparative evalution of GdCOB and YCOB nonlinear-optical properties, in principal and out of principal plane configurations, for the 1064 nm Nd:YAG laser frequency conversion. Proc. SPIE **3928**, 108–114 (2000).

[8] D.A. Hammons, M. Richardson, B.H.T. Chai, A.K. Chin, R. Jollay: Scaling of longitudinally diode-pumped self-frequency-doubling Nd:YCOB lasers. IEEE J. Quant. Electr. **36(8)**, 991–999 (2000).

[9] J. Luo, S.J. Fan, H.Q. Xie, K.C. Xiao, S.X. Qian, Z.W. Zhong, G.X. Qiang, R.Y. Sun, J.Y. Xu: Thermal and nonlinear optical properties of $Ca_4YO(BO_3)_3$. Cryst. Res. Technol. **36(11)**, 1215–1221 (2001).

[10] N. Umemura, H. Nakao, H. Furuya, M. Yoshimura, Y. Mori, T. Sasaki, K. Yoshida, K. Kato: 90° phase-matching properties of $YCa_4O(BO_3)_3$ and $Gd_xY_{1-x}Ca_4O(BO_3)_3$. Jpn. J. Appl. Phys. **40(2A)**, 596–600 (2001).

[11] H. Furuya, M. Yoshimura, T. Kobayashi, K. Murase, Y. Mori, T. Sasaki: Crystal growth and characterization of $Gd_xY_{1-x}Ca_4O(BO_3)_3$ crystal. J. Cryst. Growth **198–199**, 560–563 (1999).

[12] M. Yoshimura, T. Kobayashi, H. Furuya, K. Murase, Y. Mori, T. Sasaki: Crystal growth and optical properties of yttrium calcium oxyborate $YCa_4O(BO_3)_3$. In: *Advanced Solid-State Lasers, OSA Trends in Optics and Photonics Series, Vol. 19*, ed. by W.R. Bosenberg, M.M. Fejer (OSA, Washington DC, 1998), pp. 561–564.

[13] J. Liu, C. Wang, S. Zhang, C. Du, J. Lu, J. Wang, H. Chen, Z. Shao, M. Jiang: Investigation on intracavity second-harmonic generation at 1.06 μm in $YCa_4O(BO_3)_3$ by using an end-pumped Nd:YVO_4 laser. Opt. Commun. **182(1–3)**, 187–191 (2000).

[14] N. Umemura, K. Yoshida, H. Furuya, Y. Mori, T. Sasaki, E. Takaoka, K. Kato: New data on the phase-matching properties of $YCa_4O(BO_3)_3$. In: *Advanced Solid-State Lasers, OSA Trends in Optics and Photonics Series, Vol. 34*, ed. by H. Injeyan, U. Keller, C. Marshall (OSA, Washington DC, 2000), pp. 501–505.

[15] Z. Shao, J. Lu, Z. Wang, J. Wang, M. Jiang: Anisotropic properties of Nd:ReCOB (Re = Y, Gd): a low symmetry self-frequency doubling crystal. Progr. Cryst. Growth Character. Mater. **40(1–4)**, 63–73 (2000).

[16] G. Aka, A. Kahn-Harari, F. Mougel, D. Vivien, F. Salin, P. Coquelin, P. Colin, D. Pelenc, J.P. Damelet: Linear and nonlinear-optical properties of a new gadolinium calcium oxoborate crystal, $Ca_4GdO(BO_3)_3$. J. Opt. Soc. Am. B **14(9)**, 2238–2247 (1997).

[17] Z.P. Wang, J.H. Liu, R.B. Song, H.D. Jiang, S.J. Zhang, K. Fu, C.Q. Wang, J.Y. Wang, Y.G. Liu, J.Q. Wei, H.C. Chen, Z.S. Shao: Anisotropy of nonlinear-optical property of RCOB (R = Gd, Y) crystal. Chin. Phys. Lett. **18(3)**, 385–387 (2001).

[18] C. Chen, Z. Shao, J. Jiang, J. Wei, J. Lin, J. Wang, N. Ye, L. Lu, B. Wu, M. Jiang, M. Yoshimura, Y. Mori, T. Sasaki: Determination of the nonlinear optical coefficients of $YCa_4O(BO_3)_3$ crystal. J. Opt. Soc. Am. B **17(4)**, 566–571 (2000).

[19] G. Aka, F. Mougel, D. Vivien, R. Klein, G. Kugel, B. Ferrand, D. Pelenc: Conversion efficiency and absolute effective nonlinear optical coefficients of YCOB and GdCOB measured for different type I SHG phase matching configurations. In: *Advanced Solid-State Lasers, OSA Trends in Optics and Photonics Series, Vol. 50*, ed. by C. Marshall (OSA, Washington DC, 2001), pp. 548–553.

[20] H. Nakao, S. Makio, H. Furuya, K. Kawamura, S. Yasuda, Y.K. Yap, M. Yoshimura, Y. Mori, T. Sasaki: Crystal growth of GdYCOB for non-critical phase-matched second-harmonic generation at 860 nm. J. Cryst. Growth **237–239**, 632–836 (2002).

[21] Z. Wang, K. Fu, X. Xu, X. Sun, H. Jiang, R. Song, J. Liu, J. Wang, Y. Liu, J. Wei, Z. Shao: The optimum configuration for the third-harmonic generation of 1.064 μm in a YCOB crystal. Appl. Phys. B **72(7)**, 839–842 (2001).

[22] M. Yoshimura, H. Furuya, I. Yamada, K. Murase, H. Nakao, M. Yamazaki, Y. Mori, T. Sasaki: Noncritically phase-matched second-harmonic generation of a Nd:YAG laser in GdYCOB crystal. In: *Advanced Solid-State Lasers, OSA Trends in Optics and Photonics Series, Vol. 26*, ed. by M.M. Fejer, H. Injeyan, U. Keller (OSA, Washington DC, 1999), pp. 702–706.

[23] M. Yoshimura, H. Furuya, T. Kobayashi, K. Murase, Y. Mori, T. Sasaki: Noncritically phase-matched frequency conversion in $Gd_xY_{1-x}Ca_4O(BO_3)_3$ crystal. Opt. Lett. **24(4)** 193–197 (1999).

[24] E. Reino, E. Verdier, G. Aka, J.M. Benitez, D. Vivien: Frequency conversion for blue laser emission in $Gd_{1-x}Y_xCOB$. In: *Advanced Solid-State Lasers, OSA Trends in Optics and Photonics Series, Vol. 68*, ed. by M.E. Fermann, L.R. Marshall (OSA, Washington DC, 2002), pp. 32–36.

[25] H. Furuya, H. Nakao, I. Yamada, Y.F. Ruan, Y.K. Yap, M. Yoshimura, Y. Mori, T. Sasaki: Alleviation of photoinduced damage in $Gd_xY_{1-x}Ca_4O(BO_3)_3$ at elevated temperature for noncritically phase-matched 355-nm generation. Opt. Lett. **25(21)** 1588–1590 (2000).
[26] X. Chen, M. Huang, Z. Luo, Y. Huang: Determination of the optimum phase-matching directions for the self-frequency conversion of Nd:GdCOB and Nd:YCOB crystals. Opt. Commun. **196(1–6)**, 299–307 (2001).
[27] C. Du, Z. Wang, J. Liu, X. Xu, K. Fu, J. Wang, Z. Shao: Investigation of intracavity third-harmonic generation at 1.06 μm in $YCa_4O(BO_3)_3$ crystals. Appl. Phys. B **74(2)**, 125–127 (2002).

6.8 $Gd_xY_{1-x}Ca_4O(BO_3)_3$, Gadolinium–Yttrium Calcium Oxyborate (GdYCOB)

Negative biaxial crystal.
Point group: m
Lattice constants for $x = 0.24$ [1]:
$a = 8.067$ Å
$b = 15.991$ Å
$c = 3.531$ Å
$\beta = 101.18°$
Assignment of dielectric and crystallographic axes for $x = 0.24$:
$Y \| b$, the axes a and c lie in XZ plane, the angle between them is $\beta = 101.18°$, the angle between the axes Z and a is 23.8°, the angle between the axes X and c is 12.6° [1]
Melting point: ≈ 1773 K [2]
High transmittance range: 0.32–2.5 μm [2]
Sellmeier equations ($T = 293\ K$, λ in μm, 0.4129 μm < λ < 1.3382 μm) [3]:

$$n_X^2\,(Gd_xY_{1-x}COB) = (1-x)\,n_X^2\,(YCOB) + xn_X^2(GdCOB)$$

$$n_Y^2\,(Gd_xY_{1-x}COB) = (1-x)\left(1+0.00198x^2\right)^2 n_Y^2\,(YCOB) + xn_Y^2\,(GdCOB)$$

$$n_Z^2\,(Gd_xY_{1-x}COB) = (1-x)\left(1+0.00732x^2\right)^2 n_Z^2\,(YCOB) + xn_Z^2\,(GdCOB)$$

where the refractive indices of YCOB and GdCOB are given by the following dispersion relations [3]:

YCOB

$$n_X^2 = 2.7697 + \frac{0.02034}{\lambda^2 - 0.01779} - 0.00643\,\lambda^2$$

$$n_Y^2 = 2.8741 + \frac{0.02213}{\lambda^2 - 0.01871} - 0.01078\,\lambda^2$$

$$n_Z^2 = 2.9107 + \frac{0.02232}{\lambda^2 - 0.01887} - 0.01256\,\lambda^2$$

GdCOB

$$n_X^2 = 2.8063 + \frac{0.02315}{\lambda^2 - 0.01378} - 0.00537\,\lambda^2$$

$$n_Y^2 = 2.8959 + \frac{0.02398}{\lambda^2 - 0.01389} - 0.01132\,\lambda^2$$

$$n_Z^2 = 2.9248 + \frac{0.02410}{\lambda^2 - 0.01406} - 0.01139\,\lambda^2$$

Expressions for effective second-order nonlinear coefficient in the principal planes of GdYCOB crystal (approximation of small walk-off angle Kleinman symmetry conditions are valid: $d_{12} = d_{26}$, $d_{13} = d_{35}$, $d_{15} = d_{31}$, $d_{24} = d_{32}$) [4], [5]:

XY plane, $\theta = 90°$

$d_{ooe} = d_{13} \sin\phi$

$d_{eoe} = d_{oee} = d_{31} \sin^2\phi + d_{32} \cos^2\phi$

YZ plane, $\phi = 90°$

$d_{eeo} = d_{13} \sin^2\theta + d_{12} \cos^2\theta$

$d_{oeo} = d_{eoo} = d_{31} \sin\theta$

XZ plane, $\phi = 0°$, $V_z > \theta > 0°$

$d_{ooe} = d_{12} \cos\theta - d_{32} \sin\theta$

XZ plane, $\phi = 0°$, $90° > \theta > V_z$

$d_{oeo} = d_{eoo} = d_{12} \cos\theta - d_{32} \sin\theta$

XZ plane, $\phi = 0°$, $180° - V_z > \theta > 90°$; or $\phi = 180°$, $90° > \theta > V_z$

$d_{oeo} = d_{eoo} = d_{12} \cos\theta + d_{32} \sin\theta$

XZ plane, $\phi = 0°$, $180° > \theta > 180° - V_z$; or $\phi = 180°$, $V_z > \theta > 0°$

$d_{ooe} = d_{12} \cos\theta + d_{32} \sin\theta$

Experimental values of phase-matching angle in principal planes of GdYCOB crystal

Interacting wavelengths [μm]	Compositional parameter x	Ref.	Note
along Y axis, $\phi = 90°$, $\theta = 90°$			
SHG, type I			
$0.7735 \Rightarrow 0.38675$	0.68	[6]	$T = 240\,°C$
SHG, type II			
$1.0642 \Rightarrow 0.5321$	0.275	[7]	
	≈0.28	[8]	$T = 52\,°C$
SFG, type I			
$1.0642 + 0.5321 \Rightarrow 0.3547$	0.24	[2]	
	0.28	[1]	
along Z axis, $\phi = 0°$, $\theta = 0°$			
SHG, type I			
$0.8435 \Rightarrow 0.42175$	0.15	[9]	

Interacting wavelengths [μm]	Compositional parameter x	Ref.	Note
$0.8612 \Rightarrow 0.4306$	0.32	[9]	
$0.925 \Rightarrow 0.4625$	0.48	[10]	
$0.9293 \Rightarrow 0.46465$	0.84	[11]	
$0.946 \Rightarrow 0.473$	0.87	[12]	

Experimental values of internal angular and temperature bandwidths for some specific interactions along Y axis of GdYCOB crystal (compositional parameter $x = 0.275$ in the case of SHG and $x = 0.28$ in the case of SFG)

Interacting wavelengths [μm]	T [°C]	ΔT [°C]	$\Delta\theta^{\text{int}}$ [deg]	$\Delta\phi^{\text{int}}$ [deg]	Ref.
SHG, type II					
$1.0642 \Rightarrow 0.5321$	27	32.4	6.8	4.0	[7]
SFG, type I					
$1.0642 + 0.5321 \Rightarrow 0.3547$	21	6.6	3.8	2.2	[1], [13], [14]

Experimental values of internal angular bandwidths for SHG along Z axis of GdYCOB crystal (compositional parameter $x = 0.87$) [12]

Interacting wavelengths [μm]	$\Delta\theta^{\text{int}}$ [deg]
SHG, type I	
$0.946 \Rightarrow 0.473$	0.53

Experimental values of effective second-order nonlinear coefficient for some specific interactions along Y axis of GdYCOB crystal

Interacting wavelengths [μm]	Compositional parameter x	d_{eff} [pm/V]	Ref.
SHG, type II			
$1.0642 \Rightarrow 0.5321$	0.275	0.35 (d_{31})	[7]
SFG, type I			
$1.0642 + 0.5321 \Rightarrow 0.3547$	0.28	0.55 (d_{13})	[1], [13], [14]

Laser-induced bulk damage threshold

λ [μm]	τ_p [ns]	I_{thr} [GW/cm^2]	Ref.	Note
0.355	10	0.002–0.003	[14]	62.5 kHz, gray-track formation
1.064	5	>0.45	[8]	5 Hz
	0.035	>0.45	[8]	10 Hz

Note: The gray-track formation could be eliminated by keeping the GdYCOB crystal at elevated temperatures (at $T = 240$°C [15]). The total recovery from this damage can be realized by annealing at 150°C during 25 hours [14].

About the crystal

It is known that the YCOB crystal experiences the type I NCPM along the Y axis for the fundamental wavelength 724 nm and along the Z axis for the one at 832 nm [9]. At the same time, the GdCOB crystal possesses the similar interactions along the Y and the Z axes for the wavelengths of 826 and 961 nm, respectively [9]. It is clear that the solid solution between these two crystals, namely $Gd_xY_{1-x}Ca_4O(BO_3)_3$ (GdYCOB), depending on compositional parameter x, will display the NCPM properties along the Y and the Z axes for *any* wavelength in the ranges 724–826 nm and 832–961 nm, respectively. Using this approach, in [6] the type I NCPM SHG of 773.5 nm in GdYCOB ($x = 0.68$) was realized along Y axis. In [7], [8], the type II NCPM SHG for Nd:YAG laser radiation ($\lambda = 1.0642\,\mu m$) along the Y axis was demonstrated for GdYCOB with $x = 0.28$. Finally, the type I NCPM THG of Nd:YAG laser radiation along the same axis was also demonstrated for a GdYCOB crystal with $x = 0.24$ [2].

References

[1] M. Yoshimura, H. Furuya, T. Kobayashi, K. Murase, Y. Mori, T. Sasaki: Noncritically phase-matched frequency conversion in $Gd_xY_{1-x}Ca_4O(BO_3)_3$ crystal. Opt. Lett. **24(4)**, 193–197 (1999).

[2] H. Furuya, M. Yoshimura, T. Kobayashi, K. Murase, Y. Mori, T. Sasaki: Crystal growth and characterization of $Gd_xY_{1-x}Ca_4O(BO_3)_3$ crystal. J. Cryst. Growth **198–199**, 560–563 (1999).

[3] N. Umemura, H. Nakao, H. Furuya, M. Yoshimura, Y. Mori, T. Sasaki, K. Yoshida, K. Kato: 90° phase-matching properties of $YCa_4O(BO_3)_3$ and $Gd_xY_{1-x}Ca_4O(BO_3)_3$. Jpn. J. Appl. Phys. **40(2A)**, 596–600 (2001).

[4] G. Aka, A. Kahn-Harari, F. Mougel, D. Vivien, F. Salin, P. Coquelin, P. Colin, D. Pelenc, J.P. Damelet: Linear and nonlinear-optical properties of a new gadolinium calcium oxoborate crystal, $Ca_4GdO(BO_3)_3$. J. Opt. Soc. Am. B **14(9)**, 2238–2247 (1997).

[5] Z.P. Wang, J.H. Liu, R.B. Song, H.D. Jiang, S.J. Zhang, K. Fu, C.Q. Wang, J.Y. Wang, Y.G. Liu, J.Q. Wei, H.C. Chen, Z.S. Shao: Anisotropy of nonlinear-optical property of RCOB (R = Gd, Y) crystal. Chin. Phys. Lett. **18(3)**, 385–387 (2001).

[6] H. Kitano, H. Kawai, K. Miramitsu, S. Owa, M. Yoshimura, Y. Mori, T. Sasaki: 387-nm generation in $Gd_xY_{1-x}Ca_4O(BO_3)_3$ crystal and its utilization for 193-nm light source. Jpn. J. Appl. Phys. **42(2B)**, L166–L169 (2003).

[7] M. Yoshimura, H. Furuya, I. Yamada, K. Murase, H. Nakao, M. Yamazaki, Y. Mori, T. Sasaki: Noncritically phase-matched second-harmonic generation of a Nd:YAG laser in GdYCOB crystal. In: *Advanced Solid-State Lasers, OSA Trends in Optics and Photonics Series, Vol. 26*, ed. by M.M. Fejer, H. Injeyan, U. Keller (OSA, Washington DC, 1999), pp. 702–706.

[8] A. Zoubir, J. Eichenholz, E. Fujiwara, D. Grojo, E. Baleine, A. Rapaport, M. Bass, B. Chai, M. Richardson: Non-critical phase-matched second harmonic generation in $Gd_{1-x}Y_xCOB$. Appl. Phys. B **77(4)**, 437–440 (2003).

[9] H. Nakao, S. Makio, H. Furuya, K. Kawamura, S. Yasuda, Y.K. Yap, M. Yoshimura, Y. Mori, T. Sasaki: Crystal growth of GdYCOB for non-critical phase-matched

second-harmonic generation at 860 nm. J. Cryst. Growth **237–239**, 632–836 (2002).

[10] M. Yoshimura, T. Kobayashi, H. Furuya, K. Murase, Y. Mori, T. Sasaki: Crystal growth and optical properties of yttrium calcium oxyborate $YCa_4O(BO_3)_3$. In: *Advanced Solid-State Lasers, OSA Trends in Optics and Photonics Series, Vol. 19*, ed. by W.R. Bosenberg, M.M. Fejer (OSA, Washington DC, 1998), pp. 561–564.

[11] P.B.W. Burmester, T. Kellner, K. Petermann, G. Huber, R. Uecker, P. Reiche: Type-I noncritically phase-matched second-harmonic generation in $Gd_{1-x}Y_xCa_4O(BO_3)_3$. Appl. Phys. B **68(6)**, 1143–1146 (1999).

[12] E. Reino, E. Verdier, G. Aka, J.M. Benitez, D. Vivien: Frequency conversion for blue laser emission in $Gd_{1-x}Y_xCOB$. In: *Advanced Solid-State Lasers, OSA Trends in Optics and Photonics Series, Vol. 68*, ed. by M.E. Fermann, L.R. Marshall (OSA, Washington DC, 2002), pp. 32–36.

[13] M. Yoshimura, H. Furuya, I. Yamada, K. Murase, H. Nakao, M. Yamazaki, Y. Mori, T. Sasaki: Noncritically phase-matched ultraviolet generation in $Gd_xY_{1-x}Ca_4O(BO_3)_3$. In: *Advanced Solid-State Lasers, OSA Trends in Optics and Photonics Series, Vol. 26*, ed. by M.M. Fejer, H. Injeyan, U. Keller (OSA, Washington DC, 1999), pp. 82–88.

[14] H. Furuya, H.Nakao, I. Yamada, Y.F. Ruan, Y.K. Yap, M. Yoshimura, Y. Mori, T. Sasaki: Alleviation of photoinduced damage in $Gd_xY_{1-x}Ca_4O(BO_3)_3$ crystal at elevated crystal temperature for noncritically phase-matched 355-nm generation. Opt. Lett. **25(21)**, 1588–1590 (2000).

[15] H. Furuya, H. Nakao, I. Yamada, Y. Ruan, Y.K. Yap, M. Yoshimura, Y. Mori, T. Sasaki: Photoinduced damage in GdYCOB and its circumvention. In: *Advanced Solid-State Lasers, OSA Trends in Optics and Photonics Series, Vol. 34*, ed. by H. Injeyan, U. Keller, C. Marshall (OSA, Washington DC, 2000), pp. 404–408.

6.9 $Li_2B_4O_7$, Lithium Tetraborate (LB4)

Negative uniaxial crystal: $n_o > n_e$
Molecular mass: 169.118
Specific gravity: 2.45 g/cm^3 [1]
Point group: $4mm$
Lattice constants:
$a = 9.477$ Å [2]; 9.47 Å [3]; 9.479 Å [4]
$c = 10.286$ Å [2]; 10.26 Å [3]; 10.297 Å [4]
Mohs hardness: 5 [4]; 6 [5]
Melting point: 1190 K [1]

Linear thermal expansion coefficient α_t [4]

$\alpha_t \times 10^6$ [K^{-1}], $\parallel c$	$\alpha_t \times 10^6$ [K^{-1}], $\perp c$
3.74	11.1

Transparency range at "0" transmittance level: 0.16–3.5 μm [6]

Experimental values of refractive indices at 298 K and 10,325 Pa [6]

λ [μm]	n_o	n_e	λ [μm]	n_o	n_e
0.184887	1.774654	1.699128	0.70652	1.606162	1.549767
0.202548	1.733360	1.662581	0.85211	1.602303	1.546566
0.214438	1.714118	1.645491	1.01398	1.598952	1.543901
0.253652	1.674704	1.610421	1.12864	1.596794	1.542245
0.365015	1.632529	1.572896	1.52958	1.589202	1.536671
0.435835	1.621944	1.563516	1.97009	1.579263	1.529652
0.54607	1.612982	1.555638	2.32542	1.569365	1.522829
0.63282	1.608779	1.551997			

Temperature derivative of refractive indices for temperature range 233–373 K and spectral range 0.43584–0.64385 μm [in 10^{-6} K^{-1}] [6]:

T [K]							
λ [μm]	233–253	253–273	273–293	293–313	313–333	333–353	353–373
$\frac{dn_o}{dT}$							
0.43584	3.1	2.6	2.1	1.7	1.2	0.7	0.2
0.47999	2.9	2.4	1.9	1.4	0.9	0.4	−0.1
0.54607	2.7	2.2	1.7	1.2	0.7	0.2	−0.4
0.58929	2.7	2.2	1.6	1.1	0.6	0.1	−0.5
0.63282	2.6	2	1.5	1.0	0.5	0	−0.5
0.64385	2.6	2	1.5	1.0	0.5	−0.1	−0.6
$\frac{dn_e}{dT}$							
0.43584	4.6	4.2	3.8	3.4	3.0	2.6	2.2
0.47999	4.4	4	3.6	3.2	2.8	2.4	2.0
0.54607	4.3	3.8	3.4	3.0	2.6	2.2	1.8
0.58929	4.2	3.8	3.3	2.9	2.5	2.1	1.6
0.63282	4.1	3.7	3.3	2.8	2.4	2.0	1.6
0.64385	4.1	3.7	3.3	2.8	2.4	2.0	1.5

Best set of Sellmeier equations ($T = 298$ K, λ in μm) [6]:

$$n_o^2 = 2.56431 + \frac{0.012337}{\lambda^2 - 0.013103} - 0.019075\,\lambda^2$$

$$n_e^2 = 2.38651 + \frac{0.010664}{\lambda^2 - 0.012878} - 0.012813\,\lambda^2$$

Expressions for the effective second-order nonlinear coefficient (Kleinman symmetry conditions are valid, $d_{15} = d_{24} = d_{31} = d_{32}$) [7]:

$$d_{ooe} = d_{31} \sin\theta$$

Absolute value of second-order nonlinear coefficients [2], [8]:
$d_{31}(1.0642\,\mu\text{m}) = 0.12 \pm 0.03\text{pm/V}$
$d_{33}(1.0642\,\mu\text{m}) = 0.47 \pm 0.09\text{pm/V}$

Calculated values of phase-matching and "walk-off" angles

Interacting wavelengths [μm]	θ_{pm} [deg]	ρ_3 [deg]
SHG, o + o ⇒ e		
0.488 ⇒ 0.244	87.83	0.16
0.5106 ⇒ 0.2553	71.57	1.30
0.5145 ⇒ 0.25725	70.15	1.38
0.5321 ⇒ 0.26605	64.95	1.66
0.5782 ⇒ 0.2891	55.90	2.00
0.8 ⇒ 0.4	37.63	2.06
1.0642 ⇒ 0.5321	30.97	1.86
1.3188 ⇒ 0.6594	29.92	1.81
SFG, o + o ⇒ e		
1.0642 + 0.26605 ⇒ 0.21284	73.84	1.21
1.0642 + 0.35473 ⇒ 0.26605	52.83	2.11
1.0642 + 0.5321 ⇒ 0.35473	40.28	2.12

Laser-induced bulk damage threshold

λ [μm]	τ_p [ns]	I_{thr} [GW/cm^2]	Ref.	Note
0.532	10	>0.1	[6]	10 Hz
1.064	10	40	[5]	10 Hz

Laser-induced surface damage threshold [3]

λ [μm]	τ_p [ns]	I_{thr} [GW/cm^2]	Note
0.266	10	0.83	10 Hz
0.532	10	1.9	10 Hz
1.064	10	8.4	10 Hz

About the crystal

Though acoustic applications of LB4 were already known 20 years ago [9], it was not used much in nonlinear optics until now. The main reason for this is the rather small nonlinear coefficient of $Li_2B_4O_7$. Nevertheless, this material could find some applications due to its very short UV cutoff (around 160 nm) and high bulk damage threshold (at 1.064 nm four times more than that of fused silica) [5], [6]. Another advantage of $Li_2B_4O_7$ is its very low hygroscopicity. Therefore, this material has prospects for UV and deep-UV applications. Using an LB4 crystal, Japanese scientists managed to generate the fourth and fifth harmonics of a nanosecond Nd:YAG laser with pulse energies 0.16 and 0.07 J, respectively [6]. Very recently, employing the

cascade FoHG scheme (three quadrupler crystals), a total energy of 0.43 J at 266 nm was achieved, which corresponds to a 30.5% conversion efficiency from 532 nm radiation. Moreover, generation of 4 W UV power during 15 hours was demonstrated.

LB4 is conventionally produced by the Czochralski method [5]. Very recently, using the modified Bridgman technique, a Japanese group grew LB4 crystals of excellent optical quality, up to 10 cm in diameter and 20 cm in length [1], [10].

References

[1] N. Tsutsui, Y. Ino, K. Imai, N. Senguttuvan, M. Ishii: Growth of high quality 4in diameter $Li_2B_4O_7$ single crystals. J. Cryst. Growth **229(1–4)**, 283–288 (2001).

[2] S.-I. Furusawa, O. Chikagawa, S. Tange, T. Ishidate, H. Orihara, Y. Ishibashi, K. Miwa: Second harmonic generation in $Li_2B_4O_7$. J. Phys. Soc. Japan **60(8)**, 2691–2693 (1991).

[3] T. Sugawara, R. Komatsu, S. Uda: Surface damage and radiation resistance of lithium tetraborate single crystals. Opt. Mater. **13(2)**, 225–229 (1999).

[4] Data sheet of Molecular Technology GmbH, Available at www.mt-berlin.com.

[5] R. Komatsu, T. Sugawara, K. Sassa, N. Sarukura, Z. Liu, S. Izumida, Y. Segawa, S. Uda, T. Fukuda, K. Yamanouchi: Growth and ultraviolet application of $Li_2B_4O_7$ crystals: generation of the fourth and fifth harmonics of Nd:$Y_3Al_5O_{12}$ lasers. Appl. Phys. Lett. **70(26)**, 3492–3494 (1997).

[6] T. Sugawara, R. Komatsu, S. Uda: Linear and nonlinear optical properties of lithium tetraborate. Solid State Commun. **107(5)**, 233–237 (1998).

[7] J.E. Midwinter, J. Warner: The effects of phase matching method and of uniaxial crystal symmetry on the polar distribution of second-order non-linear optical polarization. Brit. J. Appl. Phys. **16(11)**, 1135–1142 (1965).

[8] K. Hagimoto, A. Mito: Determination of the second-order susceptibility of ammonium dihydrogen phosphate and α-quartz at 633 and 1064 nm. Appl. Opt. **34(36)**, 8276–8282 (1995).

[9] R.W. Whatmore, N.M. Shorrocks, C. O'Hara, F.W. Ainger, I.M. Young: Lithium tetraborate: a new temperature-compensated SAW substrate material. Electr. Lett. **17(1)**, 11–12 (1981).

[10] N. Tsutsui, Y. Ino, K. Imai, N. Senguttuvan, M. Ishii: Growth of large size LBO ($Li_2B_4O_7$) single crystals by modified Bridgman technique. J. Cryst. Growth **211(1–4)**, 271–275 (2000).

6.10 $LiRbB_4O_7$, Lithium Rubidium Tetraborate (LRB4)

Negative biaxial crystal: $2V_z = 130°$ at $\lambda = 0.532\,\mu m$ [1]
Molecular mass: 247.644
Specific gravity: $2.63\,g/cm^3$ (calculated) [2]
Point group: 222
Lattice constants:
$a = 8.6257 \pm 0.0012$ Å [2]
$b = 11.2576 \pm 0.0013$ Å [2]
$c = 12.8531 \pm 0.0015$ Å [2]
Assignment of dielectric and crystallographic axes: $X, Y, Z \Rightarrow b, c, a$

Transparency range at 0.01 transmittance level for 1.5-cm-long crystal: 0.187 – 3.468 μm [1]

Experimental values of refraction indices at room temperature [1]

λ [μm]	n_X	n_Y	n_Z	λ [μm]	n_X	n_Y	n_Z
0.4005	1.52660	1.55276	1.55924	0.5605	1.51425	1.53967	1.54584
0.4105	1.52570	1.55165	1.55814	0.5695	1.51375	1.53926	1.54533
0.42	1.52440	1.54965	1.55684	0.5805	1.51325	1.53857	1.54484
0.431	1.52345	1.54956	1.55553	0.5875	1.51290	1.53826	1.54433
0.441	1.52300	1.54926	1.55533	0.6	1.51230	1.53746	1.54384
0.452	1.52145	1.54766	1.55333	0.6095	1.51200	1.53706	1.54354
0.458	1.52080	1.54687	1.55263	0.6215	1.51160	1.53686	1.54324
0.4685	1.52000	1.54605	1.55193	0.633	1.51110	1.53615	1.54254
0.479	1.51915	1.54507	1.55093	0.6405	1.51095	1.53586	1.54254
0.5005	1.51770	1.54367	1.54943	0.652	1.51045	1.53556	1.54184
0.509	1.51690	1.54256	1.54863	0.661	1.51025	1.53516	1.54184
0.5185	1.51640	1.54217	1.54803	0.67	1.50990	1.53465	1.54144
0.532	1.51590	1.54176	1.54763	0.678	1.50970	1.53476	1.54114
0.541	1.51520	1.54075	1.54673	0.6895	1.50945	1.53435	1.54074
0.548	1.51475	1.54025	1.54633	0.7005	1.50925	1.53365	1.54054

Sellmeier equations (λ in μm, $T = 293$ K) [1]:

$$n_X^2 = 1 + \frac{1.2610153\,\lambda^2}{\lambda^2 - 0.0087354} - 0.0135545\,\lambda^2$$

$$n_Y^2 = 1 + \frac{1.3458727\,\lambda^2}{\lambda^2 - 0.0080394} - 0.0330918\,\lambda^2$$

$$n_Z^2 = 1 + \frac{1.3510711\,\lambda^2}{\lambda^2 - 0.0091806} - 0.0074562\,\lambda^2$$

Expressions for the effective second-order nonlinear coefficient in the principal planes of LRB4 crystal (Kleinman symmetry conditions are valid, $d_{14} = d_{25} = d_{36}$) [3]:

XY plane

$d_{\mathrm{eoe}} = d_{\mathrm{oee}} = d_{14} \sin 2\phi$

YZ plane

$d_{\mathrm{eeo}} = d_{14} \sin 2\theta$

XZ plane, $\theta < V_z$

$d_{\mathrm{eoe}} = d_{\mathrm{oee}} = -d_{14} \sin 2\theta$

XZ plane, $\theta > V_z$

$d_{\mathrm{eeo}} = -d_{14} \sin 2\theta$

Second-order nonlinear coefficient:

$d_{14}(1.064\,\mu\mathrm{m}) = 1.15 \times d_{36}(\mathrm{KDP}) = 0.45\mathrm{pm/V}$[1], [4]

About the crystal

A recently grown material, an analog of LB4, with a slightly higher value of the second-order nonlinear coefficient.

References

[1] R. Komatsu, Y. Ono, T. Kajatani, F. Rotermund, V. Petrov: Optical properties of a new nonlinear borate crystal $LiRbB_4O_7$. J. Cryst. Growth **257(1–2)**, 165–168 (2003).
[2] Y. Ono, M. Nakaya, T. Sugawara, N. Watanabe, H. Siraishi, R. Komatsu, T. Kajitani: Structural study of $LiKB_4O_7$ and $LiRbB_4O_7$: new nonlinear optical crystals. J. Cryst. Growth **229(1–4)**, 472–476 (2001).
[3] B.V. Bokut: Optical mixing in biaxial crystals. Zh. Prikl. Spektrosk. **7(4)**, 621–624 (1967) [In Russian, English trans.: J. Appl. Spectrosc. **7(4)**, 425–429 (1967)].
[4] D.A. Roberts: Simplified characterization of uniaxial and biaxial nonlinear optical crystals: a plea for standardization of nomenclature and conventions. IEEE J. Quant. Electr. **28(10)**, 2057–2074 (1992).

6.11 $CdHg(SCN)_4$, Cadmium Mercury Thiocyanate (CMTC)

Negative uniaxial crystal: $n_o > n_e$
Molecular mass: 545.221
Specific gravity (calculated): 3.25 g/cm^3 [1]; 3.54 g/cm^3 [2]
Specific gravity (observed): 3.06 g/cm^3 [3]
Point group: $\bar{4}$
Lattice constants [1]:
$a = 11.48 \pm 0.02$ Å [3]; 11.487 ± 0.003 Å [1]
$c = 4.33 \pm 0.02$ Å [3]; 4.218 ± 0.001 Å [1]
Mohs hardness: 2.9 [1]; 2.7 ($\parallel c$) [4]; 2.9 ($\perp c$) [4]
Decomposition temperature: 537 K [4]

Mean value of linear thermal expansion coefficient [4]

T [K]	$\alpha_t \times 10^6$ [K^{-1}], $\parallel c$	$\alpha_t \times 10^6$ [K^{-1}], $\perp c$
298–473	228	−19.3

Specific heat capacity c_p at $P = 0.101325$ MPa [4]

T [K]	c_p [J/kgK]
293	758.8

Transparency range at 0.5 transmittance level for 0.22-cm-long crystal is 0.4 to >2.35 μm [1].
First infrared absorption band is at 2.35 μm [1].
The UV transmission cutoff is at 0.38 μm [5], [6].

Experimental values of refraction indices at $T = 293$ K [5]

λ[μm]	n_o	n_e
0.4358	2.073	1.8069
0.4471	2.0619	
0.5461	1.997	1.7668
0.5875	1.9819	1.7586
0.5893	1.9814	1.7583
0.6563	1.9636	1.7489
0.6678	1.9621	1.7476
0.7065	1.9543	1.7439

Sellmeier equations (λ in μm, $T = 293$ K) [1], [5], [7]:

$$n_o^2 = 3.661861 + \frac{0.077588}{\lambda^2 - 0.069737} - 0.045487\,\lambda^2$$

$$n_e^2 = 2.950921 + \frac{0.041337}{\lambda^2 - 0.058791} - 0.007592\,\lambda^2$$

There is a mistake in sign of the last member in the expression for n_o, published in [1], [7].

The form of Sellmeier equations given in [5] is incorrect.

Expressions for the effective second-order nonlinear coefficient (Kleinman symmetry conditions are valid, $d_{15} = d_{31}$ and $d_{14} = d_{25} = d_{36}$) [8]:

$d_{ooe} = d_{36} \sin\theta \sin 2\phi + d_{31} \sin\theta \cos 2\phi$

$d_{eoe} = d_{oee} = d_{36} \sin 2\theta \cos 2\phi - d_{31} \sin 2\theta \sin 2\phi$

Values of second-order nonlinear coefficients:

$|d_{31}(1.064\,\mu\text{m})| = (1.3 \pm 0.1) \times d_{33}(\text{LiIO}_3) = 6.0 \pm 0.9$ pm/V [3], [9], [10]

$|d_{31}(1.064\,\mu\text{m})| = (16.0 \pm 3.0) \times d_{36}(\text{KDP}) = 6.2 \pm 1.2$ pm/V [5], [11]

$|d_{36}(1.064\,\mu\text{m})| = (0.3 \pm 0.1) \times d_{33}(\text{LiIO}_3) = 1.4 \pm 0.6$ pm/V [3], [9], [10]

$|d_{36}(1.064\,\mu\text{m})| = (3.7 \pm 1.0) \times d_{36}(\text{KDP}) = 1.4 \pm 0.4$ pm/V [5], [11]

Experimental values of phase-matching angle ($T = 293$ K)

Interacting wavelengths [μm]	θ_{exp} [deg]	Ref.
SHG, $o + o \Rightarrow e$		
$0.809 \Rightarrow 0.4045$	47.7	[1]
	48.4	[5]
SHG, $e + o \Rightarrow e$		
$0.946 \Rightarrow 0.473$	$\approx$54	[12]
$0.809 \Rightarrow 0.4045$	72.7	[5]
SFG, $o + e \Rightarrow e$		
$0.946 + 0.9385 \Rightarrow 0.4711$	$\approx$54	[13]
$0.946 + 0.808 \Rightarrow 0.4358$	$\approx$60	[6]

About the crystal

The nonlinear optical properties of the organometallic complex CMTC crystal were known from 1970 [3]. Recently, the quality of this nonlinear material was improved significantly [1], [2], which allowed the application of CMTC for SHG of CW laser diodes. In [7], 11.8-mW of CW blue output at 404 nm was generated at a fundamental frequency power of 2 W.

References

[1] D. Yuan, D. Xu, M. Liu, F. Qi, W. Yu, W. Hou, Y. Bing, S. Sun, M. Jiang: Structure and properties of a complex crystal for laser diode frequency doubling: cadmium mercury thiocyanate. Appl. Phys. Lett. **70(5)**, 544–546 (1997).

[2] D. Yuan, Z. Zhong, M. Liu, D. Xu, Q. Fang, Y. Bing, S. Sun, M. Jiang: Growth of cadmium mercury thiocyanate single crystal for laser diode frequency doubling. J. Cryst. Growth **186(1–2)**, 240–244 (1998).

[3] J.G. Bergman, Jr., J.H. McFee, G.R. Crane: Nonlinear optical properties of $CdHg(SCN)_4$ and $ZnHg(SCN)_4$. Mat. Res. Bull. **5(11)**, 913–918 (1970).

[4] D. R. Yuan, D. Xu, G.-H. Zhang, M.-G. Liu, S.-Y. Guo, F.-Q. Meng, M.-K. Lu, Q. Fang, M.-H. Jiang: Thermal and mechanical properties of a complex nonlinear optical material: cadmium mercury thiocyanate crystal. Chin. Phys. Lett. **17(9)**, 669–671 (2000).

[5] G. Zhang, M. Liu, D. Xu, D. Yuan, W. Sheng, J. Yao: Blue-violet light second harmonic generation with CMTC crystals. J. Mat. Sci. Lett. **19(14)**, 1255–1257 (2000).

[6] C.Q. Wang, Y.T. Chow, W.A. Gambling, D.R. Yuan, D. Xu, G.H. Zhang, M.H. Jiang: A continuous-wave tunable solid-state blue laser based on intracavity sum-frequency mixing and pump-wavelength tunung. Appl. Phys. Lett. **75(13)**, 1821–1823 (1999).

[7] J. Jin, S. Guo, F. Lu, Q. Jiao, J. Yao, G. Zhang: Blue-violet light by direct frequency doubling of laser diode. Proc. SPIE **3928**, 228–231 (2000).

[8] J.E. Midwinter, J. Warner: The effects of phase matching method and of uniaxial crystal symmetry on the polar distribution of second-order non-linear optical polarization. Brit. J. Appl. Phys. **16(11)**, 1135–1142 (1965).

[9] J. Jerphagnon: Optical nonlinear susceptibilities of lithium iodate. Appl. Phys. Lett. **16(8)**, 298–299 (1970).

[10] R.J. Gehr, A.V. Smith: Separated-beam nonphase-matched second-harmonic method of characterizing nonlinear optical coefficients. J. Opt. Soc. Am. B **15(8)**, 2298–2307 (1998).

[11] D.A. Roberts: Simplified characterization of uniaxial and biaxial nonlinear optical crystals: a plea for standardization of nomenclature and conventions. IEEE J. Quant. Electr. **28(10)**, 2057–2074 (1992).

[12] C.Q. Wang, Y.T. Chow, W.A. Gambling, D. Yuan, D. Xu, G. Zhang, M. Liu, M. Jiang: Intracavity-frequency-doubling of a 946 nm ND:YAG laser with cadmium mercury thiocyanate crystal. Opt. Laser Technol. **30(5)**, 291–293 (1998).

[13] C.Q. Wang, Y.T. Chow, D.R. Yuan, D. Xu, G.H. Zhang, M.G. Liu, J.R. Lu, Z.S. Shao, M.H. Jiang: CW dual-wavelength Nd:YAG laser at 946 and 938.5 nm and intracavity nonlinear frequency conversion with a CMTC crystal. Opt. Commun. **165(4–6)**, 231–235 (1999).

6.12 Nb:KTiOPO$_4$, Niobium-Doped KTP ($Nb_xK_{1-x}Ti_{1-x}OPO_4$ or NbKTP)

Positive biaxial crystal: $2V_Z = 37.8°$ at $\lambda = 0.6328\,\mu m$ (7.5 mol% Nb)
Molecular mass: 198.393 (7.5 mol% Nb)
Point group: $mm2$
Lattice constants
for 3.4 mol% Nb-doped KTP crystal [1]:
$a = 12.828$ Å
$b = 6.409$ Å
$c = 10.592$ Å
for 7.9 mol% Nb-doped KTP crystal [2]:
$a = 12.819$ Å
$b = 6.411$ Å
$c = 10.599$ Å
Assignment of dielectric and crystallographic axes: $X, Y, Z \Rightarrow a, b, c$
UV cutoff wavelength for 3.4 mol% Nb-doped KTP crystal is at $0.35\,\mu m$ ($\|a$) or at $0.37\,\mu m$ ($\|c$) [1]
IR transmission cutoff for 3.4 mol% Nb-doped KTP crystal is at $4.38\,\mu m$ [1]

Experimental values of refractive indices at $T = 293$ K (7.5 mol% Nb) [3], [4]

λ [μm]	n_X	n_Y	n_Z
0.53975	1.7791	1.7918	1.9024
0.6328	1.7640	1.7751	1.8790
1.0795	1.7389	1.7479	1.8409
1.3414	1.7326	1.7412	1.8318

Sellmeier equations (λ in μm, $T = 293$ K) (3.4 mol% Nb) [1]:

$$n_X^2 = 3.0028 + \frac{0.04113}{\lambda^2 - 0.04341} - 0.01049\,\lambda^2$$

$$n_Y^2 = 3.0359 + \frac{0.04399}{\lambda^2 - 0.04843} - 0.01070\,\lambda^2$$

$$n_Z^2 = 3.3467 + \frac{0.06282}{\lambda^2 - 0.06153} - 0.01328\,\lambda^2$$

Sellmeier equations (λ in μm, $T = 293$ K) (7.5 mol% Nb) [3]:

$$n_X^2 = 3.0060 + \frac{0.038424}{\lambda^2 - 0.056149} - 0.014512\,\lambda^2$$

$$n_Y^2 = 3.0351 + \frac{0.041414}{\lambda^2 - 0.061208} - 0.015125\,\lambda^2$$

$$n_Z^2 = 3.3575 + \frac{0.061421}{\lambda^2 - 0.061847} - 0.020850\,\lambda^2$$

The same data for 7.5 mol% Nb-doped KTP crystal were published also in [4], [5], [6], [7], [8].
Sellmeier equations for different Nb concentrations (3, 5, 7.5 and 10 mol%) are given in [8].

Thermal derivatives of refractive indices of 7.5 mol% NbKTP [3], [7]

λ [μm]	$dn_X/dT \times 10^5$ [K^{-1}]	$dn_Y/dT \times 10^5$ [K^{-1}]	$dn_Z/dT \times 10^5$ [K^{-1}]
0.53975	1.45	2.57	4.86
0.6328	1.35	2.22	4.03
1.0795	1.01	1.75	3.09
1.3414	1.04	1.75	3.43

Note: Slightly different values are presented (by the same group) in [5], [4]

Temperature derivatives of refractive indices for 7.5 mol% NbKTP for $T = 293$–416 K and for spectral range $0.53975\,\mu\text{m} < \lambda < 1.3414\,\mu\text{m}$ (λ in μm) [4], [6]:

$$\frac{dn_X}{dT} = \left(-\frac{0.42291}{\lambda^3} + \frac{1.8404}{\lambda^2} - \frac{2.1315}{\lambda} + 1.7414\right) \times 10^{-5}\,\text{K}^{-1}$$

$$\frac{dn_Y}{dT} = \left(\frac{0.35971}{\lambda^3} - \frac{0.38911}{\lambda^2} - \frac{0.16181}{\lambda} + 1.9378\right) \times 10^{-5}\,\text{K}^{-1}$$

$$\frac{dn_Z}{dT} = \left(-\frac{3.0680}{\lambda^3} + \frac{13.5595}{\lambda^2} - \frac{17.4293}{\lambda} + 10.0987\right) \times 10^{-5}\,\text{K}^{-1}$$

Expressions for the effective second-order nonlinear coefficient in principal planes of NbKTP crystal (Kleinman symmetry conditions are not valid) [9]:

XY plane

$d_{\text{eoe}} = d_{\text{oee}} = d_{15}\sin^2\phi + d_{24}\cos^2\phi$

YZ plane

$d_{\text{oeo}} = d_{\text{eoo}} = d_{15}\sin\theta$

XZ plane, $\theta < V_z$

$d_{\text{ooe}} = d_{32}\sin\theta$

XZ plane, $\theta > V_z$

$d_{\text{oeo}} = d_{\text{eoo}} = d_{24}\sin\theta$

Expressions for the effective second-order nonlinear coefficient in principal planes of NbKTP crystal (Kleinman symmetry conditions are valid, $d_{15} = d_{31}$ and $d_{24} = d_{32}$) [9]:

XY plane

$d_{\text{eoe}} = d_{\text{oee}} = d_{31}\sin^2\phi + d_{32}\cos^2\phi$

YZ plane

$d_{\text{oeo}} = d_{\text{eoo}} = d_{31}\sin\theta$

XZ plane, $\theta < V_z$

$d_{\text{ooe}} = d_{32}\sin\theta$

XZ plane, $\theta > V_z$

$d_{\text{oeo}} = d_{\text{eoo}} = d_{32}\sin\theta$

Effective second-order nonlinear coefficient for three-wave interactions in the arbitrary direction of NbKTP crystal is given in [9]

Values of second-order nonlinear coefficients (3.4 mol% Nb) [1], [10]:

$d_{15}(1.064\,\mu\text{m}) = (0.8 \pm 0.1) \times d_{15}(\text{KTP}) = 1.5 \pm 0.2\,\text{pm/V}$

$d_{24}(1.064\,\mu\text{m}) = (2.2 \pm 0.1) \times d_{15}(\text{NbKTP}) = 3.3 \pm 0.4\,\text{pm/V}$

Values of second-order nonlinear coefficients (7.9 mol% Nb) [2], [10]:

$d_{15}(1.064\,\mu\text{m}) = 0.75 \times d_{15}(\text{KTP}) \pm 10\% = 1.4 \pm 0.2\,\text{pm/V}$

$d_{24}(1.064\,\mu\text{m}) = 1.13 \times d_{24}(\text{KTP}) \pm 10\% = 4.2 \pm 0.4\,\text{pm/V}$

$d_{33}(1.064\,\mu\text{m}) = 0.9 \times d_{33}(\text{KTP}) \pm 10\% = 13.1 \pm 1.3\,\text{pm/V}$

Experimental values of phase-matching angle for 3.4 mol% Nb-doped KTP [1]

Interacting wavelengths [μm]	θ_{exp} [deg]
YZ plane, $\phi = 90°$	
SHG, $o + e \Rightarrow o$	
1.0642 ⇒ 0.5321	62.9
SFG, $o + e \Rightarrow o$	
1.3188 + 0.6594 ⇒ 0.4396	60.1
XZ plane, $\phi = 0°$, $\theta > V_z$	
SHG, $o + e \Rightarrow o$	
1.0642 ⇒ 0.5321	80.8
1.1523 ⇒ 0.57615	67.6
1.3188 ⇒ 0.6594	57.0
1.5791 ⇒ 0.78955	49.7
SFG, $o + e \Rightarrow o$	
1.3188 + 0.6594 ⇒ 0.4396	78.1
1.5791 + 0.6358 ⇒ 0.4533	63.3
1.5791 + 1.0642 ⇒ 0.6358	51.8

Experimental values of phase-matching angle for 7.5 mol% Nb-doped KTP [3]

Interacting wavelengths [μm]	θ_{pm} [deg]
XZ plane, $\phi = 0°$, $\theta > V_z$	
SHG, $o + e \Rightarrow o$	
1.0642 ⇒ 0.5321	81.4
1.0795 ⇒ 0.53975	77.6

Note: The same data on phase-matching angle values for 7.5 mol% Nb-doped KTP crystal were published also in [4], [5], [6], [7], [8], [11]

Experimental value of temperature bandwidth for 3.4 mol% Nb-doped KTP [1]

Interacting wavelengths [μm]	ΔT [°C]
XZ plane, $\phi = 0°$, $\theta > V_z$	
SHG, $o + e \Rightarrow o$	
1.0642 ⇒ 0.5321	16.4

Calculated values of internal angular, temperature and spectral bandwidth for 7.5 mol% Nb-doped KTP crystal [6]

Interacting wavelengths [μm]	ϕ_{pm} [deg]	θ_{pm} [deg]	$\Delta\phi^{int}$ [deg]	$\Delta\theta^{int}$ [deg]	ΔT [°C]	$\Delta\nu$ [cm^{-1}]
XY plane, $\theta = 90°$						
SHG, $e + o \Rightarrow e$						
$0.98 \Rightarrow 0.49$	65.1		0.38	1.70	10.5	1.9
$0.9656 \Rightarrow 0.4828$	90		4.02	1.76	6.6	1.8
XZ plane, $\phi = 0°$, $\theta > V_z$						
SHG, $o + e \Rightarrow o$						
$1.3414 \Rightarrow 0.6707$		56.6	2.72	0.08	42.6	4.4
$1.0642 \Rightarrow 0.5321$		81.5	1.89	0.19	20.6	2.2
$1.0511 \Rightarrow 0.52555$		90	4.45	1.76	18.3	2.1

About the crystal

The doping of KTP with niobium leads to the increase of birefringence and to the blue shift of the shortest available SH wavelength [2]. For example, 7.5 mol.% doping shifts the SHG cutoff wavelength from 0.994 to 0.9656 μm [6]. This is important for some applications like frequency doubling of semiconductor lasers. However, very high doping levels are unsuitable, as they simultaneously lead to the decrease of second-order nonlinear coefficients [2].

References

[1] K. Kato, N. Umemura, M. Saga: Second-harmonic and sum-frequency generation in Nb doped KTP. In: *Advanced Solid-State Lasers, OSA Trends in Optics and Photonics Series, Vol. 19*, ed. by W.R. Bosenberg, M.M. Fejer (OSA, Washington DC, 1998), pp. 82–84.

[2] L.T. Cheng, L.K. Cheng, R.L. Harlow, J.D. Bierlein: Blue light generation using bulk single crystals of niobium-doped KTiOPO$_4$. Appl. Phys. Lett. **64(2)**, 155–157 (1994).

[3] H. Shen, D. Zhang, W. Liu, W. Chen, G. Zhang, G. Zhang, W. Lin: Measurement of refractive indices and thermal refractive-index coefficients of 7.5-mol% Nb:KTiOPO$_4$ crystal. Appl. Opt. **38(6)**, 987–990 (1999).

[4] D.Y. Zhang, H.Y. Shen, W. Liu, G.F. Zhang, W.Z. Chen, G. Zhang, R.R. Zeng, C.H. Huang, W.X. Lin, J.K. Liang: The thermal refractive index coefficients of 7.5 mol% Nb:KTiOPO$_4$ crystals. J. Appl. Phys. **86(7)**, 3516–3518 (1999).

[5] D.Y. Zhang, H.Y. Shen, W. Liu, G.F. Zhang, W.Z. Chen, G. Zhang, R.R. Zeng, C.H. Huang, W.X. Lin, J.K. Liang: The expressions of the principal thermal refractive index coefficients of 7.5 mol% Nb:KTiOPO$_4$ crystals. Opt. Commun. **168(1–4)**, 111–115 (1999).

[6] D.Y. Zhang, H.Y. Shen, W. Liu, G.F. Zhang, W.Z. Chen, G. Zhang, R.R. Zeng, C.H. Huang, W.X. Lin, J.K. Liang: Study of the nonlinear optical properties of 7.5 mol% Nb:KTP crystals. IEEE J. Quant. Electr. **35(10)**, 1447–1450 (1999).

[7] W. Liu, H.Y. Shen, G.F. Zhang, D.Y. Zhang, G. Zhang, W.X. Lin, R.R. Zeng, C.H. Huang: Studies on the phase-matching condition and the cut-off wavelength of Nb:KTiOPO$_4$ crystal. Opt. Commun. **185(1–3)**, 191–196 (2000).

[8] D.Y. Zhang, H.Y. Shen, W. Liu, G.F. Zhang, W.Z. Chen, G. Zhang, R.R. Zeng, C.H. Huang, W.X. Lin, J.K. Liang: The principal refractive indices and nonlinear optical phase matched properties of Nb:KTP crystals. Opt. Mater. **15(2)**, 99–102 (2000).
[9] V.G. Dmitriev, D.N. Nikogosyan: Effective nonlinearity coefficients for three-wave interactions in biaxial crystals of $mm2$ point group symmetry. Opt. Commun. **95(1–3)**, 173–182 (1993).
[10] I. Shoji, T. Kondo, A. Kitamoto, M. Shirane, R. Ito: Absolute scale of second-order nonlinear-optical coefficients. J. Opt. Soc. Am. B **14(9)**, 2268–2294 (1997).
[11] D.Y. Zhang, H.Y. Shen, W. Liu, W.Z. Chen, G.F. Zhang, G. Zhang, R.R. Zeng, C.H. Huang, W.X. Lin, J.K. Liang: Crystal growth, X-ray diffraction and nonlinear optical properties of Nb:$KTiOPO_4$ crystal. J. Cryst. Growth **218(1)**, 98–102 (2000).

6.13 $RbTiOPO_4$, Rubidium Titanyl Phosphate (RTP)

Positive biaxial crystal: $2V_z = 39°$ at $\lambda = 0.8\,\mu m$ [1]
Molecular mass: 244.318
Specific gravity: 3.64 g/cm^3 [1]
Point group: $mm2$
Lattice constants:
$a = 12.964$ Å [2]; 12.980 Å [3]
$b = 6.4985$ Å [2]; 6.509 Å [3]
$c = 10.563$ Å [2]; 10.578 Å [3]
Assignment of dielectric and crystallographic axes: $X, Y, Z \Rightarrow a, b, c$
Vickers hardness at indenter load 50 g: 640 kgf/mm^2 (along [100] direction) [3]
Melting point: 1213 K [1]
Decomposition temperature: 1374 K [2]
Transparency range at "0" transmittance level: $0.35 - 4.5\,\mu m$ [1] with the orthophosphate overtone at $3.5\,\mu m$ [4]
UV transmission cutoff ($\alpha = 2 cm^{-1}$) is at $0.360\,\mu m$ ($\mathbf{E}\|X$); $0.370\,\mu m$ ($\mathbf{E}\|Y$); $0.384\,\mu m$ ($\mathbf{E}\|Z$) [4].

Linear absorption coefficient α [4]

λ [μm]	α [cm^{-1}]	Note
0.473	0.108	$\mathbf{E}\|X$
	0.163	$\mathbf{E}\|Y$
	0.279	$\mathbf{E}\|Z$
0.532	0.069	$\mathbf{E}\|X$
	0.087	$\mathbf{E}\|Y$
	0.151	$\mathbf{E}\|Z$

Experimental values of refractive indices at room temperature [1]

λ [μm]	n_X	n_Y	n_Z
0.4047	1.8551	1.8765	1.9972
0.4254	1.8429	1.8621	1.9764
0.4358	1.8377	1.8560	1.9672

λ [μm]	n_X	n_Y	n_Z
0.4916	1.8169	1.8321	1.9328
0.5322	1.8067	1.8205	1.9160
0.5461	1.8037	1.8172	1.9117
0.5770	1.7981	1.8110	1.9029
0.6104	1.7930	1.8053	1.8952
0.6708	1.7860	1.7975	1.8843
0.6925	1.7839	1.7952	1.8811
1.0644	1.7652	1.7749	1.8536

Sellmeier equations (λ in μm, $0.50\,\mu m < \lambda < 4.22\,\mu m$ for n_X, $0.56\,\mu m < \lambda < 4.24\,\mu m$ for n_Y, $0.94\,\mu m < \lambda < 3.40\,\mu m$ for n_Z) [1]:

$$n_X^2 = 2.1982 + \frac{0.89948}{1-(0.2152/\lambda)^{1.9727}} + \frac{1.5433}{1-(11.585/\lambda)^{1.9505}}$$

$$n_Y^2 = 2.2804 + \frac{0.84585}{1-(0.22963/\lambda)^{1.9696}} + \frac{1.1009}{1-(9.6602/\lambda)^{1.9369}}$$

$$n_Z^2 = 2.3412 + \frac{1.0609}{1-(0.26461/\lambda)^{2.0585}} + \frac{0.9714}{1-(8.149/\lambda)^{2.0038}}$$

Other sets of dispersion relations are given in [5], [6], [7].

Linear electrooptic coefficients measured at low frequencies (well below the acoustic resonances of RTA crystal, i.e., for the "free" crystal) at room temperature [5], [6]

λ [μm]	r_{13}^T [pm/V]	r_{23}^T [pm/V]	r_{33}^T [pm/V]
0.6328	10.9 ± 1.1	15.0 ± 1.5	33.0 ± 3.3

Coercive field value: 3–3.5 kV/mm [8]
Expressions for the effective second-order nonlinear coefficient in principal planes of RTP crystal (Kleinman symmetry conditions are not valid) [9]:

XY plane

$d_{eoe} = d_{oee} = d_{15}\sin^2\phi + d_{24}\cos^2\phi$

YZ plane

$d_{oeo} = d_{eoo} = d_{15}\sin\theta$

XZ plane, $\theta < V_z$

$d_{ooe} = d_{32}\sin\theta$

XZ plane, $\theta > V_z$

$d_{oeo} = d_{eoo} = d_{24}\sin\theta$

Expressions for the effective second-order nonlinear coefficient in principal planes of RTP crystal (Kleinman symmetry conditions are valid, $d_{15} = d_{31}$ and $d_{24} = d_{32}$) [9]:

XY plane

$d_{eoe} = d_{oee} = d_{31}\sin^2\phi + d_{32}\cos^2\phi$

YZ plane
$d_{oeo} = d_{eoo} = d_{31} \sin\theta$
XZ plane, $\theta < V_z$
$d_{ooe} = d_{32} \sin\theta$
XZ plane, $\theta > V_z$
$d_{oeo} = d_{eoo} = d_{32} \sin\theta$
Effective second-order nonlinear coefficient for three-wave interactions in the arbitrary direction of RTP crystal is given in [9].
The signs of RTP second-order nonlinear coefficients are probably all the same [10].
Absolute values of second-order nonlinear coefficients [5], [6]:
$d_{31}(1.064\,\mu\text{m}) = 3.3 \pm 0.6\text{pm/V}$
$d_{32}(1.064\,\mu\text{m}) = 4.1 \pm 0.8\text{pm/V}$
$d_{33}(1.064\,\mu\text{m}) = 17.1 \pm 3.4\text{pm/V}$

Experimental values of phase-matching angle

Interacting wavelengths [μm]	ϕ_{pm} [deg]	θ_{pm} [deg]	Ref.
XY plane, $\theta = 90°$			
SHG, $e + o \Rightarrow e$			
1.064 ⇒ 0.532	60.0		[5]
	58.0		[7]
	57.4		[11]
1.079 ⇒ 0.5395	48.5		[7]
YZ plane, $\phi = 90°$			
SHG, $o + e \Rightarrow o$			
1.064 ⇒ 0.532		76.0	[7]
1.079 ⇒ 0.5395		73.5	[7]

Experimental values of internal angular and temperature bandwidths [7],

Interacting wavelengths [μm]	ϕ_{pm} [deg]	$\Delta\phi^{int}$ [deg]	ΔT [°C]
XY plane, $\theta = 90°$			
SHG, $e + o \Rightarrow e$			
1.0642 ⇒ 0.5321	58	0.42	40

Laser-induced damage threshold

λ[μm]	τ_p [ns]	I_{thr} [GW/cm^2]	Ref.	Note
1.0642	15	0.9	[7]	10 Hz
	10	>0.2	[11]	10 Hz

About the crystal

As a KTP analog, the RTP crystal has not received much attention in past decade, though it was shown that it possesses a 1.8 times higher laser damage threshold than KTP itself [7]. Recently, QPM SHG in PPRTP was demonstrated [12].

References

[1] Y. Guillien, B. Menaert, J.P. Feve, P. Segonds, J. Douady, B. Boulanger, O. Pacaud: Crystal growth and refined Sellmeier equations over the complete transparency range of $RbTiOPO_4$. Opt. Mater. **22(2)**, 155–162 (2003).

[2] L.K. Cheng, E.M. McCarron III, J. Calabrese, J.D. Bierlein, A.A. Ballman: Development of the nonlinear optical crystal $CsTiOAsO_4$. I. Structural stability. J. Cryst. Growth **132(1–2)**, 280–288 (1993).

[3] C.V. Kannan, S. Ganesa Moorthy, V. Kannan, C. Subramanian, P. Ramasamy: TSSG of $RbTiOPO_4$ single crystals from phosphate flux and their characterization. J. Cryst. Growth **245(3–4)**, 289–296 (2002).

[4] G. Hansson, H. Karlsson, S. Wang, F. Laurell: Transmission measurements in KTP and isomorphic compounds. Appl. Opt. **39(27)**, 5058–5069 (2000).

[5] L.-T. Cheng, L.K. Cheng, J.D. Bierlein: Linear and nonlinear optical properties of the arsenate isomorphs of KTP. Proc. SPIE **1863**, 43–53 (1993).

[6] L.K. Cheng, L.T. Cheng, J. Galperin, P.A. Morris Hotsenpiller, J.D. Bierlein: Crystal growth and characterization of $KTiOPO_4$ isomorphs from the self-fluxes. J. Cryst. Growth **137(1–2)**, 107–115 (1994).

[7] Y.S. Oseledchik, A.I. Pisarevsky, A.L. Prosvirnin, V.V. Starshenko, N.V. Svitanko: Nonlinear optical properties of the flux grown $RbTiOPO_4$ crystal. Opt. Mater. **3(4)**, 237–242 (1994).

[8] H. Karlsson, F. Laurell: Electric field poling of flux grown $KTiOPO_4$. Appl. Phys. Lett. **71(24)**, 3474–3476 (1997).

[9] V.G. Dmitriev, D.N. Nikogosyan: Effective nonlinearity coefficients for three-wave interactions in biaxial crystals of mm2 point group symmetry. Opt. Commun. **95(1–3)**, 173–182 (1993).

[10] A. Anema, T. Rasing: Relative signs of the nonlinear coefficients of potassium titanyl phosphate. Appl. Opt. **36(24)**, 5902–5904 (1997).

[11] U. Chatterjee, P. Kumbhakar, A.K. Chaudhary, G.C. Bhar: Tunable mid-infrared generation in rubidium titanyl phosphate crystal by difference frequency mixing. Nonl. Opt. **28(1–2)**, 95–106 (2001).

[12] H. Karlsson, F. Laurell, L.K. Cheng: Periodic poling of $RbTiOPO_4$ for quasi-phase matched blue light generation. Appl. Phys. Lett. **74(11)**, 1519–1521 (1999).

6.14 $LiInS_2$, Lithium Thioindate (LIS)

Negative biaxial crystal: $2V_z = 137°$ at $\lambda = 0.5321\,\mu m$ [1]
Molecular mass: 185.881
Specific gravity: 3.54 g/cm^3 [2]; 3.52 g/cm^3 for as-grown yellowish crystals [3], [4]; 3.44 g/cm^3 for annealed rose crystals [3], [4]
Point group: $mm2$
Lattice constants
for as-grown yellowish crystals:
$a = 6.890 \pm 0.001$ Å [3], [4]
$b = 8.053 \pm 0.001$ Å [3], [4]
$c = 6.478 \pm 0.002$ Å [3], [4]

for annealed rose crystals:
$a = 6.896 \pm 0.001$ Å [3], [4]; 6.893 Å [1]
$b = 8.058 \pm 0.002$ Å [3], [4]; 8.0578 Å [1]
$c = 6.484 \pm 0.004$ Å [3], [4]; 6.4816 Å [1]
Assignment of dielectric and crystallographic axes: $X, Y, Z \Rightarrow b, a, c$
Mohs hardness: 3–4 [5]
Melting point: 1273 K [2], [6]

Linear thermal expansion coefficient α_t [7]

T [K]	$\alpha_t \times 10^6$ [K^{-1}], $\parallel X$	$\alpha_t \times 10^6$ [K^{-1}], $\parallel Y$	$\alpha_t \times 10^6$ [K^{-1}], $\parallel Z$
293	16.4	9.1	6.8

Temperature dependence of linear thermal expansion coefficient α_t for temperature range 253–393 K (T in K) [7]:

$$\alpha_t\,(\parallel X) = 1.61 \times 10^{-5} + 1.44 \times 10^{-8}\,(T - 273)$$

$$\alpha_t\,(\parallel Y) = 0.89 \times 10^{-5} + 0.72 \times 10^{-8}\,(T - 273)$$

$$\alpha_t\,(\parallel Z) = 0.66 \times 10^{-5} + 0.93 \times 10^{-8}\,(T - 273)$$

Specific heat capacity c_p at $P = 0.101325$ Mpa [6]

T [K]	c_p [J/kgK]
300	500 ± 6

Thermal conductivity coefficient [6]

κ [W/mK], $\parallel X$	κ [W/mK], $\parallel Y$	κ [W/mK], $\parallel Z$
6.2	6	7.6

Band-gap energy at room temperature: $E_g = 3.56$ eV [8]; 3.57 eV [1], [6], 3.59 eV [2], [9]; 3.6 eV [3]
Transparency range:
at 0.5 transmittance level: 0.43–11.5 μm [4]; 0.5–11 μm [5]; 0.57–8.97 μm [7]
at 0.1 transmittance level: 0.4–12.5 μm [5]
at "0" transmittance level: 0.34–13.2 μm [3], [5]

Linear absorption coefficient α

λ [μm]	α [cm^{-1}]	Ref.
0.6	0.23	[4]
0.76–0.9	0.15	[4]
1.064	<0.04	[6]
1–8	0.1–0.25	[5]

λ [μm]	α [cm^{-1}]	Ref.
	0.1–0.15	[6]
	<0.2	[4]
1.27	0.09	[4]
2.53	0.05	[4]
	<0.05	[6]
9.2–10.8	1.1–2.3	[5]

Two-photon absorption coefficient β [1]

λ [μm]	τ_p [ns]	$\beta \times 10^{11}$ [cm/W]
0.8	0.0002	<5

Experimental values of refractive indices for as-grown LIS [10]

λ [μm]	n_X	n_Y	n_Z	λ [μm]	n_X	n_Y	n_Z
0.425	2.3472	2.4126	2.4208	2.800	2.0999	2.1339	2.1411
0.450	2.3096	2.3685	2.3766	3.000	2.0987	2.1325	2.1398
0.500	2.2580	2.3095	2.3175	3.200	2.0976	2.1314	2.1386
0.550	2.2244	2.2720	2.2793	3.400	2.0965	2.1305	2.1372
0.600	2.2011	2.2455	2.2536	3.600	2.0954	2.1291	2.1361
0.650	2.1841	2.2265	2.2344	3.800	2.0941	2.1280	2.1348
0.700	2.1712	2.2119	2.2199	4.000	2.0930	2.1266	2.1335
0.750	2.1610	2.2010	2.2085	4.500	2.0900	2.1237	2.1304
0.800	2.1530	2.1918	2.1996	5.000	2.0867	2.1204	2.1271
0.850	2.1465	2.1849	2.1923	5.500	2.0828	2.1166	2.1229
0.900	2.1409	2.1789	2.1863	6.000	2.0789	2.1128	2.1189
0.950	2.1364	2.1737	2.1812	6.500	2.0750	2.1086	2.1143
1.000	2.1325	2.1696	2.1769	7.000	2.0701	2.1040	2.1096
1.100	2.1268	2.1630	2.1706	7.500	2.0650	2.0990	2.1043
1.200	2.1223	2.1579	2.1655	8.000	2.0595	2.0937	2.0987
1.400	2.1158	2.1508	2.1585	8.500	2.0534	2.0876	2.0924
1.600	2.1115	2.1463	2.1538	9.000	2.0470	2.0816	2.0856
1.800	2.1082	2.1430	2.1501	9.500	2.0398	2.0749	2.0783
2.000	2.1057	2.1405	2.1475	10.000	2.0319	2.0666	2.0703
2.200	2.1039	2.1384	2.1454	10.500	2.0238	2.0585	2.0619
2.400	2.1026	2.1367	2.1440	11.000	2.0146	2.0501	2.0522
2.600	2.1012	2.1353	2.1425				

Temperature derivatives of refractive indices at $\lambda = 1.064\,\mu m$ [6]:

$dn_X/dT = 3.72 \times 10^{-5}\,K^{-1}$

$dn_Y/dT = 4.55 \times 10^{-5}\,K^{-1}$

$dn_Z/dT = 4.47 \times 10^{-5}\,K^{-1}$

Best set of dispersion relations (λ in μm, $T = 293$ K) [11]:

$$n_X^2 = 6.6819 + \frac{0.1294}{\lambda^2 - 0.0611} + \frac{2037.53}{\lambda^2 - 897.77}$$

$$n_Y^2 = 7.0969 + \frac{0.1433}{\lambda^2 - 0.0660} + \frac{2511.13}{\lambda^2 - 988.03}$$

$$n_Z^2 = 7.2555 + \frac{0.1443}{\lambda^2 - 0.0661} + \frac{2625.82}{\lambda^2 - 9.8397}$$

Different Sellmeier equations were deduced by Ebbers and have been presented in [1], [5]. Other dispersion relations are given in [6], [12].

Linear electrooptic coefficients measured at low frequencies (well below the acoustic resonances of LIS crystal, i.e., for the "free" crystal) at room temperature [7]

λ [μm]	r_{13}^{T} [pm/V]	r_{23}^{T} [pm/V]	r_{33}^{T} [pm/V]
1.064	0.97 ± 0.1	0.42 ± 0.04	-1.33 ± 0.13

Expressions for the effective second-order nonlinear coefficient in principal planes of LIS crystal (approximation of small walk-off angle, Kleinman symmetry conditions are valid, $d_{15} = d_{31}$ and $d_{24} = d_{32}$) [13]:

XY plane

$d_{\mathrm{eoe}} = d_{\mathrm{oee}} = d_{32} \sin^2 \phi + d_{31} \cos^2 \phi$

YZ plane

$d_{\mathrm{oeo}} = d_{\mathrm{eoo}} = d_{32} \sin \theta$

XZ plane, $\theta < V_z$

$d_{\mathrm{ooe}} = d_{31} \sin \theta$

XZ plane, $\theta > V_z$

$d_{\mathrm{oeo}} = d_{\mathrm{eoo}} = d_{31} \sin \theta$

Effective second-order nonlinear coefficient for three-wave interactions in the arbitrary direction of LIS crystal is given in [13].

Values of second-order nonlinear coefficients:

$d_{31}(2.3\,\mu\mathrm{m}) = 7.2 \pm 0.4$ pm/V [6]

$d_{32}(2.3\,\mu\mathrm{m}) = 5.7 \pm 0.6$ pm/V [6]

$d_{33}(2.3\,\mu\mathrm{m}) = -16 \pm 4$ pm/V [6]

$d_{31}(10.6\,\mu\mathrm{m}) = 0.074 \times d_{36}(\mathrm{GaAs}) \pm 15\% = 6.1 \pm 0.9$ pm/V [10], [14]

$d_{32}(10.6\,\mu\mathrm{m}) = 0.064 \times d_{36}(\mathrm{GaAs}) \pm 15\% = 5.3 \pm 0.8$ pm/V [10], [14]

$d_{33}(10.6\,\mu\mathrm{m}) = 0.118 \times d_{36}(\mathrm{GaAs}) \pm 15\% = 9.8 \pm 1.5$ pm/V [10], [14]

Experimental values of phase-matching angle and internal angular bandwidth

Interacting wavelengths [μm]	ϕ_{pm} [deg]	θ_{pm} [deg]	$\Delta\varphi^{\mathrm{int}}$ [deg]	$\Delta\theta^{\mathrm{int}}$ [deg]	Ref.
XY plane, $\theta = 90°$					
SHG, $e + o \Rightarrow e$					
$2.366 \Rightarrow 1.183$	82.1				[6]
$2.469 \Rightarrow 1.2345$	73.1				[6]
$2.481 \Rightarrow 1.2405$	72.4				[4]

Interacting wavelengths [μm]	ϕ_{pm} [deg]	θ_{pm} [deg]	$\Delta\varphi^{int}$ [deg]	$\Delta\theta^{int}$ [deg]	Ref.
2.527 ⇒ 1.2635	69.8				[6]
2.583 ⇒ 1.2915	67.4				[6]
2.590 ⇒ 1.295	66.2		0.48		[6]
2.611 ⇒ 1.3055	66.3		0.4		[4]
			0.44		[15]
2.90 ⇒ 1.45	57.9				[6]
3.4 ⇒ 1.7	50.7				[6]
3.7 ⇒ 1.85	48.3				[6]
3.9 ⇒ 1.95	49.0				[6]
4.45 ⇒ 2.225	51.6				[6]
4.95 ⇒ 2.475	56.3				[6]
5.0 ⇒ 2.5	57.0		0.92		[9]
5.35 ⇒ 2.675	62.8				[6]
5.55 ⇒ 2.775	66.0				[6]
5.75 ⇒ 2.875	69.1				[6]
5.90 ⇒ 2.95	71.4				[6]
YZ plane, $\phi = 90°$					
SHG, $o + e \Rightarrow o$					
2.5427 ⇒ 1.37135		35.4			[6]
2.5527 ⇒ 1.27635		34.0			[6]
2.5704 ⇒ 1.2852		31.0			[6]
2.582 ⇒ 1.291		28.0			[7]
2.587 ⇒ 1.2935		28.7			[6]
2.590 ⇒ 1.295		27.9		2.9	[6]
2.6023 ⇒ 1.30115		25.9			[6]
2.6067 ⇒ 1.30335		25.1			[6]
2.6314 ⇒ 1.3157		19.6			[6]

Laser-induced damage threshold

λ [μm]	τ_p [ns]	I_{thr} [GW/cm^2]	Ref.	Note
0.8	0.0002	>140	[1]	surface damage
1.064	10	0.1	[6]	10 Hz, bulk damage
5.0	0.0005	0.44	[9]	10 Hz, train of 5000 pulses, bulk damage
		>6	[9]	10 Hz, train of 125 pulses, bulk damage
9.55	36	>0.18	[5]	

About the crystal

LIS is one of a very few newly developed IR nonlinear materials. At the moment, LIS is the only crystal that allows the direct down-conversion of Ti:sapphire laser radiation to the 5–11-μm range in one single step.

References

[1] F. Rotermund, V. Petrov, F. Noack, L. Isaenko, A. Yelisseyev, S. Lobanov: Optical parametric generation of femtosecond pulses up to 9 μm with $LiInS_2$ pumped at 800 nm. Appl. Phys. Lett. **78(18)**, 2623–2625 (2001).

[2] L. Isaenko, A. Yelisseyev, S. Lobanov, V. Petrov, F. Rotermund, J.-J. Zondy, G.H.M. Knippels: $LiInS_2$: a new nonlinear crystal for the mid-IR. J. Mater. Sci. Semicond. Process. **4(6)**, 665–668 (2002).

[3] L. Isaenko, I. Vasilyeva, A. Yelisseyev, V. Malakhov, L. Dovlitova, J.-J. Zondy, I. Kavun: Growth and characterization of $LiInS_2$ single crystals. J. Cryst. Growth **218(2–4)**, 313–322 (2000).

[4] A. Yelisseyev, L. Isaenko, S. Lobanov, J.-J. Zondy, A. Douillet, I. Thenot, P. Kupecek, G. Mennerat, J. Mangin, S. Fossier, S. Salaü: New ternary sulfide for double application in laser schemes. In: *Advanced Solid-State Lasers, OSA Trends in Optics and Photonics Series, Vol. 34*, ed. by H. Injeyan, U. Keller, C. Marshall (OSA, Washington DC, 2000), pp. 561–568.

[5] Y.M. Andreev, L.G. Geiko, P.P. Geiko, S.G. Grechin: Optical properties of a nonlinear $LiInS_2$ crystal. Kvant. Elektron. **31(7)**, 647–648 (2001) [In Russian, English trans.: Quantum Electron. **31(7)**, 647–648 (2001)].

[6] S. Fossier, S. Salaü, J. Mangin, O. Bidault, I. Thenot, J.-J. Zondy, W. Chen, F. Rotermund, V. Petrov, P. Petrov, J. Henningsen, A. Yelisseyev, L. Isaenko, S. Lobanov, O. Balachninaite, G. Slekys, V. Sirutkaitis: Optical, vibrational, thermal, electrical, damage and phase-matching properties of lithium thioindate. J. Opt. Soc. Am. B **21(11)**, 1981–2007 (2004).

[7] J. Mangin, S. Salaü, S. Fossier, P. Strimer, J.-J. Zondy, L. Isaenko, A. Yelisseyev: Optical properties of lithium thioindate. Proc. SPIE **4268**, 49–57 (2001).

[8] A. Eifler, V. Riede, J. Brükner, S. Weise, V. Krämer, G. Lippold, W. Schmitz, K. Bente, W. Grill: Band gap energies and lattice vibrations of the lithium ternary compounds $LiInSe_2$, $LiInS_2$, $LiGaSe_2$ and $LiGaS_2$. Jpn. J. Appl. Phys. **39(Suppl. 1)**, 279–281 (2000).

[9] G.M.H. Knippels, A.F.G. van der Meer, A.M. Macleod, A. Yelisseyev, L. Isaenko, S. Lobanov, I. Thenot, J.-J. Zondy: Mid-infrared (2.75 − 6.0-μm) second-harmonic generation in $LiInS_2$. Opt. Lett. **26(9)**, 617–619 (2001).

[10] G.D. Boyd, H.M. Kasper, J.H. McFee: Linear and nonlinear optical properties of $LiInS_2$. J. Appl. Phys. **44(6)**, 2809–2812 (1973).

[11] K. Suzuki, E. Takaoka, T. Mikami, T. Hikoso, K. Kato, N. Umemura: Fourth harmonic generation of the CO_2 laser frequency in $LiInS_2$. In: *Proceedings of Autumn Meeting of Japan Society of Applied Physics* (JSAP, Nagoya, 2002) [In Japanese].

[12] V.V. Badikov, V.I. Chizhikov, V.V. Efimenko, T.D. Efimenko, V.L. Panyutin, G.S. Shevyrdyaeva, S.I. Scherbakov: Optical properties of lithium indium selenide. Opt. Mater. **23(3–4)**, 575–581 (2003).

[13] V.G. Dmitriev, D.N. Nikogosyan: Effective nonlinearity coefficients for three-wave interactions in biaxial crystals of *mm*2 point group symmetry. Opt. Commun. **95(1–3)**, 173–182 (1993).

[14] D.A. Roberts: Simplified characterization of uniaxial and biaxial nonlinear optical crystals: a plea for standardization of nomenclature and conventions. IEEE J. Quant. Electr. **28(10)**, 2057–2074 (1992).

[15] L. Isaenko, A. Yelisseyev, J.-J. Zondy, G. Knippels, I. Thenot, S. Lobanov: Growth and characterization of single crystals of ternary chalcogenides for laser applications. Opto-Electron. Rev. **9(2)**, 135–141 (2001).

6.15 $LiInSe_2$, Lithium Indium Selenide (LISe)

Negative biaxial crystal: $2V_z = 140°$ at $\lambda = 0.5321\,\mu m$ [1]
Molecular mass: 279.561
Point group: $mm2$
Lattice constants:
for as-grown yellow crystals:
$a = 7.1917 \pm 0.0008$ Å [1]
$b = 8.4116 \pm 0.0010$ Å [1]
$c = 6.7926 \pm 0.0008$ Å [1]
Assignment of dielectric and crystallographic axes: $X, Y, Z \Rightarrow b, a, c$
Band-gap energy at room temperature: $E_g = 2.83$ eV [2]; 2.87 eV ($\mathbf{E}\|a$) [1]; 2.86 eV ($\mathbf{E}\|b$) [1]
Transparency range for as-grown yellow crystal:
at $\alpha = 15\,cm^{-1}$ level: $0.46 - 14\,\mu m$ [1]
at $\alpha = 1\,cm^{-1}$ level: $0.72 - 10.4\,\mu m$ [1]

Two-photon absorption coefficient β [3]

λ [μm]	τ_p [ns]	$\beta \times 10^{11}$ [cm/W]
0.82	0.00022	60

Experimental values of refractive indices for as-grown lithium indium selenide [1]

λ [μm]	n_X	n_Y	n_Z	λ [μm]	n_X	n_Y	n_Z
0.500	2.5228	—	2.6035	0.950	2.3037	—	2.3550
0.525	2.4849	—	2.5594	1.000	2.2977	2.3390	2.3486
0.550	2.4549	2.5178	2.5248	2.000	2.2530	2.2913	2.2988
0.575	2.4313	—	2.4977	3.000	2.2434	2.2842	2.2891
0.600	2.4118	—	2.4758	4.100	2.2398	2.2799	2.2842
0.650	2.3818	2.4331	2.4422	5.000	2.2370	2.2772	2.2818
0.700	2.3601	2.4079	2.4174	6.000	2.2323	2.2718	2.2765
0.750	2.3436	2.3893	2.3989	7.000	2.2271	2.2688	2.2715
0.800	2.3306	2.3746	2.3843	8.000	2.2202	2.2612	2.2649
0.850	2.3196	—	2.3725	10.000	2.2015	2.2522	2.2566
0.900	2.3109	2.3533	2.3632	11.000	2.1935	2.2352	2.2380

Sellmeier equations (λ in μm, $T = 293$ K) [1]:

$$n_X^2 = 5.0370599 + \frac{0.2165833\,\lambda^2}{\lambda^2 - 0.0856929} - 0.0018534\,\lambda^2$$

$$n_Y^2 = 5.2026545 + \frac{0.2422470\,\lambda^2}{\lambda^2 - 0.0899151} - 0.0015069\,\lambda^2$$

$$n_Z^2 = 5.2399142 + \frac{0.2414178\,\lambda^2}{\lambda^2 - 0.0917890} - 0.0017645\,\lambda^2$$

Other dispersion relations are given in [4].
Expressions for the effective second-order nonlinear coefficient in principal planes of $LiInSe_2$ crystal (approximation of small walk-off angle, Kleinman symmetry conditions are valid, $d_{15} = d_{31}$ and $d_{24} = d_{32}$) [5]:

XY plane

$$d_{eoe} = d_{oee} = d_{32} \sin^2 \phi + d_{31} \cos^2 \phi$$

YZ plane

$$d_{oeo} = d_{eoo} = d_{32} \sin \theta$$

XZ plane, $\theta < V_z$

$$d_{ooe} = d_{31} \sin \theta$$

XZ plane, $\theta > V_z$

$$d_{oeo} = d_{eoo} = d_{31} \sin \theta$$

Effective second-order nonlinear coefficient for three-wave interactions in the arbitrary direction of $LiInSe_2$ crystal is given in [5].
Values of second-order nonlinear coefficients:

$d_{31}(2.8\,\mu m) = 0.76 \times d_{36}(AgGaS_2) = 10.4 \pm 1.7\,pm/V$ [1], [6]

$d_{32}(2.1 - -2.45\,\mu m) = 3 \times d_{24}(KTP) = 7.8 \pm 0.3\,pm/V$ [1], [7]

Experimental values of phase-matching angle [1]

Interacting wavelengths [μm]	θ_{pm} [deg]
XZ plane, $\phi = 0°$	
SHG, $o + o \Rightarrow e$	
$2.119 \Rightarrow 1.0595$	10
$2.191 \Rightarrow 1.0955$	17
$2.292 \Rightarrow 1.146$	21
$2.456 \Rightarrow 1.228$	25

About the crystal

An analog of LIS with slightly higher values of the nonlinear coefficients d_{31} and d_{32}.

References

[1] L. Isaenko, A. Yelisseyev, S. Lobanov, V. Petrov, F. Rotermund, G. Slekys, J.-J. Zondy: $LiInSe_2$: a biaxial ternary chalcogenide crystal for nonlinear optical applications in mid-infrared. J. Appl. Phys. **91(12)**, 9475–9480 (2002).

[2] A. Eifler, V. Riede, J. Brükner, S. Weise, V. Krämer, G. Lippold, W. Schmitz, K. Bente, W. Grill: Band gap energies and lattice vibrations of the lithium ternary compounds $LiInSe_2$, $LiInS_2$, $LiGaSe_2$ and $LiGaS_2$. Jpn. J. Appl. Phys. **39(Suppl. 1)**, 279–281 (2000).

[3] V.V. Petrov, F. Noack, L. Isaenko, A. Yelisseyev, S. Lobanov, A. Titov, F. Rotermund, J.-J. Zondy: Mid-infrared optical parametric generation in lithium-containing ternary compounds $LiAB_2$ (A = Ga, In; B = S, Se). In: *Conference on Lasers and Electrooptics CLEO/QELS 2003, Technical Digest* (OSA, Washington DC, 2003), paper CTuN5.

[4] V.V. Badikov, V.I. Chizhikov, V.V. Efimenko, T.D. Efimenko, V.L. Panyutin, G.S. Shevyrdyaeva, S.I. Scherbakov: Optical properties of lithium indium selenide. Opt. Mater. **23(3–4)**, 575–581 (2003).
[5] V.G. Dmitriev, D.N. Nikogosyan: Effective nonlinearity coefficients for three-wave interactions in biaxial crystals of $mm2$ point group symmetry. Opt. Commun. **95(1–3)**, 173–182 (1993).
[6] J.-J. Zondy, D. Touahri, O. Acef: Absolute value of the d_{36} nonlinear coefficient of $AgGaS_2$: prospect for a low-threshold doubly resonant oscillator-based 3:1 frequency divider. J. Opt. Soc. Am. B **14(10)**, 2481–2497 (1997).
[7] I. Shoji, T. Kondo, A. Kitamoto, M. Shirane, R. Ito: Absolute scale of second-order nonlinear-optical coefficients. J. Opt. Soc. Am. B **14(9)**, 2268–2294 (1997).

6.16 $LiGaS_2$, Lithium Thiogallate (LGS)

Negative biaxial crystal.
Molecular mass: 140.781
Specific gravity: 2.94 g/cm^3 (calculated) [1]
Point group: $mm2$
Lattice constants:

$a = 6.519 \pm 0.006$ Å [2]; 6.5133 ± 0.0006 Å [1]
$b = 7.872 \pm 0.007$ Å [2]; 7.8629 ± 0.0008 Å [1]
$c = 6.238 \pm 0.004$ Å [2]; 6.2175 ± 0.0005 Å [1]

Assignments of dielectric and crystallographic axes:

$X, Y, Z \Rightarrow b, a, c$ ($\lambda < 6.5\,\mu$m)
$X, Y, Z \Rightarrow b, c, a$ ($\lambda > 6.5\,\mu$m)

Band-gap energy at room temperature: $E_g = 4.15$ eV [1]; 3.62 eV [3]
Transparency range at $\alpha = 5\,\text{cm}^{-1}$ level: $0.32 - 11.6\,\mu$m [1]
Dispersion relations at room temperature (λ in μm) [1]:

$$n_X^2 = 4.326834 + \frac{0.1030907}{\lambda^2 - 0.0309876} - 0.0037015\,\lambda^2$$

$$n_Y^2 = 4.478907 + \frac{0.120426}{\lambda^2 - 0.0346160} - 0.0035119\,\lambda^2$$

$$n_Z^2 = 4.493881 + \frac{0.1177452}{\lambda^2 - 0.0337004} - 0.0037767\,\lambda^2$$

Expressions for the effective second-order nonlinear coefficient in principal planes of LGS crystal (approximation of small walk-off angle, Kleinman symmetry conditions are valid, $d_{15} = d_{31}$ and $d_{24} = d_{32}$) [4]:

XY plane

$$d_{\text{eoe}} = d_{\text{oee}} = d_{32}\sin^2\phi + d_{31}\cos^2\phi$$

YZ plane

$$d_{\text{oeo}} = d_{\text{eoo}} = d_{32}\sin\theta$$

XZ plane, $\theta < V_z$

$d_{ooe} = d_{31} \sin\theta$

XZ plane, $\theta > V_z$

$d_{oeo} = d_{eoo} = d_{31} \sin\theta$

Effective second-order nonlinear coefficient for three-wave interactions in the arbitrary direction of LGS crystal is given in [4].

About the crystal

A very recently proposed IR nonlinear material with a wurtzite-type structure and UV transmission down to 0.32 μm.

References

[1] L. Isaenko, A. Yelisseyev, S. Lobanov, A. Titov, V. Petrov, J.-J. Zondy, P. Krinitsin, A. Merkulov, V. Vedenyapin, J. Smirnova: Growth and properties of $LiGaX_2$ (X = S, Se, Te) single crystals for nonlinear optical applications in the mid-IR. Cryst. Res. Technol. **38(3–5)**, 379–387 (2003).

[2] J. Leal-Gonzalez, S.S. Melibary, A.J. Smith: Structure of lithium gallium sulfide, $LiGaS_2$. Acta Crystallogr. C **46(11)**, 2017–2019 (1990).

[3] A. Eifler, V. Riede, J. Brükner, S. Weise, V. Krämer, G. Lippold, W. Schmitz, K. Bente, W. Grill: Band gap energies and lattice vibrations of the lithium ternary compounds $LiInSe_2$, $LiInS_2$, $LiGaSe_2$ and $LiGaS_2$. Jpn. J. Appl. Phys. **39(Suppl. 1)**, 279–281 (2000).

[4] V.G. Dmitriev, D.N. Nikogosyan: Effective nonlinearity coefficients for three-wave interactions in biaxial crystals of $mm2$ point group symmetry. Opt. Commun. **95(1–3)**, 173–182 (1993).

6.17 $LiGaSe_2$, Lithium Gallium Selenide (LGSe)

Negative biaxial crystal.
Molecular mass: 234.461
Specific gravity: 4.24 g/cm^3 (calculated) [1]
Point group: $mm2$
Lattice constants:
$a = 6.833$ Å [2]; 6.832 ± 0.001 Å [1]
$b = 8.227$ Å [2]; 8.237 ± 0.001 Å [1]
$c = 6.541$ Å [2]; 6.535 ± 0.001 Å [1]
Assignments of dielectric and crystallographic axes:
$X, Y, Z \Rightarrow b, a, c$ ($\lambda < 8$ μm)
$X, Y, Z \Rightarrow b, c, a$ ($\lambda > 8$ μm)
Melting point: 1119 K [2]
Band-gap energy at room temperature: $E_g = 3.65$ eV [2]; 3.13 eV [3]; 3.34 eV [1]
Transparency range at $\alpha = 5\,\text{cm}^{-1}$ level: $0.37 - 13.2$ μm [1]

Dispersion relations at room temperature (λ in μm) [1]:

$$n_X^2 = 4.99592 + \frac{0.15130}{\lambda^2 - 0.08989} - 0.00233\,\lambda^2$$

$$n_Y^2 = 5.20896 + \frac{0.18632}{\lambda^2 - 0.07687} - 0.00211\,\lambda^2$$

$$n_Z^2 = 5.22442 + \frac{0.18365}{\lambda^2 - 0.07493} - 0.00232\,\lambda^2$$

Expressions for the effective second-order nonlinear coefficient in principal planes of $LiGaSe_2$ crystal (approximation of small walk-off angle, Kleinman symmetry conditions are valid, $d_{15} = d_{31}$ and $d_{24} = d_{32}$) [4]:

XY plane

$d_{\mathrm{eoe}} = d_{\mathrm{oee}} = d_{32}\sin^2\phi + d_{31}\cos^2\phi$

YZ plane

$d_{\mathrm{oeo}} = d_{\mathrm{eoo}} = d_{32}\sin\theta$

XZ plane, $\theta < V_z$

$d_{\mathrm{ooe}} = d_{31}\sin\theta$

XZ plane, $\theta > V_z$

$d_{\mathrm{oeo}} = d_{\mathrm{eoo}} = d_{31}\sin\theta$

Effective second-order nonlinear coefficient for three-wave interactions in the arbitrary direction of $LiGaSe_2$ crystal is given in [4].

About the crystal

A very recently proposed IR nonlinear material with a wurtzite-type structure and UV transmission down to 0.37 μm.

References

[1] L. Isaenko, A. Yelisseyev, S. Lobanov, A. Titov, V. Petrov, J.-J. Zondy, P. Krinitsin, A. Merkulov, V. Vedenyapin, J. Smirnova: Growth and properties of $LiGaX_2$ (X = S, Se, Te) single crystals for nonlinear optical applications in the mid-IR. Cryst. Res. Technol. **38(3–5)**, 379–387 (2003).

[2] K. Kuriyama, T. Nozaki: Single-crystal growth and characterization of $LiGaSe_2$. J. Appl. Phys. **52(10)**, 6441–6443 (1981).

[3] A. Eifler, V. Riede, J. Brükner, S. Weise, V. Krämer, G. Lippold, W. Schmitz, K. Bente, W. Grill: Band gap energies and lattice vibrations of the lithium ternary compounds $LiInSe_2$, $LiInS_2$, $LiGaSe_2$ and $LiGaS_2$. Jpn. J. Appl. Phys. **39(Suppl. 1)**, 279–281 (2000).

[4] V.G. Dmitriev, D.N. Nikogosyan: Effective nonlinearity coefficients for three-wave interactions in biaxial crystals of mm2 point group symmetry. Opt. Commun. **95(1–3)**, 173–182 (1993).

6.18 $AgGa_xIn_{1-x}Se_2$, Silver Gallium–Indium Selenide (AGISe)

Negative uniaxial crystal: $n_o > n_e$.
Point group: $\bar{4}2m$

Mean value of linear thermal expansion coefficient α_t for $x = 0.58$ [1]

T [K]	$\alpha_t \times 10^6$ [K^{-1}], $\parallel c$	$\alpha_t \times 10^6$ [K^{-1}], $\perp c$
298–633	−12.1	16.8

The UV transmission cutoff is at 0.85 μm and the IR transmission cutoff is at 19 μm ($x = 0.65$) [2].

Linear absorption coefficient α

λ [μm]	α [cm^{-1}]	Ref.	Note
1.06	<0.01	[3]	typical crystals
	0.002	[3]	best crystals
2.09	0.01	[4]	o-wave, $x = 0.474$
	0.02	[4]	e-wave, $x = 0.474$
4.655–4.82	0.08	[5]	$x = 0.6$
5	0.157	[2]	$x = 0.65$
9.31–9.64	0.06	[5]	$x = 0.6$
10	0.158	[2]	$x = 0.65$

Sellmeier equations ($x = 0.526$, λ in μm, $T = 293$ K) [4]:

$$n_o^2 = 6.9082 + \frac{0.5586}{\lambda^2 - 0.2870} - 0.00108\,\lambda^2$$

$$n_e^2 = 6.8262 + \frac{0.6044}{\lambda^2 - 0.3736} - 0.00111\,\lambda^2$$

Other dispersion relations are given in [5] (for $x = 0.1$ to 1.0) and in [1] (for $x = 0.58$).
Expressions for the effective second-order nonlinear coefficient in general case (Kleinman symmetry conditions are valid, $d_{14} = d_{25} = d_{36}$) [6]:

$d_{ooe} = -d_{36} \sin(\theta + \rho) \sin 2\phi$

$d_{eoe} = d_{oee} = 2d_{36} \sin(\theta + \rho) \cos(\theta + \rho) \cos 2\phi$

Simplified expressions for the effective second-order nonlinear coefficient (approximation of small birefringence angle, Kleinman symmetry conditions are valid, $d_{14} = d_{25} = d_{36}$) [7]:

$d_{ooe} = -d_{36} \sin\theta \sin 2\phi$

$d_{eoe} = d_{oee} = d_{36} \sin 2\theta \cos 2\phi$

Value of second-order nonlinear coefficient:

$d_{36}(9 - 10\,\mu\text{m}) \approx 40$ pm/V for $x = 0.6$ [5]

Experimental values of phase-matching angle ($T = 293$ K)

Interacting wavelengths [μm]	θ_{exp} [deg]	Ref.	Note
SHG, $o + o \Rightarrow e$			
$9.27 \Rightarrow 4.635$	90	[1]	$x = 0.58$
$9.31 \Rightarrow 4.655$	76.8 ± 1.7	[5]	$x = 0.6$
$9.55 \Rightarrow 4.775$	83.3 ± 1.7	[5]	$x = 0.6$
$9.64 \Rightarrow 4.82$	87.3 ± 1.7	[5]	$x = 0.6$
	90	[8]	$x = 0.65$
SFG, $o + o \Rightarrow e$			
$9.2714 + 4.6357 \Rightarrow 3.09047$	88.5	[4]	$x = 0.526$
$9.5525 + 4.77625 \Rightarrow 3.18417$	84	[4]	$x = 0.526$
$10.2466 + 5.1233 \Rightarrow 3.41553$	84.7	[4]	$x = 0.526$
$10.591 + 5.2955 \Rightarrow 3.53033$	86.6	[4]	$x = 0.526$

Experimental values of internal angular and temperature bandwidths [4]

Interacting wavelengths [μm]	$\Delta\theta^{int}$ [deg]	ΔT [°C]	Note
SFG, $o + o \Rightarrow e$			
$10.2466 + 5.1233 \Rightarrow 3.41553$	8.3 ± 0.2	105 ± 5	$x = 0.526$

Laser-induced surface-damage threshold [3]

λ [μm]	τ_p [ns]	I_{thr} [GW/cm^2]	Note
10.7	70	>30	$x = 0.75$

About the crystal

This mixed chalcopyrite crystal was synthesized to realize the noncritically phase-matched (NCPM) SHG [1], [5], [8] and THG [4] of CO_2 laser radiation.

References

[1] P.G. Schunemann, S.D. Setzler, T.M. Pollak: Phase-matched crystal growth of $AgGaSe_2$ and $AgGa_{1-x}In_xSe_2$. J. Cryst. Growth **211(1–4)**, 257–264 (2000).

[2] G.C. Bhar, S. Das, U. Chatterjee, P.K. Datta, Y.N. Andreev: Noncritical second harmonic generation of CO_2 laser radiation in mixed chalcopyrite crystal. Appl. Phys. Lett. **63(10)**, 1316–1318 (1993).

[3] V.V. Badikov, V.I. Chizhikov, V.B. Laptev, V.L. Panyutin, G.S. Shevyrdyaeva, S.I. Scherbakov: $AgGa_{1-x}In_xSe_2$ nonlinear crystals for noncritical phase matching processes. Proc. SPIE **4972**, 139–144 (2003).

[4] E. Takaoka, K. Kato: 90° phase-matched third-harmonic generation of CO_2 laser frequencies in $AgGa_{1-x}In_xSe_2$. Opt. Lett. **24(13)**, 902–904 (1999).

[5] Y.M. Andreev, I.S. Baturin, P.P. Geiko, A.I. Gusamov: Frequency doubling of CO_2-laser radiation in new nonlinear crystal $AgGa_xIn_{1-x}Se_2$. Kvant. Elektron. **29(1)**, 66–70 (1999) [In Russian, English trans.: Quantum Electron. **29(10)**, 904–908 (1999)].

[6] R.C. Eckardt, H. Masuda, Y.X. Fan, R.L. Byer: Absolute and relative nonlinear optical coefficients of KDP, KD*P, BaB_2O_4, $LiIO_3$, MgO:$LiNbO_3$, and KTP measured by phase-matched second-harmonic generation. IEEE J. Quant. Electr. **26(5)**, 922–933 (1990).
[7] J.E. Midwinter, J. Warner: The effects of phase matching method and of uniaxial crystal symmetry on the polar distribution of second-order non-linear optical polarization. Brit. J. Appl. Phys. **16(11)**, 1135–1142 (1965).
[8] G.C. Bhar, S. Das, D.V. Satyanarayan, P.K. Datta, U. Nundy, Y.N. Andreev: Efficient generation of mid-infrared radiation in an $AgGa_xIn_{1-x}Se_2$ crystal. Opt. Lett. **20(20)**, 2057–2059 (1995).

6.19 Tl_4HgI_6, Thallium Mercury Iodide (THI)

Positive uniaxial crystal: $n_e > n_o$
Molecular mass: 1779.127
Point group: $4mm$
Melting point: 669 K [1]
Transparency range at "0" transmittance level: 1.0–60 μm [1]
Linear absorption coefficient α in the transparency region is about 0.5 cm^{-1} [1]

Experimental values of refractive indices

λ [μm]	n_o	n_e	λ [μm]	n_o	n_e
1.2	2.4360	2.5087	6.0	2.3872	2.4554
1.3	2.4284	2.5003	8.0	2.3850	2.4532
1.4	2.4229	2.4953	9.0	2.3834	2.4526
1.5	2.4183	2.4897	10.0	2.3815	2.4512
1.6	2.4153	2.4864	15.0	2.3696	2.4385
1.7	2.4116	2.4823	20.0	2.3534	2.4225
1.8	2.4075	2.4780	25.0	2.3312	2.4006
2.0	2.4035	2.4736	30.0	2.3015	2.3712
3.0	2.3950	2.4630	35.0	2.2623	2.3319
4.0	2.3912	2.4592	40.0	2.2101	2.2792
5.0	2.3895	2.4574			

Dispersion equations (λ in μm, 1.2 μm < λ < 40 μm) [1]:

$$n_o^2 = 8.500975 + \frac{0.2989675}{\lambda^2 - 0.1379023} + \frac{19684.543}{\lambda^2 - 7043}$$

$$n_e^2 = 8.642436 + \frac{0.3401912}{\lambda^2 - 0.1266011} + \frac{17056.32}{\lambda^2 - 6547}$$

Expression for the effective second-order nonlinear coefficient (Kleinman symmetry conditions are valid, $d_{15} = d_{24} = d_{31} = d_{32}$) [2]:

$$d_{eoo} = d_{oeo} = d_{31} \sin\theta$$

About the crystal

THI is a new nonlinear crystal with unique transparency in the IR region up to 60 μm [1].

References

[1] K.I. Avdienko, D.V. Badikov, V.V. Badikov, V.I. Chizhikov, V.L. Panyutin, G.S. Shevyrdyaeva, S.I. Scherbakov, E.S. Scherbakova: Optical properties of thallium mercury iodide. Opt. Mater. **23(3–4)**, 569–573 (2003).

[2] J.E. Midwinter, J. Warner: The effects of phase matching method and of uniaxial crystal symmetry on the polar distribution of second-order non-linear optical polarization. Brit. J. Appl. Phys. **16(11)**, 1135–1142 (1965).

7

Self-Frequency-Doubling Crystals

This chapter relates to self-frequency-doubling crystals, which are the nonlinear optical materials doped with an active trivalent ion (usually Nd^{3+} or Yb^{3+}) and possessing both lasing and frequency-converting properties. As a result, they generate IR radiation and simultaneously double the frequency of the fundamental radiation. Among these crystals are neodymium-doped yttrium aluminum tetraborate (NYAB), ytterbium-doped yttrium aluminum tetraborate (Yb:YAB), neodymium– and magnesium-oxide–doped lithium niobate (NdMgLN), neodymium-doped gadolinium calcium oxyborate (Nd:GdCOB), neodymium-doped yttrium calcium oxyborate (Nd:YCOB), and others.

7.1 Nd:MgO:$LiNbO_3$, Neodymium– and Magnesium-Oxide–Doped Lithium Niobate (NdMgLN)

Negative uniaxial crystal: $n_o > n_e$
Point group: $3m$
Main absorption bands of Nd^{3+} in MgO:LN are at 0.52–0.54 μm, 0.58–0.61 μm, 0.74–77 μm, and 0.81–0.82 μm [1], [2].

Linear absorption coefficient α

λ [μm]	α [cm^{-1}]	Ref.	Note
0.464	0.9	[3]	$\mathbf{E}\perp a$, 0.5 wt% Nd_2O_3 and 0.8 wt% MgO
0.7525	1.2	[4]	$\mathbf{E}\parallel c$, 0.5 wt% Nd_2O_3
	2.0	[4]	$\mathbf{E}\perp c$, 0.5 wt% Nd_2O_3
0.809	1.27	[5]	$\mathbf{E}\perp c$, 0.2 wt% Nd_2O_3 and 5 mol% MgO
0.81	1.39	[3]	$\mathbf{E}\perp a$, 0.5 wt% Nd_2O_3 and 0.8 wt% MgO
0.813	1.76	[5]	$\mathbf{E}\parallel c$, 0.2 wt% Nd_2O_3 and 5 mol% MgO
	2.23	[6]	$\mathbf{E}\parallel c$, 0.2 at.% Nd and 3.3 mol% MgO
1.084	0.42	[3]	$\mathbf{E}\perp a$, 0.5 wt% Nd_2O_3 and 0.8 wt% MgO

Experimental values of refractive indices for NdMgLN with 0.34 at.% Nd and 2.56 mol% MgO [7]

λ [μm]	n_o	n_e
0.4416	2.3854	2.2798
0.488	2.3457	2.2479
0.54607	2.314	2.2213
0.577	2.3012	2.2103
0.6328	2.2842	2.1958
0.6764	2.2735	2.1868
1.064	2.23	2.1495

Dispersion relations for NdMgLN with 0.34 mol% Nd and 2.56 mol% MgO (λ in μm) [7]:

$$n_o^2 = 4.9001 + \frac{0.115737}{\lambda^2 - 0.048182} - 0.030052\,\lambda^2$$

$$n_e^2 = 4.5581 + \frac{0.097078}{\lambda^2 - 0.044267} - 0.023873\,\lambda^2$$

Other dispersion relations are given in [6] (for 0.2 at.% Nd and 3.3 mol% MgO, $T = 300$ K) and in [8] (for 0.6 at.% Nd and 5 mol% MgO, $T = 294$ K).
Expressions for the effective second-order nonlinear coefficient in general case (Kleinman symmetry conditions are valid, $d_{15} = d_{24} = d_{31} = d_{32}$) [9]:

$$d_{ooe} = d_{31}\sin(\theta + \rho) - d_{22}\cos(\theta + \rho)\sin 3\phi$$
$$d_{eoe} = d_{oee} = d_{22}\cos^2(\theta + \rho)\cos 3\phi$$

Simplified expressions for the effective second-order nonlinear coefficient (approximation of small birefringence angle, Kleinman symmetry conditions are valid, $d_{15} = d_{24} = d_{31} = d_{32}$) [10]:

$$d_{ooe} = d_{31}\sin\theta - d_{22}\cos\theta\sin 3\phi$$
$$d_{eoe} = d_{oee} = d_{22}\cos^2\theta\cos 3\phi$$

Absolute values of second-order nonlinear coefficients for 5 mol% MgO:$LiNbO_3$ [11]:

$$|d_{31}(0.852\,\mu\text{m})| = 4.9\,\text{pm/V}$$

$$|d_{33}(0.852\,\mu\text{m})| = 28.4\,\text{pm/V}$$

$$|d_{31}(1.064\,\mu\text{m})| = 4.4\,\text{pm/V}$$

$$|d_{33}(1.064\,\mu\text{m})| = 25.0\,\text{pm/V}$$

$$|d_{31}(1.313\,\mu\text{m})| = 3.4\,\text{pm/V}$$

$$|d_{33}(1.313\,\mu\text{m})| = 20.3\,\text{pm/V}$$

Experimental value of phase-matching angle at room temperature

Interacting wavelengths [μm]	θ_{exp} [deg]	Ref.	Note
SHG, $o + o \Rightarrow e$			
$1.093 \Rightarrow 0.5465$	70.8	[6]	0.2 at.% Nd and 3.3 mol% MgO
		[8]	0.6 at.% Nd and 5 mol% MgO

Experimental value of NCPM temperature [1]

Interacting wavelengths [μm]	T [°C]	Note
SHG, $o + o \Rightarrow e$		
$1.093 \Rightarrow 0.5465$	152	1.0 at.% Nd and 5 mol% MgO

Fluorescence lifetime of $^4F_{3/2}$ level

λ [μm]	τ [μs]	Ref.	Note
1.09	80–85	[12]	1 wt% Nd_2O_3
	100 ± 5	[4]	any polarization, 0.5 wt% Nd_2O_3
	102	[1]	1.0 at.% Nd and 5 mol% MgO
	120	[1]	0.5 at.% Nd and 5 mol% MgO

Laser transition wavelengths and corresponding emission cross-section values (in 10^{-20} cm^2) [1]

Transition	λ [μm]	σ ($\mathbf{E}\parallel c$)	σ ($\mathbf{E}\perp c$)	Note
$^4F_{3/2} \Rightarrow {}^4I_{11/2}$	1.085	18		1.0 at.% Nd and 5 mol% MgO
	1.093		5.1	1.0 at.% Nd and 5 mol% MgO

About the crystal

LN was the first nonlinear optical crystal in which self-frequency doubling was demonstrated [13], [14]. Later, in order to prevent photorefractive damage, MgO doping was used and the first CW self-frequency doubling was realized [1]. Nowadays, NdMgLN crystal finds its application for QPM SHG [2], [15] and QPM SFG [3], [16]. Independently, YbMgLN (Yb:MgO:$LiNbO_3$) crystal was developed [17]. The self-frequency doubling (58 mW of CW green output) was recently demonstrated in this bulk material [18], [19], as well as in the periodically poled crystal, YbPPMgLN [20], where the self-pumped OPO was also realized [21].

References

[1] T.Y. Fan, A. Cordova-Plaza, M.J.F. Digonnet, R.L. Byer, H.J. Shaw: Nd:MgO:$LiNbO_3$ spectroscopy and laser devices. J. Opt. Soc. Am. B **3(1)**, 140–147 (1986).

[2] Y.Q. Lu, J.J. Zheng, Y.L. Lu, N.B. Ming: Spectral properties and quasi-phase-matched second-harmonic generation in a new active medium: optical superlattice Nd:MgO:$LiNbO_3$. Appl. Phys. B **67(1)**, 29–32 (1998).
[3] G.D. Laptev, A.A. Novikov, V.V. Firsov: Quasi-phase-matched self-frequency summing in a periodically poled Nd:Mg::$LiNbO_3$. Proc. SPIE **4972**, 42–49 (2003).
[4] I.P. Kaminow, L.W. Stulz: Nd:$LiNbO_3$ laser. IEEE J. Quant. Electr. **QE-11(6)**, 306–308 (1975).
[5] A. Cordova-Plaza, T.Y. Fan, M.J.F. Digonnet, R.L. Byer, H.J. Shaw: Nd:MgO:$LiNbO_3$ continuous-wave laser pumped by a laser diode. Opt. Lett. **13(3)**, 209–211 (1988).
[6] S. Ishibashi, H. Itoh, T. Kaino, I. Yokohama, K. Kubodera: New cavity configurations of Nd:MgO:$LiNbO_3$ self-frequency-doubled lasers. Opt. Commun. **125(1–3)**, 177–185 (1996).
[7] G.K. Kitaeva, I.I. Naumova, A.A. Mikhailovsky, P.S. Losevsky, A.N. Penin: Visible and infrared dispersion of the refractive indices in periodically poled and single domain Nd:Mg:$LiNbO_3$. Appl. Phys. B **66(2)**, 201–205 (1998).
[8] M. Gong, G. Xu, K. Han, G. Zhai: Nd:MgO:$LiNbO_3$ self-frequency-doubled laser pumped by a flashlamp at room temperature. Electron. Lett. **26(25)**, 2062–2063 (1990).
[9] I. Shoji, H. Nakamura, K. Ohdaira, T. Kondo, R. Ito, T. Okamoto, K. Tatsuki, S. Kubota: Absolute measurement of second-order nonlinear-optical coefficients of β-BaB_2O_4 for visible to ultraviolet second-harmonic wavelengths. J. Opt. Soc. Am. B **16(4)**, 620–624 (1999).
[10] J.E. Midwinter, J. Warner: The effects of phase matching method and of uniaxial crystal symmetry on the polar distribution of second-order non-linear optical polarization. Brit. J. Appl. Phys. **16(11)**, 1135–1142 (1965).
[11] I. Shoji, T. Kondo, A. Kitamoto, M. Shirane, R. Ito: Absolute scale of second-order nonlinear-optical coefficients. J. Opt. Soc. Am. B **14(9)**, 2268–2294 (1997).
[12] L.I. Ivleva, A.A. Kaminskii, Y.S. Kuzminov, V.N. Shpakov: Absorption, luminescence, and induced emission of $LiNbO_3$:Nd^{3+} crystals. Doklady AN SSSR **183(5)**, 1068–1071 (1968) [In Russian, English trans.: Sov. Phys. - Doklady **13(12)**, 1185–1187 (1969)].
[13] L.F. Johnson, A.A. Ballman: Coherent emission from rare earth ions in electrooptic crystals. J. Appl. Phys. **40(1)**, 297–302 (1969).
[14] V.G. Dmitriev, E.V. Raevskii, L.N. Rashkovich, N.M. Rubinina, O.O. Selichev, A.A. Fomichev: Simultaneous emission at the fundamental frequency and the second harmonic in an active nonlinear medium: neodymium-doped lithium metaniobate. Pisma Zh. Tech. Fiz. **5(21–22)**, 1400–1402 (1979) [In Russian, English trans.: Sov. Tech. Phys. Lett. **5(11)**, 590–591 (1979)].
[15] N.V. Kravtsov, G.D. Laptev, E.Y. Morozov, I.I. Naumova, V.V. Firsov: Quasi-phase-matched self-doubling of the frequency in an Nd:Mg:$LiNbO_3$ laser with a regular domain structure. Kvant. Elektron. **29(2)**, 95–96 (1999) [In Russian, English trans.: Quantum Electron. **29(11)**, 933–934 (1999)].
[16] N.V. Kravtsov, G.D. Laptev, I.I. Naumova, A.A. Novikov, V.V. Firsov, A.S. Chirkin: Intracavity quasi-phase matched frequency summing in a laser based on a periodically poled active nonlinear Nd:Mg:$LiNbO_3$ crystal. Kvant. Elektron. **32(10)**, 923–924 (2002) [In Russian, English trans.: Quantum Electron. **32(10)**, 923–924 (2002)].
[17] E. Montoya, A. Lorenzo, L.E. Bausa: Optical characterization of $LiNbO_3$:Yb^{3+} crystals. J. Phys.: Condens. Matter **11(1)**, 311–320 (1999).
[18] E. Montoya, J. Capmany, L.E. Bausa, T. Kellner, A. Diening, G. Huber: Infrared and self-frequency doubled laser action in Yb^{3+}-doped $LiNbO_3$:MgO. Appl. Phys. Lett. **74(21)**, 3113–3115 (1999).

[19] E. Montoya, J.A. Sanz-Garcia, J. Capmany, L.E. Bausa, A. Diening, T. Kellner, G. Huber: Continuous wave infrared laser action, self-frequency doubling, and tunability of Yb^{3+}:MgO:$LiNbO_3$. J. Appl. Phys. **87(9)**, 4056–4062 (2000).
[20] J. Capmany, E. Montoya, V. Bermudez, D. Callejo, E. Dieguez: Self-frequency doubling in Yb^{3+} doped periodically poled $LiNbO_3$:MgO bulk crystal. Appl. Phys. Lett. **76(11)**, 1374–1376 (2000).
[21] J. Capmany, D. Callejo, V. Bermudez, E. Dieguez, D. Artigas, L. Torner: Continuous-wave self-pumped optical parametric oscillator based on Yb^{3+}-doped bulk periodically poled $LiNbO_3$ (MgO). Appl. Phys. Lett. **79(3)**, 293–295 (2001).

7.2 Nd:$YAl_3(BO_3)_4$, Neodymium-Doped Yttrium Aluminum Tetraborate ($Nd_xY_{1-x}Al_3(BO_3)_4$, or NYAB)

Negative uniaxial crystal: $n_o > n_e$

Correlation between the atomic concentation of Nd relative to Y and Nd^{3+} volume concentration

[Nd] [at.%]	$[Nd^{3+}] \times 10^{-20}$ [cm^3]
4.0	2.21
4.6	2.54
5.5	3.04
10	5.53
20	11.06

Specific gravity: 3.70 g/cm^3 (without Nd doping) [1]; 3.72 g/cm^3 (without Nd doping) [2]; 3.75 g/cm^3 (4 at.% Nd) [3]
Point group: 32

Lattice constants of $Nd_xY_{1-x}Al_3(BO_3)_4$ versus atomic concentration of Nd ions

[Nd] [at.%]	a [Å]	c [Å]	Ref.
0	9.287	7.256	[1]
	9.295 ± 0.003	7.243 ± 0.002	[4]
3–4	9.293	7.245	[5]
4–8	9.293	7.245	[6]
5.6	9.293	7.245	[7]
9	9.295 ± 0.003	7.243 ± 0.001	[2]
24	9.303 ± 0.003	7.281 ± 0.002	[2]
39	9.307 ± 0.003	7.257 ± 0.001	[2]
56	9.314 ± 0.005	7.278 ± 0.001	[2]
63	9.316 ± 0.002	7.294 ± 0.001	[2]
	9.320	7.284	[8]
71	9.322 ± 0.006	7.299 ± 0.001	[2]

[Nd] [at.%]	a [Å]	c [Å]	Ref.
72	9.323 ± 0.003	7.294 ± 0.002	[2]
100	9.3416 ± 0.0006	7.3066 ± 0.0008	[4]

Mohs hardness: 7.5 (without Nd doping) [1]; 7.5–8 [9]; 8 (4 at.% Nd) [5]
Melting point (incongruent melting): 1463–1553 K [8]

Thermal conductivity coefficient [10]

T [K]	κ [W/mK]
300	3–4

UV transmission cut-off wavelength of NYAB is at 0.325 μm (at e^{-1} level) [11].
Main absorption bands of Nd^{3+} in YAB are at 0.36 μm, 0.52–0.53 μm, 0.59 μm, 0.75 μm, 0.8–0.81 μm and 0.88 μm [11], [12].
High transmittance region: 1.0–2.3 μm [5]

Linear absorption coefficient α

λ [μm]	α [cm^{-1}]	Ref.	Note
0.355	7.6	[9]	5 at.% Nd
0.530	0.94	[5]	4 at.% Nd
0.531	1.2	[13]	3.9 at.% Nd
	1.39	[3]	4 at.% Nd
	2.4	[14]	
	3	[15]	4 at.% Nd
	≈3	[16]	20 at.% Nd
0.532	3.5	[9]	5 at.% Nd
0.588	9.36	[17]	4.6 at.% Nd
0.659	<0.05	[9]	5 at.% Nd
0.748	4.5	[18]	5.5 at.% Nd
0.801	5.03	[5]	4 at.% Nd
0.804	6.8	[19]	4 at.% Nd
	7.8	[13]	12 ± 4 at.% Nd
0.808	8.3	[19]	4 at.% Nd
	8.4	[13]	12 ± 4 at.% Nd
1.061	0.04	[5]	4 at.% Nd
1.064	<0.05	[9]	5 at.% Nd
1.318	<0.001	[9]	5 at.% Nd

Experimental values of refractive indices for 5 at.% Nd [9]

λ [μm]	n_o	n_e
0.355	1.821	1.738
0.436	1.797	1.718

λ [μm]	n_o	n_e
0.532	1.786	1.710
0.546	1.784	1.708
0.578	1.782	1.706
0.633	1.780	1.705
0.659	1.778	1.704
1.064	1.765	1.694
1.152	1.763	1.693
1.318	1.762	1.693

Experimental values of refractive indices for 10 at.% Nd [14]

λ [μm]	n_o	n_e
0.4047	1.80674	1.72924
0.4358	1.79271	1.71475
0.4861	1.78539	1.70889
0.5461	1.77999	1.70455
0.5893	1.77691	1.70179
0.6563	1.77284	1.69867
0.7065	1.77234	1.69913

Dispersion relations for 10 at.% Nd (λ in μm) [20]:

$$n_o^2 = 1 + \frac{2.08192923\,\lambda^2}{\lambda^2 - (0.1098684)^2}$$

$$n_e^2 = 1 + \frac{1.83465945\,\lambda^2}{\lambda^2 - (0.1067225)^2}$$

Other dispersion relations are given in [6] (for 4–8 at.% Nd) and in [21] (for 5.6 at.% Nd).
Temperature-dependent dispersion relation for 5.6% Nd (λ in μm, $0.4\,\mu\text{m} < \lambda < 0.7\,\mu\text{m}$, T in K, $293\,\text{K} < T < 473\,\text{K}$) [21]:

$$n_o^2 = 1 + \frac{172.4727}{(0.10985 + 7.7 \times 10^{-7}\,T - 2.38 \times 10^{-9}\,T^2)^{-2} - \lambda^{-2}}$$

$$n_e^2 = 1 + \frac{161.08069}{(0.10669 + 1.3 \times 10^{-6}\,T - 3.2 \times 10^{-9}\,T^2)^{-2} - \lambda^{-2}}$$

Expression for the effective second-order nonlinear coefficient (Kleinman symmetry conditions are valid, $d_{11} = -d_{12} = -d_{26}$) [22]:

$d_{ooe} = d_{11} \cos\theta \cos 3\phi$

$d_{eoe} = d_{oee} = d_{11} \cos^2\theta \sin 3\phi$

Values of second-order nonlinear coefficient:

$d_{11}(0.71\,\mu\text{m}) = 1.68 \pm 0.34\,\text{pm/V}$ [9]

$d_{11}(1.062\,\mu\text{m}) = 1.43\,\text{pm/V}$ [23]

$d_{11}(1.062\,\mu\text{m}) = 3.9 \times d_{36}(\text{KDP}) = 1.52\,\text{pm/V}$ [14], [24]
$d_{11}(1.062\,\mu\text{m}) = 1.7\,\text{pm/V}$ [3]
$d_{11}(1.064\,\mu\text{m}) = 1.51 \pm 0.25\,\text{pm/V}$ [9]
$d_{11}(1.318\,\mu\text{m}) = 1.42 \pm 0.17\,\text{pm/V}$ [9]

Experimental values of phase-matching angle ($T = 293\,\text{K}$)

Interacting wavelengths [μm]	θ_{exp} [deg]	Ref.	Note
SHG, $o + o \Rightarrow e$			
$1.06 \Rightarrow 0.53$	30	[21]	5.6 at.% Nd
		[16]	20 at.% Nd
	30.7	[5]	4 at.% Nd
$1.061 \Rightarrow 0.5305$	30.7	[7]	5.6 at.% Nd
$1.062 \Rightarrow 0.531$	30.7	[15]	4 at.% Nd
	32.9	[13]	12 ± 4 at.% Nd
$1.064 \Rightarrow 0.532$	30	[9]	5 at.% Nd
	32.9	[3]	4 at.% Nd
		[6]	4–8 at.% Nd
	34.5	[14]	10 at.% Nd
$1.318 \Rightarrow 0.659$	27	[9]	5 at.% Nd
$1.338 \Rightarrow 0.669$	27	[25]	5.5 at.% Nd
	27	[16]	20 at.% Nd
SHG, $e + o \Rightarrow e$			
$1.06 \Rightarrow 0.53$	45.6	[5]	4 at.% Nd
$1.064 \Rightarrow 0.532$	43	[9]	5 at.% Nd
	51	[6]	4–8 at.% Nd
	50.6	[14]	10 at.% Nd
$1.318 \Rightarrow 0.659$	36	[9]	5 at.% Nd
SFG, $o + o \Rightarrow e$			
$1.064 + 0.532 \Rightarrow 0.355$	41	[9]	5 at.% Nd
$1.062 + 0.590 \Rightarrow 0.3793$	39.5	[17]	4.6 at.% Nd
$1.062 + 0.750 \Rightarrow 0.4396$	$\approx$36	[18]	5.5 at.% Nd
$1.062 + 0.807 \Rightarrow 0.4586$	35	[20]	5.5 at.% Nd
$1.338 + 0.807 \Rightarrow 0.4799$	30.8	[25]	5.5 at.% Nd
SFG, $e + o \Rightarrow e$			
$1.064 + 0.532 \Rightarrow 0.355$	62	[9]	5 at.% Nd

Experimental values of internal angular, spectral, and temperature bandwidths

Interacting wavelengths [μm]	$\Delta\theta^{\text{int}}$ [deg]	ΔT [°C]	$\Delta\nu_2$ [cm^{-1}]	Ref.	Note
SHG, $o + o \Rightarrow e$					
$1.064 \Rightarrow 0.532$	0.037	26		[26]	4 at.% Nd
	0.038			[9]	5 at.% Nd

Interacting wavelengths [μm]	$\Delta\theta^{\text{int}}$ [deg]	ΔT [°C]	$\Delta\nu_2$ [cm^{-1}]	Ref.	Note
1.318 ⇒ 0.659	0.057			[9]	5 at.% Nd
1.338 ⇒ 0.669	0.069	50		[27]	5.6 at.% Nd
SHG, $e + o \Rightarrow e$					
1.064 ⇒ 0.532	0.058			[9]	5 at.% Nd
1.318 ⇒ 0.659	0.087			[9]	5 at.% Nd
SFG, $o + o \Rightarrow e$					
1.064 + 0.532 ⇒ 0.355	0.019			[9]	5 at.% Nd
1.062 + 0.750 ⇒ 0.4396			24.9	[18]	5.5 at.% Nd
SFG, $e + o \Rightarrow e$					
1.064 + 0.532 ⇒ 0.355	0.029			[9]	5 at.% Nd

Temperature variation of phase-matching angle near room temperature [21]

Interacting wavelengths [μm]	θ_{pm} [deg]	$d\theta_{\text{pm}}/dT$ [deg/K]	Note
SHG, $o + o \Rightarrow e$			
1.06 ⇒ 0.53	30	1.52×10^{-3}	5.6 at.% Nd

Fluorescence lifetime of $^4F_{3/2}$ level

λ [μm]	τ [μs]	Ref.	Note
1.061	50	[6]	4–8 at.% Nd
	53	[28]	5.6 at.% Nd
	60	[3]	4 at.% Nd
		[5]	4 at.% Nd
		[29]	10 at.% Nd
		[13]	12 ± 4 at.% Nd
	65	[23]	
1.338	56	[19]	4 at.% Nd

Laser transition wavelengths and corresponding emission cross-section values (in 10^{-20} cm^2)

Transition	λ [μm]	σ	σ (**E**∥c)	σ (**E**⊥c)	Ref.	Note
$^4F_{3/2} \Rightarrow {}^4I_{11/2}$	1.061		14	10	[28]	5.6 at.% Nd
		20			[13]	12 ± 4 at.% Nd
		20.1			[29]	10 at.% Nd
		45			[19]	4 at.% Nd
		100			[6]	4–8 at.% Nd
		100 ± 20			[16]	20 at.% Nd
$^4F_{3/2} \Rightarrow {}^4I_{13/2}$	1.338		2.56	2.46	[27]	5.6 at.% Nd
		18 ± 3.6			[16]	20 at.% Nd

Laser-induced damage threshold

λ [μm]	τ_p [ns]	I_{thr} [GW/cm^2]	Ref.
0.8	50	>0.4	[23]
1.06	10	>0.4–0.6	[2]

About the crystal

This SFD crystal was proposed in 1981 [16] and it is still quite popular [15], [30], besides some disadvantages like the lack of the high-quality crystals, concentration quenching, low quantum efficiency, unfavorable heating effects, and significant absorption in the green spectral range. Recently, 225 mW of CW green output ($\lambda = 530.5$ nm) was generated in 0.5-cm-long NYAB crystal with 1.6-W diode-pumping at 807 nm [15]. In the same crystal, pumped by 2.2 W of 807 nm diffraction-limited Ti:sapphire laser radiation, 450 mW of CW green radiation was generated [15].

References

[1] A.A. Filimonov, N.I. Leonyuk, L.B. Meissner, T.I. Timchenko, I.S. Rez: Nonlinear optical properties of isomorphic family of crystals with yttrium-aluminium borate (YAB) structure. Kristall und Technik **9(1)**, 63–66 (1974).

[2] N.I. Leonyuk, L.I. Leonyuk: Growth and characterization of $RM_3(BO_3)_4$ crystals. Progr. Cryst. Growth Character. Mater. **31(3–4)**, 179–278 (1995).

[3] S. Amano, S. Yokoyama, H. Koyama, S. Amano, T. Mochizuki: Diode pumped NYAB green laser. Rev. Laser Eng. **17(12)**, 895–898 (1989) [In Japanese].

[4] N.I. Leonyuk, E.V. Koporulina, Y.Y. Wang, X.B. Hu, A.V. Mokhov: Neodymium and chromium segregation at high-temperature crystallization of $(Nd,Y)Al_3(BO_3)_4$ and $(Nd,Y)Ca_4O(BO_3)_3$ doped with Cr^{3+}. J. Cryst. Growth **252(1–3)**, 174–179 (2003).

[5] Y.X. Fan, R. Schlecht, M.W. Qiu, D. Luo, A.D. Jiang, Y.C. Huang: Spectroscopic and nonlinear-optical properties of a self-frequency-doubling NYAB crystal. In: *OSA Proceedings on Advanced Solid-State Lasers, Vol. 13*, ed. by L.L. Chase, A.A. Pinto (OSA, Washington DC, 1992), pp. 371–375.

[6] Z.D. Luo, J.T. Lin, A.D. Jiang, Y.C. Huang, M.W. Qui: Features and applications of a new self-frequency-doubling laser crystal—NYAB. Proc. SPIE **1104**, 132–141 (1989).

[7] D. Jaque, J. Capmany, J. Garcia Sole, Z.D. Luo, A.D. Jiang: Continuous-wave laser properties of the self-frequency-doubling $YAl_3(BO_3)_4$:Nd crystal. J. Opt. Soc. Am. B **15(6)**, 1656–1662 (1998).

[8] E.V. Koporulina, N.I. Leonyuk, S.N. Barilo, L.A. Kurnevich, G.L. Bychkov, A.V. Mokhov, G. Bocelli, L. Righi: Flux growth, composition, structural and thermal characteristics of $(R_xY_{1-x})Al_3(BO_3)_4$ (R = Nd, Gd; x = 1, 0.6, 0.65, 0.7, and 0.75) crystals. J. Cryst. Growth **198–199**, 460–465 (1999).

[9] L.M. Dorozhkin, I.I. Kuratev, V.A. Zhitnyuk, A.V. Shestakov, V.D. Shigorin, G.P. Shipulo: Nonlinear optical properties of neodymium-yttrium-aluminum borate. Kvant. Elektron. **10(7)**, 1497–1498 (1983) [In Russian, English trans.: Sov. J. Quantum Electron. **13(7)**, 978–980 (1983)].

[10] T. Omatsu, Y. Kato, M. Shimosegawa, A. Hasegawa, I. Ogura: Thermal effects in laser diode pumped self-frequency-doubled $Nd_xY_{1-x}Al_3(BO_3)_4$ (NYAB) microchip laser. Opt. Commun. **118(3–4)**, 302–308 (1995).

[11] D. Jaque: Optimum conditions for ultraviolet-laser generation based on self-frequency sum mixing in Nd^{3+}-activated borate crystals. J. Opt. Soc. Am. B **19(6)**, 1326–1334 (2002).
[12] I. Schütz. I. Freitag, R. Wallenstein: Miniature self-frequency-doubling CW Nd:YAB laser pumped by a diode-laser. Opt. Commun. **77(2–3)**, 221–225 (1990).
[13] H. Hemmati: Diode-pumped self-frequency-doubled neodymium yttrium aluminum borate (NYAB) laser. IEEE J. Quant. Electr. **28(4)**, 1169–1171 (1992).
[14] B.-S. Lu, J. Wang, H.-F. Pan, M.-H. Jiang, E.-Q. Liu, X.-Y. Hou: Laser self-doubling in neodymium yttrium aluminum borate. J. Appl. Phys. **66(12)**, 6052–6054 (1989).
[15] J. Bartschke, R. Knappe, K.-J. Boller, R. Wallenstein: Investigation of efficient self-frequency-doubling Nd:YAB lasers. IEEE J. Quant. Electr. **33(12)**, 2295–2300 (1997).
[16] L.M. Dorozhkin, I.I. Kuratev, N.I. Leonyuk, T.I. Timchenko, A.V. Shestakov: Optical second-harmonic generation in a new nonlinear active medium: neodymium-yttrium-aluminum borate crystals. Pisma Zh. Tekh. Fiz. **7(21)**, 1297–1300 (1981) [In Russian, English trans.: Sov. Tech. Phys. Lett. **7(11)**, 555–556 (1981)].
[17] A. Brenier, G. Boulon: Self-frequency summing NYAB laser for tunable UV generation. J. Luminesc. **86(2)**, 125–128 (2000).
[18] A. Brenier, G. Boulon, D. Jaque, J. Garcia Sole: Self-frequency-summing NYAB laser for tunable blue generation. Opt. Mater. **13(3)**, 311–317 (1999).
[19] S. Amano, T. Mochizuki: Diode-pumped NYAB green laser. Nonl. Opt. **1(4)**, 297–306 (1991).
[20] D. Jaque, J. Capmany, F. Molero, J. Garcia Sole: Blue-light laser source by sum-frequency mixing in Nd:$YAl_3(BO_3)_4$. Appl. Phys. Lett. **73(25)**, 3659–3661 (1998).
[21] D. Jaque, J. Capmany, J. Rams, J. Garcia Sole: Effects of pump heating on laser and spectroscopic properties of the Nd:[$YAl_3(BO_3)_4$] self-frequency-doubling laser. J. Appl. Phys. **87(3)**, 1042–1048 (2000).
[22] J.E. Midwinter, J. Warner: The effects of phase matching method and of uniaxial crystal symmetry on the polar distribution of second-order non-linear optical polarization. Brit. J. Appl. Phys. **16(11)**, 1135–1142 (1965).
[23] R.E. Stone, R.C. Spitzer, S.C. Wang: A Q-switched diode-pumped neodymium yttrium aluminum borate laser. IEEE Photon. Technol. Lett. **2(11)**, 769–771 (1990).
[24] I. Shoji, T. Kondo, A. Kitamoto, M. Shirane, R. Ito: Absolute scale of second-order nonlinear-optical coefficients. J. Opt. Soc. Am. B **14(9)**, 2268–2294 (1997).
[25] D. Jaque, J. Capmany, J. Garcia Sole: Red, green, and blue laser light from a single Nd:$YAl_3(BO_3)_4$ crystal based on laser oscillation at 1.3 μm. Appl. Phys. Lett. **75(3)**, 325–327 (1999).
[26] M.-Y. Hwang, J.T. Lin: Temperature dependence of second harmonic generation in NYAB crystals. Opt. Commun. **95(1–3)**, 103–108 (1993).
[27] D. Jaque, J. Capmany, J. Garcia Sole: Continuous wave laser radiation at 669 nm from a self-frequency-doubled laser of $Yal_3(BO_3)_4$:Nd^{3+}. Appl. Phys. Lett. **74(13)**, 1788–1790 (1999).
[28] D. Jaque, J. Capmany, Z.D. Luo, J. Garcia Sole: Optical bands and energy levels of Nd^{3+} ion in the $YAl_3(BO_3)_4$ nonlinear laser crystal. J. Phys.: Condens. Matter **9(44)**, 9715–9729 (1997).
[29] H.-F. Pan, M.-G. Liu, J. Xue, B.-S. Lu: The spectra and sensitization of laser self-frequency-doubling $Nd_xY_{1-x}Al_3(BO_3)_4$ crystal. J. Phys.: Condens. Matter **2(19)**, 4525–4530 (1990).
[30] Y.F. Chen, S.C. Wang, C.F. Kao, T.M. Huang: Investigation of fiber-coupled laser-diode-pumped NYAB green laser performance. IEEE Photon. Technol. Lett. **8(10)**, 1313–1315 (1996).

7.3 Nd:$GdAl_3(BO_3)_4$, Neodymium-Doped Gadolinium Aluminum Tetraborate ($Nd_xGd_{1-x}Al_3(BO_3)_4$ or NGAB)

Negative uniaxial crystal: $n_o > n_e$

Correlation between the atomic concentation of Nd relative to Gd and Nd^{3+} volume concentration

[Nd] [at.%]	$[Nd^{3+}] \times 10^{-20}$ [cm^3]	Ref.
3	1.63	[1], [2]
10	5.6	[3]

Point group: 32
Lattice constants:
for 3 at.% Nd:
$a = 9.3416$ Å [1]
$a = 7.3066$ Å [1]
for 10 at.% Nd
$a = 9.305 \pm 0.008$ Å [3]
$c = 7.258 \pm 0.001$ Å [3]
UV transmission cut-off wavelength of NYAB is at 0.32 μm (at e^{-1} level) [3].
Main absorption bands of Nd^{3+} in GAB are at 0.36 μm, 0.53 μm, 0.588 μm, 0.748 μm, 0.807 μm, and 0.88 μm [4].

Linear absorption coefficient α

λ [μm]	α [cm^{-1}]	Ref.	Note
0.353	4.34	[3]	10 at.% Nd
0.432	2.23	[3]	10 at.% Nd
0.475	2.22	[3]	10 at.% Nd
0.537	3.19	[3]	10 at.% Nd
0.588	8.69	[3]	10 at.% Nd
0.689	2.05	[3]	10 at.% Nd
0.749	10.22	[3]	10 at.% Nd
0.808	9.30	[3]	10 at.% Nd
0.811	2.55	[5]	3.35 at.% Nd
0.881	2.61	[3]	10 at.% Nd

Absorption cross-section for 3 at.% Nd (in 10^{-20} cm^2) [1]

λ [μm]	σ ($\mathbf{E} \| c$)
0.44	0.31
0.531	0.45

Experimental values of refractive indices for 5 at.% Nd [4]

λ [μm]	n_o	n_e
0.4368	1.7921	1.7144
0.4861	1.7851	1.7089
0.5321	1.7801	1.7050
0.5461	1.7792	1.7036
0.5893	1.7760	1.7012
0.6328	1.7733	1.6991
0.6563	1.7723	1.6980
0.7065	1.7694	1.6955
1.0642	1.7603	1.6884

Experimental values of refractive indices for 10 at.% Nd [3]

λ [μm]	n_o	n_e
0.4047	1.8142	1.7352
0.4358	1.8026	1.7253
0.4861	1.7959	1.7178
0.5461	1.7920	1.7141
0.5893	1.7890	1.7122
0.6563	1.7856	1.7099
0.7363	1.7841	1.7087

Temperature dependence of refractive indices at $\lambda = 0.5893\,\mu$m for 5 at.% Nd [4]

T [K]	n_o	n_e
290	1.7760	1.7011
293	1.7761	1.7012
303	1.7761	1.7013
321	1.7762	1.7014
338.5	1.7764	1.7016
355	1.7766	1.7018
376	1.7768	1.7020

Temperature derivative of refractive indices for 5 at.% Nd [4]

λ [μm]	$dn_o/dT \times 10^5$ [K^{-1}]	$dn_e/dT \times 10^5$ [K^{-1}]
0.5893	0.93	1.05

Dispersion relations for 5 at.% Nd (λ in μm, $T = 293$ K) [4], [6]:

$$n_o^2 = 3.07289 + \frac{0.03079}{\lambda^2 + 0.03265}$$

$$n_e^2 = 2.82998 + \frac{0.0242}{\lambda^2 + 0.03127}$$

Dispersion relations for 10 at.% Nd (λ in μm) [3]:

$$n_o^2 = 3.2087 + \frac{0.0034}{\lambda^2 - 0.1271} - 0.0656\,\lambda^2$$

$$n_e^2 = 2.9150 + \frac{0.0048}{\lambda^2 - 0.1147} - 0.0124\,\lambda^2$$

Expression for the effective second-order nonlinear coefficient (Kleinman symmetry conditions are valid, $d_{11} = -d_{12} = -d_{26}$) [7]:

$d_{ooe} = d_{11} \cos\theta \cos 3\phi$

$d_{eoe} = d_{oee} = d_{11} \cos^2\theta \sin 3\phi$

Experimental values of phase-matching angle ($T = 293$ K)

Interacting wavelengths [μm]	θ_{exp} [deg]	Ref.	Note
SHG, $o + o \Rightarrow e$			
1.062 $\Rightarrow$ 0.531	30.1	[1], [8]	
	30.3	[9]	
1.064 $\Rightarrow$ 0.532	30.6	[4]	5 at.% Nd
1.338 $\Rightarrow$ 0.669	24.4	[2]	
SHG, $e + o \Rightarrow e$			
1.064 $\Rightarrow$ 0.532	44.1	[4]	5 at.% Nd
SFG, $o + o \Rightarrow e$			
1.062 + 0.588 $\Rightarrow$ 0.3785	38.2	[10]	3 at.% Nd
1.062 + 0.7482 $\Rightarrow$ 0.4389	35	[1], [8]	
1.062 + 0.811 $\Rightarrow$ 0.4598	34	[5]	3.35 at.% Nd
1.062 + 0.807 $\Rightarrow$ 0.4586	34.1	[6]	3.4 at.% Nd
1.338 + 0.7482 $\Rightarrow$ 0.4799	31	[2]	
DFG, $e - o \Rightarrow o$			
0.588 − 1.062 $\Rightarrow$ 1.3174	27.3	[10]	3 at.% Nd

Fluorescence lifetime of $^4F_{3/2}$ level

λ [μm]	τ [μs]	Ref.	Note
1.062	48 ± 3	[4]	
	55.6	[1]	3 at.% Nd

Laser transition wavelengths and corresponding emission cross-section values (in 10^{-20} cm^2)

Transition	λ [μm]	σ	Ref.	Note
$^4F_{3/2} \Rightarrow {}^4I_{11/2}$	1.062	20.8	[9]	
		30	[1]	3 at.% Nd
$^4F_{3/2} \Rightarrow {}^4I_{13/2}$	1.338	5.04	[9]	
		5.5	[2]	3 at.% Nd

About the crystal

NGAB is an analog of Nd:YAB which recently was used for difference-frequency generation [10]. The pump (near 588 nm) and resulting IR ($^4F_{3/2} \Rightarrow {}^4I_{11/2}$ transition, 1.0619 μm) radiations were mixed in a 0.43-cm NGAB crystal doped with 3 at.% Nd. The obtained tuning range was extended from 1.305 to 1.365 μm.

References

[1] A. Brenier, C. Tu, M. Qiu, A. Jiang, J. Li, B. Wu: Spectroscopic properties, self-frequency doubling, and self-sum frequency mixing in $GdAl_3(BO_3)_4$:Nd^{3+}. J. Opt. Soc. Am. B **18(8)**, 1104–1110 (2001).

[2] A. Brenier, C. Tu, J. Li, Z. Zhu, B. Wu: Spectroscopy, laser operation and self-frequency doubling in $GdAl_3(BO_3)_4$:Nd^{3+}. Opt. Commun. **200(1–6)**, 355–358 (2001).

[3] H.-D. Jiang, J.-Y. Wang, X.-B. Hu, S.-T. Li, B. Teng, C.-Q. Zhang: Absorption spectrum and optical parameters of Nd-doped gadolinium aluminium tetraborate crystals. Jpn. J. Appl. Phys. **40(10)**, 5981–5984 (2001).

[4] C. Tu, M. Qiu, Y. Huang, X. Chen, A. Jiang, Z. Luo: The study of a self-frequency-doubling laser crystal Nd^{3+}:$GdAl_3(BO_3)_4$. J. Cryst. Growth **208(1–4)**, 487–492 (2000).

[5] Y. Chen, M. Huang, Y. Huang, Z. Luo: Simultaneous green and blue laser radiation based on a nonlinear laser crystal Nd:$GdAl_3(BO_3)_4$ and a nonlinear optical crystal KTP. Opt. Commun. **218(4–6)**, 379–384 (2003).

[6] M. Huang, Y. Chen, X. Chen, Y. Huang, Z. Luo: A CW blue laser emission by self-sum-frequency mixing in Nd^{3+}:$GdAl_3(BO_3)_4$. Opt. Commun. **208(1–3)**, 163–166 (2002).

[7] J.E. Midwinter, J. Warner: The effects of phase matching method and of uniaxial crystal symmetry on the polar distribution of second-order non-linear optical polarization. Brit. J. Appl. Phys. **16(11)**, 1135–1142 (1965).

[8] G. Aka, A. Brenier: Self-frequency conversion in nonlinear optical crystals. Opt. Mater. **22(2)**, 89–94 (2003).

[9] M. Huang, Y. Chen, X. Chen, Y. Huang, Z. Luo: Study on CW fundamental and self-frequency doubling laser of Nd^{3+}:$GdAl_3(BO_3)_4$ crystal. Opt. Commun. **204(1–6)**, 333–338 (2002).

[10] A. Brenier, C. Tu, J. Li, Z. Zhu, B. Wu: Self-sum- and -difference-frequency mixing in $GdAl_3(BO_3)_4$:Nd^{3+} for generation of tunable ultraviolet and infrared radiation. Opt. Lett. **27(4)**, 240–242 (2002).

7.4 Nd:$GdCa_4O(BO_3)_3$, Neodymium-Doped Gadolinium Calcium Oxyborate (Nd_xGd_{1-x}COB or Nd:GdCOB)

Negative biaxial crystal

Correlation between the atomic concentation of Nd relative to Gd and Nd^{3+} volume concentration

[Nd] [at.%]	$[Nd^{3+}] \times 10^{-20}$ [cm^3]
4	1.8
5	2.2
7	3.1

Point group: m
Lattice constants for Nd:GdCOB crystal with 5 at.% Nd [1]:
$a = 8.0998 \pm 0.0016$ Å
$b = 16.0312 \pm 0.0026$ Å
$c = 3.5625 \pm 0.0008$ Å
$\beta = 101.242° \pm 0.024°$
Assignment of dielectric and crystallographic axes Nd:GdCOB crystal with 7 at.% Nd: $Y \| b$, the axes a and c lie in XZ plane, the angle between them is $\beta = 101.27°$, the angle between the axes Z and a is 27.1°, the angle between the axes X and c is 16.1° [2].
Mohs hardness: 6.5 [3]

Linear thermal expansion coefficient for Nd:GdCOB crystal with 7 at.% Nd [2]

$\alpha_t \times 10^6$ [K^{-1}], $\|a$	$\alpha_t \times 10^6$ [K^{-1}], $\|b$	$\alpha_t \times 10^6$ [K^{-1}], $\|c$
7	5	11.3

Mean value of linear thermal expansion coefficient for Nd:GdCOB crystal with 5.2 at.% Nd [4]

T [K]	$\alpha_t \times 10^6$ [K^{-1}], $\|X$	$\alpha_t \times 10^6$ [K^{-1}], $\|Y$	$\alpha_t \times 10^6$ [K^{-1}], $\|Z$
298–572.5	11.6	5.4	5.9

Specific heat capacity c_p at $P = 0.101325$ MPa (for 5.2 at.% Nd) [4]

T [K]	c_p [J/kgK]
330	665

High transmittance range: 0.9–2.6 μm [2].

Linear absorption coefficient α

λ [μm]	α [cm^{-1}]	Ref.	Note
0.461	0.37–0.42	[5]	5 at.% Nd, depending on polarization
0.465	0.43–0.46	[5]	7 at.% Nd, depending on polarization
0.53	0.41	[3]	4 at.% Nd
	0.73	[6]	7 at.% Nd
0.81	1.78	[3]	4 at.% Nd
1.06	0.02	[3]	4 at.% Nd

Absorption cross-section σ (in 10^{-20} cm^2)

λ [μm]	σ ($\mathbf{E}\|X$)	σ ($\mathbf{E}\|Y$)	σ ($\mathbf{E}\|Z$)	Ref.	Note
0.530	0.17	0.31	0.27	[3]	4 at.% Nd
	0.22	0.35	0.22	[7]	4 at.% Nd
	0.27	0.21	0.43	[2]	7 at.% Nd

λ [μm]	σ ($\mathbf{E}\|X$)	σ ($\mathbf{E}\|Y$)	σ ($\mathbf{E}\|Z$)	Ref.	Note
0.545	<0.1	<0.1	<0.1	[7]	4 at.% Nd
0.811	1.86	1.57	2.23	[3], [8]	4 at.% Nd
	0.52	0.35	0.64	[2]	7 at.% Nd

Note: The labeling of X and Z axes given in [3], [8] is incorrect. The σ values given in [2] are underestimated.

Sellmeier equations for Nd:GdCOB crystal with 9 at.% Nd (λ in μm) [9]:

$$n_X^2 = 2.85005 + \frac{0.00651}{\lambda^2 - 0.11688} - 0.00001\,\lambda^2$$

$$n_Y^2 = 2.93898 + \frac{0.00674}{\lambda^2 - 0.11711} - 0.00001\,\lambda^2$$

$$n_Z^2 = 2.96538 + \frac{0.00839}{\lambda^2 - 0.10739} - 0.00001\,\lambda^2$$

For small Nd concentrations, the refractive indices of Nd:GdCOB are very near to those of GdCOB [5].
Expressions for effective second-order nonlinear coefficient in the principal planes of Nd:GdCOB crystal (approximation of small walk-off angle Kleinman symmetry conditions are valid: $d_{12} = d_{26}$, $d_{13} = d_{35}$, $d_{15} = d_{31}$, $d_{24} = d_{32}$) [10], [11]:

XY plane, $\theta = 90°$

$d_{\mathrm{ooe}} = d_{13} \sin\phi$

$d_{\mathrm{eoe}} = d_{\mathrm{oee}} = d_{31} \sin^2\phi + d_{32} \cos^2\phi$

YZ plane, $\phi = 90°$

$d_{\mathrm{eeo}} = d_{13} \sin^2\theta + d_{12} \cos^2\theta$

$d_{\mathrm{oeo}} = d_{\mathrm{eoo}} = d_{31} \sin\theta$

XZ plane, $\phi = 0°$, $V_{\mathrm{z}} > \theta > 0°$

$d_{\mathrm{ooe}} = d_{12} \cos\theta - d_{32} \sin\theta$

XZ plane, $\phi = 0°$, $90° > \theta > V_{\mathrm{z}}$

$d_{\mathrm{oeo}} = d_{\mathrm{eoo}} = d_{12} \cos\theta - d_{32} \sin\theta$

XZ plane, $\phi = 0°$, $180° - V_{\mathrm{z}} > \theta > 90°$; or $\phi = 180°$, $90° > \theta > V_{\mathrm{z}}$

$d_{\mathrm{oeo}} = d_{\mathrm{eoo}} = d_{12} \cos\theta + d_{32} \sin\theta$

XZ plane, $\phi = 0°$, $180° > \theta > 180° - V_{\mathrm{z}}$; or $\phi = 180°$, $V_{\mathrm{z}} > \theta > 0°$

$d_{\mathrm{ooe}} = d_{12} \cos\theta + d_{32} \sin\theta$

Experimental values of phase-matching angle

Interacting wavelengths [μm]	ϕ_{pm} [deg]	Ref.
XY plane, $\theta = 90°$		
SHG, $o + o \Rightarrow e$		
1.091 $\Rightarrow$ 0.5455	44	[12]
1.0642 $\Rightarrow$ 0.5321	46.02	[5]
1.061 $\Rightarrow$ 0.5305	46	[6], [8], [9], [12], [13], [14], [15]
0.936 $\Rightarrow$ 0.468	58.7	[16]

Interacting wavelengths [μm]	ϕ_{pm} [deg]	Ref.
SFG, $o + o \Rightarrow e$		
$1.061 + 0.811 \Rightarrow 0.45965$	60	[12]

Experimental value of effective second-order nonlinear coefficient for some specific phase-matching directions (SHG, type I) in Nd:GdCOB crystal

Phase-matching direction	d_{eff} [pm/V]	Ref.
$\theta = 90°$, $\phi = 46°$ (XY plane)	0.7	[15]
$\theta = 66.3°$, $\phi = 134.4°$	1.5	[15]
	2.6	[1]

Note: The properties of d_{eff} in the case of Nd:GdCOB crystal include mirror and inversion symmetries. This means that the spatial distribution of d_{eff} can fully be described by choosing two independent quadrants, for example, ($0° < \theta < 90°$, $0° < \phi < 90°$) and ($0° < \theta < 90°$, $90° < \phi < 180°$). After that, the d_{eff} value in each (θ, ϕ) direction in these two quadrants is equal to that in ($180° - \theta$, $180° - \phi$) direction and vice versa. For example, the directions ($\theta = 66.3°$, $\phi = 134.4°$) and ($\theta = 113.7°$, $\phi = 45.6°$) possess equal d_{eff} values.

Experimental values of SHG conversion efficiency (type I, 1.0642 μm ⇒ 0.5321 μm, $I = 0.03\,\mathrm{GW/cm^2}$, $l = 0.8\,\mathrm{cm}$) for some specific phase-matching directions in Nd:GdCOB crystal [13]

Phase-matching direction	SHG conversion efficiency [%]
$\theta = 90°$, $\phi = 46°$ (XY plane)	3.9
$\theta = 66.3°$, $\phi = 134.4°$	19.5

See the note to the previous table.

Fluorescence lifetime of $^4F_{3/2}$ level [3]

λ [μm]	τ [μs]	Note
1.06	98	1–2 at.% Nd
	90	7 at.% Nd
	82	10 at.% Nd
	60	20 at.% Nd

Laser transition wavelengths and corresponding emission cross-section values (in $10^{-20}\,\mathrm{cm^2}$)

Transition	λ [μm]	σ ($\mathbf{E}\|X$)	σ ($\mathbf{E}\|Y$)	σ ($\mathbf{E}\|Z$)	Ref.	Note
$^4F_{3/2} \Rightarrow {}^4I_{9/2}$	0.936	0.54	0.44	0.16	[16]	7 at.% Nd
$^4F_{3/2} \Rightarrow {}^4I_{11/2}$	1.061	2.0	2.1	4.2	[3], [6], [8]	4 at.% Nd

Note: The labeling of X and Z axes given in [3], [6], [8] is incorrect.

About the crystal

The newly developed Nd:GdCOB crystal can be used for efficient self-frequency doubling. In [17], [18], 115 mW of CW green output ($\lambda = 530.5/545$ nm) were generated in a 0.4-cm-long, 5 at.% Nd-doped crystal ($\theta = 90°$, $\phi = 46°$) at 1.3 W of absorbed pump power delivered by a 810 nm laser diode. The 545-nm line was produced due to accompanying self-sum-frequency mixing process (1061 nm + 810 nm $\Rightarrow$ 545 nm). In [19], a 0.7-cm-long Nd:GdCOB crystal, cut at $\theta = 66.3°$, $\phi = 134.4°$, and containing 8 at.% Nd, was used for type I self-frequency doubling. The maximum power of generated CW green light at 530.5 nm under Ti:sapphire laser pumping ($\lambda = 812$ nm, absorbed pump power 1.56 W) reached 225 mW. In [18], 1.2 mW of CW blue light ($\lambda = 465$ nm) was generated by the self-sum-frequency mixing between the 1090-nm laser radiation and the remaining part of the 812 nm pump (CW Ti:sapphire laser).

References

[1] A. Brenier, A. Majchrowski, E. Michalski, T. Lukasiewicz: Evaluation of GdCOB:Nd^{3+} for self-frequency doubling in the optimum phase matching direction. Opt. Commun. **217(1–6)**, 395–400 (2003).

[2] S. Zhang, Z. Cheng, J. Han, G. Zhou, Z. Shao, C. Wang, Y.T. Chow, H. Chen: Growth and investigation of efficient self-frequency-doubling $Nd_xGd_{1-x}Ca_4O(BO_3)_3$ crystal. J. Cryst. Growth **206(3)**, 197–202 (1999).

[3] F. Mougel, G. Aka, A. Kahn-Harari, H. Hubert, J.M. Benitez, D. Vivien: Infrared laser performance and self-frequency doubling of Nd:$Ca_4GdO(BO_3)_3$ (Nd:GdCOB). Opt. Mater. **8(3)**, 161–173 (1997).

[4] C. Wang, H. Zhang, X. Meng, L. Zhu, Y.T. Chow, X. Liu, R. Cheng, Z. Yang, S. Zhang, L. Sun: Thermal, spectroscopic properties and laser performance at 1.06 and 1.33 μm of Nd:$Ca_4YO(BO_3)_3$ and Nd:$Ca_4GdO(BO_3)_3$ crystals. J. Cryst. Growth **220(1–2)**, 114–120 (2000).

[5] F. Mougel, G. Aka, A. Kahn-Harari, D. Vivien: CW blue laser generation by self sum-frequency mixing in Nd:$Ca_4GdO(BO_3)_3$ (Nd:GdCOB) single crystal. Opt. Mater. **13(3)**, 293–297 (1999).

[6] F. Mougel, F. Auge, G. Aka, A. Kahn-Harari, D. Vivien, F. Balembois, P. Georges, A. Brun: New green self-frequency-doubling diode-pumped Nd:$Ca_4GdO(BO_3)_3$ laser. Appl. Phys. B **67(5)**, 533–535 (1998).

[7] C. Maunier, J.L. Doualan, G. Aka, J. Landais, E. Antic-Fidancev, R. Moncorge, D. Vivien: Excited state absorption of the self-frequency doubling laser material: Nd:GdCOB. Opt. Commun. **184(1–4)**, 209–214 (2000).

[8] R. Auge, F. Mougel, G. Aka, A. Kahn-Harari, D. Vivien, F. Balembois, P. Georges, A. Brun: Self-frequency doubling of Nd:$Ca_4GdO(BO_3)_3$ (Nd:GdCOB) laser pumped by CW Ti:sapphire or laser diode. In: *Advanced Solid-State Lasers, OSA Trends in Optics and Photonics Series, Vol. 19*, ed. by W.R. Bosenberg, M.M. Fejer (OSA, Washington DC, 1998), pp. 53–55.

[9] J. Wang, Z. Shao, J. Wei, X. Hu, Y. Liu, B. Gong, G. Li, J. Lu, M. Guo, M. Jiang: Research on growth and self-frequency doubling of Nd:ReCOB (Re = Y or Gd) crystals. Progr. Cryst. Growth Character. Mater. **40(1–4)**, 17–31 (2000).

[10] G. Aka, A. Kahn-Harari, F. Mougel, D. Vivien, F. Salin, P. Coquelin, P. Colin, D. Pelenc, J.P. Damelet: Linear and nonlinear-optical properties of a new gadolinium calcium oxoborate crystal, $Ca_4GdO(BO_3)_3$. J. Opt. Soc. Am. B **14(9)**, 2238–2247 (1997).
[11] Z.P. Wang, J.H. Liu, R.B. Song, H.D. Jiang, S.J. Zhang, K. Fu, C.Q. Wang, J.Y. Wang, Y.G. Liu, J.Q. Wei, H.C. Chen, Z.S. Shao: Anisotropy of nonlinear-optical property of RCOB (R = Gd, Y) crystal. Chin. Phys. Lett. **18(3)**, 385–387 (2001).
[12] G. Aka, A. Brenier: Self-frequency conversion in nonlinear optical crystals. Opt. Mater. **22(2)**, 89–94 (2003).
[13] J. Lu, G. Li, J. Liu, S. Zhang, H. Chen, M. Jiang, Z. Shao: Second harmonic generation and self-frequency doubling performance in $Nd:GdCa_4O(BO_3)_3$ crystal. Opt. Commun. **168(5–6)**, 405–408 (1999).
[14] F. Auge, S. Auzanneau, G. Lukas-Leclin, F. Balembois, P. Georges, A. Brun, F. Mougel, G. Aka, A. Kahn-Harari, D. Vivien: Efficient self-frequency-doubling Nd:GdCOB crystal pumped by a high brightness laser diode. In: *Advanced Solid-State Lasers, OSA Trends in Optics and Photonics Series, Vol. 26*, ed. by M.M. Fejer, H. Injeyan, U. Keller (OSA, Washington DC, 1999), pp. 77–81.
[15] Z. Shao, J. Lu, Z. Wang, J. Wang, M. Jiang: Anisotropic properties of Nd:ReCOB (Re = Y, Gd): a low symmetry self-frequency doubling crystal. Progr. Cryst. Growth Character. Mater. **40(1–4)**, 63–73 (2000).
[16] F. Auge, G. Lukas-Leclin, F. Balembois, P. Georges, A. Brun, F. Mougel, G. Aka, A. Kahn-Harari, D. Vivien: Blue laser emission by self-frequency-doubling of the $^4F_{3/2} \Rightarrow {}^4I_{9/2}$ transition (936 nm) in Nd:GdCOB. In: *Advanced Solid-State Lasers, OSA Trends in Optics and Photonics Series, Vol. 34*, ed. by H. Injeyan, U. Keller, C. Marshall (OSA, Washington DC, 2000), pp. 335–341.
[17] G. Lucas-Leclin, F. Auge, S.C. Auzanneau, F. Balembois, P. Georges, A. Brun, F. Mougel, G. Aka, D. Vivien: Diode-pumped self-frequency-doubling $Nd:GdCa_4O(BO_3)_3$ lasers: toward green microchip lasers. J. Opt. Soc. Am. **17(9)**, 1526–1530 (2000).
[18] D. Vivien, F. Mougel, F. Auge, G. Aka, A. Kahn-Harari, F. Balembois, G. Lucas-Leclin, P. Georges, A. Brun, P. Aschehoug, J.-M. Benitez, N. Le Nain, M. Jacquet: Nd:GdCOB: overview of its infrared, green and blue laser performances. Opt. Mater. **16(1–2)**, 213–220 (2001).
[19] C.Q. Wang, Y.T. Chow, W.A. Gambling, S.J. Zhang, Z.X. Cheng, Z.S. Shao, H.C. Chen: Efficient self-frequency doubling of Nd:GdCOB crystal by type-I phase matching out of its principal planes. Opt. Commun. **174(5–6)**, 471–474 (2000).

7.5 $Nd:YCa_4O(BO_3)_3$, Neodymium-Doped Yttrium Calcium Oxyborate ($Nd_xY_{1-x}COB$ or Nd:YCOB)

Negative biaxial crystal

Correlation between the atomic concentration of Nd relative to Y and Nd^{3+} volume concentration

[Nd] [at.%]	$[Nd^{3+}] \times 10^{-20}$ [cm^3]
4	1.8
5	2.2
7	3.1

Point group: m
Lattice constants for Nd:YCOB crystal with 4.4 at.% Nd [1]:
$a = 8.076 \pm 0.007$ Å
$b = 16.020 \pm 0.010$ Å
$c = 3.527 \pm 0.002$ Å
$\beta = 101.23°$
Mohs hardness: 6–6.5 [2]

Mean value of linear thermal expansion coefficient (for 7 at.% Nd) [3]

T [K]	$\alpha_t \times 10^6$ [K^{-1}], $\parallel X$	$\alpha_t \times 10^6$ [K^{-1}], $\parallel Y$	$\alpha_t \times 10^6$ [K^{-1}], $\parallel Z$
298–572.5	10.9	4.2	5.9

Specific heat capacity c_p at $P = 0.101325$ MPa (for 7 at.% Nd) [3]

T [K]	c_p [J/kgK]
330	774

Linear absorption coefficient α

λ [μm]	α [cm^{-1}]	Ref.	Note
0.530	<0.43	[4], [5]	$\mathbf{E}\perp Z$, 5 at.% Nd
	0.46	[6]	$\mathbf{E}\perp Z$, 5 at.% Nd
0.468	0.03	[4]	$\mathbf{E}\perp Z$, 5 at.% Nd
	0.12	[4]	$\mathbf{E}\perp Y$, 5 at.% Nd
0.666	0.03	[4]	$\mathbf{E}\perp Z$, 5 at.% Nd
	0.12	[4]	$\mathbf{E}\perp Y$, 5 at.% Nd
0.794	1.00	[7]	$\mathbf{E}\parallel Z$, 2 at.% Nd
	2.36	[1]	4.4 at.% Nd
	3.0	[5]	$\mathbf{E}\parallel Z$, 5 at.% Nd
0.812	0.84	[7]	$\mathbf{E}\parallel Z$, 2 at.% Nd
	2.88	[1]	4.4 at.% Nd
	1.9	[5], [8]	$\mathbf{E}\parallel X$, 5 at.% Nd
	1.55	[5], [8]	$\mathbf{E}\parallel Y$, 5 at.% Nd
	2.6	[5], [8]	$\mathbf{E}\parallel Z$, 5 at.% Nd
1.061	3.8	[6]	$\mathbf{E}\parallel Z$, 5 at.% Nd, $\theta = 90°$, $\phi = 35°$
1.332	2.9	[6]	$\mathbf{E}\parallel Z$, 5 at.% Nd, $\theta = 90°$, $\phi = 28°$

Absorption cross-section σ (in 10^{-20} cm^2) [4]

λ [μm]	σ ($\mathbf{E}\parallel Z$)	Note
0.7945	2.65	5 at.% Nd
0.8115	2.38	5 at.% Nd

Experimental values of refractive indices [2]

λ [μm]	n_X	n_Y	n_Z
1.061	1.6844	1.7152	1.7256

For small Nd concentrations, the refractive indices of Nd:YCOB are very near to those of YCOB.

Expressions for effective second-order nonlinear coefficient in the principal planes of Nd:YCOB crystal (approximation of small walk-off angle Kleinman symmetry conditions are valid: $d_{12} = d_{26}$, $d_{13} = d_{35}$, $d_{15} = d_{31}$, $d_{24} = d_{32}$) [9], [10]:

XY plane, $\theta = 90°$

$d_{\mathrm{ooe}} = d_{13} \sin\phi$

$d_{\mathrm{eoe}} = d_{\mathrm{oee}} = d_{31} \sin^2\phi + d_{32} \cos^2\phi$

YZ plane, $\phi = 90°$

$d_{\mathrm{eeo}} = d_{13} \sin^2\theta + d_{12} \cos^2\theta$

$d_{\mathrm{oeo}} = d_{\mathrm{eoo}} = d_{31} \sin\theta$

XZ plane, $\phi = 0°$, $V_z > \theta > 0°$

$d_{\mathrm{ooe}} = d_{12} \cos\theta - d_{32} \sin\theta$

XZ plane, $\phi = 0°$, $90° > \theta > V_z$

$d_{\mathrm{oeo}} = d_{\mathrm{eoo}} = d_{12} \cos\theta - d_{32} \sin\theta$

XZ plane, $\phi = 0°$, $180° - V_z > \theta > 90°$; or $\phi = 180°$, $90° > \theta > V_z$

$d_{\mathrm{oeo}} = d_{\mathrm{eoo}} = d_{12} \cos\theta + d_{32} \sin\theta$

XZ plane, $\phi = 0°$, $180° > \theta > 180° - V_z$; or $\phi = 180°$, $V_z > \theta > 0°$

$d_{\mathrm{ooe}} = d_{12} \cos\theta + d_{32} \sin\theta$

Experimental values of phase-matching angle

Interacting wavelengths [μm]	ϕ_{pm} [deg]	Ref.
XY plane, $\theta = 90°$		
SHG, $o + o \Rightarrow e$		
$1.332 \Rightarrow 0.666$	28	[4]
$1.061 \Rightarrow 0.5305$	33	[1]
	33.63	[6]
	33.95	[5]
	35	[4]

Experimental values of second-harmonic pulse energy for some specific phase-matching directions (SHG, type I, 1.0642 μm ⇒ 0.5321 μm) in Nd:YCOB crystal [11]

Phase-matching direction	ϵ [mJ]
$\theta = 90°$, $\phi = 33.6°$ (*XY* plane)	1.65
$\theta = 32°$, $\phi = 0°$ (*XZ* plane)	2.3
$\theta = 66.8°$, $\phi = 144.6°$	3.95

Note: The properties of d_{eff} in the case of Nd:YCOB crystal include mirror and inversion symmetries. This means that the spatial distribution of d_{eff} can fully be described by choosing two independent quadrants, for example, $(0° < \theta < 90°$,

$0° < \phi < 90°$) and ($0° < \theta < 90°$, $90° < \phi < 180°$). After that, the d_{eff} value in each (θ, ϕ) direction in these two quadrants is equal to that in ($180° - \theta$, $180° - \phi$) direction and vice versa. For example, the directions ($\theta = 66.8°$, $\phi = 144.6°$) and ($\theta = 113.2°$, $\phi = 35.4°$) possess equal d_{eff} values.

Fluorescence lifetime of $^4F_{3/2}$ level

λ [μm]	τ [μs]	Ref.	Note
1.06	102	[4], [6]	2 at.% Nd
	100	[4]	5 at.% Nd
	96	[12]	5 at.% Nd
		[4]	10 at.% Nd
	95	[6]	10 at.% Nd

Laser transition wavelengths and polarization of strongest emission lines [4]

Transition	λ [μm]	Polarization
$^4F_{3/2} \Rightarrow {}^4I_{9/2}$	0.936	$\mathbf{E} \parallel Y$
$^4F_{3/2} \Rightarrow {}^4I_{11/2}$	1.061	$\mathbf{E} \parallel Z$
$^4F_{3/2} \Rightarrow {}^4I_{13/2}$	1.332	$\mathbf{E} \parallel Z$

About the crystal

The self-doubling of $^4F_{3/2} \Rightarrow {}^4I_{11/2}$ transition ($\lambda = 1.061$ μm) in Nd:YCOB at 812-nm CW diode-pumping was investigated in [5], [6]. In the latter experiment, 245 mW of CW green output was generated in a type I, 0.5-cm-long crystal cut at $\theta = 90°$, $\phi = 33.6°$ and doped with 5 at.% Nd. The absorbed pump power constituted 3.8 W. The self-doubling of $^4F_{3/2} \Rightarrow {}^4I_{13/2}$ transition ($\lambda = 1.332$ μm) with the same AlGaAs diode-pumping was achieved in [4]. About 16 mW of CW red power at 666 nm was generated in a 0.5-cm-long, 5 at.% doped type I Nd:YCOB crystal ($\theta = 90°$, $\phi = 28°$) at 0.95 W of absorbed pump power.

References

[1] H.J. Zhang, X.L. Meng, L. Zhu, C.Q. Wang, R.P. Cheng, W.T. Yu, S.J. Zhang, L.K. Sun, Y.T. Chow, W.L. Zhang, H. Wang, K.S. Wong: Growth and laser properties of Nd:$Ca_4YO(BO_3)_3$ crystal. Opt. Commun. **160(4–6)**, 273–276 (1999).

[2] Q. Ye, B.H.T. Chai: Crystal growth of $YCa_4O(BO_3)_3$ and its orientation. J. Cryst. Growth **197(1–2)**, 228–235 (1999).

[3] C. Wang, H. Zhang, X. Meng, L. Zhu, Y.T. Chow, X. Liu, R. Cheng, Z. Yang, S. Zhang, L. Sun: Thermal, spectroscopic properties and laser performance at 1.06 and 1.33 μm of Nd:$Ca_4YO(BO_3)_3$ and Nd:$Ca_4GdO(BO_3)_3$ crystals. J. Cryst. Growth **220(1–2)**, 114–120 (2000).

[4] Q. Ye, L. Shah, J. Eichenholz, D. Hammons, R. Peale, M. Richardson, A. Chin, B.H.T. Chai: Investigation of diode-pumped, self-frequency doubled RGB lasers from Nd:YCOB crystals. Opt. Commun. **164(1–3)**, 33–37 (1999).

[5] J.M. Eichenholz, D.A. Hammons, L. Shah, Q. Ye, R.E. Peale, M. Richardson, B.H.T. Chai: Diode-pumped self-frequency doubling in a Nd^{3+}:$YCa_4O(BO_3)_3$ laser. Appl. Phys. Lett. **74(14)**, 1954–1956 (1999).
[6] D.A. Hammons, M. Richardson, B.H.T. Chai, A.K. Chin, R. Jollay: Scaling of longitudinally diode-pumped self-frequency-doubling Nd:YCOB lasers. IEEE J. Quant. Electr. **36(8)**, 991–999 (2000).
[7] B.H.T. Chai, J.M. Eichenholz, Q. Ye, D.A. Hammons, W.K. Jang, L. Shah, G.M. Luntz, M. Richardson: Self-frequency doubled Nd:YCOB laser. In: *Advanced Solid-State Lasers, OSA Trends in Optics and Photonics Series, Vol. 19*, ed. by W.R. Bosenberg, M.M. Fejer (OSA, Washington DC, 1998), pp. 56–58.
[8] Q. Ye, L. Shah, J.M. Eichenholz, D.A. Hammons, R.E. Peale, M. Richardson, B.H.T. Chai, A. Chin: Diode-pumped, self-frequency doubled red Nd:YCOB laser. In: *Advanced Solid-State Lasers, OSA Trends in Optics and Photonics Series, Vol. 26*, ed. by M.M. Fejer, H. Injeyan, U. Keller (OSA, Washington DC, 1999), pp. 100–103.
[9] G. Aka, A. Kahn-Harari, F. Mougel, D. Vivien, F. Salin, P. Coquelin, P. Colin, D. Pelenc, J.P. Damelet: Linear and nonlinear-optical properties of a new gadolinium calcium oxoborate crystal, $Ca_4GdO(BO_3)_3$. J. Opt. Soc. Am. B **14(9)**, 2238–2247 (1997).
[10] Z.P. Wang, J.H. Liu, R.B. Song, H.D. Jiang, S.J. Zhang, K. Fu, C.Q. Wang, J.Y. Wang, Y.G. Liu, J.Q. Wei, H.C. Chen, Z.S. Shao: Anisotropy of nonlinear-optical property of RCOB (R = Gd, Y) crystal. Chin. Phys. Lett. **18(3)**, 385–387 (2001).
[11] J. Wang, Z. Shao, J. Wei, X. Hu, Y. Liu, B. Gong, G. Li, J. Lu, M. Guo, M. Jiang: Research on growth and self-frequency doubling of Nd:ReCOB (Re = Y or Gd) crystals. Progr. Cryst. Growth Character. Mater. **40(1–4)**, 17–31 (2000).
[12] H. Zhang, X. Meng, L. Zhu, P. Wang, X. Liu, R. Cheng, J. Dawes, P. Dekker, S. Zhang, L. Sun: Growth and laser properties of Yb:$Ca_4YO(BO_3)_3$ crystal. J. Cryst. Growth **200(1–2)**, 335–338 (1999).

7.6 Nd:$LaBGeO_5$, Neodymium-Doped Lanthanum Borogermanate ($Nd_xLa_{1-x}BGeO_5$ or NdLBGO)

Positive uniaxial crystal: $n_e > n_o$
Molecular mass (for $LaBGeO_5$): 302.213
Point group: 3
Lattice constants (without Nd doping):
$a = 7.020 \pm 0.005$ Å [1]
$c = 6.879 \pm 0.004$ Å [1]
Melting point: 1473 K [2]
Transparency range at "0" transmittance level for 0.1-cm-long $LaBGeO_5$ crystal: 0.19–4.5 μm [1]

Experimental values of refractive indices for undoped $LaBGeO_5$ crystal at 296 K [1]

λ [μm]	n_o	n_e
0.4047	1.8504	1.8925
0.4358	1.8422	1.8836
0.4880	1.8322	1.8729
0.4920	1.8318	1.8722

λ [μm]	n_o	n_e
0.5321	1.8263	1.8663
0.5461	1.8247	1.8646
0.5770	1.8216	1.8613
0.5893	1.8201	1.8596
0.6328	1.8166	1.8558
1.0642	1.8023	1.8359
1.1524	1.8012	1.8391

Dispersion relations for undoped $LaBGeO_5$ crystal at 296 K (λ in μm) [1]:

$$n_o^2 = 1 + \frac{2.2209\,\lambda^2}{\lambda^2 - (0.1173)^2}$$

$$n_e^2 = 1 + \frac{2.3567\,\lambda^2}{\lambda^2 - (0.1197)^2}$$

Expression for the effective second-order nonlinear coefficient (Kleinman symmetry conditions are valid, $d_{15} = d_{31}$, $d_{14} = d_{25} = 0$) [3]:

$d_{eeo} = (d_{11}\sin 3\phi + d_{22}\cos 3\phi)\cos^2\theta$

$d_{oeo} = d_{eoo} = (d_{11}\cos 3\phi - d_{22}\sin 3\phi)\cos\theta + d_{15}\sin\theta$

Values of second-order nonlinear coefficient from [1], recalculated using new absolute values for $d_{11}(SiO_2)$ and d_{36}(KDP) from [4]:

$d_{11}(1.064\,\mu\text{m}) = 0.46 \pm 0.07$ pm/V

$d_{22}(1.064\,\mu\text{m}) = 0.23 \pm 0.04$ pm/V

$d_{31}(1.064\,\mu\text{m}) = 0.41 \pm 0.06$ pm/V

$d_{33}(1.064\,\mu\text{m}) = 0.35 \pm 0.05$ pm/V

Experimental values of phase-matching angle ($T = 293$ K)

Interacting wavelengths [μm]	θ_{exp} [deg]	Ref.	Note
SHG, $e + e \Rightarrow o$			
0.849 $\Rightarrow$ 0.4245	90	[5]	1.4 at.% Nd
1.048 $\Rightarrow$ 0.524	$\approx$54	[5], [6]	1.4 at.% Nd
	54 $\pm$ 0.5	[1]	no doping
1.314 $\Rightarrow$ 0.657	$\approx$35	[7]	1.4 at.% Nd
1.341 $\Rightarrow$ 0.6705	$\approx$40	[1]	
1.386 $\Rightarrow$ 0.693	$\approx$35	[7]	1.4 at.% Nd
SHG, $e + o \Rightarrow o$			
1.386 $\Rightarrow$ 0.693	$\approx$60	[7]	1.4 at.% Nd

Experimental values of internal angular and temperature bandwidths [5]

Interacting wavelengths [μm]	$\Delta\theta^{int}$ [deg]	ΔT [°C]	Note
SHG, $e + e \Rightarrow o$			
1.048 $\Rightarrow$ 0.524	0.084	10.1	1.4 at.% Nd

Fluorescence lifetime of $^4F_{3/2}$ level at 300 K

λ [μm]	τ [μs]	Ref.	Note
1.048	275 ± 15	[2]	0.1 at.% Nd
	280 ± 5	[1]	0.1 at.% Nd
	280	[8]	

Laser transition wavelengths and corresponding emission cross-section values (in 10^{-20} cm^2)

Transition	λ [μm]	σ (**E**∥c)	σ (**E**⊥c)	Ref.	Note
$^4F_{3/2} \Rightarrow {}^4I_{11/2}$	1.0482	26		[1]	1.4 at.% Nd
		26		[2]	2.0 at.% Nd
		24		[6]	1.4 at.% Nd
	1.0711		21	[1]	1.4 at.% Nd
			21	[2]	2.0 at.% Nd
			18	[6]	1.4 at.% Nd
$^4F_{3/2} \Rightarrow {}^4I_{13/2}$	1.3141	7		[1]	1.4 at.% Nd
		9		[7]	1.4 at.% Nd
	1.3868		6.5	[1]	1.4 at.% Nd
			3	[7]	1.4 at.% Nd

Laser-induced damage threshold

λ [μm]	τ_p [ns]	I_{thr} [GW/cm^2]	Ref.	Note
1.0642	10	>0.2	[6]	10 Hz
		>0.5	[1]	

About the crystal

A CW green output (λ = 524 nm) of about 0.1 mW power was demonstrated in a self-frequency-doubled, 0.4-cm-long NdLBGO crystal at an absorbed pump power of 0.6 W, delivered by a Ti:sapphire laser (λ = 800 nm) [9], [10]. In another experiment, made by the same Spanish group, the self-frequency doubling of another lasing transition, $^4F_{3/2} \Rightarrow {}^4I_{13/2}$, was performed [7]. About 0.8 mW of CW red radiation (λ = 657 nm) was generated in a 0.2-cm crystal at an absorbed pump power of 1.6 W.

References

[1] A.A. Kaminskii, A.V. Butashin, I.A. Maslyanizin, B.V. Mill, V.S. Mironov, S.P. Rozov, S.E. Sarkisov, V.D. Shigorin: Pure and Nd^{3+}-, Pr^{3+}-ion doped trigonal acentric $LaBGeO_5$ single crystals. Phys. Stat. Solidi A **125(2)**, 671–696 (1991).

[2] A.A. Kaminskii, B.V. Mill, A.V. Butashin: Stimulated emission from Nd^{3+} ions in acentric $LaBGeO_5$ crystals. Phys. Stat. Solidi A **118(1)**, K59–K64 (1990).

[3] J.E. Midwinter, J. Warner: The effects of phase matching method and of uniaxial crystal symmetry on the polar distribution of second-order non-linear optical polarization. Brit. J. Appl. Phys. **16(11)**, 1135–1142 (1965).

[4] I. Shoji, T. Kondo, A. Kitamoto, M. Shirane, R. Ito: Absolute scale of second-order nonlinear-optical coefficients. J. Opt. Soc. Am. B **14(9)**, 2268–2294 (1997).
[5] J. Capmany, J. Garcia Sole: Second harmonic generation in $LaBGeO_5$:Nd^{3+}. Appl. Phys. Lett. **70(19)**, 2517–2519 (1997).
[6] J. Capmany, L.E. Bausa, J. Garcia Sole, R. Moncorge, A.V. Butashin, B.V. Mill, A.A. Kaminskii: Fluorescence and 1.06–0.53 μm second harmonic generation in Nd^{3+} doped $LaBGeO_5$. J. Luminesc. **60–61**, 78–80 (1994).
[7] J. Capmany, D. Jaque, J. Garcia Sole: Continuous wave laser radiation at 1314 and 1386 nm and infrared to red self-frequency doubling in nonlinear $LaBGeO_5$:Nd^{3+} crystal. Appl. Phys. Lett. **75(18)**, 2722–2724 (1999).
[8] D. Jaque, J. Capmany, Z.D. Luo, J. Garcia Sole: Optical bands and energy levels of Nd^{3+} ion in the $YAl_3(BO_3)_4$ nonlinear laser crystal. J. Phys.: Condens. Matter **9(44)**, 9715–9729 (1997).
[9] J. Capmany, L.E. Bausa, D. Jaque, J. Garsia Sole, A.A. Kaminskii: CW end-pumped Nd^{3+}:$LaBGeO_5$ mini laser for self-frequency doubling. J. Luminesc. **72–74**, 816–818 (1997).
[10] J. Capmany, D. Jaque, J. Garcia Sole, A.A. Kaminskii: Continuous wave laser radiation at 524 nm from a self-frequency-doubled laser of $LaBGeO_5$:Nd^{3+}. Appl. Phys. Lett. **72(5)**, 531–533 (1998).

7.7 Nd:$Gd_2(MoO_4)_3$, Neodymium-Doped Gadolinium Molybdate ($Nd_{2x}Gd_{2-2x}(MoO_4)_3$ or NdGMO)

Positive biaxial crystal: $2V_z = 9.9°$ at $\lambda = 0.5321\,\mu m$
Molecular mass for $Gd_2(MoO_4)_3$: 794.313

Correlation between the atomic concentration of Nd relative to Gd and Nd^{3+} volume concentration

[Nd] [at.%]	$[Nd^{3+}] \times 10^{-20}$ [cm^3]
2.5	1.74
5.0	3.49

Specific gravity: 4.6 g/cm^3 (without Nd doping) [1], [2]; 4.65 g/cm^3 (without Nd doping) [3]
Point group: $mm2$
Lattice constants of $Gd_2(MoO_4)_3$ at $T = 293$ K [4]:
$a = 10.392$ Å
$b = 10.416$ Å
$c = 10.696$ Å
Assignment of dielectric and crystallographic axes: $X, Y, Z \Rightarrow b, a, c$
Curie temperature:
for $x = 0$: 432 K [1]
for $x = 0.03$: 432 K [1]

Melting point:
for $x = 0$: 1438 K [4]
for NdGMO 1428 K [4]

Specific heat capicity c_p at $P = 0.101325$ MPa (without Nd doping) [5]

T [K]	c_p [J/kgK]
373	429
473	461

Transparency range at "0" transmittance level (without doping): 0.31–5.13 μm [4]; 0.32–5.5 μm [4]; 0.32–5.2 μm [3]; 0.3–6 μm [6], [7]

Linear absorption coefficient α

λ [μm]	α [cm^{-1}]	Ref.	Note
0.53	4.34	[8]	15 at.% Nd
0.807	12.35	[2]	3 at.% Nd

Experimental values of refractive indices for $Gd_2(MoO_4)_3$ [9]

λ [μm]	n_X	n_Y	n_Z
0.4579	1.8758	1.8762	1.9342
0.4765	1.8694	1.8699	1.9270
0.4880	1.8659	1.8663	1.9229
0.4965	1.8634	1.8639	1.9201
0.5017	1.8621	1.8625	1.9185
0.5145	1.8588	1.8593	1.9148
0.5321	1.8545	1.8549	1.9102
0.6328	1.8385	1.8390	1.8915
1.0642	1.8142	1.8146	1.8637

Dispersion relations for $Gd_2(MoO_4)_3$ (λ in μm, 0.46 μm < λ < 1.06 μm) [9]:

$$n_X^2 = 1 + \frac{2.2450\,\lambda^2}{\lambda^2 - 0.022693}$$

$$n_Y^2 = 1 + \frac{2.24654\,\lambda^2}{\lambda^2 - 0.0226803}$$

$$n_Z^2 = 1 + \frac{2.41957\,\lambda^2}{\lambda^2 - 0.0245458}$$

Same dispersion relations are given in [4] with mistake.
Expressions for the effective second-order nonlinear coefficient in principal planes of NdGMO crystal (Kleinman symmetry conditions are valid, $d_{15} = d_{31}$ and $d_{24} = d_{32}$) [10]:

XY plane

$$d_{eoe} = d_{oee} = d_{32}\sin^2\phi + d_{31}\cos^2\phi$$

YZ plane
$d_{oeo} = d_{eoo} = d_{32} \sin\theta$
XZ plane, $\theta < V_z$
$d_{ooe} = d_{31} \sin\theta$
XZ plane, $\theta > V_z$
$d_{oeo} = d_{eoo} = d_{31} \sin\theta$

Effective second-order nonlinear coefficient for three-wave interactions in the arbitrary direction of NdGMO crystal is given in [10].

Values of second-order nonlinear coefficient (without doping) [14], recalculated using new absolute values for $d_{11}(SiO_2)$ [11]:
$d_{31}(1.06\,\mu m) = -2.3 \pm 0.6\,pm/V$
$d_{32}(1.06\,\mu m) = 2.3 \pm 0.6\,pm/V$
$d_{33}(1.06\,\mu m) = -0.035 \pm 0.009\,pm/V$

Values of second-order nonlinear coefficient ($x = 0.15$) [8], recalculated using new absolute values for $d_{11}(SiO_2)$ [11]:
$d_{31}(1.06\,\mu m) = -2.5\,pm/V$
$d_{32}(1.06\,\mu m) = 2.5\,pm/V$

Experimental values of phase-matching angle ($T = 293$ K, uniaxial approximation)

Interacting wavelengths [μm]	θ_{exp} [deg]	Ref.	Note
SHG, $e + e \Rightarrow o$			
0.974 ⇒ 0.487	90	[12]	no doping
1.064 ⇒ 0.532	68.3	[13]	no doping
1.06 ⇒ 0.53	65	[4]	no doping

Note: In [12] no difference in phase matching angle of doped ($x = 0.025$) and undoped GMO crystals was found.

Experimental values of internal angular, spectral and temperature bandwidths for undoped NdGMO (uniaxial approximation)

Interacting wavelengths [μm]	$\Delta\theta^{int}$ [deg]	ΔT [°C]	$\Delta\nu_2$ [cm^{-1}]	Ref.
SHG, $e + e \Rightarrow o$				
0.974 ⇒ 0.487			42	[12]
1.053 ⇒ 0.5265	0.08			[4]
1.064 ⇒ 0.532	0.07	5.6		[13]

Laser transition wavelengths at $T = 300$ K for NdGMO crystals ($x = 0.03$) of different orientation [1], [2]

Transition	λ [μm]	Note
$^4F_{3/2} \Rightarrow {}^4I_{11/2}$	1.0606	$\mathbf{E} \parallel c$
	1.0701	$\mathbf{E} \perp c$

Fluorescence lifetime of $^4F_{3/2}$ level at 300 K

λ [μm]	τ [μs]	Ref.	Note
1.0701	150	[2]	1 at.% Nd
	150 ± 10	[1]	≈1 at.% Nd

Laser-induced damage threshold

λ [μm]	τ_p [ns]	I_{thr} [GW/cm^2]	Ref.
1.0642	6	>0.13	[13]
	0.12	>1900 (?)	[6]

About the crystal

Nonlinear optical properties of gadolinium molybdate (GMO) and infrared laser generation in Nd^{3+}:$Gd_2(MO_4)_3$ were investigated in the 1970s [1], [8], [14]. Nevertheless in 1996–1997, Kamiskii with multiple coauthors claimed that NdGMO is a "new nonlinear optical material for self-frequency doubling" [4], [6], [7], though no SFD effect was demonstrated in this crystal.

References

[1] K.S. Bagdasarov, G.A. Bogomolova, A.A. Kaminskii, A.M. Prokhorov, T.M. Prokhortseva: Laser and spectral properties of $Gd_2(MoO_4)_3$:Nd^{3+} crystal. Doklady AN SSSR **197(3)**, 557–560 (1971) [In Russian, English trans.: Sov. Phys. - Doklady **16(3)**, 216–218 (1971)].

[2] A.A. Kamiskii: New room-temperature laser-diode pumped efficient quasi-CW and CW single-mode laser based on ferroelectric and ferroelastic $Gd_2(MoO_4)_3$:Nd^{3+} crystal. Phys. Stat. Solidi **149(1)**, K39–K42 (1995).

[3] *Handbook of Optical Materials*, ed. by M.J. Weber (CRC Press, Boca Raton, 2003), pp. 1–512.

[4] A.A. Kaminskii, A.V. Butashin, H.-J. Eichler, D. Grebe, R. Macdonald, K. Ueda, H. Nishioka, W. Odajima, M. Tateno, J. Song, M. Musha, S.N. Bagaev, A.A. Pavlyuk: Orthorhombic ferroelectric and ferroelastic $Gd_2(MoO_4)_3$ crystal—a new many-purposed nonlinear and optical material: efficient multiple stimulated Raman scattering and CW and tunable second harmonic generation. Opt. Mater. **7(3)**, 59–73 (1997).

[5] A. Fouskova: The specific heat of $Gd_2(MoO_4)_3$. J. Phys. Soc. Japan **27(6)**, 1699 (1969).

[6] A.A. Kaminskii, K. Ueda, S.N. Bagaev, A.A. Pavlyuk, J. Song, H. Nishioka, N. Uehara, M. Musha: Orthorhombic dadolinium molybdate—a new nonlinear crystal for frequency doubling of one-micron CW laser emission. Kvant. Elektron. **23(5)**, 389–390 (1996) [In Russian, English trans.: Quantum Electron. **26(5)**, 379–380 (1996)].

[7] A.A. Kaminskii, H.-J. Eichler, S.N. Bagaev, D. Grebe, R. Macdonald, A.V. Butashin, A.A. Pavlyuk, F.A. Kuznetsov: Orthorhombic $Gd_2(MoO_4)_3$ crystal as a new nonlinear laser material for efficient second-harmonic generation. Kvant. Elektron. **23(2)**, 99–100 (1996) [In Russian, English trans.: Quantum Electron. **26(2)**, 95–96 (1996)].

[8] R. Bonneville, F. Auzel: Linear and nonlinear susceptibilities of rare earth ferroic molybdates. J. Appl. Phys. **67(10)**, 4597–4602 (1977).

[9] S. Singh: Nonlinear optical materials. In: *Handbook of Lasers with Selected Data on Optical Technology*, ed. by R.J. Pressley (Chemical Rubber Co., Cleveland, 1971), pp. 489–525.
[10] V.G. Dmitriev, D.N. Nikogosyan: Effective nonlinearity coefficients for three-wave interactions in biaxial crystals of $mm2$ point group symmetry. Opt. Commun. **95(1–3)**, 173–182 (1993).
[11] I. Shoji, T. Kondo, A. Kitamoto, M. Shirane, R. Ito: Absolute scale of second-order nonlinear-optical coefficients. J. Opt. Soc. Am. B **14(9)**, 2268–2294 (1997).
[12] H. Nishioka, W. Odajima, T. Tateno, K. Ueda, A.A. Kaminskii, A.V. Butashin, S.N. Bagaev, A.A. Pavlyuk: Femtosecond continuously tunable second harmonic generation over entire-visible range in orthorhombic acentric $Gd_2(MoO_4)_3$ crystals. Appl. Phys. Lett. **70(11)**, 1366–1368 (1997).
[13] S.I. Kim, J. Kim, S.C. Kim, S.I. Yun, T.Y. Kwon: Second harmonic generation in the $Gd_2(MoO_4)_3$ crystal grown by the Czochralski method. Mat. Lett. **25(5–6)**, 195–198 (1995).
[14] R.C. Miller, W.A. Nordland, K. Nassau: Nonlinear optical properties of $Gd_2(MoO_4)_3$ and $Tb_2(MoO_4)_3$. Ferroelectrics **2(2)**, 97–99 (1971).

7.8 Yb:$YAl_3(BO_3)_4$, Ytterbium-Doped Yttrium Aluminum Tetraborate ($Yb_xY_{1-x}Al_3(BO_3)_4$ or Yb:YAB)

Negative uniaxial crystal: $n_o > n_e$

Correlation between the atomic concentration of Yb relative to Y and Yb^{3+} volume concentration

[Yb] [at.%]	$[Yb^{3+}] \times 10^{-20}$ [cm^3]
4.0	2.21
4.6	2.54
5.5	3.04
10	5.53
20	11.06

Specific gravity: 3.70 g/cm^3 (without Yb doping) [1]; 3.72 g/cm^3 (without Yb doping) [2]; 3.844 g/cm^3 (with 8 at.% Yb doping) [3]; 4.574 g/cm^3 (100 at.% Yb) [4]
Point group: 32

Lattice constants of $Yb_xY_{1-x}Al_3(BO_3)_4$ versus atomic concentration of Yb ions

[Yb] [at.%]	a [Å]	c [Å]	Ref.
0	9.287	7.256	[1]
	9.295 ± 0.003	7.243 ± 0.002	[5]
5.6	9.277	7.224	[6]
8	9.931 (?)	7.240 (?)	[3]
100	9.2512	7.1893	[4]

Mohs hardness: 7.5 (without Nd doping) [1]
Melting point (incongruent melting): 1563 K [4]

Mean value of linear thermal expansion coefficient [7]

T [K]	$\alpha_t \times 10^6$ [K^{-1}], $\parallel c$	$\alpha_t \times 10^6$ [K^{-1}], $\perp c$	[Yb] [at.%]
298–573	8.1	1.4	1 at.% Yb
	8.5	1.2	10 at.% Yb
	9.7	2.0	25 at.% Yb

Specific heat capacity c_p at $P = 0.101325$ MPa [7]

T [K]	c_p [J/kgK]	[Yb] [at.%]
298	760	1 at.% Yb
	700	10 at.% Yb
	680	25 at.% Yb
373	910	1 at.% Yb
	870	10 at.% Yb
	750	25 at.% Yb
473	1150	1 at.% Yb
	1050	10 at.% Yb
	1280	25 at.% Yb
560	1220	1 at.% Yb
	1080	10 at.% Yb
	1390	25 at.% Yb

Thermal conductivity coefficient [8]

T [K]	κ [W/mK]	Note
300	4.7	5.6 at.% Yb

UV transmission cutoff wavelength of Yb:YAB is at 0.252 μm [3].
Main absorption bands of Yb^{3+} in YAB are at 0.938 μm, 0.975 μm and 0.981 μm [4].

Linear absorption coefficient α

λ [μm]	α [cm^{-1}]	Ref.	Note
0.937	2.3	[6]	5.6 at.% Yb, $\mathbf{E}\perp c$
0.975	10.4	[6]	5.6 at.% Yb, $\mathbf{E}\perp c$
	6	[6]	5.6 at.% Yb, $\mathbf{E}\parallel c$
0.976	17.05	[3]	8 at.% Yb
	15	[9]	10 at.% Yb, $\mathbf{E}\perp c$
	12	[9]	10 at.% Yb, $\mathbf{E}\parallel c$
0.98	118	[4]	100 at.% Yb
0.981	8	[6]	5.6 at.% Yb, $\mathbf{E}\perp c$
0.998	1.18	[6]	5.5 at.% Yb
1.040	0.12	[6]	5.5 at.% Yb

λ [μm]	α [cm^{-1}]	Ref.	Note
1.040	0.28	[9]	10 at.% Yb
1.061	<0.07	[9]	10 at.% Yb

Experimental values of refractive indices for 8 at.% Yb [3]

λ [μm]	n_o	n_e
0.40467	1.80158	1.72928
0.43584	1.78507	1.71848
0.48613	1.78017	1.70996
0.54607	1.77699	1.70478
0.58960	1.77462	1.70188
0.65628	1.77179	1.69862
0.70625	1.76912	1.69705

Dispersion relations for 8 at.% Yb (λ in μm) [3]:

$$n_o^2 = 3.1762 + \frac{0.0013}{\lambda^2 - 0.1480} - 0.0971\,\lambda^2$$

$$n_e^2 = 2.8632 + \frac{0.0090}{\lambda^2 - 0.0937} - 0.0083\,\lambda^2$$

Other dispersion relations are given in [10].
Expression for the effective second-order nonlinear coefficient (Kleinman symmetry conditions are valid, $d_{11} = -d_{12} = -d_{26}$) [11]:

$d_{ooe} = d_{11} \cos\theta \cos 3\phi$

$d_{eoe} = d_{oee} = d_{11} \cos^2\theta \sin 3\phi$

Value of second-order nonlinear coefficient:

$d_{11}(1.04\,\mu\text{m}) = 1.42\,\text{pm/V}$ [12]

Experimental values of phase-matching angle

Interacting wavelengths [μm]	θ_{exp} [deg]	Ref.	Note
SHG, $o + o \Rightarrow e$			
$1.0 \Rightarrow 0.5$	≈31	[9]	10 at.% Yb
$1.04 \Rightarrow 0.52$	32.8	[6]	
	34.6	[10]	
$1.064 \Rightarrow 0.532$	31	[3]	8 at.% Yb
SHG, $e + o \Rightarrow e$			
$1.04 \Rightarrow 0.52$	52.4	[6]	

Experimental values of internal angular and temperature bandwidths [13]

Interacting wavelengths [μm]	$\Delta\theta^{int}$ [deg]	ΔT [°C]	Note
SHG, $o + o \Rightarrow e$			
$1.064 \Rightarrow 0.532$	0.077	28	10 at.% Yb

Fluorescence lifetime of $^2F_{5/2}$ level

λ [μm]	τ [μs]	Ref.
1.03	1400	[10]
1.04	600	[12]
	680	[6]

Laser transition wavelength with corresponding emission cross-section value [6]

Transition	λ [μm]	σ [cm^2]	Note
$^2F_{5/2} \Rightarrow {}^2F_{7/2}$	1.04	0.8×10^{20}	5.6 at.% Nd

About the crystal

Yb:YAB is one of most successful SFD crystals. The radius of Yb^{3+} ions (0.870 Å) is very close to that of Y^{3+} ions (0.893 Å), and therefore it is easy to incorporate the ytterbium ions into the YAB matrix. There is no concentration quenching, no excited-state absorption, and no absorption on doubled wavelength. In addition, YbYAB crystals offer high quantum efficiency, low quantum defects, reduced thermal effects, and a potentially broad gain bandwidth. The wide pump band in Yb:YAB crystals is well matched to high-power InGaAs diodes. This together with a high second-order nonlinearity results in broad-band tuning of self-frequency-doubled radiation.

Recently, the Australian–Chinese group generated 1.1 W of CW green output ($\lambda = 530.5$ nm) via SFD in a type I Yb:YAB crystal (0.3-cm-long, 8–10 at.% Yb, $\theta = 31°$) with 11 W InGaAs diode-pumping at 976 nm [3], [14]. This is the highest green power reported for any diode-pumped SFD laser to date. The same group reported the tuning of self-frequency-doubled radiation between 517 and 540 nm at a 50-mW level [13].

References

[1] A.A. Filimonov, N.I. Leonyuk, L.B. Meissner, T.I. Timchenko, I.S. Rez: Nonlinear optical properties of isomorphic family of crystals with yttrium-aluminium borate (YAB) structure. Kristall und Technik **9(1)**, 63–66 (1974).

[2] N.I. Leonyuk, L.I. Leonyuk: Growth and characterization of $RM_3(BO_3)_4$ crystals. Progr. Cryst. Growth Character. Mater. **31(3–4)**, 179–278 (1995).

[3] H. Jiang, J. Li, J. Wang, X.-B. Hu, H. Liu, B. Teng, C.-Q. Zhang, P. Dekker, P. Wang: Growth of Yb:$YAl_3(BO_3)_4$ crystals and their optical and self-frequency-doubling properties. J. Cryst. Growth **233(1–2)**, 248–252 (2001).

[4] Y. Xu, X. Gong, Y. Chen, M. Huang, Z. Luo, Y. Huang: Crystal growth and optical properties of $YbAl_3(BO_3)_4$: a promising stoichiometric laser crystal. J. Cryst. Growth **252(1–3)**, 241–245 (2003).

[5] N.I. Leonyuk, E.V. Koporulina, Y.Y. Wang, X.B. Hu, A.V. Mokhov: Neodymium and chromium segregation at high-temperature crystallization of $(Nd,Y)Al_3(BO_3)_4$ and $(Nd,Y)Ca_4O(BO_3)_3$ doped with Cr^{3+}. J. Cryst. Growth **252(1–3)**, 174–179 (2003).

[6] P. Wang, J.M. Dawes, P. Dekker, D.S. Knowles, J.A. Piper, B. Lu: Growth and evaluation of ytterbium-doped yttrium aluminum borate as a potential self-doubling laser crystal. J. Opt. Soc. Am. B **16(1)**, 63–69 (1999).
[7] J. Li, J. Wang, X. Cheng, X. Hu, P.A. Burns, J.M. Dawes: Thermal and laser properties of Yb:$YAl_3(BO_3)_4$ crystal. J. Cryst. Growth **250(3–4)**, 458–462 (2003).
[8] J.L. Blows, P. Dekker, P. Wang, J.M. Dawes, T. Omatsu: Thermal lensing measurements and thermal conductivity of Yb:YAB. Appl. Phys. B **76(3)**, 289–292 (2003).
[9] P. Wang, P. Dekker, J.M. Dawes, J.A. Piper, Y. Liu, J. Wang: Efficient continuous-wave self-frequency-doubling green diode-pumped Yb:$YAl_3(BO_3)_4$ lasers. Opt. Lett. **25(10)**, 731–733 (2000).
[10] L. Tian, J. Wang, J. Wei, H. Pan, Y. Liu: Growth and optical properties of Yb:YAB crystal. J. Synth. Cryst. **27(3)**, 225–228 (1998) [In Chinese].
[11] J.E. Midwinter, J. Warner: The effects of phase matching method and of uniaxial crystal symmetry on the polar distribution of second-order non-linear optical polarization. Brit. J. Appl. Phys. **16(11)**, 1135–1142 (1965).
[12] P. Dekker, J. Blows, P. Wang, J. Dawes, J. Piper, T. Omatsu, Y. Liu, J. Wang: Yb:$YAl_3(BO_3)_4$: an efficient green self-frequency-doubled laser source. In: *Advanced Solid-State Lasers*, *OSA Trends in Optics and Photonics Series, Vol. 50*, ed. by C. Marshall (OSA, Washington DC, 2001), pp. 476–483.
[13] P. Dekker, P.A. Burns, J.M. Dawes, J.A. Piper, J. Li, X. Hu, J. Wang: Widely tunable yellow-green lasers based on the self-frequency-doubling material Yb:YAB. J. Opt. Soc. Am. B **20(4)**, 706–712 (2003).
[14] P. Dekker, J.M. Dawes, J.A. Piper, Y. Liu, J. Wang: 1.1 W CW self-frequency-doubled diode-pumped Yb:$YAl_3(BO_3)_4$ laser. Opt. Commun. **195(56)**, 431–436 (2001).

7.9 Yb:$GdCa_4O(BO_3)_3$, Ytterbium-Doped Gadolinium Calcium Oxyborate (Yb_xGd_{1-x} COB or Yb:GdCOB)

Negative biaxial crystal

Correlation between the atomic concentration of Yb relative to Gd and Yb^{3+} volume concentration

[Yb] [at.%]	$[Yb^{3+}] \times 10^{-20}$ [cm^3]
4	1.8
5	2.2
7	3.1
15	6.6

Point group: *m*
Assignment of dielectric and crystallographic axes for Yb:GdCOB equals to that of GdCOB crystal [1], [2].
Mohs hardness: 6.5 [3]
Melting point: ≈1753 K [3]

Linear absorption coefficient α

λ [μm]	α [cm^{-1}]	Ref.	Note
0.902	2.7	[4]	15 at.% Yb, $\mathbf{E}\parallel Z$
	3	[5]	15 at.% Yb, $\mathbf{E}\parallel Z$
0.976	4	[6]	15 at.% Yb, $\mathbf{E}\parallel Z$
	5.5	[5]	

Absorption cross-section σ (in 10^{-20} cm^2)

λ [μm]	σ ($\mathbf{E}\parallel X$)	σ ($\mathbf{E}\parallel Y$)	σ ($\mathbf{E}\parallel Z$)	Ref.	Note
0.9015	0.31	0.19	0.41	[7]	7 at.% Yb
	0.38	0.16	0.37	[3]	7 at.% Yb
0.976			1.15	[8]	7 at.% Yb
			1.12	[4]	

The refractive indices of Yb:GdCOB are very near to those of GdCOB [3].
Expressions for effective second-order nonlinear coefficient in the principal planes of Yb:GdCOB crystal (approximation of small walk-off angle Kleinman symmetry conditions are valid: $d_{12} = d_{26}$, $d_{13} = d_{35}$, $d_{15} = d_{31}$, $d_{24} = d_{32}$) [9], [10]:

XY plane, $\theta = 90°$

$d_{\mathrm{ooe}} = d_{13} \sin\phi$

$d_{\mathrm{eoe}} = d_{\mathrm{oee}} = d_{31} \sin^2\phi + d_{32} \cos^2\phi$

YZ plane, $\phi = 90°$

$d_{\mathrm{eeo}} = d_{13} \sin^2\theta + d_{12} \cos^2\theta$

$d_{\mathrm{oeo}} = d_{\mathrm{eoo}} = d_{31} \sin\theta$

XZ plane, $\phi = 0°$, $V_z > \theta > 0°$

$d_{\mathrm{ooe}} = d_{12} \cos\theta - d_{32} \sin\theta$

XZ plane, $\phi = 0°$, $90° > \theta > V_z$

$d_{\mathrm{oeo}} = d_{\mathrm{eoo}} = d_{12} \cos\theta - d_{32} \sin\theta$

XZ plane, $\phi = 0°$, $180° - V_z > \theta > 90°$; or $\phi = 180°$, $90° > \theta > V_z$

$d_{\mathrm{oeo}} = d_{\mathrm{eoo}} = d_{12} \cos\theta + d_{32} \sin\theta$

XZ plane, $\phi = 0°$, $180° > \theta > 180° - V_z$; or $\phi = 180°$, $V_z > \theta > 0°$

$d_{\mathrm{ooe}} = d_{12} \cos\theta + d_{32} \sin\theta$

Experimental value of phase-matching angle [3]

Interacting wavelengths [μm]	ϕ_{pm} [deg]
XY plane, $\theta = 90°$	
SHG, $o + o \Rightarrow e$	
$1.043 \Rightarrow 0.5215$	$\approx$43

Experimental value of effective second-order nonlinear coefficient for some specific phase-matching directions (SHG, type I) in Yb:GdCOB crystal [11]

Phase-matching direction	d_{eff} [pm/V]
$\theta = 66.8°$, $\phi = 132.6°$	2.3

Fluorescence lifetime of $^2F_{5/2}$ level at room temperature

λ [μm]	τ [μs]	Ref.	Note
1.032	2300	[5]	15 at.% Yb
	2440	[6]	
	2500	[7]	7 at.% Yb
	2600	[3]	7 at.% Yb

Laser transition wavelength and corresponding emission cross-section values (in 10^{-20} cm^2)

Transition	λ [μm]	σ (**E**‖Z)	Ref.	Note
$^2F_{5/2} \Rightarrow {}^2F_{7/2}$	1.032	0.55	[3], [7]	7 at.% Yb
		0.36	[12]	

About the crystal

Yb:GdCOB was recently used for efficient CW IR generation around 1.04 μm [6], [13]. Using a 0.3-cm-long, 15 at.% Yb-doped crystal, pumped by a 976-nm fiber-coupled diode, an output power at 1043 nm of 3.2 W was produced at an absorbed pump power of 5.2 W. Furthermore, the generated IR light is continuously tunable between 1018 and 1086 nm, with more than 1 W of output power over a bandwidth of 30 nm. In [13], [14] the broad emission spectrum has been used to develop a diode-pumped Yb:GdCOB femtosecond laser ($\lambda = 1045$ nm, $\tau = 90$ fs, $P_{av} = 40$ mW, $\Delta f = 100$ MHz). Though the self-doubling effect in Yb:GdCOB crystal was already reported in early work [3], no quantitative measurements have been made up to date.

References

[1] Z. Wang, J. Liu, R. Song, X. Xu, X. Sun, H. Jiang, K. Fu, J. Wang, Y. Liu, J. Wei, Z. Shao: The second-harmonic-generation property of $GdCa_4O(BO_3)_3$ crystal with various phase-matching directions. Opt. Commun. **187(4–6)**, 401–405 (2001).

[2] Z. Shao, J. Lu, Z. Wang, J. Wang, M. Jiang: Anisotropic properties of Nd:ReCOB (Re = Y, Gd): a low symmetry self-frequency doubling crystal. Progr. Cryst. Growth Character. Mater. **40(1–4)**, 63–73 (2000).

[3] F. Mougel, K. Dardenne, G. Aka, A. Kahn-Harari, D. Vivien: Ytterbium-doped $Ca_4GdO(BO_3)_3$: an efficient infrared laser and self-frequency doubling crystal. J. Opt. Soc. Am. B **16(1)**, 164–172 (1999).

[4] F. Auge, F. Balembois, P. Georges, A. Brun, F. Mougel, G. Aka, A. Kahn-Harari, D. Vivien: High-efficiency CW diode-pumped lasing and tunability of Yb:GdCOB (Yb^{3+}:$Ca_4GdO(BO_3)_3$). In: *Advanced Solid-State Lasers, OSA Trends in Optics and Photonics Series, Vol. 26*, ed. by M.M. Fejer, H. Injeyan, U. Keller (OSA, Washington DC, 1999), pp. 298–302.

[5] F. Auge, F. Druon, F. Balembois, P. Georges, A. Brun, F. Mougel, G. Aka, D. Vivien: Theoretical and experimental investigations of a diode-pumped quasi-three-level laser: the Yb^{3+}-doped $Ca_4GdO(BO_3)_3$ (Yb:GdCOB) laser. IEEE. J. Quant. Electr. **36(5)**, 598–606 (2000).

[6] S. Chenais, F. Druon, F. Balembois, G. Lucas-Leclin, P. Georges, A. Brun, M. Zavelani-Rossi, F. Auge, J.P. Chambaret, G. Aka, D. Vivien: Multiwatt, tunable, diode-pumped CW Yb:GdCOB laser. Appl. Phys. B **72(4)**, 389–393 (2001).
[7] D. Martrou, F. Mougel, K. Dardenne, G. Aka, A. Kahn-Harari, D. Vivien, B. Viana: Laser performance of an ytterbium doped new single crystal: Yb^{3+}:$Ca_4GdO(BO_3)_3$ (Yb:GdCOB) under end pumped titanium sapphire. In: *Advanced Solid-State Lasers, OSA Trends in Optics and Photonics Series, Vol. 19*, ed. by W.R. Bosenberg, M.M. Fejer (OSA, Washington DC, 1998), pp. 454–458.
[8] F. Auge, F. Balembois, P. Georges, A. Brun, F. Mougel, G. Aka, A. Kahn-Harari, D. Vivien: Efficient and tunable continuous-wave diode-pumped Yb^{3+}:$Ca_4GdO(BO_3)_3$ laser. Appl. Opt. **38(6)**, 976–979 (1999).
[9] G. Aka, A. Kahn-Harari, F. Mougel, D. Vivien, F. Salin, P. Coquelin, P. Colin, D. Pelenc, J.P. Damelet: Linear and nonlinear-optical properties of a new gadolinium calcium oxoborate crystal, $Ca_4GdO(BO_3)_3$. J. Opt. Soc. Am. B **14(9)**, 2238–2247 (1997).
[10] Z.P. Wang, J.H. Liu, R.B. Song, H.D. Jiang, S.J. Zhang, K. Fu, C.Q. Wang, J.Y. Wang, Y.G. Liu, J.Q. Wei, H.C. Chen, Z.S. Shao: Anisotropy of nonlinear-optical property of RCOB (R = Gd, Y) crystal. Chin. Phys. Lett. **18(3)**, 385–387 (2001).
[11] S. Zhang, Z. Cheng, S. Zhang, J. Liu, J. Han, J. Wang, H. Chen: Growth and second-harmonic generation properties of Tm^{3+}-, Yb^{3+}-, Bi^{3+}-, and Li^{+}-doped $GdCa_4O(BO_3)_3$ crystals. Chin. Phys. Lett. **18(3)**, 388–389 (2001).
[12] A. Aron, G. Aka, B. Viana, A. Kahn-Harari, D. Vivien, F. Druon, F. Balembois, P. Georges, A. Brun, N. Lenain, M. Jacquet: Spectroscopic properties and laser performances of Yb:YCOB and potential of the Yb:LaCOB material. Opt. Mater. **16(1–2)**, 181–188 (2001).
[13] F. Druon, S. Chenais, F. Balembois, P. Georges, A. Brun, A. Courjaud, C. Hönninger, F. Salin, M. Zavelani-Rossi, F. Auge, J.P. Chambaret, A. Aron, F. Mougel, G. Aka, D. Vivien: High-power diode-pumped Yb:GdCOB laser: from continuous-wave to femtosecond regime. Opt. Mater. **19(1)**, 73–80 (2002).
[14] F. Druon, F. Balembois, P. Georges, A. Brun, A. Courjaud, C. Hönninger, F. Salin, A. Aron, F. Mougel, G. Aka, D. Vivien: Generation of 90-fs pulses from a mode-locked diode-pumped Yb^{3+}:$Ca_4GdO(BO_3)_3$ laser. Opt. Lett. **25(6)**, 423–425 (2000).

7.10 Yb:$YCa_4O(BO_3)_3$, Ytterbium-Doped Yttrium Calcium Oxyborate (Yb_xY_{1-x}COB or Yb:YCOB)

Negative biaxial crystal

Correlation between the atomic concentration of Nd relative to Y and Nd^{3+} volume concentration

[Yb] [at.%]	$[Yb^{3+}] \times 10^{-20}$ [cm^3]
4	1.8
5	2.3
7	3.2
10	4.5
20	9.0

Specific gravity: 3.39 g/cm^3 for 10 at.% Yb [1]
Point group: m
Assignment of dielectric and crystallographic axes for Yb:YCOB equals to that of YCOB crystal [2].

Absorption cross-section σ (in 10^{-20} cm^2)

λ [μm]	σ ($\mathbf{E}\|X$)	σ ($\mathbf{E}\|Y$)	σ ($\mathbf{E}\|Z$)	Ref.	Note
0.900			0.4	[1]	10 at.% Yb
	0.42	0.30	0.53	[3]	18.3 at.% Yb
	0.31	0.13	0.43	[4], [5]	20 at.% Yb
0.976			1.2	[1]	10 at.% Yb
	0.77	0.87	0.81	[4], [5]	20 at.% Yb

The refractive indices of Yb:YCOB are very near to those of YCOB.
Expressions for effective second-order nonlinear coefficient in the principal planes of Yb:YCOB crystal (approximation of small walk-off angle Kleinman symmetry conditions are valid: $d_{12} = d_{26}$, $d_{13} = d_{35}$, $d_{15} = d_{31}$, $d_{24} = d_{32}$) [6], [7]:

XY plane, $\theta = 90°$

$d_{\mathrm{ooe}} = d_{13} \sin\phi$

$d_{\mathrm{eoe}} = d_{\mathrm{oee}} = d_{31} \sin^2\phi + d_{32} \cos^2\phi$

YZ plane, $\phi = 90°$

$d_{\mathrm{eeo}} = d_{13} \sin^2\theta + d_{12} \cos^2\theta$

$d_{\mathrm{oeo}} = d_{\mathrm{eoo}} = d_{31} \sin\theta$

XZ plane, $\phi = 0°$, $V_z > \theta > 0°$

$d_{\mathrm{ooe}} = d_{12} \cos\theta - d_{32} \sin\theta$

XZ plane, $\phi = 0°$, $90° > \theta > V_z$

$d_{\mathrm{oeo}} = d_{\mathrm{eoo}} = d_{12} \cos\theta - d_{32} \sin\theta$

XZ plane, $\phi = 0°$, $180° - V_z > \theta > 90°$; or $\phi = 180°$, $90° > \theta > V_z$

$d_{\mathrm{oeo}} = d_{\mathrm{eoo}} = d_{12} \cos\theta + d_{32} \sin\theta$

XZ plane, $\phi = 0°$, $180° > \theta > 180° - V_z$; or $\phi = 180°$, $V_z > \theta > 0°$

$d_{\mathrm{ooe}} = d_{12} \cos\theta + d_{32} \sin\theta$

Experimental values of phase-matching angle in principal planes of Yb:YCOB crystal

Interacting wavelengths [μm]	ϕ_{pm} [deg]	θ_{pm} [deg]	Ref.
XY plane, $\theta = 90°$			
SHG, $o + o \Rightarrow e$			
1.090 $\Rightarrow$ 0.545	$\approx$36.2		[4]
1.064 $\Rightarrow$ 0.532	34		[8]
XZ plane, $\phi = 0°$			
SHG, $o + o \Rightarrow e$			
1.070 $\Rightarrow$ 0.535		$\approx$31.7	[9]

Fluorescence lifetime of $^2F_{5/2}$ level at room temperature

λ [μm]	τ [μs]	Ref.	Note
1.032	2100	[10]	2 at.% Yb
	2500	[1]	1 at.% Yb
	2700	[10]	5 at.% Yb
	2800	[10]	10 at.% Yb
	2850	[1]	10 at.% Yb
	3000	[4], [10]	20 at.% Yb
		[10]	25 at.% Yb
		[10]	45 at.% Yb

Laser transition wavelengths and corresponding emission cross-section values (in 10^{-20} cm^2)

Transition	λ [μm]	σ (**E**‖Z)	Ref.	Note
$^2F_{5/2} \Rightarrow {}^2F_{7/2}$	1.018	0.30	[1]	10 at.% Yb
	1.032	0.36	[3]	18.3 at.% Yb
		0.39	[9]	
	1.050	0.18	[9]	
	1.082	0.12	[1]	10 at.% Yb
	1.084	0.10	[9]	
	1.085	0.76 (?)	[3]	18.3 at.% Yb

Laser-induced bulk damage threshold [8]

λ [μm]	τ_p [ns]	I_{thr} [GW/cm^2]
1.064	10	>0.06

About the crystal

The CW infrared laser performance of Yb:YCOB at around 1085 nm was reported in [4]. An X-cut 1.3-cm-long, 20 at.% Yb-doped crystal was pumped by a CW Ti:sapphire laser tuned to 900 nm. Output radiation of 300 mW was achieved at 1.2 W of absorbed pump power. With CW diode pumping at $\lambda = 976$ nm of a Y-cut, 0.186-cm-long, 20 at.% Yb-doped crystal, 446 mW of IR laser output at 0.76 W absorbed pump power was reported in [3].

In the first self-frequency-doubling experiment with Yb:YCOB, less than 1 mW of 543-nm light was generated in a 20 at.% Yb-doped crystal ($\theta = 90°$, $\phi = 36.2°$) at 0.9 W absorbed pump power [4]. In later work [9], a 35 at.% Yb-doped crystal ($\theta = 31.7°$, $\phi = 0°$) was used, which produced a similar level of CW green output.

References

[1] V.A. Lebedev, I.V. Voroshilov, A.N. Gavrienko, B.V. Ignatiev: Kinetic and spectroscopic investigations of Yb:$YCa_4O(BO_3)_3$ (Yb:YCOB) single crystals. Opt. Mater. **14(2)**, 171–173 (2000).

[2] F. Mougel, G. Aka, F. Salin, D. Pelenc, B. Ferrand, A.Kahn-Harari, D.Vivien: Accurate second harmonic generation phase matching angles prediction and evaluation of nonlinear coefficients of $YCa_4O(BO_3)_3$ (YCOB) crystal. In: *Advanced Solid State Lasers, OSA Trends in Optics and Photonics Series, Vol. 26*, ed. by M.M. Fejer, H. Injeyan, U. Keller (OSA, Washington DC, 1999), pp. 709–714.

[3] P. Wang, J.M. Dawes, P. Dekker, H. Zhang, X. Meng: Spectral characterization and diode-pumped laser performance of Yb:YCOB. In: *Advanced Solid State Lasers, OSA Trends in Optics and Photonics Series, Vol. 26*, ed. by M.M. Fejer, H. Injeyan, U. Keller (OSA, Washington DC, 1999), pp. 631–634.

[4] D.A. Hammons, J.M. Eichenholz, Q. Ye, B.H.T. Chai, L. Shah, R.E. Peale, M. Richardson, H. Qiu: Laser action in Yb^{3+}:YCOB (Yb:$YCa_4O(BO_3)_3$). Opt. Commun. **156(4–6)**, 327–330 (1998).

[5] D.A. Hammons, L. Shah, J. Eichenholz, Q. Ye, M. Richardson, B.H.T. Chai, A. Chin, J. Cary: 980 nm diode pumped laser operation and wavelength tunability performance in Yb^{3+}:YCOB. In: Advanced Solid State Lasers, OSA Trends in Optics and Photonics Series, Vol. 26, ed. by M.M. Fejer, H. Injeyan, U. Keller (OSA, Washington DC, 1999), pp. 286–290.

[6] G. Aka, A. Kahn-Harari, F. Mougel, D. Vivien, F. Salin, P. Coquelin, P. Colin, D. Pelenc, J.P. Damelet: Linear and nonlinear-optical properties of a new gadolinium calcium oxoborate crystal, $Ca_4GdO(BO_3)_3$. J. Opt. Soc. Am. B **14(9)**, 2238–2247 (1997).

[7] Z.P. Wang, J.H. Liu, R.B. Song, H.D. Jiang, S.J. Zhang, K. Fu, C.Q. Wang, J.Y. Wang, Y.G. Liu, J.Q. Wei, H.C. Chen, Z.S. Shao: Anisotropy of nonlinear-optical property of RCOB (R = Gd, Y) crystal. Chin. Phys. Lett. **18(3)**, 385–387 (2001).

[8] W.K. Jang, Q. Ye, J. Eichenholz, M.C. Richardson, B.H.T. Chai: Second harmonic generation in Yb doped $YCa_4O(BO_3)_3$. Opt. Commun. **155(4–6)**, 332–334 (1998).

[9] A. Aron, G. Aka, B. Viana, A. Kahn-Harari, D. Vivien, F. Druon, F. Balembois, P. Georges, A. Brun, N. Lenain, M. Jacquet: Spectroscopic properties and laser performances of Yb:YCOB and potential of the Yb:LaCOB material. Opt. Mater. **16(1–2)**, 181–188 (2001).

[10] B.H.T. Chai, D.A. Hammons, J.M. Eichenholz, Q. Ye, W.K. Yang, L. Shah, G.M. Luntz, M. Richardson, H. Qiu: Lasing, second harmonic conversion and self-frequency doubling of Yb:YCOB (Yb:$YCa_4B_3O_{10}$). In: *Advanced Solid-State Lasers, OSA Trends in Optics and Photonics Series, Vol. 19*, ed. by W.R. Bosenberg, M.M. Fejer (OSA, Washington DC, 1998), pp. 59–61.

8

Rarely Used and Archive Crystals

This chapter comprises 18 relatively rarely used or old-fashioned crystals.

8.1 $KB_5O_8 \cdot 4H_2O$, Potassium Pentaborate Tetrahydrate (KB5)

Positive biaxial crystal: $2V_z = 126.3°$ at $\lambda = 0.5461\,\mu m$ [1]
Molecular mass: 293.210
Specific gravity: 1.74 g/cm^3 [2]
Point group: $mm2$
Lattice constants [2]:
$a = 11.065 \pm 0.002$ Å
$b = 11.171 \pm 0.001$ Å
$c = 9.054 \pm 0.006$ Å
Assignment of dielectric and crystallographic axes: $X, Y, Z \Rightarrow a, b, c$
Mohs hardness: 2.5 [2]

Vickers hardness (in kgf/mm^2) [3], [4]

Indenter load 5 g	Indenter load 10 g	Indenter load 25 g	Note
64.4	59.7	49.7	along a
82.5	74.2	68.8	along b
78.7	75.7	68.1	along c

Transparency range at "0" transmittance level: 0.162–1.5 μm [5]

Linear absorption coefficient α

λ [μm]	α [cm^{-1}]	Ref.	Note
0.2128	0.18	[6]	o-wave, XY plane, FiHG direction
	0.14	[7]	o-wave, XY plane, FiHG direction
0.2314	0.12	[1]	o-wave, XY plane, THG direction

λ [μm]	α [cm^{-1}]	Ref.	Note
0.2661	0.12	[6]	*e*-wave, *XY* plane, FiHG direction
	0.06	[7]	*e*-wave, *XY* plane, FiHG direction
0.3472	0.04	[1]	*e*-wave, *XY* plane, THG direction
0.3547	<0.01	[8]	along *Y*
0.5321	0.02	[7]	*XY* plane, FiHG direction
	<0.01	[8]	along *Y*
0.6943	0.03	[1]	*e*-wave, *XY* plane, THG direction
1.0642	0.06	[7]	*e*-wave, *XY* plane, FiHG direction

Two-photon absorption coefficient β (along *b* axis) [9]

λ [μm]	τ_p [ns]	$\beta \times 10^{11}$ [cm/W]
0.216	0.015	65 ± 10
0.270	0.015	35 ± 5

Experimental values of refractive indices

λ [μm]	n_X	n_Y	n_Z	Ref.
0.217			1.4969	[10]
0.220			1.4938	[10]
0.225			1.4891	[10]
0.230			1.4848	[10]
0.2345		1.4930		[11]
0.235			1.4809	[10]
0.240			1.4774	[10]
0.245			1.4740	[10]
0.250			1.4708	[10]
0.390	1.5021	1.4457	1.4327	[11]
0.400	1.5005	1.4453	1.4320	[11]
0.420	1.4984	1.4438	1.4303	[11]
0.450	1.4956	1.4414	1.4280	[11]
0.500	1.4917	1.4380	1.4251	[11]
0.546	1.4888	1.4357	1.4230	[11]
0.600	1.4859	1.4334	1.4211	[11]
0.650	1.4839	1.4319	1.4196	[11]
0.700	1.4823	1.4306	1.4182	[11]
0.730	1.4815	1.4297	1.4176	[11]
0.765	1.4813	1.4292	1.4171	[11]

Best set of Sellmeier equations (λ in μm, $T = 293$ K) [12]:

$$n_X^2 = 1.99191 + \frac{0.009253}{\lambda^2 - 0.009329}$$

$$n_Y^2 = 2.02998 + \frac{0.009464}{\lambda^2 - 0.009188}$$

$$n_Z^2 = 2.17908 + \frac{0.010354}{\lambda^2 - 0.008781}$$

Other sets of dispersion relations are given in [11], [13].
Expressions for the effective second-order nonlinear coefficient in principal planes of KB5 crystal (Kleinman symmetry conditions are not valid) [14]:

XY plane

$d_{eeo} = d_{31} \sin^2 \phi + d_{32} \cos^2 \phi$

YZ plane

$d_{ooe} = d_{31} \sin \theta$

XZ plane, $\theta < V_z$

$d_{oeo} = d_{eoo} = d_{24} \sin \theta$

XZ plane, $\theta > V_z$

$d_{ooe} = d_{32} \sin \theta$

Expressions for the effective second-order nonlinear coefficient in principal planes of KB5 crystal (Kleinman symmetry conditions are valid, $d_{15} = d_{31}$ and $d_{24} = d_{32}$) [14]:

XY plane

$d_{eeo} = d_{31} \sin^2 \phi + d_{32} \cos^2 \phi$

YZ plane

$d_{ooe} = d_{31} \sin \theta$

XZ plane, $\theta < V_z$

$d_{oeo} = d_{eoo} = d_{32} \sin \theta$

XZ plane, $\theta > V_z$

$d_{ooe} = d_{32} \sin \theta$

Expressions for the effective second-order nonlinear coefficient for three-wave interaction in an arbitrary direction inside KB5 crystal are given in [14].
Second-order nonlinear coefficients [15]:

$d_{31}(0.5321\ \mu m) = 0.04\ pm/V$

$d_{32}(0.5321\ \mu m) = 0.003\ pm/V$

$d_{33}(0.5321\ \mu m) = 0.05\ pm/V$

Experimental values of phase-matching angle ($T = 293$ K)

Interacting wavelengths [μm]	ϕ_{exp} [deg]	θ_{exp} [deg]	Ref.
XY plane, $\theta = 90°$			
SHG, $e + e \Rightarrow o$			
$0.434 \Rightarrow 0.217$	90		[10]
$0.4342 \Rightarrow 0.2171$	90		[16]
$0.4384 \Rightarrow 0.2192$	80.5		[17]
$0.4597 \Rightarrow 0.22985$	67.2		[18]
$0.4765 \Rightarrow 0.23825$	60.2		[18]

Interacting wavelengths [μm]	ϕ_{exp} [deg]	θ_{exp} [deg]	Ref.
0.488 ⇒ 0.244	56.6		[18]
0.5 ⇒ 0.25	52.8		[10]
0.5145 ⇒ 0.25725	50.2		[18]
0.63 ⇒ 0.315	31		[16]
0.6943 ⇒ 0.34715	26.5		[18]
SFG, $e + e \Rightarrow o$			
0.5398 + 0.35987 ⇒ 0.21592	50.4		[19]
0.5435 + 0.3511 ⇒ 0.2133	90		[20]
0.6943 + 0.3472 ⇒ 0.2314	57		[21]
0.5737 + 0.3345 ⇒ 0.2113	90		[20]
0.6522 + 0.3261 ⇒ 0.2174	68		[8]
0.6219 + 0.3110 ⇒ 0.2073	90		[8]
0.6943 + 0.30519 ⇒ 0.2120	70		[22]
0.6943 + 0.28409 ⇒ 0.2016	90		[22]
0.78971 + 0.26604 ⇒ 0.1990	75		[23]
0.75322 + 0.26604 ⇒ 0.1966	90		[23]
0.79737 + 0.25725 ⇒ 0.1945	84		[24]
0.79235 + 0.25725 ⇒ 0.1942	90		[24]
0.9 + 0.23287 ⇒ 0.185	90		[25]
1.06415 + 0.26604 ⇒ 0.2128	53		[7]
1.06415 + 0.21283 ⇒ 0.17736	80		[12]
1.0796 + 0.2699 ⇒ 0.21592	80		[19]
1.31417 + 0.19 ⇒ 0.166	90		[26], [27]
YZ plane, $\phi = 90°$			
SHG, $o + o \Rightarrow e$			
0.4346 ⇒ 0.2173		90	[21]
0.4690 ⇒ 0.2345		17	[21]
0.4796 ⇒ 0.2398		0	[16]
SFG, $o + o \Rightarrow e$			
0.5634 + 0.3511 ⇒ 0.2163		63	[20]
0.5948 + 0.3345 ⇒ 0.2141		63	[20]
0.6264 + 0.3132 ⇒ 0.2088		68	[8]
0.7621 + 0.26604 ⇒ 0.1972		68	[23]
1.06415 + 0.21283 ⇒ 0.17736		68.5	[12]

Experimental values of NCPM temperature

Interacting wavelengths [μm]	T [°C]	Ref.
along *b* axis		
SFG, type I		
0.6943 + 0.28334 ⇒ 0.20122	−15	[22]
0.6943 + 0.28361 ⇒ 0.20136	0	[22]
0.6943 + 0.28405 ⇒ 0.20158	20	[22]
0.6943 + 0.28449 ⇒ 0.20180	35	[22]

Interacting wavelengths [μm]	T [°C]	Ref.
$0.79202 + 0.25725 \Rightarrow 0.19418$	25	[24]
$0.79344 + 0.25725 \Rightarrow 0.19427$	40	[24]

Laser-induced surface-damage threshold

λ [μm]	τ_p [ns]	I_{thr} [GW/cm^2]	Ref.	Note
0.1774	12	0.000003	[12]	10 Hz, 50 hours
0.2661	8	>0.043	[7]	10 Hz
	0.03	>0.48	[28]	1 Hz
0.311	10	>0.013	[8]	10 Hz
0.3472	8	>0.09	[1]	
0.45	7	1	[21]	15 Hz
0.622	10	>0.04	[8]	10 Hz
0.6943	10	>0.08	[1]	
0.74–0.91	30	>0.05	[25]	
1.0642	12	>0.085	[7]	10 Hz

About the crystal

KB5 was very popular in the seventies for UV and deep-UV sum-frequency generation.

References

[1] K. Kato: Phase-matched generation of 2314 Å in $KB_5O_8 \cdot 4H_2O$. Appl. Phys. Lett. **29(9)**, 562–563 (1976).

[2] W.R. Cook, Jr., H. Jaffe: The crystallographic, elastic, and piezoelectric properties of ammonium pentaborate and potassium pentaborate. Acta Crystallogr. **10(11)**, 705–707 (1957).

[3] K. Thamizharasan, S. Xavier Jesu Raja, F.P. Xavier, P. Sagayaraj: Growth, thermal and microhardness studies of single crystals of potassium penta borate (KB5). J. Cryst. Growth **218(2–4)**, 323–326 (2000).

[4] S.A. Rajasekar, K. Thamizharasan, A. Joseph Arul Pragasam, J. Pakiam Julius, P. Sagayaraj: Growth and characterization of pure and doped potassium pentaborate (KB5) single crystals. J. Cryst. Growth **247(1–2)**, 199–206 (2003).

[5] J.A. Paisner, M.L. Spaeth, D.C. Gerstenberger, I.W. Ruderman: Generation of tunable radiation below 2000Å by phase-matched sum-frequency mixing in $KB_5O_8 \cdot 4H_2O$. Appl. Phys. Lett. **32(8)**, 476–478 (1978).

[6] K.B. Petrosyan, A.L. Pogosyan, K.M. Pokhsraryan: Generation of ultrashort light pulses in the UV region by up-conversion of radiation in potassium pentaborate. Izv. Akad. Nauk SSSR, Ser. Fiz. **47(8)**, 1619–1621 (1983) [In Russian, English trans.: Bull. Acad. Sci. USSR, Phys. Ser. **47(8)**, 155–157 (1983)].

[7] K. Kato: Phase matched generation of 2128 Å in $KB_5O_8 \cdot 4H_2O$. Opt. Commun. **19(3)**, 332–333 (1976).

[8] K. Kato: Efficient ultraviolet generation of 2073–2174 Å in $KB_5O_8 \cdot 4H_2O$. IEEE J. Quant. Electr. **QE-13(7)**, 544–546 (1977).

[9] G.G. Gurzadyan, R.K. Ispiryan: Two-photon absorption in potassium dihydrophosphate, potassium pentaborate and quartz crystals at 270 and 216 nm. Int. J. Nonl. Opt. Phys. **1(3)**, 533–540 (1992).

[10] H. Zacharias, A. Anders, J.B. Halpern, K.H. Welge: Frequency doubling and tuning with $KB_5O_8 \cdot 4H_2O$ and application to NO ($A^2\Sigma^+$) excitation. Opt. Commun. **19(1)**, 116–119 (1976).

[11] W.R. Cook, Jr., L.M. Hubby, Jr.: Indices of refraction of potassium pentaborate. J. Opt. Soc. Am. **66(1)**, 72–73 (1976).

[12] N. Umemura, K. Kato: Phase-matched UV generation at 0.1774 μm in $KB_5O_8 \cdot 4H_2O$. Appl. Opt. **35(27)**, 5332–5335 (1996).

[13] F.B. Dunning, R.E. Stickel, Jr.: Sum frequency mixing in potassium pentaborate as a source of tunable coherent radiation at wavelengths below 217 nm. Appl. Opt. **15(12)**, 3131–3134 (1976).

[14] V.G. Dmitriev, D.N. Nikogosyan: Effective nonlinearity coefficients for three-wave interactions in biaxial crystals of $mm2$ point group symmetry. Opt. Commun. **95(1–3)**, 173–182 (1993).

[15] D.A. Roberts: Simplified characterization of uniaxial and biaxial nonlinear optical crystals: a plea for standardization of nomenclature and conventions. IEEE J. Quant. Electr. **28(10)**, 2057–2074 (1992).

[16] H.J. Dewey: Second-harmonic generation in $KB_5O_8 \cdot 4H_2O$ from 217.1 to 315.0 nm. IEEE J. Quant. Electr. **QE-12(5)**, 303–306 (1976).

[17] E. Fill, J. Wildenauer: Generation of the fifth and sixth harmonics of iodine laser pulses. Opt. Commun. **47(6)**, 412–413 (1983).

[18] T.S. Chen, W.P. White: Second-harmonic generation in $KB_5O_8 \cdot 4H_2O$. IEEE J. Quant. Electr. **QE-12(7)**, 436–437 (1976).

[19] A.G. Arutyunyan, G.G. Gurzadyan, R.K. Ispiryan: Generation of the fifth harmonic of picosecond yttrium aluminate laser radiation. Kvant. Elektron. **16(12)**, 2493–2495 (1989) [In Russian, English trans.: Sov. J. Quantum Electron. **19(12)**, 1602–1603 (1989)].

[20] R.E. Stickel, Jr., S. Blit, G.F. Hildebrandt, E.D. Dahl, F.B. Dunning, F.K. Tittel: Generation of coherent UV radiation tunable from 211 nm to 216 nm. Appl. Opt. **17(15)**, 2270 (1978).

[21] C.F. Dewey, Jr., W.R. Cook, Jr., R.T. Hodgson, J.J. Wynne: Frequency doubling in $KB_5O_8 \cdot 4H_2O$ and $NH_4B_5O_8 \cdot 4H_2O$ to 217.3 nm. Appl. Phys. Lett. **26(12)**, 714–716 (1975).

[22] R.E. Stickel, Jr., F.B. Dunning: Generation of coherent radiation tunable from 201 nm to 212 nm. Appl. Opt. **16(9)**, 2356–2358 (1977).

[23] K. Kato: Tunable UV generation in $KB_5O_8 \cdot 4H_2O$ to 1966 Å. Appl. Phys. Lett. **30(11)**, 583–584 (1977).

[24] H. Hemmati, J.C. Bergquist, W.M. Itano: Generation of continuous-wave 194 nm radiation by sum-frequency mixing in an external ring cavity. Opt. Lett. **8(2)**, 73–75 (1983).

[25] R.E. Stickel, Jr., F.B. Dunning: Generation of tunable coherent vacuum UV radiation in KB5. Appl. Opt. **17(7)**, 981–982 (1978).

[26] V. Petrov, F. Rotermund, F. Noack: Generation of femtosecond pulses down to 166 nm by sum-frequency mixing in $KB_5O_8 \cdot 4H_2O$. Electron. Lett. **34(18)**, 1748–1750 (1998).

[27] V. Petrov, F. Rotermund, F. Noack, J. Ringling, O. Kittelmann, R. Komatsu: Frequency conversion of Ti:sapphire-based femtosecond laser systems to the 200-nm spectral region using nonlinear optical crystals. IEEE J. Sel. Topics Quant. Electr. **5(6)** 1532–1542 (1999).

[28] A.G. Arutyunyan, V.G. Atanesyan, K.B. Petrosyan, K.M. Pokhsraryan: Frequency multiplication of ultrashort light pulses in potassium pentaborate. Pisma Zh. Tekh. Fiz. **6(5–6)**, 277–280 (1980) [In Russian, English trans.: Sov. Tech. Phys. Lett. **6(3)**, 120–121 (1980)].

8.2 CsB_3O_5, Cesium Triborate (CBO)

Positive biaxial crystal: $2V_z = 79.0°$ at $\lambda = 0.5321\,\mu m$ [1]
Molecular mass: 245.335
Specific gravity (calculated): 3.357 g/cm^3 [2]
Point group: 222
Lattice constants:
$a = 6.213 \pm 0.001$ Å [2]
$b = 8.521 \pm 0.001$ Å [2]
$c = 9.170 \pm 0.002$ Å [2]
Assignment of dielectric and crystallographic axes: $X, Y, Z \Rightarrow c, a, b$
Transparency range at "0" transmittance level: 0.17–3.0 μm [3]

Experimental values of refractive indices [3]

λ [μm]	n_X	n_Y	n_Z
0.3547	1.5499	1.5849	1.6145
0.4765	1.5370	1.5758	1.6031
0.4880	1.5367	1.5736	1.6009
0.4965	1.5362	1.5716	1.5996
0.5145	1.5349	1.5690	1.5974
0.5321	1.5328	1.5662	1.5936
0.6328	1.5294	1.5588	1.5864
1.0642	1.5194	1.5505	1.5781

Sellmeier equations (λ in μm, $T = 293$ K) [1]:

$$n_X^2 = 2.3035 + \frac{0.01378}{\lambda^2 - 0.01498} - 0.00612\,\lambda^2$$

$$n_Y^2 = 2.3704 + \frac{0.01528}{\lambda^2 - 0.01581} - 0.00939\,\lambda^2$$

$$n_Z^2 = 2.4753 + \frac{0.01806}{\lambda^2 - 0.01752} - 0.01654\,\lambda^2$$

Other set of dispersion relations is given in [3].
Expressions for the effective second-order nonlinear coefficient in the principal planes of CBO crystal (Kleinman symmetry conditions are valid, $d_{14} = d_{25} = d_{36}$) [4]:

XY plane

$$d_{eoe} = d_{oee} = d_{14} \sin 2\phi$$

YZ plane
$d_{eeo} = d_{14} \sin 2\theta$
XZ plane, $\theta < V_z$
$d_{eoe} = d_{oee} = -d_{14} \sin 2\theta$
XZ plane, $\theta > V_z$
$d_{eeo} = -d_{14} \sin 2\theta$
Values of second-order nonlinear coefficient:
$d_{14}(1.0642\,\mu\text{m}) = 0.468 \times d_{22}(\text{BBO}) = 1.08\,\text{pm/V}$ [3], [5]
$d_{14}(1.0642\,\mu\text{m}) = 0.468 \times d_{22}(\text{BBO}) = 1.03\,\text{pm/V}$ [3], [6]
$d_{14}(1.0642\,\mu\text{m}) = (0.53 \pm 0.05) \times d_{22}(\text{BBO}) = (1.17 \pm 0.11)\,\text{pm/V}$ [1], [6]

Experimental values of phase-matching angle and temperature phase-matching bandwidth in the principal planes of CBO crystal ($T = 293$ K) [1]

Interacting wavelengths [μm]	ϕ_{exp} [deg]	θ_{exp} [deg]	ΔT [°C]
XY plane, $\theta = 90°$			
SHG, $e + o \Rightarrow e$			
$1.0642 \Rightarrow 0.5321$	12.9		18.7
SFG, $e + o \Rightarrow e$			
$1.0642 + 0.5321 \Rightarrow 0.35473$	40.3		5.7
YZ plane, $\phi = 90°$			
SFG, $e + e \Rightarrow o$			
$1.0642 + 0.5321 \Rightarrow 0.35473$		25.5	
$1.0642 + 0.35473 \Rightarrow 0.26605$		52.3	4.0
XZ plane, $\phi = 0°, \theta > V_z$			
SHG, $e + e \Rightarrow o$			
$1.0642 \Rightarrow 0.5321$		58.2	10.8
SFG, $e + e \Rightarrow o$			
$1.0642 + 0.5321 \Rightarrow 0.35473$		77.9	7.8

Experimental value of internal angular bandwidth [3]

Interacting wavelengths [μm]	θ_{pm} [deg]	$\Delta\theta^{int}$ [deg]
XZ plane, $\phi = 0°, \theta > V_z$		
SHG, $e + e \Rightarrow o$		
$1.0642 \Rightarrow 0.5321$	60.2	0.064

Laser-induced damage threshold

λ [μm]	τ_p [ns]	I_{thr} [GW/cm^2]	Ref.
1.053	1	26	[3]
1.0642	0.035	>10	[7]

About the crystal

The nonlinear optical properties of CBO was investigated by Chen and co-workers in 1993 [3]. However, this crystal did not attract much interest and was soon forgotten.

References

[1] K. Kato: Tunable UV generation to 0.185 μm in CsB_3O_5. IEEE J. Quant. Electr. **31(1)**, 169–171 (1995).

[2] J. Krogh-Moe: Refinement of the crystal structure of caesium triborate, $Cs_2O{\cdot}3B_2O_5$. Acta Crystallogr. B **30(5)**, 1178–1180 (1974).

[3] Y. Wu, T. Sasaki, S. Nakai, A. Yokotani, H. Tang, C. Chen: CsB_3O_5: a new nonlinear crystal. Appl. Phys. Lett. **62(21)**, 2614–2615 (1993).

[4] B.V. Bokut: Optical mixing in biaxial crystals. Zh. Prikl. Spektrosk. **7(4)**, 621–624 (1967) [In Russian, English trans.: J. Appl. Spectrosc. **7(4)**, 425–429 (1967)].

[5] D.A. Roberts: Simplified characterization of uniaxial and biaxial nonlinear optical crystals: a plea for standardization of nomenclature and conventions. IEEE J. Quant. Electr. **28(10)**, 2057–2074 (1992).

[6] I. Shoji, H. Nakamura, K. Ohdaira, T. Kondo, R. Ito, T. Okamoto, K. Tatsuki, S. Kubota: Absolute measurements of second-order nonlinear-optical coefficients of β-BaB_2O_4 for visible to ultraviolet second-harmonic wavelengths. J. Opt. Soc. Am. B **16(4)**, 620–624 (1999).

[7] Y. Wu, P. Fu, J. Wang, Z. Xu, L. Zhang, Y. Kong, C. Chen: Characterization of CsB_3O_5 crystal for ultraviolet generation. Opt. Lett. **22(24)**, 1840–1842 (1997).

8.3 $C_4H_7D_{12}N_4PO_7$, Deuterated *L*-Arginine Phosphate Monohydrate (DLAP)

Chemical formula [1]

Negative biaxial crystal: $2V_z = 142.6°$ at $\lambda = 0.5321\,\mu m$ [2]

Molecular mass: 302.286

Specific gravity: 1.591 g/cm^3 [3]

Point group: 2

Lattice constants for *L*-arginine phosphate monohydrate (LAP) [4]:

$a = 10.85 \pm 0.02$ Å

$b = 7.91 \pm 0.01$ Å

$c = 7.32 \pm 0.02$ Å

$\beta = 98.0° \pm 0.1°$

Lattice constants for deuterated *L*-arginine phosphate monohydrate (DLAP):

$a = 10.75$ Å [5]; 10.87 Å [6]

$b = 7.91$ Å [5]; 7.92 Å [6]

$c = 7.32$ Å [5]; 7.38 Å [6]

Assignment of dielectric and crystallographic axes (for LAP):

$Y \| b$, the axes a and c lie in XZ plane, the angle between them is $\beta = 98°$, the angle between the axes Z and c is $\alpha = 35°$ [2].

Mohs hardness: 3

Chemical decomposition temperature: 403 K [2]; 380–410 K [5]

Mean values of linear thermal expansion coefficient α_t (in 10^{-6} K^{-1}) [3]

T [K]	α_{11} ($\|a$)	α_{22} ($\|b$)	α_{33} ($\|c$)	$\alpha_{13} = \alpha_{31}$
298–373	57.4 ± 0.8	8.7 ± 0.5	18.3 ± 0.6	5.0 ± 0.8

Transparency range at "0" transmittance level: 0.22–1.30 μm [2]

Linear absorption coefficient α

λ [μm]	α [cm^{-1}]	Ref.	Note
0.266	0.074	[2]	along X
	0.131	[2]	along Y
	0.184	[2]	along Z
0.3547	0.025	[2]	along X
	0.053	[2]	along Y
	0.039	[2]	along Z
0.5265	0.01	[7]	
0.5321	0.01	[1]	
	<0.01	[2]	
0.910	0.028	[2]	along X
	0.037	[2]	along Y
	0.044	[2]	along Z
1.040	0.012	[2]	along X
	0.014	[2]	along Y
	0.009	[2]	along Z
1.053	0.02	[7]	
1.064	0.02	[1]	
	0.012	[2]	along X
	0.014	[2]	along Y
	0.009	[2]	along Z
1.180	0.385	[2]	along X
	0.394	[2]	along Y
	0.557	[2]	along Z

Temperature derivatives of refraction indices [8]

λ [μm]	$dn_X/dT \times 10^5$ [K^{-1}]	$dn_Y/dT \times 10^5$ [K^{-1}]	$dn_Z/dT \times 10^5$ [K^{-1}]
0.5321	-3.64 ± 0.17	-5.34 ± 0.17	-6.69 ± 0.17
1.0642	-3.73 ± 0.17	-5.30 ± 0.17	-6.30 ± 0.17

Sellmeier equations (λ in μm, $T = 298$ K) [2]:

$$n_X^2 = 2.2352 + \frac{0.0118}{\lambda^2 - 0.0146} - 0.00683\,\lambda^2$$

$$n_Y^2 = 2.4313 + \frac{0.0151}{\lambda^2 - 0.0214} - 0.0143\,\lambda^2$$

$$n_Z^2 = 2.4484 + \frac{0.0172}{\lambda^2 - 0.0229} - 0.0115\,\lambda^2$$

Expressions for effective second-order nonlinear coefficient in the principal planes of DLAP crystal (approximation of small walk-off angle, Kleinman symmetry conditions are valid, $d_{14} = d_{25} = d_{36}$, $d_{16} = d_{21}$ and $d_{23} = d_{34}$) [2], [9]:

XY plane

$d_{\mathrm{ooe}} = d_{23}\cos\phi$

$d_{\mathrm{eoe}} = d_{\mathrm{oee}} = d_{14}\sin 2\phi$

YZ plane

$d_{\mathrm{eeo}} = d_{14}\sin 2\theta$

$d_{\mathrm{oeo}} = d_{\mathrm{eoo}} = d_{16}\cos\theta$

XZ plane, $\phi = 0°$, $V_z > \theta > 0°$

$d_{\mathrm{eoe}} = d_{\mathrm{oee}} = d_{16}\cos^2\theta + d_{23}\sin^2\theta - d_{14}\sin 2\theta$

XZ plane, $\phi = 0°$, $90° > \theta > V_z$

$d_{\mathrm{eeo}} = d_{16}\cos^2\theta + d_{23}\sin^2\theta - d_{14}\sin 2\theta$

XZ plane, $\phi = 0°$, $180° - V_z > \theta > 90°$; or $\phi = 180°$, $90° > \theta > V_z$

$d_{\mathrm{eeo}} = d_{16}\cos^2\theta + d_{23}\sin^2\theta + d_{14}\sin 2\theta$

XZ plane, $\phi = 0°$, $180° > \theta > 180° - V_z$; or $\phi = 180°$, $V_z > \theta > 0°$

$d_{\mathrm{eoe}} = d_{\mathrm{oee}} = d_{16}\cos^2\theta + d_{23}\sin^2\theta + d_{14}\sin 2\theta$

Second-order nonlinear coefficients [2], [10]:

$d_{14}(1.0642\,\mu\mathrm{m}) = -0.59\,\mathrm{pm/V}$

$d_{16}(1.0642\,\mu\mathrm{m}) = 0.40\,\mathrm{pm/V}$

$d_{22}(1.0642\,\mu\mathrm{m}) = 0.37\,\mathrm{pm/V}$

$d_{23}(1.0642\,\mu\mathrm{m}) = 0.83\,\mathrm{pm/V}$

Experimental values of phase-matching angle at $T = 297\,\mathrm{K}$ [8]

Interacting wavelengths [μm]	ϕ_{exp} [deg]	θ_{exp} [deg]
XY plane, $\theta = 90°$		
SHG, $o + o \Rightarrow e$		
$1.0642 \Rightarrow 0.5321$	22.2	
SHG, $e + o \Rightarrow e$		
$1.0642 \Rightarrow 0.5321$	37.5	
XZ plane, $\phi = 0°$, $\theta < V_z$		
SHG, $e + o \Rightarrow e$		
$1.0642 \Rightarrow 0.5321$		42.8

Experimental values of internal angular, temperature and spectral bandwidths [11]

Interacting wavelengths [μm]	ϕ_{pm} [deg]	$\Delta\phi^{int}$ [deg]	ΔT [°C]	$\Delta\nu$ [cm^{-1}]
XY plane, $\theta = 90°$				
SHG, $o + o \Rightarrow e$				
1.0642 ⇒ 0.5321	22.2	0.036	5.4	20.2
SHG, $e + o \Rightarrow e$				
1.0642 ⇒ 0.5321	37.5	0.072	14.6	20.1

Laser-induced damage threshold

λ [μm]	τ_p [ns]	I_{thr} [GW/cm^2]	Ref.
0.308	17	0.03	[12]
0.5265	20	38	[7]
	0.6	67	[7]
1.053	25	33	[7]
	1	87	[7]
1.0642	14	>1.4	[1]
	1	9–13	[2]

About the crystal

DLAP was one of the first thoroughly investigated nonlinear optical crystals belonging to the low-symmetry point group *2*.

References

[1] M. Yoshimura, Y. Mori, T. Sasaki, H. Yoshida, M. Nakatsuka: Efficient stimulated Brillouin scattering in the organic crystal deuterated L-arginine phosphate monohydrate. J. Opt. Soc. Am. B **15(1)**, 446–450 (1998).

[2] D. Eimerl, S. Velsko, L. Davis, F. Wang, G. Loiacono, G. Kennedy: Deuterated L-arginine phosphate: a new efficient nonlinear crystal. IEEE J. Quant. Electr. **25(2)**, 179–193 (1989).

[3] D. Eimerl, J. Marion, E.K. Graham, H.A. McKinstry, S. Haussühl: Elastic components and thermal fracture of $AgGaSe_2$ and *d*-LAP. IEEE J. Ouant. Electr. **27(1)**, 142–145 (1991).

[4] K. Aoki, K. Nagano, Y. Iitaka: The crystal structure of L-arginine phosphate monohydrate. Acta Crystallogr. B **27(1)**, 11–23 (1971).

[5] A.S. Haja Hameed, G. Ravi, R. Jayavel, P. Ramasamy: Nucleation kinetics, growth and characterization of dLAP, dLAP:KF and dLAP:NaN_3 crystals. J. Cryst. Growth **250(1–2)**, 126–133 (2003).

[6] A.S. Haja Hameed, G. Ravi, R. Ilangovan, A. Nixon Azariah, P. Ramasamy: Growth and characterization of deuterated analog of L-arginine phosphate single crystals. J. Cryst. Growth **237–239**, 890–893 (2002).

[7] A. Yokotani, T. Sasaki, K. Yoshida, S. Nakai: Extremely high damage threshold of a new nonlinear crystal L-arginine phosphate and its deuterium compound. Appl. Phys. Lett. **55(26)**, 2692–2693 (1989).

[8] C.E. Barker, D. Eimerl, S.P. Velsko: Temperature-insensitive phase-matching for second-harmonic generation in deuterated L-arginine phosphate. J. Opt. Soc. Am. B **8(12)**, 2481–2492 (1991).
[9] B.V. Bokut: Optical mixing in biaxial crystals. Zh. Prikl. Spektrosk. **7(4)**, 621–624 (1967) [In Russian, English trans.: J. Appl. Spectrosc. **7(4)**, 425–429 (1967)].
[10] D.A. Roberts: Simplified characterization of uniaxial and biaxial nonlinear optical crystals: a plea for standardization of nomenclature and conventions. IEEE J. Quant. Electr. **28(10)**, 2057–2074 (1992).
[11] R.B. Andreev, K.V. Vetrov, V.N. Voitsechovskii, V.D. Volosov, I.V. Nikiforuk, B.P. Nikolaeva, V.E. Yakobson: Growth of *d*-LAP crystals and study of their primary nonlinear optical properties. Izv. Akad. Nauk SSSR, Ser. Fiz. **54(12)**, 2491–2493 (1990) [In Russian, English trans.: Bull. Acad. Sci. USSR, Phys. Ser. **54(12)**, 187–189 (1990)].
[12] G. Robertson, M.H. Dunn: Excimer pumped deuterated L-arginine phosphate optical parametric oscillator. Appl. Phys. Lett. **62(26)**, 3405–3407 (1993).

8.4 α-Iodic Acid (α-HIO_3)

Negative biaxial crystal: $2V_z = 47°$ [1]
Molecular mass: 175.911
Specific gravity: 4.63 g/cm^3 [1]
Point group: 222
Assignment of dielectric and crystallographic axes: $X, Y, Z \Rightarrow b, c, a$
Transparency range at "0" transmittance level: 0.32–1.7 μm ($\|c$), 0.32–2.3 μm ($\perp c$) [1]
Linear absorption coefficient α: $< 0.5\,\mathrm{cm}^{-1}$ in the range 0.35–1.3 μm [2]

Experimental values of refraction indices at $T = 293$ K [3]

λ [μm]	n_X	n_Y	n_Z	λ [μm]	n_X	n_Y	n_Z
0.35	2.1485	2.1265	1.9612	0.62	1.9884	1.9632	1.8388
0.36	2.1330	2.1077	1.9474	0.64	1.9854	1.9589	1.8368
0.37	2.1171	2.0917	1.9360	0.66	1.9821	1.9560	1.8348
0.38	2.1053	2.0782	1.9257	0.68	1.9791	1.9529	1.8328
0.39	2.0929	2.0662	1.9154	0.70	1.9763	1.9506	1.8311
0.40	2.0808	2.0545	1.9086	0.80	1.9668	1.9409	1.8248
0.41	2.0715	2.0465	1.9020	0.85	1.9634	1.9377	1.8222
0.42	2.0637	2.0394	1.8952	0.90	1.9602	1.9346	1.8202
0.44	2.0494	2.0246	1.8847	0.95	1.9569	1.9314	1.8184
0.46	2.0378	2.0119	1.8753	1.00	1.9541	1.9286	1.8150
0.48	2.0292	2.0026	1.8685	1.10	1.9486	1.9260	1.8114
0.50	2.0194	1.9926	1.8624	1.20	1.9436	1.9229	1.8088
0.52	2.0126	1.9883	1.8562	1.30	1.9390	1.9206	1.8063
0.54	2.0065	1.9829	1.8522	1.40	1.9348	1.9180	1.8038
0.56	2.0010	1.9763	1.8476	1.50	1.9310	1.9157	1.8018
0.58	1.9960	1.9712	1.8436	1.60		1.9132	1.7998
0.60	1.9918	1.9665	1.8405				

Optical activity at $T = 300\,\mathrm{K}$ [1]

λ [μm]	ρ [deg/mm]
0.4360	74.5
0.5461	58.7

Best set of Sellmeier equations (λ in μm, $T = 293\,\mathrm{K}$) [4]:

$$n_X^2 = 3.739 + \frac{0.07128}{\lambda^2 - 0.05132}$$

$$n_Y^2 = 3.654 + \frac{0.06721}{\lambda^2 - 0.04234}$$

$$n_Z^2 = 3.239 + \frac{0.05353}{\lambda^2 - 0.017226}$$

Other sets of dispersion relations are given in [3], [5].

Linear electrooptic coefficients measured at low frequencies (well below the acoustic resonances of α-HIO_3 crystal, i.e., for the "free" crystal) at room temperature [6]

λ [μm]	r_{41}^{T} [pm/V]	r_{52}^{T} [pm/V]	r_{63}^{T} [pm/V]
0.6328	6.6 ± 0.3	7.0 ± 0.5	6.0 ± 0.3

Expressions for the effective second-order nonlinear coefficient in the principal planes of α-HIO_3 crystal (Kleinman symmetry conditions are valid, $d_{14} = d_{25} = d_{36}$) [7]:

XY plane

$d_{\mathrm{eeo}} = -d_{14} \sin 2\phi$

YZ plane

$d_{\mathrm{eoe}} = d_{\mathrm{oee}} = -d_{14} \sin 2\theta$

XZ plane, $\theta < V_z$

$d_{\mathrm{eeo}} = d_{14} \sin 2\theta$

XZ plane, $\theta > V_z$

$d_{\mathrm{eoe}} = d_{\mathrm{oee}} = d_{14} \sin 2\theta$

Values of second-order nonlinear coefficient:

$d_{14}(1.064\,\mu\mathrm{m}) = 20 \times d_{11}(SiO_2) \pm 25\% = 6.0 \pm 1.5\,\mathrm{pm/V}$ [1], [8]

$d_{14}(1.1523\,\mu\mathrm{m}) = 10.9 \times d_{36}(\mathrm{ADP}) \pm 14\% = 5.0 \pm 0.7\,\mathrm{pm/V}$ [9], [10]

Experimental values of phase-matching angle ($T = 293\,\mathrm{K}$)

Interacting wavelengths [μm]	θ_{exp} [deg]	Ref.
YZ plane, $\phi = 90°$		
SHG, $e + o \Rightarrow e$		
$0.976 \Rightarrow 0.488$	57.9	[11]
$1.029 \Rightarrow 0.5145$	52.7	[11]

Interacting wavelengths [μm]	θ_{exp} [deg]	Ref.
1.0642 ⇒ 0.5321	50.4	[12]
1.065 ⇒ 0.5325	52	[1]
XZ plane, $\phi = 0°, \theta > V_z$		
SHG, $e + o \Rightarrow e$		
0.976 ⇒ 0.488	72.2	[11]
1.029 ⇒ 0.5145	66.1	[11]
1.06 ⇒ 0.53	64.9	[13]
1.065 ⇒ 0.5325	66	[1]

Experimental values of internal angular and spectral bandwidths [14]

Interacting wavelengths [μm]	θ_{pm} [deg]	$\Delta\theta^{int}$ [deg]	$\Delta\nu$ [cm^{-1}]
XZ plane, $\phi = 0°, \theta > V_z$			
SHG, $e + o \Rightarrow e$			
1.06 ⇒ 0.53	66	0.035	3.38

Temperature tuning of critical SFG process [11]

Interacting wavelength [μm]	θ_{pm} [deg]	$d\lambda_2/dT$ [nm/K]
XZ plane, $\phi = 0°, \theta > V_z$		
SHG, $e + o \Rightarrow e$		
1.9226 + 0.654 ⇒ 0.488	50	0.055

Laser-induced surface-damage threshold

λ [μm]	τ_p [ns]	I_{thr} [GW/cm^2]	Ref.	Note
0.488	CW	>0.00025	[1]	
0.528	0.007	>7	[15]	2 Hz
0.53	15	0.055	[13]	
	0.006	>0.8	[16]	
0.532	0.03	>0.8	[17]	25 Hz
		>5.5	[18]	
	0.035	8–10	[19]	1 Hz
		4–5	[19]	12.5 Hz

About the crystal

α-HIO_3 was probably the first biaxial crystal of the 222 point group used in nonlinear optics.

References

[1] S.K. Kurtz, T.T. Perry, J.G. Bergman, Jr.: Alpha-iodic acid: a solution-grown crystal for nonlinear optical studies and applications. Appl. Phys. Lett. **12(5)**, 186–188 (1967).

[2] V.I. Bespalov, I.A. Batyreva, L.A. Dmitrenko, V.V. Korolikhin, S.P. Kuznetsov, M.A. Novikov: Investigation of the absorption of near infrared radiation in partly deuterated KDP and α-HIO_3 crystals. Kvant. Elektron. **4(7)**, 1563–1566 (1977) [In Russian, English trans.: Sov. J. Quantum Electron. **7(7)**, 885–887 (1977)].

[3] H. Naito, H. Inaba: Measurement of the refractive indices of α – iodic acid, HIO_3, crystal. Opto-electron. **4(3)**, 335–337 (1972).

[4] S.K. Kurtz: Nonlinear Optical Materials. In: *Laser Handbook*, Vol. 1, ed. by F.T. Arecchi, E.O. Schulz-Dubois (North-Holland, Amsterdam, 1972), pp. 923–974.

[5] R.A. Andrews: IR image parametric up-conversion. IEEE J. Quant. Electr. **QE-6(1)**, 68–80 (1970).

[6] E.N. Volkova, V.A. Dianova, A.L. Zueva, A.N. Izrailenko, A.C. Lipatov, V.N. Parygin, L.N. Rashkovich, L.E. Chirkov: Electro-optical and piezoelectric properties of α-HIO_3 crystals. Kristallogr. **16(2)**, 346–349 (1971) [In Russian, English trans.: Sov. Phys. - Crystallogr. **16(2)**, 284–287 (1971)].

[7] B.V. Bokut: Optical mixing in biaxial crystals. Zh. Prikl. Spektrosk. **7(4)**, 621–624 (1967) [In Russian, English trans.: J. Appl. Spectrosc. **7(4)**, 425–429 (1967)].

[8] D.A. Roberts: Simplified characterization of uniaxial and biaxial nonlinear optical crystals: a plea for standardization of nomenclature and conventions. IEEE J. Quant. Electr. **28(10)**, 2057–2074 (1992).

[9] J.E. Bjorkholm: Relative measurement of the optical nonlinearities of KDP, ADP, $LiNbO_3$, and α-HIO_3. IEEE J. Quant. Electr. **QE-4(11)**, 970–972 (1968).

[10] K. Hagimoto, A. Mito: Determination of the second-order susceptibility of ammonium dihydrogen phosphate and α-quartz at 633 and 1064 nm. Appl. Opt. **34(36)**, 8276–8282 (1995).

[11] V.A. Kiselev, V.F. Kitaeva, L.A. Kulevskii, Y.N. Polivanov, S.N. Poluektov: Investigation of spontaneous parametric emission in biaxial crystal α-HIO_3. Zh. Eksp. Teor. Fiz. **62(4)**, 1291–1301 (1972) [In Russian, English trans.: Sov. Phys. - JETP **35(4)**, 687–691 (1972)].

[12] H. Ito, H. Naito, H. Inaba: Generalized study on angular dependence of induced second-order nonlinear optical polarizations and phase matching in biaxial crystals. J. Appl. Phys. **46(9)**, 3992–3998 (1975).

[13] A.I. Izrailenko, A.I. Kovrigin, P.V. Nikles: Parametric generation of light in high-efficiency nonlinear $LiIO_3$ and α-HIO_3 crystals. Pisma Zh. Eksp. Teor. Fiz. **12(10)**, 475–478 (1970) [In Russian, English trans.: JETP Lett. **12(10)**, 331–333 (1970)].

[14] R.B. Andreev, V.D. Volosov, A.G. Kalintsev: Spectral, angular, and temperature characteristics of HIO_3, $LiIO_3$, CDA, DKDP, KDP and ADP non-linear crystals in second- and fourth-harmonic generation. Opt. Spektrosk. **37(2)**, 294–299 (1974) [In Russian, English trans.: Opt. Spectrosc. USSR **37(2)**, 169–171 (1974)].

[15] G. Dikchyus, E. Zhilinskas, A. Piskarskas, V. Sirutkaitis: Statistical properties and stabilization of a picosecond phosphate-glass laser with 2 Hz repetition frequency. Kvant. Elektron. **6(8)**, 1610–1619 (1979) [In Russian, English trans.: Sov. J. Quantum Electron. **9(8)**, 950–955 (1979)].

[16] G.A. Dikchyus, V.I. Kabelka, A.S. Piskarskas, A.Y. Stabinis: Single-pass parametric generation of light in an α-HIO_3 crystal pumped with ultrashort pulses. Kvant. Elektron. **1(11)**, 2513–2515 (1974) [In Russian, English trans.: Sov. J. Quantum Electron. **4(11)**, 1402–1403 (1974)].

[17] G. Dikchyus, R. Danielius, V. Kabelka, A. Piskarskas, T. Tomkiavichyus, A. Stabinis: Kvant. Elektron. **3(4)**, 779–784 (1976) [In Russian, English trans.: Sov. J. Quantum Electron. **6(4)**, 425–428 (1976)].

[18] R. Danielius, G. Dikchyus, V. Kabelka, A. Piskarskas: High efficiency, picosecond parametric light source with narrow output spectrum and high pulse rate. Zh. Tekh. Fiz. **47(5)**, 1075–1077 (1977) [In Russian, English trans.: Sov. Phys. - Tech. Phys. **22(5)**, 642–643 (1977)].

[19] R. Danielius, G. Dikchyus, V. Kabelka, A. Piskarskas, A. Stabinis, Y. Yasevichyute: Parametric excitation of light in the picosecond range. Kvant. Elektron. **4(11)**, 2379–2395 (1977) [In Russian, English trans.: Sov. J. Quantum Electron. **7(11)**, 1360–1368 (1977)].

8.5 LiCOOH · H_2O, Lithium Formate Monohydrate (LFM)

Negative biaxial crystal: $2V_z = 123.8°$ at $\lambda = 0.5321\,\mu m$ [1]
Molecular mass: 69.974
Specific gravity: $1.46\,g/cm^3$ [1]
Point group: $mm2$
Lattice constants [1]:
$a = 4.85$ Å
$b = 6.49$ Å
$c = 10.01$ Å
Assignment of dielectric and crystallographic axes: $X, Y, Z \Rightarrow a, b, c$
Transparency range at "0" transmittance level: 0.23–1.56 μm [1], [2]

Linear absorption coefficient $\alpha(\theta = 90°, \phi = 10°)$ [3]

λ [μm]	α [cm^{-1}]
0.3547	0.025
0.5321	0.012
1.0642	0.017

Experimental values of refractive indices [4]

λ [μm]	n_X	n_Y	n_Z	λ [μm]	n_X	n_Y	n_Z
0.35	1.3810	1.5073	1.5540	0.54	1.3666	1.4827	1.5219
0.36	1.3791	1.5051	1.5510	0.56	1.3657	1.4813	1.5200
0.37	1.3777	1.5034	1.5484	0.58	1.3647	1.4804	1.5187
0.38	1.3767	1.5017	1.5458	0.60	1.3643	1.4796	1.5174
0.39	1.3758	1.4999	1.5432	0.62	1.3638	1.4787	1.5161
0.40	1.3748	1.4981	1.5405	0.64	1.3633	1.4778	1.5152
0.42	1.3729	1.4955	1.5367	0.66	1.3628	1.4768	1.5144
0.44	1.3714	1.4928	1.5332	0.68	1.3625	1.4760	1.5135
0.46	1.3705	1.4902	1.5301	0.70	1.3623	1.4751	1.5126
0.48	1.3696	1.4880	1.5279	0.80	1.3614	1.4729	1.5099
0.50	1.3686	1.4862	1.5257	0.90	1.3604	1.4711	1.5077
0.52	1.3677	1.4845	1.5236	1.00	1.3595	1.4694	1.5055

λ [μm]	n_X	n_Y	n_Z	λ [μm]	n_X	n_Y	n_Z
1.10	1.3590	1.4675	1.5032	1.40	1.3583	1.4630	1.4970
1.20	1.3587	1.4658	1.5011	1.50	1.3581	1.4617	
1.30	1.3585	1.4644	1.4987				

Sellmeier equations (λ in μm, $T = 293$ K) [4]:

$$n_X^2 = 1.4376 + \frac{0.4045\,\lambda^2}{\lambda^2 - 0.01692601} - 0.0005\,\lambda^2$$

$$n_Y^2 = 1.6586 + \frac{0.5006\,\lambda^2}{\lambda^2 - 0.023409} - 0.0127\,\lambda^2$$

$$n_Z^2 = 1.6714 + \frac{0.5928\,\lambda^2}{\lambda^2 - 0.02534464} - 0.0153\,\lambda^2$$

Expressions for the effective second-order nonlinear coefficient in principal planes of LFM crystal (Kleinman symmetry conditions are not valid) [5]:

XY plane

$d_{\mathrm{eoe}} = d_{\mathrm{oee}} = d_{15}\sin^2\phi + d_{24}\cos^2\phi$

YZ plane

$d_{\mathrm{oeo}} = d_{\mathrm{eoo}} = d_{15}\sin\theta$

XZ plane, $\theta < V_z$

$d_{\mathrm{ooe}} = d_{32}\sin\theta$

XZ plane, $\theta > V_z$

$d_{\mathrm{oeo}} = d_{\mathrm{eoo}} = d_{24}\sin\theta$

Expressions for the effective second-order nonlinear coefficient in principal planes of LFM crystal (Kleinman symmetry conditions are valid, $d_{15} = d_{31}$ and $d_{24} = d_{32}$) [5]:

XY plane

$d_{\mathrm{eoe}} = d_{\mathrm{oee}} = d_{31}\sin^2\phi + d_{32}\cos^2\phi$

YZ plane

$d_{\mathrm{oeo}} = d_{\mathrm{eoo}} = d_{31}\sin\theta$

XZ plane, $\theta < V_z$

$d_{\mathrm{ooe}} = d_{32}\sin\theta$

XZ plane, $\theta > V_z$

$d_{\mathrm{oeo}} = d_{\mathrm{eoo}} = d_{32}\sin\theta$

Expressions for the effective second-order nonlinear coefficient in arbitrary direction inside the LFM crystal are given in [5]. The formulas given in [2] are incorrect.

Absolute values of second-order nonlinear coefficients [6]:

$d_{31}(1.0642\,\mu\mathrm{m}) = 0.13\,\mathrm{pm/V}$

$d_{32}(1.0642\,\mu\mathrm{m}) = -0.60\,\mathrm{pm/V}$

$d_{33}(1.0642\,\mu\mathrm{m}) = 0.94\,\mathrm{pm/V}$

Experimental values of phase-matching angle

Interacting wavelengths [μm]	ϕ_{exp} [deg]	θ_{exp} [deg]	Ref.
XY plane, $\theta = 90°$			
SFG, $e + o \Rightarrow e$			
$1.0642 + 0.5321 \Rightarrow 0.3547$	8.2		[3]
XZ plane, $\phi = 0°$			
SHG, $o + o \Rightarrow e$			
$0.486 \Rightarrow 0.243$		38.5	[7]
$1.0642 \Rightarrow 0.5321$		55.1	[1]
SHG, $o + e \Rightarrow e$			
$1.0642 \Rightarrow 0.5321$		82.0	[1]

Experimental value of internal angular bandwidth [3]

Interacting wavelengths [μm]	ϕ_{pm} [deg]	$\Delta\varphi^{int}$ [deg]
XY plane, $\theta = 90°$		
SFG, $e + o \Rightarrow e$		
$1.0642 + 0.5321 \Rightarrow 0.3547$	8.2	0.04

Laser-induced surface-damage threshold

λ [μm]	τ_p [ns]	I_{thr} [GW/cm^2]	Ref.
0.475	330	0.15	[8]
0.488	CW	>0.000001	[1]
0.490	330	0.15	[8]

About the crystal

LFM is one of the first biaxial nonlinear optical crystals, belonging to the *mm*2 point group.

References

[1] S. Singh, W.A. Bonner, J.R. Potopowicz, L.G. van Uitert: Non-linear optical susceptibility of lithium formate monohydrate. Appl. Phys. Lett. **17(7)**, 292–294 (1970).

[2] H. Ito, H. Naito, H. Inaba: New phase-matchable nonlinear optical crystals of the formate family. IEEE J. Quant. Electr. **QE-10(2)**, 247–252 (1974).

[3] K. Kato: Third-harmonic generation of Nd:YAG laser in lithium formate monohydrate. Opt. Quant. Electron. **8(3)**, 261–262 (1976).

[4] H. Naito, H. Inaba: Measurement of the refractive indices of crystalline lithium formate HCOOLI·H_2O. Opto-electron. **5(3)**, 256–259 (1973).

[5] V.G. Dmitriev, D.N. Nikogosyan: Effective nonlinearity coefficients for three-wave interactions in biaxial crystals of *mm*2 point group symmetry. Opt. Commun. **95(1–3)**, 173–182 (1993).

[6] D.A. Roberts: Simplified characterization of uniaxial and biaxial nonlinear optical crystals: a plea for standardization of nomenclature and conventions. IEEE J. Quant. Electr. **28(10)**, 2057–2074 (1992).

[7] S.J. Bastow, M.H. Dunn: The generation of tunable UV radiation from 238–249 nm by intracavity frequency doubling of Coumarin 102 dye laser. Opt. Commun. **35(2)**, 259–263 (1980).
[8] L. Armstrong, S.E. Neister, R. Adhav: Measuring CFP dye laser damage thresholds on UV doubling crystals. Laser Focus **18(12)**, 49–53 (1982).

8.6 CsH_2AsO_4, Cesium Dihydrogen Arsenate (CDA)

Negative uniaxial crystal: $n_o > n_e$
Molecular mass: 273.840
Specific gravity: 3.53 g/cm^3 [1]
Point group: $\bar{4}2m$
Lattice constants [2]:
$a = 7.9852 \pm 0.0004$ Å at $T = 298$ K
$c = 7.8928 \pm 0.0003$ Å at $T = 298$ K
Curie temperature: 143 K [2]

Linear thermal expansion coefficient [2]

$\alpha_t \times 10^6$ [K^{-1}], $\parallel c$	$\alpha_t \times 10^6$ [K^{-1}], $\perp c$
49	12

Transparency range at 0.5 level for 17.5-mm-long crystal cut at $\theta = 90°$, $\phi = 45°$: 0.26–1.43 μm [3]
UV edge of transparency range at "0" transmittance level: 0.216 μm [4]
IR edge of transparency range at "0" transmittance level: 1.87 μm for *o*-wave, 1.67 μm for *e*-wave [5]

Linear absorption coefficient α

λ [μm]	α [cm^{-1}]	Ref.
0.35–1.4	0.6	[4]
1.062	0.041	[6]
1.064	0.041	[3]

Two-photon absorption coefficient β [7]

λ [μm]	$\beta \times 10^{11}$ [cm/W]	Note
0.355	2.81	*e*-wave, $\theta = 90°$, $\phi = 45°$

Experimental values of refraction indices [3]

λ [μm]	n_o	n_e
0.3472	1.6027	1.5722
0.5321	1.5733	1.5514

λ [μm]	n_o	n_e
0.6943	1.5632	1.5429
1.0642	1.5516	1.5330

Temperature derivatives of refraction indices [8]

λ [μm]	$dn_o/dT \times 10^5$ [K^{-1}]	$dn_e/dT \times 10^5$ [K^{-1}]
0.405	−3.15	−1.89
0.436	−3.05	−2.09
0.546	−2.59	−2.12
0.578	−2.76	−2.39
0.633	−2.80	−2.56

Best set of dispersion relations (λ in μm, $T = 293$ K) [5]:

$$n_o^2 = 1.8776328 - 0.03602222\,\lambda^2 + 0.005234121\,\lambda^4 + \frac{0.5503951\,\lambda^2}{\lambda^2 - (0.1625700)^2}$$

$$n_e^2 = 1.6862889 - 0.01372244\,\lambda^2 + 0.003948463\,\lambda^4 + \frac{0.6694571\,\lambda^2}{\lambda^2 - (0.1464712)^2}$$

Other dispersion relations are given in [8], [9].
Expressions for the effective second-order nonlinear coefficient in general case (Kleinman symmetry conditions are valid, $d_{14} = d_{25} = d_{36}$) [10]:

$$d_{ooe} = -d_{36}\sin(\theta + \rho)\sin 2\phi$$
$$d_{eoe} = d_{oee} = 2d_{36}\sin(\theta + \rho)\cos(\theta + \rho)\cos 2\phi$$

Simplified expressions for the effective second-order nonlinear coefficient (approximation of small birefringence angle, Kleinman symmetry conditions are valid, $d_{14} = d_{25} = d_{36}$) [11]:

$$d_{ooe} = -d_{36}\sin\theta\sin 2\phi$$
$$d_{eoe} = d_{oee} = d_{36}\sin 2\theta\cos 2\phi$$

Absolute value of second-order nonlinear coefficient:

$d_{36}(1.0642\,\mu\text{m}) = 0.40 \pm 0.05$ pm/V [3]

Experimental values of phase-matching angle ($T = 293$ K)

Interacting wavelengths [μm]	θ_{exp} [deg]	Ref.
SHG, $o + o \Rightarrow e$		
$1.05 \Rightarrow 0.525$	90	[12]
$1.052 \Rightarrow 0.526$	90	[8]
$1.06 \Rightarrow 0.53$	87	[13], [14]
$1.0642 \Rightarrow 0.5321$	83.5	[15], [16]
	84.2	[3]
	84.4	[17]

Experimental values of NCPM temperature

Interacting wavelengths [μm]	T [°C]	Ref.	Note
SHG, $o + o \Rightarrow e$			
1.05 ⇒ 0.525	20	[12]	
1.052 ⇒ 0.526	20	[8]	
1.06 ⇒ 0.53	31	[13]	
1.0642 ⇒ 0.5321	39.6	[3]	20 Hz
	40.3	[18]	10 Hz
	41	[16]	
	42	[19]	
	43	[17]	
	44.5	[20]	
	45	[6]	
	46	[15]	12.5 Hz
	48	[3]	0.1–1 Hz
	49.2	[21]	10 Hz
1.073 ⇒ 0.5365	61	[19]	
1.078 ⇒ 0.539	100	[12]	

Experimental values of internal angular and temperature bandwidths

Interacting wavelengths [μm]	T [°C]	θ_{pm} [deg]	$\Delta\theta^{int}$ [deg]	ΔT [°C]	Ref.
SHG, $o + o \Rightarrow e$					
1.06 ⇒ 0.53	22	87	≈0.4		[13]
	31	90	≈3.8	≈3	[13]
	20	87	0.43		[14]
	63 (?)	90	3.03		[14]
1.062 ⇒ 0.531	45	90	2.85	6.5	[6]
1.0642 ⇒ 0.5321	40.3	90		6.8	[18]
	24	83.5	0.86	∼8	[15]
	46	90	3.2		[15]
	20	84.15	0.70		[3]
	48	90	2.91	6 ± 0.2	[3]
	20	84.4	0.70		[17]
	43	90	≈3		[17]

Experimental values of spectral bandwidth [14]

Interacting wavelengths [μm]	T [°C]	θ_{pm} [deg]	$\Delta\nu$ [cm^{-1}]
SHG, $o + o \Rightarrow e$			
1.06 ⇒ 0.53	20	87	199
	63 (?)	90	158

Temperature variation of phase-matching angle

Interacting wavelengths [μm]	T [°C]	θ_{pm} [deg]	$d\theta_{pm}/dT$ [deg/K]	Ref.
SHG, $o + o \Rightarrow e$				
1.06 ⇒ 0.53	20	87	0.085	[14]
	63 (?)	90	0.481	[14]
1.0642 ⇒ 0.5321	24	83.5	0.129	[15]
	20	84.4	0.131	[17]
	35	86.5	0.194	[17]
	39	87.6	0.251	[17]
	41	88.3	0.537	[17]

Temperature tuning of noncritical SHG [8]

Interacting wavelengths [μm]	$d\lambda_1/dT$ [nm/K]
SHG, $o + o \Rightarrow e$	
1.052 ⇒ 0.526	0.308

Temperature variation of birefringence for noncritical SHG process (1.0642 μm ⇒ 0.5321 μm, $o + o \Rightarrow e$):

$d(n_2^e - n_1^o)/dT = 7.2 \times 10^{-6}\,K^{-1}$ [18]

$d(n_2^e - n_1^o)/dT = (8.0 \pm 0.2) \times 10^{-6}\,K^{-1}$ [3]

Laser-induced bulk-damage threshold

λ [μm]	τ_p [ns]	I_{thr} [GW/cm^2]	Ref.	Note
0.532	10	>0.3	[21]	
1.062	0.007	>4	[6]	
1.064	12	>0.26	[3]	10–20 Hz
	10	0.35	[15]	12.5 Hz
	18	0.4	[18]	2–50 Hz

About the crystal

CDA (together with its deuterated analog DCDA) was widely used in the 1970s for NCPM of Nd:YAG laser radiation.

References

[1] V.G. Dmitriev, G.G. Gurzadyan, D.N. Nikogosyan: *Handbook of Nonlinear Optical Crystals, Third Revised Edition* (Springer, Berlin, 1999).

[2] W.R. Cook, Jr.: Thermal expansion of crystals with KH_2PO_4 structure. J. Appl. Phys. **38(4)**, 1637–1642 (1967).

[3] K. Kato: Second-harmonic generation in CDA and CD*A. IEEE J. Quant. Electr. **QE-10(8)**, 616–618 (1974).

[4] A.S. Sonin, A.S. Vasilevskaya: *Elektrooptic Crystals* (Atomizdat, Moscow, 1971) [In Russian].

[5] D. Eimerl: Electro-optic, linear and nonlinear optical properties of KDP and its isomorphs. Ferroelectrics **72(1–4)**, 95–139 (1987).
[6] T.A. Rabson, H.J. Ruiz, P.L. Shah, F.K. Tittel: Efficient second harmonic generation of picosecond laser pulses. Appl. Phys. Lett. **20(8)**, 282–284 (1972).
[7] P. Liu, W.L. Smith, H. Lotem, J.H. Bechtel, N. Bloembergen, R.S. Adhav: Absolute two-photon absorption coefficients at 355 and 266 nm. Phys. Rev. B **17(12)**, 4620–4632 (1978).
[8] N.P. Barnes, D.J. Gettemy, R.S. Adhav: Variations of the refractive index with temperature and the tuning rate for KDP isomorphs. J. Opt. Soc. Am. **72(7)**, 895–898 (1982).
[9] K.W. Kirby, L.G. DeShazer: Refractive indices of 14 nonlinear crystals isomorphic to KH_2PO_4. J. Opt. Soc. Am. B **4(7)**, 1072–1078 (1987).
[10] R.C. Eckardt, H. Masuda, Y.X. Fan, R.L. Byer: Absolute and relative nonlinear optical coefficients of KDP, KD*P, BaB_2O_4, $LiIO_3$, MgO:$LiNbO_3$, and KTP measured by phase-matched second-harmonic generation. IEEE J. Quant. Electr. **26(5)**, 922–933 (1990).
[11] J.E. Midwinter, J. Warner: The effects of phase matching method and of uniaxial crystal symmetry on the polar distribution of second-order non-linear optical polarization. Brit. J. Appl. Phys. **16(11)**, 1135–1142 (1965).
[12] R.S. Adhav: Materials for optical harmonic generation. Laser Focus **19(6)**, 73–78 (1983).
[13] V.S. Suvorov, I.S. Rez: Second-harmonic generation without birefringence in CDA (CsH_2AsO_4) crystal at room temperature. Opt. Spektrosk. **27(1)**, 181–183 (1969) [English trans.: Opt. Spectrosc. USSR **27(1)**, 94–95 (1969)].
[14] R.B. Andreev, V.D. Volosov, A.G. Kalintsev: Spectral, angular, and temperature characteristics of HIO_3, $LiIO_3$, CDA, DKDP, KDP and ADP non-linear crystals in second- and fourth-harmonic generation. Opt. Spektrosk. **37(2)**, 294–299 (1974) [English trans.: Opt. Spectrosc. USSR **37(2)**, 169–171 (1974)].
[15] Y.D. Golyaev, V.G. Dmitriev, I.Y. Itskhoki, V.N. Krasnyanskaya, I.S. Rez, E.A. Shalaev: Efficient frequency doubler utilizing a cesium dihydrogen arsenate crystal. Kvantovaya Elektron. **No. 1**, 122–123 (1973) [English trans.: Sov. J. Quantum Electron. **3(1)**, 72–73 (1973)].
[16] R.S. Adhav, A.D. Vlassopoulos: Guide to efficient doubling. Laser Focus **10(5)**, 47–48 (1974).
[17] K.V. Vetrov, V.D. Volosov, A.G. Kalintsev: Nonlinear characteristics of CDA and DCDA in neodymium-laser second-harmonic generation. Izv. Akad. Nauk SSSR, Ser. Fiz. **52(2)**, 301–303 (1988) [English trans.: Bull. Acad. Sci. USSR, Ser. Phys. **52(2)**, 78–79 (1988)].
[18] K. Kato: Efficient second harmonic generation in CDA. Opt. Commun. **9(3)**, 249–251 (1973).
[19] R.S. Adhav, R.W. Wallace: Second harmonic generation in 90° phase-matched KDP isomorphs. IEEE J. Quant. Electr. **QE-9(8)**, 855–856 (1973).
[20] G.A. Massey, M.D. Jones, J.C. Johnson: Generation of pulse bursts at 212.8 nm by intracavity modulation of an Nd:YAG laser. IEEE J. Quant. Electr. **QE-14(7)**, 527–532 (1978).
[21] G.A. Massey, R.A. Elliot: Tunable infrared parametric generation in cesium dihydrogen arsenate. IEEE J. Quant. Electr. **QE-10(12)**, 899–900 (1974).

8.7 CsD_2AsO_4, Deuterated Cesium Dihydrogen Arsenate (DCDA)

Negative uniaxial crystal: $n_o > n_e$
Molecular mass: 275.853

Specific gravity: 3.53 g/cm^3 [1]
Point group: $\bar{4}2m$
Transparency range at 0.5 level for 13.5-mm-long crystal cut at $\theta = 90°$, $\phi = 45°$: 0.27–1.66 μm [2]
IR edge of transparency range at "0" transmittance level: 2.03 μm for *o*-wave, 1.78 μm for *e*-wave [3]

Linear absorption coefficient α

λ [μm]	α [cm^{-1}]	Ref.
1.062	0.01	[4]
1.064	0.02	[2]

Two-photon absorption coefficient β [5]

λ [μm]	$\beta \times 10^{11}$ [cm/W]	Note
0.355	8.0	*o*-wave, $\theta = 90°$, $\phi = 45°$
	5.1	*e*-wave, $\theta = 90°$, $\phi = 45°$

Experimental values of refraction indices [2]

λ [μm]	n_o	n_e
0.3472	1.5895	1.5685
0.5321	1.5681	1.5495
0.6943	1.5596	1.5418
1.0642	1.5503	1.5326

Temperature derivatives of refraction indices [6]

λ [μm]	$dn_o/dT \times 10^5$ [K^{-1}]	$dn_e/dT \times 10^5$ [K^{-1}]
0.405	−2.26	−1.77
0.436	−2.26	−1.51
0.546	−2.47	−1.64
0.578	−2.31	−1.71
0.633		−1.70

Best set of dispersion relations (λ in μm, $T = 293$ K) [3]:

$$n_o^2 = 1.6278496 - 0.018220310\,\lambda^2 + 0.0002813331\,\lambda^4 + \frac{0.7808170\,\lambda^2}{\lambda^2 - (0.1407699)^2}$$

$$n_e^2 = 1.6236063 - 0.009338692\,\lambda^2 + 0.0019654130\,\lambda^4 + \frac{0.7249589\,\lambda^2}{\lambda^2 - (0.1414850)^2}$$

Other dispersion relations are given in [6], [7].

Expressions for the effective second-order nonlinear coefficient in general case (Kleinman symmetry conditions are valid, $d_{14} = d_{25} = d_{36}$) [8]:

$d_{ooe} = -d_{36} \sin(\theta + \rho) \sin 2\phi$

$d_{eoe} = d_{oee} = 2d_{36} \sin(\theta + \rho) \cos(\theta + \rho) \cos 2\phi$

Simplified expressions for the effective second-order nonlinear coefficient (approximation of small birefringence angle, Kleinman symmetry conditions are valid, $d_{14} = d_{25} = d_{36}$) [9]:

$d_{ooe} = -d_{36} \sin\theta \sin 2\phi$

$d_{eoe} = d_{oee} = d_{36} \sin 2\theta \cos 2\phi$

Absolute value of second-order nonlinear coefficient:

$d_{36}(1.0642\,\mu\text{m}) = 0.40 \pm 0.05\,\text{pm/V}$ [2]

Experimental values of phase-matching angle ($T = 293$ K)

Interacting wavelengths [μm]	θ_{exp} [deg]	Ref.
SHG, $o + o \Rightarrow e$		
1.034 ⇒ 0.517	90	[10]
1.037 ⇒ 0.5185	90	[6]
1.0642 ⇒ 0.5321	79.35	[2]
	80.8	[11]

Experimental values of NCPM temperature

Interacting wavelengths [μm]	T [°C]	Ref.	Note
SHG, $o + o \Rightarrow e$			
1.034 ⇒ 0.517	20	[10]	
1.037 ⇒ 0.5185	20	[6]	
1.0642 ⇒ 0.5321	96.4	[11]	70% deuteration
	102	[12], [13]	
	108	[10]	
	109.8	[2]	90% deuteration, 20 Hz
	112.3	[2]	90% deuteration, <1 Hz

Experimental values of internal angular and temperature bandwidths

Interacting wavelengths [μm]	T [°C]	θ_{pm} [deg]	$\Delta\theta^{int}$ [deg]	ΔT [°C]	Ref.
SHG, $o + o \Rightarrow e$					
1.0642 ⇒ 0.5321	20	79.35	0.41		[2]
	20	80.8	0.50		[11]
	96.4	90	≈3.5		[11]
	112.3	90	2.90	6.1 ± 0.1	[2]

Temperature variation of phase-matching angle [11]

Interacting wavelengths [μm]	T [°C]	θ_{pm} [deg]	$d\theta_{pm}/dT$ [deg/K]
SHG, $o + o \Rightarrow e$			
1.0642 ⇒ 0.5321	20	80.8	0.042
	66.3	84.3	0.081
	80	86.4	0.270
	87.7	88.1	0.533

Temperature tuning of noncritical SHG [6]

Interacting wavelengths [μm]	$d\lambda_1/dT$ [nm/K]
SHG, $o + o \Rightarrow e$	
1.037 ⇒ 0.5185	0.317

Temperature variation of birefringence for noncritical SHG process (1.0642 μm ⇒ 0.5321 μm, $o + o \Rightarrow e$):

$d(n_2^e - n_1^o)/dT = (7.8 \pm 0.2) \times 10^{-6}\,K^{-1}$ [2]

Laser-induced bulk-damage threshold

λ [μm]	τ_p [ns]	I_{thr} [GW/cm^2]	Ref.	Note
1.064	12	>0.26	[2]	10–20 Hz
		>0.25	[14]	0.1–20 Hz

About the crystal

DCDA (together with its analog CDA) was widely used in the 1970s for NCPM of Nd:YAG laser radiation.

References

[1] V.G. Dmitriev, G.G. Gurzadyan, D.N. Nikogosyan: *Handbook of Nonlinear Optical Crystals, Third Revised Edition* (Springer, Berlin, 1999).

[2] K. Kato: Second-harmonic generation in CDA and CD*A. IEEE J. Quant. Electr. **QE-10(8)**, 616–618 (1974).

[3] D. Eimerl: Electro-optic, linear and nonlinear optical properties of KDP and its isomorphs. Ferroelectrics **72(1–4)**, 95–139 (1987).

[4] T.A. Rabson, H.J. Ruiz, P.L. Shah, F.K. Tittel: Efficient second harmonic generation of picosecond laser pulses. Appl. Phys. Lett. **20(8)**, 282–284 (1972).

[5] P. Liu, W.L. Smith, H. Lotem, J.H. Bechtel, N. Bloembergen, R.S. Adhav: Absolute two-photon absorption coefficients at 355 and 266 nm. Phys. Rev. B **17(12)**, 4620–4632 (1978).

[6] N.P. Barnes, D.J. Gettemy, R.S. Adhav: Variations of the refractive index with temperature and the tuning rate for KDP isomorphs. J. Opt. Soc. Am. **72(7)**, 895–898 (1982).

[7] K.W. Kirby, L.G. DeShazer: Refractive indices of 14 nonlinear crystals isomorphic to KH_2PO_4. J. Opt. Soc. Am. B **4(7)**, 1072–1078 (1987).

[8] R.C. Eckardt, H. Masuda, Y.X. Fan, R.L. Byer: Absolute and relative nonlinear optical coefficients of KDP, KD*P, BaB_2O_4, $LiIO_3$, MgO:$LiNbO_3$, and KTP measured by phase-matched second-harmonic generation. IEEE J. Quant. Electr. **26(5)**, 922–933 (1990).
[9] J.E. Midwinter, J. Warner: The effects of phase matching method and of uniaxial crystal symmetry on the polar distribution of second-order non-linear optical polarization. Brit. J. Appl. Phys. **16(11)**, 1135–1142 (1965).
[10] R.S. Adhav: Materials for optical harmonic generation. Laser Focus **19(6)**, 73–78 (1983).
[11] K.V. Vetrov, V.D. Volosov, A.G. Kalintsev: Nonlinear characteristics of CDA and DCDA in neodymium-laser second-harmonic generation. Izv. Akad. Nauk SSSR, Ser. Fiz. **52(2)**, 301–303 (1988) [In Russian, English trans.: Bull. Acad. Sci. USSR, Ser. Phys. **52(2)**, 78–79 (1988)].
[12] R.S. Adhav, R.W. Wallace: Second harmonic generation in 90° phase-matched KDP isomorphs. IEEE J. Quant. Electr. **QE-9(8)**, 855–856 (1973).
[13] R.S. Adhav, A.D. Vlassopoulos: Guide to efficient doubling. Laser Focus **10(5)**, 47–48 (1974).
[14] K. Kato: Conversion of high power Nd:YAG laser radiation to the UV at 2661 Å. Opt. Commun. **13(4)**, 361–362 (1975).

8.8 RbH_2PO_4, Rubidium Dihydrogen Phosphate (RDP)

Negative uniaxial crystal: $n_o > n_e$
Molecular mass: 182.454
Specific gravity: 2.805 g/cm^3 [1]
Point group: $\bar{4}2m$
Lattice constants [2]:
$a = 7.608 \pm 0.008$ Å
$c = 7.296 \pm 0.007$ Å
Curie temperature: 147 K [3], [4]

Linear thermal expansion coefficient [4]

$\alpha_t \times 10^6$ [K^{-1}], $\parallel c$	$\alpha_t \times 10^6$ [K^{-1}], $\perp c$
42.5	19

Transparency range at 0.5 level for 15.3-mm-long crystal cut at $\theta = 50°$, $\phi = 45°$: 0.19–1.38 μm [5]
IR edge of transparency range at "0" transmittance level: 1.65 μm for *o*-wave, 1.87 μm for *e*-wave [6]

Linear absorption coefficient α

λ [μm]	α [cm^{-1}]	Ref.	Note
0.25–1.25	<0.03	[7]	
0.3547	0.015	[5]	$\theta = 50°$, $\phi = 45°$
0.5321	0.01	[5]	$\theta = 50°$, $\phi = 45°$
1.0642	0.041	[5]	$\theta = 50°$, $\phi = 45°$

Two-photon absorption coefficient β [8]

λ [μm]	$\beta \times 10^{11}$ [cm/W]	Note
0.355	0.59	e-wave, $\theta = 90°$, $\phi = 45°$

Experimental values of refraction indices

λ [μm]	n_o	n_e	Ref.	λ [μm]	n_o	n_e	Ref.
0.3472	1.5284	1.4969	[9]	0.5321	1.5106	1.4811	[10]
0.4358	1.5165	1.4857	[9]	0.5468	1.5082	1.4790	[9]
0.4765	1.5140	1.4861	[10]	0.5500	1.5093	1.4804	[3]
0.4880	1.5132	1.4832	[10]	0.5893	1.5053	1.4765	[9]
0.4965	1.5126	1.4827	[10]	0.6000	1.5067	1.4784	[3]
0.5000	1.5125	1.4813	[3]	0.6500	1.5046	1.4767	[3]
0.5017	1.5121	1.4825	[10]	0.6943	1.5020	1.4735	[9]
0.5145	1.5116	1.4820	[10]	1.0642	1.4926	1.4700	[10]

λ [μm]	n_o	Ref.	λ [μm]	n_e	Ref.
0.4699	1.5148	[11]	0.4658	1.4851	[11]
0.4950	1.5128	[11]	0.4780	1.4845	[11]
0.5120	1.5117	[11]	0.4950	1.4833	[11]
0.5329	1.5104	[11]	0.5324	1.4810	[11]
0.5851	1.5074	[11]	0.5577	1.4798	[11]
0.5980	1.5069	[11]	0.5878	1.4787	[11]
0.6245	1.5056	[11]	0.6165	1.4776	[11]
0.6474	1.5047	[11]	0.6521	1.4766	[11]
0.6662	1.5042	[11]	0.6640	1.4763	[11]

Temperature derivatives of refraction indices [12]

λ [μm]	$dn_o/dT \times 10^5$ [K^{-1}]	$dn_e/dT \times 10^5$ [K^{-1}]
0.405	−3.69	−2.67
0.436	−3.86	−2.76
0.546	−3.72	−2.54
0.578	−3.72	−2.80
0.633	−3.72	−2.89

Best set of dispersion relations (λ in μm, $T = 293$ K) [13]:

$$n_o^2 = 2.249885 + \frac{3.688005\,\lambda^2}{\lambda^2 - (11.27829)^2} + \frac{0.010560}{\lambda^2 - (0.088207)^2}$$

$$n_e^2 = 2.159913 + \frac{0.988431\,\lambda^2}{\lambda^2 - (11.30013)^2} + \frac{0.009515}{\lambda^2 - (0.092076)^2}$$

Other dispersion relations are given in [6], [10], [12].

Linear electrooptic coefficients measured at low frequencies (well below the acoustic resonances of RDP crystal, i.e., for the "free" crystal) at $T = 295$ K [3]

λ [μm]	r_{41}^{T} [pm/V]	r_{63}^{T} [pm/V]
0.6328	12.5 ± 0.2	7.7 ± 0.3

Expressions for the effective second-order nonlinear coefficient in general case (Kleinman symmetry conditions are valid, $d_{14} = d_{25} = d_{36}$) [14]:

$$d_{\mathrm{ooe}} = -d_{36} \sin(\theta + \rho) \sin 2\phi$$
$$d_{\mathrm{eoe}} = d_{\mathrm{oee}} = 2d_{36} \sin(\theta + \rho) \cos(\theta + \rho) \cos 2\phi$$

Simplified expressions for the effective second-order nonlinear coefficient (approximation of small birefringence angle, Kleinman symmetry conditions are valid, $d_{14} = d_{25} = d_{36}$) [15]:

$$d_{\mathrm{ooe}} = -d_{36} \sin\theta \sin 2\phi$$
$$d_{\mathrm{eoe}} = d_{\mathrm{oee}} = d_{36} \sin 2\theta \cos 2\phi$$

Values of second-order nonlinear coefficient:

$$d_{36}(0.6943\,\mu\mathrm{m}) = 1.04 \times d_{36}(\mathrm{KDP}) \pm 15\% = 0.41 \pm 0.06\,\mathrm{pm/V}\ [16], [17]$$
$$d_{36}(0.6943\,\mu\mathrm{m}) = 0.92 \times d_{36}(\mathrm{KDP}) \pm 10\% = 0.36 \pm 0.04\,\mathrm{pm/V}\ [17], [18]$$

Experimental values of phase-matching angle ($T = 293$ K)

Interacting wavelengths [μm]	θ_{exp} [deg]	Ref.
SHG, $o + o \Rightarrow e$		
$0.626 \Rightarrow 0.313$	90	[12]
$0.627 \Rightarrow 0.3135$	90	[19]
$0.6275 \Rightarrow 0.31375$	90	[20]
$0.6294 \Rightarrow 0.3147$	86.6	[20]
$0.6328 \Rightarrow 0.3164$	83.2	[21]
$0.6386 \Rightarrow 0.3193$	78.9	[20]
$0.6550 \Rightarrow 0.3275$	73.9	[20]
$0.6700 \Rightarrow 0.3350$	70.8	[20]
$0.6943 \Rightarrow 0.34715$	66	[9]
$1.0642 \Rightarrow 0.5321$	50.8	[5], [22]
	50.9	[23]
$1.1523 \Rightarrow 0.57615$	51	[21]
SHG, $e + o \Rightarrow e$		
$1.0642 \Rightarrow 0.5321$	83.1	[22]
$1.1523 \Rightarrow 0.57615$	77.1	[21]
THG, $o + o \Rightarrow e$		
$1.0642 + 0.5321 \Rightarrow 0.3547$	61.2	[5]

Experimental values of NCPM temperature

Interacting wavelengths [μm]	T [°C]	Ref.
SHG, $o + o \Rightarrow e$		
0.627 ⇒ 0.3135	20	[19], [23]
0.6275 ⇒ 0.31375	20	[20]
0.635 ⇒ 0.3175	100	[19], [23]
0.637 ⇒ 0.3185	98	[20]

Experimental values of internal angular bandwidth at $T = 293$ K

Interacting wavelengths [μm]	θ_{pm} [deg]	$\Delta\theta^{int}$ [deg]	Ref.
SHG, $o + o \Rightarrow e$			
0.6275 ⇒ 0.31375	90	1.73	[20]
0.6943 ⇒ 0.34715	66	0.14	[24]
1.0642 ⇒ 0.5321	50.8	0.10	[22]
		0.11	[5]
SHG, $e + o \Rightarrow e$			
1.0642 ⇒ 0.5321		0.40	[25]
	83.1	0.54	[22]
THG, $o + o \Rightarrow e$			
1.0642 + 0.5321 ⇒ 0.3547	61.2	0.08	[5]

Temperature tuning of noncritical SHG

Interacting wavelengths [μm]	$d\lambda_1/dT$ [nm/K]	Ref.
SHG, $o + o \Rightarrow e$		
0.626 ⇒ 0.313	0.12	[12]
0.6275 ⇒ 0.31375	0.123	[20]

Experimental value of temperature bandwidth for noncritical SHG process (0.6275 μm ⇒ 0.31375 μm, $o + o \Rightarrow e$):

$\Delta T = 2.5 \pm 0.3$°C [20]

Temperature variation of birefringence for noncritical SHG process (0.6275 μm ⇒ 0.31375 μm, $o + o \Rightarrow e$):

$d(n_2^e - n_1^o)/dT = (1.1 \pm 0.1) \times 10^{-5}\,K^{-1}$ [20]

Laser-induced bulk-damage threshold

λ [μm]	τ_p [ns]	I_{thr} [GW/cm^2]	Ref.	Note
0.6281	330	0.55	[26]	
0.6943	10	>0.18	[24]	
1.0642	12	>0.26	[22]	10–20 Hz

About the crystal

RDP was rather often used in the late 1960s to the mid-1970s for SHG of ruby and dye laser radiations. As these lasers came out of fashion, the RDP applications also stopped.

References

[1] V.G. Dmitriev, G.G. Gurzadyan, D.N. Nikogosyan: *Handbook of Nonlinear Optical Crystals, Third Revised Edition* (Springer, Berlin, 1999).

[2] S. Haussühl: Elastische und thermoelastische Eigenschaften von KH_2PO_4, KH_2AsO_4, $NH_4H_2PO_4$, $NH_4H_2AsO_4$ und RbH_2PO_4. Z. Kristallogr. **120(6)**, 401–414 (1964) [In German].

[3] E.N. Volkova, B.M. Berezhnoi, A.N. Izrailenko, A.V. Mishchenko, L.N. Rashkovich: Electro-optic and optical properties of partly deuterated rubidium dihydrogen phosphate crystals. Izv. Akad. Nauk SSSR, Ser. Fiz. **35(9)**, 1858–1861 (1971) [In Russian, English trans.: Bull. Acad. Sci. USSR, Ser. Phys. **35(9)**, 1690–1693 (1971)].

[4] W.R. Cook, Jr.: Thermal expansion of crystals with KH_2PO_4 structure. J. Appl. Phys. **38(4)**, 1637–1642 (1967).

[5] K. Kato: Efficient UV generation at 3547Å in RDP. Appl. Phys. Lett. **25(6)**, 342–343 (1974).

[6] D. Eimerl: Electro-optic, linear and nonlinear optical properties of KDP and its isomorphs. Ferroelectrics **72(1–4)**, 95–139 (1987).

[7] A.S. Sonin, A.S. Vasilevskaya: *Elektrooptic Crystals* (Atomizdat, Moscow, 1971) [In Russian].

[8] P. Liu, W.L. Smith, H. Lotem, J.H. Bechtel, N. Bloembergen, R.S. Adhav: Absolute two-photon absorption coefficients at 355 and 266 nm. Phys. Rev. B **17(12)**, 4620–4632 (1978).

[9] A.S. Vasilevskaya, M.F. Koldobskaya, L.G. Lomova, V.P. Popova, T.A. Regulskaya, I.S. Rez, Y.P. Sobesskii, A.S. Sonin, V.S. Suvorov: Some physical properties of rubidium dihydrogen phosphate single crystals. Kristallogr. **12(3)**, 447–450 (1967) [In Russian, English trans.: Sov. Phys. - Crystallogr. **12(3)**, 383–385 (1967)].

[10] S. Singh: Nonlinear Optical Materials. In: *Handbook of Lasers*, ed. by R.G. Pressley (The Chemical Rubber Co., Cleveland, 1971), pp. 489–525.

[11] E.N. Volkova, S.L. Faerman: Refractive indices of $KD_{2x}H_{2(1-x)}PO_4$ and $RbD_{2x}H_{2(1-x)}PO_4$ crystals. Kvant. Elektron. **3(11)**, 2508–2511 (1976) [In Russian, English trans.: Sov. J. Quantum Electron. **6(11)**, 1380–1382 (1976)].

[12] N.P. Barnes, D.J. Gettemy, R.S. Adhav: Variations of the refractive index with temperature and the tuning rate for KDP isomorphs. J. Opt. Soc. Am. **72(7)**, 895–898 (1982).

[13] K.W. Kirby, L.G. DeShazer: Refractive indices of 14 nonlinear crystals isomorphic to KH_2PO_4. J. Opt. Soc. Am. B **4(7)**, 1072–1078 (1987).

[14] R.C. Eckardt, H. Masuda, Y.X. Fan, R.L. Byer: Absolute and relative nonlinear optical coefficients of KDP, KD^*P, BaB_2O_4, $LiIO_3$, MgO:$LiNbO_3$, and KTP measured by phase-matched second-harmonic generation. IEEE J. Quant. Electr. **26(5)**, 922–933 (1990).

[15] J.E. Midwinter, J. Warner: The effects of phase matching method and of uniaxial crystal symmetry on the polar distribution of second-order non-linear optical polarization. Brit. J. Appl. Phys. **16(11)**, 1135–1142 (1965).

[16] V.S. Suvorov, A.S. Sonin, I.S. Rez: Some nonlinear optical properties of crystals of the KDP group. Zh. Eksp. Teor. Fiz. **53(1)**, 49–55 (1967) [In Russian, English trans.: Sov. Phys. - JETP **26(1)**, 33–37 (1968)].
[17] D.A. Roberts: Simplified characterization of uniaxial and biaxial nonlinear optical crystals: a plea for standardization of nomenclature and conventions. IEEE J. Quant. Electr. **28(10)**, 2057–2074 (1992).
[18] J.E. Pearson, G.A. Evans, A.Yariv: Measurement of the relative nonlinear coefficients of KDP, RDP, RDA, and $LiIO_3$. Opt. Commun. **4(5)**, 366–367 (1972).
[19] R.S. Adhav: Materials for optical harmonic generation. Laser Focus **19(6)**, 73–78 (1983).
[20] K. Kato: Highly efficient frequency doubling of visible dye laser radiation in RDP. J. Appl. Phys. **46(6)**, 2721–2722 (1975).
[21] M.P. Golovey, I.N. Kalinkina, G.I. Kosourov: On the nonlinear properties of RDP crystal. Opt. Spektrosk. **28(5)**, 991–992 (1970) [In Russian, English trans.: Opt. Spectrosc. USSR **28(5)**, 535–536 (1970)].
[22] K. Kato, S. Nakao: Frequency doubling of Nd:YAG laser radiation in RDP. Jpn. J. Appl. Phys. **13(10)**, 1681–1682 (1974).
[23] R.S. Adhav, A.D. Vlassopoulos: Guide to efficient doubling. Laser Focus **10(5)**, 47–48 (1974).
[24] K. Kato, A.J. Alcock, M.C. Richardson: Conversion of high power ruby laser radiation to the UV in RDP. Opt. Commun. **11(1)**, 5–7 (1974).
[25] E.V. Nilov, I.L. Yachnev: Some results on investigating RDP (RbH_2PO_4) crystal as laser frequency doubler. Zh. Prikl. Spektrosk. **7(6)**, 943–945 (1967) [In Russian, English trans.: J. Appl. Spectrosc. **7(6)**, 628–630 (1967)].
[26] L. Armstrong, S.E. Neister, R. Adhav: Measuring CFP dye laser damage thresholds on UV doubling crystals. Laser Focus **18(12)**, 49–53 (1982).

8.9 $CsTiOAsO_4$, Cesium Titanyl Arsenate (CTA)

Positive biaxial crystal: $2V_z = 52.9°$ at $\lambda = 0.5321\,\mu m$ [1]
Molecular mass: 335.704
Specific gravity: $4.511\,g/cm^3$ [2]
Point group: $mm2$
Lattice constants:
$a = 13.486$ Å [3]; 13.494 Å [4]
$b = 6.8616$ Å [3]; 6.8627 Å [4]
$c = 10.688$ Å [3]; 10.699 Å [4]
Assignment of dielectric and crystallographic axes: $X, Y, Z \Rightarrow a, b, c$
Curie temperature: 917 K [5]
Melting point: 1322 K [6]
Transparency range at "0" transmittance level: 0.35–5.3 μm [5]; 0.37–5.3 μm [4]; 0.38–5.3 μm [7]

Experimental values of refractive indices at room temperature [8]

λ [μm]	n_X	n_Y	n_Z
0.66	1.8771	1.8939	1.9519
1.32	1.8441	1.8590	1.9150

Traditional Sellmeier equations (λ in μm, $T = 293$ K) [1]:

$$n_X^2 = 2.34498 + \frac{1.04863\,\lambda^2}{\lambda^2 - (0.22044)^2} - 0.01483\,\lambda^2$$

$$n_Y^2 = 2.74440 + \frac{0.70733\,\lambda^2}{\lambda^2 - (0.26033)^2} - 0.01526\,\lambda^2$$

$$n_Z^2 = 2.53666 + \frac{1.10600\,\lambda^2}{\lambda^2 - (0.24988)^2} - 0.01711\,\lambda^2$$

More accurate dispersion relations (λ in μm, $0.4\,\mu\text{m} < \lambda < 5.3\,\mu\text{m}$ for n_X and n_Y, $0.4\,\mu\text{m} < \lambda < 2.1\,\mu\text{m}$ for n_Z, $T = 293$ K) [9], [10]

$$n_X^2 = 2.0408 + \frac{1.2924\,\lambda^{2.0008}}{\lambda^{2.0008} - 0.047575} + \frac{1.9304\,\lambda^{1.9874}}{\lambda^{1.9874} - 156.5049}$$

$$n_Y^2 = 2.4330 + \frac{0.9591\,\lambda^{1.9853}}{\lambda^{1.9853} - 0.068339} + \frac{4.2292\,\lambda^{1.9338}}{\lambda^{1.9338} - 305.9224}$$

$$n_Z^2 = 2.5723 + \frac{1.0532\,\lambda^{2.0297}}{\lambda^{2.0297} - 0.080077} + \frac{0.6178\,\lambda^{1.9934}}{\lambda^{1.9934} - 40.7806}$$

Other sets of dispersion relations are given in [11], [12], [13].

Linear electrooptic coefficients measured at low frequencies (well below the acoustic resonances of CTA crystal, i.e., for the "free" crystal) at room temperature [1]

λ [μm]	r_{13}^{T} [pm/V]	r_{23}^{T} [pm/V]	r_{33}^{T} [pm/V]
0.6328	14.2 ± 1.4	18.5 ± 1.9	38 ± 3.8

Expressions for the effective second-order nonlinear coefficient in principal planes of CTA crystal (approximation of small walk-off angle, Kleinman symmetry conditions are valid, $d_{15} = d_{31}$ and $d_{24} = d_{32}$) [14]:

XY plane

$d_{\mathrm{eoe}} = d_{\mathrm{oee}} = d_{31}\sin^2\phi + d_{32}\cos^2\phi$

YZ plane

$d_{\mathrm{oeo}} = d_{\mathrm{eoo}} = d_{31}\sin\theta$

XZ plane, $\theta < V_z$

$d_{\mathrm{ooe}} = d_{32}\sin\theta$

XZ plane, $\theta > V_z$

$d_{\mathrm{oeo}} = d_{\mathrm{eoo}} = d_{32}\sin\theta$

Effective second-order nonlinear coefficient for three-wave interactions in the arbitrary direction of CTA crystal is given in [14].

The signs of CTA second-order nonlinear coefficients are probably all the same [15].

Absolute values of second-order nonlinear coefficients:

$d_{31}(1.064\,\mu\text{m}) = 2.1 \pm 0.4$ pm/V [1]

$d_{32}(1.064\,\mu\text{m}) = 3.4 \pm 0.7$ pm/V [1]

$d_{33}(1.064\,\mu m) = 18.1 \pm 1.8\,pm/V$ [1]
$d_{31}(1.32\,\mu m) = 1.1 \pm 0.1\,pm/V$ [8]
$d_{32}(1.32\,\mu m) = 1.7 \pm 0.6\,pm/V$ [8]

Experimental values of phase-matching angle and internal angular bandwidth

Interacting wavelengths [μm]	ϕ_{pm} [deg]	θ_{pm} [deg]	$\Delta\varphi^{int}$ [deg]	$\Delta\theta^{int}$ [deg]	Ref.
XY plane, $\theta = 90°$					
SHG, $e + o \Rightarrow e$					
$1.3188 \Rightarrow 0.6594$	64.5		0.52		[11]
	64				[12]
	59		0.60		[8]
DFG, $e - o \Rightarrow e$					
$0.5309 - 0.7822 \Rightarrow 1.6525$	41				[16]
YZ plane, $\phi = 90°$					
SHG, $o + e \Rightarrow o$					
$1.3188 \Rightarrow 0.6594$		76			[12]
		73.1		0.29	[8]

About the crystal

An analog of KTA and RTA, CTA did not find any practical application.

References

[1] L.T. Cheng, L.K. Cheng, J.D. Bierlein, F.C. Zumsteg: Nonlinear optical and electro-optical properties of single crystal $CsTiOAsO_4$. Appl. Phys. Lett. **63(19)**, 2618–2620 (1993).

[2] B.H.T. Chai: Optical Crystals. In: *CRC Handbook of Laser Science and Technology, Supplement 2: Optical Materials*, ed. by M.J. Weber (CRC Press, Boca Raton, 1995), pp. 3–65.

[3] J. Protas, G. Marnier, B. Boulanger, B. Menaert: Structure crystalline de $CsTiOAsO_4$. Acta Crystallogr. C **45(8)**, 1123–1125 (1989).

[4] D.T. Reid, M. Ebrahimzade, W. Sibbett: Design criteria and comparison of femtosecond optical parametric oscillators based on $KTiOPO_4$ and $RbTiOAsO_4$. J. Opt. Soc. Am. B **12(11)**, 2168–2179 (1995).

[5] L.K. Cheng, J.D. Bierlein: KTP and isomorphs—recent progress in device and material development. Ferroelectrics **142(1–2)**, 209–228 (1993).

[6] L.K. Cheng, E.M. McCarron III, J. Calabrese, J.D. Bierlein, A.A. Ballman: Development of the nonlinear optical crystal $CsTiOAsO_4$. I. Structural stability. J. Cryst. Growth **132(1–2)**, 280–288 (1993).

[7] J. Nordborg, G. Svensson, R.J. Bolt, J. Albertson: Top seeded solution growth of $[Rb,Cs]TiOAsO_4$. J. Cryst. Growth **224(3–4)**, 256–268 (2001).

[8] B. Boulanger, J.P. Feve, G. Marnier, G.M. Loiacono, D.N. Loiacono C. Bonnin: SHG and internal conical refraction experiments in $CsTiOAsO_4$: comparison with $KTiOPO_4$ and $KTiOAsO_4$ for 1.32-μm type II SHG. IEEE J. Quant. Electr. **33(6)**, 945–949 (1997).

[9] J.P. Feve, B. Boulanger, O. Pacaud, I. Rousseau, B. Menaert, G. Marnier: Refined Sellmeier equations from phase-matching measurements over the complete transparency range of $KTiOAsO_4$, $RbTiOAsO_4$, and $CsTiOAsO_4$. In: *Advanced Solid-State Lasers, OSA Trends in Optics and Photonics Series, Vol. 34*, ed. by H. Injeyan, U. Keller, C. Marshall (OSA, Washington DC, 2000), pp. 575–577.

[10] J.-P. Feve, B. Boulanger, O. Pacaud, I. Rousseau, B. Menaert, G. Marnier, P. Villeval, C. Bonnin, G.M. Loiacono, D.N. Loiacono: Phase-matching measurements and Sellmeier equations over the complete transparency range of $KTiOAsO_4$, $RbTiOAsO_4$, and $CsTiOAsO_4$. J. Am. Opt. Soc. B **17(5)**, 775–780 (2000).

[11] L.K. Cheng, L.T. Cheng, F.C. Zumsteg, J.D. Bierlein, J. Galperin: Development of the nonlinear optical crystal $CsTiOAsO_4$. II. Crystal growth and characterization. J. Cryst. Growth **132(1–2)**, 289–296 (1993).

[12] L.-T. Cheng, L.K. Cheng, J.D. Bierlein: Linear and nonlinear optical properties of the arsenate isomorphs of KTP. Proc. SPIE **1863**, 43–53 (1993).

[13] L.K. Cheng, L.T. Cheng, J. Galperin, P.A. Morris Hotsenpiller, J.D. Bierlein: Crystal growth and characterization of $KTiOPO_4$ isomorphs from the self-fluxes. J. Cryst. Growth **137(1–2)**, 107–115 (1994).

[14] V.G. Dmitriev, D.N. Nikogosyan: Effective nonlinearity coefficients for three-wave interactions in biaxial crystals of $mm2$ point group symmetry. Opt.Commun. **95(1–3)**, 173–182 (1993).

[15] A. Anema, T. Rasing: Relative signs of the nonlinear coefficients of potassium titanyl phosphate. Appl. Opt. **36(24)**, 5902–5904 (1997).

[16] B. Lai, N.C. Wong, L.K. Cheng: Continuous-wave tunable light source at 1.6 μm by difference-frequency mixing in $CsTiOAsO_4$. Opt. Lett. **20(17)**, 1779–1781 (1995).

8.10 $Ba_2NaNb_5O_{15}$, Barium Sodium Niobate (BNN)

Negative biaxial crystal: $2V_z = 13°$ [1]

Molecular mass: 1002.173

Specific gravity: 5.4 g/cm^3 [2]; 5.4076 g/cm^3 [1], 5.42 g/cm^3 [3]

Point group: $mm2$

Lattice constants at 298 K [4]:

$a = 17.62560 \pm 0.00005$ Å

$b = 17.59182 \pm 0.00001$ Å

$c = 3.994915 \pm 0.000004$ Å

Assignment of dielectric and crystallographic axes: $X, Y, Z \Rightarrow a, b, c$

Melting point: 1703 K [2]

Curie temperature: 833 K [2]

Thermal conductivity coefficient [3]: $\kappa = 3.5$ W/mK

Transparency range at "0" transmittance level: 0.37–5 μm [1], [5]

Linear absorption coefficient α

λ [μm]	α [cm^{-1}]	Ref.	Note
0.5321	0.04	[3]	NCSHG direction
	0.051–0.067	[6]	along a axis
1.0642	<0.002	[3]	NCSHG direction
	0.003	[6]	along a axis
	0.002	[7]	along b axis

Experimental values of refraction indices [1]

λ [μm]	n_X	n_Y	n_Z
0.4579	2.4284	2.4266	2.2931
0.4765	2.4094	2.4076	2.2799
0.4880	2.3991	2.3974	2.2727
0.4965	2.3920	2.3903	2.2678
0.5017	2.3879	2.3862	2.2649
0.5145	2.3786	2.3767	2.2583
0.5321	2.3672	2.3655	2.2502
0.6328	2.3222	2.3205	2.2177
1.0642	2.2580	2.2567	2.1700

Temperature derivatives of n_X and n_Z at $\lambda = 1.064\,\mu\text{m}$ (n_Y depends on T only slightly) [1]:

$dn_X/dT = -2.5 \times 10^{-5}\,\text{K}^{-1}$

$dn_Z/dT = +8.0 \times 10^{-5}\,\text{K}^{-1}$

Best set of dispersion relations (λ in μm, $T = 293\,\text{K}$) [1]:

$$n_X^2 = 1 + \frac{3.9495\,\lambda^2}{\lambda^2 - 0.04038894}$$

$$n_Y^2 = 1 + \frac{3.9495\,\lambda^2}{\lambda^2 - 0.04014012}$$

$$n_Z^2 = 1 + \frac{3.6008\,\lambda^2}{\lambda^2 - 0.03219871}$$

Other set of dispersion relation is given in [8].

Expressions for the effective second-order nonlinear coefficient in principal planes of BNN crystal (Kleinman symmetry conditions are not valid) [9]:

XY plane

$d_{\text{eeo}} = d_{31}\sin^2\phi + d_{32}\cos^2\phi$

YZ plane

$d_{\text{ooe}} = d_{31}\sin\theta$

XZ plane, $\theta < V_z$

$d_{\text{oeo}} = d_{\text{eoo}} = d_{24}\sin\theta$

XZ plane, $\theta > V_z$

$d_{\text{ooe}} = d_{32}\sin\theta$

Expressions for the effective second-order nonlinear coefficient in principal planes of BNN crystal (Kleinman symmetry conditions are valid, $d_{15} = d_{31}$ and $d_{24} = d_{32}$) [9]:

XY plane

$d_{eeo} = d_{31} \sin^2 \phi + d_{32} \cos^2 \phi$

YZ plane

$d_{ooe} = d_{31} \sin \theta$

XZ plane, $\theta < V_z$

$d_{oeo} = d_{eoo} = d_{32} \sin \theta$

XZ plane, $\theta > V_z$

$d_{ooe} = d_{32} \sin \theta$

Expressions for the effective second-order nonlinear coefficient in arbitrary direction inside the BNN crystal are given in [9].

Values of second-order nonlinear coefficients:

$d_{31}(1.064\,\mu\text{m}) = 40 \times d_{11}(SiO_2) \pm 5\% = 12 \pm 0.6\,\text{pm/V}$ [1], [10]

$d_{32}(1.064\,\mu\text{m}) = 40 \times d_{11}(SiO_2) \pm 10\% = 12 \pm 1.2\,\text{pm/V}$ [1], [10]

$d_{33}(1.064\,\mu\text{m}) = 55 \times d_{11}(SiO_2) \pm 7\% = 16.5 \pm 1.2\,\text{pm/V}$ [1], [10]

Experimental values of phase-matching angle ($T = 293\,\text{K}$) [1]

Interacting wavelengths [μm]	θ_{exp} [deg]
YZ plane, $\phi = 90°$	
SHG, $o + o \Rightarrow e$	
$1.0642 \Rightarrow 0.5321$	73.8
XZ plane, $\phi = 0°$, $\theta > V_z$	
SHG, $o + o \Rightarrow e$	
$1.0642 \Rightarrow 0.5321$	75.4

Note: The PM angle values are strongly dependent on melt stoichiometry.

Experimental values of NCPM temperature and temperature bandwidth

Interacting wavelengths [μm]	T [°C]	ΔT [°C]	Ref.
along *a* axis			
SHG, $o + o \Rightarrow e$			
$1.0642 \Rightarrow 0.5321$	85	0.45–0.47	[6]
	85		[11]
	86–87	0.45	[12]
	89	0.5	[1]
$1.08 \Rightarrow 0.54$		0.42	[13]
along *b* axis			
SHG, $o + o \Rightarrow e$			
$1.0642 \Rightarrow 0.5321$	97		[14]
	101	0.5	[1]

Note: The NCPM temperature values are strongly dependent on melt stoichiometry.

Temperature variation of birefringence for noncritical SHG process [1]:
along b axis (1.0642 μm ⇒ 0.5321 μm)
$d[n_Z(2\omega) - n_X(\omega)]/dT = 1.05 \times 10^{-4}\,\mathrm{K}^{-1}$

Laser-induced damage threshold

λ [μm]	τ_p [ns]	I_{thr} [GW/cm^2]	Ref.	Note
0.5321	CW	>0.00005	[14]	
	450	0.0002	[15]	2 kHz
	0.05	0.072	[16]	1 kHz
1.0642	450	0.004	[15]	2 kHz
	0.08	>0.0025	[6]	500 MHz

About the crystal

Due to a high effective second-order nonlinearity, BNN crystal attracted much attention in the late 1960s and 1970s. However, it is difficult to grow perfect barium sodium niobate, and some undesirable properties like cracks and twins limit its practical application. Quite recently, it was discovered that Nd doping of BNN ($Nd_xBa_{2-2x}Na_{1-x}Nb_5O_{15}$, $x = 0.025$) allows the production of high-quality crystals [17]. Other properties of Nd:BNN are as follows: point group, $4mm$; lattice constants, $a = 12.446 \pm 0.001$ Å, $c = 3.991 \pm 0.001$ Å; Mohs hardness, 5; specific gravity, 5.43 g/cm^3; specific heat, 300 J/kgK; melting point, 1773 K; and Curie temperature, 810 K [17]. In [18], Nd:BNN was successfully used for self-frequency doubling.

References

[1] S. Singh, D.A. Draegert, J.E. Geusic: Optical and ferroelectric properties of barium sodium niobate. Phys. Rev. B **2(7)**, 2709–2724 (1970).

[2] L.G. van Uitert, J.J. Rubin, W.A. Bonner: Growth of $BaNaNb_5O_{15}$ single crystals for optical applications. IEEE J. Quant. Electr. **QE-4(10)**, 622–627 (1968).

[3] J.D. Barry, C.J. Kennedy: Thermo-optical effects of intracavity $Ba_2Na(NbO_3)_5$ on a frequency-doubled Nd:YAG laser. IEEE J. Quant. Electr. **QE-11(8)**, 575–579 (1975).

[4] M. Ferriol: Crystal growth and structure of pure and rare-earth doped barium sodium niobate (BNN). Progr. Cryst. Growth Character. Mater. **43(2–3)**, 221–244 (2001).

[5] J.E. Geusic, H.J. Levinstein, J.J. Rubin, S. Singh, L.G. van Uitert: The nonlinear optical properties of $Ba_2NaNb_5O_{15}$. Appl. Phys. Lett. **11(9)**, 269–271 (1967).

[6] J.E. Murray, R.J. Pressley, J.H. Boyden, R.B. Webb: CW mode-locked source at 0.532 μm. IEEE J. Quant. Electr. **QE-10(2)**, 263–267 (1974).

[7] Y. Uematsu, T. Fukuda: Characteristics and performance of $KNbO_3$–Nd:YAG intracavity second harmonic generation. Jpn. J. Appl. Phys. **12(6)**, 841–844 (1973).

[8] R.A. Andrews: IR image parametric up-conversion. IEEE J. Quant. Electr. **QE-6(1)**, 68–80 (1970).

[9] V.G. Dmitriev, D.N. Nikogosyan: Effective nonlinearity coefficients for three-wave interactions in biaxial crystals of $mm2$ point group symmetry. Opt. Commun. **95(1–3)**, 173–182 (1993).

[10] D.A. Roberts: Simplified characterization of uniaxial and biaxial nonlinear optical crystals: a plea for standardization of nomenclature and conventions. IEEE J. Quant. Electr. **28(10)**, 2057–2074 (1992).
[11] J.E. Geusic, H.J. Levinstein, S. Singh, R.G. Smith, L.G. van Uitert: Continuous 0.532 μm solid-state source using $Ba_2NaNb_5O_{15}$. Appl. Phys. Lett. **12(9)**, 306–308 (1968).
[12] V.A. Dyakov, V.I. Pryalkin, A.I. Kholodnykh: Potassium niobate optical parametric oscillator pumped by the second harmonic of a garnet laser. Kvant. Elektron. **8(4)**, 715–721 (1981) [In Russian, English trans.: Sov. J. Quantum Electron. **11(4)**, 433–436 (1981)].
[13] F.R. Nash, E.H. Turner, P.M. Bridenbaugh, J.M. Dziedzic: Measurements of second-harmonic generation and the variations in the free and clamped values of the dielectric constants and electro-optic coefficients in barium sodium niobate. J. Appl. Phys. **43(1)**, 1–9 (1972).
[14] R.G. Smith, J.E. Geusic, H.J. Levinstein, J.J. Rubin, S. Singh, L.G. van Uitert: Continuous optical parametric oscillation in $Ba_2NaNb_5O_{15}$. Appl. Phys. Lett. **12(9)**, 308–310 (1968).
[15] R.B. Chesler, M.A. Karr, J.E. Geusic: An experimental and theoretical study of high repetition rate Q-switched Nd:YAG lasers. Proc. IEEE **58(12)**, 1899–1914 (1970).
[16] A. Piskarskas, V. Smilgevichius, A. Umbrasas: The parametric generation of bandwidth-limited picosecond light pulses. Opt. Commun. **73(4)**, 322–324 (1989).
[17] H.R. Xia, L.J. Hu, C.J. Wang, L.X. Li, S.B. Yue, X.L. Meng, L. Zhu, Z.H. Yang, J.Y. Wang: Energy state of Nd^{3+} doped in barium sodium niobate. J. Appl. Phys. **83(5)**, 2560–2562 (1998).
[18] A.A. Kaminskii, D. Jaque, S.N. Bagayev, K.-I. Ueda, S.J. Garsia, J. Capmany: New nonlinear-laser properties of ferroelectric Nd^{3+}:$Ba_2NaNb_5O_{15}$–CW stimulated emission ($^4F_{3/2} \Rightarrow {}^4I_{11/2}$ and $^4F_{3/2} \Rightarrow {}^4I_{13/2}$), collinear and diffuse self-frequency doubling and summation. Kvant. Elektron. **26(2)**, 95–97 (1999) [In Russian, English trans.: Quantum Electron. **29(2)**, 95–97 (1999)].

8.11 $K_3Li_2Nb_5O_{15}$, Potassium Lithium Niobate (KLN)

Negative uniaxial crystal: $n_o > n_e$
Point group: $4mm$
Molecular mass: 4.3 g/cm^3 [1]; 4.42 ± 0.07 g/cm^3 [2]

Lattice constants

a [Å]	c [Å]	Ref.	Note
12.583	4.041	[3]	$[K_2O] : [Li_2O] : [Nb_2O_5] = 31\% : 26\% : 43\%$
12.542	4.033	[4]	$[K_2O] : [Li_2O] : [Nb_2O_5] = 32\% : 24\% : 44\%$
12.58	4.01	[5]	$[K_2O] : [Li_2O] : [Nb_2O_5] = 33.4\% : 17.8\% : 48.8\%$
12.60	3.99	[6]	$[K_2O] : [Li_2O] : [Nb_2O_5] = 28.9\% : 18.1\% : 53.0\%$

Curie temperature:
678 K (for molar ratio $[K_2O] : [Li_2O] : [Nb_2O_5]$ = 33.4% : 17.8% : 48.8%) [5]
725 K (for molar ratio $[K_2O] : [Li_2O] : [Nb_2O_5]$ = 30% : 25% : 45%) [7]
765 K (for molar ratio $[K_2O] : [Li_2O] : [Nb_2O_5]$ = 32% : 23% : 45%) [7]
771 K (for molar ratio $[K_2O] : [Li_2O] : [Nb_2O_5]$ = 33% : 23% : 44%) [8]

786 K (for molar ratio $[K_2O] : [Li_2O] : [Nb_2O_5] = 32\% : 24\% : 44\%$) [4]
794 K (for molar ratio $[K_2O] : [Li_2O] : [Nb_2O_5] = 32\% : 24\% : 44\%$) [7]
813 K (for molar ratio $[K_2O] : [Li_2O] : [Nb_2O_5] = 31\% : 26\% : 43\%$) [3]
Band-gap energy at room temperature: $E_g = 3.2$ eV [9]
Transparency range: 0.35–5 μm [10], [11]; 0.4–5 μm [12]

Linear absorption coefficient α

λ [μm]	α [cm^{-1}]	Ref.
0.38	3.0	[6]
1.064	0.004	[11]

Experimental values of refraction indices at $T = 303$ K [10], [13]

λ [μm]	n_o	n_e	λ [μm]	n_o	n_e
0.4500	2.4049	2.2512	0.6000	2.2899	2.1720
0.4750	2.3751	2.2315	0.6250	2.2799	2.1645
0.5000	2.3546	2.2144	0.6328	2.2770	2.1630
0.5250	2.3349	2.2010	0.6500	2.2711	2.1586
0.5321	2.3260	2.1975	0.6750	2.2631	2.1529
0.5500	2.3156	2.1900	1.0642	2.2080	2.1120
0.5750	2.3016	2.1801			

Sellmeier equations ($T = 303$ K) [13]:

$$n_o^2 = 1 + \frac{3.708\,\lambda^2}{\lambda^2 - 0.04601}$$

$$n_e^2 = 1 + \frac{3.349\,\lambda^2}{\lambda^2 - 0.03564}$$

Expression for the effective second-order nonlinear coefficient (Kleinman symmetry conditions are valid, $d_{15} = d_{24} = d_{31} = d_{32}$) [14]:

$d_{ooe} = d_{31} \sin\theta$

Second-order nonlinear coefficients:

$d_{31}(0.8\,\mu\text{m}) = 11.8$ pm/V [11]
$d_{31}(1.06\,\mu\text{m}) = (1.7 \pm 0.3) \times d_{31}(\text{LN}) = 7.8 \pm 1.4$ pm/V [15], [16]
$d_{31}(1.0642\,\mu\text{m}) = 19.3 \times d_{11}(SiO_2) \pm 20\% = 5.8 \pm 1.2$ pm/V [10], [17]
$d_{33}(1.0642\,\mu\text{m}) = 35 \times d_{11}(SiO_2) \pm 15\% = 10.5 \pm 1.5$ pm/V [10], [17]

Experimental values of interacting wavelengths at noncritical phase-matching ($T = 293$ K)

Interacting wavelengths [μm]	Ref.	Note
SHG, $o + o \Rightarrow e$		
$0.82 \Rightarrow 0.41$	[11]	

Interacting wavelengths [μm]	Ref.	Note
0.8274 ⇒ 0.4137	[7]	$[K_2O] : [Li_2O] : [Nb_2O_5] = 32\% : 25\% : 43\%$
0.833 ⇒ 0.4165	[7]	$[K_2O] : [Li_2O] : [Nb_2O_5] = 31\% : 26\% : 43\%$
0.8334 ⇒ 0.4167	[3]	$[K_2O] : [Li_2O] : [Nb_2O_5] = 31\% : 26\% : 43\%$
0.8595 ⇒ 0.42975	[7]	$[K_2O] : [Li_2O] : [Nb_2O_5] = 32\% : 24\% : 44\%$
0.870 ⇒ 0.435	[7]	$[K_2O] : [Li_2O] : [Nb_2O_5] = 31\% : 25\% : 44\%$
0.9203 ⇒ 0.46015	[7]	$[K_2O] : [Li_2O] : [Nb_2O_5] = 32\% : 23\% : 45\%$
0.929 ⇒ 0.4645	[7]	$[K_2O] : [Li_2O] : [Nb_2O_5] = 31.5\% : 23.5\% : 45\%$
0.953 ⇒ 0.4765	[7]	$[K_2O] : [Li_2O] : [Nb_2O_5] = 31\% : 24\% : 45\%$
0.959 ⇒ 0.4795	[7]	$[K_2O] : [Li_2O] : [Nb_2O_5] = 30.5\% : 24.5\% : 45\%$
0.974 ⇒ 0.487	[7]	$[K_2O] : [Li_2O] : [Nb_2O_5] = 30\% : 25\% : 45\%$

Experimental values of temperature and spectral bandwidths at noncritical phase-matching

Interacting wavelengths [μm]	T [°C]	ΔT [°C]	$\Delta\nu$ [cm^{-1}]	Ref.
SHG, $o + o \Rightarrow e$				
0.8334 ⇒ 0.4167	20		1.9 (?)	[3]
0.8382 ⇒ 0.4191	50	0.4 (?)		[3]
0.8595 ⇒ 0.42975	20		3.9	[7]
0.8695 ⇒ 0.43475	60	0.8	3.2	[4]
0.8898 ⇒ 0.4449	20		≈3.0	[18]
0.9203 ⇒ 0.46015	20		4.2	[7]

About the crystal

KLN is one of the "old" nonlinear materials: it was discovered in the mid-1960s simultaneously with LN and BNN [10], [1]. However, until now it was difficult to grow KLN crystals of decent quality and size. Very recently, high-quality crack-free KLN crystals were finally synthesized by Singaporean and Japanese scientists [3], [4], [7], [18].

References

[1] L.G. van Uitert, J.J. Rubin, W.A. Bonner: Growth of $BaNaNb_5O_{15}$ single crystals for optical applications. IEEE J. Quant. Electr. **QE-4(10)**, 622–627 (1968).

[2] S.C. Abrahams, P.B. Jamieson, J.L. Bernstein: Ferroelectric tungsten bronze-type crystal structures. III. Potassium lithium niobate $K_{(6-x-y)}Li_{(4+x)}Nb_{(10+y)}O_{30}$. J. Chem. Phys. **54(6)**, 2355–2364 (1971).

[3] T.C. Chong, X.W. Xu, G.Y. Zhang, H. Kumagai: Blue SHG characteristics and homogeneity of the TSSG grown potassium lithium niobate (KLN) crystal with high Li_2O content. J. Cryst. Growth **225(2–4)**, 489–494 (2001).

[4] X.-W. Xu, T.-C. Chong, G.-Y. Zhang, H. Kumagai: Second-harmonic generation of ferroelectric potassium lithium niobate crystals. Jpn. J. Appl. Phys. **40(7)**, 4540–4543 (2001).

[5] M. Adachi, A. Kawabata: Elastic and piezoelectric properties of potassium lithium niobate (KLN) crystals. Jpn. J. Appl. Phys. **17(11)**, 1969–1973 (1978).

[6] J. Xu, S. Fan, Y. Lin, X. Xu: Bridgeman growth and properties of potassium lithium niobate single crystals. Progr. Cryst. Growth Character. Mater. **40(1–4)**, 137–144 (2000).
[7] X.W. Xu, T.C. Chong, G.Y. Zhang, H. Kumagai: Influence of [K]/[Li] and [Li]/[Nb] ratios in melts on the TSSG growth and SHG characteristics of potassium lithium niobate crystals. J. Cryst. Growth **225(2–4)**, 458–464 (2001).
[8] G.Y. Kang, J.K. Yoon: The growth of potassium lithium niobate (KLN) with low Nb_2O_5 content. J. Cryst. Growth **193(4)**, 615–622 (1998).
[9] J. Xu, S. Fan, Y. Lin, Y. Fei: Growth and characterization of potassium lithium niobate crystals. Proc. SPIE **3556**, 24–30 (1998).
[10] L.G. van Uitert, S. Singh, H.J. Levinstein, J.E. Geusic, W.A. Bonner: A new and stable nonlinear optical material. Appl. Phys. Lett. **11(5)**, 161–163 (1967); Erratum. Appl. Phys. Lett. **12(6)**, 224 (1968).
[11] J.J.E. Reid: Resonantly enhanced, frequency doubling of an 820 nm GaAlAs diode laser in a potassium lithium niobate crystal. Appl. Phys. Lett. **62(1)**, 19–21 (1993).
[12] T. Fukuda: Growth and crystallographic characteristics of $K_3Li_2Nb_5O_{15}$ single crystals. Jpn. J. Appl. Phys. **8(1)**, 122 (1969).
[13] S. Singh: "Nonlinear Optical Materials" in *Handbook of Lasers*, ed. by R.G. Pressley (The Chemical Rubber Co., Cleveland, 1971), pp. 489–525.
[14] J.E. Midwinter, J. Warner: The effects of phase matching method and of uniaxial crystal symmetry on the polar distribution of second-order non-linear optical polarization. Brit. J. Appl. Phys. **16(11)**, 1135–1142 (1965).
[15] A.W. Smith, G. Burns, B.A. Scott, H.D. Edmonds: Nonlinear optical properties of potassium-lithium niobates. J. Appl. Phys. **42(2)**, 684–686 (1971).
[16] I. Shoji, T. Kondo, A. Kitamoto, M. Shirane, R. Ito: Absolute scale of second-order nonlinear-optical coefficients. J. Opt. Soc. Am. B **14(9)**, 2268–2294 (1997).
[17] D.A. Roberts: Simplified characterization of uniaxial and biaxial nonlinear optical crystals: a plea for standardization of nomenclature and conventions. IEEE J. Quant. Electr. **28(10)**, 2057–2074 (1992).
[18] L. Li, T.C. Chong, X.W. Wu, H. Kumagai, M. Hirano: Growth of potassium lithium niobate (KLN) single crystals for second harmonic generation (SHG) application. J. Cryst. Growth **211(1–4)**, 281–285 (2000).

8.12 $CO(NH_2)_2$, Urea

Positive uniaxial crystal: $n_e > n_o$
Molecular mass: 60.055
Specific gravity: 1.318 g/cm^3 [1]
Point group: $\bar{4}2m$
Mohs hardness: <2.5
Transparency range at 0.5 level for 0.5-cm-long crystal cut at $\theta = 74°$: 0.2–1.43 μm [2]

Linear absorption coefficient α [2]

λ [μm]	α [cm^{-1}]	Note
0.213	0.10	*o*-wave, FiHG direction
0.266	0.04	*e*-wave, FiHG direction
1.064	0.02	*e*-wave, FiHG direction

The graph of n_o and n_e dependences versus wavelength is given in [3], [4].

Best set of dispersion relations (λ in μm, $T = 293$ K) [5], [6]:

$$n_o^2 = 2.1548 + \frac{0.01310}{\lambda^2 - 0.0318}$$

$$n_e^2 = 2.5527 + \frac{0.01784}{\lambda^2 - 0.0294} + \frac{0.0288\,(\lambda - 1.5)}{(\lambda - 1.5)^2 + 0.03371}$$

Other sets of dispersion relations are given in [7], [8].

Expressions for the effective second-order nonlinear coefficient in general case (Kleinman symmetry conditions are valid, $d_{14} = d_{25} = d_{36}$) [9], [10]:

$$d_{eeo} = 2d_{36}\sin(\theta + \rho)\cos(\theta + \rho)\cos 2\phi$$

$$d_{oeo} = d_{eoo} = -d_{36}\sin(\theta + \rho)\sin 2\phi$$

Simplified expressions for the effective second-order nonlinear coefficient (approximation of small birefringence angle, Kleinman symmetry conditions are valid, $d_{14} = d_{25} = d_{36}$) [10]:

$$d_{eeo} = d_{36}\sin 2\theta\cos 2\phi$$

$$d_{oeo} = d_{eoo} = -d_{36}\sin\theta\sin 2\phi$$

Values of second-order nonlinear coefficient:

$d_{36}(1.0642\,\mu\text{m}) \approx 3 \times d_{36}(\text{KDP}) = 1.2$ pm/V [3], [11]

$d_{36}(0.6328\,\mu\text{m}) = 2.4 \times d_{36}(\text{ADP}) \pm 8\% = 1.3 \pm 0.1$ pm/V [6], [12]

Experimental values of phase-matching angle ($T = 293$ K)

Interacting wavelengths [μm]	θ_{exp} [deg]	Ref.
SHG, $e + e \Rightarrow o$		
$0.476 \Rightarrow 0.238$	90	[7]
$0.500 \Rightarrow 0.250$	67.6	[7]
$0.550 \Rightarrow 0.275$	54	[7]
$0.600 \Rightarrow 0.300$	46.6	[7]
SFG, $e + e \Rightarrow o$		
$0.6943 + 0.34715 \Rightarrow 0.23143$	77	[2]
$1.0642 + 0.26605 \Rightarrow 0.21284$	72	[2]
SHG, $o + e \Rightarrow o$		
$0.597 \Rightarrow 0.2985$	90	[7]
$0.650 \Rightarrow 0.325$	63.6	[7]
$0.700 \Rightarrow 0.350$	55.6	[7]
SFG, $o + e \Rightarrow o$		
$1.0642 + 0.29146 \Rightarrow 0.2288$	90	[7]
$1.0642 + 0.29668 \Rightarrow 0.2320$	80	[7]
$1.0642 + 0.30656 \Rightarrow 0.2380$	70.4	[7]
$1.0642 + 0.42792 \Rightarrow 0.3052$	47.5	[7]

Interacting wavelengths [μm]	θ_{exp} [deg]	Ref.
$1.0642 + 0.63501 \Rightarrow 0.3977$	37.7	[7]
$0.720 + 0.53764 \Rightarrow 0.3078$	63	[13]
$0.646 + 0.58793 \Rightarrow 0.3078$	69	[14]
$0.62875 + 0.5321 \Rightarrow 0.2882$	90	[7]
$0.63980 + 0.5321 \Rightarrow 0.2905$	80.5	[7]
$0.66406 + 0.5321 \Rightarrow 0.2954$	73.4	[7]
SFG, $e + o \Rightarrow o$		
$1.0642 + 0.50787 \Rightarrow 0.3438$	90	[7]
$1.0642 + 0.53 \Rightarrow 0.3538$	72.2	[7]
$1.0642 + 0.575 \Rightarrow 0.3733$	62.5	[7]
$1.0642 + 0.63195 \Rightarrow 0.3965$	53.5	[7]

Experimental value of internal angular bandwidth [2]

Interacting wavelengths [μm]	$\Delta\theta^{int}$ [deg]
FiHG, $e + e \Rightarrow o$	
$1.064 + 0.266 \Rightarrow 0.213$	0.017

Temperature tuning for noncritical SHG [7]

Interacting wavelengths [μm]	$d\lambda_1/dT$ [nm/K]
SHG, $e + o \Rightarrow e$	
$0.597 \Rightarrow 0.2985$	−0.013

Laser-induced bulk-damage threshold

λ [μm]	τ_p [ns]	I_{thr} [GW/cm^2]	Ref.	Note
0.266	10	0.5	[15]	single pulse
0.355	10	1.4	[15]	single pulse
		0.15	[16]	3000 pulses
0.532	10	3	[15]	single pulse
1.064	10	5	[15]	single pulse

About the crystal

Urea is one of the few organic nonlinear crystals, developed in the 1970s. There was no practical application of this material in the past 15 years.

References

[1] V.G. Dmitriev, G.G. Gurzadyan, D.N. Nikogosyan: *Handbook of Nonlinear Optical Crystals, Third Revised Edition* (Springer, Berlin, 1999).

[2] K. Kato: High-efficiency high-power UV generation at 2128Å in urea. IEEE J. Quant. Electr. **QE-16(8)**, 810–811 (1980).

[3] D. Bauerle, K. Betzler, H. Hesse, S. Kapphan, P. Loose: Phase-matched second harmonic generation in urea. Phys. Status Solidi A **42(2)**, K119–K121 (1977).
[4] K. Betzler, H. Hesse, P. Loose: Optical second harmonic generation in organic crystals: urea and ammonium-malate. J. Mol. Struct. **47**, 393–396 (1978).
[5] W.R. Donaldson, C.L. Tang: Urea optical parametric oscillator. Appl. Phys. Lett. **44(1)**, 25–27 (1984).
[6] M.J. Rosker, C.L. Tang: Widely tunable optical parametric oscillator using urea. J. Opt. Soc. Am. B **2(5)**, 691–696 (1985).
[7] J.-M. Halbout, S. Blit, W. Donaldson, C.L. Tang: Efficient phase-matched second-harmonic generation and sum-frequency mixing in urea. IEEE J. Quant. Electr. **QE-15(10)**, 1176–1180 (1979).
[8] M.J. Rosker, K. Cheng, C.L. Tang: Practical urea optical parametric oscillator for tunable generation throughout the visible and near-infrared. IEEE J. Quant. Electr. **QE-21(10)**, 1600–1606 (1985).
[9] R.C. Eckardt, H. Masuda, Y.X. Fan, R.L. Byer: Absolute and relative nonlinear optical coefficients of KDP, KD*P, BaB_2O_4, $LiIO_3$, MgO:$LiNbO_3$, and KTP measured by phase-matched second-harmonic generation. IEEE J. Quant. Electr. **26(5)**, 922–933 (1990).
[10] J.E. Midwinter, J. Warner: The effects of phase matching method and of uniaxial crystal symmetry on the polar distribution of second-order non-linear optical polarization. Brit. J. Appl. Phys. **16(11)**, 1135–1142 (1965).
[11] D.A. Roberts: Simplified characterization of uniaxial and biaxial nonlinear optical crystals: a plea for standardization of nomenclature and conventions. IEEE J. Quant. Electr. **28(10)**, 2057–2074 (1992).
[12] K. Hagimoto, A. Mito: Determination of the second-order susceptibility of ammonium dihydrogen phosphate and α-quartz at 633 and 1064 nm. Appl. Opt. **34(36)**, 8276–8282 (1995).
[13] M. Ebrahimzadeh, M.H. Dunn, F. Akerboom: Highly efficient visible urea optical parametric oscillator pumped by a XeCl excimer laser. Opt. Lett. **14(11)**, 560–562 (1989).
[14] M. Ebrahimzadeh, M.H. Dunn: Optical parametric fluorescence and oscillation in urea using an excimer laser. Opt. Commun. **69(2)**, 161–165 (1988).
[15] C. Cassidy, J.M. Halbout, W. Donaldson, C.L. Tang: Nonlinear optical properties of urea. Opt. Commun. **29(2)**, 243–246 (1979).
[16] M.J. Rosker: Recent developments in urea. Proc. SPIE **681**, 10–11 (1986).

8.13 $LiIO_3$, Lithium Iodate

Negative uniaxial crystal: $n_o > n_e$
Molecular mass: 181.844
Specific gravity: 4.48 g/cm^3 at $T = 293$ K [1];
4.487 g/cm^3 [2]; 4.49 g/cm^3 [3]
Point group: 6
Lattice constants:
$a = 5.4815 \pm 0.0003$ Å [1]; 5.4813 Å [4]
$c = 5.1709 \pm 0.0004$ Å [1]; 5.1717 Å [4]
Mohs hardness: 3.5 [2]; 3.5–4.0 [1]; 4.0 [4]

Solubility in 100 g H_2O [1]

T [K]	s [g]
283.1	89.4
293.4	84.7
298.1	82.9
313.2	79.0
348.7	74.9

Melting point: 692 K [1]

Linear thermal expansion coefficient

T [K]	$\alpha_t \times 10^6$ [K^{-1}], $\parallel c$	$\alpha_t \times 10^6$ [K^{-1}], $\perp c$	Ref.
100	25	14	[5]
150	32	17	[5]
200	40	21	[5]
250	47	25	[5]
273	45	25	[1]
298	48	28	[6]
300	50	25	[5]
323	49	26	[7]
350	51	25	[5]
373	51	26	[7]
400	51	28	[5]
423	54	27	[7]
450	53	29	[5]
473	56	31	[7]

Temperature dependence of linear thermal expansion coefficient (T in K) [5]:

for temperature range 80–253 K

$$\alpha_t(\parallel c) = 2.5 \times 10^{-5} + 1.5 \times 10^{-7}\, T$$
$$\alpha_t(\perp c) = 1.4 \times 10^{-5} + 7.5 \times 10^{-8}\, T$$

for temperature range 273–470 K

$$\alpha_t(\parallel c) = 4.9 \times 10^{-5} + 3 \times 10^{-8}\, T$$

for temperature range 353–470 K

$$\alpha_t(\perp c) = 2.7 \times 10^{-5} + 1.4 \times 10^{-8}\, T$$

Specific heat capacity c_p at $P = 0.101325$ MPa: 365 J/kgK [3]; 569 J/kgK [1]

Thermal conductivity coefficient:
$\kappa = 1.47$ W/mK [3]

T [K]	κ [W/mK], $\parallel c$	κ [W/mK], $\perp c$	Ref.
300	0.65	1.27	[5]
400	0.70	1.20	[5]

Band-gap energy at room temperature: $E_g = 4.0$ eV [2]; 4.37 ± 0.03 eV [8]
Transparency range at "0" transmittance level: 0.28–6 μm [9], [10]

Linear absorption coefficient α

λ [μm]	α [cm^{-1}]	Ref.	Note
0.325	≈0.4	[11]	
0.34715	0.1	[12]	$\parallel c$
	0.3	[12]	e-wave, $\perp c$
0.5145	0.0024	[13]	$\parallel c$
	0.0025	[13]	e-wave, $\perp c$
0.5321	0.3	[14]	e-wave
0.5422	0.37	[10]	
0.650	≈0.001	[11]	
0.6594	0.0007–0.0023	[13]	$\parallel c$
	0.0006–0.0017	[13]	e-wave, $\perp c$
1.0642	0.1	[14]	o-wave
	0.25	[14]	e-wave
	<0.0002	[13]	$\parallel c$
	0.0008	[13]	e-wave, $\perp c$
1.0845	0.06	[10]	
1.315	0.0005	[3]	
1.3188	0.0008–0.0036	[13]	$\parallel c$
	0.0007–0.0010	[13]	e-wave, $\perp c$

Two-photon absorption coefficient β

λ [μm]	τ_p [ns]	$\beta \times 10^{11}$ [cm/W]	Ref.
0.53	0.03–0.1	<3	[15]
0.5321	10	<40	[16]

Experimental values of refractive indices

λ [μm]	n_o	n_e	Ref.	λ [μm]	n_o	n_e	Ref.
0.3547	1.9822	1.8113	[17]	0.4727	1.9122	1.7600	[8]
0.3669	1.9706	1.8026	[17]	0.4765	1.9100	1.7583	[8]
0.3712	1.9671	1.8000	[17]	0.4800	1.9109	1.7579	[17]
0.3795	1.9600	1.7947	[17]	0.4880	1.9083	1.7556	[8]
0.3877	1.9544	1.7905	[17]	0.5017	1.9053	1.7537	[8]
0.3996	1.9464	1.7842	[17]	0.5086	1.9031	1.7514	[17]
0.4047	1.9443	1.7826	[18]	0.5145	1.9012	1.7487	[8]
0.4358	1.9275	1.7702	[17]	0.5320	1.8975	1.7475	[17]
0.4545	1.9184	1.7638	[8]	0.5461	1.8950	1.7455	[19]
0.4579	1.9170	1.7630	[8]	0.5600	1.8921	1.7433	[17]
0.4658	1.9141	1.7611	[8]	0.5791	1.8894	1.7413	[18]

λ [μm]	n_o	n_e	Ref.	λ [μm]	n_o	n_e	Ref.
0.5800	1.8889	1.7403	[17]	1.1000	1.8559	1.7160	[19]
0.5896	1.8875	1.7400	[18]	1.2000	1.8536	1.7143	[19]
0.6000	1.8859	1.7383	[17]	1.3000	1.8517	1.7130	[19]
0.6200	1.8828	1.7361	[17]	1.3674	1.8508	1.7122	[18]
0.6328	1.8815	1.7351	[20]	1.5296	1.8482	1.7101	[18]
0.6438	1.8807	1.7346	[18]	1.6920	1.8464	1.7089	[18]
0.6560	1.8789	1.7332	[19]	1.9701	1.8431	1.7072	[18]
0.7000	1.8746	1.7300	[19]	2.2493	1.8385	1.7050	[18]
0.7660	1.8694	1.7261	[19]	2.5000	1.8378	1.7037	[20]
0.8000	1.8673	1.7245	[19]	3.0000	1.8319	1.7001	[20]
0.8630	1.8640	1.7220	[19]	3.5000	1.8266	1.6971	[20]
0.9000	1.8623	1.7207	[19]	4.0000	1.8140	1.6897	[20]
1.0000	1.8587	1.7180	[19]	5.0000	1.7940	1.6783	[20]

Optical activity at $T = 300\,\mathrm{K}$

λ [μm]	ρ [deg/mm]	Ref.	λ [μm]	ρ [deg/mm]	Ref.
0.286	1052.9	[21]	0.429	222.46	[21]
0.290	964.99	[21]	0.448	198.72	[21]
0.295	886.65	[21]	0.470	175.75	[21]
0.299	814.39	[21]	0.492	153.61	[21]
0.304	748.76	[21]	0.520	133.02	[21]
0.310	687.46	[21]	0.546	117.42	[21]
0.317	630.44	[21]	0.551	113.36	[21]
0.324	579.01	[21]	0.600	95.27	[21]
0.331	532.44	[21]	0.628	86.80	[21]
0.339	489.47	[21]	1.084	25.0	[10]
0.347	448.42	[21]	1.1	23.83	[22]
0.355	410.37	[21]	1.6	11.00	[22]
0.363	374.34	[21]	2.1	6.33	[22]
0.374	340.18	[21]	2.6	4.12	[22]
0.386	308.07	[21]	3.1	2.89	[22]
0.399	277.45	[21]	3.6	2.32	[22]
0.412	249.32	[21]			

Temperature derivative of refractive indices at $T = 300\,\mathrm{K}$

λ [μm]	$dn_o/dT \times 10^6$ [K^{-1}]	$dn_e/dT \times 10^6$ [K^{-1}]	Ref.
0.5321	−96	−86	[13]
0.657	−79	−71	[7]
0.6594	−95	−84	[13]
1.0642	−89	−75	[13]
1.3188	−94	−85	[13]

Best set of dispersion relations (λ in μm, $T = 293$ K) [23], [24]:

$$n_o^2 = 3.4132 + \frac{0.0476}{\lambda^2 - 0.0338} - 0.0077\,\lambda^2$$

$$n_e^2 = 2.9211 + \frac{0.0346}{\lambda^2 - 0.0320} - 0.0042\,\lambda^2$$

Other sets of dispersion relations are given in [17], [20], [25], [26], [27], [28].

Linear electrooptic coefficients measured at high frequencies (well above the acoustic resonances of $LiIO_3$ crystal, i.e., for the "clamped" crystal) at room temperature [10]

λ [μm]	r_{13}^S [pm/V]	r_{33}^S [pm/V]	r_{41}^S [pm/V]	r_{51}^S [pm/V]
0.6328	$+4.1 \pm 0.6$	$+6.4 \pm 1.0$	1.4 ± 0.2	$+3.3 \pm 0.7$

Verdet constant ($\|c$) [29]

λ [μm]	T [K]	V [degree/Tm]
0.6328	295	757

Expressions for the effective second-order nonlinear coefficient in general case (Kleinman symmetry conditions are valid, $d_{15} = d_{24} = d_{31} = d_{32}$) [30]:

$d_{ooe} = d_{31} \sin(\theta + \rho)$

Simplified expressions for the effective second-order nonlinear coefficient (approximation of small birefringence angle, Kleinman symmetry conditions are valid, $d_{15} = d_{24} = d_{31} = d_{32}$) [31]:

$d_{ooe} = d_{31} \sin\theta$

Absolute and relative values of second-order nonlinear coefficients:

$d_{31}(1.319\,\mu\text{m}) = 3.9 \pm 0.2$ pm/V [32]

$d_{31}(1.0642\,\mu\text{m}) = 4.1 \pm 0.4$ pm/V [30]; 4.4 ± 0.3 pm/V [33]

$d_{31}(0.806\,\mu\text{m}) = 5.2 \pm 0.5$ pm/V [32]

$d_{33}(1.318\,\mu\text{m}) = 0.99 \times d_{31}(1.318\,\mu\text{m}) = 3.9 \pm 0.2$ pm/V [20], [32]

$d_{33}(1.0642\,\mu\text{m}) = 1.04 \times d_{31}(1.0642\,\mu\text{m}) = 4.6 \pm 0.3$ pm/V [14], [33]

Experimental values of phase-matching angle ($T = 293$ K)

Interacting wavelengths [μm]	θ_{exp} [deg]	Ref.
SHG, $o + o \Rightarrow e$		
$0.586 \Rightarrow 0.293$	90	[23]
$0.5863 \Rightarrow 0.29315$	90	[28]
$0.6 \Rightarrow 0.3$	75.6	[28]

Interacting wavelengths [μm]	θ_{exp} [deg]	Ref.
0.62 ⇒ 0.31	68.2	[28]
0.6943 ⇒ 0.34715	52	[9], [34]
0.946 ⇒ 0.473	34.3	[35]
1.06 ⇒ 0.53	30	[36]
1.0642 ⇒ 0.5321	30.2	[30], [37]
	30	[27], [38]
1.0845 ⇒ 0.54225	28.9	[10]
1.1523 ⇒ 0.57615	27.2	[10]
1.3886 ⇒ 0.6943	23.1	[39]
1.746 ⇒ 0.873	20	[40]
SFG, $o + o \Rightarrow e$		
5.33 + 1.32969 ⇒ 1.0642	21	[27]
4.44 + 1.39968 ⇒ 1.0642	20.2	[27]
5.2 + 0.80129 ⇒ 0.6943	19.5	[41]
2.5 + 0.96126 ⇒ 0.6943	21	[42]
5.0 + 0.66251 ⇒ 0.585	20.3	[43]
2.0 + 0.82686 ⇒ 0.585	25.1	[43]
4.16 + 0.61015 ⇒ 0.5321	21.6	[44]
2.66 + 0.66514 ⇒ 0.5321	24.5	[44]
0.946 + 0.5484 ⇒ 0.34715	50	[45]
2.67 + 0.6943 ⇒ 0.55102	24.4	[46]
1.98 + 0.6943 ⇒ 0.51405	27.4	[46]
1.2013 + 0.6943 ⇒ 0.44	35.1	[39]
3.3913 + 0.5145 ⇒ 0.44673	24	[47]
2.38 + 0.4880 ⇒ 0.40497	30.5	[48]
1.0642 + 0.5321 ⇒ 0.35473	47.5	[37]

Experimental values of internal angular, temperature, and spectral bandwidths ($T = 293$ K)

Interacting wavelengths [μm]	θ_{pm} [deg]	$\Delta\theta^{int}$ [deg]	ΔT [°C]	$\Delta\nu$ [cm^{-1}]	Ref.
SHG, $o + o \Rightarrow e$					
0.586 ⇒ 0.293	90	0.5–0.58		2.04	[23]
0.6943 ⇒ 0.34715	52	0.018			[9]
1.06 ⇒ 0.53	30	0.019		6.27	[19]
1.0642 ⇒ 0.5321	30	0.022			[38]
	30	0.022	40		[49]
	30	0.024	52.4		[50]
	30	0.026			[30]
1.0845 ⇒ 0.54225	29	0.020			[10]

Temperature variation of phase-matching angle

Interacting wavelengths [μm]	θ_{pm} [deg]	$d\theta_{pm}/dT$ [deg/K]	Ref.
SHG, $o + o \Rightarrow e$			
1.0845 ⇒ 0.54225	29	$< -1.3 \times 10^{-3}$	[10]
1.0642 ⇒ 0.5321	30	-8.4×10^{-4}	[50]

Laser-induced bulk-damage threshold

λ [μm]	τ_p [ns]	I_{thr} [GW/cm^2]	Ref.	Note
0.44–0.62	200–300	0.01	[51]	
0.53	20	0.07–0.08	[52]	
	15	0.04–0.05	[36]	
0.5321	12	0.03	[27]	
	0.1	1	[15]	
	0.035	4–5	[53]	12.5 Hz
		8–10	[53]	1 Hz
	0.032	10–12	[54]	25 Hz
	0.031	5	[15]	
0.64	330	0.004	[55]	
0.6943	20	0.025	[39]	500 pulses
		0.13	[12]	10 pulses
	10	0.12	[42]	
1.0642	180,000	>0.05	[42]	50 Hz
	300	0.002	[38]	1 kHz
	12	0.12	[27]	
	10	0.12	[56]	100 Hz
	0.13	8	[15]	
	0.045	19	[15]	

Laser-induced surface damage threshold [57]

λ [μm]	τ_p [ns]	I_{thr} [GW/cm^2]	Note
1.0642	12	3.2	$\theta = 30°$, 30-μm beam-waist diameter

About the crystal

This crystal, due to an easy growth procedure and relatively high value of second-order nonlinear coefficient, was very popular in the 1960s and 1970s. However, lithium iodate is hygroscopic, and its value of laser-induced bulk damage threshold is rather low. These circumstances limit the applications of this material in modern laser technology.

References

[1] K.I. Avdienko, S.V. Bogdanov, S.M. Arkhipov, B.I. Kidyarov, V.V. Lebedev, Y.E. Nevskii, V.I. Trunov, D.V. Sheloput, R.M. Shklovskaya: *Lithium Iodate. Growth, Properties and Applications* (Nauka, Novosibirsk, 1980) [In Russian].

[2] B.H.T. Chai: Optical Crystals. In: *CRC Handbook of Laser Science and Technology, Supplement 2: Optical Materials*, ed. by M.J. Weber (CRC Press, Boca Raton, 1995), pp. 3–65.

[3] G.D. Hager, S.A. Hanes, M.A. Dreger: Continuous wave frequency doubling of a high energy 1315 nm laser. IEEE J. Quant. Electr. **28(11)**, 2573–2576 (1992).

[4] Data sheet of Molecular Technology GmbH. Available at www.mt-berlin.com.

[5] Y.V. Burak, K.Y. Borman, I.S. Girnyk: Characteristics of the temperature dependences of thermal properties of α-$LiIO_3$. Fiz. Tverd. Tela **26(12)**, 3692–3694 (1984) [In Russian, English trans.: Sov. Phys. - Solid State **26(12)**, 2223–2224 (1984)].

[6] Data sheet of Cleveland Crystals Inc. Available at www.clevelandcrystals.com.

[7] J.M. Thierry, E. Coquet, J.M. Crettez: Interferometric measurement of thermal expansion coefficients and birefringence of α-$LiIO_3$ with temperature. Opt. Commun. **16(3)**, 417–419 (1976).

[8] J.M. Crettez, J. Comte, E. Coquet: Optical properties of α- and β-lithium iodate in the visible range. Opt. Commun. **6(1)**, 26–29 (1972).

[9] G. Nath, S. Haussühl: Strong second harmonic generation of a ruby laser in lithium iodate. Phys. Lett. A **29(2)**, 91–92 (1969).

[10] F.R. Nash, J.G. Bergman, G.D. Boyd, E.H. Turner: Optical nonlinearities in $LiIO_3$. J. Appl. Phys. **40(13)**, 5201–5206 (1969).

[11] T. Laurila, R. Hernberg: Frequency-doubled diode laser for ultraviolet absorption spectroscopy at 325 nm. Appl. Phys. Lett. **83(5)**, 845–847 (2003).

[12] G. Nath, H. Mehmanesch, M. Gsänger: Efficient conversion of a ruby laser radiation to 0.347 μm in low-loss lithium iodate. Appl. Phys. Lett. **17(7)**, 286–288 (1970).

[13] D.J. Gettemy, W.C. Harker, G. Lindholm, N.P. Barnes: Some optical properties of KTP, $LiIO_3$, and $LiNbO_3$. IEEE J. Quant. Electr. **24(11)**, 2231–2237 (1988).

[14] J. Jerphagnon: Optical nonlinear susceptibilities of lithium iodate. Appl. Phys. Lett. **16(8)**, 298–299 (1970).

[15] E.W. van Stryland, W.E. Williams, M.J. Soileau, A.L. Smirl: Laser-induced damage, nonlinear absorption and doubling efficiency of $LiIO_3$. IEEE J. Quant. Electr. **QE-20(4)**, 434–439 (1984).

[16] N.M. Bityurin, V.I. Bredikhin, V.N. Genkin: Nonlinear optical absorption and energy structure of $LiNbO_3$ and α-$LiIO_3$ crystals. Kvant. Elektron. **5(11)**, 2453–2457 (1978) [In Russian, English trans.: Sov. J. Quantum Electron. **8(11)**, 1377–1379 (1978)].

[17] K. Takizawa, M. Okada, S. Ieiri: Refractive indices of paratellurite and lithium iodate in the visible and ultraviolet regions. Opt. Commun. **23(2)**, 279–281 (1977).

[18] S. Umegaki, S.I. Tanaka, T. Uchiyama, S. Yabumoto: Refractive indices of lithium iodate between 0.4 and 2.2 μm. Opt. Commun. **3(4)**, 44–245 (1971).

[19] R.B. Andreev, V.D. Volosov, A.G. Kalintsev: Spectral, angular, and temperature characteristics of HIO_3, $LiIO_3$, CDA, DKDP, KDP and ADP non-linear crystals in second- and fourth-harmonic generation. Opt. Spektrosk. **37(2)**, 294–299 (1974) [In Russian, English trans.: Opt. Spectrosc. USSR **37(2)**, 169–171 (1974)].

[20] M.M. Choy, R.L. Byer: Accurate second-order susceptibility measurements of visible and infrared nonlinear crystals. Phys. Rev. B **14(4)**, 1693–1706 (1976).

[21] Z.B. Perekalina, G.F. Dobrzhansky, I.A. Spilko: The rotation of the plane of polarization in $LiIO_3$ crystals. Kristallogr. **15(6)**, 1252–1253 (1970) [In Russian, English trans.: Sov. Phys. - Crystallogr. **15(6)**, 1095 (1970)].
[22] V.A. Kizel, V.I. Burkov: Gyrotropy of Crystals (Nauka, Moscow, 1980) [In Russian].
[23] I.M. Beterov, V.I. Stroganov, V.I. Trunov, B.Y. Yurshin: Excitation of optical harmonics in lithium iodate and formate crystals by CW dye laser radiation. Kvant. Elektron. **2(11)**, 2440–2443 (1975) [In Russian, English trans.: Sov. J. Quantum Electron. **5(11)**, 1329–1331 (1975)].
[24] S.G. Karpenko, N.E. Kornienko, V.L. Strizhevskii: Use of diverging and nonmonochromatic pump waves in nonlinear spectroscopy of infrared radiation. Kvant. Elektron. **1(8)**, 1768–1779 (1974) [In Russian, English trans.: Sov. J. Quantum Electron. **4(8)**, 979–985 (1974)].
[25] V.I. Kabelka, V.G. Kolomiets, A.S. Piskarskas, A.Y.Stabinis: Features of parametric interaction of ultra-short light packets in a $LiIO_3$ crystal. Zh. Prikl. Spektrosk. **21(5)**, 947–950 (1974) [In Russian, English trans.: J. Appl. Spectrosc. **21(5)**, 582–585 (1974)].
[26] V.I. Kabelka, A.S. Piskarskas, A.Y. Stabinis, R.L. Sher: Group phase matching of interacting light pulses in nonlinear crystals. Kvant. Elektron. **2(2)**, 434–436 (1975) [In Russian, English trans.: Sov. J. Quantum Electron. **5(2)**, 255–256 (1975)].
[27] K. Kato: High-power difference-frequency generation at 4.4–5.7 μm. IEEE J. Quant. Electr. **QE-21(2)**, 119–120 (1985).
[28] H. Buesener, A. Renn, M. Brieger, F. von Moers, A. Hese: Frequency doubling of CW ring-dye-laser radiation in lithium iodate crystals. Appl. Phys. B **39(2)**, 77–81 (1986).
[29] M. Koralewski: Magnetooptical phenomena in $LiIO_3$ crystals. Phys. Stat. Solidi A **61(2)**, K151-K154 (1980).
[30] R.C. Eckardt, H. Masuda, Y.X. Fan, R.L. Byer: Absolute and relative nonlinear optical coefficients of KDP, KD*P, BaB_2O_4, $LiIO_3$, MgO:$LiNbO_3$, and KTP measured by phase-matched second-harmonic generation. IEEE J. Quant. Electr. **26(5)**, 922–933 (1990).
[31] J.E. Midwinter, J. Warner: The effects of phase matching method and of uniaxial crystal symmetry on the polar distribution of second-order non-linear optical polarization. Brit. J. Appl. Phys. **16(11)**, 1135–1142 (1965).
[32] W.J. Alford, A.V. Smith: Wavelength variation of the second-order nonlinear coefficients of $KNbO_3$, $KTiOPO_4$, $KtiOAsO_4$, $LiNbO_3$, $LiIO_3$, β-BaB_2O_4, KH_2PO_4, and LiB_3O_5 crystals: a test of Miller wavelength scaling. J. Opt. Soc. Am. B **18(4)**, 524–533 (2001).
[33] R.J. Gehr, A.V. Smith: Separated-beam nonphase-matched second-harmonic method of characterizing nonlinear optical coefficients. J. Opt. Soc. Am. B **15(8)**, 2298–2307 (1998).
[34] J.E. Pearson, G.A. Evans, A. Yariv: Measurement of the relative nonlinear coefficient of KDP, RDP, RDA and $LiIO_3$. Opt. Commun. **4(5)**, 366–367 (1972).
[35] T. Kellner, F. Heine, G. Huber: Efficient laser performance of Nd:YAG at 946 nm and intracavity frequency doubling with $LiJO_3$, β-BaB_2O_4, and LiB_3O_5. Appl. Phys. B **65(6)**, 789–792 (1997).
[36] A.I. Izrailenko, A.I. Kovrigin, P.V. Nikles: Parametric generation of light in high-efficiency nonlinear $LiIO_3$ and α-HIO_3 crystals. Pisma Zh. Eksp. Teor. Fiz. **12(10)**, 475–478 (1970) [In Russian, English trans.: JETP Lett. **12(10)**, 331–333 (1970)].
[37] M. Okada, S. Ieiri: Kleinman's symmetry relation in nonlinear optical coefficient of $LiIO_3$. Phys. Lett. A **34(1)**, 63–64 (1971).
[38] R.B. Chesler, M.A. Karr, J.E. Geusic: Repetitively Q-switched Nd:YAG–$LiIO_3$ 0.53 μm harmonic source. J. Appl. Phys. **41(10)**, 4125–4127 (1970).
[39] A.J. Campillo, C.L. Tang: Extending the tuning range of tunable oscillators by upconversion. Appl. Phys. Lett. **19(2)**, 36–38 (1971).

[40] A.J. Campillo: Properties of a pulsed $LiIO_3$ doubly resonant parametric oscillator. IEEE J. Quant. Electr. **QE-8(10)**, 809–811 (1972).

[41] D.W. Meltzer, L.S. Goldberg: Tunable IR difference frequency generation in $LiIO_3$. Opt. Commun. **5(3)**, 209–211 (1972).

[42] L.S. Goldberg: Optical parametric oscillation in lithium iodate. Appl. Phys. Lett. **17(11)**, 489–491 (1970).

[43] T.M. Jedju, L. Rothberg: Tunable femtosecond radiation in the mid-infrared for time-resolved absorption in semiconductors. Appl. Opt. **27(3)**, 615–618 (1988).

[44] F. Huisken, A. Kulcke, D. Voelkel, C. Laush, J.M. Lisy: New infrared injection-seeded optical parametric oscillator with high energy and narrow bandwidth output. Appl. Phys. Lett. **62(8)**, 805–807 (1993).

[45] G. Nath, G. Pauli: Efficient pulsed optical parametric oscillator with a tuning range from 0.415 to 2.1 μm. Appl. Phys. Lett. **22(2)**, 75–76 (1973).

[46] D. Malz, J. Bergmann, J. Heise: Up-conversion of thermal IR-radiation in $LiIO_3$ with a pulsed ruby-laser. Exp. Techn. Phys. **23(4)**, 379–388 (1975).

[47] Y.C. See, J. Falk: Lithium iodate, intracavity upconversion. Appl. Phys. Lett. **36(7)**, 503–505 (1980).

[48] D. Malz, J. Bergmann, J. Heise: Up-conversion of thermal IR-radiation in $LiIO_3$ with a CW argon laser. Exp. Techn. Phys. **23(5)**, 495–498 (1975).

[49] B.I. Kidyarov, I.V. Nikolaev, E.V. Pestryakov, V.M. Tarasov: Aluminium iodate octahydrate as a new nonlinear-optical crystal. Izv. Ross. Akad. Nauk, Ser. Fiz. **58(2)**, 131–134 (1994) [In Russian, English trans.: Bull. Russian Acad. Sci.: Physics **58(2)**, 294–296 (1994)]

[50] M. Webb, S.P. Velsko: Temperature sensitivity of phase-matched second-harmonic generation in $LiIO_3$. IEEE J. Quant. Electr. **26(8)**, 1394–1398 (1990).

[51] H. Gerlach: Difference frequency generation in $LiIO_3$ using two tunable dye lasers. Opt. Commun. **12(4)**, 405–408 (1974).

[52] R.B. Andreev, V.D. Volosov, V.N. Krylov: Parametric generation of high-power nanosecond light pulses at 0.74–1.85 μm. Pisma Zh. Tekh. Fiz. **4(5–6)**, 256–258 (1978) [In Russian, English trans.: Sov. Tech. Phys. Lett. **4(3)**, 105–106 (1978)].

[53] R. Danielius, G. Dikchyus, V. Kabelka, A. Piskarskas, A. Stabinis, Y. Yasevichyute: Parametric excitation of light in the picosecond range. Kvant. Elektron. **4(11)**, 2379–2395 (1977) [In Russian, English trans.: Sov. J. Quantum Electron. **7(11)**, 1360–1368 (1977)].

[54] A. Arutyunyan, G. Arzumanyan, R. Danielius, V. Kabelka, R. Sharkhatunyan, Y. Yasevichyute: Investigation of parametric superluminescence of $LiIO_3$ crystals in the picosecond band. Lit. Fiz. Sbornik **18(2)**, 255–263 (1978) [In Russian, English trans.: Sov. Phys. - Collection **18(2)**, 62–67 (1978)].

[55] L. Armstrong, S.E. Neister, R. Adhav: Measuring CFP dye laser damage thresholds on UV doubling crystals. Laser Focus **18(12)**, 49–53 (1982).

[56] V.G. Dmitriev, V.N. Krasnyanskaya, M.F. Koldobskaya, I.S. Rez, E.A. Shalaev, E.M. Shvom: Frequency multiplication in nonlinear lithium iodate crystals. Kvant. Elektron. **No. 2**, 64–66 (1973) [In Russian, English trans.: Sov. J. Quantum Electron. **3(2)**, 126–127 (1973)].

[57] M. Bass, H.H. Barrett: Avalanche breakdown and the probabilistic nature of laser-induced damage. IEEE J. Quant. Electr. **QE-8(3)**, 338–343 (1972).

8.14 Ag_3AsS_3, Proustite

Negative uniaxial crystal: $n_o > n_e$
Molecular mass: 494.724
Specific gravity: 5.49 g/cm^3 [1]; 5.629 g/cm^3 [2]; 5.635 g/cm^3 at $T = 293$ K [3]; 5.65 g/cm^3 [4]
Point group: $3m$
Lattice constants:
$a = 10.74$ Å [5]; 10.756 Å [6]; 10.82 Å [4]
$c = 8.64$ Å [5]; 8.652 Å [6]; 8.69 Å [4]
Mohs hardness: 2–2.5 [3]
Solubility in water: insoluble [3]
Melting point: 769 K [6]

Linear thermal expansion coefficient [3]

T [K]	$\alpha_t \times 10^6$ [K^{-1}], $\parallel c$	$\alpha_t \times 10^6$ [K^{-1}], $\perp c$
300	12	16

Thermal conductivity coefficient κ [2]

T [K]	κ [W/mK], $\parallel c$	κ [W/mK], $\perp c$
300	0.113	0.092

Band-gap energy at room temperature for indirect transition
$E_g = 2.067$ eV for $\mathbf{E}\perp c$ [2]
$E_g = 2.100$ eV for $\mathbf{E}\parallel c$ [2]
Band-gap energy at room temperature for direct transition:
$E_g = 2.177$ eV for $\mathbf{E}\perp c$ [2]
$E_g = 2.235$ eV for $\mathbf{E}\parallel c$ [2]
Transparency range at $\alpha = 1$ cm^{-1} level:
0.63–12.5 μm ($\mathbf{E}\perp c$) [5]
0.61–13.3 μm ($\mathbf{E}\parallel c$) [5]

Linear absorption coefficient α

λ [μm]	α [cm^{-1}]	T [K]	Ref.	Note
0.593	0.89	77	[7]	e-wave
0.6328	0.81	77	[7]	o-wave
	0.64	77	[7]	e-wave
0.6789	0.64	77	[7]	o-wave
9.31	0.25	77	[7]	e-wave
0.576	36 ± 1	300	[5]	e-wave, $\perp c$

λ [μm]	α [cm^{-1}]	T [K]	Ref.	Note
0.593	16.1	300	[7]	*e*-wave
0.6328	1.83	300	[7]	*o*-wave
	1.59	300	[7]	*e*-wave
0.6358	1.88	300	[8]	*e*-wave
0.6764	0.95	300	[8]	*o*-wave
0.6789	0.83	300	[7]	*o*-wave
0.6943	0.1	300	[9]	
	0.2	300	[10]	*o*-wave, $\parallel c$
1.06	0.1	300	[10]	*o*-wave, $\parallel c$
1.0642	0.02	300	[9]	
5.3	0.3	300	[11]	*e*-wave
	0.32	300	[12]	*e*-wave
9.2	0.29	300	[13]	*o*-wave
9.3	0.53	300	[7]	*e*-wave
9.55	<0.1	300	[14]	SHG direction
10.2	1.2	300	[5]	*o*-wave, $\perp c$
	1.3	300	[15]	*o*-wave
10.6	0.16	300	[16]	*o*-wave
	0.38	300	[12]	*o*-wave
	0.45	300	[8]	*o*-wave
	0.6	300	[11]	*o*-wave
	0.8	300	[17]	*o*-wave
	1	300	[18]	*o*-wave
11.6	0.5	300	[15]	*o*-wave
14.5	≈70	300	[15]	*o*-wave
15.2–20.8	<20	300	[19]	*o*-wave

Two-photon absorption coefficient β ($\parallel c$)

λ [μm]	τ_p [ns]	$\beta \times 10^{11}$ [cm/W]	Ref.
0.6943	∼20	10,000	[10]
	25	2000	[9]
1.06	∼20	3000	[10]
1.0642	20	<300	[9]

Experimental values of refractive indices at $T = 293$ K [5]

λ [μm]	n_o	n_e
0.5876		2.7896
0.6328	3.0190	2.7391
0.6678	2.9804	2.7094
1.014	2.8264	2.5901
1.129	2.8067	2.5756
1.367	2.7833	2.5570

λ [μm]	n_o	n_e
1.530	2.7728	2.5485
1.709	2.7654	2.5423
2.50	2.7478	2.5282
3.56	2.7379	2.5213
4.62	2.7318	2.5178

Best set of Sellmeier equations (λ in μm, $T = 293\,\mathrm{K}$) [20]:

$$n_o^2 = 9.220 + \frac{0.4454}{\lambda^2 - 0.1264} + \frac{1733}{\lambda^2 - 1000}$$

$$n_e^2 = 7.007 + \frac{0.3230}{\lambda^2 - 0.1192} + \frac{660}{\lambda^2 - 1000}$$

Other sets of dispersion relations are given in [5], [21].

Linear electrooptic coefficient measured at high frequencies (well above the acoustic resonances of Ag_3AsS_3 crystal, i.e., for the "clamped" crystal) at room temperature [22]

λ [μm]	r_{22}^S [pm/V]
0.6328	1.1

Expressions for the effective second-order nonlinear coefficient in general case (Kleinman symmetry conditions are valid, $d_{15} = d_{24} = d_{31} = d_{32}$) [23]:

$$d_{ooe} = d_{31}\sin(\theta + \rho) - d_{22}\cos(\theta + \rho)\sin 3\phi$$

$$d_{eoe} = d_{oee} = d_{22}\cos^2(\theta + \rho)\cos 3\phi$$

Simplified expressions for the effective second-order nonlinear coefficient (Kleinman symmetry conditions are valid, $d_{15} = d_{24} = d_{31} = d_{32}$) [24]:

$$d_{ooe} = d_{31}\sin\theta - d_{22}\cos\theta\sin 3\phi$$

$$d_{eoe} = d_{oee} = d_{22}\cos^2\theta\cos 3\phi$$

Second-order nonlinear coefficients [17], [25]:

$$|d_{22}(10.6\,\mu\mathrm{m})| = (0.2 \pm 0.03) \times |d_{36}(\mathrm{GaAs})| = 16.6 \pm 2.5\,\mathrm{pm/V}$$

$$|d_{31}(10.6\,\mu\mathrm{m})| = (1.6 \pm 0.1)^{-1} \times |d_{22}(\mathrm{Ag_3AsS_3})| = 10.4 \pm 2.2\,\mathrm{pm/V}$$

Experimental values of phase-matching angle ($T = 293\,\mathrm{K}$)

Interacting wavelengths [μm]	θ_{exp} [deg]	Ref.
SHG, $o + o \Rightarrow e$		
$10.6 \Rightarrow 5.3$	23.6	[26]
$10.59 \Rightarrow 5.295$	21.5	[17]
$9.2 \Rightarrow 4.6$	19.9	[13]

Interacting wavelengths [μm]	θ_{exp} [deg]	Ref.
2.13 ⇒ 1.065	29.5	[27]
2.1284 ⇒ 1.0642	29.4	[28]
SFG, $o + o \Rightarrow e$		
12.2 + 1.064 ⇒ 0.9786	17.2	[29]
8.9 + 1.064 ⇒ 0.9504	20.0	[29]
6.3 + 1.064 ⇒ 0.9103	23.5	[29]
10.57 + 0.6943 ⇒ 0.6515	25.3	[30]
10.6 + 0.6764 ⇒ 0.6358	25.7	[8]
10.6935 + 0.6726 ⇒ 0.6328	25.81	[31]
10.5881 + 0.6730 ⇒ 0.6328	25.93	[31]
10.3006 + 0.6742 ⇒ 0.6328	26.12	[31]
10.1918 + 0.6747 ⇒ 0.6328	26.36	[31]
9.5333 + 0.6778 ⇒ 0.6328	27.09	[31]
9.2688 + 0.6792 ⇒ 0.6328	27.43	[31]
6.3552 + 0.7028 ⇒ 0.6328	32.90	[32]
6.2571 + 0.7040 ⇒ 0.6328	33.16	[32]
6.1629 + 0.7052 ⇒ 0.6328	33.37	[32]
5.9079 + 0.7087 ⇒ 0.6328	34.06	[32]
5.7375 + 0.7112 ⇒ 0.6328	34.53	[32]
5.5393 + 0.7144 ⇒ 0.6328	35.12	[32]
5.2578 + 0.7194 ⇒ 0.6328	36.00	[32]
SFG, $e + o \Rightarrow e$		
10.59 + 1.064 ⇒ 0.967	20.0	[33]
10.59 + 0.6943 ⇒ 0.6516	27.7	[34]
9.31 + 0.6789 ⇒ 0.6328	29.0	[35]
SFG, $o + e \Rightarrow e$		
7.8 + 2.47 ⇒ 1.8759	33	[36]

Experimental values of internal angular bandwidth

Interacting wavelengths [μm]	$\Delta\theta^{int}$ [deg]	Ref.
SHG, $o + o \Rightarrow e$		
10.6 ⇒ 5.3	0.098	[11]
9.2 ⇒ 4.6	0.082	[13]
SFG, $e + o \Rightarrow e$		
10.6 + 0.6943 ⇒ 0.6516	0.031	[34]

Laser-induced surface-damage threshold

λ [μm]	τ_p [ns]	I_{thr} [GW/cm^2]	Ref.
0.6943	1,000,000	0.000006	[37]
	14	0.003	[38]
1.0642	CW	0.0000001	[37]
	18	>0.012	[38]

λ [μm]	τ_p [ns]	I_{thr} [GW/cm^2]	Ref.
2.098	200	>0.01	[38]
9.55	30	0.18	[14]
10.6	190	>0.046	[38]
	150	0.053	[11]

About the crystal

Proustite was introduced in 1967 [5] and during the next decade was extensively used for nonlinear frequency conversion to the IR range and for IR up-conversion. However, this material is not free from drawbacks, such as low value of surface damage threshold and difficulty in obtaining large uniform monocrystals. In the 1980s, this crystal was replaced by other materials (i.e., by AGS and GaSe).

References

[1] B.H.T. Chai: Optical Crystals. In: *CRC Handbook of Laser Science and Technology, Supplement 2: Optical Materials*, ed. by M.J. Weber (CRC Press, Boca Raton, 1995), pp. 3–65.

[2] *Physical-Chemical Properties of Semiconductors. Handbook* (Nauka, Moscow, 1979) [In Russian].

[3] A.A. Blistanov, V.S. Bondarenko, N.V. Perelomova, F.N. Strizhevskaya, V.V. Tchkalova, M.P. Shaskolskaya: *Acoustic Crystals* (Nauka, Moscow, 1982) [In Russian].

[4] D.M. Bercha, Y.V. Voroshilov, V.Y. Slivka, I.D. Turyanitsa: *Complex Chalcogenides and Chalcohalogenides*, ed. by D.V. Chepur (Vishcha Shkola, Lvov, 1983) [In Russian].

[5] K.F. Hulme, O. Jones, P.H. Davies, M.V. Hobden: Synthetic proustite (Ag_3AsS_3): a new crystal for optical mixing. Appl. Phys. Lett. **10(4)**, 133–135 (1967).

[6] M.I. Holovey, I.D. Olexeyuk, M.I. Gurzan, I.S. Rez, V.V. Panko, Y.V. Voroshilov, M.Y. Rigan, I.G. Ganeyev, A.V. Bagdanova: Preparation and some properties of synthetic proustite single crystals. Kristall und Technik **6(5)**, 631–637 (1971).

[7] N. Ito: Sum-frequency mixing of CO_2 and He-Ne lasers in proustite. Opt. Lett. **7(2)**, 63–65 (1982).

[8] E.N. Antonov, V.R. Mironenko, D.N. Nikogosyan, M.I. Golovey: Conversion of CO_2 laser radiation to the visible range in a proustite crystal. Kvant. Elektron. **1(8)**, 1742–1746 (1974) [In Russian, English trans.: Sov. J. Quantum Electron. **4(8)**, 963–965 (1974)].

[9] D.S. Hanna, A.J. Turner: Nonlinear absorption measurements in proustite (Ag_3AsS_3) and CdSe. Opt. Quant. Electron. **8(3)**, 213–217 (1976).

[10] V.V. Berezovskii, Y.A. Bykovskii, S.N. Potanin, I.S. Rez: Two-photon absorption in proustite. Kvant. Elektron. **No. 2**, 74–75 (1973) [In Russian, English trans.: Sov. J. Quantum Electron. **3(2)**, 134–135 (1973)].

[11] D.N. Nikogosyan, A.P. Sukhorukov, M.I. Golovey: Saturation of second harmonic generation of TEA CO_2 laser radiation in a proustite crystal. Kvant. Elektron. **2(3)**, 609–612 (1975) [In Russian, English trans.: Sov. J. Quantum Electron. **5(3)**, 344–346 (1975)].

[12] V.V. Berezovskii, Y.A.Bykovskii, M.I. Goncharov, I.S. Rez: Nonlinear polarization coefficients of proustite and tellurium. Kvant. Elektron. **No. 2**, 105–107 (1972) [In Russian, English trans.: Sov. J. Quantum Electron. **2(2)**, 180–182 (1972)].

[13] G.J. Ernst, W.J. Witteman: Second-harmonic generation in proustite with a CW CO_2 laser. IEEE J. Quant. Electr. **QE-8(3)**, 382–383 (1972).

[14] Y.M. Andreev, V.V. Badikov, V.G. Voevodin, L.G. Geiko, P.P. Geiko, M.V. Ivashchenko, A.I. Karapuzikov, I.V. Sherstov: Radiation resistance of nonlinear crystals at a wavelength of 9.55 μm. Kvant. Elektron. **31(12)**, 1075–1078 (2001) [In Russian, English trans.: Quantum Electron. **31(12)**, 1075–1078 (2001)].

[15] L.O. Hocker, C.F. Dewey: Difference frequency generation in proustite from 11 to 23 μm. Appl. Phys. **11(2)**, 137–140 (1976).

[16] N.P. Barnes, R.C. Eckardt, D.J. Gettemy, L.B. Edgett: Absorption coefficients and the temperature variation of the refractive index difference of nonlinear optical crystals. IEEE J. Quant. Electr. **QE-15(10)**, 1074–1076 (1979).

[17] D.S. Chemla, P.J. Kupeček, C.A. Schwartz: Redetermination of the nonlinear optical coefficients of proustite by comparison with pyrargyrite and gallium selenide. Opt. Commun. **7(3)**, 225–228 (1973).

[18] P.J. Kupeček, C.A. Schwartz, D.S. Chemla: Silver thiogallate ($AgGaS_2$)—Part I: nonlinear optical properties. IEEE J. Quant. Electr. **QE-10(7)**, 540–545 (1974).

[19] D. Cotter, D.C. Hanna, B. Luther-Davies, R.C. Smith: Backward-wave medium infrared down-conversion in proustite. Opt. Commun. **11(1)**, 54–56 (1974).

[20] M.V. Hobden: The dispersion of the refractive indices of proustite (Ag_3AsS_3). Optoelectron. **1(3)**, 159 (1969).

[21] R.A. Andrews: IR image parametric up-conversion. IEEE J. Quant. Electr. **QE-6(1)**, 68–80 (1970).

[22] G.W.C. Kaye, T.H. Laby: *Tables of Physical and Chemical Constants* (Longman Group Ltd., London, 1995).

[23] I. Shoji, H. Nakamura, K. Ohdaira, T. Kondo, R. Ito, T. Okamoto, K. Tatsuki, S. Kubota: Absolute measurement of second-order nonlinear-optical coefficients of β-BaB_2O_4 for visible to ultraviolet second-harmonic wavelengths. J. Opt. Soc. Am. B **16(4)**, 620–624 (1999).

[24] J.E. Midwinter, J. Warner: The effects of phase matching method and of uniaxial crystal symmetry on the polar distribution of second-order non-linear optical polarization. Brit. J. Appl. Phys. **16(11)**, 1135–1142 (1965).

[25] D.A. Roberts: Simplified characterization of uniaxial and biaxial nonlinear optical crystals: a plea for standardization of nomenclature and conventions. IEEE J. Quant. Electr. **28(10)**, 2057–2074 (1992).

[26] Y.A. Gorokhov, D.P. Krindach, D.N. Nikogosyan, A.P. Sukhorukov: Influence of thermal self-actions on second harmonic generation of continuous-wave radiation. Kvant. Elektron. **1(3)**, 679–683 (1974) [In Russian, English trans.: Sov. J. Quantum Electron. **4(3)**, 382–384 (1974)].

[27] D.C. Hanna, B. Luther-Davies, H.N. Rutt, R.C. Smith: Reliable operation of a proustite parametric oscillator. Appl. Phys. Lett. **20(1)**, 34–36 (1972).

[28] T. Elsaesser, A. Seilmeier, W. Kaiser: Parametric generation of tunable picosecond pulses in proustite between 1.2 and 8 μm. Opt. Commun. **44(4)**, 293–296 (1983).

[29] J. Falk, J.M. Yarborough: Detection of room-temperature blackbody radiation by parametric upconversion. Appl. Phys. Lett. **19(3)**, 68–70 (1971).

[30] D.N. Nikogosyan: The up-conversion efficiency of CO_2 laser radiation in a proustite crystal pumped by ultrashort light pulses. Kvant. Elektron. **2(11)**, 2524–2525 (1975) [In Russian, English trans.: Sov.J.Quantum Electron. **5(11)**, 1378–1379(1975)].

[31] E.K. Pfitzer, H.D. Riccius, K.J. Siemsen: Fabry-Perot photographs of CO_2 laser lines up-converted in proustite. Opt. Commun. **3(4)**, 277–278 (1971).

[32] H.D. Riccius, K.J. Siemsen: Up-conversion of CO laser lines by difference-frequency mixing in proustite (Ag_3AsS_3). Phys. Lett. A **45(5)**, 377–378 (1973).

[33] A.J. Alcock, A.C. Walker: Fast linear detection system for TE CO_2 lasers. Appl. Phys. Lett. **23(8)**, 467–468 (1973).

[34] J. Warner: Photomultiplier detection of 10.6 μm radiation using optical up-conversion in proustite. Appl. Phys. Lett. **12(6)**, 222–224 (1968).

[35] N. Ito: Sum-frequency mixing of CO_2 and He-Ne lasers in proustite. Opt. Lett. **7(2)**, 63–65 (1982).

[36] G.C. Bhar, D.C. Hanna, B. Luther-Davies, R.C. Smith: Tunable down-conversion from an optical parametric oscillator. Opt. Commun. **6(4)**, 323–326 (1972).

[37] A.F. Milton: Upconversion—a systems view. Appl. Opt. **11(10)**, 2311–2330 (1972).

[38] D.C. Hanna, B. Luther-Davies, H.N. Rutt, R.C. Smith, C.R. Stanley: Q-switched laser damage of infrared nonlinear materials. IEEE J. Quant. Electr. **QE-8(3)**, 317–324 (1972).

8.15 $HgGa_2S_4$, Mercury Thiogallate

Negative uniaxial crystal: $n_o > n_e$
Molecular mass: 468.180
Specific gravity: 4.95 g/cm^3 [1]
Point group: $\bar{4}$
Lattice constants [2]:
$a = 5.506$ Å
$c = 10.299$ Å
Mohs hardness: 3–3.5

Specific heat capacity at $P = 0.101325$ MPa [3]

T [K]	c_p [J/kgK]
293	350–490

Thermal conductivity coefficient κ [3]

T [K]	κ [W/mK], $\parallel c$	κ [W/mK], $\perp c$
293	2.5–2.9	2.3–2.4

Band-gap energy at room temperature: $E_g = 2.84$ eV [4]
Transparency range: 0.55–11 μm [5], 0.55–12.4 μm [6], 0.55–13 μm [7]
The UV transmission cutoff is at 0.51 μm for "yellow" crystals and 0.55 μm for "orange" ones [8].

Linear absorption coefficient α

λ [μm]	α [cm^{-1}]	Ref.	Note
0.53	8	[9]	*e*-wave, SHG direction
	11	[7]	
0.9–8.5	0.1–0.2	[8]	
0.96	0.25	[10]	*e*-wave, SFG direction
1.06	0.1	[9]	*o*-wave, SHG direction
1.064	0.25	[10]	*o*-wave, SFG direction
4.34	0.15	[3]	orange crystal
9.55	<0.2–0.3	[11]	SHG direction
10.6	1.2	[10]	*o*-wave, SFG direction
	0.44	[3]	orange crystal

Experimental values of refraction indices at $T = 293$ K [2]

λ [μm]	n_o	n_e
0.5495	2.6592	2.5979
0.5747	2.6334	2.5748
0.6009	2.6112	2.5549
0.6328	2.5890	2.5349
0.6500	2.5796	2.5264
1.0760	2.477	2.432
1.1500	2.472	2.428
2.6500	2.444	2.403
3.5400	2.439	2.398
7.1500	2.414	2.372
8.7300	2.400	2.358
10.400	2.380	2.337
11.000	2.369	2.329

Sellmeier equations (λ in μm, $T = 293$ K) [6]:

$$n_o^2 = 5.9405 + \frac{0.2361}{\lambda^2 - 0.0929} - 0.00257\,\lambda^2$$

$$n_e^2 = 5.7412 + \frac{0.2138}{\lambda^2 - 0.0897} - 0.00247\,\lambda^2$$

Other dispersion relations are given in [2], [3], [8], [12].
Expressions for the effective second-order nonlinear coefficient (Kleinman symmetry conditions are valid, $d_{15} = d_{31}$ and $d_{14} = d_{25} = d_{36}$) [13]:

$$d_{ooe} = d_{36} \sin\theta \sin 2\phi + d_{31} \sin\theta \cos 2\phi$$

$$d_{eoe} = d_{oee} = d_{36} \sin 2\theta \cos 2\phi - d_{31} \sin 2\theta \sin 2\phi$$

Values of second-order nonlinear coefficients:

$|\, d_{36}(1.064\,\mu\text{m})\, | = 80 \times d_{11}(SiO_2) \pm 30\% = 24.0 \pm 7.2$ pm/V [7], [14]

$|\, d_{36}(1.064\,\mu\text{m})\, | = 1.8 \times d_{36}(AgGaS_2) \pm 15\% = 24.7 \pm 7.6$ pm/V [9], [15]

$| d_{36}(1.064\,\mu m) | = 1.8 \times d_{36}(AgGaS_2) \pm 15\% = 31.5 \pm 4.7$ pm/V [9], [14], [16]
$| d_{31}(1.064\,\mu m) | = 0.33 \times | d_{36}(HgGa_2S_4) | = 8.1 \pm 2.5$ pm/V [9], [15]
$| d_{31}(1.064\,\mu m) | = 0.33 \times | d_{36}(HgGa_2S_4) | = 10.4 \pm 1.6$ pm/V [9], [14], [16]

Experimental value of phase-matching angle ($T = 293$ K) [8]

Interacting wavelengths [μm]	θ_{exp} [deg]
SHG, $o + o \Rightarrow e$	
$9.55 \Rightarrow 4.775$	67.5

Laser-induced surface-damage threshold

λ [μm]	τ_p [ns]	I_{thr} [GW/cm^2]	Ref.	Note
0.82	0.00022	>170	[4]	1 kHz
1.064	30	0.04	[3]	
		~0.06	[10]	12.5 Hz, 10 pulses
1.25	0.00016	>160	[4]	1 kHz
9.55	30	0.3	[11]	
10.6	CW	>0.000000016	[10]	

About the crystal

Though mercury thiogallate was introduced in the 1970s [2], [7], due to rather low optical quality it found a very little application. Recently, the performance of $HgGa_2S_4$ was significantly improved, and the first OPO, using this nonlinear material, was demonstrated [17].

References

[1] *Physical-Chemical Properties of Semiconductors. Handbook* (Nauka, Moscow, 1979) [In Russian].
[2] V.V. Badikov, I.N. Matveev, V.L. Panyutin, S.M. Pshenichnikov, T.M. Repyakhova, O.V. Rychik, A.E. Rozenson, N.K. Trotsenko, N.D. Ustinov: Growth and optical properties of mercury thiogallate. Kvant. Elektron. **6(8)**, 1807–1810 (1979) [In Russian, English trans.: Sov. J. Quantum Electron. **9(8)**, 1068–1069 (1979)].
[3] V. Badikov, K. Mitin, A. Seryogin, E. Ryabov, V. Laptev, A. Malinovsky: $HgGa_2S_4$ crystals for mid-infrared optical parametric oscillators pumped by Nd:YAG lasers. Proc. SPIE **4972**, 131–138 (2003).
[4] V. Petrov, F. Rotermund, V.V. Badikov, G.S. Shevyrdyaeva: Mixed nonlinear crystal $Cd_xHg_{1-x}Ga_2S_4$ used for optical parametric amplification. In: *Conference on Lasers and Electrooptics CLEO/QELS 2003, Technical Digest* (OSA, Washington DC, 2003), paper CMA5.
[5] P.G. Schunemann, P.G. Pollak: Synthesis and growth of $HgGa_2S_4$ crystals. J. Cryst. Growth **174(1–4)**, 278–282 (1997).
[6] E. Takaoka, K. Kato: Second-harmonic generation in $HgGa_2S_4$. In: *CLEO/Europe 1998, Technical Digest* (OSA, Washington DC, 1998), p. 387, paper CFH7.

[7] B.F. Levine, C.G. Bethea, H.M. Kasper, F.A. Thiel: Nonlinear optical susceptibilities of $HgGa_2S_4$. IEEE J. Quant. Electr. **QE-12(6)**, 367–368 (1976).
[8] Y.M. Andreev, P.P. Geiko, V.V. Badikov, G.C. Bhar, S. Das, A.K. Chaudhury: Nonlinear optical properties of defect tetrahedral crystals $HgGa_2S_4$ & $AgGaGeS_4$ and mixed chalcopyrite crystal $Cd_{0.4}Hg_{0.6}Ga_2S_4$. Nonl. Opt. **29(1)**, 19–27 (2002).
[9] V.V. Badikov, I.N. Matveev, S.M. Pshenichnikov, O.V. Rychik, N.K. Trotsenko, N.D. Ustinov, S.I. Shcherbakov: Growth and nonlinear properties of $HgGa_2S_4$. Kvant. Elektron. **7(10)**, 2235–2237 (1980) [In Russian, English trans.: Sov. J. Quantum Electron. **10(10)**, 1300–1301 (1980)].
[10] S.A. Andreev, N.P. Andreeva, V.V. Badikov, I.N. Matveev, S.M. Pschenichnikov: Frequency up-conversion in a mercury thiogallate crystal. Kvant. Elektron. **7(9)**, 2003–2006 (1980) [In Russian, English trans.: Sov. J. Quantum Electron. **10(9)**, 1157–1158 (1980)].
[11] Y.M. Andreev, V.V. Badikov, V.G. Voevodin, L.G. Geiko, P.P. Geiko, M.V. Ivashchenko, A.I. Karapuzikov, I.V. Sherstov: Radiation resistance of nonlinear crystals at a wavelength of 9.55 μm. Kvant. Elektron. **31(12)**, 1075–1078 (2001) [In Russian, English trans.: Quantum Electron. **31(12)**, 1075–1078 (2001)].
[12] G.G. Matvienko, Y.M. Andreev, V.V. Badikov, P.P. Geiko, S.G. Grechin, A.I. Karapuzikov: Wide band frequency converters for lidar systems. Proc. SPIE **4546**, 119–126 (2002).
[13] J.E. Midwinter, J. Warner: The effects of phase matching method and of uniaxial crystal symmetry on the polar distribution of second-order non-linear optical polarization. Brit. J. Appl. Phys. **16(11)**, 1135–1142 (1965).
[14] D.A. Roberts: Simplified characterization of uniaxial and biaxial nonlinear optical crystals: a plea for standardization of nomenclature and conventions. IEEE J. Quant. Electr. **28(10)**, 2057–2074 (1992).
[15] J.-J. Zondy, D. Touahri, O. Acef: Absolute value of the d_{36} nonlinear coefficient of $AgGaS_2$: prospect for a low-threshold doubly resonant oscillator-based 3:1 frequency divider. J. Opt. Soc. Am. B **14(10)**, 2481–2497 (1997).
[16] F. Rotermund, V. Petrov: Mercury thiogallate mid-infrared femtosecond optical parametric generator pumped at 1.25 μm by a Cr: forsterite regenerative amplifier. Opt. Lett. **25(10)**, 746–748 (2000).
[17] V.V. Badikov, A.K. Don, K.V. Mitin, A.M. Seregin, V.V. Sinaiskii, N.I. Shchebetova: A $HgGa_2S_4$ optical parametric oscillator. Kvant. Elektron. **33(9)**, 831–832 (2003) [In Russian, English trans.: Quantum Electron. **33(9)**, 831–832 (2003).

8.16 $CdGeAs_2$, Cadmium Germanium Arsenide (CGA)

Positive uniaxial crystal: $n_e > n_o$
Molecular mass: 334.753
Specific gravity: 5.60 g/cm^3 [1]
Point group: $\bar{4}2m$
Mohs hardness: 3.5–4
Knoop (or Vickers) hardness: 485 at indenter load 50 g [2]
Melting point: 933 K [3]

Mean value of linear thermal expansion coefficient [2]

ΔT [K]	$\alpha_t \times 10^6$ [K^{-1}], $\parallel c$	$\alpha_t \times 10^6$ [K^{-1}], $\perp c$
293–673	1.0	11.4

Thermal conductivity coefficient [1]: $\kappa = 4.18$ W/mK (or 6.69 W/mK)
Band-gap energy at room temperature: $E_g = 0.52$ eV [4]; 0.54 eV [5]
Transparency range at "0" transmittance level: 2.3–18 μm [3]; 2.4–18 μm [6]; 2.45–18.1 μm [3]; multiphonon absorption peaks exist at 12.5 μm and 13.5 μm [3]

Linear absorption coefficient α

λ [μm]	T [K]	α [cm^{-1}]	Ref.	λ [μm]	T [K]	α [cm^{-1}]	Ref.
2.8	300	1.5	[7]	9–11	300	0.23	[9]
3.39	300	5.7	[8]	9.2	300	0.30	[11]
4–18	300	<0.9	[9]	9.27	77	0.002 (?)	[12]
4.5	300	0.7	[10]		300	0.44	[12]
4.6	300	0.17	[11]	9.55	80	0.1	[13]
4.635	77	0.32	[12]		295	0.66	[13]
	300	1.03	[12]		300	0.42	[17]
4.755	80	0.3	[13]	10	300	0.2	[7]
	295	0.99	[13]	10.6	77	0.1	[14]
5.3	77	0.4	[14]		300	0.4	[6]
	300	1.3	[8]		300	0.5	[8]
5.5	300	0.46	[3]		300	2.4	[18]
5.85	77	0.42	[15]	10.6–11.7	77	0.14	[15]
	300	1.5	[15]		300	0.5	[15]
8.6–12	77	<0.2	[16]	11	300	<0.2	[10]
	300	<0.5	[16]	12.3	300	0.4	[4]

Two-photon absorption coefficient β [7]

λ [μm]	τ_p [ns]	$\beta \times 10^{11}$ [cm/W]	Note
2.8	0.1	25,000	*o*-wave

Experimental values of refraction indices [19]

λ [μm]	n_o	n_e	λ [μm]	n_o	n_e
2.3	3.6076		3.6	3.5503	3.6508
2.4	3.5973	3.7545	3.8	3.5468	3.6454
2.5	3.5895	3.7316	4.0	3.5440	3.6402
2.6	3.5823	3.7156	4.2	3.5415	3.6368
2.7	3.5773	3.7030	4.4	3.5391	3.6329
2.8	3.5721	3.6926	4.6	3.5372	3.6299
2.9	3.5684	3.6846	4.8	3.5354	3.6273
3.0	3.5645	3.6775	5.0	3.5336	3.6249
3.1	3.5615	3.6714	5.5	3.5285	3.6178
3.2	3.5581	3.6661	6.0	3.5251	3.6134
3.4	3.5536	3.6574	6.5	3.5223	3.6104

λ [μm]	n_o	n_e	λ [μm]	n_o	n_e
7.0	3.5200	3.6073	10.0	3.5078	3.5942
7.5	3.5175	3.6050	10.5	3.5054	3.5922
8.0	3.5157	3.6030	11.0	3.5031	3.5896
8.5	3.5140	3.6009	11.5	3.5004	3.5871
9.0	3.5120	3.5988	12.0	3.4977	
9.5	3.5098	3.5966	12.5	3.4950	

Best set of Sellmeier equations (λ in μm, $T = 293\,\mathrm{K}$) [20]:

$$n_o^2 = 12.4008 + \frac{2.1603}{\lambda^2 - 2.0617} - 0.00133\,\lambda^2$$

$$n_e^2 = 13.0079 + \frac{3.2613}{\lambda^2 - 2.8382} - 0.00126\,\lambda^2$$

The authors of [10], [21] represent these equations with slightly changed last coefficient for n_e, namely, 0.00125 instead of 0.00126.
Other sets of Sellmeier equations are given in [6], [9], [22].
Temperature derivatives of the refractive indices upon heating from room temperature to T[K] for the spectral range 2.65–10.6 μm [20]:

$$dn_o/dT = \left(26.51/\lambda^2 - 6.45/\lambda + 19.17\right) \times 10^{-5} \times \left[1 + 9.0 \times 10^{-4}\,(T - 293)\right]$$

$$dn_e/dT = \left(22.62/\lambda^2 - 5.35/\lambda + 15.20\right) \times 10^{-5} \times \left[1 + 6.1 \times 10^{-4}\,(T - 293)\right]$$

Expressions for the effective second-order nonlinear coefficient in general case (Kleinman symmetry conditions are valid, $d_{14} = d_{25} = d_{36}$) [23], [24]:

$$d_{eeo} = 2d_{36}\sin(\theta + \rho)\cos(\theta + \rho)\cos 2\phi$$

$$d_{oeo} = d_{eoo} = -d_{36}\sin(\theta + \rho)\sin 2\phi$$

Simplified expressions for the effective second-order nonlinear coefficient (approximation of small birefringence angle, Kleinman symmetry conditions are valid, $d_{14} = d_{25} = d_{36}$) [24]:

$$d_{eeo} = d_{36}\sin 2\theta\cos 2\phi$$

$$d_{oeo} = d_{eoo} = -d_{36}\sin\theta\sin 2\phi$$

Second-order nonlinear coefficient:

$d_{36}(10.6\,\mu\mathrm{m}) = (4.7 \pm 0.4) \times d_{36}(AgGaSe_2) = 186 \pm 16\,\mathrm{pm/V}$ [20], [25]

Experimental values of phase-matching angle ($T = 293$ K)

Interacting wavelengths [μm]	θ_{exp} [deg]	Ref.
SHG, $e + e \Rightarrow o$		
$9 \Rightarrow 4.5$	32.2	[21]
$10 \Rightarrow 5.0$	32	[21]
$10.6 \Rightarrow 5.3$	32	[8]
	32.6	[20]
	33.8	[15]
	34	[16]
	35	[19]
$11 \Rightarrow 5.5$	32.5	[21]
$11.7 \Rightarrow 5.85$	35.7	[15]
SHG, $o + e \Rightarrow o$		
$10.6 \Rightarrow 5.3$	48.4	[9]
	49	[8]
	49.3	[20]
	50.7	[9]
	51.6	[19]
	52	[6]
SFG, $o + e \Rightarrow o$		
$16.4 + 9.54 \Rightarrow 6.03$	47	[9]
$12.9 + 9.59 \Rightarrow 5.5$	46.1	[9]

Experimental values of internal angular and temperature bandwidths

Interacting wavelengths [μm]	$\Delta\theta^{int}$ [deg]	ΔT [K]	Ref.
SHG, $e + e \Rightarrow o$			
$10.6 \Rightarrow 5.3$	0.84		[16]
SHG, $o + e \Rightarrow o$			
$10.6 \Rightarrow 5.3$	0.29		[6]
		41	[20]
DFG, $o - e \Rightarrow e$			
$5.3 - 9.3 \Rightarrow 12.32$	0.98		[4]

Laser-induced surface-damage threshold

λ [μm]	τ_p [ns]	I_{thr} [GW/cm^2]	Ref.	Note
2.8	0.1	2.7	[7]	
5	0.0006	>6	[21]	10 Hz, 100 pulses in train
9.55	30	0.16	[17]	
10.6	CW	>0.00013	[14]	T = 77 K
	CW	>0.000001	[6]	
	160	>0.004	[6]	
	160	0.038	[9]	
	150	0.033–0.04	[26]	

About the crystal

Though cadmium germanium arsenide possesses one of the highest second-order nonlinear coefficients, good optical quality crystals of this material are difficult to grow. Recently, Schunemann succeeded in growing CGA crystals with absorption coefficients less than $0.1\,cm^{-1}$ at 4.6- and 9.2-μm wavelengths [11], which were used in DFG [10] and OPG [21] applications by Vodopyanov.

References

[1] *Physical-Chemical Properties of Semiconductors. Handbook* (Nauka, Moscow, 1979) [In Russian].

[2] I.I. Kozhina, A.S. Borshchevskii: High-temperature x-ray investigations of $A^{II}B^{IV}C_2^{V}$ compounds. Vestnik LGU **No. 22**, 87–92 (1971) [In Russian].

[3] P.G. Schunemann, T.M. Pollak: Ultralow gradient HGF-grown $ZnGeP_2$ and $CdGeAs_2$ and their optical properties. MRS Bulletin **23(7)**, 23–27 (1998).

[4] R.G. Harrison, P.K. Gupta, M.R. Taghizadeh, A.K. Kar: Efficient multikilowatt mid infrared difference frequency generation in $CdGeAs_2$. IEEE J. Quant. Electr. **QE-18(8)**, 1239–1242 (1982).

[5] G.C. Bhar, R.C. Smith: Optical properties of II-IV-V_2 and I-III-VI_2 crystals with particular reference to transmission limits. Phys. Stat. Solidi A **13(1)**, 157–168 (1972).

[6] R.L. Byer, H. Kildal, R.S. Feigelson: $CdGeAs_2$—a new nonlinear crystal phasematchable at 10.6 μm. Appl. Phys. Lett. **19(7)**, 237–240 (1971).

[7] K.L. Vodopyanov, S.B. Mirov, V.G. Voevodin, P.G. Schunemann: Two-photon absorption in GaSe and $CdGeAs_2$. Opt. Commun. **155(1–3)**, 47–50 (1998).

[8] D.S. Chemla, R.F. Begley, R.L. Byer: Experimental and theoretical studies of third harmonic generation in chalcopyrite $CdGeAs_2$. IEEE J. Quant. Electr. **QE-10(1)**, 71–81 (1974).

[9] H. Kildal, J.C. Mikkelsen: Efficient doubling and CW difference frequency mixing in the infrared using the chalcopyrite $CdGeAs_2$. Opt. Commun. **10(4)**, 306–309 (1974).

[10] K.L. Vodopyanov, P.G. Schunemann: Efficient difference-frequency generation of 7–20 μm radiation in $CdGeAs_2$. Opt. Lett. **23(14)**, 1096–1098 (1998).

[11] P.G. Schunemann, S.D. Setzler, T.M. Pollak: Crystal growth of low-loss $CdGeAs_2$. In: *Advanced Solid-State Lasers, OSA Trends in Optics and Photonics Series, Vol. 50*, ed. by C. Marshall (OSA, Washington DC, 2001), pp. 632–634.

[12] P.G. Schunemann, K.L. Schepler, P.A. Budni: Nonlinear frequency conversion performance of $AgGaSe_2$, $ZnGeP_2$, and $CdGeAs_2$. MRS Bulletin **23(7)**, 45–49 (1998).

[13] A. Zakel, J.L. Blackshire, P.G. Schunemann, S.D. Setzler, J. Goldstein, S. Guha: Temperature and pulse-duration dependence of second-harmonic generation in $CdGeAs_2$. Appl. Opt. **41(12)**, 2299–2303 (2002).

[14] N. Menyuk, G.W. Iseler, A. Mooradian: High-efficiency high-average-power second-harmonic generation with $CdGeAs_2$. Appl. Phys. Lett. **29(7)**, 422–424 (1976).

[15] Y.M. Andreev, V.G. Voevodin, P.P. Geiko, A.I. Gribenyukov, A.P. Dyadkin, S.V. Pigulsky, A.I. Starodubtsev: Efficient generation of the second harmonic of NH_3 laser radiation in $CdGeAs_2$. Kvant. Elektron. **14(4)**, 784–786 (1987) [In Russian, English trans.: Sov. J. Quantum Electron. **17(4)**, 491–493 (1987)].

[16] V.E. Zuev, M.V. Kabanov, Y.M. Andreev, V.G. Voevodin, P.P. Geiko, A.I. Gribenyukov, V.V. Zuev: Applications of efficient parametric IR-laser frequency converters. Izv. Akad.

Nauk SSSR, Ser. Fiz. **52(6)**, 1142–1148 (1988) [In Russian, English trans.: Bull. Acad. Sci. USSR, Phys. Ser. **52(6)**, 87–92 (1988)].
[17] Y.M. Andreev, V.V. Badikov, V.G. Voevodin, L.G. Geiko, P.P. Geiko, M.V. Ivashchenko, A.I. Karapuzikov, I.V. Sherstov: Radiation resistance of nonlinear crystals at a wavelength of 9.55 μm. Kvant. Elektron. **31(12)**, 1075–1078 (2001) [In Russian, English trans.: Quantum Electron. **31(12)**, 1075–1078 (2001)].
[18] N.P. Barnes, R.C. Eckardt, D.J. Gettemy, L.B. Edgett: Absorption coefficients and the temperature variation of the refractive index difference of nonlinear optical crystals. IEEE J. Quant. Electr. **QE-15(10)**, 1074–1076 (1979).
[19] G.D. Boyd, E. Buehler, F.G. Storz, J.H. Wernick: Linear and nonlinear optical properties of ternary $A^{II}B^{IV}C_2^{V}$ chalcopyrite semiconductors. IEEE J. Quant. Electr. **QE-8(4)**, 419–426 (1972).
[20] E. Tanaka, K. Kato: Second-harmonic and sum-frequency generation in $CdGeAs_2$. In: *MRS Symposium Proceedings, Vol. 384, Infrared Applications of Semiconductors II*, ed by D.L. McDaniel, Jr., M.O. Manasreh, R.H. Miles, S. Sivananthan (Materials Research Society, Warrendale, PA, 1998), pp. 475–479.
[21] K.L. Vodopyanov, G.M.H. Knippels, A.F.G. van der Meer, J.P. Maffetone, I. Zweiback: Optical parametric generation in CGA crystal. Opt. Commun. **202(1–3)**, 205–208 (2002).
[22] G.C. Bhar: Refractive index interpolation in phase-matching. Appl. Opt. **15(2)**, 305–307 (1976).
[23] R.C. Eckardt, H. Masuda, Y.X. Fan, R.L. Byer: Absolute and relative nonlinear optical coefficients of KDP, KD*P, BaB_2O_4, $LiIO_3$, MgO:$LiNbO_3$, and KTP measured by phase-matched second-harmonic generation. IEEE J. Quant. Electr. **26(5)**, 922–933 (1990).
[24] J.E. Midwinter, J. Warner: The effects of phase matching method and of uniaxial crystal symmetry on the polar distribution of second-order non-linear optical polarization. Brit. J. Appl. Phys. **16(11)**, 1135–1142 (1965).
[25] A. Harasaki, K. Kato: New data on the nonlinear optical constant, phase-matching, and optical damage of $AgGaS_2$. Jpn. J. Appl. Phys. **36(2)**, 700–703 (1997).
[26] H. Kildal, G.W. Iseler: Laser-induced surface damage of infrared nonlinear materials. Appl. Opt. **15(12)**, 3062–3065 (1976).

8.17 Tl_3AsSe_3, Thallium Arsenic Selenide (TAS)

Negative uniaxial crystal: $n_o > n_e$
Molecular mass: 784.002
Specific gravity: 7.83 g/cm^3 [1]
Point group: $3m$
Lattice constants [2]:
$a = 9.80$ Å
$c = 7.08$ Å
Mohs hardness: 2–3 [2]
Melting point: 584 K [1]

Linear thermal expansion coefficient [3]

T [K]	$\alpha_t \times 10^6$ [K^{-1}], $\parallel c$	$\alpha_t \times 10^6$ [K^{-1}], $\perp c$
300	18.2	28

Transparency range at 0.5 level for 6-mm-long crystal: 1.28–17 μm [2]

Linear absorption coefficient α

λ [μm]	α [cm^{-1}]	Ref.	Note
2–12	<0.02	[1]	
9.6	0.0005	[4]	
10.6	0.082	[5]	SHG direction
	0.038	[2]	

Experimental values of refraction indices at 300 K [3]

λ [μm]	n_o	n_e	λ [μm]	n_o	n_e
2.056	3.419	3.227	7.854	3.345	3.162
3.059	3.380	3.190	9.016	3.340	3.158
4.060	3.364	3.177	9.917	3.336	3.155
5.035	3.357	3.171	10.961	3.331	3.152
5.856	3.354	3.168	12.028	3.327	3.147
6.945	3.349	3.164			

Temperature derivatives of refraction indices for $\lambda = 2$ to 10.6 μm ($T = 80$ to 300 K) [3]:

$$\frac{dn_o}{dT} = -4.52 \times 10^{-5}\,\mathrm{K}^{-1}$$

$$\frac{dn_e}{dT} = +3.55 \times 10^{-5}\,\mathrm{K}^{-1}$$

Sellmeier equations (λ in μm, $T = 300$ K) [3]:

$$n_o^2 = 1 + \frac{10.210\,\lambda^2}{\lambda^2 - 0.197136} + \frac{0.522\,\lambda^2}{\lambda^2 - 625}$$

$$n_e^2 = 1 + \frac{8.933\,\lambda^2}{\lambda^2 - 0.197136} + \frac{0.308\,\lambda^2}{\lambda^2 - 625}$$

Other set of dispersion relations is given in [2].

Expressions for the effective second-order nonlinear coefficient in general case (Kleinman symmetry conditions are valid, $d_{15} = d_{24} = d_{31} = d_{32}$) [6]:

$d_{ooe} = d_{31}\sin(\theta + \rho) - d_{22}\cos(\theta + \rho)\sin 3\phi$

$d_{eoe} = d_{oee} = d_{22}\cos^2(\theta + \rho)\cos 3\phi$

Simplified expressions for the effective second-order nonlinear coefficient (approximation of small birefringence angle, Kleinman symmetry conditions are valid, $d_{15} = d_{24} = d_{31} = d_{32}$) [7]:

$d_{ooe} = d_{31}\sin\theta - d_{22}\cos\theta\sin 3\phi$

$d_{eoe} = d_{oee} = d_{22}\cos^2\theta\cos 3\phi$

Maximal second-order nonlinear coefficient for type I interaction, $d_+ = |d_{31}\sin\theta| + |d_{22}\cos\theta|$:

$d_+(10.6\,\mu\text{m}) = (3.47 \pm 1.04) \times d_+(Ag_3AsS_3) = 68 \pm 31\,\text{pm/V}$ [2], [8], [9]

$d_+(10.6\,\mu\text{m}) = (3.3 \pm 1.0) \times d_+(Ag_3SbS_3) = 37 \pm 13\,\text{pm/V}$ [2], [9], [10]

$d_+(10.6\,\mu\text{m}) = 20$ to $30\,\text{pm/V}$ [4]

Experimental values of phase-matching angle and internal angular bandwidth

Interacting wavelengths [μm]	θ_{pm} [deg]	$\Delta\theta^{int}$ [deg]	Ref.
SHG, $o + o \Rightarrow e$			
$4.8 \Rightarrow 2.4$	27		[11]
$9.6 \Rightarrow 4.8$	19	0.21	[11]
$10.6 \Rightarrow 5.3$		0.30	[12]
SFG, $o + o \Rightarrow e$			
$9.6 + 4.8 \Rightarrow 3.2$	21		[11]
$9.6 + 2.4 \Rightarrow 1.92$	28		[11]

Laser-induced surface-damage threshold

λ [μm]	τ_p [ns]	I_{thr} [GW/cm^2]	Ref.	Note
9.25	20	>0.00001	[4]	10 kHz
9.6	70	>0.01	[11]	
10.6	20	>0.27	[12]	
	150	0.01–0.017	[13]	
	200	0.016	[2]	

About the crystal

TAS is a rather exotic IR nonlinear crystal. It was developed during the 1970s [1], [2], [3] and since then was used mainly for SHG of CO_2 laser radiation. Recently, a 6-W quasi CW output at 4.625 μm was achieved in this crystal via SHG of 20-ns, 30-kHz CO_2 laser pulses [4].

References

[1] M. Gottlieb, T.J. Isaacs, J.D. Feichtner, G.W. Roland: Acousto-optic properties of some chalcogenide crystals. J. Appl. Phys. **45(12)**, 5145–5151 (1974).

[2] J.D. Feichtner, G.W. Roland: Optical properties of a new nonlinear optical material: Tl_3AsSe_3. Appl. Opt. **11(5)**, 993–998 (1972).

[3] M.D. Ewbank, P.R. Newman, N.L. Mota, S.M. Lee, W.L. Wolfe, A.G. DeBell, W.A. Harrison: The temperature dependence of optical and mechanical properties of Tl_3AsSe_3. J. Appl. Phys. **51(7)**, 3848–3852 (1980).

[4] D.R. Suhre, L.H. Taylor: Six-watt mid-infrared laser using harmonic generation with Tl_3AsSe_3. Appl. Phys. B **63(3)**, 225–228 (1996).

[5] N.P. Barnes, R.C. Eckardt, D.J. Gettemy, L.B. Edgett: Absorption coefficients and the temperature variation of the refractive index difference of nonlinear optical crystals. IEEE J. Quant. Electr. **QE-15(10)**, 1074–1076 (1979).

[6] I. Shoji, H. Nakamura, K. Ohdaira, T. Kondo, R. Ito, T. Okamoto, K. Tatsuki, S. Kubota: Absolute measurement of second-order nonlinear-optical coefficients of β-BaB_2O_4 for visible to ultraviolet second-harmonic wavelengths. J. Opt. Soc. Am. B **16(4)**, 620–624 (1999).
[7] J.E. Midwinter, J. Warner: The effects of phase matching method and of uniaxial crystal symmetry on the polar distribution of second-order non-linear optical polarization. Brit. J. Appl. Phys. **16(11)**, 1135–1142 (1965).
[8] D.S. Chemla, P.J. Kupeček, C.A. Schwartz: Redetermination of the nonlinear optical coefficients of proustite by comparison with pyrargyrite and gallium selenide. Opt. Commun. **7(3)**, 225–228 (1973).
[9] D.A. Roberts: Simplified characterization of uniaxial and biaxial nonlinear optical crystals: a plea for standardization of nomenclature and conventions. IEEE J. Quant. Electr. **28(10)**, 2057–2074 (1992).
[10] J.H. McFee, G.D. Boyd, P.H. Schmidt: Redetermination of the nonlinear optical coefficients of Te and GaAs by comparison with Ag_3SbS_3. Appl. Phys. Lett. **17(2)**, 57–59 (1970).
[11] R.C.Y. Auyeung, D.M. Zielke, B.J. Feldman: Multiple harmonic conversion of pulsed CO_2 laser radiation in Tl_3AsSe_3. Appl. Phys. B **48(4)**, 293–297 (1989).
[12] D.R. Suhre: Efficient second-harmonic generation in Tl_3AsSe_3 using pulsed CO_2 laser radiation. Appl. Phys. B **52(6)**, 367–370 (1991).
[13] H. Kildal, G.W. Iseler: Laser-induced surface damage of infrared nonlinear materials. Appl. Opt. **15(12)**, 3062–3065 (1976).

8.18 CdSe, Cadmium Selenide

Positive uniaxial crystal: $n_e > n_o$
Molecular mass: 191.370
Specific gravity: 5.81 g/cm^3 at $T = 288$ K [1], [2], [3]
Point group: $6mm$
Lattice constants:
$a = 4.30$ Å [4]; 4.2985 Å [5]; 4.2999 Å [6]
$c = 7.01$ Å [4]; 7.0150 Å [5]; 7.0109 Å [6]
Mohs hardness: 3.25 [4]
Knoop hardness: 44–90 [7]; 71 at indenter load 20 g [4]; 90 at indenter load 20 g [5]
Solubility in water: insoluble [5]
Melting point: 1512 K [1]; 1525 K [2]; 1531 K [2]

Mean value of linear thermal expansion coefficient [2]

T [K]	$\alpha_t \times 10^6$ [K^{-1}], $\parallel c$	$\alpha_t \times 10^6$ [K^{-1}], $\perp c$
77–298	2.45	4.4

Specific heat capacity c_p at P = 0.101325 MPa [1]

T [K]	c_p [J/kgK]
298	258

Thermal conductivity coefficient [8]

T [K]	κ [W/mK], $\parallel c$	κ [W/mK], $\perp c$
293	6.9	6.2

Band-gap energy at room temperature (direct transition):
$E_g = 1.67$ eV [2]; 1.7 eV [9], [10]; 1.74 eV [1], [11], [12], [13], [14], [15], [16]; 1.75 eV [17]; 1.8 eV [3]
Transparency range at "0" transmittance level: 0.7–24 μm [3]

Linear absorption coefficient α

λ [μm]	α [cm^{-1}]	Ref.
0.75–20	<0.1	[18]
0.1–10	0.01–0.02	[19]
1.06	0.062 ± 0.006	[20]
1.0642	0.013 ± 0.001	[21]
	0.02	[22], [23]
1.32	0.01	[22]
3.39	0.01	[24]
4	0.04	[25]
10.6	0.0005	[26]
	0.016	[25]
	0.032	[27]

Two-photon absorption coefficient β

λ [μm]	τ_p [ns]	$\beta \times 10^{11}$ [cm/W]	Ref.	Note
1.06	~20	$90{,}000 \pm 9000$	[28]	$\mathbf{E}\perp c$
		$39{,}000 \pm 4000$	[28]	$\mathbf{E}\parallel c$
	20	14,000	[29]	$\perp c$, $\mathbf{E}\perp c$
		14,000	[29]	$\parallel c$, $\mathbf{E}\perp c$
		6000	[29]	$\perp c$, $\mathbf{E}\parallel c$
1.0642	0.03	3000 ± 500	[23]	
	0.038	1800	[30]	$\parallel c$
	0.040	3500	[31]	
	11	2500 ± 800	[21]	
	15	8000	[32]	$\perp c$, $\mathbf{E}\parallel c$
		16,000	[32]	$\perp c$, $\mathbf{E}\perp c$
		16,000	[32]	$\parallel c$, $\mathbf{E}\perp c$
	16	5000 ± 1400	[20]	$\parallel c$
	~20	23,000	[33]	$\mathbf{E}\perp c$
		21,000	[33]	$\mathbf{E}\parallel c$
	26	3800 ± 1100	[21]	
1.15	0.003	199	[34]	$\perp c$, $\mathbf{E}\parallel c$

λ [μm]	τ_p [ns]	$\beta \times 10^{11}$ [cm/W]	Ref.	Note
1.22	0.003	215	[34]	$\perp c$, $\mathbf{E} \parallel c$
1.30	0.003	304	[34]	$\perp c$, $\mathbf{E} \parallel c$
1.3188	80	6700 ± 2000	[21]	
1.37	0.003	355	[34]	$\perp c$, $\mathbf{E} \parallel c$
1.42	0.003	8	[34]	$\perp c$, $\mathbf{E} \parallel c$
1.44	0.000083	20	[35]	$\parallel c$
1.46	0.003	5	[34]	$\perp c$, $\mathbf{E} \parallel c$
1.50	0.003	10	[34]	$\perp c$, $\mathbf{E} \parallel c$

Experimental values of refractive indices

λ [μm]	n_o	n_e	Ref.	λ [μm]	n_o	n_e	Ref.
0.8	2.6448	2.6607	[36]	3.2	2.4532	2.4726	[36]
0.9	2.5826	2.6027	[36]	3.4	2.4518	2.4714	[36]
1.0	2.5502	2.5696	[36]	3.6	2.4509	2.4702	[36]
1.0139	2.5481	2.5677	[27]	3.8	2.4498	2.4694	[36]
1.1287	2.5246	2.5444	[27]	4.0	2.4491	2.4685	[36]
1.2	2.5132	2.5331	[36]		2.449	2.470	[37]
1.3673	2.4971	2.5170	[27]	5.0	2.4464	2.4657	[27]
1.4	2.4929	2.5133	[36]	6.0	2.445	2.466	[37]
1.5295	2.4861	2.5059	[27]		2.4434	2.4625	[27]
1.6	2.4818	2.5008	[36]	7.0	2.4398	2.4586	[27]
1.7109	2.4776	2.4974	[27]	8.0	2.4367	2.4552	[27]
1.8	2.4732	2.4930	[36]	9.0	2.4333	2.4514	[27]
2.0	2.4682	2.4873	[36]	10.0	2.431	2.452	[37]
	2.468	2.489	[37]		2.4294	2.4475	[27]
2.2	2.4642	2.4840	[36]	11.0	2.4252	2.4430	[27]
2.3253	2.4627	2.4823	[27]	12.0	2.4204	2.4379	[27]
2.4	2.4612	2.4798	[36]	14.0	2.410	2.431	[37]
2.6	2.4590	2.4784	[36]	16.0	2.399	2.419	[37]
2.8	2.4562	2.4757	[36]	20.0	2.376	2.390	[37]
3.0	2.4553	2.4748	[27]	22.0	2.339	2.351	[37]
		2.4741	[36]	24.0	2.291		[37]

Best set of dispersion relations (λ in μm, $T = 293$ K) [38]:

$$n_o^2 = 4.2243 + \frac{1.7680\,\lambda^2}{\lambda^2 - 0.2270} + \frac{3.1200\,\lambda^2}{\lambda^2 - 3380}$$

$$n_e^2 = 4.2009 + \frac{1.8875\,\lambda^2}{\lambda^2 - 0.2171} + \frac{3.6461\,\lambda^2}{\lambda^2 - 3629}$$

Other sets of dispersion relations are given in [39], [40].
Sellmeier equations for the temperatures 73 K, 173 K, 373 K, 573 K are given in [40].

Nonlinear refractive index γ

λ [μm]	$\gamma \times 10^{15}$ [cm^2/W]	Ref.
1.0642	−15	[14]
1.44–1.54	130	[35]

Linear electrooptic coefficients measured at high frequencies (well above the acoustic resonances of CdSe crystal, i.e., for the "clamped" crystal) at room temperature [41]

λ [μm]	r_{13}^{S} [pm/V]	r_{33}^{S} [pm/V]
3.3913	1.8	4.3

Expression for the effective second-order nonlinear coefficient (Kleinman symmetry conditions are valid, $d_{15} = d_{24} = d_{31} = d_{32}$) [42]:

$d_{oeo} = d_{eoo} = d_{31} \sin\theta$

Second-order nonlinear coefficients:

$d_{33}(2.12\,\mu\text{m}) = 40\,\text{pm/V}$ [43], [44]

$d_{31}(10.6\,\mu\text{m}) = -18\,\text{pm/V}$ [45]

$d_{33}(10.6\,\mu\text{m}) = 36\,\text{pm/V}$ [45]

Experimental values of phase-matching angle ($T = 293$ K)

Interacting wavelengths [μm]	θ_{exp} [deg]	Ref.
SFG, $o + e \Rightarrow o$		
$16.4 + 3.479 \Rightarrow 2.87$	73.7	[26]
$15.96 + 2.28 \Rightarrow 1.995$	62.2	[46]
$14.1 + 3.604 \Rightarrow 2.87$	70.9	[26]
$13.7 + 2.8492 \Rightarrow 2.3587$	65	[47]
$10.6 + 2.72 \Rightarrow 2.1646$	70.5	[24]
$10.361 + 2.227 \Rightarrow 1.833$	78	[48]
$9.871 + 2.251 \Rightarrow 1.833$	84	[48]
$9.776 + 2.256 \Rightarrow 1.833$	90	[48]
$8.278 + 4.3 \Rightarrow 2.83$	84	[25]
$8.253 + 4.4 \Rightarrow 2.87$	84	[25]
$8.236 + 4.5 \Rightarrow 2.91$	84	[25]
$7.88 + 3.36 \Rightarrow 2.3587$	90	[47]
$7.86 + 3.37 \Rightarrow 2.3587$	90	[18]

Experimental value of internal angular bandwidth [24]

Interacting wavelengths [μm]	$\Delta\theta^{int}$ [deg]
SFG, $o + e \Rightarrow o$	
$10.6 + 2.72 \Rightarrow 2.1646$	1.24

Experimental value of spectral bandwidth [24]

Interacting wavelengths [μm]	$\Delta\nu$ [cm^{-1}]
SFG, $o + e \Rightarrow o$	
$10.6 + 2.72 \Rightarrow 2.1646$	15

Laser-induced surface-damage threshold

λ [μm]	τ_p [ns]	I_{thr} [GW/cm^2]	Ref.
0.6943	30	0.008	[49]
	500000	<0.000002	[50]
1.833	200	0.03	[27]
1.995	20	>0.05	[46]
2.29–2.52	0.005	>0.22	[51]
2.36	35	0.05	[18]
2.596	22	>0.009	[52]
2.79	50	>0.014	[53]
2.797	0.1	>4	[19]
9.55	30	0.13	[54]
10.6	200	0.06	[55]

About the crystal

Main feature of this crystal is IR transmission up to 24 μm. In the 1970s, CdSe was widely employed for OPO, DFG, and up-conversion; it is still in use nowadays [19], [51], [53].

References

[1] *Physical-Chemical Properties of Semiconductors. Handbook* (Nauka, Moscow, 1979) [In Russian].

[2] *Physical Quantities. Handbook*, ed. by I.S. Grigoriev, E.Z. Meilikhov (Energoatomizdat, Moscow, 1991) [In Russian].

[3] B.H.T. Chai: Optical Crystals. In: *CRC Handbook of Laser Science and Technology, Supplement 2: Optical Materials*, ed. by M.J. Weber (CRC Press, Boca Raton, 1995), pp. 3–65.

[4] E.M. Voronkova, B.N. Grechushnikov, G.I. Distler, I.P. Petrov: *Optical Materials for Infrared Technique* (Nauka, Moscow, 1965) [In Russian].

[5] A.A. Blistanov, V.S. Bondarenko, N.V. Perelomova, F.N. Strizhevskaya, V.V. Tchkalova, M.P. Shaskolskaya: *Acoustic Crystals* (Nauka, Moscow, 1982) [In Russian].

[6] *Handbook of Optical Constants of Solids II*, ed. by E.D. Palik (Academic Press, Boston, 1991).

[7] M.J. Weber: Optical Crystals. In: *CRC Handbook of Laser Science and Technology, Vol. IV, Optical Materials: Part 2*, ed. by M.J. Weber (CRC Press, Boca Raton, 1987), pp. 5–14.

[8] J.D. Beasley: Thermal conductivities of some novel nonlinear optical materials. Appl. Opt. **33(6)**, 1000–1003 (1994).

[9] B. Jensen, A. Torabi: Refractive index of hexagonal II–VI compounds CdSe, CdS, and $CdSe_xS_{1-x}$. J. Opt. Soc. Am. B **3(6)**, 857–863 (1986).

[10] K.J. Bachmann: *The Materials Science of Microelectronics* (VCH Publishers, New York, 1995).

[11] E.W. van Stryland, M.A. Woodall, H. Vanherzeele, M.J. Soileau: Energy band-gap dependence of two-photon absorption. Opt. Lett. **10(10)**, 490–492 (1985).

[12] S.S. Mitra, L.M. Narducci, R.A. Shatas, Y.F. Tsay, A. Vaidyanathan: Nonlinear absorption in direct-gap semiconductors. Appl. Opt. **14(12)**, 3038–3042 (1975).

[13] A. Miller, G.S. Ash: Two-photon absorption and short pulse stimulated recombination in $AgGaSe_2$. Opt. Commun. **33(3)**, 297–300 (1980).

[14] M. Sheik-Bahae, D.C. Hutchings, D.J. Hagan, E.W. van Stryland: Dispersion of bound electron nonlinear refraction in solids. IEEE J. Quant. Electr. **27(6)**, 1296–1309 (1991).

[15] E.W. van Stryland, L.L. Chase: Two-Photon Absorption. Inorganic Materials. In: *CRC Handbook of Laser Science and Technology, Supplement 2: Optical Materials*, ed. by M.J. Weber (CRC Press, Boca Raton, 1995), pp. 299–328.

[16] C. Kittel: *Introduction to Solid State Physics, Seventh Edition* (John Wiley & Sons, New York, 1996).

[17] M. Schäffner, X. Bao, A. Penzkofer: Principal optical constants measurement of uniaxial crystal CdSe in the wavelength region between 380 and 950 nm. Appl. Opt. **31(22)**, 4546–4552 (1992).

[18] A.A. Davydov, L.A. Kulevskii, A.M. Prokhorov, A.D. Saveliev, V.V. Smirnov: Parametric generation with CdSe crystal pumped by CaF_2:Dy^{2+}. Pisma Zh. Eksp. Teor. Fiz. **15(12)**, 725–727 (1972) [In Russian, English trans.: JETP Lett. **15(12)**, 513–514 (1972)].

[19] K.L. Vodopyanov: Megawatt peak power 8–13 μm CdSe optical parametric generator pumped at 2.8 μm. Opt. Commun. **150(1–6)**, 210–212 (1998).

[20] M. Bass, E.W. van Stryland, A.F. Stewart: Laser calorimetric measurement of two-photon absorption. Appl. Phys. Lett. **34(2)**, 142–144 (1979).

[21] A.F. Stewart, M. Bass: Intensity-dependent absorption in semiconductors. Appl. Phys. Lett. **37(11)**, 1040–1043 (1980).

[22] D.S. Hanna, A.J. Turner: Nonlinear absorption measurements in proustite (Ag_3AsS_3) and CdSe. Opt. Quant. Electron. **8(3)**, 213–217 (1976).

[23] J.H. Bechtel, W.L. Smith: Two-photon absorption in semiconductors with picosecond light pulses. Phys. Rev. B **13(8)**, 3515–3522 (1976).

[24] A. Ferrario, M. Garbi: Efficient up-conversion in CdSe. Opt. Commun. **17(2)**, 158–159 (1976).

[25] J.A. Weiss, L.S. Goldberg: Singly resonant CdSe parametric oscillator pumped by an HF laser. Appl. Phys. Lett. **24(8)**, 389–391 (1974).

[26] R.G. Wenzel, G.P. Arnold: Parametric oscillator: HF oscillator-amplifier pumped CdSe parametric oscillator tunable from 14.1 μm to 16.4 μm. Appl. Opt. **15(5)**, 1322–1326 (1976).

[27] R.L. Herbst, R.L. Byer: Efficient parametric mixing in CdSe. Appl. Phys. Lett. **19(12)**, 527–530 (1971).

[28] A.Z. Grasyuk, I.G. Zubarev, A.N. Menzer: Anisotropy of two-photon absorption upon optical excitation of CdSe semiconductor lasers. Fiz. Tverd. Tela **10(2)**, 543–549 (1968) [In Russian, English trans.: Sov. Phys. - Solid State **10(2)**, 427–431 (1968)].

[29] F. Brkiner, V.S. Dneprovskii, V.U. Khattatov: Two-photon absorption in cadmium selenide. Kvant. Elektron. **1(6)**, 1360–1364 (1974) [In Russian, English trans.: Sov. J. Quantum Electron. **4(6)**, 749–751 (1974)].

[30] E.W. van Stryland, H. Vanherzeele, M.A. Woodall, M.J. Soileau, A.L. Smirl, S. Guha, T.F. Boggess: Two photon absorption, nonlinear refraction, and optical limiting in semiconductors. Opt. Eng. **24(4)**, 613–623 (1985).

[31] W.L. Smith: Two-Photon Absorption in Condensed Media. In: *CRC Handbook of Laser Science and Technology, Vol. III, Optical Materials: Part 1*, ed. by M.J. Weber (CRC Press, Boca Raton, 1986), pp. 229–258.

[32] V.S. Dneprovskii, S.M. Ok: Role of absorption by nonequillibrium carriers in determination of two-photon absorption of CdSe and GaAs crystals. Kvant. Elektron. **3(3)**, 559–562 (1976) [In Russian, English trans.: Sov. J. Quantum Electron. **6(3)**, 298–300 (1976)].

[33] J.M. Ralston, R.K. Chang: Nd:laser induced absorption in semiconductors and aqueous $PrCl_3$ and $NdCl_3$. Opto-electron. **1(4)**, 182–188 (1969).

[34] I.B. Zotova, Y.J. Ding: Spectral measurements of two-photon absorption coefficients for CdSe and GaSe crystals. Appl. Opt. **40(36)**, 6654–6658 (2001).

[35] G.-M. Schucan, R.G. Ispasoiu, A.M. Fox, J.F. Ryan: Ultrafast two-photon nonlinearities in CdSe near 1.5 μm studied by interferometric autocorrelation. IEEE J. Quant. Electr. **34(8)**, 1374–1379 (1998).

[36] W.L. Bond: Measurement of the refractive indices of several crystals. J. Appl. Phys. **36(5)**, 1674–1677 (1965).

[37] M.P. Lisitsa, L.F. Gudymenko, V.N. Malinko, S.F. Terekhova: Dispersion of the refractive indices and birefringence of CdS_xSe_{1-x} single crystals. Phys. Stat. Solidi **31(1)**, 389–399 (1969).

[38] G.C. Bhar: Refractive index interpolation in phase-matching. Appl. Opt. **15(2)**, 305–307 (1976).

[39] G.C. Bhar, D.C. Hanna, B. Luther-Davies, R.C. Smith: Tunable down-conversion from an optical parametric oscillator. Opt. Commun. **6(4)**, 323–326 (1972).

[40] G.C. Bhar, G.C. Ghosh: Temperature dependent phase-matched nonlinear optical devices using CdSe and $ZnGeP_2$. IEEE J. Quant. Electr. **QE-16(8)**, 838–843 (1980).

[41] I.P. Kaminow: Tables of Linear Electrooptic Coefficients. In: *CRC Handbook of Laser Science and Technology, Vol. III, Optical Materials: Part 2*, ed. by M.J. Weber (CRC Press, Boca Raton, 1986), pp. 253–278.

[42] J.E. Midwinter, J. Warner: The effects of phase matching method and of uniaxial crystal symmetry on the polar distribution of second-order non-linear optical polarization. Brit. J. Appl. Phys. **16(11)**, 1135–1142 (1965).

[43] M.M. Choy, R.L. Byer: Accurate second-order susceptibility measurements of visible and infrared nonlinear crystals. Phys. Rev. B **14(4)**, 1693–1706 (1976).

[44] W.J. Alford, A.V. Smith: Wavelength variation of the second-order nonlinear coefficients of $KNbO_3$, $KTiOPO_4$, $KTiOAsO_4$, $LiNbO_3$, $LiIO_3$, β-BaB_2O_4, KH_2PO_4, and LiB_3O_5 crystals: a test of Miller wavelength scaling. J. Opt. Soc. Am. B **18(4)**, 524–533 (2001).

[45] D.A. Roberts: Simplified characterization of uniaxial and biaxial nonlinear optical crystals: a plea for standardization of nomenclature and conventions. IEEE J. Quant. Electr. **28(10)**, 2057–2074 (1992).

[46] D. Andreou: 16 μm tunable source using parametric processes in non-linear crystals. Opt. Commun. **23(1)**, 37–43 (1977).

[47] A.A. Davydov, L.A. Kulevskii, A.M. Prokhorov, A.D. Saveliev, V.V. Smirnov, A.V. Shirkov: A tunable infrared parametric oscillator in a CdSe crystal. Opt. Commun. **9(3)**, 234–236 (1973).

[48] R.L. Herbst, R.L. Byer: Singly resonant CdSe infrared parametric oscillator. Appl. Phys. Lett. **21(5)**, 189–191 (1972).

[49] M. Birnbaum, T.L. Stocker: Reflectivity enhancement of semiconductors by Q-switched ruby lasers. J. Appl. Phys. **39(13)**, 6032–6036 (1968).

[50] M. Bertolotti, F. de Pasquale, P. Marietti, D. Sette, G.Vitali: Laser damage on semiconductor surfaces. J. Appl. Phys. **38(10)**, 4088–4090 (1967).

[51] M.A. Watson, M.V. O'Connor, D.P. Shepherd, D.C. Hanna: Synchronously pumped CdSe optical parametric oscillator in the 9–10 μm region. Opt. Lett. **28(20)**, 1957–1959 (2003).

[52] J.M. Fukumoto: Three-stage optical parametric oscillator conversion from 1 μm to the 8–12 μm region. In: *Advanced Solid-State Lasers, OSA Trends in Optics and Photonics Series, Vol. 68*, ed. by M.E. Fermann, L.R. Marshall (OSA, Washington DC, 2002), pp. 558–562.

[53] T.H. Allik, S. Chandra, D.M. Rines, P.G. Schunemann, J.A. Hutchinson, R. Utano: Tunable 7–12-μm optical parametric oscillator using a Cr,Er:YSGG laser to pump CdSe and $ZnGeP_2$ crystals. Opt. Lett. **22(9)**, 597–599 (1997).

[54] Y.M. Andreev, V.V. Badikov, V.G. Voevodin, L.G. Geiko, P.P. Geiko, M.V. Ivashchenko, A.I. Karapuzikov, I.V. Sherstov: Radiation resistance of nonlinear crystals at a wavelength of 9.55 μm. Kvant. Elektron. **31(12)**, 1075–1078 (2001) [In Russian, English trans.: Quantum Electron. **31(12)**, 1075–1078 (2001)].

[55] D.C. Hanna, B. Luther-Davies, H.N. Rutt, R.C. Smith, C.R. Stanley: Q-switched laser damage of infrared nonlinear materials. IEEE J. Quant. Electr. **QE-8(3)**, 317–324 (1972).

9

Some Recent Applications

This chapter contains seven short reviews discussing modern applications of common and novel nonlinear materials.

9.1 Deep-UV Light Generation

In 1986, Kato found that the shortest wavelength generated by frequency doubling (NCPM SHG) was equal to 204.8 nm [1]. This record, achieved in BBO, was surpassed only 10 years later. In 1996, a Chinese group reported the new nonlinear crystal potassium fluoroboratoberyllate (KBBF) [2], which allows direct SHG down to 172.5 nm [3]. However, KBBF possesses a plate-like nature, and the growth of crystals thicker than a millimeter is extremely difficult. This makes the angular tuning of phase-matching angle difficult. Especially for deep-UV applications of this crystal, an optical contact approach via two CaF_2 prisms coupling was proposed [3], which is rather inconvenient and cannot be used for very efficient nonlinear conversion.

An alternative way to reach very short UV wavelengths (below 205 nm) is to use the sum-frequency generation. This approach was developed in the mid-1970s [4], [5]. In order to satisfy phase matching conditions, the summing wavelengths should differ as much as possible in frequencies; that is, one of them should lie near the UV edge of transmission range and the other near the IR edge. Recently, a German group, using SFG between the near IR idler wavelengths from OPO, pumped by a Ti:sapphire femtosecond laser and the UV fourth harmonic of the same laser, reached 175-nm wavelength in CLBO [6], 172.7 nm in LBO [7], 170 nm in LB4 [8], and 166 nm in KB5 [9]. For the review of their results, see [10].

A few powerful quasi-CW deep-UV sources were demonstrated recently, using CLBO for the final sum-frequency mixing stage. In [11], the mean power of 250 mW at 205 nm was generated, in [12] a 1-W source at 196.3 nm was developed, while in [13] the absolute maximum of 1.5 W mean power at the same wavelength was achieved.

A nanosecond widely tunable deep-UV source was reported in [14]. Using a set of BBO harmonic generators and a broadly tunable Ti:sapphire laser with amplifier,

the authors generated pulses with more than 1 mJ energy in the 193–233 nm spectral range with a repetition rate of 10 Hz.

References

[1] K. Kato: Second-harmonic generation to 2048Å in β-BaB_2O_4. IEEE J. Quant. Electr. **QE-22(7)**, 1013–1014 (1986).

[2] B. Wu, D. Tang, N. Ye, C. Chen: Linear and nonlinear optical properties of the $KBe_2BO_3F_2$ (KBBF) crystal. Opt. Mater. **5(1–2)**, 105–109 (1996).

[3] T. Togashi, T. Kanai, T. Sekikawa, S. Watanabe, C. Chen, C. Zhang, Z. Xu, J. Wang: Generation of vacuum-ultraviolet light by an optically contacted, prism-coupled $KBe_2BO_3F_2$ crystal. Opt. Lett. **28(4)**, 254–256 (2003).

[4] F.B. Dunning, R.E. Stickel, Jr.: Sum frequency mixing in potassium pentaborate as a source of tunable coherent radiation at wavelengths below 217 nm. Appl. Opt. **15(12)**, 3131–3134 (1976).

[5] G.A. Massey, J.C. Johnson: Wavelength-tunable optical mixing experiments between 208 nm and 259 nm. IEEE J. Quant. Electr. **QE-12(11)**, 721–727 (1976).

[6] V. Petrov, F. Noack, F. Rotermund, M. Tanaka, Y. Okada: Sum-frequency generation of femtosecond pulses in $CsLiB_6O_{10}$ down to 175 nm. Appl. Opt. **39(27)**, 5076–5079 (2000).

[7] F. Seifert, J. Ringling, F. Noack, V. Petrov, O. Kittelmann: Generation of tunable femtosecond pulses to as low as 172.7 nm by sum-frequency mixing in lithium triborate. Opt. Lett. **19(19)**, 1538–1540 (1994).

[8] V. Petrov, F. Rotermund, F. Noack, R. Komatsu, T. Sugawara, S. Uda: Vacuum ultraviolet application of $Li_2B_4O_7$ crystals: generation of 100 fs pulses down to 170 nm. J. Appl. Phys. **84(11)**, 5887–5892 (1998).

[9] V. Petrov, F. Rotermund, F. Noack: Generation of femtosecond pulses down to 166 nm by sum-frequency mixing in $KB_5O_8 \cdot 4H_2O$. Electron. Lett. **34(18)**, 1748–1750 (1998).

[10] V. Petrov, F. Rotermund, F. Noack, J. Ringling, O. Kittelmann, R. Komatsu: Frequency conversion of Ti:sapphire-based femtosecond laser systems to the 200-nm spectral region using nonlinear optical crystals. IEEE J. Sel. Topics Quant. Electr. **5(6)**, 1532–1542 (1999).

[11] K.F. Wall, J.S. Smucz, B. Pati, Y. Isyanova, P. Moulton, J.G. Manni: A quasi-continuous-wave deep ultraviolet laser source. IEEE J. Quant. Electr. **39(9)**, 1160–1169 (2003).

[12] J. Sakuma, A. Finch, Y. Ohsako, K. Deki, M. Yoshino, M. Horiguchi, T. Yokota, Y. Mori, T. Sasaki: All-solid-state, 1-W, 5-kHz laser source below 200 nm. In: *Advanced Solid-State Lasers, OSA Trends in Optics and Photonics Series, Vol. 26*, ed. by M.M. Fejer, H. Injeyan, U. Keller (OSA, Washington DC, 1999), pp. 89–92.

[13] J. Sakuma, K. Deki, A. Finch, Y. Ohsako, T. Yokota: All-solid-state, high-power, deep-UV laser system based on cascaded sum-frequency mixing in $CsLiB_6O_{10}$ crystals. Appl. Opt. **39(30)**, 5505–5511 (2001).

[14] A.V. Kachynski, V.A. Orlovich, A.A. Bui, V.D. Kopachevsky, A.V. Kudryakov, W. Kiefer: All solid-state pulsed ultraviolet laser widely tunable down to 188.5 nm. Opt. Commun. **218(4–6)**, 351–357 (2003).

9.2 Terahertz-Wave Generation by DFG

One of most common applications of nonlinear optical crystals is difference frequency generation to the IR range. Even during the early years of quantum electronics,

attempts were made to generate submillimeter radiation via this approach. In 1971, Yajima and Takeuchi experimentally proved the possibility of tunable far IR generation in $LiNbO_3$ via DFG between two spectral components of spectrally wide 1.06-μm radiation of a mode-locked Nd:glass laser [1]. Using lithium niobate (LN) crystal and changing the phase-matching angle from 18° to 16.2°, they managed to receive far infrared radiation, tunable in the 521–645 μm (0.58–0.47 THz) range. The next year, the American group from Bell Labs observed phase-matched DFG between the frequencies of two CO_2 lasers in $ZnGeP_2$ [2]. The obtained tuning range was 91–143 μm (3.3–2.1 THz), and the power conversion efficiency at 120 μm was 1.3×10^{-8}.

Three decades later, when the development of compact and efficient THz sources became actual for the applications in molecular spectroscopy, radio astronomy, biomedical imaging, electronics, and so forth, the old DFG technique of THz-wave generation was revived. A Japanese group [3] used for DFG two signal waves from two OPOs created in one PPLN crystal with two domains of slightly different poling period. When pumping the PPLN crystal with a Q-switched Nd:YAG laser radiation ($\lambda = 1.064$ μm), two waves near 1.5 μm were generated; the frequency difference between them was controlled by the temperature of the crystal. For DFG, the organic nonlinear crystal DAST was used. As a result, far IR radiation in the range 120–160 μm (2.5–1.87 THz) with a rather low power conversion efficiency of 3.8×10^{-10} was obtained. American scientists Shi and Ding decided to use the much better developed inorganic nonlinear crystals GaSe and $ZnGeP_2$ (ZGP) for DFG. Using angular-tuned phase matching in a 1.5-cm-long GaSe crystal (type II interaction, $e - e \Rightarrow o$), they managed to produce coherent THz radiation in the extremely wide range of 56.8–1618 μm (5.27–0.18 THz), with power conversion efficiency 1.8×10^{-4} at 196 μm [4]. In a 1.2-cm-long ZGP crystal, both type I ($o - e \Rightarrow e$) and type II ($o - e \Rightarrow o$) interactions were realized with tuning ranges of 66.5–300 μm (4.51–1.0 THz) and 72.7–237 μm (4.13–1.26 THz), respectively [5]. The measured power conversion efficiency values were 6.7×10^{-5} (at 97 μm) and 3.6×10^{-5} (at 123 μm) for $o - e \Rightarrow e$ and $o - e \Rightarrow o$ interactions, respectively.

A recently published review [6] deals with nonlinear optical crystals suitable for submillimeter wave generation. Together with the DFG method of THz-wave generation, both forward and backward OPO approaches are considered.

References

[1] T. Yajima, N. Takeuchi: Spectral properties and tunability of far-infrared difference-frequency radiation produced by picosecond light pulses. Jpn. J. Appl. Phys. **10(7)**, 907–915 (1971).

[2] G.D. Boyd, T.J. Bridges, C.K.N. Patel, E. Buehler: Phase-matched submillimeter wave generation by difference-frequency mixing in $ZnGeP_2$. Appl. Phys. Lett. **21(11)**, 553–555 (1972).

[3] K. Kawase, T. Hatanaka, H. Takahashi, K. Nakamura, T. Taniuchi, H. Ito: Tunable terahertz-wave generation from DAST crystal by dual signal-wave parametric oscillation of periodically poled lithium niobate. Opt. Lett. **25(23)**, 1714–1716 (2000).

[4] W. Shi, Y.J. Ding, N. Fernelius, K. Vodopyanov: Efficient, tunable, and coherent 0.18–5.27-THz source based on GaSe crystal. Opt. Lett. **27(16)**, 1454–1456 (2002).

[5] W. Shi, Y.J. Ding: Continuously tunable and coherent terahertz radiation by means of phase-matched difference-frequency generation in zinc germanium phosphide. Appl. Phys. Lett. **83(5)**, 848–851 (2003).
[6] Y.J. Ding, I.B. Zotova: Second-order nonlinear optical materials for efficient generation and amplification of temporally-coherent and narrow-linewidth terahertz waves. Opt. Quant. Electron. **32(4–5)**, 531–552 (2000).

9.3 Ultrashort Laser Pulse Compression via SHG

In 1990, Australian scientists proposed the new effect of pulsewidth shortening in the course of type II SHG of 1-ps, 1-μm pulse in a KDP type crystal [1]. The idea behind this method is to introduce an optimal "predelay" between the ordinary and extraordinary interacting fundamental pulses by using another thin type II KDP crystal ("predelay" crystal) of the same cut, set out of phase matching direction and with its axes aligned at 90° to the SHG crystal. Owing to the difference in group velocities of the *o*- and *e*-polarized fundamental pulses at the entrance of the SHG crystal, a much longer nonlinear-interaction length should be attained. This should lead to the compression of the second-harmonic pulse by up to a factor of 5 and an increase in the power conversion efficiency.

Both predictions were experimentally verified in the works of the same Australian group [2], [3]. In [3], the shortening of 1.2-ps, 1.053-μm pulses from a Nd:YLF laser with an almost Gaussian shape was investigated. The 15-mm-thick "predelay" DKDP crystal introduced a 1.4-ps delay between the extraordinary and ordinary components of the 1.053-μm pulse at the entrance of the 25-mm-thick KDP type II SHG crystal. At the incident intensity of $7\,\mathrm{GW/cm^2}$, the green second-harmonic pulse was compressed to 250 fs (by about 5 times) and the power conversion efficiency raised by 240%, compared to the standard 40% observed without a predelay. Similar results were obtained in a later work [4] where compression by more than 2.5 times was reported.

Simultaneously with the shortening of second-harmonic pulses in the type II SHG, any interacting fundamental pulses (*o* or *e*) could be compressed if the proper intensity ratio between them is chosen. In [5], the shortening of an *o*-polarized fundamental beam from 1.3 ps to 280 fs was demonstrated. Concerning the limitations of this technique, it was mentioned [2] that from the whole range of nonlinear optical crystals, only KDP and its closest analog DKDP could provide the correct relationship between the group velocities of the fundamental and second-harmonic pulses and, moreover, only for SHG at wavelengths close to 1 μm (Nd-doped lasers). In [6], a more than 20-fold compression was demonstrated for the relatively long 11-ps Nd:YAG laser pulse.

The development of this method is possible, if employing for group velocities adjustment the pulse front tilting (see the pioneering works [7], [8]). This allows the use of another nonlinear crystal for SHG compression of a 1.3-ps Nd:glass laser pulse, for example BBO, for which 9-fold compression was reported [9]. Furthermore, the tilting compression technique could be transferred to THG and even to type I

interactions. In [10], the satellite-free pulse-shortening at 351 nm from 1.3 ps to 350 fs was achieved.

References

[1] Y. Wang, R. Dragila: Efficient conversion of picosecond laser pulses into second-harmonic frequency using group-velocity dispersion. Phys. Rev. A **41(10)**, 5645–5649 (1990).

[2] Y. Wang, B. Luther-Davies, Y.-H. Chuang, R.S. Craxton, D.D. Meyerhofer: Highly efficient conversion of picosecond laser pulses with the use of group-velocity-mismatched frequency doubling in KDP. Opt. Lett. **16(23)**, 1862–1864 (1991).

[3] Y. Wang, B. Luther-Davies: Frequency-doubling pulse compressor for picosecond high-power neodymium laser pulses. Opt. Lett. **17(20)**, 1459–1461 (1992).

[4] T. Zhang, H. Daido, Y. Kato, L.B. Sharma, Y. Izawa, S. Nakai: Second-harmonic generation of a picosecond laser pulse at high intensities with time predelay. Jpn. J. Appl. Phys. **34(7A)**, 3546–3551 (1995).

[5] A. Dubietis, G. Valiulis, R. Danielius, A. Piskarskas: Fundamental-frequency pulse compression through cascaded second-order processes in a type II phase-matched second-harmonic generator. Opt. Lett. **21(6)**, 1262–1264 (1996).

[6] A. Umbrasas, J.-C. Diels, J. Jacob, G. Valiulis, A. Piskarskas: Generation of femtosecond pulses through second-harmonic compression of the output of a Nd:YAG laser. Opt. Lett. **20(21)**, 2228–2230 (1995).

[7] M.R. Topp, G.C. Orner: Group dispersion effects in picosecond spectroscopy. Opt. Commun. **13(3)**, 276–281 (1975).

[8] Z. Bor, B. Racz: Group velocity dispersion in prisms and its application to pulse compression and traveling-wave excitation. Opt. Commun. **54(3)**, 165–170 (1985).

[9] A. Dubietis, G. Valiulis, G. Tamošauskas, R. Danielius, A. Piskarskas: Nonlinear second-harmonic pulse compression with tilted pulses. Opt. Lett. **22(14)**, 1071–1073 (1997).

[10] A. Dubietis, G. Valiulis, G. Tamošauskas, R. Danielius, A. Piskarskas: Nonlinear pulse compression in the ultraviolet. Opt. Commun. **144(1–3)**, 55–59 (1997).

9.4 Self-Frequency-Doubling Crystals

The idea of self-frequency doubling (SFD) is very simple. A nonlinear optical crystal, doped with a trivalent rare-earth ion (which is usually Nd or Yb), generates the fundamental radiation and simultaneously converts it into the second harmonic. This idea was first realized in LN, doped with Tm [1] and Nd [2]. Later, other host crystals, such as YAB [3], $MgO:LiNbO_3$ [4], $LaBGeO_5$ [5], and GAB [6], were probed for self-frequency doubling. From the practical point of view, the most important implications of SFD are those related to diode pumping, which has been available since the early 1990s.

First we will list the best results on SFD, obtained in Nd:YAB (NYAB), and also in recently discovered neodymium-doped gadolinium and yttrium calcium oxyborates crystals (GdCOB [7], [8], [9] and YCOB [9], [10], [11], respectively). The second harmonic wavelength of ${}^4F_{3/2} \Rightarrow {}^4I_{11/2}$ transition of the Nd^{3+}-ion in these crystal matrices corresponds to 530.5 nm. Using a 0.5-cm-long NYAB crystal (4 at.%Nd),

cut for type I SHG ($\theta = 30.7°$), and 1.6-W diode-pumping at 807 nm, 225 mW of CW green radiation was generated in [12]. In [13], [14], using an 0.8-cm-long Nd:GdCOB crystal (7 at.% Nd), cut for type I SHG ($\theta = 90°$, $\phi = 46°$), and 1.25-W (absorbed power) diode-pumping at 810 nm, 115 mW at 530.5 nm was obtained. A similar experiment with Nd:YCOB (0.5-cm-long, 5 at.% Nd, $\theta = 90°$, $\phi = 33.6°$) yielded 245 mW of CW green light at 3.8 W (absorbed power) diode-pumping at 812 nm [15].

The combined Australian–Chinese group investigated SFD in a type I Yb:YAB crystal (0.3-cm-long, 8–10 at.% Yb, $\theta = 31°$). With moderate 1.4-W InGaAs diode-pumping at 976 nm, 160 mW of CW green output was obtained [16]. At high pumping power of 11 W, 1.1 W at 530.5 nm was generated [17], [18]. This is the highest green power reported for any diode-pumped SFD laser to date.

In [19], the self-doubling of another Nd^{3+}-ion transition, ${}^4F_{3/2} \Rightarrow {}^4I_{13/2}$ ($\lambda =$ 1332 nm), was performed in a Nd:YCOB crystal. About 16 mW CW red output was generated with 0.9 W absorbed fundamental power at 812 nm.

Besides the SFD, the sum- and the difference-frequency mixing processes could also be realized in self-frequency-doubling nonlinear crystals [20], [21]. The simultaneous occurrence of SFD and SFM channels in one crystal is also possible [22], [23]; in the latter work, the CW light at wavelengths corresponding to the three fundamental colors red (669 nm), green (505 nm) and blue (481 nm) was generated in NYAB crystal using a combination of two different pump wavelengths (755 and 807 nm).

References

[1] L.F. Johnson, A.A. Ballman: Coherent emission from rare earth ions in electro-optic crystals. J. Appl. Phys. **40(1)**, 297–302 (1969).

[2] V.G. Dmitriev, E.V. Raevskii, L.N. Rashkovich, N.M. Rubinina, O.O. Selichev, A.A. Fomichev: Simultaneous emission at the fundamental frequency and the second harmonic in an active nonlinear medium: neodymium-doped lithium metaniobate. Pisma Zh. Tech. Fiz. **5(21–22)**, 1400–1402 (1979) [In Russian, English trans.: Sov. Tech. Phys. Lett. **5(11)**, 590–591 (1979)].

[3] L.M. Dorozhkin, I.I. Kuratev, N.I. Leonyuk, T.I. Timchenko, A.V. Shestakov: Optical second-harmonic generation in a new nonlinear active medium: neodymium-yttrium-aluminum borate crystals. Pisma Zh. Tekh. Fiz. **7(21)**, 1297–1300 (1981) [In Russian, English trans.: Sov. Tech. Phys. Lett. **7(11)**, 555–556 (1981)].

[4] T.Y. Fan, A. Cordova-Plaza, M.J.F. Digonnet, R.L. Byer, H.J. Shaw: Nd:MgO:$LiNbO_3$ spectroscopy and laser devices. J. Opt. Soc. Am. B **3(1)**, 140–147 (1986).

[5] J. Capmany, D. Jaque, J. Garcia Sole, A.A. Kaminskii: Continuous wave laser radiation at 524 nm from a self-frequency-doubled laser of $LaBGeO_5$:Nd^{3+}. Appl. Phys. Lett. **72(5)**, 531–533 (1998).

[6] C. Tu, M. Qiu, Y. Huang, X. Chen, A. Jiang, Z. Luo: The study of a self-frequency-doubling laser crystal Nd^{3+}:$GdAl_3(BO_3)_4$. J. Cryst. Growth **208(1–4)**, 487–492 (2000).

[7] G. Aka, L. Bloch, J.M. Benitez, P. Crochet, A. Kahn-Harari, D. Vivien, F. salin, P. Coquelin, D. Colin: A new non linear oxoborate crystal, characterized by using femtosecond broadband pulses. In: *Advanced Solid-State Lasers, OSA Trends in Optics and Photonics Series, Vol. 1*, ed. by S.A. Payne, C. Pollock (OSA, Washington DC, 1996), pp. 336–340.

[8] G. Aka, A. Kahn-Harari, D. Vivien, J.-M. Benitez, F. Salin, J. Godard: A new nonlinear and neodymium laser self-frequency doubling crystal with congruent melting: $Ca_4GdO(BO_3)_3$ (GdCOB). Eur. J. Solid State Inorg. Chem. **33(8)**, 727–736 (1996).

[9] M. Iwai, T. Kobayashi, H. Furuya, Y. Mori, T. Sasaki: Crystal growth and optical characterization of rare-earth (Re) calcium oxyborate $ReCa_4O(BO_3)_3$ (Re = Y or Gd) as new nonlinear optical material. Jpn. J. Appl. Phys. **36(3A)**, L276–L279 (1997).

[10] M. Yoshimura, T. Kobayashi, H. Furuya, K. Murase, Y. Mori, T. Sasaki: Crystal growth and optical properties of yttrium calcium oxyborate $YCa_4O(BO_3)_3$. In: *Advanced Solid-State Lasers, OSA Trends in Optics and Photonics Series, Vol. 19*, ed. by W.R. Bosenberg, M.M. Fejer (OSA, Washington DC, 1998), pp. 561–564.

[11] Q. Ye, B.H.T. Chai: Crystal growth of $YCa_4O(BO_3)_3$ and its orientation. J. Cryst. Growth **197(1–2)**, 228–235 (1999).

[12] J. Bartschke, R. Knappe, K.-J. Boller, R. Wallenstein: Investigation of efficient self-frequency-doubling Nd:YAB lasers. IEEE J. Quant. Electr. **33(12)**, 2295–2300 (1997).

[13] F. Auge, S. Auzanneau, G. Lukas-Leclin, F. Balembois, P. Georges, A. Brun, F. Mougel, G. Aka, A. Kahn-Harari, D. Vivien: Efficient self-frequency-doubling Nd:GdCOB crystal pumped by a high brightness laser diode. In: *Advanced Solid-State Lasers, OSA Trends in Optics and Photonics Series, Vol. 26*, ed. by M.M. Fejer, H. Injeyan, U. Keller (OSA, Washington DC, 1999), pp. 77–81.

[14] D. Vivien, F. Mougel, F. Auge, G. Aka, A. Kahn-Harari, F. Balembois, G. Lucas-Leclin, P. Georges, A. Brun, P. Aschehoug, J.-M. Benitez, N. Le Nain, M. Jacquet: Nd:GdCOB: overview of its infrared, green and blue laser performances. Opt. Mater. **16(1-2)**, 213–220 (2001).

[15] D.A. Hammons, M. Richardson, B.H.T. Chai, A.K. Chin, R. Jollay: Scaling of longitudinally diode-pumped self-frequency-doubling Nd:YCOB lasers. IEEE J. Quant. Electr. **36(8)**, 991–999 (2000).

[16] P. Wang, P. Dekker, J.M. Dawes, J.A. Piper, Y. Liu, J. Wang: Efficient continuous-wave self-frequency-doubling green diode-pumped $Yb:YAl_3(BO_3)_4$ lasers. Opt. Lett. **25(10)**, 731–733 (2000).

[17] P. Dekker, J.M. Dawes, J.A. Piper, Y. Liu, J. Wang: 1.1 W CW self-frequency-doubled diode-pumped $Yb:YAl_3(BO_3)_4$ laser. Opt. Commun. **195(5–6)**, 431–436 (2001).

[18] H. Jiang, J. Li, J. Wang, X.-B. Hu, H. Liu, B. Teng, C.-Q. Zhang, P. Dekker, P. Wang: Growth of $Yb:YAl_3(BO_3)_4$ crystals and their optical and self-frequency-doubling properties. J. Cryst. Growth **233(1–2)**, 248–252 (2001).

[19] Q. Ye, L. Shah, J. Eichenholz, D. Hammons, R. Peale, M. Richardson, A. Chin, B.H.T. Chai: Investigation of diode-pumped, self-frequency doubled RGB lasers from Nd:YCOB crystals. Opt. Commun. **164(1–3)**, 33–37 (1999).

[20] F. Mougel, G. Aka, A. Kahn-Harari, D. Vivien: CW blue laser generation by self sum-frequency mixing in $Nd:Ca_4GdO(BO_3)_3$ (Nd:GdCOB) single crystal. Opt. Mater. **13(3)**, 293–297 (1999).

[21] A. Brenier, C. Tu, J. Li, Z. Zhu, B. Wu: Self-sum- and difference-frequency mixing in $GdAl_3(BO_3)_4:Nd^{3+}$ for generation of tunable ultraviolet and infrared radiation. Opt. Lett. **27(4)**, 240–242 (2002).

[22] Y. Chen, M. Huang, Y. Huang, Z. Luo: Simultaneous green and blue laser radiation based on a nonlinear laser crystal $Nd:GdAl_3(BO_3)_4$ and a nonlinear optical crystal KTP. Opt. Commun. **218(4–6)**, 379–384 (2003).

[23] D. Jaque, J. Capmany, J. Garcia Sole: Red, green, and blue laser light from a single $Nd:Yal_3(BO_3)_4$ crystal based on laser oscillation at 1.3 μm. Appl. Phys. Lett. **75(3)**, 325–327 (1999).

9.5 Periodically Poled Crystals

The introduction of periodically poled crystals is probably the most important breakthrough in the field of nonlinear optics in the past decade. Since 1991, hundreds of experimental works have been devoted to the applications of periodically poled nonlinear materials. What is surprising is that until now, there was not any special monography devoted to such materials, not even any mention of them in the standard textbooks on nonlinear optics, even though the history of these crystals already counts more than 40 years.

In 1961, the first observation of SHG in crystalline quartz was made by Franken *et al.* [1]. The power of the SH wave was very small due to the absence of phase matching between the interaction waves. Two years later, Giordmaine [2] and Maker *et al.* [3] proposed the birefringent phase matching (BPM), which utilizes the difference in phase velocities between waves with different polarizations at second-harmonic and fundamental frequencies. This kind of phase matching was generally used in applied nonlinear optics during next three decades. However, as early as 1962, Bloembergen *et al.* proposed another way of phase matching, so-called quasi-phase matching (QPM) [4]. QPM refers to a periodic modulation of the nonlinear susceptibility of nonlinear material in the direction of light wave (waves) propagation, which keeps the phase mismatch around the zero value. Three decades later, the emergence of an electric-field poling technique allowed the periodical reversing of ferroelectric domain polarity, which led to the practical implementation of the QPM approach. At present, the periodically poled crystals PPLN, PPLT, PPKTP, and PPRTA are used most often. For the reviews on QPM, see [5], [6], [7].

There are several advantages of quasi-phase matching over BPM. First, there is no restriction imposed on material and polarization. Second, it is possible to use the highest second-order nonlinear coefficient [e.g., for LN $d_{33}(1.064\,\mu\text{m}) = 25.2\,\text{pm/V}$, which is much higher than $d_{31}(1.064\,\mu\text{m}) = 4.6\,\text{pm/V}$, usually used in BPM. Therefore, polarizing all interacting waves along the Z axis results in the highest effective nonlinearity. It should be emphasized that such interaction could not be realized through BPM]. In the case of PPLN, there are additional advantages like smaller susceptibility to photorefractive effect (compared with LN) and longwave IR cutoff for the extraordinary wave; this last property allows realization of PPLN-based OPO with idler tunability up to 6.6 μm [8], 6.8 μm [9], and even 7.3 μm [10].

We will shortly list the most important recent technical achievements in applications of periodically poled nonlinear materials. In [11], SHG of a CW Nd:YAG laser ($\lambda = 1.064\,\mu\text{m}$, $P = 6.5\,\text{W}$) in a 5.3-cm-long PPLN crystal with a 6.5-μm domain period was investigated. The measured green output power was 2.7 W. Another transition of a Nd:YAG laser ($\lambda = 0.946\,\mu\text{m}$, $P = 2.6\,\text{W}$) was used for second-harmonic generation in [12]. The CW blue power reached in a 0.9-cm-long PPKTP with a 6.09-μm domain period equaled 0.74 W. In [13], the SHG of picosecond pulses, emitted by an InGaAs MOPA ($\lambda = 920\,\text{nm}$), was studied in a 1-cm-long PPKTP with a 5-μm domain period. The obtained average SH power was 0.25 W. The sum-frequency generation between two lines of a diode-pumped Nd:YVO_4 laser ($\lambda_1 = 1.064\,\mu\text{m}$, $P_1 = 1.2\,\text{W}$, $\lambda_2 = 1.342\,\mu\text{m}$, $P_2 = 1.0\,\text{W}$) in a 1.9-cm-long PPLN crystal with a

9.5-μm domain period was investigated in [14]. The generated CW yellow output power at 593 nm was 78 mW. In [15], a 5-cm-long PPLN crystal with a 30.3-μm domain period was used simultaneously for OPO (pumped by CW Nd:YAG laser, $\lambda = 1.064\,\mu m$) and DFG between the signal (1.7 μm) and idler (2.8 μm) wavelengths. The power of CW IR output reached 150 mW at 4.3 μm.

Now we will consider the OPO results obtained with periodically poled crystals. In [16], a diode-pumped Nd:YVO_4 laser pumped the OPO based on 5-cm-long PPLN crystal with 8 domain periods from 28.5 to 29.9 μm. The OPO tuning in the 1.461–1.601-μm range for signal wave and 3.173–3.917 μm for idler wave was accomplished by the grating change and/or by raising the crystal temperature from 91 °C to 173 °C. The system produced signal pulses with 34-ps duration, repetition rate 235 MHz, and output average signal power of 1 W. In [17], a similar pump laser but with smaller repetition rate (20 kHz) was used. Two 1-cm-long, periodically poled crystals were employed: PPKTP with a 37.8-μm domain period and PPRTA with 40.2-μm domain period. At room temperature, the PPKTP-based OPO generated the signal wave at 1.72 μm and idler wave at 2.79 μm with total output power of 2 W. The PPRTA-based OPO produced the signal wave at 1.58 μm and idler wave at 3.26 μm with total output power of 1.3 W. In [18], 1.6 W of signal power (1.56–1.64 μm) and 0.8 W of idler power (3.34–3.03 μm) were generated in a 5.5-cm-long PPLN crystal with a 29.75-μm domain period. The PPLN-based OPG is pumped by 10-ns pulses of a Q-switched Nd:YVO_4 laser, operating at a 10-kHz repetition rate. The tuning is accomplished by the changing of the PPLN temperature from 140 °C to 250 °C. In [19], the maximal total OPG output power of 8.9 W was achieved. The OPG was pumped by a mode-locked Nd:YVO_4 oscillator-amplifier system, which generated 7-ps pulses with a repetition rate of 82.3 MHz and an average power of 24 W. A 5.5-cm-long PPLN crystal with 29.75-μm domain period was employed. In [20], the maximal tuning range for OPO using periodically poled nonlinear crystals was reached. The OPO was pumped by the second harmonic of a CW Nd:YVO_4 laser ($\lambda = 532$ nm, $P = 0.8$–3.3 W). As a nonlinear element, 2.4-cm-long PPKTP crystals or 2.5-cm-long PPLN crystals were used with different domain periods: 19 periods from 8.96 to 12.194 μm for PPKTP and 23 periods from 6.51 to 9.59 μm for PPLN. The tuning in the ranges 656–1035 nm for signal wave and 1096–2830 nm for idler wave was accomplished by the changing of gratings and/or the temperature of nonlinear crystal. For the PPKTP crystal, the temperature varied from 20 °C to 80 °C and for the PPLN crystal from 140 °C to 200 °C.

Changing the temperature of a periodically poled nonlinear material is a rather slow method of OPO tuning. Another way of OPO tuning is through the change of domain period (choosing different superlattices in a multigrating crystal), and this needs mechanical translational devices and hence it is also slow. In [21], the method of electrooptic tuning was proposed. The idea is very simple: the periodically poled crystal is divided into 3 equal segments, the first and the last being poled with a 50% duty cycle, whereas the central segment remains unpoled and carries a pair of electrodes. A high voltage is applied across the central segment to change electrooptically the refractive index of the periodically poled crystal, which modifies the spectral shape of the parametric gain and thereby shifts the gain-maximum and

the oscillation wavelength. Changing the applied voltage from −180 to +1050 V, the fast tuning of a PPLN-based OPO in the 1562–1664-nm range was demonstrated. Similar results were reported in [22].

Some authors utilize double grating domain structures [23], [24] or partly periodically poled nonlinear crystal [25]. In [23], with picosecond 532-nm pumping (by SH of Nd:YAG laser) in the first structure (PPLT, 2 cm of 11.9-μm domain period), the optical parametric generation takes place, whereas in the second structure (PPLT, 1 cm of 8.8-μm domain period), the SFG between the OPG idler and pump radiation occurs. As a result, red light at 631 nm and blue light at 460 nm are produced. In [24], with 1342-nm pumping (diode-pumped Nd:YVO_4 laser, 35 ns, 10 kHz) in the first structure (PPLT, 2 cm of 14.9-μm domain period, working temperature 74.6 °C), SHG takes place, whereas in the second structure (PPLT, 1 cm of 4.9-μm domain period, working temperature 74.6 °C) THG occurs. As a result, the red (671 nm) and the blue (447 nm) radiations are generated with average powers 0.75 W and 0.15 W, respectively. Finally, in [25], only part of the nonlinear crystal was periodically poled (1.5 cm of 3.0-cm-long KTP with 16.46-μm domain period), in which QPM SHG of 1.327-μm radiation took place, whereas in the remaining unpoled 1.5 cm of KTP crystal, the usual birefringent THG occurred.

In [26], a special two-component quasi-periodic optical superlattice, which allows the third-harmonic generation at any desired wavelength, is proposed. The corresponding grating contains the sequence of two building blocks A and B with the lengths D_A and D_B. Each block consists of two inverse ferroelectric domains, the widths of the positive ones being equal to L. The calculations made for LT, fundamental wavelength of 1.44 μm, and crystal temperature of 30 °C show the maximum of THG conversion for $D_A = 13.12$ μm, $D_B = 18.65$ μm, $L = 9.31$ μm, and the block sequence ABBBBABBBAB... In the experiment, the 27% THG conversion efficiency was obtained in 1.5-cm-long PPLT crystal at 27.8 °C; the measured blue output power at 480 nm equaled 4 mW.

References

[1] P.A. Franken, A.E. Hill, C.W. Peters, G. Weinreich: Generation of optical harmonics. Phys. Rev. Lett. **7(4)**, 118–119 (1961).

[2] J.A. Giordmaine: Mixing of light beams in crystals. Phys. Rev. Lett. **8(1)**, 19–20 (1962).

[3] P.D. Maker, R.W. Terhune, M. Nisenoff, C.M. Savage: Effects of dispersion and focusing on the production of optical harmonics. Phys. Rev. Lett. **8(1)**, 21–22 (1962).

[4] J.A. Armstrong, N. Bloembergen, J. Ducuing, P.S. Pershan: Interactions between light waves in a nonlinear dielectric. Phys. Rev. **127(6)**, 1918–1939 (1962).

[5] M.M. Fejer, G.A. Magel, D.H. Jundt, R.L. Byer: Quasi-phase-matched second harmonic generation: tuning and tolerances. IEEE. J. Quant. Electr. **28(11)**, 2631–2654 (1992).

[6] L.E. Myers, R.C. Eckardt, M.M. Fejer, R.L. Byer, W.R. Bosenberg, J.W. Pierce: Quasi-phase-matched optical parametric oscillators in bulk periodically poled $LiNbO_3$. J. Opt. Soc. Am. B **12(11)**, 2102–2116 (1995).

[7] L.E. Myers, W.R. Bosenberg: Periodically poled lithium niobate and quasi-phase-matched optical parametric oscillators. IEEE. J. Quant. Electr. **33(10)**, 1663–1672 (1997).

[8] M. Sato, T. Hatanaka, S. Izumi, T. Taniuchi, H. Ito: Generation of 6.6-μm optical parametric oscillation with periodically poled $LiNbO_3$. Appl. Opt. **38(12)**, 2560–2563 (1999).

[9] P. Loza-Alvarez, C.T.A. Brown, D.T. Reid, W. Sibbett, M. Missey: High-repetition-rate ultrashort-pulse optical parametric oscillator continuously tunable from 2.8 to 6.8 μm. Opt. Lett. **24(21)**, 1523–1525 (1999).

[10] M.A. Watson, M.V. O'Connor, P.S. Lloyd, D.P. Shepard, D.C. Hanna, C.B.E. Gavith, L. Ming, P.G.R. Smith, O. Balachninaite: Extended operation of synchronously pumped optical parametric oscillators to longer idler wavelengths. Opt. Lett. **27(23)**, 2106–2108 (2002).

[11] G.D. Miller, R.G. Batchko, W.M. Tulloch, D.R.Weise, M.M. Fejer, R.L. Byer: 42%-efficient single-pass CW second-harmonic generation in periodically poled lithium niobate. Opt. Lett. **22(24)**, 1834–1836 (1997).

[12] M. Pierrou, F. Laurell, H. Karlsson, T. Kellner, C. Czeranowsky, G. Huber: Generation of 740 mW of blue light by intracavity frequency doubling with a first-order quasi-phase-matched $KTiOPO_4$ crystal. Opt. Lett. **24(4)**, 205–207 (1999).

[13] D. Woll, J. Schumacher, A. Robertson, M.A. Tremont, R. Wallenstein, M. Katz, D. Eger, A. Englander: 250 mW of coherent blue 460-nm light generated by single-pass frequency doubling of the output of a mode-locked high-power diode laser in periodically poled KTP. Opt. Lett. **27(12)**, 1055–1057 (2002).

[14] Y.F. Chen, S.W. Tsai, S.C. Wang, Y.C. Huang, T.C. Lin, B.C. Wong: Efficient generation of continuous-wave yellow light by single-pass sum-frequency mixing of a diode-pumped Nd:YVO_4 dual-wavelength laser with periodically poled lithium niobate. Opt. Lett. **27(20)**, 1809–1811 (2002).

[15] D.-W. Chen, K. Masters: Continuous-wave 4.3-μm intracavity difference frequency generation in an optical parametric oscillator. Opt. Lett. **26(1)**, 25–27 (2001).

[16] T. Graf, G. McConnell, A.I. Ferguson, E. Bente, D. Burns, M.D. Dawson: Synchronously pumped optical parametric oscillation in periodically poled lithium niobate with 1-W average output power. Appl. Opt. **38(15)**, 3324–3328 (1999).

[17] M. Peltz, U. Bäder, A. Borsutzky, R. Wallenstein, J. Hellström, H. Karlsson, V. Pasiskevicius, F. Laurell: Optical parametric oscillators for high pulse energy and high average power operation based on large aperture periodically poled KTP and RTA. Appl. Phys. B **73(7)**, 663–670 (2001).

[18] U. Bäder, T. Mattern, T. Bauer, J. Batschke, M. Rahm, A. Borsutzky, R. Wallenstein: Pulsed nanosecond optical parametric generator based on periodically poled lithium niobate. Opt. Commun. **217(1–6)**, 375–380 (2003).

[19] B. Köhler, U. Bäder, A. Nebel, J.-P. Meyn, R. Wallenstein: A 9.5-W 82-MHz-repetition-rate picosecond optical parametric generator with CW diode laser injection seeding. Appl. Phys. B **75(1)**, 31–34 (2002).

[20] U. Strößner, J.-P. Meyn, R. Wallenstein, P. Urenski, A. Arie, G. Rosenman, J. Mlynek, S, Schiller, A. Peters: Single-frequency continuous-wave optical parametric oscillator system with an ultrawide tuning range of 550 to 2830 nm. J. Opt. Soc. Am. B **19(6)**, 1419–1424 (2002).

[21] P. Gross, M.E. Klein, H. Ridderbusch, D.-H. Lee, J.-P. Meyn, R. Wallenstein, K.-J. Boller: Wide wavelength tuning of an optical parametric oscillator through electro-optic shaping of the gain spectrum. Opt. Lett. **27(16)**, 1433–1435 (2002).

[22] S. Haidar, Y. Sasaki, E. Niwa, K. Masumoto, H. Ito: Electro-optic tuning of a periodically poled $LiNbO_3$ optical parametric oscillator and mixing its output waves to generate mid-IR tunable from 9.4 to 10.5 μm. Opt. Commun. **229(1–6)**, 325–330 (2004).

[23] Z.-W. Liu, S.-N. Zhu, Y.-Y. Zhu, H.-T. Wang, G.-Z. Luo, H. Liu, N.-B. Min, X.-Y. Liang, Z.-Y. Xu: Red and blue light generation in an $LiTaO_3$ crystal with a double grating domain structure. Chin. Phys. Lett. **18(4)**, 539–540 (2001).

[24] J.-L. He, X.-P. Hu, S.-N. Zhu, Y.-Y. Zhu, N.-B. Min: Efficient generation of red and blue light in a dual-structure periodically poled $LiTaO_3$ crystal. Chin. Phys. Lett. **20(2)**, 2175–2177 (2003).
[25] X. Mu, Y.J. Ding: Efficient third-harmonic generation in partly periodically poled $KTiOPO_4$ crystal. Opt. Lett. **26(9)**, 623–625 (2001).
[26] C. Zhang, H. Wei, Y.-Y. Zhu, H.-T. Wang, S.-N. Zhu, N.-B. Ming: Third-harmonic generation in a general two-component quasi-periodic optical superlattice. Opt. Lett. **26(12)**, 899–901 (2001).

9.6 Photonic Band-Gap Crystals

Photonic band-gap crystals (or photonic crystals, both terms seem to be unsuccessful) are simply nonlinear crystals where the nonlinearity is varying in two dimensions. It should be remembered that periodically poled nonlinear crystals are materials with periodical *one-dimensional* change of the sign of second-order nonlinearity. Recently, Berger proposed [1], [2] to extend the idea of quasi-phase matching to multiple spatial dimensions. The first *two-dimensional periodically poled* nonlinear crystal was experimentally realized by a UK group [3], who fabricated a periodic structure with hexagonal symmetry in lithium niobate (so-called HeXLN). The resulting hexagonal lattice of hexagonal inverted domains had a period of 18.05 μm, a total inverted area of about 30%, and was designed for QPM SHG of 1531-nm fundamental radiation in ΓM direction (X axis) at 150 °C. The propagation length in this direction was 1.4 cm. The HeXLN crystal was placed in the oven to eliminate the photorefractive damage. At low input intensities ($\sim$0.2 GW/cm^2) of 4 ps, 1.531-μm fundamental radiation, the output consists of multiple output beams of different colors, emerging from the crystals at different angles. These beams correspond to SH radiation, emerging at symmetrical $\pm(1.1 \pm 0.1)^\circ$ angles from fundamental beam direction (ΓM direction) as well as to cascaded THG and FoHG radiations. At higher intensities, the SH spots remained in the same positions, whereas the THG light started to be emitted over a wide range of angles. The maximum external SHG conversion efficiency (at intensities $\sim$0.2 GW/cm^2) was around 60%.

A more detailed investigation of SHG and cascaded THG and FoHG in HeXLN was conducted later by the same group, using a less-powerful nanosecond IR source (1.520–1.560 μm, 5 ns, 2 kHz, 5–16 MW/cm^2) and a shorter, 1-cm-long, HeXLN crystal [4]. At relatively low intensities, the obtained SHG temperature bandwidth for 1536-nm fundamental radiation in HeXLN was 8.5 °C, which is considerably larger than that for PPLN of the same length and same period (4.2 °C). At higher irradiation intensities (14–16 MW/cm^2), besides the SHG beam at 768 nm, the authors of [4] observed green and blue beams, emerging from the crystal, and corresponding to cascaded THG and FoHG. An additional green beam, corresponding to birefringent type II THG, was also discovered. The authors of [4] state that HeXLN is "highly suited for the simultaneous phase matching of multiple nonlinear interactions." A similar statement was made by the authors of [5], who theoretically considered harmonic generation in nonlinear photonic crystals and suggested that two-dimensional

photonic crystals "are ideal candidates for experimental observation of simultaneous generation of several harmonics and different effects associated with the multistep cascading processes." Unfortunately, this remarkable feature of HeXLN will probably limit its practical application in nonlinear optics.

In [6], the SHG of 1.536-μm fundamental radiation in a HeXLN-based waveguide was investigated. The best value of internal conversion efficiency (46%) was found for $TM_0(\omega) \Rightarrow TM_1(2\omega)$ SHG process. However, the simultaneous damage of the crystal due to the third-harmonic generation was also observed.

References

[1] V. Berger: Nonlinear photonic crystals. Phys. Rev. Lett. **81(19)**, 4136–4139 (1998).
[2] V. Berger: From photonic band gaps to refractive index engineering. Opt. Mater. **11(2–3)**, 131–142 (1999).
[3] N.G.R. Broderick, G.W. Ross, H.L. Offerhaus, D.J. Richardson, D.C. Hanna: Hexagonally poled lithium niobate: a two-dimensional nonlinear photonic crystal. Phys. Rev. Lett. **84(19)**, 4345–4348 (2000).
[4] N.G.R. Broderick, R.T. Bratfalean, T.M. Monro, D.J. Richardson, C.M. de Sterke: Temperature and wavelength tuning of second-, third-, and fourth-harmonic generation in a two-dimensional hexagonally poled nonlinear crystal. J. Opt. Soc. Am. B **19(9)**, 2263–2272 (2002).
[5] S. Saltiel, Y.S. Kivshar: Phase matching in nonlinear $\chi^{(2)}$ photonic crystals. Opt. Lett. **25(16)**, 1204–1206 (2000).
[6] K. Gallo, R.T. Bratfalean, A.C. Peacock, N.G.R. Broderick, C.B.E. Gavith, L. Ming, P.G.R. Smith, D.J. Richardson: Second-harmonic generation in hexagonally-poled lithium niobate slab waveguides. Electron. Lett. **39(1)**, 75–76 (2003).

9.7 THG via $\chi^{(3)}$ Nonlinearity

All described in this book, until now, referred to so-called three-wave interactions, utilizing the second-order nonlinear susceptibility tensor $\chi^{(2)}$. The four-wave interactions, using $\chi^{(3)}$ nonlinearity, could also be of practical interest, especially in the case of THG (as they employ one nonlinear crystal instead of two). The effective third-order nonlinear coefficients for uniaxial and isotropic crystals were derived by Midwinter and Warner [1] in 1967. Later, the corresponding expressions for biaxial crystals were obtained by a Chinese group [2]. In [3], the third-order nonlinear coefficients of lithium iodate, c_{35} and c_{12} were measured relative to the third-order nonlinear coefficients of ADP and KDP.

Qiu and Penzkofer [4] investigated the THG of 5-ps, 1.054-μm radiation in a BBO crystal and obtained 0.8% conversion efficiency at input intensity of $50\,GW/cm^2$. The authors claimed that the observed third-harmonic radiation could be due to the direct third-order nonlinear process or to cascaded second-order processes and state that both processes have a similar yield. A decade later, THG in a KTP crystal was investigated simultaneously by two groups [5], [6]. They obtained similar results on efficiency: 2.4% in a 0.49-cm crystal at $28\,GW/cm^2$ incident intensity of 22-ps,

1.618-μm fundamental radiation and 1% at 20 GW/cm^2 incident intensity of 30–40-ps, 1.6–1.8-μm fundamental radiation, respectively. However, the conclusions of both groups contradict each other: whereas the first group claims that "the quadratic contribution is only 10%," the second group proves that "the cascaded second-order process is the dominant process for THG in KTP."

Recently, an American group reached a 6% THG efficiency value in a 0.3-cm-long BBO at 200 GW/cm^2 incident intensity ($\lambda = 1.055\,\mu\text{m}$, $\tau_p = 350\,\text{fs}$) using either type I or type II phase matching [7], [8]. Their conclusion: "the cascaded SHG and SFG processes, even though non-phase-matched, can contribute significantly and even play the dominant role in phase-matched single-crystal SHG in nonlinear materials with a second-order response."

References

[1] J.E. Midwinter, J. Warner: The effects of phase matching method and of crystal symmetry on the polar dependence of third-order non-linear optical polarization. Brit. J. Appl. Phys. **16(11)**, 1667–1674 (1965).

[2] S.-W. Xie, X.-L. Yang, W.-Y. Jia, Y.-L. Chen: Phase-matched third-harmonic generation in biaxial crystals. Opt. Commun. **118(5–6)**, 648–656 (1995).

[3] M. Okada: Third-order nonlinear optical coefficients of $LiIO_3$. Appl. Phys. Lett. **18(10)**, 451–452 (1971).

[4] P. Qiu, A. Penzkofer: Picosecond third-harmonic light generation in β-BaB_2O_4. Appl. Phys. B **45(4)**, 225–236 (1988).

[5] J.P. Feve, B. Boulanger, Y. Guillien: Efficient energy conversion for cubic third-harmonic generation that is phase-matched in $KTiOPO_4$. Opt. Lett. **25(18)**, 1373–1375 (2000).

[6] Y. Takagi, S. Muraki: Third-harmonic generation in a noncentrosymmetrical crystal: direct third-order or cascaded second-order process? J. Lumunesc. **87–89**, 865–867 (2000).

[7] P.S. Banks, M.D. Feit, M.D. Perry: High-intensity third-harmonic generation in beta barium borate through second-order and third-order susceptibilities. Opt. Lett. **24(1)**, 4–6 (1999).

[8] P.S. Banks, M.D. Feit, M.D. Perry: High-intensity third-harmonic generation. J. Opt. Soc. Am. B **19(1)**, 102–118 (2002).

10

Concluding Remarks

Even though during my work on this book I took all conceivable precautions to minimize the number of mistakes and misprints, it is difficult, if not impossible, to exclude them all. Therefore, I wish to apologize for all possible errors and ask the readers in the case of their discovery to inform me by post or e-mail (niko@phys.ucc.ie). I would also be grateful for any comments regarding this book, which will be taken into account in future editions.

Appendix A

Full Titles of Listed Journals

Acta Crystallogr.
Acta Crystallographica
Appl. Opt.
Applied Optics
Appl. Phys.
Applied Physics
Appl. Phys. Lett.
Applied Physics Letters
Atmos. Oceanic Opt.
Atmospheric and Oceanic Optics (Russia)
Brit. J. Appl. Phys.
British Journal of Applied Physics
Bull. Mater. Sci.
Bulletin of Materials Science (India)
Bull. Acad. Sci. USSR, Phys. Ser.
Bulletin of USSR Academy of Sciences: Physical Series
Bull. Russian Acad. Sci.: Physics
Bulletin of the Russian Academy of Sciences: Physics
Chin. Phys. Lett.
Chinese Physics Letters
Cryst. Res. Technol.
Crystal Research and Technology
Doklady AN SSSR
Doklady Akademii Nauk SSSR (USSR)
Electron. Lett.
Electronics Letters
Exp. Techn. Phys.
Experimentelle Technik der Physik
Eur. J. Solid State Inorg. Chem.
European Journal of Solid State and Inorganic Chemistry

Fiz. Tekh. Poluprov.
Fizika i Tekhnuka Poluprovodnikov (USSR, Russia)
Fiz. Tverd. Tela
Fizika Tverdogo Tela (USSR, Russia)
IEEE J. Quant. Electr.
IEEE Journal of Quantum Electronics
IEEE J. Sel. Topics Quant. Electr.
IEEE Journal of Selected Topics in Quantum Electronics
IEEE Photon. Technol. Lett.
IEEE Photonics Technology Letters
Int. J. Nonl. Opt. Phys.
International Journal of Nonlinear Optical Physics
Int. Mater. Rev.
International Materials Reviews
Izv. Akad. Nauk SSSR, Ser. Fiz.
Izvestiya Akademii Nauk SSSR, Seriya Fizicheskaya (USSR)
Izv. Ross. Akad. Nauk, Ser. Fiz.
Izvestiya Rossiiskoi Akademii Nauk, Seriya Fizicheskaya (Russia)
JETP Lett.
JETP Letters
J. Am. Ceram. Society
Journal of American Ceramic Society
J. Appl. Phys.
Journal of Applied Physics
J. Appl. Spectrosc.
Journal of Applied Spectroscopy
J. Cryst. Growth
Journal of Crystal Growth
J. Korean Phys. Soc.
Journal of the Korean Physical Society
J. Luminesc.
Journal of Luminescence
J. Mat. Sci. Lett.
Journal of Materials Science Letters
J. Mater. Sci. Semicond. Process.
Journal of Material Science in Semiconductor Processing
J. Mol. Struct.
Journal of Molecular Structure
J. Opt. Soc. Am.
Journal of Optical Society of America
J. Opt. Technol.
Journal of Optical Technology (Russia)
J. Phys.
Journal of Physics

J. Phys. Chem. Solids
Journal of Physics and Chemistry of Solids
J. Phys.: Condens. Matter
Journal of Physics: Condensed Matter
J. Phys. Soc. Japan
Journal of the Physical Society of Japan
J. Synth. Cryst.
Journal of Synthetic Crystals (China)
Jpn. J. Appl. Phys.
Japanese Journal of Applied Physics
Kratkie Soobshch. Fiz.
Kratkie Soobshcheniya po Fizike (USSR, Russia)
Kristallogr.
Kristallografiya (USSR, Russia)
Kvant. Elektron.
Kvantovaya Elektronika (USSR, Russia)
Laser Phys.
Laser Physics (Russia)
Lit. Fiz. Sbornik
Litovskii Fizicheskii Sbornik (Lithuania)
Mater. Lett.
Materials Letters
MRS Bulletin
Materials Research Society Bulletin
Mater. Res. Bull.
Materials Research Bulletin
Mater. Sci. Eng.
Materials Science and Engineering
Nonl. Opt.
Nonlinear Optics
Opt. Commun.
Optics Communications
Opto-electron.
Opto-electronics
Opto-Electron. Rev.
Opto-Electronics Review
Opt. Eng.
Optical Engineering
Opt. Laser Technol.
Optics & Laser Technology
Opt. Lett.
Optics Letters
Opt. Mater.
Optical Materials

Opt. Mekh. Promyshl.
Optiko-Mekhanicheskaya Promyshlennost (USSR, Russia)
Opt. Quant. Electron.
Optical and Quantum Electronics
Opt. Spectrosc. USSR
Optics and Spectroscopy USSR
Opt. Spektrosk.
Optika i Spektroskopiya (USSR, Russia)
Pisma Zh. Eksp. Teor. Fiz.
Pisma v Zhurnal Eksperimentalnoi i Teoreticheskoi Fiziki (USSR, Russia)
Pisma Zh. Tekh. Fiz.
Pisma v Zhurnal Tekhnicheskoi Fiziki (USSR, Russia)
Progr. Cryst. Growth Character. Mater.
Progress in Crystal Growth and Characterization of Materials
Phys. Lett.
Physics Letters
Phys. Rev.
Physical Review
Phys. Rev. Lett.
Physical Review Letters
Phys. Stat. Solidi
Physica Status Solidi
Pure Appl. Opt.
Pure and Applied Optics
Proc SPIE
Proceedings SPIE
Quantum Electron.
Quantum Electronics (Russia)
Rev. Laser Eng.
Review of Laser Engineering
Russ. J. Inorgan. Chem.
Russian Journal of Inorganic Chemistry
Solid State Commun.
Solid State Communications
Sov. J. Opt. Technol.
Soviet Journal of Optical Technology
Sov. J. Quantum Electron.
Soviet Journal of Quantum Electronics
Sov. Phys. - Crystallogr.
Soviet Physics - Crystallography
Sov. Phys. - Doklady
Soviet Physics - Doklady
Sov. Phys. - JETP
Soviet Physics - JETP

Sov. Phys. - Semicond.
Soviet Physics - Semiconductors
Sov. Phys. - Solid State
Soviet Physics - Solid State
Sov. Phys. - Tech. Phys.
Soviet Physics - Technical Physics
Sov. Tech. Phys. Lett.
Soviet Technical Physics Letters
Z. Kristallogr.
Zeitschrift für Kristallographie
Zh. Eksp. Teor. Fiz.
Zhurnal Eksperimentalnoi I Teoreticheskoi Fiziki (USSR, Russia)
Zh. Neorg. Khim.
Zhurnal Neorganicheskoi Khimii (USSR, Russia)
Zh. Prikl. Spektrosk.
Zhurnal Prikladnoi Spektroskopii (USSR, Russia)
Zh. Tekh. Fiz.
Zhurnal Tekhnicheskoi Fiziki (USSR, Russia)

Appendix B

Recent References added at Proof Reading

To Chapter 2. Basic nonlinear optical crystals

[1] H. Wang, A.M. Weiner: Efficiency of short-pulse type-I second-harmonic generation with simultaneous spatial walk-off, temporal walk-off, and pump depletion. IEEE J. Quant. Electr. **39(12)**, 1600–1618 (2003).

[2] A.-Y. Yao, W. Hou, X.-C. Lin, Y. Bi, R.-N. Li, D.-F. Cui, Z.-Y. Xu: High power red laser at 671 nm by intracavity-doubled Nd:YVO_4 laser using LiB_3O_5. Opt. Commun. **231(1–6)**, 413–416 (2004).

[3] H.Q. Li, H.B. Zhang, Z. Bao, J. Zhang, Z.P. Sun, Y.P. Kong, Y. Bi, X.C. Lin, A.Y. Yao, G.L. Wang, W. Hou, R.N. Li, D.F. Cui, Z.Y. Xu: High-power nanosecond optical oscillator based on a long LiB_3O_5 crystal. Opt. Commun. **232(1–6)**, 411–415 (2004).

[4] X.-C. Lin, Y. Zhang, Y.-P. Kong, J. Zhang, A.-Y. Yao, W. Hou, D.-F. Cui, R.-N. Li, Z.-Y. Xu, J. Li: Low-threshold mid-infrared optical parametric oscillator using periodically poled $LiNbO_3$. Chin. Phys. Lett. **21(1)**, 98–100 (2004).

[5] M.V. Pack, D.J. Armstrong, A.V. Smith: Measurements of the $\chi^{(2)}$ tensors of $KTiOPO_4$, $KTiOAsO_4$, $RbTiOPO_4$ and $RbTiOAsO_4$ crystals. Appl. Opt. **43(16)**, 3319–3323 (2004).

To Chapter 3. Main infrared materials

[6] W. Shi, Y.J. Ding, P.G. Schunemann: Coherent terahertz waves based on difference-frequency generation in an annealed zinc-germanium phosphide crystal: improvements on tuning ranges and peak powers. Opt. Commun. **233(1–3)**, 183–189 (2004).

[7] P. Kumbhakar, T. Kobayashi, G.C. Bhar: Sellmeier dispersion for phase-matched terahertz generation in $ZnGeP_2$. Appl. Opt. **43(16)**, 3324–3328 (2004).

[8] R.S. Dubinkin, X. Mu, Y.J. Ding: Spectrum of two-photon absorption coefficients for $ZnGeP_2$. In: *International Quantum Electronics Conference CLEO/IQEC 2004, Technical Digest* (OSA, Washington DC 2004) paper IMD6.

To Chapter 4. Often used crystals

[9] I.A. Begishev, M. Kalashnikov, V. Karpov, P. Nickles, H. Schönnagel, I.A. Kulagin, T. Usmanov: Limitation of second-harmonic generation of femtosecond Ti:sapphire laser pulses. J. Opt. Soc. Am. B **21(2)**, 318–322 (2004).

[10] J. Sakuma, Y. Asakawa, M. Obara: Generation of 5-W deep-UV continuous-wave radiation at 266 nm by an external cavity with a $CsLiB_6O_{10}$ crystal. Opt. Lett. **29(1)**, 92–94 (2004).

[11] N. Pavel, I. Shoji, T. Taira, K. Mizuuchi, A. Morikawa, T. Sugita, K. Yamamoto: Room-temperature, continuous-wave 1-W green power by single-pass frequency doubling in a bulk periodically poled $MgO:LiNbO_3$ crystal. Opt. Lett. **29(8)**, 830–832 (2004).

[12] K. Kato, N. Umemura: Sellmeier and thermo-optic dispersion formulas for $KTiOAsO_4$. In: *Conference on Lasers and Electrooptics CLEO/IQEC 2004, Technical Digest* (OSA, Washington DC 2004) paper CThT35.

[13] J. Hirohashi, K. Yamada, H. Kamio, S. Shichijyo: Embryonic nucleation method for fabrication of uniform periodically poled structures in potassium niobate for wavelength conversion devices. Jpn. J. Appl. Phys. **43(2)**, 559–566 (2004).

[14] S.S. Saltiel, K. Koynov, B. Agate, W. Sibbett: Second-harmonic generation with focused beams under conditions of large group-velocity mismatch. J. Opt. Soc. Am. B **21(3)**, 591–598 (2004).

To Chapter 5. Periodically poled crystals and "wafer" materials

[15] I. Yutsis, B. Kirshner, A. Arie: Temperature-dependent dispersion relations for $RbTiOPO_4$ and $RbTiOAsO_4$. Appl. Phys. B **79(1)**, 77–81 (2004).

[16] T. Skauli, P.S. Kuo, K.L. Vodopyanov, T.J. Pinguet, O. Levi, L.A. Eyres, J.S. Harris, M.M. Fejer, B. Gerard, L. Becouarn, E. Lallier: Improved dispersion relations for GaAs and applications to nonlinear optics. J. Appl. Phys. **94(10)**, 6447–6455 (2003).

To Chapter 6. Newly-developed and prospective crystals

[17] P. Segonds, B. Boulanger, J.-P. Feve, B. Menaert, J. Zaccaro, G. Aka, D. Pelenc: Linear and nonlinear optical properties of the monoclinic $Ca_4YO(BO_3)_3$ crystal. J. Opt. Soc. Am. B **21(4)**, 765–769 (2004).

[18] P. Kumbhakar, T. Kobayashi: Nonlinear optical properties of $Li_2B_4O_7$ (LB4) crystal for the generation of tunable ultra-fast laser radiation by optical parametric amplification. Appl. Phys. B **78(2)**, 165–170 (2004).

[19] V. Petrov, A. Yelisseyev, L. Isaenko, S. Lobanov, A. Titov, J.-J. Zondy: Second harmonic generation and optical parametric amplification in the mid-IR with orthorhombic biaxial crystals $LiGaS_2$ and $LiGaSe_2$. Appl. Phys. B **78(5)**, 543–546 (2004).

To Chapter 7. Self-frequency-doubling crystals

[20] A. Brenier, C. Tu, Z. Zhu, J. Li, Y. Wang, Z. You, B. Wu: Self-frequency tripling from two-cascaded second-order nonlinearities in $GdAl_3(BO_3)_4$: Nd^{3+}. Appl. Phys. Lett. **84(1)**, 16–18 (2004).
[21] A. Brenier, C. Tu, Z. Zhu, B. Wu: Red-green-blue generation from a lone dual-wavelength $GdAl_3(BO_3)_4$:Nd^{3+} laser. Appl. Phys. Lett. **84(12)**, 2034–2036 (2004).

To Chapter 8. Rare-used and archive crystals

[22] V. Petrov, V. Badikov, V. Panyutin, G. Shevyrdyaeva, S. Sheina, F. Rotermund: Mid-IR optical parametric amplification with femtosecond pumping near 800 nm using $Cd_xHg_{1-x}Ga_2S_4$. Opt. Commun. **235(1–3)**, 219–226 (2004).
[23] A.A. Mani, Z.D. Schultz, A.A. Gewirth, J.O. White, Y. Caudano, C. Humbert, L. Dreesen, P.A. Thiry, A. Peremans: Picosecond laser for performance of efficient nonlinear spectroscopy from 10 to 21 μm. Opt. Lett. **29(3)**, 274–276 (2004).

To Chapter 9. Some recent applications

[24] T. Kanai, T. Kanda, T. Sekikawa, S. Watanabe, T. Togashi, C. Chen, C. Zhang, Z. Xu, J. Wang: Generation of vacuum-ultraviolet light below 160 nm in a KBBF crystal by the fifth harmonic of a single-mode Ti:sapphire laser. J. Opt. Soc. Am. B **21(2)**, 370–375 (2004).
[25] W. Shi, Y.J. Ding: A monochromatic and high-power terahertz source tunable in the ranges of 2.7–38.4 and 58.2–3540 μm for variety of potential applications. Appl. Phys. Lett. **84(10)**, 1635–1637 (2004).
[26] P. Ni, B. Ma, S. Feng, B. Cheng, D. Zheng: Multiple-wavelength second-harmonic generations in a two-dimensional periodically poled lithium niobate. Opt. Commun. **233(1–3)**, 199–203 (2004).
[27] E.H.G. Backus, S. Roke, A.W. Kleyn, M. Bonn: Cascading second-order versus direct third-order nonlinear optical processes in a uniaxial crystal. Opt. Commun. **234(1–6)**, 404–417 (2004).

Subject Index